Synthesis and biophysical properties of Nucleic acid analogues bearing 5-atom achiral amide- and chiral D/L-amino acid-derived linkages

Thesis Submitted to
The University of Pune for the degree of

Doctor of Philosophy
in
Chemistry

BY

SEEMA BAGMARE

Research Supervisor
Dr. Vaijayanti A. Kumar

Division Of Organic Chemistry
National Chemical Laboratory
Pune-411008

December, 2012

CERTIFICATE

This is to certify that the work presented in the thesis entitled "**Synthesis and biophysical properties of Nucleic acid analogues bearing 5-atom achiral amide- and chiral D/L-amino acid-derived linkages**" submitted by Seema Bagmare, was carried out by the candidate at the National Chemical Laboratory Pune, under my supervision. Such materials as obtained from other sources have been duly acknowledged in the thesis.

Dr. Vaijayanti A. Kumar **December 2012**

(Research Supervisor)
Division of Organic Chemistry
National Chemical Laboratory
Pune 411008

CANDIDATE'S DECLARATION

I hereby declare that the thesis entitled "**Synthesis and biophysical properties of Nucleic acid analogues bearing 5-atom achiral amide- and chiral D/L-amino acid-derived linkages"** submitted for the award of degree of ***Doctor of Philosophy*** in Chemistry to the University of Pune has not been submitted by me to any other university or institution. This work was carried out by me at the National Chemical Laboratory, Pune, India. Such materials as obtained from other sources have been duly acknowledged in the thesis.

Seema Bagmare **December 2012**

National Chemical Laboratory
Pune- 411 008

Dedicated to
all my family members

Acknowledgement

It gives me an immense pleasure to express my deep and sincere gratitude to my research guide Dr. (Mrs.) Vaijayanti A. Kumar for all the advice, guidance and encouragement during every stage of this work. I am thankful for the confidence she had on me which encouraged me to pursue different scientific ideas during my research period. She challenged me to set my benchmark even higher and to look for solutions to problems rather than focus on the problem. I learned to believe in my future, my work and myself.

"Thank you doesn't seem sufficient but it is said with all respect"

Dr. (Mrs.) Moneesha deserves special thanks. Her encouragement, understanding and suggestions were invaluable during my stay in the lab and went a long way towards the completion of this thesis.

My sincere thanks to Mrs. Anita Gunjal for her help during the course of this work. I am also thankful to Dr. Anil Kumar, Dr. (Mrs.) V. S. Pore, Dr. M N Deshmukh, Prof. D. D. Dhavale and for their advice, various kinds of help and encouragement during the course of this work. I am also thankful to Mrs. M. V. Mane and Mrs. S. S. Kunte for HPLC analysis, and also special thanks to Dr Mahesh Kulkarni and Mrs Shanta Kumari for the MALDI-TOF and LC-MS experiments. The kind support from NMR group is greatly acknowledged and I am specially thankful to Dr.Rajmohanan, Shrikant, Snehal and Roshan. Thanks to Dr. (Mrs.) Puranik for the X-ray analysis.

I admire the co-operation of my seniors and colleagues who have taught me many things. I thank Dr Raman, Dr.Nilkantha, Dr Amit, Dr.Sathe, Dr.Shengte, Shridhar, Pradnya, Dr.Ashwani, Dr.Mahesh, Dr.Gitali, Dr.Roopa, Dr.Manaswini, Deepak, Nitin.

I thank Dr. Khirud Gogoi, Dr.Madhuri, Dr.Sachin,, Namrata, Parameshwar, Harshal, Harshit, Kiran, Venu, Manoj, Anjan, Tanya, Govind and Amit for their support and help, who made workplace fun, lively and made each other forget their worries even for a while. Thanks you all, for making my last period of work fun, enjoyable and sometimes unforgettable.I thank Bhumkar for the laboratory assistance.

My special thanks go to my beloved friends Shital, Ravi, Kishore, Rahul, Dr.Sunita, Archana, Aaliya, Suchita, Pravin, Sachin, Yogesh, Deepa, Madhav, Madhuru, Gowri, Roshna, Lalit, Pitamber and Soni for their individual support and encouragement during my carrier.

I would like to express my deep sense of gratitude to my husband, Prashant for providing me unflinching encouragement and support which made this dissertation possible. This piece of work will never be accomplished without him being behind me for guiding and accompanying me through thick and thin.

I want to thank my Parents, Mrs. Indumati Bagmare, without her continuous support and encouragement I never would have been able to achieve my goals and Late. Mr. Rameshappa Bagmare for giving me unconditional love all the way. I thank my all family members for their constant support and encouragement. I warmly appreciate the generosity and understanding of my In-laws Mrs. Bharatbai Mengshetti and Mr. Sharnappa Mengshetti for the support provided to me. Without the support of all family members, my ambition can hardly be realized.

My greatest regards to the Almighty for bestowing upon me the courage to face the complexities of life and complete this dissertation successfully and for inculcating in me the dedication and discipline to do whatever I undertake well.

I offer my sincere regards to people who have inspired me directly or indirectly in research and life during my doctoral study.

I am grateful to UGC, New Delhi, for awarding the senior research fellowship and Dr. Sourav Pal, present Director, and Dr. Shivram, former director, National Chemical Laboratory to carry out my research works, extending all infrastructural facilities and to submit this work in the form of a thesis for the award of Ph. D degree.

Seema Bagmare

Contents

Publication /Symposia		**i**
Abbreviations		**ii**
Abstract		**v**
1	**Chapter 1: Introduction: Recent advances in the area of nucleic acid modification**	
1.1	Introduction	
	1.1.1 Primary structure of DNA and RNA	1
	1.1.2 Base pairing *via* hydrogen bonding	2
	1.1.3 Sugar Puckering	3
	1.1.4 DNA Secondary conformation	4
	1.1.5 Structure of RNA	6
	1.1.6 Sense and antisense strand	6
1.2	Antisense Technologies	6
	1.2.1 Disruptive antisense approach	7
	1.2.2 Corrective antisense approach	8
1.3	Spectroscopic methods for studying DNA/RNA Interactions	11
	1.3.1 Ultraviolet spectroscopy	11
	1.3.2 Circular Dichroism	13
1.4	Modified Oligonucleotides	14
	1.4.1 Modifications of phosphate linkage	14
	1.4.2 N3'-P5'/P3'-N5' phosphoramidates	15
	1.4.3 Enantio-DNA and other stereoisomers of DNA/RNA	17
	1.4.4 Sugar 2'-Modifications	18
	1.4.5 Locked nucleic acids and its analogs	19
	1.4.6 Substituted sugar analogs	21
	1.4.7 L-Threofuranosyl nucleic acid (TNA) and Hexitol nucleic acids (HNA)	22
	1.4.8 Six membered carbocyclic analogs	24
	1.4.9 Oligonucleotides with dephosphono backbone	25
	1.4.9.1 Artificial DNA with amide backbone	25
	1.4.9.2 3', 5'-Guanidino linkers	27
1.5	Sugar-Phosphate modified oligonucleotides	28
	1.4.1 Morpholino nucleotides	28
	1.4.2 Peptide Nucleic Acids	29
	1.4.3.1 PNA modifications for selective RNA targeting	30
1.6	The present Work	32
1.7	References	34
2	**Chapter 2: Design and synthesis of oligonucleotide analogs with controlled backbone chirality**	49

2.1 Synthesis of T-$_{(\alpha\text{-amino Acid})}$-T dimers using L-Proline, D-Proline and Glycine 50

2.1.1 Introduction 50
2.1.2 Rationale, design and objectives of the present work 51
2.1.3 Methodolgy, results and discussion 54
2.1.3a Synthesis of amine component 55
2.1.3b Synthesis of acid component 56
2.1.3c Synthesis of T-$_{(\alpha\text{-amino acid})}$-T dimers 57
2.1.3d Synthesis of T-$_{(\alpha\text{-amino acid})}$-T phosphoramidite derivatives 58
2.1.4 Assignments of ^{1}H NMR of T-$_{(\alpha\text{-amino acid})}$-T dimer blocks with free 5', 3'-OH group 58
2.1.4a Conformation about the glycosidic bond 60
2.1.5 Conformation of the sugar ring 71
2.1.6 Cis trans isomers in proline containging dimer units 74
2.1.7 Summary 76

2.2 Synthesis of T-$_{(D\text{-Proline})}$-U$^{2'\text{-OMe}}$ dimer and T-$_{(\alpha\text{-Amino Acid})}$-T dimers using L-Lysine, D-Lysine

2.2.1: Introduction 77
2.2.2 Rationale, design and objectives of the present work 78
2.2.3 Methodolgy, results and discussion 81
2.2.3a Synthesis of T-$_{D\text{-Proline}}$-U$^{2'\text{-OMe}}$ dimer 81
2.2.3b Synthesis of T-$_{L\text{-Lysine}}$-T dimer and T-$_{D\text{-Lysine}}$-T dimer 83
2.2.4 Assignments by ^{1}H NMR of 3'-, 5'-OH free T-$_{D\text{-proline}}$-U$^{2'\text{-OMe}}$ and T-$_{Lysine}$-T dimer blocks 85
2.2.4a Conformation about the glycosidic bond 87
2.2.5 Conformation of the sugar ring 94
2.2.6 Summary 96

2.3 CD studies for the dimers and biophysical studies of sequences containing T-$_{(\alpha\text{-Amino Acid})}$-T and T-$_{D\text{-Proline}}$-U$^{2'\text{OMe}}$ dimers 97

2.3.1 CD analysis of building units, dimers and comparison study of base-stacking interactions in dimers 97
2.3.2 Solid phase synthesis of DNA Oligonucleotides by phosphoramidite method 101
2.3.2a Purification and MALDI-TOF characterization of modified oligomers 103
2.3.2b Synthesis of complementary oligonucleotides 104
2.3.3 Biophysical studies of T-$_{(\alpha\text{-amino acid})}$-T/U$^{2'\text{-OMe}}$ modified oligomers 105
2.3.3a UV-T_m of T-$_{(\alpha\text{-amino acid})}$-T/U$^{2'\text{-OMe}}$ modified 18mer oligonucleotides 105
2.3.3b UV-T_m of T-$_{(\alpha\text{-amino acid})}$-T/U$^{2'\text{-OMe}}$ modified 18mer oligonucleotides 109
2.3.4 Summary 112

2.4 Experimental 113

2.5	Appendix	130
2.6	References	176
3	**Chapter 3. Synthesis of all four Nucleoside-based-β-amino acid monomers for the synthesis of polyamide-DNA with alternating α-amino acid and nucleoside-β-amino-acids**	184
3.1	Introduction	185
3.2	Rational, Design and Objectives of the Present Work	185
3.3	Methodology, Results and Discussion	187
	3.3.1 Synthesis of Thymine monomer	188
	3.3.2 Synthesis of 5-methylcytosine monomer	189
	3.3.3 Synthesis of Adenine monomer	190
	3.3.4 Synthesis of Guanine monomer	191
3.4	Solid Phase synthesis of polyamide DNA oligomer	192
	3.4.1 Pre-loading of MBHA resin	193
	3.4.2 Solid Phase synthesis of model tetramer	193
	3.4.3 Cleavage and purification of tetramer	194
3.5	Conclusion	195
3.6	Summary	195
3.7	Experimental	196
3.8	Appendix	206
3.9	**References**	224
4	**Chapter 4: α-L-DNA: A DNA mimic with a compact backbone like RNA**	229
4.1	Introduction	230
4.2	Rational, Design and present work	234
4.3	Methodology, Results and Discussion	235
	4.3.1 Synthesis of α-L-DNA monomer	235
	4.3.2 Sugar conformation and crystal structure	237
4.4	Solid phase synthesis of modified oligonucleotide by phosphoroamidite method	240
	4.4.1 Purification and MALDI-TOF characterization of modified oligomers	241
4.5	Biophysical studies of α-L-DNA modified oligomers	241
4.6	RNase H digestion assay	243
4.7	Summary	245
4.8	Experimental	246
4.9	Appendix	255
4.10	**References**	267

List of Research Publications:

1. "Effect of chirality of L/D-proline and prochiral glycine as the linker amino acid in five-atom linked thymidinyl-(α-amino acid)-thymidine dimers" **Seema Bagmare**, Moneesha D'Costa and Vaijayanti A. Kumar., **Chem. Commun., 2009,** 6646–6648.

2. "Synthesis of all four nucleoside-based β-amino acids as protected precursors for the synthesis of polyamide-DNA with alternating α-amino acid and nucleoside-β-amino acids" **Seema Bagmare**, Manojkumar varada, Anjan Banerjee and Vaijayanti A. Kumar. Tetrahedron. article in press. http://dx.doi.org/10.1016/j.tet.2012.11.028

3. "Investigation of the effect of amino acid chirality in the internucleoside linker on DNA:DNA and DNA:RNA duplex stability" Seema Bagmare, Anita D.Gunjal and Vaijayanti A. Kumar., manuscript under preparation.

Symposia Attended/Poster/Oral Presentations:

1. Attended 4th INSA-KOSEF Symposium in Organic Chemistry. Contemporary Organic chemistry and its future directions. National Chemical Laboratory, Pune India, January 12-13, 2009.
2. Attended 11th CRSI National Symposium in Chemistry. National Chemical Laboratory, Pune India, February 5-8, 2009.
3. Attended National Seminar on Biocatalysis and Biomimetic Catalysis in Organic Chemistry. Dr. Babasaheb Ambedkar Marathwada University, Aurangabad India, March 20-21, 2009.
4. 5th J-NOST Conference, Indian Institute of Technology, Kanpur, India, December 4 -7, 2009 : Oral Presentation on "Effect of chirality of L/D-proline and prochiral glycine as the linker amino acid in five atom linked thymidinyl-(α-amino acid)-thymidine dimers" **Seema Bagmare,** Moneesha D'Costa, Anita Gunjal and Vaijayanti A. Kumar.
5. National Science Day, NCL Research Foundation, National chemical Laboratory, Pune. February 28, 2010; Poster Presentation on "Linker Chirality: Directs Base stacking in T-(α-amino acid)-T dimer" **Seema Bagmare,** Moneesha D'Costa and Vaijayanti A. Kumar.
6. XIX International Round Table on Nucleosides, Nucleotides and Nucleic Acids held in Lyon, France. August 31st to September 03rd, 2010 ; Poster presentation on "Investigation of the effect of amino acid chirality in the internucleoside linker on DNA:DNA and DNA:RNA duplex stability" **Seema Bagmare**, Moneesha D'Costa, Anita Gunjal and Vaijayanti A. Kumar
7. National Science Day, NCL Research Foundation, National chemical Laboratory, Pune. February 24-25, 2010; Poster Presentation on "Synthesis of nucleoside β-amino acids" **Seema Bagmare,** Anjan Banarjee and Vaijayanti A. Kumar

Abbreviations

A	Adenine
Ac_2O	Acetic anhydride
aeg	Aminoethylglycine
aq.	Aqueous
BAIB	[Bis(acetoxy)iodo] benbene
bep	Backbone extended PNA
Bz	Benzoyl
C	Cytosine
Calc.	calulated
Cat	Catalytic/catalyst
CD	Circular Dichroism
2'-dA	Deoxyadenosine
DCA	Dichloroacetic acid
DCM	Dichloromethane
dG	2'-Deoxyguanosine
DIPEA/DIEA	Diisopropylethylamine
DMAP	4',4'-Dimethylaminopyridine
DMF	*N*,*N*-dimethylformamide
DMSO	*N*,*N*-Dimethyl sulfoxide
DNA	2'-deoxyribonucleic acid
ds	Double stranded
EDTA	Ethylenediaminetetraacetic acid
Et	Ethyl
EtOAc	Ethyl acetate
Fmoc	9-Fluorenylmethoxycarbonyl
FT	Fourier Transform
g	gram
G	Guanine
hrs	Hours

HBTU	2-(1H-Benzotriazole-1-yl)-1,1,3,3-tetramethyluronum hexafluorophosphate
HIV	Human Immuno Difficiency Virus
HOBt	1-Hydroxybenzotriazole
HPLC	High Performance Liquid Chromatography
Hz	Hertz
Ibu	Isobutyryl
IBX	2-Iodoxybenzoic acid
IR	Infra red
L-	Levo-
LC-MS	Liquid Chromatography-Mass Spectrometry
Lys	Lysine
MALDI-TOF	Matrix Assisted Laser Desorption Ionisation-Time of Flight
MBHA	4-Methyl benzhydryl amine
MF	Molecular formula
mg	milligram
MHz	Megahertz
mins	minutes
µL	Microlitre
µM	Micromolar
mL	millilitre
mM	millimolar
mmol	millimoles
m.p	melting point
MS	Mass spectrometry
MW	Molecular weight
N	Normal
nm	Nanometer

NMR	Nuclear Magnetic Resonance
POM	Pyrrolidine –amide linked oligonucleotides mimics
PPh_3	Triphenyl Phosphine
ppm	Parts per million
Pro	Proline
PPTS	Pyridinium p-toluene sulphonate
PS-oligo	Phosphorothioate-oligo
Py	Pyridine
PNA	Peptide Nucleic Acid
pet	pyrolidinylethyl
R	Rectus
R_f	Retention factor
RP	Reversed Phase
rt	Room temperature
S	Sinister
SPPS	Solid Phase Peptide Synthesis
t-Boc	*tert*-Butoxycarbonyl
T	Thymine
TANA	Thio acetamido Nucleic Acids
TBTU	O-(Benzotriazol-1-yl)-N,N,N',N'-tetramethyluronium tetrafluoroborate
TEMPO	2,2,6,6-tetramethyl-1-piperidinyloxyl
TEA/Et_3N	Triethylamine
TFA	Trifluoroacetic acid
TFMSA	Trifluoromethane sulfonic acid
THF	Tetrahydrofuran
TLC	Thin layer chromatography
T_m	Melting temperature
U	Uridine

Abstract

The Thesis entitled ‘‘**Synthesis and biophysical properties of Nucleic acid analogues bearing 5-atom achiral amide- and chiral D/L-amino acid-derived linkages** ” has been divided into four chapters.

Chapter 1: Introduction: Recent advances in the area of nucleic acid modification

Chapter 2 : Design and synthesis of oligonucleotide analogs with controlled backbone chirality

Section 2.1: Synthesis of T-$_{(\alpha\text{-amino Acid})}$-T dimers using L-Proline, D-Proline and Glycine

Section 2.2: Synthesis of T-$_{(D\text{-Proline})}$-U$^{2'\text{-OMe}}$ dimer and T-$_{(\alpha\text{-Amino Acid})}$-T dimers using L-Lysine, D-Lysine

Section 2.3: CD studies for the dimers and biophysical studies of sequences containing T-$_{(\alpha\text{-Amino Acid})}$-T and T-$_{D\text{-Proline}}$-U$^{2'OMe}$ dimers

Chapter 3: Synthesis of all four Nucleoside-based-β-amino acid monomers for the synthesis of polyamide-DNA with alternating α-amino acid and nucleoside-β-aminoacids

Chapter 4: α-L-DNA: A DNA mimic with a compact backbone like RNA

Chapter 1. Introduction: Recent advances in the area of nucleic acid modification

The potential of modified oligonucleotides to act as antisense agents that can inhibit the expression of a target gene in a sequence-specific manner may be used for therapeutic and other biological applications. Besides having a specific binding affinity to a complementary target polynucleotide sequence, antisense oligonucleotide (ASON) desirably should meet the requirements for therapeutic purposes, e.g., potency, bioavailability, low toxicity and low cost. Several modifications have been developed over the last two decades to enhance the effectiveness of antisense oligonucleotides. The sites of the modifications include sugar, base and phosphate groups. A major shortcoming of oligonucleotide analogues used for antisense applications is that the modifications mostly lead to elimination of the RNase H activation of ONs, which

degrades the RNA strand of the RNA:ASON duplex. It is desirable to provide ON analog with enhanced nuclease resistance and cellular uptake, while retaining the property of activating RNase H.

Several analogs containing modifications in the phosphodiester linkage have been studied, e.g., phosphorothioates, phosphoramidates and methyl phosphonates. Though these display better resistance towards the nucleases, the chirality at the phosphorus leads to mixture of diastereomeric oligomers and resulting conformational heterogeneity leads to the lowering of the melting temperatures. Replacement of the phosphorus atom with an achiral, neutral or positively charged moiety is an alternative approach to avoid the problem associated with the modification on the prochiral phosphorus moiety and negative charge repulsions. This class includes Morpholino, aeg PNA and other PNA modifications. Modifications of sugar units to conformationally lock or freeze into 3'-endo geometries include LNA. This chapter reviews the literature that is focused on DNA backbone modifications as well as sugar ring modifications.

Chapter 2. Design and synthesis of oligonucleotide analogs with controlled backbone chirality

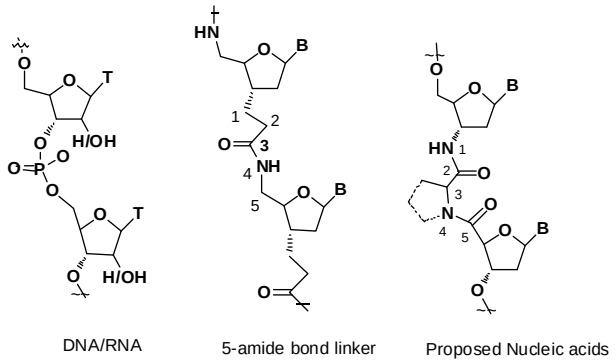

Figure 1. Structures of DNA/RNA and proposed nucleic acids

It is known that in DNA, the phosphate group connecting the two nucleosides is prochiral and when rendered chiral due to substitution at phosphorus, affects DNA/RNA recognition processes. The partial replacement of the DNA/RNA phosphodiester linker by five-atom amide linkers has been found to be very useful for RNA recognition. Also chirality of amide linkers was found to affect the binding strength of modified oligomers to target sequences. Considering the importance of

replacement of the phosphate group with a 5-atom linker and also the chirality at the phosphorus, a chiral amino-acetamido linker was proposed (Figure 1). One novel aspect of our approach is that an amino acid is used as the internucleoside linker. The amino acid linker motif was chosen based on chemical stability and chirality. Consequently the nucleic acid-amino acid conjugate could be converted to dimer blocks. In this Chapter, we describe the design and synthesis of the thyminyl dimer blocks (TT) having 5-atom chiral acetamido internucleoside linkage amenable for their incorporation in chimeric DNA, characterization of dimers using 2D NMR techniques, CD studies and sugar puckering and *cis/trans* isomerism in dimers.

Section A: Synthesis of T-$_{(\alpha\text{-Amino Acid})}$-T dimers using D-Proline, L-Proline and Glycine

Following three T-$_{(\alpha\text{-amino acid})}$-T dimers have been synthesized using L/D-proline and a glycine unit as internucleoside linker (Figure 2).

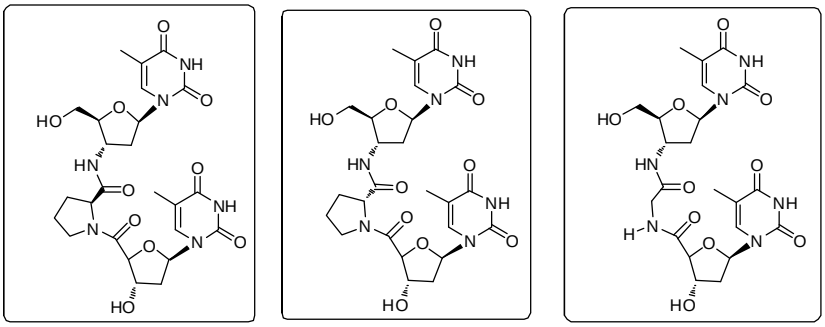

Figure 2. T-$_{(\alpha\text{-amino acid})}$-T dimers using L/D-Proline and a glycine unit as internucleoside linker.

Synthesis of amine component The amine component was synthesized starting from 3'- Azido thymidine as shown in scheme 1

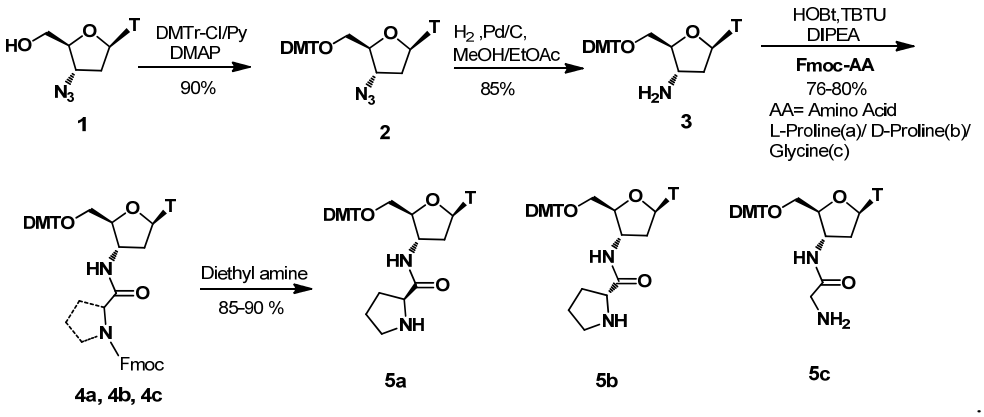

Scheme 1. Synthesis of amine component **5a, 5b and 5c**

Synthesis of acid Component

The acid component was synthesized starting from Thymidine using TEMPO-BAIB method for oxidation of 5'- hydroxy group (scheme 2)

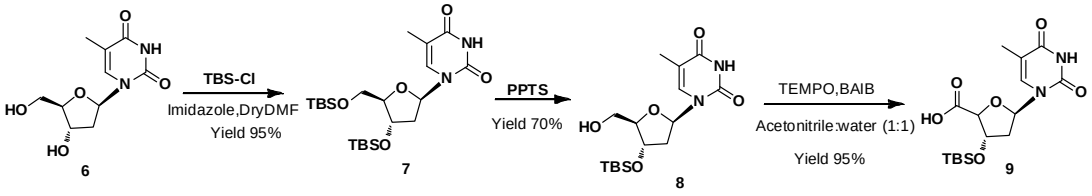

Scheme 2. Synthesis of 4' carboxylic acid Thymine monomer

Synthesis of phosphoramidite dimers

Coupling of amino component (**5a/5b/5c**) with acid component **9** gave dimer blocks **10a/10b/10c** respectively as shown in scheme 3.

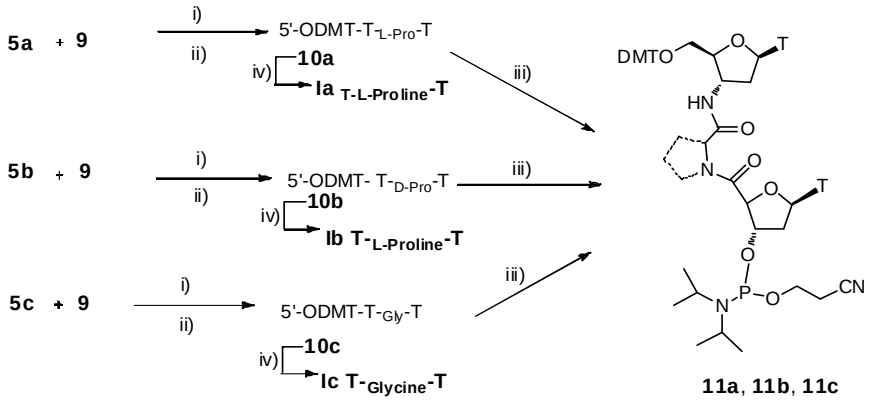

i) TBTU/HOBt, DIPEA, ACN, DMF ii) 1N TBAF in THF iii) N,N'-diisopropylcyanoethyl chlorophosphine iv) 3% Dichloroacetic acid in DCM

Scheme 3. Synthesis of T-$_{D\text{-}Proline}$-T, T-$_{L\text{-}Proline}$-T, T-$_{Glycine}$-T dimers and their phosphoramidites

Sugar conformations of dimers

Conformational preference of the sugar ring in these dimers were determined by ^{1}H NMR. The %S character for sugar ring was calculated from empirical formula

$$\% S = (\Sigma H1'\text{-}9.8)/5.9 \times 100 \text{ where } \Sigma H1' = J_{1'2'} + J_{1'2''}$$

Table 1. N-type and S-type preference for the compound **3**, **9** and dimers **Ia**, **Ib**, **Ic**

Compound		$J_{H1'H2'}$ (Hz)	$J_{H1'H2''}$ (Hz)	%S	%N	
3		5.5	5.8	25	75	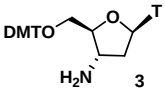
9		5.0	9.3	78	22	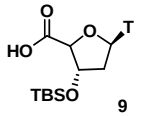
Ia $T\text{-}_{\text{L-Proline}}\text{-}T$	Ring A	5.6	9.0	82	18	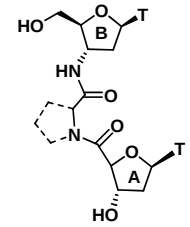
	Ring B	5.7	7.1	50	50	
Ib $T\text{-}_{\text{D-Proline}}\text{-}T$	Ring A	5.5	8.6	72	28	
	Ring B	5.5	6.5	36	64	
Ic $T\text{-}_{\text{Glycine}}\text{-}T$	Ring A	6.9	7.2	73	27	
	Ring B	5.6	6.8	44	56	

Ia, **Ib**, **Ic**

In all the three dimers **Ia**, **Ib** and **Ic**, the 3'-sugar exhibited higher S-type geometry uniformly as compared to the 5'-thymidinyl units. The percentage of N character was found to be higher where C3' of the sugar ring was substituted by nitrogen in the ring B (50–64%) as compared to the 3'-OH sugar (18–28%) in ring A.

Section 2.2. Synthesis of $T\text{-}_{(\alpha\text{-Amino Acid})}\text{-}T$ dimers using D-Lysine, L-Lysine and $T\text{-}_{(D\text{-Proline})}$-2'-OMe U dimer

A 2'-*O*-alkyl substitution in a ribonucleoside having a phosphodiester or phosphorothioate backbone favors the C3'-*endo* conformation of the five membered ring. 2'-*O*-Methyl oligoribonucleotide binds to RNA targets with much higher melting temperatures (Tm values) than corresponding 2'-deoxy oligoribonucleotide. To see the effect of 2'-O-alkyl substitutionin the present case, we have synthesized a dimer with the amide modification which carries an additional 2'-OMe substitution on one of the sugar ring. Also this section report the synthesis of dimer using positively charged amino acids D-Lysine and L-Lysine as internucleosidic linker. Lysine provides a

covalently linked amino group to the nucleic acid which could be protonated under physiological condition and may neutralize an anionic phosphate group. This could lead to decreased electrostatic repulsions between two single strands in duplexes.

Synthesis of $T\text{-}_{D\text{-}Proline}\text{-}U^{2'\text{-}OMe}$ dimer

The synthesis of amine component was accomplished as described in section **A**. The acid component **12** having 2'-OMe substitution was accomplished using TEMPO-BAIB method. The dimer was then converted the phosphoramidite 16 (Scheme 4).

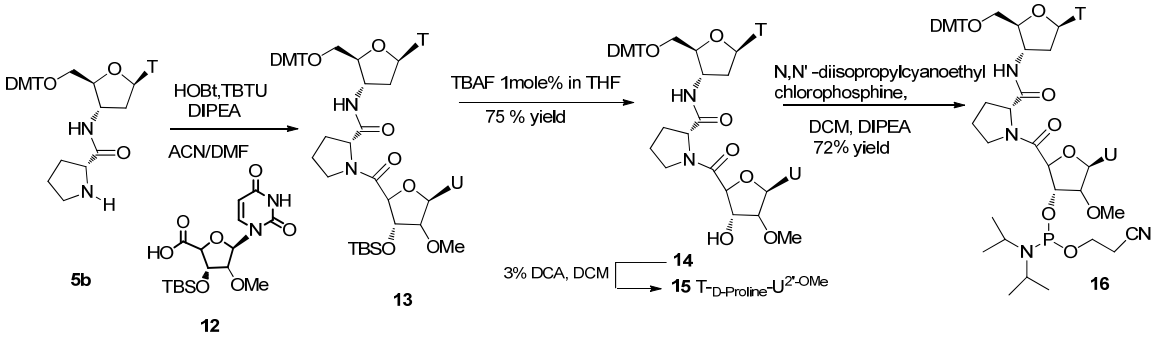

Scheme 4. Synthesis of $T\text{-}_{D\text{-}Proline}\text{-}\ U^{2'OMe}$ dimer and its phosphoramidite derivatve

Synthesis of $T\text{-}_{D\text{-}Lysine}$-T dimer and $T\text{-}_{L\text{-}Lysine}$-T dimers

The synthesis of T-Lysine-T dimer units was accomplished following the same reaction sequence as in section A. In this case orthogonal protection for the amino groups of lysine compatible with the synthetic strategy of the dimers and during the synthesis of oligomer on automated DNA synthesizer was a prerequisite. The orthogonally protected D-Lysine and L-Lysine using trifluoroacetyl group for protection of ε-amino group functionality was synthesized (Scheme 5). Choice of trifluoroacetyl protection for ε-amino function of lysine was based on the fact that it can be cleaved during final deprotection of the ONs. The dimer blocks were then synthesized using D/L-Lysine as a linker group as shown in scheme 6.

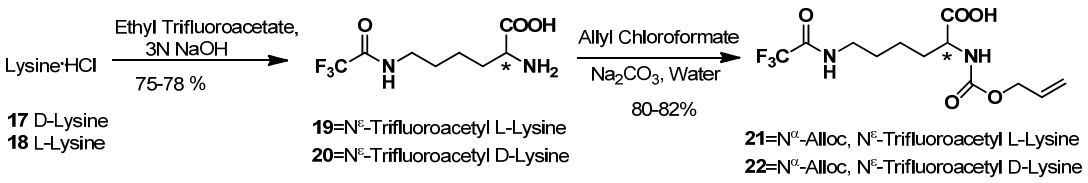

Scheme 5: Orthogonal protection of D-Lysine and L-Lysine

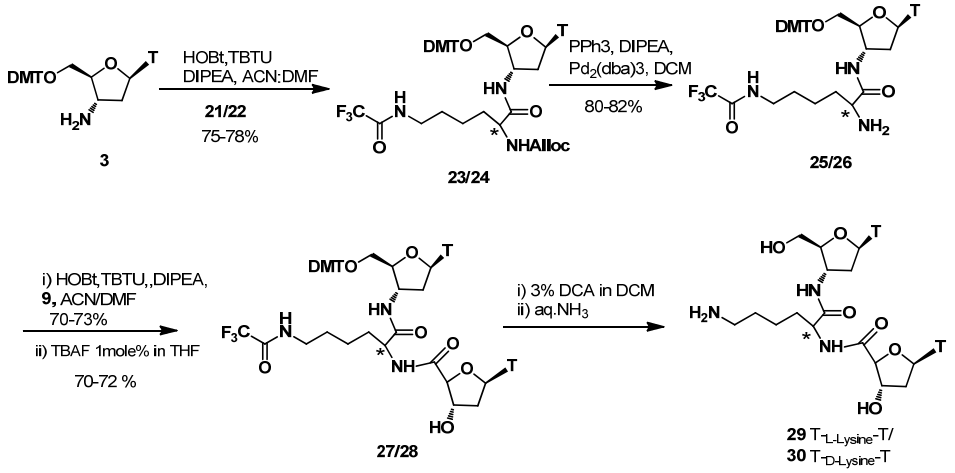

Scheme 6. Synthesis of T-$_{D\text{-}Lysine}$-T dimer and T-$_{L\text{-}Lysine}$-T dimers

Conformational preference of the sugar ring in these dimers were determined by ^{1}H NMR.

Table 2. N-type and S-type preference for the compound **3**, **9, 16** , **Ib, 20, 37 and 38**

Compound		$J_{H1'H2'}$ (Hz)	$J_{H1'H2''}$ (Hz)	%S	%N
3		5.5	5.8	25	75
9		5.0	9.3	78	22
16		6.0	-	73	27
Ib **T-$_{D\text{-}Proline}$-T**	Ring A	5.5	8.6	72	28
	Ring B	5.5	6.5	36	64
20 **T-$_{D\text{-}Proline}$-U$^{2'\text{-}OMe}$**	Ring A	5.0	-	58	42
	Ring B	5.8	7	51	49
37 **T-$_{L\text{-}Lysine}$-T**	Ring A	6.8	7	68	32
	Ring B	6.5	6.2	49	51
38 **T-$_{D\text{-}Lysine}$-T**	Ring A	6.8	7	68	32
	Ring B	5.8	6.5	42	58

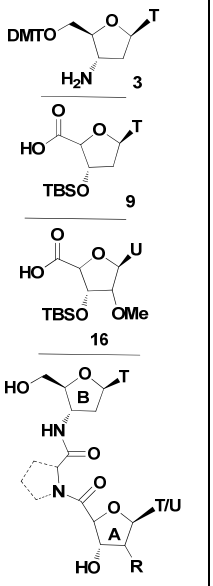

Section 2.3. **Biophysical Studies of sequences containing T-$_{(\alpha\ Amino\ Acid)}$-T and T$_{D\text{-}pro}$U$^{2'OMe}$ dimers**

CD studies were carried out in order to study the nucleobase stacking interaction. The chirality of the α-amino acid as the internucleoside linker in the dimers was found to exert profound effect on the CD signal. Temperature dependent CD studies showed that

both D-Proline and L-proline containing dimer are well stacked as compared to glycine containing dimer (Figure 3). CD studies for dimers **16**, **29 and 30** were also carried out.

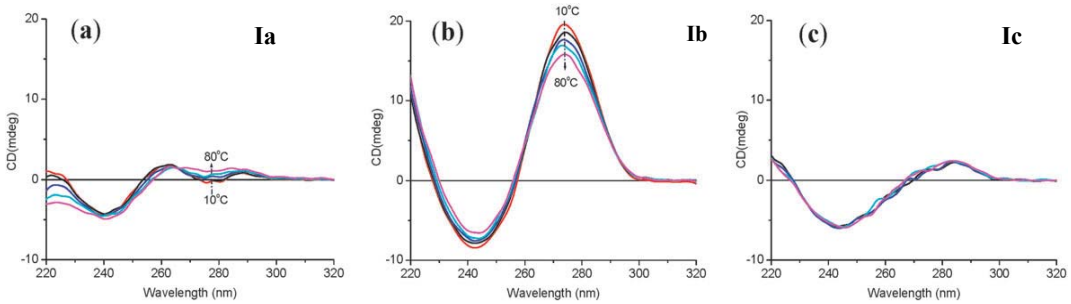

Figure 3. Temperature-dependent CD studies of thymine dimers containing (a) L-proline (**Ia**), (b) D-proline (**Ib**) and (c) glycine (**Ic**) at 100 mM concentration in water

Phosphoramidite derivatives **11a**,**11b**,**11c** and **16** (Scheme 3 and 4) were incorporated into DNA oligomers using the automated DNA synthesizer. These modified oligomers were purified by Reverse phase HPLC and characterized by MALDI-TOF spectrometry and are listed in Table 3.

Table 3. Oligomers synthesized with their HPLC retention times and MALDI -TOF values

Code	Sequences	HPLC t_R (min)	Exp Mass	Obs Mass
ON1	5'CCT CTT ACC TCA G**T$_{D\text{-}Pro}$T** ACA3'	11.2	5400.65	5403.41
ON2	5'CCT CTT ACC TCA G**T$_{L\text{-}Pro}$T** ACA3'	11.4	5400.65	5403.62
ON3	5'CCT CTT ACC TCA G**T$_{Gly}$T** ACA3	11.0	5360.62	5354.46
ON4	5'CCT CTT ACC TCA G**T$_{D\text{-}Pro}$U$^{2'OMe}$** ACA3	13.7	5416.64	5417.32
ON5	5'CCT C**T$_{D\text{-}Pro}$T** ACC TCA G**T$_{D\text{-}Pro}$T** ACA3'	11.3	5431.74	5429.07
ON6	5'CCT C**T$_{L\text{-}Pro}$T** ACC TCA G**T$_{L\text{-}Pro}$T** ACA3'	11.5	5431.74	5433.63
ON7	5'CCT C**T$_{Gly}$T** ACC TCA G**T$_{Gly}$T** ACA3'	11.2	5351.68	5341.43
ON8	5'GAA GGG CTT **T$_{D\text{-}Pro}$T**G AAC TCT T3'	10.8	5864.95	5866.67
ON9	5'GAA GGG CTT **T$_{L\text{-}Pro}$T**G AAC TCT T3'	10.9	5864.95	5868.31
ON10	5'GAA GGG CTT **T$_{Gly}$T**G AAC TCT T3'	10.6	5824.91	5814.90
ON11	5'GAA GGG CTT **T$_{D\text{-}Pro}$U$^{2'OMe}$** G AAC TCT T3'	13.1	5880.95	5880.57
ON12	5'GAA GGG C**T$_{D\text{-}Pro}$U$^{2'OMe}$ T$_{D\text{-}Pro}$U$^{2'OMe}$** G AAC TCT T3'	12.9	5928.03	5926.96

***** Bold letters in sequence indicate site of modification

UV-*T*m studies were carried out to investigate the binding efficiency of the modified oligomers to complementary DNA and RNA and the data is summarized in Table 4 and 5.

Table 4. T_m (°C) values of 18mer chimeric ONs with complementary DNA/RNA duplexes

Entry	Sequences	UV-T_m °C (ΔT_m °C)[a]	
		DNA 2	**RNA1**
DNA1	5'CCT CTT ACC TCA GTT ACA3'	52.8	56.6
ON1	5'CCT CTT ACC TCA G**T$_{D\text{-}pro}$T** ACA3'	**52.4** (-0.4)	**55.5** (-1.1)
ON2	5'CCT CTT ACC TCA G**T$_{L\text{-}pro}$T** ACA3'	47.8 (-5.0)	51.5 (-5.1)
ON3	5'CCT CTT ACC TCA G**T$_{Gly}$T** ACA3	49.6 (-3.2)	54.4 (-2.2)
ON4	5'CCT CTT ACC TCA G**T$_{D\text{-}pro}$U$^{2'OMe}$** ACA3'	**51.5** (-1.3)	**55.2** (-1.4)
ON5	5'CCT C**T$_{D\text{-}Pro}$T** ACC TCA G**T$_{D\text{-}Pro}$T** ACA3'	47.2 (-5.6)	53.2 (-3.4)
ON6	5'CCT C**T$_{L\text{-}Pro}$T** ACC TCA G**T$_{L\text{-}Pro}$T** ACA3'	40.3 (-12.5)	43.5 (-13.1)
ON7	5'CCT C**T$_{Gly}$T** ACC TCA G**T$_{Gly}$T** ACA3'	47.3 (-5.5)	48.8 (-7.8)

DNA2=5' TGT AAC TGA GGT AAG AGG 3'; **RNA1** = 5'UGU AAC UGA GGU AAG AGG 3', [a] The experiments were carried out three times with an experimental error of ± 0.5°C, $\Delta T_m = T_m - T_{m(control)}$

Table 5. T_m (°C) values of 19mer chimeric ONs with complementary DNA/RNA

Entry	Sequences	UV-T_m °C (ΔT_m °C)	
		DNA 5	**RNA3**
DNA4	5'GAA GGG CTT TTG AAC TCT T3'	55.9	56.5
ON8	5'GAA GGG CTT **T-$_{D\text{-}Pro}$TG** AAC TCT T3'	**56.5 (+0.6)**	**56.0 (-0.5)**
ON9	5'GAA GGG CTT **T-$_{L\text{-}Pro}$-T** G AAC TCT T3'	50.9 (-5.0)	50.7 (-5.8)
ON10	5'GAA GGG CTT **T-$_{Gly}$-T** G AAC TCT T3'	53.5 (-2.4)	53.1 (-3.4)
ON11	5'GAA GGG CTT **T-$_{D\text{-}Pro}$-U$^{2'OMe}$** G AAC TCT T3'	**54.5 (-1.4)**	**54.3 (-1.7)**
ON12	5'GAA GGG C**T-$_{D\text{-}Pro}$-U$^{2'OMe}$ T$_{D\text{-}pro}$U$^{2'OMe}$** G AAC TCT T3'	50.5(-5.4)	50.2(-6.3)

DNA5=5'AAG AGT TCA AAA GCC CTT C 3'; **RNA3** = 5'AAG AGU UCA AAA GCC CUU C 3', [a] The experiments were carried out three times with an experimental error of ± 0.5°C, $\Delta T_m = T_m - T_{m(control)}$

Incorporation of the single dimer block containing D-Proline was found to be well accommodated in DNA:DNA and DNA:RNA duplexes as there no change in the UV-

T_m values was observed. Incorporation of second dimer block caused destabilization of duplexes, in most cases. The intermittent replacement of the phosphodiester linkages probably causes discontinuity of the backbone structures, further destabilizing the duplexes.

Conclusions

1. T-$_{(\alpha\text{-amino acid})}$-T/U$^{2'\text{-OMe}}$ dimer blocks were synthesized and characterized by 2D COSY and NOESY NMR techniques.
2. CD studies at the dimer level showed that D-Prolin.e containing-dimer is well stacked as compared to L-Proline- or Glycine-containing dimers.
3. The stacking interactions in D-Proline and L-Proline containing dimers could be arising from differently adopted conformations due to opposite chirality of the linker.
4. Chiral amide-linked dimers were incorporated into the DNA backbone by partial replacement of selected phosphodiester linkages.
5. The UV-T_m data shows that the dimer block having D-proline as an internucleoside linker in the DNA backbone to stabilizes the ON:DNA and ON:RNA complexes better than L-Proline or glycine.

Chapter 3. Synthesis of all four Nucleoside-based-β-amino acid monomers for the synthesis of polyamide-DNA with alternating α-amino acid and nucleoside-β-aminoacids

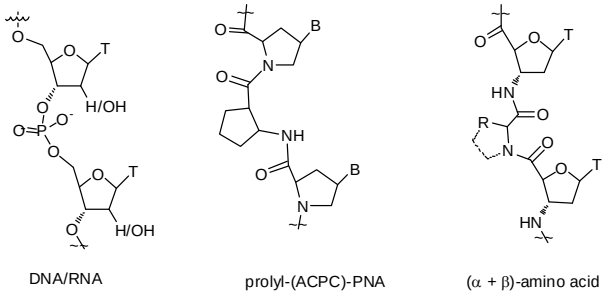

Figure 4 : DNA/RNA and modified DNA/PNA analoges

The replacement of phosphodiester linker by 5-atom amide linker has been found to be very useful for RNA recognition. Prolyl-(ACPC)-PNA consisting of alternating α-amino acid proline as a nucleobase carrier and chiral β-aminocyclopentane carboxylic acid was shown to exhibit preferential binding to complementary DNA rather than RNA. An α/β –peptide backbone oligonucleotide comprising of natural α-amino acids alternating with a β-amino acid component derived from thymidine (Figure 5, a) sequence specifically recognize DNA and RNA in triplex mode. For the synthesis of

mixed base having homogeneous backbone, synthesis of all four nucleosides to get the protected nucleoside-β-amino acids is a prerequisite. Choice of nucleobase protection and its compatibility with solid phase peptide chemistry is of utmost importance to achieve optimum yields and purity of product oligomers. We chose to use trityl protection for sugar amino function as the exocyclic amino group on the nucleobase was protected with base-labile benzoyl or isobutryl group (Figure 5, b).

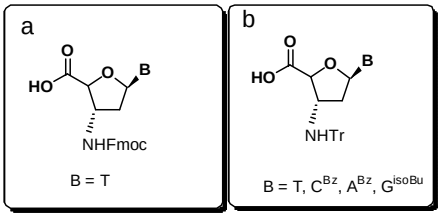

Figure 5: Nucleoside-β-amino acid monomers

The synthesis of all the four monomers with suitable protection of bases which are compatible during solid phase synthesis from commercially available starting material depicted in Scheme 7-9.

Synthesis of Thymine monomer

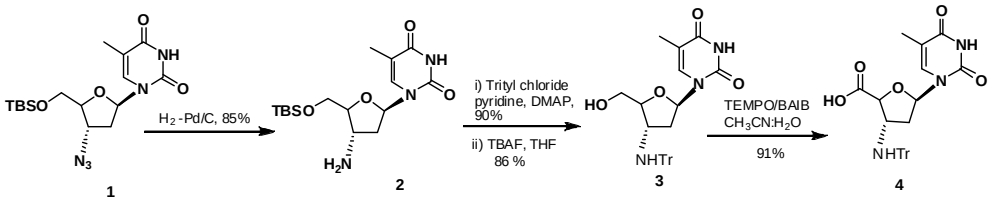

Scheme 7. Synthesis of Thymine monomer

Synthesis of 5-Methyl Cytosine monomer

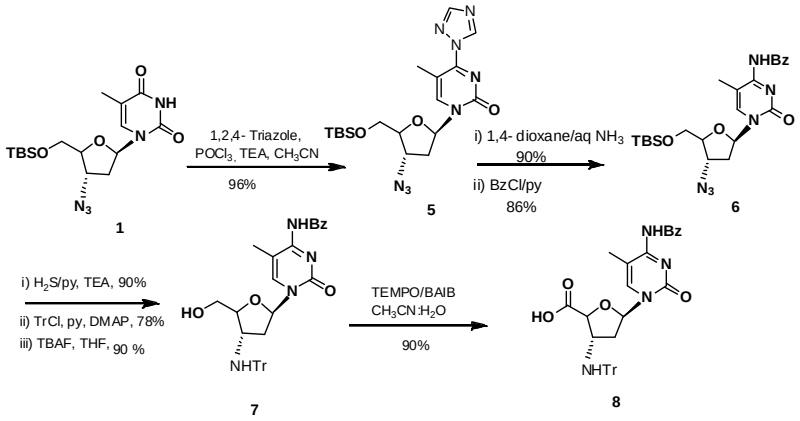

Scheme 8. Synthesis of 5-Methyl Cytosine monomer

Synthesis of Adenine and Guanine monomer

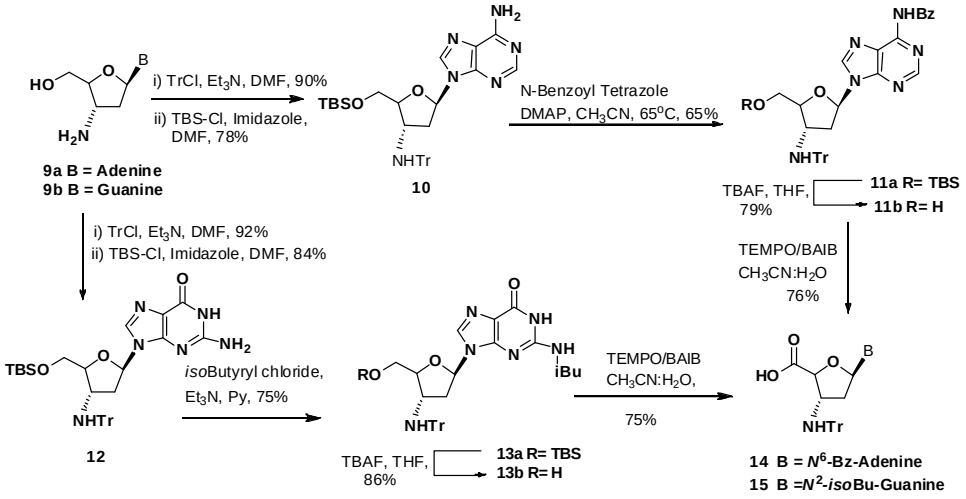

Scheme 9. Synthesis of Adenine and Guanine monomer

Synthesis of a model tetrameric nucleoside sequence 5'-C(gly)A(gly)C(gly)T (**18**) was then accomplished using synthesized monomeric units (**4/8/14/15**) and trityl glycine (**17)** as shown in Scheme 10.

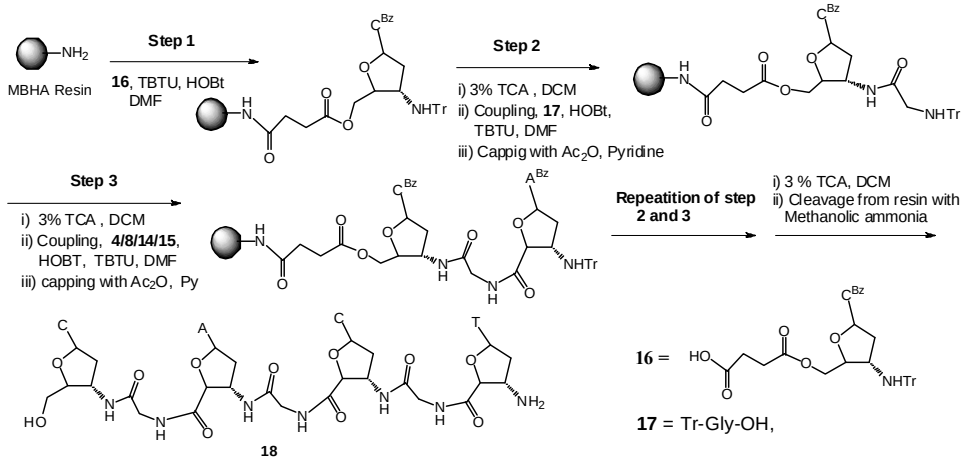

Scheme 10. Schematic representation of solid phase synthesis of (α + β amino acid) tetramer

Conclusion

1. All four nucleoside-β-amino acids were synthesized using the simple TEMPO-BAIB method for oxidation.
2. A tetrameric nucleoside sequence 5'-C(gly)A(gly)C(gly)T was accomplished using synthesized monomeric units.

Chapter 4. α-L-DNA: A DNA mimic with a compact backbone like RNA

RNase H (Ribonuclease H) cleavage of target RNA (Figure 1) is a highly effective approach and the most widely used mechanism to downregulate target genes using antisense oligonucleotides, accounting for the majority of drugs in development.

In search for oligonucleotide analogs possessing enhanced hybridization and enzyme stability as well as ability to induce RNase H activity, we have explored a sugar modification at the 4'-postion. From the consideration that the restriction of sugar puckering in nucleosides to a proper conformation would serve as an advantageous strategy to develop a desired antisense molecule, we propose a nucleotide analog in which the sugar was expected to have a 2'-*endo* (S-type) pucker (Figure 6) that is normally observed in DNA. The cis geometry of the phosphodiester linking 4'-α-CH_2OH and 3'-OH group may show internucleoside distance complementarity while binding to A-type RNA geometry. This compact backbone (5''- 3' linkage) was envisaged to be helpful in improving DNA:RNA duplex binding strength.

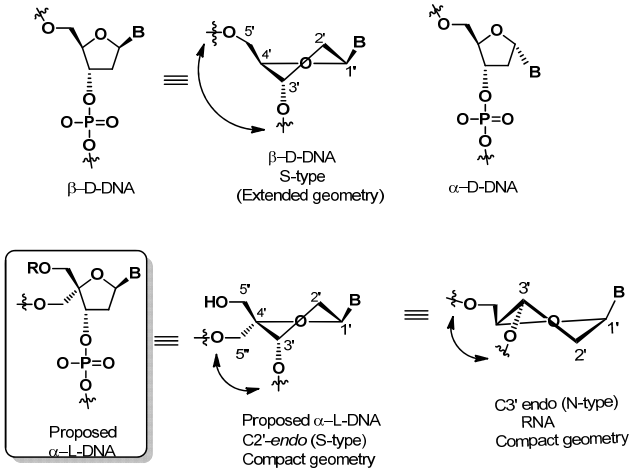

Figure 6. β-D-DNA, α-D-DNA and proposed α-L-DNA with 5''→ 3'-phosphodiester linkage

Synthesis of α-L-DNA monomer

Synthesis of monomer unit was accomplished starting from thymidine as shown in scheme 11

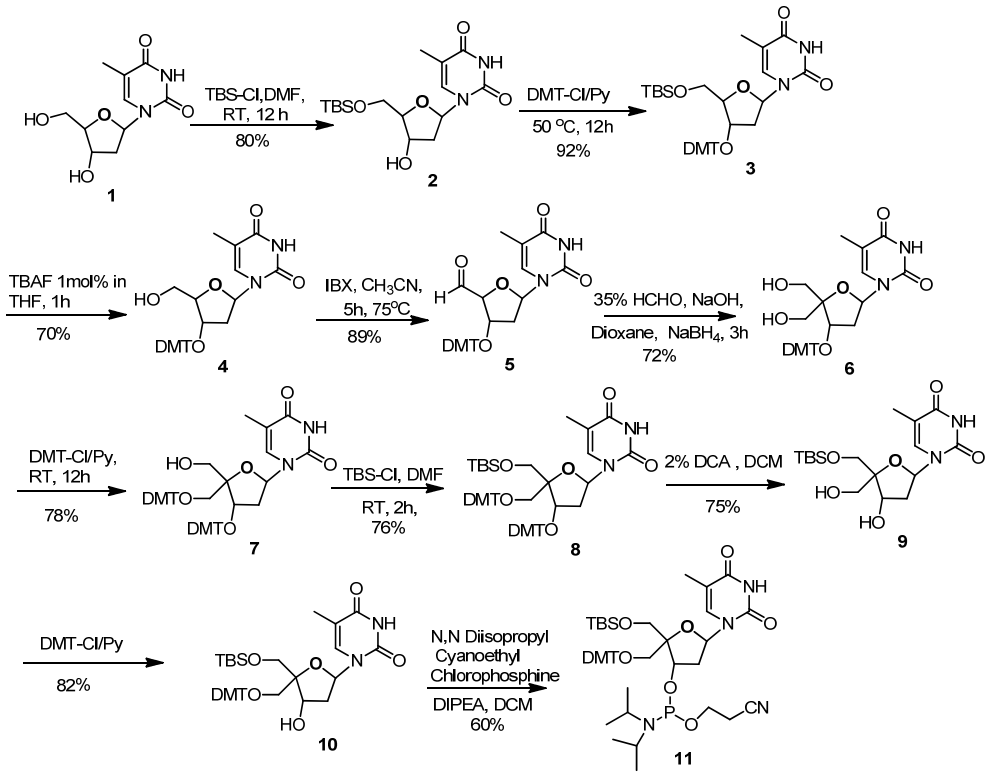

Scheme 11. Synthesis of α-L-DNA monomer

Crystal structure of compound **7** clearly shows 2'-endo pucker of the sugar ring. (Figure 7)

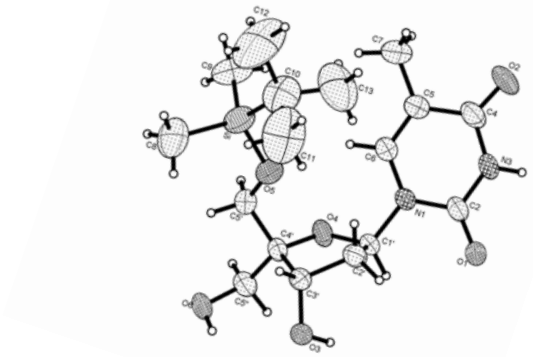

Figure 7. Crystal structure of compound **7**

Following sequences were synthesized on automated DNA synthesizer using phosphoramidite **11**. These oligomers were purified by RP- HPLC and characterized by MALDI-TOF mass spectrometry.

Table 6. Oligomers synthesized with their HPLC retention times and MALDI -TOF values

Code	Sequence	HPLC t_r	Mass	
			Calculated	Observed
ON1	5'CCT CTT ACC TCA GT**T** ACA3'	8.66	5400	5402.26
ON2	5'CCT CTT ACC **T**CA GT**T** ACA3'	7.95	5431	5434.72

Uv-T*m* studies has to carried out for these sequences to study the binding affinity of modified sequences towards complementary DNA and RNA.

Table 7. T_m (°C) values of 18mer chimeric ONs with complementary DNA/RNA duplexes

code	Sequence	UV-T_m °C	
		DNA2	RNA1
DNA1	5'CCT CTT ACC TCA GTT ACA3'	**53.1**	**56.5**
ON1	5'CCT CTT ACC **T**CA GT**T** ACA3'	50.2	50.4
ON2	5'CCT CTT ACC **T**CA GT**T** ACA3'	46.8	48.6

DNA2=5' TGT AAC TGA GGT AAG AGG 3'; **RNA1** = 5'UGU AAC UGA GGU AAG AGG 3', T= α-L-DNA monomer. The experiments were carried out three times with an experimental error of ± 0.5°C, $\Delta T_m = T_m - T_{m(control)}$

RNase H study

RNase H was carried out digestion assay for the single modified sequence in order to find out its ability to induce RNase H using electrophoretic gel experiment (Figure 8).

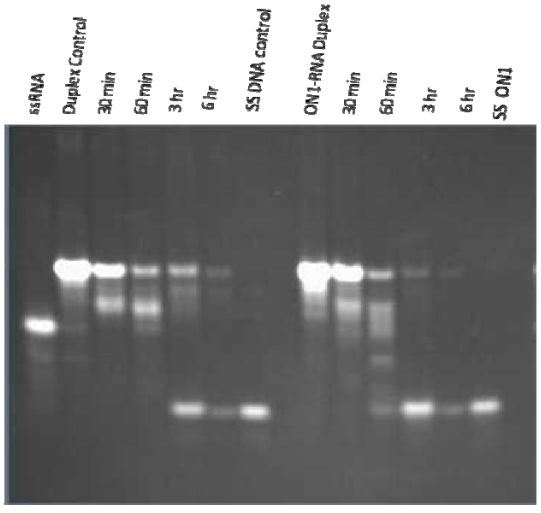

Figure 8. The PAGE analysis of RNase H hydrolysis of the hybrid duplexes control DNA and modified oligomer ON1 with RNA

Conclusion

1. The proposed nucleotide analog shows S-type sugar pucker, confirmed by NMR and crystal structure.
2. Introduction of 4'-substituted sugar monomer into oligomer destabilized complexes with both DNA and RNA.
3. Irrespective of the loss of T_m, the single modified ON1-RNA duplex was found to be as good a substrate for RNase H as the native hybrid duplex.

Chapter 1

Introduction:
Recent advances in the area of nucleic acid modification

1.1 Introduction

1.1.1 Primary structure of DNA and RNA

Nucleic acids are complex, high molecular weight biological macromolecules. The two chief types of nucleic acid are DNA (deoxyribonucleic acid) and RNA (ribonucleic acid). DNA carries the hereditary information from generation to generation and RNA functions in converting genetic information from gene into amino acid sequences of proteins. In 1953, molecular biologists J. D. Watson and F. H. Crick discovered double stranded structure[1] of DNA (Figure 1) which gave rise to entirely new research in bio-molecular area.

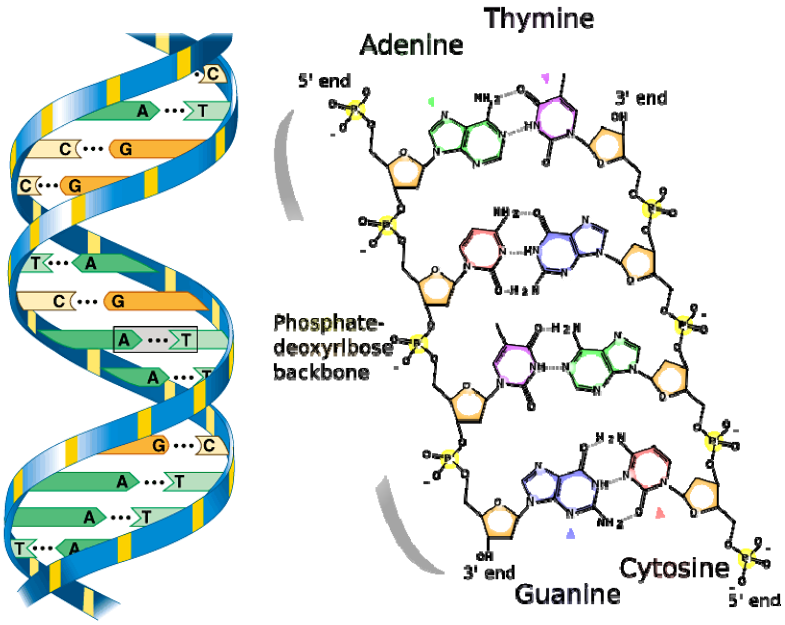

Figure 1. Double helical structure of DNA

Single stranded nucleic acids are composed of repeating smaller units, called nucleotides which are made up of a pentose sugar, a nitrogenous base which is either purine or pyrimidine and a phosphate group. The nucleotides in RNA contain ribose sugar and the pyrimidine bases are uracil and cytosine (U and C). In DNA, the nucleotides contain 2'-deoxyribose sugar and the pyrimidine bases are thymine and cytosine (T and C). The purines bases adenine (A) and guanine (G) are present in both RNA and DNA. The heterocyclic base is joined covalently (at *N*-1 of pyrimidines and *N*-9 of purines) in an *N*-*β*-glycosyl bond to the 1' carbon of the pentose and the

phosphate is in the form of diester at 3’ and 5’–hydroxy group to join the neighbouring sugars (Figure 2).

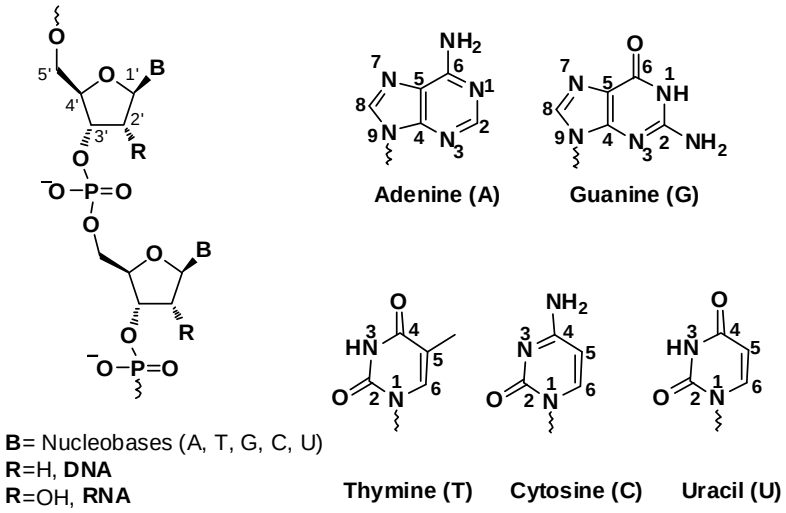

Figure 2. Structures of 3’-5’ phosphodiester linked dinucleotide and nucleobases of DNA and RNA

1.1.2 Base pairing *via* hydrogen bonding

The nitrogenous base pairs in DNA (A–T and C–G) are formed via hydrogen bonds within the antiparallel double-stranded (ds) structure for DNA. The N-H groups of the bases are the hydrogen donors, while the sp^2- hybridized electron pairs on the oxygens of the base C=O groups and the ring nitrogens are hydrogen bond acceptors, which are engaged in the formation of specific (Watson–Crick) A-T and G-C base pairs (Figure 3). A–T pairs form two hydrogen bonds while C–G pairs form three. RNA usually exists in the single-stranded (ss) form but may fold into secondary and tertiary structures through the formation of specific base pairings (A-U and C-G).

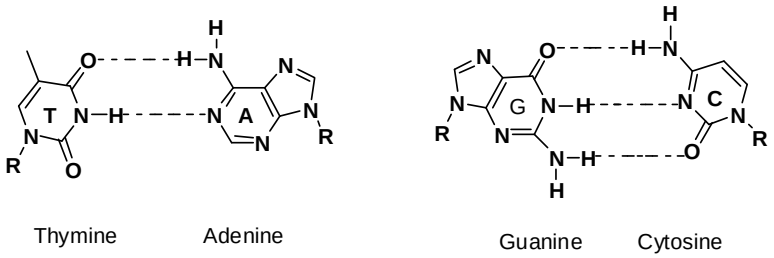

Figure 3. Watson and Crick hydrogen- bonding scheme for A: T and G: C base pair

Other significant base pairing are Hoogsteen[2a] and Wobble base pairs.[2b] In Hoogsteen base pairing, the purine rotates 180° with respect to the helix axis and adopts *syn* conformation. Hoogsteen base pairs utilize the C6-N7 face of the purine for hydrogen bonding with Watson-Crick (N3-C4) face of the pyrimidine (Figure 4, a and b). This base pairing permits the formation of triple helix DNA also called triplex or H-DNA. In Wobble base pairing, a single purine is able to recognize a non complementary pyrimidine (e.g. IU and GU, where I= Inosine, U=Uracil) [Figure 4, c and d] and these have importance in the interaction of messenger RNA (mRNA) with transfer RNA (tRNA) on the ribosome during protein synthesis (codon-anticodon interactions).

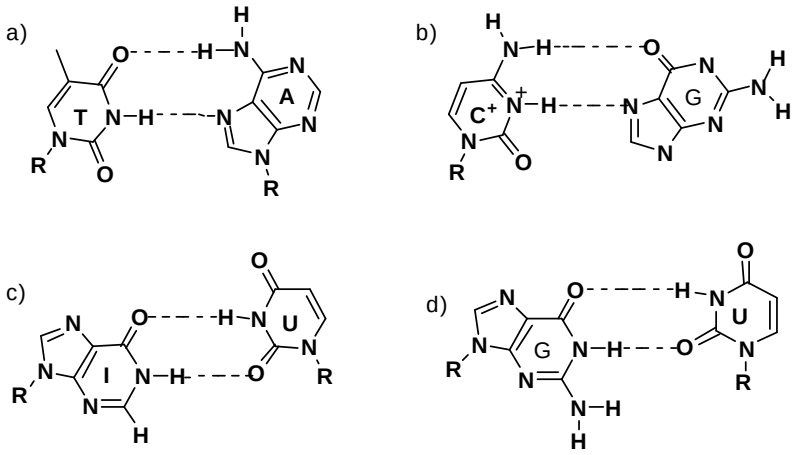

Figure 4. Hoogsteen (a,b) and Wobble (c,d) hydrogen-bonding

1.1.3 Sugar Puckering

The conformations of nucleic acids are dynamic and are stabilized by several forces. Besides base pairing, the conformational features are constrained by pseudo tortional angles for rotation around each bond. The details of the conformational structure of nucleotides are accurately defined by the torsional angles α, β, γ, δ, ε and ζ in the phosphate backbone, θ_0 to θ_4, in the furanose ring, and χ for the glycosidic bond (Figure 5a).

The pentose sugar ring in nucleic acids is inherently nonplaner. This nonplanrity is termed puckering. The ring puckering arises from the effect of nonbonded interactions between substituents at the four ring carbon atoms – the energetically most stable conformation for the ring has all substituents as far apart as possible. This '*puckering*' is described by identifying the major displacement of the carbons *C*-2' and

C-3' from the median plane of *C*1'-*O*4'-*C*4'. Thus, if the *endo*-displacement of *C*-2' is greater than the *exo*-displacement of C-3', the conformation is called *C*2'-*endo* and so on for other atoms of the ring (Figure 5, b and c). The *endo*-face of the furanose is on the same side as *C*5' and the base; the *exo*-face is on the opposite face to the base. The sugar puckers are located in the north (N) and south (S) domains of the pseudorotation cycle of the furanose ring[3]. In solution, N and S conformations are in rapid equilibrium and are separated by low energy barrier. The average position of the equilibrium is influenced by several factors such as (i) the preference of the electronegative substituents at C2' and C3' for axial orientation, (ii) the orientation of the base, and (iii) the formation of an intra-strand hydrogen-bond from O2' in one RNA residue to O4' in the next, which favors C3'-*endo*-pucker.

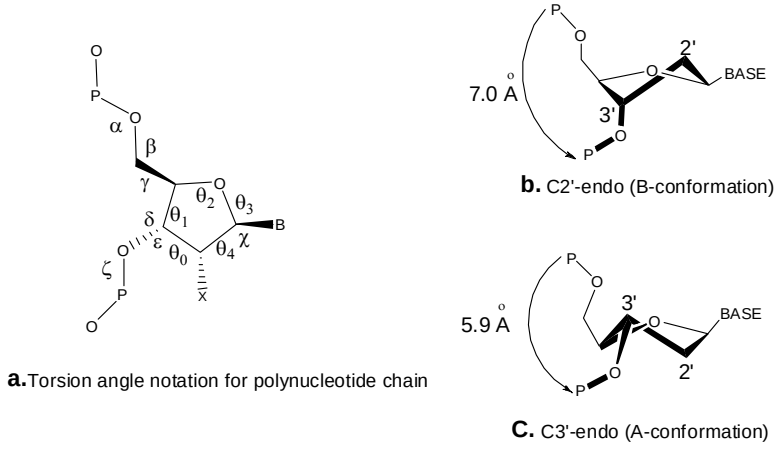

Figure 5. a) Tortional angle notations for polynucleotide chain b) C2'-*endo* sugar and c) C3'-*endo* sugar conformations

1.1.4 DNA Secondary conformation

Three DNA conformations are believed to be present in biological system, right handed A-form, right handed B-form and left handed Z-form (Figure 6). The preferred structure of DNA molecule depends on both nucleotide sequence, the solvent and salt conditions. Under physiological condition, DNA mainly adopts B-form conformation and it is stabilized under high relative humidity (> 85%). On the other hand, A- DNA is favored at relative low humidity (between 75% and 80%), and high salt concentration, especially for GC rich sequences.[3] The "B" form described by James D. Watson and Francis Crick is believed to predominate in cells.[4] B-DNA has a wide major-groove and

a narrow minor-groove where the bases are perpendicular to the helical axis. It is 23.7 Å wide and extends 34 Å per 10 base pair of sequence.

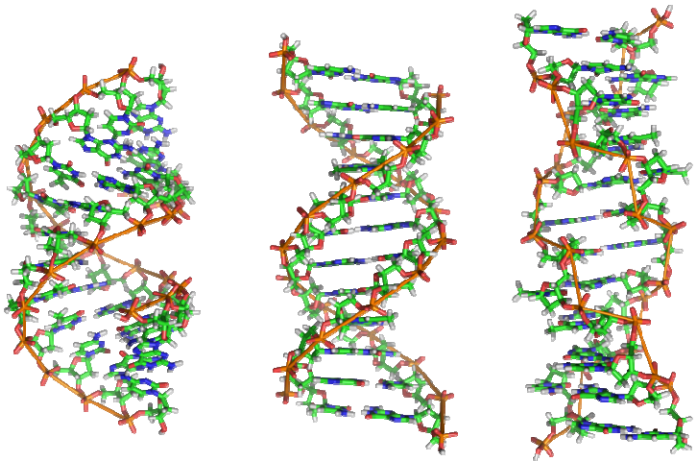

Figure 6. A, B and Z DNA

A-DNA has 11 base pairs per helical turn, base pairs are tilted to about 20°, with respect to the helical axis, the grooves are not as deep as those in B-DNA, the sugar pucker is C3' *endo* compared to C2' *endo* for B-DNA, and the base pairs are shifted to the helix periphery which creates a 9 Å hole in the helix center. In both A and B forms

Table 1. Salient features of major DNA conformations

Parameters	A Form	B Form	Z-Form
Direction of helical rotation	Right	Right	Left
Conditions	Low humidity and high salt	Dilute aqueous solutions	High salt and alternating G-C sequences
Residues per turn of helix	11	10	12 base pairs
Rotation of helix per residue (in degrees)	33	36	-30
Base tilt relative to helix axis (in degrees)	20	6	7
Rise per base pair	2.3 Å	3.4 Å	3.8 Å
Major groove (width)	narrow and deep (11.0 Å)	wide and deep (5.7 Å)	Flat (2.0 Å)
Minor groove (width)	wide and shallow (2.7 Å)	narrow and deep (11.7 Å)	narrow and deep (8.8 Å)
Orientation of N-glycosidic Bond	Anti	Anti	Anti for Py, Syn for Pu
Comments		most prevalent within cells	occurs in stretches of alternating pu-py base pairs

of DNA the Watson-Crick base pairing is maintained by *anti* glycosidic conformation of the nucleobases. Z-DNA[4e] has been mostly found in alternating purine-pyrimidine sequences $(CG)_n$ and $(TG)_n$. Because of the zigzag backbone path, some phosphate groups are closer and electrostatic repulsion between them is greater than in B-DNA. Therefore, Z-DNA is stabilized by high salt concentrations or polyvalent cations. Z-DNA forms excellent crystals. The characteristic features of major DNA conformations are summarized in Table 1.

1.1.5 Structure of RNA

Despite of the great similarity in chemical composition, DNA and RNA differs functionally. RNA actively participates in virtually all cellular metabolic processes. One important factor that enables RNA's diverse functionalities is that RNA is transcribed as single strand molecule, which in turn, can fold into secondary and tertiary structure such as stem and bubble. An example of folded RNA structure is *t*-RNA, which is the key RNA involved in the translation of genetic information from *m*-RNA to proteins. The presence of the 2'-hydroxy group in RNA hinders the formation of a B-type helix but can be accommodated within an A-type helix.

1.1.6 Sense and antisense strand

Sense strand or coding strand is the segment of double stranded DNA running from 5' - 3' that is complementary to the antisense strand or template strand. The sense strand is the strand of DNA that has the same sequence as the mRNA, and is transcribed from antisense strand as its template. The antisense DNA/RNA is defined as a short DNA/RNA sequences that lack coding capacity, but have a high degree of base sequence complementarity to the coding RNA which enables the two to hybridize.[5] The consequence is that such antisense, or complementary DNA/RNA can act as a regulator of the normal function of the targeted RNA.[5]

1.2 Antisense Technology

The potential of oligodeoxynucleotides to act as antisense agents that inhibit viral replication in cell culture was discovered by Zamecnik and Stephenson in 1978.[6] Efficient methods for gene silencing have been receiving increased attention in the era of functional genomics, since sequence analysis of the human genome and the genomes

of several model organisms revealed numerous genes, whose function is not yet known. Conceptual simplicity, the possibility of rational design, and developments in the sequencing of human genome has led to the use antisense oligonucleotides as therapeutic agents. In addition to the therapeutic applications, other common applications for this technology include characterization of the roles of specific genes, discovery and validation of new targets for therapeutics, and the production of knock-down mice. Antisense agents differs from conventional drugs, most of which bind to proteins and thereby modulate their function. In contrast, antisense agents act at the mRNA level, preventing its translation into protein. AS-ONs usually consist of 15-20 nucleotides, which are complementary to their target mRNA.

1.2.1 Disruptive antisense approach

The AS-ONs which can disrupt the translation processes at mRNA level, thus causing the disruption or down-regulation of the synthesis of disease-causing functional protein. There are four major mechanism of gene-silencing molecules[7]: (1) antisense oligonucleotide derivatives that, depending on their type, recruit RNase H to cleave the target mRNA (Figure 7A); or (2) AS-ONs that do not induce RNase H cleavage can be used to inhibit translation by steric blockage of the ribosome (Figure 7B); (3) ribozymes and deoxyribozymes- cleave the target RNA directly due to their intrinsic catalytic activities (Figure 7C); (4) RNA interference (RNAi)[7c]- small interfering double-stranded RNA (siRNA) molecules that induce mRNA degradation through a natural gene-silencing pathway (Figure 7D). In the siRNA pathway, the endonuclease enzyme Dicer processes the long dsRNA into small or short interfering RNAs (siRNAs) which are around 21 nucleotides long, of which 19 nucleotides form a helix and 2 nucleotides on each of the 3' ends are unpaired. The actual effector of the RNAi is the ribonucleoprotein complex RISC (RNA induced silencing complex), which guides by the siRNA to the complementary target RNA. The target RNA is cleaved at a specific site in the center of the duplex, 10 nucleotides from the 5' end of the siRNA strand. After the cleavage, the target RNA lacks those elements which are typically responsible for stabilizing mRNAs, namely the 5' end cap and the poly-A tail at the 3' end, so that the cleaved mRNA is rapidly degraded by RNases and the coded protein can no longer be synthesized (Figure 7D).

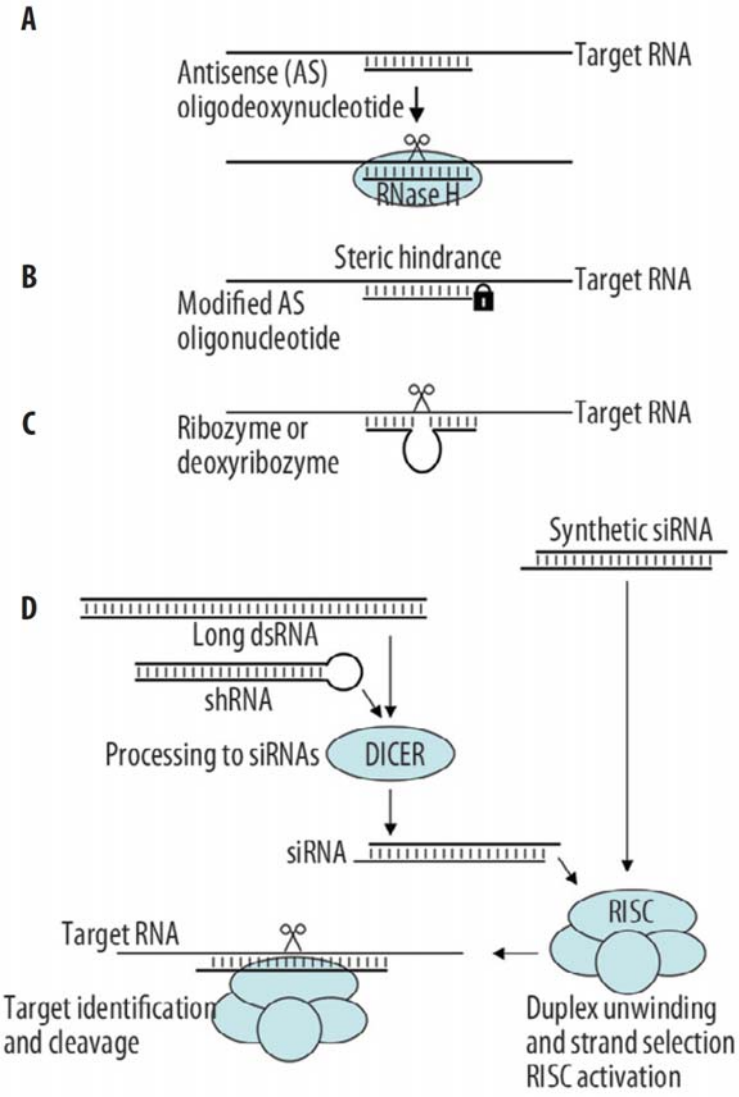

Figure 7. Mechanisms of the inhibition of gene expression through various antisense technologies

1.2.2 Corrective antisense approach

Recent research opens up an exciting possibility for the application of AS-ONs as corrective antisense[8] in the cases of certain diseases caused by genetic mutations. In this approach the AS-ONs can help restoring the viable protein production by acting at pre-mRNA levels for splice corrections[8] or to yield mRNA that is translated into viable proteins. The disruptive antisense effects could involve non-antisense, non-specific interactions leading to stimulation of immune response but corrective antisense depends upon specific and stable interactions with mRNA for the desired corrective action.

Precursor mRNA, more commonly termed pre-mRNA is an incompletely processed single strand, synthesized from a DNA template in the nucleus of a cell by transcription. Once pre-mRNA has been completely processed, it is termed "mature messenger RNA", "mature mRNA", or simply "mRNA". Pre-mRNA includes two different types of segments, exons and introns. Most of exons encode protein, while introns do not and must be excised before translation. This process is called splicing.[9] Spliceosomes are small proteins found in the nucleus and composed of protein and RNA, perform the excision. An exon is any region of DNA within a gene that is transcribed to the final mRNA molecule, rather than being spliced out from the transcribed RNA molecule. Introns are sections of DNA colinear to the mRNA sequence that will be spliced out after transcription, but before the mRNA is translated (Figure 8).

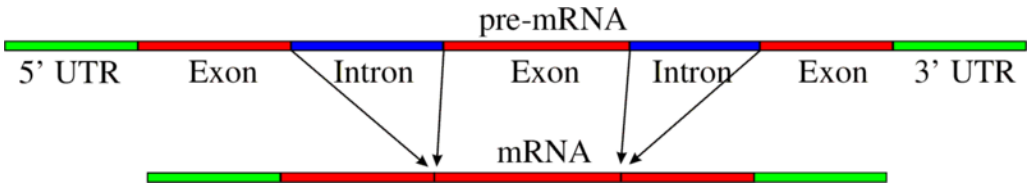

Figure 8. Simple illustration of exons and introns in pre-mRNA.The mature mRNA is formed by splicing. (UTR: Untranslated region)

The natural complexity of pre-mRNA splicing also allows the exclusion (or inclusion) of specific exons by a process known as alternative splicing[10] (Figure 9). Alternative splicing allows production of several different proteins from a single pre-mRNA resulting in an increased diversity of proteins from a limited number of transcribed genes. Mutations in the intron regions of pre-mRNA lead to alternative splicing that manifest in a number of disease states ranging from thalassemia[8] and cancer to neuromuscular disorders.[11]Approximately 15% of all genetic diseases are caused by mutations that affect RNA splicing.[12] Techniques that trick the splicing machinery to correct the alternative splicing pathways can be of high therapeutic value. Antisense technology used to specifically target complementary viral nucleic acid sequences and inhibit viral replication.[13,14] This can be adapted to correct the alternative splicing process.

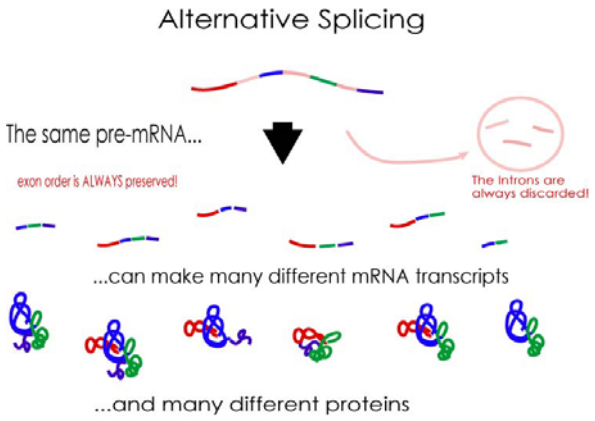

Figure 9. Alternative splicing

Kang *et al*[15] have developed an assay (Figure 10) based on fluorescent protein expression as a result of steric blockage of alternative splicing by an antisense agent (modified DNA/RNA, PNA etc). This assay is straightforward to carry out and has a very high dynamic range, such that even very low activity levels can be seen as a positive luminescence read-out. The chemistries that have been shown to work in animal models include peptide nucleic acids (PNAs), alternating locked nucleic acids (LNAs) and deoxynucleotide oligonucleotides, fully modified (non-gapmer) 2'-substituted oligonucleotides and PMO-based oligomers.[16]

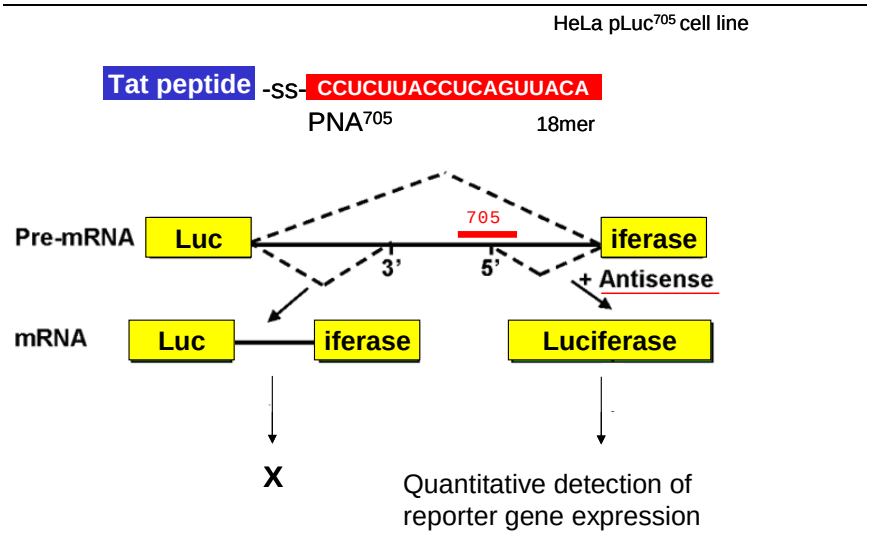

Figure 10: Kole's splice correction assay

1.3 Spectroscopic technique to study DNA/RNA interactions

Ultraviolet absorption (UV) and circular dichroism (CD) which probe electronic properties of the bases are highly useful and general tools for characterizing nucleic acids.

1.3.1 Ultraviolet spectroscopy

The absorbance of polynucleotide depends on the sum of the absorbance of the nucleotide plus the effect of the interaction among the nucleotides. The interaction cause a single strand to absorb less than the sum of its nucleotides and a double strand absorbs less than its two component single strand. The effect is called hypochromicity which results from the coupling of the transition dipoles between neighboring stacked bases and is larger in amplitude for A-U and A-T pairs.[17] In converse term, hyperchromicity refers to the increase in absorption when a double standed nucleic acid is dissociated into single strands. The UV absorption of a DNA duplex increases typically by 20-30 % when it is denatured. This transition from a stacked, hydrogen bonded double helix to an unstacked, strand-separated coil has a strong entropic component and is temperature dependent. The mid-point of this thermal transition is known as the **melting temperature** (T_m). Such a thermal dissociation of nucleic acid helices in solution to give single stranded DNA/RNA is a function of base composition, sequence, chain length as well as of temperature, salt concentration, and pH of the solvent (buffer). In particular, early observations of the relationship between T_m and base composition for different DNAs showed that A-T pairs are less stable than G-C pairs, a fact which is now expressed in a linear correlation between T_m and the gross composition of a DNA oligomer by the equation:

$$T_m = X + 0.41\ (\%\ C+ G)\ ^oC$$

The constant X is dependent on salt concentration and pH and has a value of 69.3 ºC for 0.3 M sodium ions at pH 7.[17]

A second consequence is that the steepness of the transition curve also depends on base sequence. Thus, melting curves for homooligomers have much sharper transitions than those for random-sequence oligomers. This is because A-T rich regions melt first to give unpaired regions which then extend gradually with rising temperature until; finally, even the pure G-C regions have melted. Short homooligomers melt at

lower temperatures and with broader transitions than longer homooligomers. For example for poly (rA)n-poly (rU)n, the octamer melts at 9 ºC, and the undecamer at 20 ºC, and long oligomers at 49 ºC in the same sodium cacodylate buffer at pH 6.9. Consequently, in the design of synthetic self complementary duplexes for crystallization and X-ray structure determination, G-C pairs are often placed at the ends of hexamers and octamers to stop them 'fraying'. The converse of melting is the renaturation of two separated complementary strands to form a correctly paired duplex.

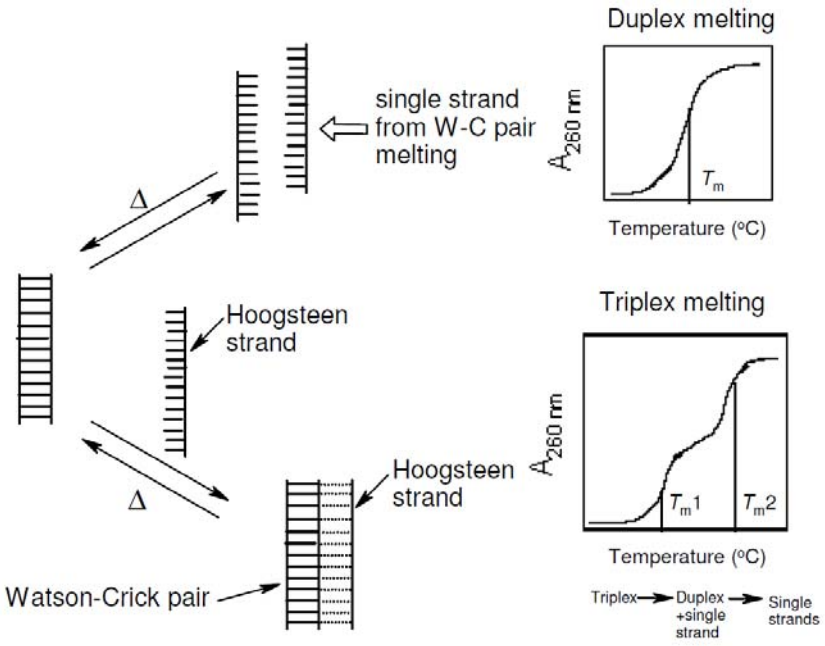

Figure 11: Schematic representation of DNA duplex and Triplex

Duplex melting: According to the 'all or none model'[18], the UV absorbance value at any given temperature is an average of the absorbance of duplex and single strands. A plot of absorbance against temperature gives a sigmoidal curve in case of duplexes and the midpoint of the sigmoidal curve (Figure 11) called as the 'melting temperature' (T_m) (equilibrium point) at which the duplex and the single strands exist in equal proportions.

Triplex melting: In the case of triplexes, the first dissociation leads to melting of triplex generating the duplex (WC duplex) and third strand (Hoogsteen strand), followed by the duplex dissociation to form two single strands. The DNA triplex melting shows characteristic double sigmoidal transition (Figure 11) and UV melting temperature for each transition is obtained from the first derivative plots. The lower melting temperature

(T_m1) corresponds to triplex to duplex transition while the second higher melting temperature (T_m2) corresponds to the transition of duplex to single strands.[19]

1.3.2 Circular Dichroism

Circular dichroism (CD) refers to the differential absorption of left and right circularly polarized light. CD is particularly useful for studying chiral molecules and has very special significance in the characterization of biomolecules (including the secondary structure of proteins and the handedness of DNA). The commonly used units in current literature are the mean residue ellipticity (degree cm^2 $dmol^{-1}$) and the difference in molar extinction coefficients called as molar circular dichroism or $\Delta\varepsilon$ (liter $mol^{-1}cm^{-1}$). The molar ellipticity [θ] is related to the difference in molar extinction coefficients by [θ] = 3298 ($\Delta\varepsilon$). In the nucleic acid, the heterocyclic bases that are principal chromophores. As these bases are planar, they don't have any intrinsic CD. CD arises from the asymmetry induced by linked sugar group. CD spectra from the dinucleotide exhibit hyperchromicity, being more intense by roughly an order of magnitude than those from monomers. It is when the bases are linked together in polynucleotide's, giving rise to many degenerate interactions and they gain additional characteristic associated with the asymmetric feature of secondary structure such as in proteins and nucleic acids.[20]

The simplest application of CD to DNA structure determination is for identification of polymorph present in the sample.[21] The CD signature of the B-form DNA as read from longer to shorter wavelength is a positive band centered at 275 nm, a negative band at 240 nm, with cross over around 258 nm. These two bands arise not from a simple degenerate exciton coupling, but as a result of superimposition of all coupling transitions from all the bases. A-DNA is characterized by a positive CD band centered at 260 nm that is larger than the corresponding B-DNA band, a fairly intense negative band at 210 nm and a very intense positive band at 190 nm. The 250-230 nm region is also usually fairly flat though not necessarily zero. Naturally occurring RNAs adopt the A-form if they are duplex.

CD denaturation (melting) and CD-Job's plots are equally important as they give T_m and binding stoichiometry of DNA/RNA complexes respectively

Stoichiometry. *The binding stoichiometry of oligonucleotide to target DNA/RNA by UV-titration (mixing)*: This is derived from Job's plot.[22] The two components of the

complex are mixed in different molar ratios, so that the total concentration of each mixture should be constant, i.e., as the concentration of one strand decreases, concentration of the second strand increases and the UV-absorbance of each mixture is recorded. The absorbance decreases in the beginning to a minimum and then again increases. The molar ratio of the two strands at which absorbance reached minimum indicates the stoichiometry of complexation.

1.4 Modified Oligonucleotides

All therapeutic oligomers should be stable to enzymatic degradation and pass efficiently through the cell membrane to the target site without degradation. Native oligomers are not suitable for this purpose because they are rapidly degraded by extra and intracellular nucleases. A vast number of chemically modified oligonucleotides have been used in antisense experiments most of which have been described in the recent review articles.[23] In general, three types of modifications of nucleic acid can be distinguished (Figure 12) analogs with unnatural bases, modified sugars (especially at the 2' position of the ribose) or altered phosphate backbones.

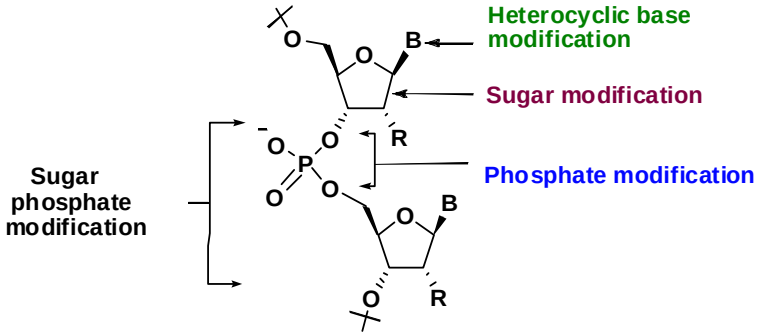

Figure 12. Different sites of modification for DNA

1.4.1 Modifications of phosphate linkage

The first generation modifications focussed attention on oligonucleotides having phosphorothioate (PS, Figure 13a)[24] phosphorodithioates, methylphosphonates[25] (Figure 13b), phosphotriesters[26](Figure 13c), boranophosphonates[27](figure 13d) and phosphoramidates[28] (Figure 13e) replacing the anionic phosphate diester linkages either with anionic or neutral linkages. Phosphorothioate and the vast majority of first generation antisense agents which possess increased hydrolytic stability are

accomplished by weaker binding affinity for their RNA or DNA targets via duplex and triplex formation.[29] The only antisense agent approved by FDA (Vitravene) so far is based on PS-oligos. However PS oligomers exhibit nonspecific effects, presumably due to adventitious protein binding.[30]

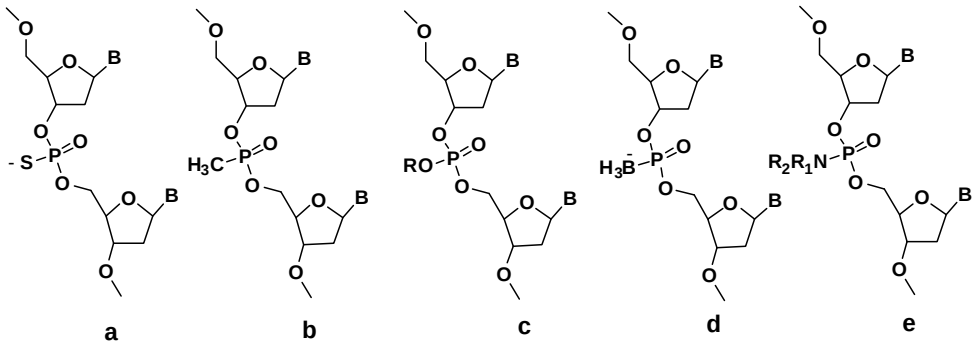

Figure 13. First generation modified antisense oligonucleotide

All these modifications also introduces additional chiral centre at phosphorus thus the oligomers are complex mixture of diastereomers and the conformational heterogeneity leads to lowering of the melting temperature. As a consequence, the search for a stereo controlled synthesis has been undertaken.[31] Synthetic diastereomerically pure phosphorothioate-containing RNA oligomers with the Rp configuration showed higher affinity for complementary RNA than the natural oligomer did, whereas Sp oligomers had similar or lower affinity.

1.4.2 N3'-P5'/P3'-N5' phosphoramidates

Uniformly modified oligonucleotide N3'-P5' phosphoramidates as DNA analogs in which 3'-hydroxyl group was substituted with 3'-amino group, bind with high affinity and in a sequence specific manner to RNA.[32] N3'-P5' phosphoramidates (Figure 14a) have shown increased efficacy relative to phosphorothioate ODNs in both cell culture assays and *in vivo* therapeutic models, despite their inability to activate RNase H.[33] Additionally, their tight binding to double stranded DNA targets have made them potentially useful as 'antigene' agents via triplex formation.[25c] N3'-P5' ribophosphoramidates[34] (Figure 14b) form stable duplexes with complementary natural phosphodiester DNA and RNA strands, as well as with 2'-deoxy N3'→P5' phosphoramidates and they are very resistant to enzymatic hydrolysis by snake venom phosphodiesterase. The 2'-ribo-fluoro substitution in phosphodiester and

phosphorothioate ONs stabilized the duplex with both DNA and RNA sequences, due to C3'-*endo* or N-type sugar puckering. In contrast, stability of 2'-arabino-fluoro ON:DNA/RNA duplexes were found to be significantly less stable.

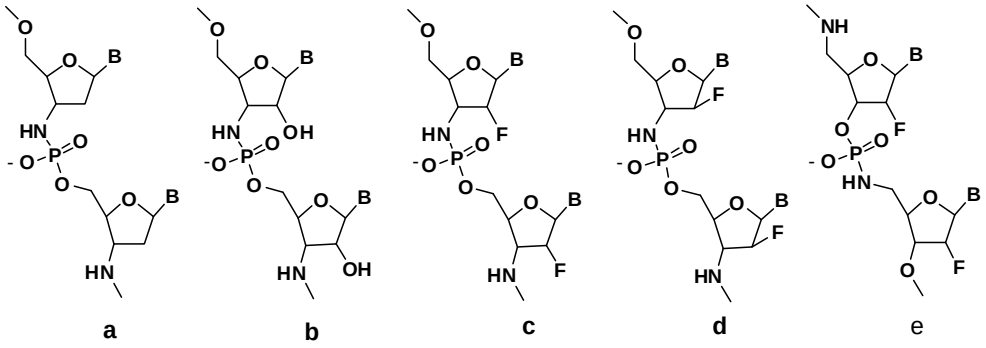

Figure 14. 3'N-P5' and 3'P-N5' phosphoramidates

The introduction of 2'-ribo-fluoro substituent in N3'-P5' phosphoramidates (Figure 14c) rendered very high stability for the complexes with RNA and the effect of 2'-ribo-fluro and 3'-amino was found to be synergistic in stabilizing the 3'-endo sugar pucker.[35] Structural analysis of apparently opposing conformational effects of 2'-arabino-fluoro and 3'-amino groups, which shift the conformational equilibrium of the nucleoside sugar puckering to C2'-*endo* (or O4'-*endo*) and C3'- *endo* forms respectively, was studied in 2'-arabino-fluoro N3'-P5' phosphoramidates backbone (Figure 14d).[36] NMR analysis revealed that the replacement of 3'-oxygen by a 3'-amino group shifted the 2'-arabino-fluoro furanose conformational equilibrium towards N type, similar to that seen for 2'-deoxy-3'-amino nucleosides. The duplexes formed by 2'-arabino-fluoro phosphoramidate and 2'-deoxy phosphoramidate ONs had similar thermal stabilities, which reflected the similarities of their sugar puckering. The most stable complexes with RNA were formed by fully modified 2'-arabino-fluoro phosphoramidates ON.

Another phosphoramidate analog in which the DNA having P3'/N5'phosphoramidate linkage (Figure 14e), exhibited largely decreased thermal stability of duplexes with DNA and RNA complements. It was found that the introduction of 5'-amino-2',5'-dideoxy-2'-ribo-fluororibonucleosides into siRNAs slightly improved thermal stabilities and also exhibited improved nuclease-resistant properties of the siRNAs without loss of their silencing efficacy.[37]

1.4.3 Enantio-DNA and other stereoisomers of DNA/RNA

A very early example towards RNA selectivity was found for short enantio-DNA sequences based on L-sugars (Figure 15b). In 1970, Ts'O *et al* found that that L-ApA interacts with poly(U).[38] Later in 1984, L-$(dUp)_{17}$ dU was shown to have no interaction with poly(dA).[39] In 1990, Shudo *et al*.[40] synthesized enatiomeric- dA_6 and showed that they bind sequence specifically with poly (U) but not with poly (dT). The thermal stability of selective enantio-DNA:RNA complexes was less than either DNA:RNA or RNA:RNA complexes.

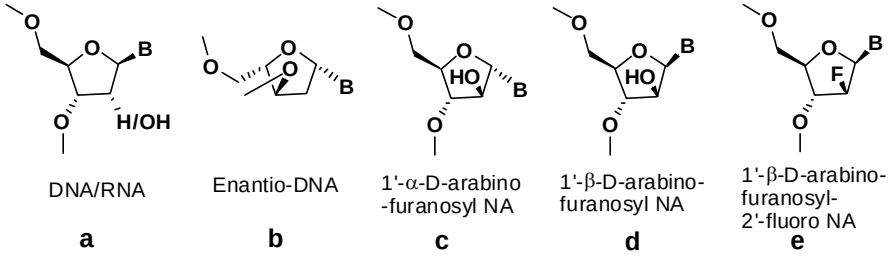

Figure 15: Enantio-DNA and other stereoisomers of DNA and RNA

Meyer, Jr. *et al*.[41] studied a 15mer sequence containing 1'-α-D-arabinofuranosylthymine (Figure 15c) which showed binding with complementary RNA as good as the natural DNA:RNA duplex but its complex with poly-dA showed substantially lower stability than the natural counterpart. The presence of arabino-D-sugar, the 2'-stereoisomer of ribose in the oligomers (ANA) (Figure 15d) allowed complex formation with both RNA and DNA, but with reduced stability.[42] This destabilization was presumed to be derived from the steric interference by the β-2'-OH group, which being oriented into the major groove of the helix, could cause slight local deformation or unstacking. Replacement of 2'-OH of ANA by 2'-Fluoro-ANA (Figure 15e) led to stabilization of 2'F-ANA:RNA duplexes. This stability was attributed to the reduced steric interactions of fluorine atom (*vs* OH groups) and higher pre-organization state of 2'FANA relative to DNA. The standard arabinose sugar pucker was shown to be almost C2'-*endo* locked due to an internal H-bonding with C5'-oxygen. The lack of such interaction in 2'FANA allowed increased variability and sugar pucker shift towards C4'-*endo*, but the overall structural geometry of 2' FANA/ANA:RNA duplexes was predicted to be similar to the native DNA:RNA substrate of RNase H.[43] Contrary to these studies, the NMR solution structural analysis showed that in either ANA:RNA or 2'FANA:RNA duplexes, the

ANA sugar residues assumed conformations in C4'-*endo* range.[44] The differential stability of 2'FANA:RNA and ANA:RNA hybrids was attributed to different extents of hydration of the 2'-OH and 2'-Fluorine groups.

1.4.4 Sugar 2'-Modifications

It has been shown that short RNA/RNA duplexes are thermally more stable than short DNA/DNA duplexes due to sugar ring in RNA is found predominantly in the C3'-*endo*-conformation which exclusively forms A-type duplexes.[45] In order to improve the RNA binding behavior of AON, second generation modifications focused mimicking RNA or C3'-*endo*-like structures. This class includes sugar 2'- modifications (Figure 16).[23b]

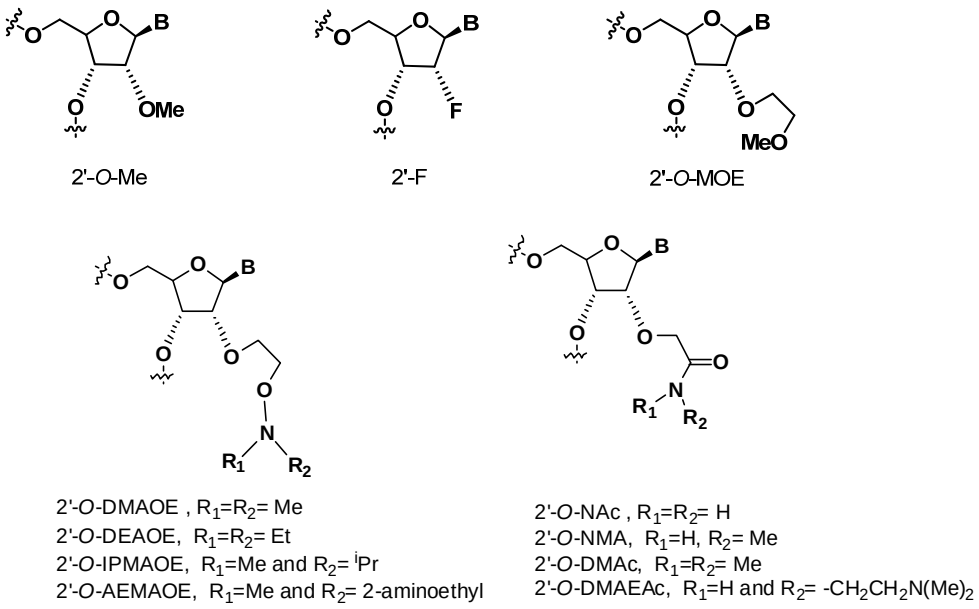

Figure 16. Sugar 2'-Modifications

Electronegative substituent's such as fluorine and oxygen shift the ribose conformational equilibrium towards the C3'-*endo* pucker.[46] The effect of 2'-substitution on the thermal stability of a DNA/RNA duplex was demonstrated with 2'-*O*-Me modification.[47] The 2'-*O*-Me modification improved thermal stability of an oligonucleotide hybridized to a complementary RNA. The 2'-deoxy-2'-fluororibonucleosides also increased the affinity of oligonucleotides toward complementary RNA.[48] However, these modifications did not confer the necessary

metabolic stability to antisense oligonucleotides. In combination with phosphorothioate backbone modification, oligonucleotides with these modifications are resistant to metabolic degradation. Oligonucleotides with 2'-*O*-alkoxy substituent's related to ethylene glycol (2'-*O*-MOE) showed equal or higher binding affinity than 2'-*O*-Me modified oligonucleotides.[49] The 2'-*O*-[2-(methoxy) ethyl] modification (Figure 16, 2'-*O*-MOE) offers +2° increase in thermal stability (*T*m) per modification compared to PS-DNA.[50] Furthermore, the 2'-*O*-MOE modification enhances the nuclease stability of oligonucleotide phosphodiesters at approximately the same level as that of PS-DNA.

Several analogs of 2'-*O*-[2-(aminooxy) ethyl] modification have been synthesized by exploiting the reactive aminooxy group present in this modification.[51] These include modifications such as 2'-*O*-{2-[(Dimethylamino)oxy]ethyl]} (Figure 16, 2'-*O*-DMAOE), 2'-*O*-(2-{[(diethyl)amino]oxy}ethyl) (Figure16, 2'-*O*-DEAOE), 2'-*O*-(2-{[(isopropyl)(methyl) amino]oxy}ethyl) (Figure 16, 2'-*O*-IPMAOE), and 2'-O-(2-{[(2-aminoethyl)(methyl)- amino]oxy}ethyl) (Figure 16, 2'-*O*-AEMAOE). A group of 2'-*O*-[2-(amino)-2- oxoethyl] modified oligonucleotides were reported such as 2'-*O*-(2-amino-2- oxoethyl) (Figure 16, 2'-*O*-NAc), 2'-*O*-[2-(methylamino)-2-oxoethyl] (Figure 16, 2'-*O*-NMA), 2'-*O*-[2-(dimethylamino)-2-oxoethyl] (Figure 16, 2'-*O*-DMAc), and 2'-*O*-(2-{[2- (dimethylamino)ethyl]amino}-2-oxoethyl) (Figure 16, 2'-*O*-DMAEAc). These 2'-modified oligonucleotides showed excellent binding affinities to complementary RNA and high nuclease stability.[52]

1.4.5 Locked nucleic acids and its analogs

The anomeric-inverted analogue of DNA (α-DNA) [Figure 17] has been demonstrated to hybridize efficiently with complementary DNA/RNA, but in parallel orientation.[53] Due to the predominant influence of the 3'-OH gauche effect [O3'-C3'-C4'-O4'] over the anomeric effect, the β-D-2'-deoxy nucleosides sugar moiety preferentially adopted S-type conformations. The sugars in α-D-2'-deoxy nucleosides were predominantly in the S-type conformation due to the co-operative influence of nucleobase as well as the gauche effect.[54]

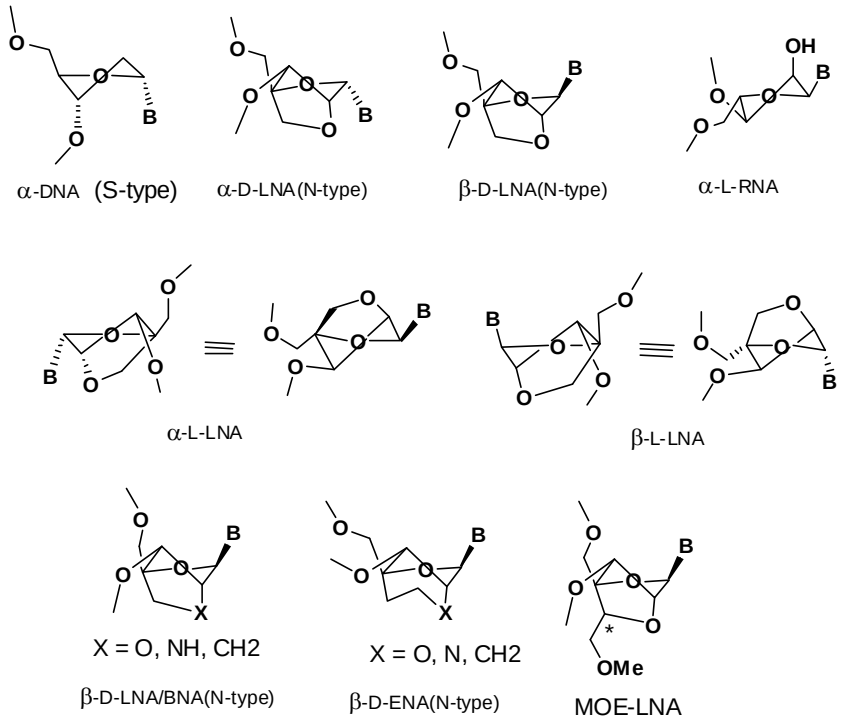

Figure 17. Locked nucleic acid and its analog

Locked nucleic acids (LNA) are a class of high-affinity RNA analogs in which the ribose ring is "locked" in 3'-*endo* conformation[55] (Figure 17). As a result, LNA oligonucleotides exhibit unprecedented thermal stability when hybridized to a complementary DNA or RNA strand. Structural studies by NMR spectroscopy have shown LNA-containing ONs to fit into an A-type duplex geometry.[56] For each incorporated LNA monomer, the melting temperature (*T*m) of the duplex increases by 2-8 ºC compared to the unmodified duplexes.[57] In addition, LNA oligonucleotides can be made shorter than traditional DNA or RNA oligonucleotides and still retain a high *T*m. This is important when the oligonucleotide is used to detect small or highly similar targets.

Koizumi *et al.*[58] synthesized ethylene-bridged nucleic acid (ENA, Figure 17) with six-membered bridged structure. ENA showed comparable duplex forming ability, triplex formation and nuclease resistance were somewhat improved compared to LNA.[59] Combining the structural elements of 2'-*O*-methoxyethyl (MOE) and LNA nucleosides as cMOE and cEt modifications of LNA hybridized complementary nucleic acids with the same affinity as LNA while greatly increasing nuclease stability (Figure 17).[60] Both ENA- and LNA-type carbocyclic analogues have sugar moiety locked in the same North

conformation as in the ENA and LNA. 8-Me/NH_2/OH modified carba-ENA-T AONs analogues are highly RNA-selective since all of them led to slight thermal stabilization effect for the AON: RNA duplex, but quite large destabilization effect for the AON: DNA duplex.[61]

The α-configured LNA was introduced as α-DNA with locked N-type sugar conformation. Fully modified α-D-LNA (Figure 17) sequences of either oligothymine or mixed oligopyrimidines displayed unprecedented recognition of parallel complementary RNA sequences whereas the complementary DNA sequences were not recognized.[62] Chimeric α-D-LNA/α-DNA sequences showed low affinity for RNA. This observation meant that the stabilization of parallel orientation in RNA:α-D-LNA was not fine-tuned in chimeric sequences probably because α-DNA units in the sequence remain in S type preferred conformation creating incoherency between N and S type conformations within the same sequence. This suggests that unlike the original LNA, the N-type conformation of α-D-LNA could not influence the conformations of neighbouring α-DNA nucleosides to adopt N-type conformations.

Wengel and co-workers investigated α-L-LNA (Figure 17), which contains the 2', 4'-bridge on the same side of the sugar as the nucleobases, along with an inversion of the 3'-OH group. This modification have nearly the same affinity for target RNA as that of LNA. Structural studies of α-L-LNA were showed that α-L-LNA assumes a DNA-like Southern conformation, resulting in H-form duplexes with target RNA.[63] Even though α-L-LNA showed Southern sugar pucker, α-L-LNA does not support RNase H, but has been utilized successfully in gapmer ASO designs.[64] α-L-LNA shows increased nuclease resistance over LNA.[65]

With LNA being RNA mimic and α-L-LNA being a DNA mimic, β-L-LNA was deduced to be a α-DNA mimic. Changing the configuration at anomeric center of α-L-LNA led to the synthesis of β-L-LNA, which was expected to mimic the characteristics of α-DNA. Thus, the β-L-LNA sequences recognized complementary RNA and DNA sequences in parallel orientation with similar stabilities of parallel α-LNA:RNA duplex.[66]

1.4.6. Substituted sugar analogs

Several substituted sugar analogs have been reported in the literature. 3'-C-(hydroxymethyl) thymidine modified ODNs causes no (middle modifications) or only

minor (3'-end modifications) destabilization of the resulting DNA: DNA duplex (Figure 18, I).

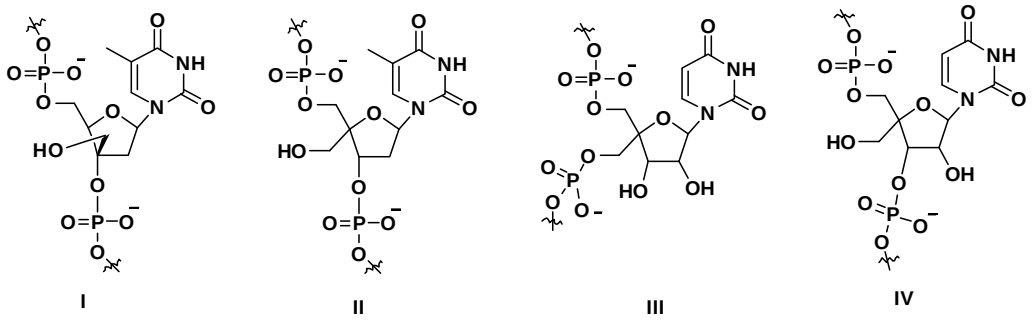

Figure 18. 3'and 4'-substituted DNA and RNA analogs

3'-End-capped sequences exhibit enhanced stability toward snake venom phosphodiesterase.[67] Several 4'-substituted nucleosides has been synthesized, screened for its HIV inhibition activity and only the fused oxetane derivative of thymidine inhibit HIV replication in A301(Alex) cells with remarkably low bone marrow toxicity.[68] Novel 4'-C-(hydroxymethyl)thymidine modified ODNs have shown excellent hybridization properties and this modification leads to significantly improved enzymatic stability[69](Figure 18, II). Incorporation of 4'-C-hydroxymethyluridine (Figure 18, III and IV) in oligonucleotides (both 5'- hydroxyl to 4'-C-hydroxymethyl backbone or 5'-hydroxyl to 3'-hydroxy backbone) showed destabilization with complementary DNA and RNA.[70] The conformations of the pentofuranose ring in the modified nucleotides III and IV are far from ideal when optimal DNA: DNA duplex stability is considered and it was confirmed by modeling studies, which revealed distortions in the sugar-phosphate backbone, especially for modification III.

1.4.7 L-Threofuranosyl nucleic acid (TNA) and Hexitol nucleic acids (HNA)

3'-2' Nucleic acids (TNA, Figure 19, I) cross paired both with RNA and DNA, but the pairing with RNA was found to be stronger in comparison with DNA. The backbone is shorter than both in DNA or RNA as the sugar moiety in TNA contains only four atoms between two adjacent P atoms as compared to five atoms in either DNA or RNA.[71] The detailed crystal structure study of the three dimensional structure provided insight into the origins preferred pairing between TNA and RNA relative to that between DNA and TNA.[72] It was found that the 3' and 2' phosphate groups

preferred to be in quasi diaxial orientation which brought the P...P distance around 5.8 Å. This distance is similar to that between A form of duplexes leading to very stable TNA: RNA structures. Cross pairing between TNA and DNA was permissible because of the allowed conformational adjustments of DNA strand in TNA: DNA duplex and not vice-versa. The close and specific distance complementarity could be the structural parameter that determined the capability of TNA ONs for preferential cross pairing.

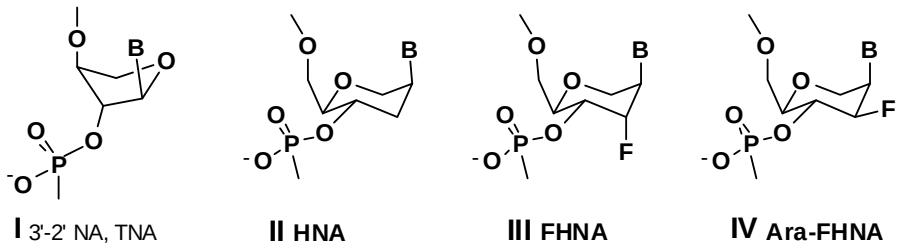

Figure 19. TNA and HNA analogs

The replacement of conformationally flexible deoxyribose by the restricted anhydrohexitol ring resulted in a structurally preorganized HNA (Figure 19, II) to form A- type helices with efficient base stacking.[73] Molecular associations between HNA and RNA were found to be more stable than those between HNA and DNA. ^{1}H NMR analysis of a HNA dimer confirmed the axial orientation of the base moiety with respect to the hexitol ring, and this was used as starting conformation for molecular dynamics study of HNA/RNA and HNA/DNA duplexes. Both complexes showed A-type geometry and very similar hydrogen bonding pattern between base pairs. The presence of 2'-OH group could be responsible for the differential hydration patterns in the minor groove of HNA: RNA and HNA: DNA duplexes. The DNA strand in HNA: DNA complex was found to be more flexible than the RNA strand in HNA: RNA duplexes. In contrast, the crystal structure of HNA: RNA hybrid suggested less-pronounced rigidity of the backbone. The differences in hydration of the HNA and RNA backbones were also observed in the HNA: RNA duplex crystal structure. The hydration of the HNA strand promoted tighter bridging of the adjacent phosphate groups by water molecules and helped alteration in adjacent P-P distances that were close to RNA than DNA. This reinforcing effect upon hydration could be the second reason for overall duplex stability of HNA: RNA duplex in addition to the conformational preorganization imposed by the six membered rings.[74]

Synthesis, biophysical and biological properties of the 3'-fluoro hexitol nucleic acid (FHNA and Ara-FHNA) modified oligonucleotides were reported recently.[75] Axial 3'-fluoro substitution (Figure 19, FHNA, III) boosts the RNA affinity of HNA, whereas fluorine in equatorial orientation (Figure 19, Ara-FHNA, IV) results in a significant destabilization relative to HNA and DNA. Crystal structure at high resolution revealed that the equatorial 3'-fluorine substituent in Ara-FHNA pushes away the 3'-flanking nucleotide thus disrupting stacking of nucleobases.

1.4.8 Six membered carbocyclic analogs

Replacement of the five-membered furanose ring by a six-membered ring is the basis for CNA (carbocyclic nucleic acid) and cyclohexenyl nucleic acids (CeNAs), which are characterized by a high degree of conformational rigidity of the oligomers. Cyclohexanyl-nucleic acid (Figure 20, CNA) was prepared in both enantiomeric (D/L) forms and D-CNA hybridizes to complementary RNA as compared to DNA with reduced affinity.[76]

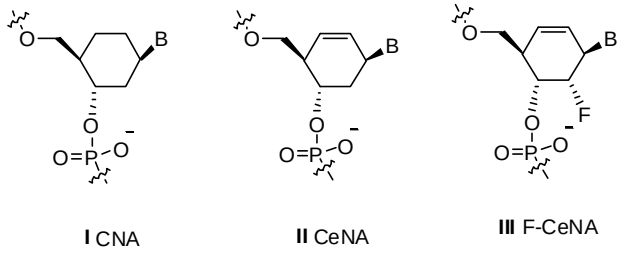

Figure 20. CNA and CeNA analogs

CeNAs form stable duplexes with complementary DNA or RNA and protect ONs against nucleolytic degradation. In addition, CeNA:RNA hybrids have been reported to activate RNase H, albeit with a 600-fold lower *K*cat compared to a DNA:RNA duplex.[77] Recently 2'-fluoro modification was reported in cyclohexenyl nucleic acid (Figure 20, F-CeNA) showed slightly lower duplex thermostability with complementary RNA as compared to that of more rigid 3'-fluoro hexitol nucleic acid.[78] However, F-CeNA modified oligonucleotides were significantly more stable against digestion by snake venom phosphodiesterase as compared to unmodified DNA, 2'-fluoro RNA, 2'-*O*-MOE and FHNA.

1.4.9 Oligonucleotides with dephosphono backbone

1.4.9.1 Artificial DNA with amide backbone

A second generation of backbone replacements for the use of antisense oligonucleotides involves elimination of phosphorous atom from the phosphodiester backbone. A common problem for all anionic analogs is the ineffective permeation of cellular membranes. Anionic ODNs are taken up by endosomes, but are unable to cross the endosomal membrane in the absence of cationic lipids.[79] Based on this observation, neutral isosteres of the phosphodiester linkage have been devised and well reviewed in the literature.[80]

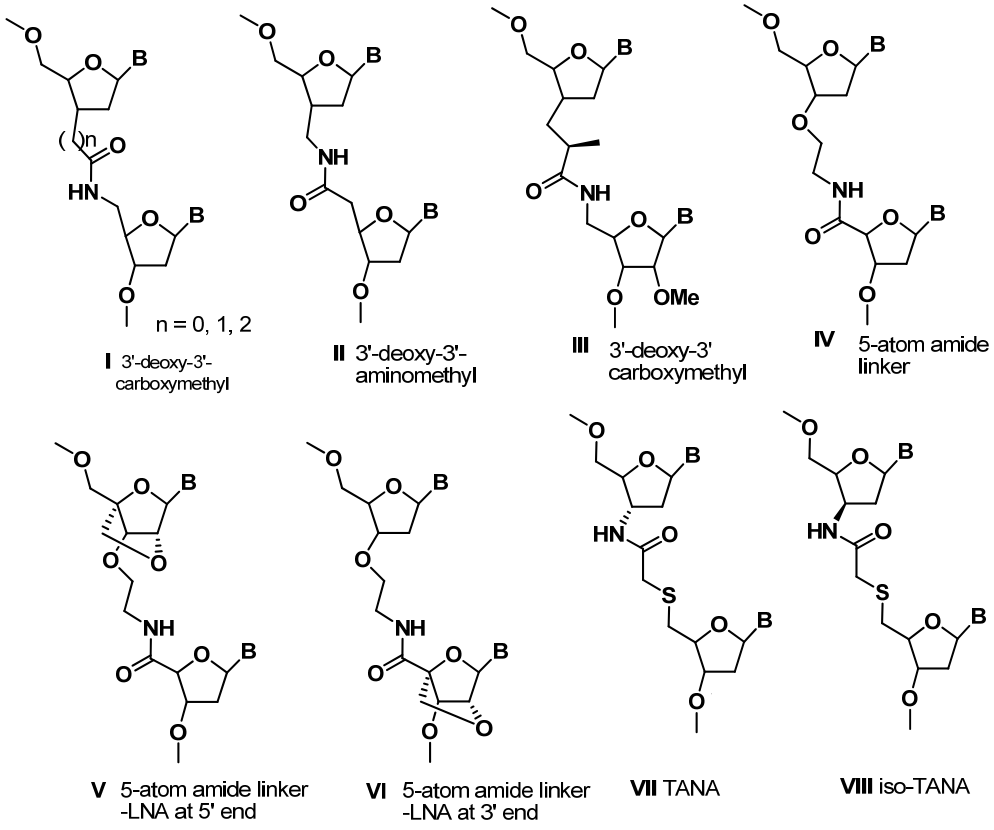

Figure 21. Replacement of phosphodiester by amide linkage

The most promising modification emerged from the replacement of phosphodiester linkage with a neutral carboxylic amide linkage. The four-atom amide substitution of four- atom phosphodiester linkage led to chimeric ONs with alternate amide-phosphodiester groups (Figure 21, II). Such chimeric ONs bound to RNA with a

moderate RNA binding selectivity and with moderately diminished DNA affinity.[81] In contrast, the full replacement of the phosphodiester in the ON by amide linkages led to the formation of much less stable duplexes with RNA compared to the duplexes with DNA.[82] The higher binding affinity in alternating amide-phosphate backbone has been partially attributed to the absence of a gauche effect arising from oxygen atoms of O4′-C4′-C3′-O3 of the native phosphodiester linkage, causing a C3′-*endo* sugar pucker in 3′- deoxy-3′-carboxymethyl nucleoside derivative. This gives the oligomer a favorable A-form like geometry in a mixed alternate amide- phosphodiester backbone. Molecular dynamics simulations of such alternate backbone DNA:RNA complexes favoured exclusive adaptation of C3′-*endo* conformation and A-type DNA: RNA hybrid geometry. The amide (Figure 21, I, n = 1) which formed the most stable backbone could be in constrained planar trans conformation and the neighboring phosphate residues (i-1 and i+2) need to compensate one less degree of rotational freedom in the constrained amide.[83] This could also be the reason for lower stability of fully amide-modified DNA: RNA duplexes. The other amide backbones with extended (Figure 21, I, n = 2) and shortened (Figure 21, I, n = 0) amide linkages in a mixed amide-phosphate backbone destabilized the complex with RNA. The amide backbone (Figure 21, I, n = 1 and II) stabilized the complexes with RNA due to the restricted number of low energy conformations compatible with the overall helical structure.

In contrast to the above discussion, an additional atom in the five-atom amide linker that provided requisite flexibility lead to the stabilization of the duplexes with RNA (Figure 21, III).[84] The amide linkers in 2'-*O*-methyl substituted furanose sugar also led to the stabilization of RNA duplexes. The replacement of 3'-O with a methylene group and addition of a methyl group in either R or S configuration (Figure 21, III) also led to stabilization of duplexes.[80b] CD studies indicated increase in A- type of duplex structure in these cases. Thermodynamic results on duplex formation of DNA/RNA ONs with multiple amide bonds show less unfavorable entropic component relative to wild type DNA: RNA despite the presence of an additional atom in the backbone. The reduced conformational flexibility of the amide bond leading to favorable pre-organization could be one reason for increased stability of the duplexes. X-ray structure of the duplex with RNA revealed a trans amide conformation and that the distance between the neighbouring base pairs was not affected by the longer backbone. An alternate, slightly different five-atom linker was introduced in the

dinucleoside. These chimeric amide-phosphate linkages resulted in destabilization of the duplexes (Figure 21, IV). Further, in order to improve the binding efficiency, LNA nucleoside was introduced as one of the dinucleoside unit in the amide dimer.[85] The LNA monomer improved binding to RNA when positioned preferably towards the 3'-end of the oligomer (Figure 21, VI). Thus, the LNA monomer could replace the destabilizing effect despite the fact that the linker had an additional atom compared to the natural phosphodiester linkage. The 3'-substituents that could exert conformational restrictions on the ribose ring also showed effective stabilization with RNA targets when positioned towards 3'-end. Some amide linked oligonucleotides were also reported by our group where a novel class of thioacetaamido backbone (Figure 21, TANA and iso TANA, VII and VIII) were found to improve the binding affinity and selectivity towards DNA/RNA recognition.[86]

1.4.9.2 3', 5'-Guanidino linkers

ONs with phosphodiester replacement by guanidine (DNG) and S-methylurea (DNmt) linkages in ONs bind to DNA and RNA with high preference for RNA binding (Figure 22).[87, 88]

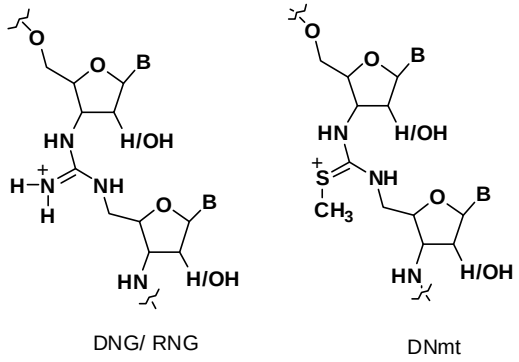

Figure 22. Guanidino and methylthioguanidino DNA/RNA analogues

Predictions based on molecular modeling studies of DNG: DNA and DNG: RNA complexes suggested that DNG in DNG: DNA duplex may primarily retain B-form structure with contracted minor groove due to electrostatic interactions between phosphate and guanidine groups on opposite strands. The DNG: RNA complex, on the other hand adopted A-type structure with furanose sugars in both the strands in C3'-*endo* conformation and also with contracted minor groove. Specific base-pairing was

observed when DNG interacted with DNA and RNA, giving highly stable complexes with RNA over DNA, both the hybrids being highly stabilized compared with their natural counterparts. The enhanced stability by electrostatic interactions was supported by experiments at varying ionic environments. Similar to DNG, the S-methylthiourea linker was designed to lessen the electrostatic attraction compared to DNG and reduce any nonspecific binding with negatively charged phosphate groups.[89] The RNG counterpart of DNG containing ribose sugar instead of deoxyribose sugar was shown to bind preferentially to DNA over RNA due to its rigid B-DNA type backbone.[90]

1.5 Sugar-Phosphate modified oligonucleotides

Morpholino nucleotides and peptide nucleic acids are the most prominent modified nucleic acid mimics that involve the replacement of the sugar-phosphate backbone.

1.5.1 Morpholino nucleotides

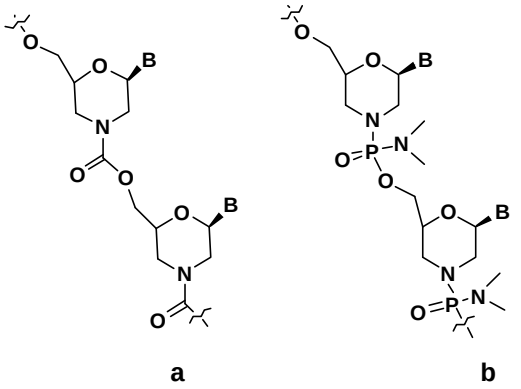

Figure 23. Morpholino ONs linked by a) carbamate, b) phosphorodiamidate

Summerton *et al*. prepared novel oligonucleotide analogues from ribonucleotide derived morpholine units linked by carbamate group (Figure 23a).[91] Cytosine hexamer with stereoregular backbone was prepared in solution phase and was shown to bind poly dG with very high affinity. Solubility characteristics of the resulting oligomer have been improved by terminal conjugation with polyethylene glycol. Fully modified morpholino oligomers where phosphorodiamidate groups are shown to be more effective antisense agents than iso-sequential PS-oligos in cell-free systems and in various cultured cells (Figure 23b). These was attributed to the fact that unlike PS-oligos, morpholino oligos do not bind to non-specific proteins and are much more sequence specific in their

binding to DNA. In one notable study, morpholino oligos were shown to be more effective than PS-oligos as sequence specific antisense inhibitors of tumor necrosis factor-α (TNF-α) in mouse macrophages, despite poor uptake into these cells.[92]

1.5.2 Peptide Nucleic Acids

Peptide nucleic acids (PNAs) [Figure 24] are neutral, achiral DNA mimics that bind to complementary DNA/RNA sequences with high affinity and sequence specificity.[93] In PNA the natural nucleobases are attached via methylene carbonyl linkers to an uncharged pseudopeptide backbone composed of repeating *N*-(2-aminoethyl)glycyl units. PNA hybridizes to complementary DNA/RNA sequences via specific base complementation to form duplexes for mixed sequences and triplexes for homopyrimidine/homopurine sequences.[94]

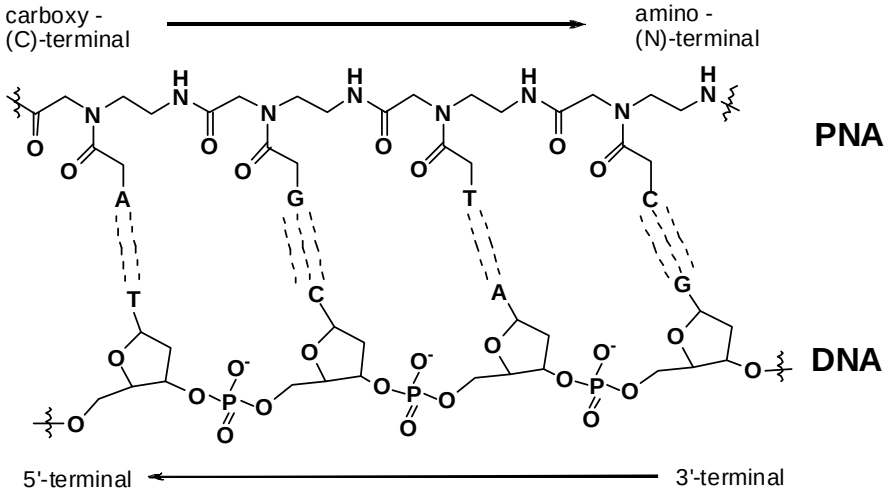

Figure 24. An antiparallel PNA: DNA duplex

The complexes of PNA with DNA/RNA sequences generally show thermal stabilities higher than the corresponding DNA-DNA/RNA complexes depending on sequence.[95] PNAs and their analogs are resistant to proteases and nucleases. Due to these exceptional properties PNAs have major applications as a tool in molecular biology[96] as lead compounds for development of gene targeted drugs via antisense/antigene technology,[97] for diagnostics, biosensors,[98] and as building blocks for designing PNA supramolecular constructs.[99]

The main limitations of PNAs are its poor water solubility and lack of cell permeability coupled with ambiguity in DNA/RNA recognition arising from its equally

facile binding in a parallel/antiparallel fashion (Figure 24) with the complementary nucleic acid sequences. These limitations are being systematically addressed with rationally modified PNA analogues.[100] The solubility of PNAs was improved through conjugation with cationic ligands such as lysine at the N/C terminus of the PNA, or guanidine in backbone without compromising the hydrogen-bonding specificity.[101] The cell penetrability has been improved by conjugation with various transfer molecules such as cell-penetrating peptides.[102] The equal binding of PNA in parallel and antiparallel orientations to DNA/RNA reduces its target specificity. This ambiguity in DNA/RNA binding would lead to recognition of nonspecific target sequences, and achieving PNA specificity in binding is a desirable goal for successful therapeutic applications. This issue was addressed by introduction of chirality into achiral PNA backbones to effect orientational selectivity in complementary DNA/ RNA binding.[103] Relatively high binding affinity of PNAs toward natural oligonucleotides is attributed to the lack of electrostatic repulsion between the uncharged PNA backbone and the negatively charged sugar-phosphate backbone of DNA/RNA. The single-stranded form of PNA, being acyclic, is conformationally flexible in its different structural segments. Consequently, formation of PNA:DNA/RNA complexes is accompanied by conformational changes in PNA to gain enthalpic advantage by hydrogen-bonding and base-stacking interactions accompanied by an undesirable decrease in entropy.[104] Any further increase in the conformational freedom in *aeg*-PNA through extended backbone[105] or side-chain structures[106] lead to substantial reduction in the stability of the resulting PNA: DNA/RNA complexes.

1.5.3.1 PNA modifications for selective RNA targeting

Introduction of chirality in PNA analogues could attain selectivity for parallel versus antiparallel binding with nucleic acids. An early example of PNA analog which induced kinetic selectivity for RNA binding was the POM-PNA, a pyrrolidine-amide oligonucleotide mimics[107] (Figure 25, I). The pyrrolidine ring in the 2*R,* 4*R* stereochemistry was selected as it was expected to adopt the sterically less demanding *trans* relative configuration making the system a stereochemical match with native nucleic acids. X-ray crystallographic data for a similar protonated pyrrolidine ring system showed that the alkyl substituent adopted the *trans* relative stereochemistry with close conformational resemblance to native RNA like C3'-*endo* sugar conformation.[92a]

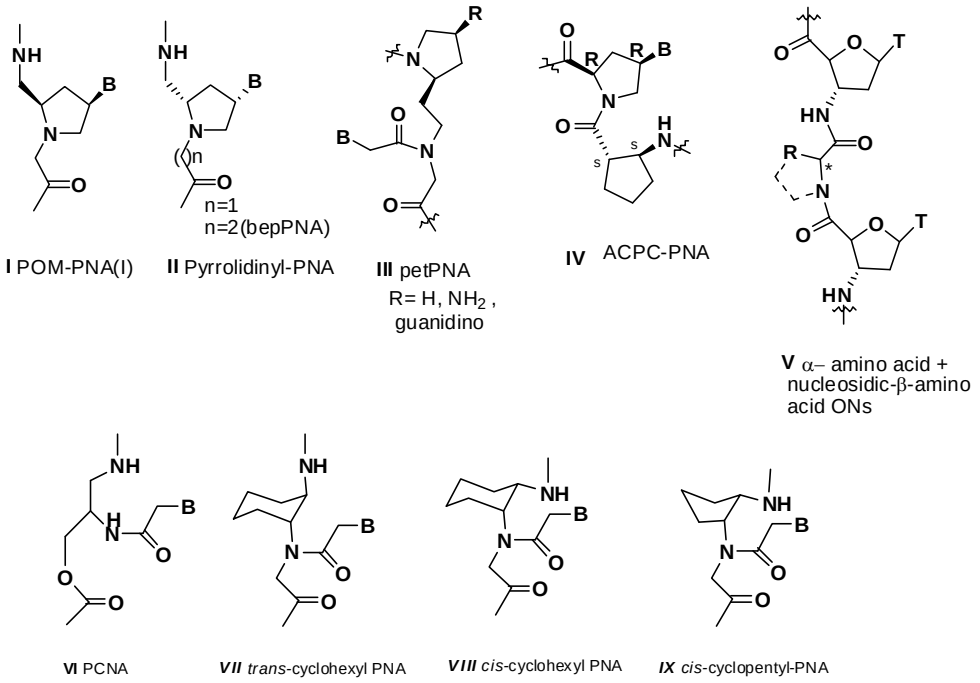

Figure 25. Conformational constrained analogs of PNA

It was found that short pentameric thyminyl-POM sequences bind much faster to RNA than to DNA. Introduction of an additional methyl group to restrict the conformational freedom in the backbone led to destabilizing effect for binding to either with DNA or RNA.[92b] The binding of oligomers of enantiomeric pyrrolidinyl-PNA with 2*S*, 4*S* stereochemistry (Figure 25**,** II**,** n = 1) were found to destabilize the complexes with either DNA or RNA.[108] In our group, the arguments of a five-atom amide linker between the nucleosides that stabilized the complexes formed with RNA to the 2*S*, 4*S*-pyrrolidinyl-PNA was extended that gave rise to backbone extended pyrrolidinyl PNA (*bep*PNA) [Figure 25, II**,** n = 2]. Indeed, alternating PNA:*bep*PNA backbone formed very stable complexes with the target RNA.[109] On the similar ground, another backbone extended pyrrolidine PNAs (petPNA, Figure 25, III) was synthesized to achieve RNA selective binding.[110] Conformationally restricted pyrrolidinyl PNAs with an α/β-dipeptide backbone consisting of a nucleobase-modified proline and a cyclic five-membered amino acid spacer such as (1S,2S)-2-aminocyclopentanecarboxylic acid (ACPC) (Figure 25, IV). ACPC- PNA also formed very stable hybrids with DNA with high Watson-Crick base pairing and exhibited high preference for binding to DNA over RNA.[111] Our group reported a similar concept but a synthetically more straightforward

(α- + β-) amino acid backbone in which the β-amino acid derived from thymidine alternated with naturally occurring α-L-amino acids such as proline, sarcosine, lysine and methionine, yielding amide-linked oligomers[112] (Figure 25, V).

Replacement of amide bond with carbamate linker endowed the polycarbamate nucleic acids with DNA binding selectivity[113] (Figure 25, VI). The most interesting results were obtained when structural constraint in the aminoethyl segment of PNA was introduced in the form of a cyclopentyl/cyclohexyl ring systems. In 1996, Nielsen *et al.* showed that a *trans* cyclohexyl system in *aeg*PNA destabilizes the PNA:DNA/RNA complexes[114] (Figure 25, VII). Comparison of the X-ray and NMR structures of PNA:DNA, PNA:RNA and PNA_2:DNA complexes revealed that the dihedral angle β could play a very important role in deciding the overall stability of these complexes.[115] The angle β remains near 60-65° in RNA:PNA duplexes and in PNA_2:DNA triplexes. The angle β was then frozen in the range 60-65° by adopting the *cis* stereochemistry in the conformationally rigid cyclohexanyl PNA analogue (Figure 25, VIII). X-ray studies on either of the *cis R, S* and *S, R* stereoisomeric cyclohexanyl PNA monomers confirmed that the angle β remains in the range of 60-65°.[116] Introduction of one to three *cis* cyclohexanyl units in the *aeg*PNA led to very strong stabilization of PNA:RNA duplexes and triplexes at the same time the PNA:DNA duplex was considerably destabilized.In contrast, the *cis*/*trans*-cyclopentanyl PNA, consisting of a conformationally flexible five-membered ring stabilized the duplex/triplex structures with both DNA and RNA[117,118] (Figure 25, IX). Some examples of α and γ substituted PNAs have also been synthesized and have better RNA selectivity, water solubility and cellular uptake.[119]

1.6 Present Work

The various DNA and PNA modifications have been reviewed in the preceding sections. All these modifications exhibit excellent properties in some way but lack some other important properties. It is known that in DNA, the phosphate group connecting the two nucleosides is prochiral and when rendered chiral due to substitution at phosphorous, affects DNA/RNA recognition. Implications of amino acid chirality in this backbone are sparingly studied. In the case of partial replacement of phosphodiester linkages with the amide dimer units, where it is necessary to keep the continuity of the backbone for synergistic stacking interactions, such studies are very important.

The thesis comprises the design, synthesis and DNA/ RNA recognition properties of backbone modified DNA analogues where a four atom phosphate linkage is replaced by five atom amide chiral linkages, synthesis of nucleoside based β-Amino acid monomers, synthesis α-L-DNA monomer and incorporation into oligomers.

Chapter 2. This Chapter has been divided into three sections

Section I: In this section we have described the synthesis of designed T-(amino acid)-T dimer blocks using L-proline, D-proline and glycine units.

Section II: In this section we have described the synthesis of designed T-(amino acid)-T dimer blocks using D-Lysine, L-Lysine and T-(amino acid)-$U^{2'\text{-}OMe}$ dimer unit using D-Proline.

Section III: NMR and CD studies were carried out to investigate the effect of backbone chiralty on the base stacking interactions of dimer building block. Dimers having D-Proline, L-Proline and Glycine as internucleoside linker were incorporated in chimeric amide-phosphate backbone, characterization of the resulting oligomers and their preference of binding with DNA/RNA is presented in this chapter.

Chapter 3. This chapter describes synthesis all four nucleoside based β-amino acid and synthetic protocol for synthesis of oligomers using these monomers.

Chapter 4. This chapter describes the synthesis of 4'-substituted α-L-nucleotide analog which has compact backbone like RNA but shows S-Type sugar pucker. Incorporation of this monomer into DNA, characterization of the resulting oligomers and their preference of binding with DNA/RNA are presented in this chapter.

1.7 References

1. Watson, J. D.; Crick, F. H. C. Molecular structure of nucleic acid. A structure for deoxyribose nucleic acid. *Nature*, **1953** *171*, 737.
2. (a) Hoogsteen, K. The crystal and molecular structure of a Hydrogen-bonded complex between 1-methyl thymine and 9-methyl adenine. *Acta. Cryst*. **1963,** *65*, 907; (b) Crick, F. H. C. Codon-anticodon pairing: The Wobble hypothesis. *J. Mol. Biol*. **1966**, *19*, 548.
3. (a) Saenger, W. Principles of nucleic acid structure. Springer-Verlag, New York. **1984** (b) Lescrinier, E.; Froeyen, M.; Herdewijn, P. Survey and summary: Difference in conformational diversity between nucleic acids with a six-membered 'sugar' unit and natural 'furanose' nucleic acids. *Nucleic Acid. Res*. **2003**, *31*, 2975.
4. (a) Richmond, T. J.; Davey C. A. The structure of DNA in the nucleosome core. *Nature*, **2003**, *423*, 145; (b) Leslie, A.G.; Arnott, S.; Chandrasekaran, R.; Ratliff, R.L. Polymorphism of DNA double helices. *J. Mol. Biol*. **1980**, *143*, 49; (c) Wahl, M.; Sundaralingam, M. Crystal structures of A-DNA duplexes. *Biopolymers,* **1997,** *44*, 45; (d) Ghosh. A.; Bansal, M. A glossary of DNA structures from A to Z. *Acta Crystallogr D Biol Crystallogr*. **2003,** *59*, 620; (e) Herbert A.; Rich A. Left-handed Z-DNA: structure and function. *Genetica*. **1999,** *106*, 37.
5. (a) Weiss, B. (ed.) Antisense Oligodeoxynucleotides and Antisense RNA : Novel Pharmacological and Therapeutic Agents, CRC Press, Boca Raton, FL. **1997** (b) Stein, C. A , Does antisense exist ?. *Nat. Med*, **1995**, *1*, 1119.
6. Zamecnik, P. C.; Stephenson, M. L. Inhibition of Rous sarcoma virus replication and cell transformation by a specific oligonucleotide. *Proc. Natl. Acad. Sci. U.S.A*. **1978,** *75*, 280.
7. (a) Kurreck, J. Antisense technologies: improvement through novel chemical modifications. *Eur. J. Biochem*. **2003**, *270*, 1628; (b) Dallas, A.; Alexander A. V. RNAi: A novel antisense technology and its therapeutic potential. *Med Sci Monit,* **2006**, *12*, 67; (c) Kurreck, J. RNA Interference: From Basic Research to Therapeutic Applications *Angew. Chem. Int. Ed*. **2009**, *48*, 1378.
8. (a) Dominski, Z.; Kole, R. Proc. Restoration of correct splicing in thalassemic pre-mRNA by antisense oligonucleotides *Nat. Acad. Sci U.S.A*. **1993**, *90*, 8673;

(b) Sazani, P.; Kole, R. Therapeutic potential of antisense oligonucleotides as modulators of alternative splicing *J. Clin. Invest*. **2003**, *112*, 481.

9. Gilbert, W. Why genes in pieces? *Nature*, **1978**, *271*, 501.
10. Matlin, A. J.; Clark, F.; Smith, C. W. Understanding alternative splicing: towards a cellular code. *Nat. Rev. Mol. Cell Biol.* **2005**, *6*, 386.
11. Wood, M. J. A.; Gait, M. J.; Yin, H. RNA targeted splice–correction for neuromuscular disease. *Brain*, **2010**, *133*, 957.
12. (a) Mironov, A. A.; Fickett, J. W.; Gelfand, M. S. Frequent alternative splicing of human genes. *Genome Res*. **1999**, *9*, 1288; (b) Faustino, N. A.; Cooper, T. A. Pre-mRNA splicing and human disease. *Genes Dev*. **2003**, *17*, 419.
13. Stephenson, M. L.; Zamecnik, P. C. Inhibition of Rous-sarcoma viral-RNA translation by a specific oligodeoxyribonucleotide. *Proc. Natl. Acad. Sci. USA* **1978**, *75*, 285.
14. Zamecnik, P. C.; Stephenson, M. L. Inhibition of Rous-sarcoma virus-replication and cell transformation by a specific oligodeoxynucleotide. *Proc. Natl. Acad. Sci. USA* **1978**, *75*, 280.
15. Kang, S. H.; Cho, M. J.; Kole, R. Up-regulation of luciferase gene expression with antisense oligonucleotides: implications and applications in functional assay development. *Biochemistry* **1998**, *37*, 6235.
16. (a) Sazani, P.; Graziewicz, M.; Kole, R.; in Antisense Drug Technology: Principles, Strategies, and Applications 2nd edn (ed. Crooke, S. T.) **2007,** 89–114 (CRC Press); (b) Lu, Q. L.; Rabinowitz, A.; Chen,Y. C. Systemic delivery of antisense oligoribonucleotide restores dystrophin expression in body-wide skeletal muscles. *Proc. Nat. Acad. Sci. USA* **2005**, *102*, 198; (c) Sazani, P.; Gemignani, F.; Kang, S. H. systemically delivered antisense oligomers upregulate gene expression in mouse tissues. *Nature Biotech*. **2002**, *20*, 1228; (d) Roberts, J.; Palma, E.; Sazani, P.; Orum, H.; Cho, M.; Kole, R. Efficient and persistent splice switching by systemically delivered LNA oligonucleotides in mice. *Mol. Ther*. **2006**, *14*, 471.
17. Blackburn, G. M.; Gait, M. J.; Loakes, D.; Williams, D. M. Nucleic acids in chemistry and biology. RSC publishing, 3rd edition,

18. Cantor, C. R.; Schimmel, P. R. (Eds) Biophysical Chemistry part III, **1971**, W. H. Freeman and Company, New Yok.

19. Plum, G. E.; Park, Y-H, Singleton, S. F.; Dervan, P. B.; Breslauer, K. J. Thermodynamic characterization of the stability and the melting behavior of a DNA triplex: A spectroscopic and calorimetric study, *Proc. Nat. Acad. Sci. USA*, **1990**, *87*, 9436.

20. Van Holde, K. E.; Brahms, J.; Michelson, M. E. Base interactions of nucleotide polymers in aqueous solutions. *J. Mol. Biol*. **1965**, *12*, 726.

21. (a) Stryer, L. Biochemistry, 3rd ed.; New York: W. H. freeman and Company, **1988**; (b) Egli, M.; Williams, L. D.; Gao, Q.; Rich, A. Structure of the pure-spermine form of Z-DNA (magnesium free) at 1-A resolution. *Biochemistry* **1991**, *30*, 11388; (c) Calladine, C. R.; Drew, H. R. Understanding DNA, The molecule and how it works; Cambridge: Academic Press LTd., **1992**; (d) Beveridge, D. L.; Jorgensen, W. L. Computer Simulation of chemical and biomolecular systems. *Ann. NY Acad. Sci*. **1986**, 482; (e) Gassner, R. V.; Frederick, C. A.; Quigley, G. J.; Rich, A.; Wang, A. H. The molecular structure of the left handed Z-DNA double helix at 1.0 A atomic resolution. Geometry, conformation, and ionic interactions of d(CGCGCG). *J. Biol. Chem.* **1989**, *264*, 7921.

22. (a) Job, P. *Annali di Chimica Applicata*. **1928**, *9*, 113; (b) Huang, C. Y. Determination of binding stoichiometry by the continuous variation method: The Job Plot. *Methods in Enzymology*, **1982**, *87*, 509.

23. (a) Kole, R.; Krainer, A. R.; Altman, S. RNA therapeutics: beyond RNA interference and antisense oligonucleotides. *Nat. Rev. Drug. Discov*. **2011**, *11*, 125; (b) Prakash T, P. An overview of sugar-modified oligonucleotides for antisense therapeutics. *Chem. Biodiversity*. **2011,** *8,* 1616; (c) Bennett, C. F and Swayze, E, E RNA Targeting therapeutics: molecular mechanisms of antisense oligonucleotides as a therapeutic platform, *Annu. Rev. Pharmacol. Toxicol*. **2010**, *50*, 259; (d) Shukla, S.; Sumaria, C.S and Pradeepkumar, P.I. Exploring chemical modifications for siRNA therapeutics: A structural and functional outlook. *Chem. Med. Chem* **2010**, *5*, 328; (e) Kumar, V. A.; Ganesh, K. N. Structure-Editing of Nucleic Acids for Selective Targeting of RNA. *Curr. Topics. Med Chem*. **2007**, *7*, 715.

24. Stein, C. A.; Cohen, J. S. Phoshorothioate oligodeoxynucleotide analogues. In Cohen, J. S. (ed.): Oligodeoxynucleotides-Antisense Inhibitors of Gene Expression. London: Macmillan Press, **1989**, 97.

25. Millar, P. S. Non-ionic antisense oligonucleotides. In Cohen, J. S. (ed.): Oligodeoxynucleotides-Antisense Inhibitors of Gene Expression. London: Macmillan Press, **1989**, 79.

26. Summers, M. F.; Powell, C.; Egan, W.; Byrd, R. A.; Wilson, W. D.; Zon, G. Alkyl phospotriester modified oligodeoxyribonucleotides. VI. NMR and UV spectroscopic studies of ethyl phosphotriester (Et) modified Rp-Rp and Sp-Sp duplexes, $(d(GGAA(Et)TTCC))_2$. *Nucleic Acid Res*. **1986**, *14*, 7421.

27. Li, H.; Huang, F.; Shaw, B. R. Conformational studies of dithymidine boranomonophosphate diastereoisomers. *Bioorg. Med. Chem*. **1997**, *5*, 787.

28. Froehler, B.; Ng, P.; Matteucci, M. Phosphoramidate analogs of DNA: Synthesis and thermal stabilities of heteroduplexes. *Nucleic Acid Res*. **1988**, *16*, 4831.

29. Kibler-Herzog, L.; Zon, G.; Uzanski, B.; Whittier, G.; Wilson, W. D. Duplex stabilities of phosphorothioate, methylphosphonate, and RNA analogs of two DNA 14-mers. *Nucleic Acids Res*. **1991**, *19*, 2979.

30. Stein, C.A.; Cheng, Y. C. Antisense oligonucleotides as therapeutic agents: Is the bullet really magical ? *Science* **1993,** *261*, 1004.

31. (a) Yano, J.; Smyth, G. E. New Antisense Strategies: Chemical Synthesis of RNA Oligomers. *Adv Polym Sci*, **2012**, *249*, 1; (b) Oka, N.; Kondo, T.; Fujiwara, S. Stereocontrolled synthesis of oligoribonucleoside phosphorothioates by an oxazaphospholidine approach. *Org. Lett*, **2009**, *11,* 967.

32. (a) Gryaznov, S.; Chen, J. K. Oligodeoxyribonucleotide N3'-P5' phosphoramidates: Synthesis and hybridization properties. *J. Am. Chem. Soc*. **1994**, *116*, 3143; (b) Gryaznov, S. M.; Lloyd, D. H.; Chen, J. K.; Schultz, R.G.; DeDionisio, L. A.; Ratmeyer, L.; Wilson, W. D. Oligonucleotide N3'-P5' phosphoramidates. *Proc. Natl. Acad. Sci. U.S.A*. **1995**. *92*, 5798.

33. a) Gryaznov, S.; Skorski, T.; Cucco, C.; Nieborowska- Skorska, M.; Chiu, C.Y.; Lloyd, D.; Chen, J.-K.; Koziolkiewicz, M.; Calabretta, B. Oligonucleotide N3'-P5'phosphoramidates as antisense agents. *Nucleic Acids Res*. **1996**, *4*, 1508; (b) Heidenreich, O.; Gryaznov, S.; Nerenberg, M. RNase H-independent antisense

activity of oligonucleotide N3'-P5' phosphoramidates. *Nucleic Acids Res*. **1997** *25,* 776; (c) DeDionisio, L.; Gryaznov, S. M. Analysis of a ribonuclease H digestion of N3'-P5'phosphoramidate- RNA duplexes by capillary gel electrophoresis. *J. Chromatogr. B. Biomed. Appl*. **1995**, *669*, 125.

34. Gryaznov S. M., Winter, H. RNA mimetics: oligoribonucleotide N3'-P5' phosphoramidates. *Nucleic Acids Res.***1998**, *26*, 4160.
35. Schultz, R. G.; Gryaznov, S. M. Oligo-2'-fluoro-2'-deoxynucleotide N3'-P5' phosphoramidates: synthesis and properties. *Nucleic Acids res*. **1996**, *24*, 2966.
36. Schultz, R. G.; Gryaznov, S. M. Arabino-fluorooligonucleotide N3'-P5' phosphoramidates: synthesis and properties. *Tet. Lett*. **2000**, *41*, 1895.
37. Ueno, Y.; Hirai, M.; Yoshikawa, K.; Kitamura, Y.; Hirata, Y.; Kiuchi, K.; Kitade, Y. Synthesis and properties of siRNAs containing 5'-amino-2',5'-dideoxy-2'α-fluororibonucleosides. *Tetrahedron*, **2008**, *64*, 11328.
38. Tazawa, I.; Tazawa, S.; Stempel, L. M.; and Ts'o, P. O. P. Conformation and interaction of dinucleoside mono- and diphosphates. L-adenylyl-(3'-5')-L-adenosine and L-adenylyl-(2'-5')-L-adenosine. *Biochemistry*, **1970**, *9*, 3499.
39. Anderson, D. J.; Reischer, R. J.; Taylor, A. J.; Wechter, W. J. Synthesis of L-(dUp)17dU and the absence of interaction of the compound with poly(dA). *Nucleosides Nucleotides*, **1984**, *3*, 499.
40. Shudo, K.; Fujimori, S. Enantio-DNA recognizes complementary RNA but not complementary DNA. *J. Am. Chem. Soc*. **1990**, *112*, 7436.
41. Adams, D. A.; Petrie, C. R.; Meyer, Jr. R. B. Preparation and hybridization of oligonucleotides containing 1-α-D-arabinofuranosylthymine. *Nucleic Acids Res*. **1991**, *19*, 3647.
42. Damha, M. J.; Wilds, C. J.; Noronha, A.; Brukner, I.; Borkow, G.; Arion, D.; Parniak, M. A. Hybrids of RNA and Arabinonucleic Acids (ANA and 2'FANA) Are Substrates of Ribonuclease H. *J. Am. Chem. Soc.,* **1998**, *120*, 12976.
43. (a) Venkateswarlu, D.; Ferguson, D. M. Effects of C2'-sbstitution on arabinonucleic acid structure and conformation. *J. Am. Chem. Soc*., **1999**, *121*, 5609; (b) Minasov, G.; Teplova, M.; Nielsen, P.; Wengel, J.; Egli, M. Structural Basis of Cleavage by RNase H of Hybrids of Arabinonucleic Acids and RNA. *Biochemistry*, **2000**, *39*, 3525.

44. Denisov, A. Y.; Noronha, A. M.; Wilds, C. J.; Trempe, J.-F.; Pon, R. T.; Gehring, K.; Damha, M. J. Solution structure of an arabinonucleic acid (ANA)/ RNA duplex in a chimeric hairpin: comparison with 2'-fluoro- ANA/RNA and DNA/RNA hybrids. *Nucleic Acids Res*. **2001**, *29*, 4284 -4293.

45. Saenger,W. Principles of Nucleic Acid Structure, Springer-Verlag, New York, **1983**

46. Guschlbauer, W.; Jankowski, K. Nucleoside conformation is determined by the electronegativity of the sugar substituent. *Nucleic Acids Res*. **1980**, *8*, 1421.

47. Inoue, H.; Hayase, Y.; Imura, A.; Iwai, S.; Miura, K.; Ohtsuka, E. Synthesis and hybridization studies on two complementary nona(2'-O-methyl) ribonucleotides. *Nucleic Acids Res*. **1987**, *15*, 6131.

48. Kawasaki, A. M.; Casper, M. D.; Freier, S. M.; Lesnik, E. A.; Zounes, M. C.; Cummins, L. L.; Gonzalez, C.; Cook, P. D. Uniformly Modified 2'-Deoxy-2'-fluoro Phosphorothioate Oligonucleotides as Nuclease-Resistant Antisense Compounds with High Affinity and Specificity for RNA Targets. *J. Med. Chem*. **1993**, *36*, 831.

49. Martin, P. 'Ein neuer Zugang zu 2'-O-Alkylribonucleosiden und Eigenschaften deren Oligonucleotide , *Helv. Chim. Acta* **1995**, *78*, 486.

50. Freier, S. M.; Altmann, K.-H. The ups and downs of nucleic acid duplex stability: structure_stability studies on chemically-modified DNA:RNA duplexes. *Nucleic Acids Res*. **1997**, *25*, 4429.

51. Prakash, T. P.; Kawasaki, A. M.; Lesnik, E. A.; Sioufi, N.; Manoharan, M. Synthesis of 2'-O-[2-(N,Ndialkylamino)oxy]ethyl]-modified oligonucleotides: hybridization affinity, resistance to nuclease and protein binding characteristics. *Tetrahedron* **2003**, *59*, 7413.

52. Prakash, T. P.; Kawasaki, A. M.; Lesnik, E. A.; Owens, S. R.; Manoharan, M. 2'-O-[2-(Amino)-2- oxoethyl] Oligonucleotides. *Org. Lett*. **2003**, *5*, 403.

53. Gagnor, C.; Rayner, B.; Leonetti, J.-P.; Imbach, J.-L.; Lebleu B. α-DNA IX: parallel annealing of α-anomeric oligodeoxyribonucleotides to natural mRNA is required for interference in RNase H mediated hydrolysis and reverse transcription. *Nucleic Acids Res*. **1989**, *17*, 5107.

54. Thibaudeau, C.; Fiildesi A.; Chattopadhyaya J. The Quantitation of the Competing Energetics of the Stereoelectronic and Steric Effects of the 3'-OH and the Aglycone in the α- versus β-D- & -L-2'-deoxyribonucleosides by 1H-NMR. *Tetrahedron*, **1998**, *54*, 1867.

55. (a) Singh, S. K.; Koshkin, A. A.; Wengel, J.; Nielsen, P. LNA (Locked Nucleic acids): synthesis and high affinity nucleic acid recognition. *Chem. Commun.* **1998**, 455; (b) Koshkin, A. A.; Singh, S. K.; Nielsen, P.; Rajwanshi, V. K; Kumar, R.; Meldgaard, M.; Olsen, C. E.; Wengel, J. LNA (Locked Nucleic Acids): Synthesis of the adenine, cytosine, guanine, 5-methylcytosine, thymine and uracil bicyclonucleoside monomers, oligomerisation and unprecedented nucleic acid recognition. *Tetrahedron*, **1998**, *54*, 3607; (c) Obika, S.; Nanbu, D.; Hari, Y.; Morio, K.-i.; In, Y.; Ishida, T.; Imanishi, T. Synthesis of 2'-*O*, 4'-C – methyleneuridine and -cytidine. Novel bicyclic nucleosides having a fixed C3'-endo sugar puckering. *Tetrahedron Lett*. **1997**, *38*, 8735.

56. (a) Petersen, M.; Bondensgaard, K.; Wengel, J.; Jacobsen, J. P. Locked Nucleic Acid (LNA) recognition of RNA: NMR solution structures of LNA: RNA hybrids. *J. Am. Chem. Soc*. **2002**, *124*, 5974; (b) Nielsen, K. E.; Rasmussen, J.; Kumar, R.; Wengel, J.; Jacobsen, J. P.; Petersen, M. NMR studies of fully modified locked nucleic acid (LNA) hybrids: solution structure of an LNA:RNA hybrid and characterization of an LNA:DNA hybrid. *Bioconjugate Chem*. **2004**, *15*, 449.

57. (a) Koshkin, A. A.; Nielsen, P.; Meldgaard, M.; Rajwanshi, V. K.; Singh, S. K. ; Wengel, J. LNA (Locked Nucleic Acid): An RNA mimic forming exceedingly stable LNA:LNA duplexes. *J. Am. Chem. Soc*.**1998**, *120*, 13252; (b) Obika, S.; Nanbu, D.; Hari, Y.; Andoh, J.-i.; Morio, K.-i.; Doi, T.; Imanishi, T. Stability and structural features of the duplexes containing nucleoside analogues with a fixed N-type conformation, 2'-*O*, 4'-C-methyleneribonucleosides. *Tetrahedron Lett*. **1998**, *39*, 5401; (c) Wengel, J. Synthesis of 3'-C- and 4'-C-branched oligodeoxynucleotides and the development of Locked Nucleic Acid (LNA). *Acc. Chem. Res*. **1999**, *32*, 301.

58. Morita, K.; Takagi, M.; Hasegawa, C.; Kaneko, M.; Tsutsumi, S.; Sone, J.; Ishikawa, T.; Imanishi, T.; Koizumi, M. Synthesis and properties of 2'-*O*,4'-C-

ethylene-bridged nucleic acids (ENA) as effective antisense oligonucleotides *Bioorg. Med. Chem*. **2003**, *11*, 2211.

59. Koizumi, M.; Morita, K.; Daigo, M.; Tsutsumi, S.; Abe, K.; Obika, S.; Imanishi, T. Triplex formation with 2'-*O*,4'-C-ethylene-bridged nucleic acids (ENA) having C3'-endo conformation at physiological pH. *Nucleic Acids Res.* **2003**, *31*, 3267.
60. Seth, P. P.; Vasquez, G.; Allerson, C. A.; Berdeja, A.; Gaus, H.; Kinberger, G. A.; Prakash, T. P.; Migawa, M. T.; Bhat, B.; Swayze E. E. Synthesis and biophysical evaluation of 2',4'-constrained 2'O-methoxyethyl and 2',4'-constrained 2'-*O*-ethyl nucleic acid analogues. *J. Org. Chem*. **2010**, *75*, 1569.
61. Liu, H.Y.; Xu, J.; Karimiahmadabadi, M.; Zhou C.; and Chattopadhyaya J. Synthesis of 2′, 4′-propylene-bridged (Carba-ENA) thymidine and its Analogues: The engineering of electrostatic and steric effects at the bottom of the minor groove for nuclease and thermodynamic stabilities and elicitation of RNase. *J. Org. Chem*. **2010**, *75*, 7112.
62. Nielsen, P.; Dalskov, K. α-LNA, locked nucleic acid with α-D-configuration. *Chem. Commun*. **2000**, 1179
63. (a) Rajwanshi, V. K.; Ha˚kansson, A. E.; Sørensen, M. D.; Pitsch, S.; Singh, S. K.; Kumar, R.; Nielsen, P.; Wengel, J. The Eight Stereoisomers of LNA (Locked Nucleic Acid): A Remarkable Family of Strong RNA Binding Molecules. *Angew. Chem., Int. Ed*. **2000**, *39*, 1656; (b) Nielsen, K. M.; Petersen, M.; Ha˚kansson, A. E.; Wengel, J.; Jacobsen, J. P. 'α-L-LNA (α-L-ribo Configured Locked Nucleic Acid) Recognition of DNA: An NMR Spectroscopic Study'*, Chemistry.* **2002**, *8*, 3001.
64. Nielsen, J. T.; Stein, P. C.; Petersen, M. NMR structure of an α-L-LNA:RNA hybrid: structural implications for RNase H recognition. *Nucleic Acids Res.* **2003,** *31*, 5858.
65. Kurreck, J.; Wyszko, E.; Gillen, C.; Erdmann, V. A. Design of antisense oligonucleotides stabilized by locked nucleic acids. *Nucleic Acids Res*. **2002**, *30*, 1911.
66. Christensen, N. K.; Bryld, T.; Sørensen, M. D.; Arar, K.; Wengel, J. and Nielsen, P. Parallel nucleic acid recognition by LNA stereoisomers β-L-LNA and α-D-LNA: Studies in the mirror image world. *Chem. Commun*. **2004**, 282.

67. Jorgensen, P. N.; Stein, P. C.; Wengel, J. Synthesis of 3'-C-(Hydroxymethyl)thymidine: Introduction of a Novel Class of Deoxynucleosides and Oligodeoxynucleotides *J. Am. Chem. Soc.* **1994**, *116*, 2231.

68. 4'-Substituted Nucleosides as Inhibitors of HIV: An Unusal Oxetane Derivative. O-Yang, C.; Kurz,W.; Elsie M. Eugui, E.M.; McRoberts, M.J.; Verheyden, J. P. H.; Kurz, L. J.; Walker, K. A. M. *Tetrahedron Lett,* **1992**, *33*, 41.

69. Fensholdt, J.; Thrane, H; Wengel, J. Synthesis of oligodeoxynucleotides containing 4'-C-(hydroxymethyl)thymidine: novel promising antisense molecules. *Tetrahedron Lett*, **1995**, *36*, 2535.

70. Nielsen, K. D.; Kirpekar, F.; Roepstorft, P.; Wengel, J. Oligonucleotide analogues containing 4'-C-(hydroxymethyl)uridine: Synthesis, evaluation and mass spectrometric analysis. *Bioorg. Med. Chem,* **1995**, *3*, 1493.

71. Schöning, K.-U.; Scholz, P., Guntha, S.; Wu, X.; Krishnamurthy, R.; Eschenmoser, A. Chemical etiology of nucleic acid structure: The α-threofuranosyl-(3'→2') oligonucleotide System. *Science*, **2000**, 1347.

72. Pallan, P. S.; Wilds, C. J.; Wawrzak, Z.; Krishnamurthy, R.; Eschenmoser, A.; and Egli, M. Why does TNA cross pair more strongly with RNA than with DNA? An answer from X-ray analysis. *Angew. Chem. Int. Ed. Engl*. **2003**, *42*, 5893.

73. De Winter, H.; Lescrinier, E.; Van Aerschot, A.; Herdewijn, P. Molecular dynamics simulation to investigate differences in minor groove hydration of HNA/RNA hybrids as compared to HNA/DNA complexes. *J. Am. Chem. Soc*. **1998**, *120*, 5381.

74. Maier, T.; Przylas, I.; Strater, N.; Herdewijn, P.; Saenger, W. Reinforced HNA backbone hydration in the crystal structure of a decameric HNA/RNA hybrid. *J. Am. Chem. Soc*. **2005**, *127*, 2937.

75. Egli, M.; Pallan, P. S.; Allerson, C. R.; Prakash, T. P.; Berdeja, A.; Yu, J.; Lee, S.; Watt, A.; Gaus H.; Bhat, B.; Swayze, E. E.; Seth, P. P. Synthesis, improved antisense activity and structural rationale for the divergent RNA affinities of 3-'Fluoro Hexitol Nucleic Acid (FHNA and Ara-FHNA) modified oligonucleotides. *J. Am. Chem. Soc*. **2011**, *133*, 16642.

76. Mourinsh, Y.; Rosemeyer, H.; Esnouf, R.; Mevedovici, A.; Wang, J.; Ceulemans, G.; Lescrinier, E.; Hendrix, C.; Busson, R.; Sandra, P.; Seela, F.; Aerschot, A. V.;

Herdewijn, P. Synthesis and purity properties of oligonucleotides containing 3-hydroxy-4-hydroxymethyl- 1-cyclohexanyl nucleosides. *Chem. Eur. J*. **1999,** *5*, 2139.

77. Wang,J.; Verbeure, B.; Luyten, I.; Lescrinier, E.; Froeyen, M.; Hendrix, C.; Rosemeyer, H.; Seela, F.; van Aerschot, A.; Herdewijn, P. Cyclohexene Nucleic Acids (CeNA): Serum stable oligonucleotides that activate RNase H and increase duplex stability with complementary RNA. *J. Am. Chem. Soc*. **2000**, *122*, 8595.

78. Seth, P. P.; Yu, J.; Jazayeri, A.; Pallan, P. S.; Allerson, C. R.; Østergaard, M.E.; Liu, F.; Herdewijn, P.; Egli, M.; Swayze, E. E. Synthesis and Antisense Properties of Fluoro Cyclohexenyl Nucleic Acid (F-CeNA), a Nuclease Stable Mimic of 2' -Fluoro RNA. *J. Org. Chem*. **2012**, *77*, 5074.

79. (a) Chin, D. J.; Green, G. A.; Zon, G.; szoka, Jr., F. C.; Straubinger, R. M: Rapid nuclear accumulation of injected oligodeoxyribonucleotides. *New Biologist* **1990**, *2*, 1091; (b) Leonetti, J. P.; Mechti, N.; Degols, G.; Gagnor, C.; Lebleu, B: Intracellular distribution of microinjected antisense oligonucleotides. *Proc. Natl. acad. Sci. USA*. **1991**, *88*, 2702.

80. (a) Micklefield, J. Backbone modification of nucleic acids: Synthesis, structure and therapeutic applications *Curr. Med. Chem.* **2001**, *8*, 1157. (b) Pallan, P. S.; Matt von, P.; Wilds, C.; Altmann, K.-H.; Egli, M. RNA binding affinities and crystal structure of oligonucleotides containing five-atom amide-based backbone structures. *Biochemistry*, **2006**, *45*, 8048.

81. (a) Lebreton, J.; De Mesmaeker, A.; Waldner, A.; Fritsch, V.; Wolf, R. M.; Freier, S. M. Synthesis of thymidine dimer derivatives containing an amide linkage and their incorporation into oligodeoxyribonucleotides. *Tetrahedron Lett*. **1993**, *34*, 6383-4386., (b) Lebreton, J.; Waldner, A.; Fritsch, F.; Wolf, R.M.; De Mesmaeker A. Comparison of two amides as backbone replacement of the phosphodiester linkage in oligodeoxynucleotides. *Tetrahedron Lett*. **1994**, *35*, 5225-5228. (c) Halford, M. H.; Jones, M. S: Synthetic analogues of polynucleotides. *Nature* **1968**, *217*, 638.

82. von Matt, P.; De Mesmaeker, A.; Pieles, U.; Zurcher, W.; Altman, K.-H. 2'-deoxyribo-PNAs: A structurally novel class of polyamide nucleic acids with good RNA and DNA binding affinity. *Tetrahedron Lett*. **1999**, *40*, 2899.

83. Nina, M.; Fonne-Pfister, R.; Beaudegnies, R.; Chekatt, H.; Jung, P. M. J.; Murphy-Kessabi, F.; Mesmaeker, A.; Wendeborn, S. Recognition of RNA by amide modified backbone nucleic acids: Molecular dynamics simulations of DNA-RNA hybrids in aqueous solution. *J. Am. Chem. Soc*., **2005**, *127*, 6027.

84. Wilds, C. J.; Minasov, G.; Natt, F.; Matt von, P.; Altmann, K.-H.; Egli, M. Studies of a chemically modified oligonucleotide containing a 5-atom backbone which exhibits improved binding to RNA. *Nucleosides Nucleotides Nucleic Acids,* **2001**, *20*, 991.

85. Lauristen, A.; Wengel, J. Oligonucleotides containing amide linked LNA type dinucleotides: synthesis and high affinity. *Chem. Commun* **2002**, 530.

86. (a) Gogoi, K.; Gunjal, A. D.; Kumar, V. A. Sugar–thioacetamide backbone in oligodeoxyribonucleosides for specific recognition of nucleic acids. *Chem. Commun*. **2006**, 2373; (b) Gokhale, S. S.; Gogoi, K.; Kumar, V. A. Probing binding preferences of DNA and RNA: backbone chirality of thioacetamido-linked nucleic acids and iso-thioacetamido-linked nucleic acids to differentiate DNA versus RNA selective binding. *J. Org. Chem*. **2010**, *75*, 7431.

87. Jain, M. L.; Bruice, P.Y.; Szabó, I. E and Thomas C. Bruice, Incorporation of Positively Charged Linkages into DNA and RNA Backbones: A Novel Strategy for Antigene and Antisense Agents, *Chem. Rev*. **2012**, 112, 1284.

88. Dempcy, R. O.; Browne, K. A.; Bruice, T. C. Synthesis of polycation thyminyl DNG, its fidelity in binding polyanionic DNA/RNA, and the stability and nature of the hybrid complexes. *J. Am. Chem. Soc*. **1995**, *117*, 6140.

89. Arya, D. P.; Bruice, T. C. Replacement of negative phosphodiester linkages of DNA by positive S-methylthiourea linkers: A novel approach to putative antisense agents. *J. Am. Chem. Soc*. **1998**, *120*, 6619.

90. Park, M.; Toporowski, J. W.; Bruice, T. C. Ribonucleic guanidine demonstrates an unexpected marked preference for complementary DNA rather than RNA. *Bioorg. Med. Chem*, **2006**, *14*, 1743.

91. (a) Summerton, J.; Stein, D.; Huang, S. B.; Matthews, P.; Weller, S.; Partridge, M. Morpholino and phosphorothioates antisense oligomers compared in cell-free and in-cell systems. *Antisense Nucleic Acid Drug Dev*. **1997**, *7*, 63; (b) Summerton, J.;

Weller, D. Morpholino antisense oligomers: Design, preparation, and properties. *Antisense Nucleic Acid Drug Dev*. **1997**, *7*, 187.

92. Toyler, M. F.; Wellar, D.D.; Kobzik, L. Effect of TNF-α antisense oligomers on cytokine production by primary murine alveolar macrophages. *Antisense Nucleic Acid Drug Dev*. **1998**, *8*, 199.
93. Nielsen, P. E.; Egholm, M.; Berg, R. H.; Buchardt, O. Sequence-selective recognition of DNA by strand displacement with a thymine-substituted polyamide. *Science*, **1991**, *254*, 1497.
94. Egholm, M.; Buchardt, O.; Christensen, L.; Behrens, C.; Freier, S. M.; Driver, D. A.; Berg, R. H.; Kim, S. K.; Nordon, B.; Nielsen, P. E. PNA hybridizes to complementary oligonucleotides obeying the Watson-Crick hydrogen-bonding rules. *Nature*, **1993**, *365*, 566.
95. Nielsen, P. E.; Egholm, M.; Buchardt, O. Peptide nucleic acid (PNA): A DNA mimic with a peptide backbone. *Bioconjugate Chem*. **1994**, *5*, 3.
96. (a) Nielsen, P. E.; Egholm, M. Peptide Nucleic Acids. Protocols and Applications; Horizon Press: Norfolk. **1999** (b) Ray, A.; Norden, B. Peptide nucleic acid: its medical and biotechnological applications and promise for the future. *FASEB J*. **2000**, *14*, 1041.
97. Good, L.; Nielsen, P. E. Antisense inhibition of gene expression in bacteria by PNA targeted to mRNA. *Nature (Biotechnology)*, **1998**, *16*, 355.
98. Nielsen, P. E. Applications of peptide nucleic acids. *Curr. Opin. Biotechnol*. **1999**, *10*, 71.
99. Nielsen, P. E Structural and Biological Properties of Peptide Nucleic Acid (PNA) *Pure Appl. Chem*. **1998,** *70*, 105; (b) Corey, D. R. Peptide nucleic acids: expanding the scope of nucleic acid recognition. *Trends Biotechnol*. **1997**, *15*, 224.
100. (a) Ganesh, K. N. and Nielsen, P. E. Peptide nucleic acids: Analogs and derivatives. *Curr. Org. Chem*. **2000**, *4*, 931; (b) Kumar, V. A. Structural pre-organization of peptide nucleic acids: chiral cationic analogues with five- or six-membered ring structures. *Eur. J. Org. Chem*. **2002**, 2021; (c) Kumar, V. A.; Ganesh K. N. Conformationally Constrained PNA Analogues: Structural Evolution toward DNA/RNA Binding Selectivity. *Acc. Chem. Res*. **2005**, *38*, 404;

(d) Uhlmann, E.; Breipohl, G.; Will, D. PNA: Synthetic polyamide nucleic acids with unusual binding properties. *Angew. Chem., Int. Ed. Engl*. **1998**, *37*, 2796.

101. Zhou, P.; Wang, M.; Du, L.; Fischer, G. W.; Waggoner, A.; Ly, D. H. Novel binding and efficient cellular uptake of guanidine based peptide nucleic acids. *J. Am. Chem. Soc*. **2003**, *125*, 6878.
102. (a) de Koning, M. C.; van der Marcel, G.; Overhand, M. Synthetic developments towards PNA-peptide conjugates. *Curr. Opin. Chem. Biol*. **2003**, *7*, 734; (b) Eriksson, M.; Nielsen, P. E.; Good, L. Cell permeabilization and uptake of antisense peptide nucleic acid into E. coli. *J. Biol. Chem*. **2002**, *277*, 7144.
103. Sforza, S.; Corradini, R.; Dossena, A.; Marchelli, R.; DNA binding of a D-lysine-based chiral PNA: Direction control and mismatch recognition. *Eur. J. Org. Chem*. **2000**, 2905.
104. Tomac, S.; Sarkar, M.; Ratilainen, T.; Wittung, P.; Nielsen, P. E.; Norden, B.; Graslund, A. Ionic effects on the stability and conformation of peptide nucleic acids. *J. Am. Chem. Soc*. **1996**, *118*, 5544.
105. Hyrup, B.; Egholm, M.; Nielsen, P. E.; Wittung, P.; Norden, B.; Buchardt, O. Structure activity studies of binding of modified peptide nucleic acids (PNAs) to DNA. *J. Am. Chem. Soc*. **1994**, *116*, 7964.
106. Hyrup, B.; Egholm, M.; Buchardt, O.; Nielsen, P. E. A flexible and positively charged PNA analogue with an ethylene-linker to the nucleobase: Synthesis and hybridization properties. *Bioorg. Med. Chem. Lett*. **1996**, *6*, 1083 and references therein.
107. (a)Hickman, D. T.; Tan, T. H. S.; Morral, J.; King, P. M. Cooper, M. A.; Mickelfield, J. *Org. Biomol. Chem*. **2003**, *1*, 3277; (b) Khan, A. I..; Tan T. H. S.; Micklefield, J. Stereospecific backbone methylation of pyrrolidine–amide oligonucleotide mimics (POM) *Chem. Commun*. **2006**, 1436.
108. Kumar, V. A.; Pallan, P. S.; Meena.; Ganesh, K. N. Pyrrolidine nucleic acids: DNA/PNA oligomers with 2-hydroxy/ aminomethyl-4-(thymin-1yl) pyrrolidine-N-acetic acid. *Org. Lett*. **2001**, *3*, 1269.
109. Govindaraju, T.; Kumar, V. A. Backbone Extended Pyrrolidine Peptide Nucleic Acids (bepPNA): Design, Synthesis and DNA/RNA binding Studies. *Chem. Commun.* **2005**, 495.

110. Gokhale, S. S.; Kumar, V. A. Amino/guanidino-functionalized N-(pyrrolidin-2-ethyl)glycine-based pet-PNA: Design, synthesis and binding with DNA/RNA *Org. Biomol. Chem*. **2010**, *8,* 3742.

111. (a) Vilaivan, T.; Srisuwannaket. C. Hybridization of pyrrolidinyl peptide nucleic acids and DNA: Selectivity, base-pairing specificity, and direction of binding. *Org. Lett*. **2006**, *8*, 1897; (b) Vilaivan, C.; Srisuwannaket, C.; Ananthanawat, C.; Suparpprom, C.; Kawakami, J.; Yamaguchi, Y.; Tanaka, Y.; Vilaivan, T. Pyrrolidinyl peptide nucleic acid with α/β-peptide backbone: A conformationally constrained PNA with unusual hybridization properties, *Artificial DNA: PNA & XNA*, **2011**, *2*, 50.

112. Gogoi, K.; Kumar, V. A. Chimeric (α-amino acid + nucleoside-β-amino acid)$_n$ peptide oligomers show sequence specific DNA/RNA recognition. *Chem. Commun*. **2008**, 706.

113. Vangala, M.; Kumar V. A. Design, synthesis and DNA/RNA binding studies of nucleic acids comprising stereoregular and acyclic polycarbamate backbone: polycarbamate nucleic acids (PCNA) *Org. Biomol. Chem*. **2010**, *8*, 3734.

114. Lagriffoule, P.; Wittung, P.; Eriksson, M.; Jensen, K.K.; Nordén, B.; Buchardt, O.; Nielsen, P.E. Peptide nucleic acids with a conformationally constrained chiral cyclohexyl-derived backbone. *Chem. Eur. J.* **1997**, *3*, 912.

115. (a)Brown, S. C.; Thomson, S. A.; Veal, J. M.; Davis, D. J. NMR solution structure of a peptide nucleic acid complexed with RNA *Science* **1994**, *265*, 777; (b) Ericksson, M.; Nielsen, P. E. Solution structure of a peptide nucleic acid-DNA duplex. *Nat. Struct. Biol*. **1996**, *3*, 410; (c) Betts, L., Josey, J. A., Veal, M., Jordan, S. R. A nucleic acid triple helix formed by a peptide nucleic acid-DNA complex. *Science* **1995**, *270*, 1838.

116. Govindaraju, T.; Gonnade, R. G.; Bhadbhade, M. M.; Kumar, V. A. ; Ganesh, K. N. (1S,2R/1R,2S)-2-Aminocyclohex-1-yl glycyl PNA Thymine monomers: Synthesis and Crystal Structures, *Org. Lett*. **2003**, *5*, 3013.

117. (a) Govindaraju, T.; Kumar, V. A.; Ganesh, K. N. (SR/RS)-Cyclohexanyl PNAs: Conformationally preorganized PNA analogues with unprecedented preference for duplex formation with RNA *J. Am. Chem. Soc*. **2005**, *127*, 4144; (b) Govindaraju, T.; Madhuri, V.; Kumar, V. A.; Ganesh, K. N. Cyclohexanyl peptide nucleic

acids (chPNA) for preferential RNA binding: Effective tuning of dihedral angle β in PNA for DNA/RNA discrimination. *J. Org. Chem*. **2006**, *71*, 14.

118. (a) Myers, M. C.; Witschi, M. A.; Larionova, N. V.; Franck, J. M.; Haynes, R. D.; Hara, T.; Grakowski A.; Appella, D. H. *Org. Lett*. **2003**, *5*, 2695; (b) Govindaraju, T.; Kumar, V. A.; Ganesh K. N. (1S,2R/1R,2S)-cis-Cyclopentyl PNA (cpPNA) as constrained PNA analogues: Synthesis and Evaluation of aeg-cpPNA chimera and Stereopreferences in hybridization with DNA/RNA. *J. Org. Chem*. **2004**, *69*, 5725.

119. (a) Englund, E. A.; Appella, D. H. γ-Substituted peptide nucleic acids constructed from l-lysine are a versatile scaffold for multifunctional display. *Angew. Chem. Int. Ed*. **2007**, *46*, 1414; (b) Sahu, B.; Sacui, I.; Rapireddy, S.; Zanotti, K. J.; Bahal, R.; Armitage, B. A. and Ly D. H. Synthesis and characterization of conformationally preorganized, (R)-diethylene glycol-containing γ-peptide nucleic acids with superior hybridization properties and water solubility *J. Org. Chem.* **2011**, *76*, 5614; (c) Rapireddy, S.; Bahal, R. and Ly, D. H. Strand Invasion of Mixed-Sequence, Double-Helical B-DNA by γ-Peptide Nucleic Acids Containing G-Clamp Nucleobases under Physiological Conditions. *Biochemistry* **2011**, *50*, 3913; (d) Yeh, J. I.; Shivachev, B.; Rapireddy, S.; Crawford, M. J.; Gil, R. R.; Du, S.; Madrid, M.; Ly, D. H. Crystal Structure of Chiral γPNA with Complementary DNA Strand: Insights into the stability and specificity of recognition and conformational preorganization. *J. Am. Chem. Soc*. **2010**, *132*, 10717; (e) Sahu, B., Chenna, V.; Lathrop, K.L.; Thomas, S.M.; Zon, G.; Livak, K, J.; Ly, D. H. Synthesis of Conformationally Preorganized and Cell-Permeable Guanidine-Based γ-Peptide Nucleic Acids (γGPNAs) *J. Org. Chem*., **2009**, *74*, 1509.

Chapter 2

Design and synthesis of oligonucleotide analogs with controlled backbone chirality

(Section-2.1)

Synthesis of T-$_{(\alpha\text{-amino Acid})}$-T dimers using L-Proline, D-Proline and Glycine

(Section-2.2)

Synthesis of T-$_{(D\text{-Proline})}$-U$^{2'\text{-OMe}}$ dimer and T-$_{(\alpha\text{-Amino Acid})}$-T dimers using L-Lysine, D-Lysine

(Section-2.3)

CD studies for the dimers and biophysical studies of sequences containing T-$_{(\alpha\text{-Amino Acid})}$-T and T-$_{D\text{-Proline}}$-U$^{2'OMe}$ dimers

Section 2.1 Synthesis of T-$_{(\alpha\text{-amino Acid})}$-T dimers using L-Proline, D-Proline and Glycine

2.1.1 Introduction

During the last two decades, the rational drug design approach offered by antisense oligonucleotides specifically designed to bind to mRNA has led to increased interest in this research area. The ever-increasing span of therapeutic interventions by oligonucleotides in antisense RNA,[1] siRNA,[1,2] miRNA,[3] splice correction,[4] etc. has further emphasized the need for the development of modified oligonucleotides. Natural oligonucleotides exhibit poor stability against nucleases and thus cannot be used as therapeutic agents. Therefore, modifications have been introduced to enhance the efficacy of oligonucleotides. Important goals in designing antisense compounds include increasing the binding affinity while maintaining fidelity of recognition, water solubility, cellular uptake, degradation of RNA by RNase-H enzyme and above all, easy synthetic methodologies. Also the design and synthesis should fulfill the requirement of the enantiomeric purity and integrity of the oligonucleotides. The design of phosphorothioate ONs, which is the only FDA approved antisense drug, leads to an inseparable mixture of diastereomers due to chirality at phosphorus. The other currently developing modifications include second and third generation antisense ONs such as 2'-*O*-alkyl, 2'-*O*-methylthioethyl, LNA, HeNA, Morpholino NA, PNA or PNA modifications. All these modifications exhibit excellent therapeutic properties in some way but lack some other important properties. In Chapter 1, we have discussed about these modifications. PNA is uncharged and achiral in nature and is sparingly soluble in water. Also, PNAs require assistance in the form of covalent conjugation with cell penetrating peptides (CPP)[5] or additional positive charges on PNA[6] to cross the cell membranes for their activity. Also, being achiral, PNA binds to DNA/RNA in parallel or antiparallel orientation with almost equal strength. The replacement of the internucleoside phosphate linkages by the robust amide bond as in PNA could be an alternate solution so that the advantages of chirality and 3'-5' directionality of the sugar can be maintained in the analogue along with the nuclease stability of the amide bond. Several four- and five-atom amide-linked oligonucleotide analogues are known in the literature, most of which are discussed in Chapter 1. The five-atom amide linkers were introduced to compensate the shorter amide bond in the dinucleoside as compared with

the four-atom phosphate linkers to maintain the internucleoside distance complementarity. The strategy was found to be successful as some of the five-atom-linked dimers when substituted in ON sequences lead to significantly higher RNA affinities compared with that of the native DNA. It has been shown by CD spectroscopy and crystal structure that the longer amide backbones do not disrupt the duplex geometries.[7]

In this section we describe the design and synthesis of the thyminyl dimer blocks (TT) having 5-atom chiral acetamido internucleoside linkage amenable for their incorporation in chimeric DNA, characterization of dimers using 2D NMR techniques, sugar puckering and *cis/trans* isomerism in dimers.

2.1.2 Rationale, Design and Objectives of the Present Work

Natural oligonucleotides (ON) with phosphodiester linkage are susceptible for hydrolysis with various enzymes like nucleases and this limits their use for various biological applications. The partial replacement of the DNA/RNA phosphodiester linker by five-atom amide linkers has been found to be very useful for RNA recognition. The chirality of the internucleoside linker such as prochiral natural phosphate, *Rp* and *Sp* chiral phosphorothioate (PS)[8] or *R*/*S* amides[7a] is known to exert large effects on the binding efficiency of the oligomers.

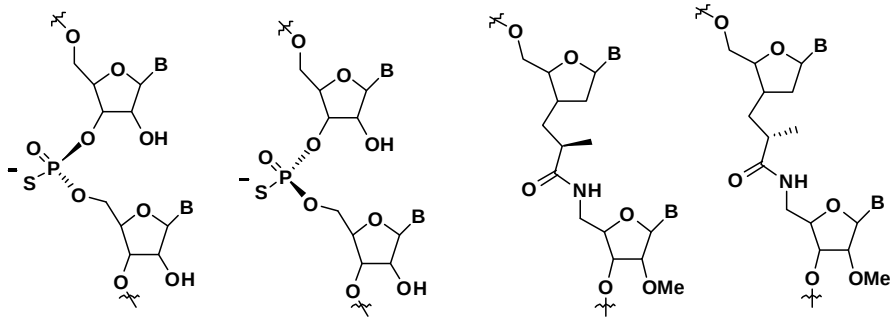

Figure 1. Chiral phosphorothioate-(I and II) and amide- (III and IV) linked ONs

ORNs (oligoribonucleotides) having all-(*Rp*)-PO/PS alternating backbone had higher affinity for complementary RNA, whereas all-(*Sp*)-PO/PS oligomers had similar or lower affinity.[9] A fully modified backbone consisting of (*R*p)-PS-linkages (Figure 1, I) slightly stabilizes a PS-ORN:ORN duplex, whereas a backbone consisting of (*S*p)-PS-

linkages (Figure 1, II) or stereorandom PS-linkages exert large destabilizing effect on the duplex.[8e] Pallan *et al*.[7a] carried out a systematic study for RNA binding affinity of modified oligonucleotides with five atom amide linked DNA analogues. They also studied the effect of configuration of the stereocenter in the amide linkage.[7a] The linkers with opposite stereochemistry at the chiral center stabilize duplexes between the modified DNA and RNA to different degrees. The amide linker with *R* stereochemistry at methyl group was found to be more favourable for RNA-DNA duplex stability than corresponding *S* configured backbone modification (Figure 1, III and IV).

Some five-atom amide-linked oligonucleotides (Figure 2, I and II) were reported by our group where thioacetamido backbone (TANA) was found to show discrimination in binding affinity towards DNA/RNA.[10] The thioacetamido (TANA, 3'-ribo configuration in 3'-amino substituted sugar) modified sequences showed better binding affinity towards RNA, whereas *iso*-TANA (3' xylo configuration in 3'-amino substituted sugar) showed preference for DNA binding. Thus RNA selectivity of binding of TANA-modified oligomers was reversed to DNA binding selectivity by the change in configuration at the 3'-amino-substituted sugar. An amino acid backbone extended DNA modification was also reported by our group where natural α-amino acids were used alternately with thyminyl β-amino acid derived from thymidine (Figure 2, III).[11] Thyminyl homo-oligomers specifically recognized both deoxy- and ribo-oligoadenylates in triplex mode.

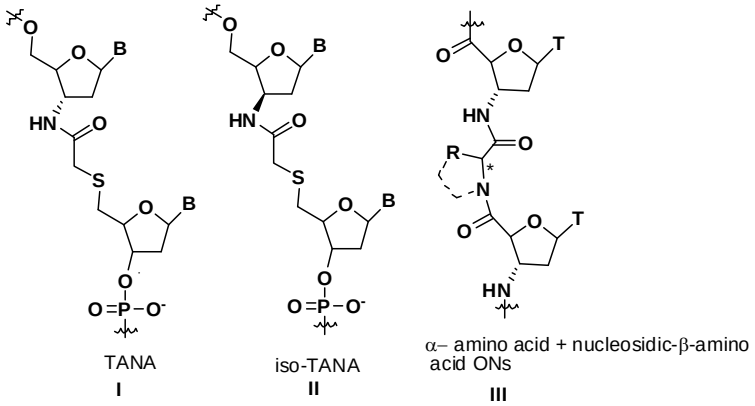

Figure 2. Five atom linked amide modification in DNA

Introduction of chirality and cyclic structures in the PNA backbone are known to reduce possible conformational states of acyclic, achiral single stranded PNAs.[12] The cyclic pyrrolidinyl based 2*S*, 4*S*-pyrrolidinyl-PNA (bepPNA) with extended backbone

(Figure 3, I) have been previously reported in our laboratory to bind sequence-specifically only to RNA.[13] A recently reported *N*-(pyrrolidin-2-ethyl) glycine-based PNA (pet-PNA) backbone, with 4-amino- or 4-guanidino-functionalized pyrrolidine ring oligomers recognized the target DNA and RNA sequences with increased sequence specificity[14] (Figure 3, II).

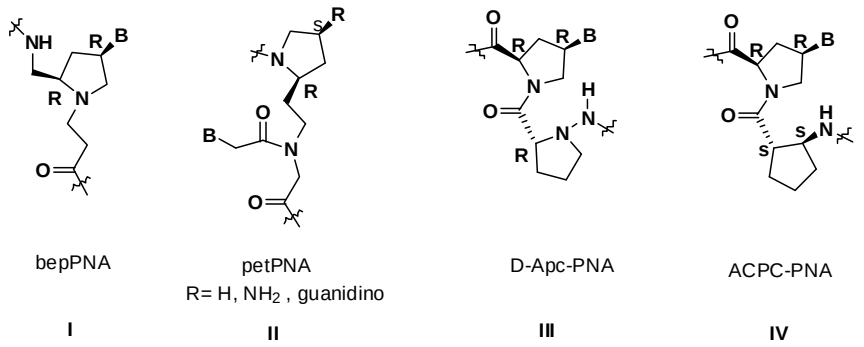

Figure 3. Pyrrolidinyl based chiral PNA modifications

Vilaivan and co-workers have developed a conformationally constrained chiral analogs of PNA based on the pyrrolidinyl PNA derived from alternating 4'*R*-thymin-1-ylpyrrolidine-2'*R*-carboxylic acid (nucleobases-modified D-proline) and aminopyrrolidine -2R-carboxylic acid (Figure 3, III). This modification showed preferential binding affinity for complementary DNA over RNA.[15] Also they have developed new conformationally constrained pyrrolidinyl PNA systems (Figure 3, IV, ACPC-PNA) based on an alternating nucleobase-subtituted proline and 2-aminocyclopentanecarboxylic acid backbone. The ACPC-PNA system with (2'*R*, 4'*R*)-proline/(1*S*, 2*S*)-2-aminocyclopentanecarboxylic acid backbone binds to DNA only in antiparallel orientation with exceptionally high affinity and sequence specificity following the Watson-Crick base pairing rules.[16]

Design of oligonucleotide analogs with controlled backbone chirality

Considering the importance of replacement of the phosphate group with a 5-atom linker and also the chirality at the phosphorus, a chiral amino-acetamido linker was proposed (Figure 4). One novel aspect of our approach is that an amino acid is used as the internucleoside linker. The amino acid linker motif was chosen based on chemical stability and chirality. Consequently the nucleic acid-amino acid conjugate could be converted to dimer blocks. To study structural differences that L- or D-amino

acids in the backbone would assert on the geometry of the derived oligomers we have replaced phosphodiester linkages partially with chiral amide dimer units. For this purpose, T-(amino acid)-T dimers are the simplest units where such effects can be investigated. This section presents the synthesis of T-(amino acid)-T dimer blocks with L-proline (Ia)/D-proline (Ib) and prochiral glycine units (Ic) [Figure 4]. L/D-Prolines were chosen because they would be devoid of an amide N–H and hence remove the influence of possible hydrogen bonds on the overall structural features.

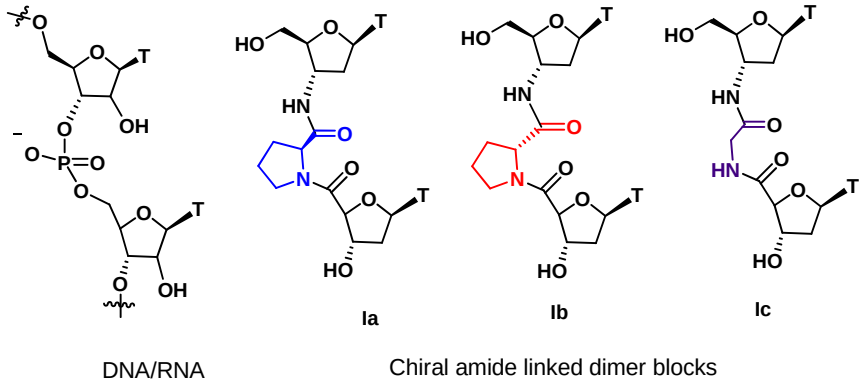

Figure 4. Structure of DNA/RNA and chiral amide linked dimers

The objectives of this section are

1. Synthesis of T-$_{(\alpha\text{-amino acid})}$-T dimer units and conversion to their phosphoramidite derivatives.
2. Characterization of dimers using 2D NMR techniques
3. Study of sugar puckering and *cis-trans* isomerism in dimers.

Section 3 of this chapter will discuss the CD of dimers and biophysical studies of the derived oligomers.

2.1.3 Methodology, Results and Discussion

Retrosynthetic analysis of the phosphoroamidite dimer building block depicted in Figure 5 shows that the T-(α-amino acid)-T dimer building blocks can be synthesized starting from 3'-azido thymidine, suitably protected α-amino acid and thymidine. The dimer blocks can easily be created by the coupling between the the 3'-amino nucleoside with α-amino acid and followed by coupling between α-amino acid and thymidine-4'-carboxylic acid derived from thymidine.

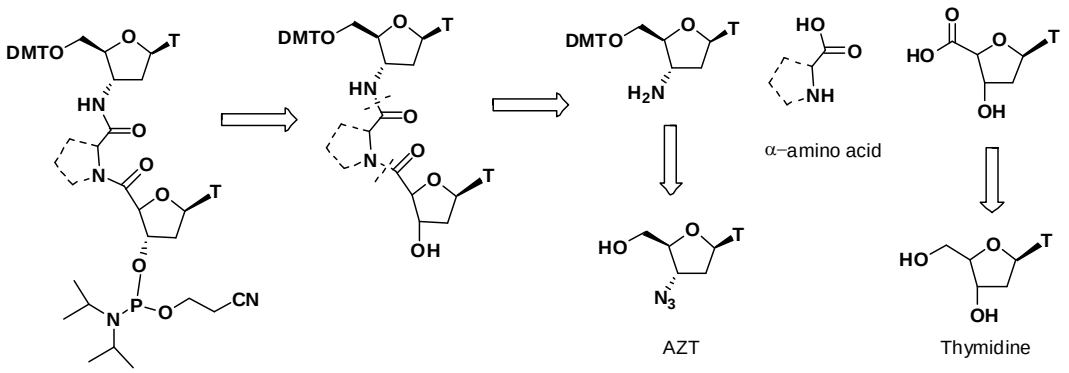

Figure 5. Retrosynthetic pathway for synthesis of chiral amide linked dimer blocks**.**

2.1.3a Synthesis of Amine component

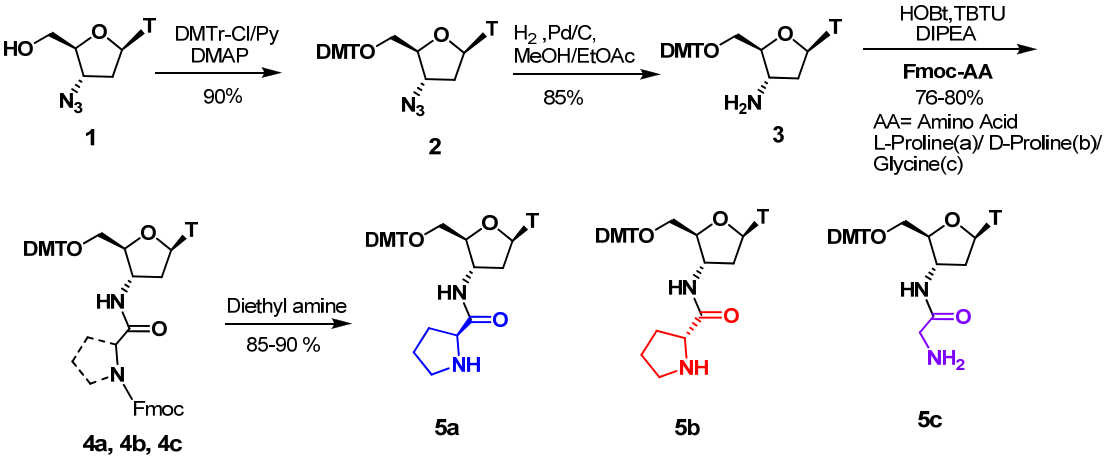

Scheme 1. Synthesis of amine component

The amine component was synthesized starting from 3'-azido thymidine (AZT) as shown in scheme 1. Azido thymidine was synthesized in the laboratory starting from thymidine by following reported procedures.[17] Protection of the 5'-hydroxy group in AZT **1** as its 5'-*O*-DMTr derivative was carried out, followed by reduction of the 3'-azide to amine by catalytic hydrogenation using Pd-C in methanol: ethyl acetate (1:1) to give **3**. Peptide coupling of **3** with Fmoc-protected α-amino acids L-Proline (a), D-Proline (b) and glycine (c) yielded **4a**, **4b**, **4c** respectively using HBTU/ HOBt as coupling reagent and DIPEA as base in acetonitrile: DMF mixture. The Fmoc function was removed using relatively volatile diethyl amine (50% DEA in DCM), in lieu of piperidine in DMF. The deprotection as monitored by TLC was found to complete in about 45 mins. Isolation of intermediate products **5a**, **5b** and **5c** with free amino group

was obtained by simple precipitation using petroleum ether and used in the next coupling step without further purification.

2.1.3b Synthesis of Acid component

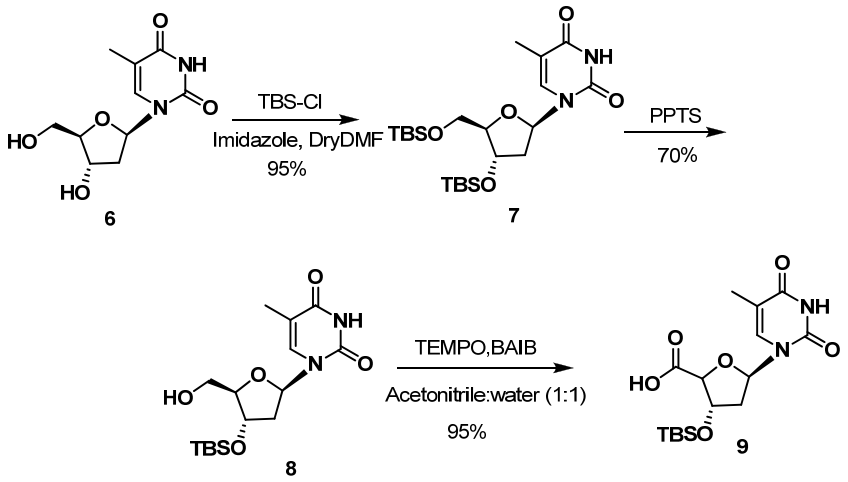

Scheme 2. Synthesis of acid component

Synthesis of acid component **9**[18] was accomplished starting from commercially available thymidine using reported procedure with minor changes in the experimental procedures. Both 3'and 5' hydroxyl group of thymidine were protected as their silyl derivative to get disilylated thymidine **7**. The 5'-silyl ether was selectively deprotected using pyridinium *p*-toluenesufonate (PPTS). PPTS was prepared according to literature procedure.[19] PPTS is weakly acidic and deprotects less hindered silyl groups easily. J. Zhang *et al.* reported the oxidation of 3'-*O*-silylthymidine using sodium persulphate and ruthenium trichloride in 1N NaOH solution and obtained product **9** in 50% yield.[20] We used highly selective, mild and efficient N-oxoammonium salt-based oxidation protocol,[21] where a catalytic amount of 2,2,6,6-tetramethyl-1-piperidinyloxyl (TEMPO) and [Bis(acetoxy)iodo]benzene was used for oxidation of 3'-*O*-silylthymidine. The active oxidant is an *N*-oxoammonium salt generated by dismutation of TEMPO; BAIB is necessary to regenerate TEMPO by oxidizing the corresponding hydroxylamine of TEMPO. 3'-*O*-silylthymidine **8** was easily converted to the corresponding acid **9** under TEMPO-BAIB oxidation conditions and the product was recovered by trituration with ether and acetone. The formation of the product was confirmed by disappearance of the peaks due to the 5' and 5'' protons in the ^{1}H NMR spectra.

2.1.3c. Synthesis of T-$_{(\alpha\text{-amino acid})}$-T dimers

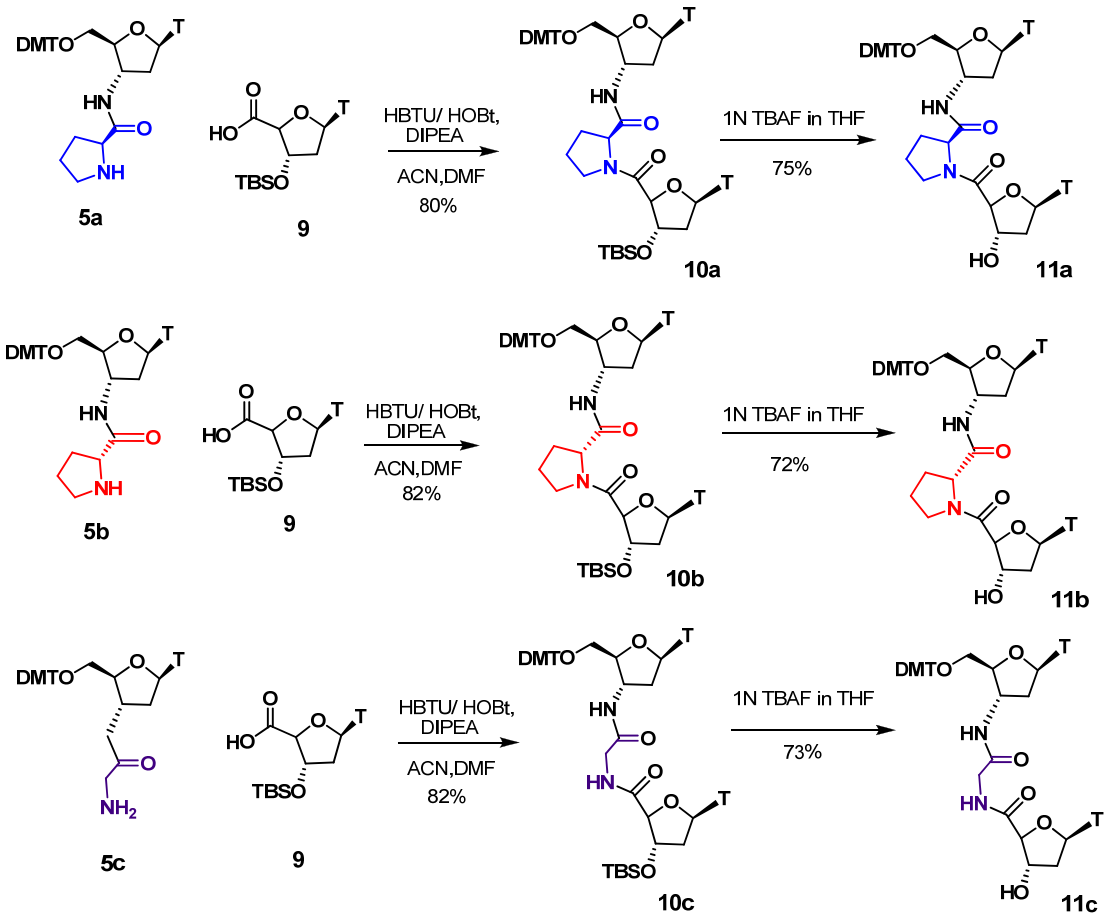

Scheme 3. Synthesis of protected T-(α-amino acid)-T dimer blocks

Synthesis of the dimer building blocks **10a, 10b and 10c** was then achieved by using peptide coupling chemistry starting from the amine **(5a, 5b and 5c)** and thymidine 4'- carboxylic acid **9**, using HBTU/ HOBt as coupling reagents and DIPEA as base in acetonitrile: DMF mixture (Scheme 3). Formation of the product was confirmed by ^{1}H NMR as well as mass spectroscopy. The desilylation of the 3'-*O*-TBS group of **10a, 10b and 10c** by using TBAF in THF gave the desilylated dimers **11a, 11b and 11c** having L-Proline, D-Proline and glycine in the internucleoside amide linkage respectively**.**

2.1.3d Synthesis of T-$_{(\alpha\text{-amino acid})}$-T phosphoramidites derivatives

Phosphitylation of the 3'-OH of **11a, 11b** and **11c** were done using the reagent N,N'-diisopropylcyanoethyl chlorophosphine and base diisopropyl ethyl amine and DCM as the solvent to give the phosphoramidites **12a, 12b** and **12c** (Scheme 4). The formation of the product was confirmed by ^{31}P NMR spectroscopy.

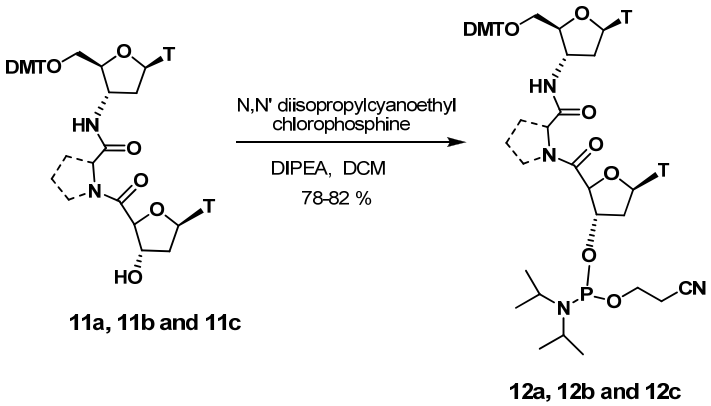

Scheme 4. Synthesis of T-$_{(\alpha\text{-amino acid})}$-T phosphoramidite derivative

2.1.4 Assignments of ^{1}H NMR of T-$_{(\alpha\text{-amino acid})}$-T dimer blocks with free 5', 3'-OH group

In order to undertake NMR and CD studies to study base-stacking interactions in aqueous medium, the 5', 3'-OH free dinucleotide (**Ia, Ib** and **Ic**) was obtained by deprotection of 5'-ODMT group of dimers **11a**, **11b** and **11c** respectively. The deprotection was done using 3% dichloroacetic acid in DCM using triethyl silane as the scavenger (Scheme 5). The free dinucleosides **Ia**, **Ib** and **Ic** formed were purified by successive trituration of the crude product with diethyl ether.

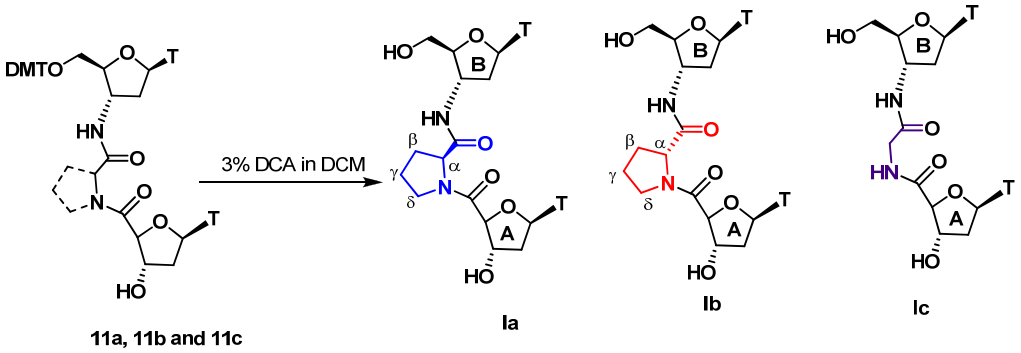

Scheme 5. Synthesis of 5', 3'-OH free T-(α-amino acid)-T dimer blocks

The ^{1}H NMR spectra were recorded using D_2O as the solvent. All the peaks were found to be well resolved for the 5', 3'-OH free dinucleoside. The 1D ^{1}H NMR spectra of dimers **Ia**, **Ib** and **Ic** were fully assigned with the aid of 2D COSY, 2D NOESY experiments and chemical shift values are reported in Table 1.

Table 1. ^{1}H Chemical shifts of dimers **Ia**, **Ib** and **Ic**

Entry	Sugar	H1'	H2'	H2''	H3'	H4'	H5'	H5''	H6	CH3	α Pro-CH	β Pro-CH_2	γ pro-CH_2	δ Pro-CH_2	Gly-CH_2
Ia	Ring A	6.4.	2.1	2.3	4.7	4.8	--	--	8.0	1.8	--	--	--	--	
	Ring B	6.2	2.5	2.4	4.4	3.9	3.7	3.8	7.6	1.8	4.4	2.1(1H) 1.8(1H)	2.02	3.7(1H) 3.6(1H)	
Ib	Ring A	6.4	2.2	2.3	4.7	4.8	--	--	8.1	1.8	--	--	--	--	
	Ring B	6.2	2.5	2.4	4.5	4.0	3.7	3.8	7.7	1.8	4.3	2.2(1H) 1.9(1H)	2.05	3.8(1H) 3.6(1H)	
Ic	Ring A	6.3	2.3	2.4	4.7	4.4	--	--	7.7	1.8					
	Ring B	6.1	2.3	2.4	4.4	3.9	3.7	3.8	7.6	1.8					3.8

H5'/H5" protons were assigned according to the Remin and Shugar rule[22] where the lower field proton is assigned as H5' while the higher field protons are assigned as the H5''. The discrimination between 2' and 2'' proton was made using the rules devised by Altona *et al*.[23] The chemical shift positions for H3' and H4' proton for thymidine-4'-carboxylic acid **9** component were determined from 2D COSY experiment (Figure 8). The H4' proton appeared as a broad singlet, possibly due to weak coupling with the H3' proton and H3' proton showed cross peak with H2' proton (Figure 8). The 5'- and 3'-terminal deoxyribose rings in the dimers were assigned by COSY experiments and distinguished by absence of 5' and 5'' protons in the 3' terminal sugar. This sugar also showed noticeable downfield shift of H3' and H4' proton. In case of dimers **Ia** and **Ib**, the H4' proton signal merged with the D_2O peak (Figure 10 and 13). Due to proline CH_2 groups resonance mixed with both 5'5'' and 2'2'' protons resonance, it was not possible to derive all the coupling constants due to spectral complexity and overlap. The two protons attached to β carbon (diasterotopic protons) and on δ carbon which is attached to tricoordinate nitrogen in proline rings showed different chemical shifts (Figure 10 and 13).

2.14a Conformation about the glycosidic bond

The bond joining the 1'-carbon of the sugar ring to the heterocyclic base is the *glycosidic* bond. Rotation about this bond gives rise to *syn* and *anti* conformations[24] (Figure 6). Rotation about this bond is restricted and the *anti* conformation is generally favoured, partly on steric grounds. The *anti* conformer has the smaller H6 (Py) or H-8 (Pu) atom above the sugar ring while the *syn* conformer has the larger O-2 (Py) or N-3 (Pu) in that position.

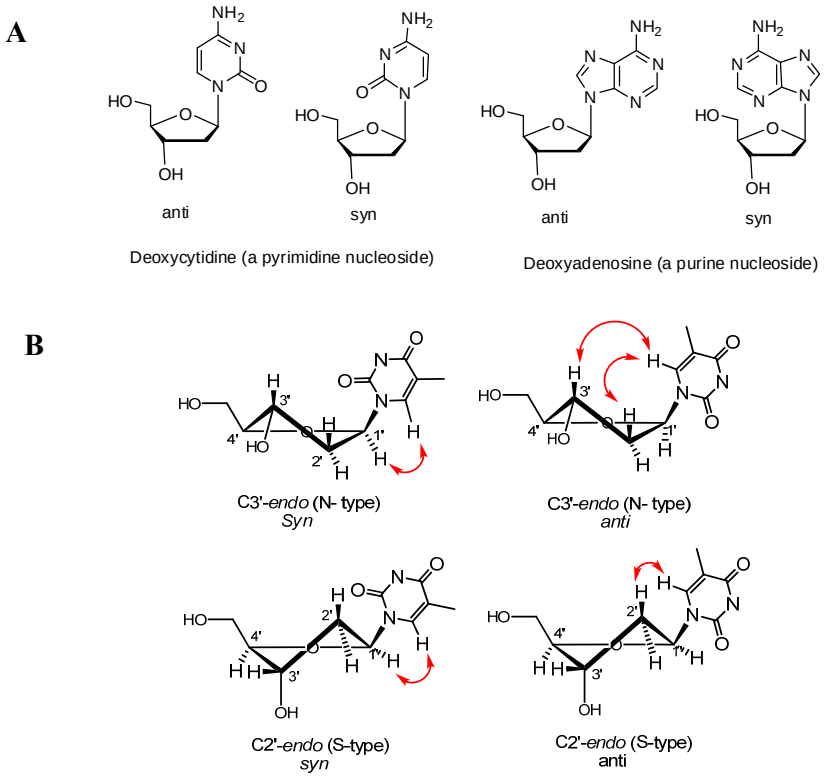

Figure 6. (A) Structure of *syn* and *anti* nucleoside conformation and (B) N-type and S type conformers showing major nOe cross peaks

The conformation about the glycosidic bond in the dimers was determined from 2D NOESY experiments. An *anti* conformation is preferred when a strong nOe between H6 of thymidine (H8 of adenosine) and H2'or H3'of the sugar ring is observed while a strong nOe between H6/H8 and H1' reveals a preferred *syn* conformation. In case of comparable nOe strength between H6 /H1' and H6/H2' or H3' a preferred *syn* conformation is attributed because of the fact that the minimum possible distance to H1' to H6/H8 is greater than H2' or H3' to H6/H8.[25] A nucleotide with an S-type sugar is in *anti* conformation when a strong nOe between H6 and H2' is observed while a

nucleotide with an N-type sugar has an *anti* conformation when a strong nOe between H6 and H3' is observed.[26]

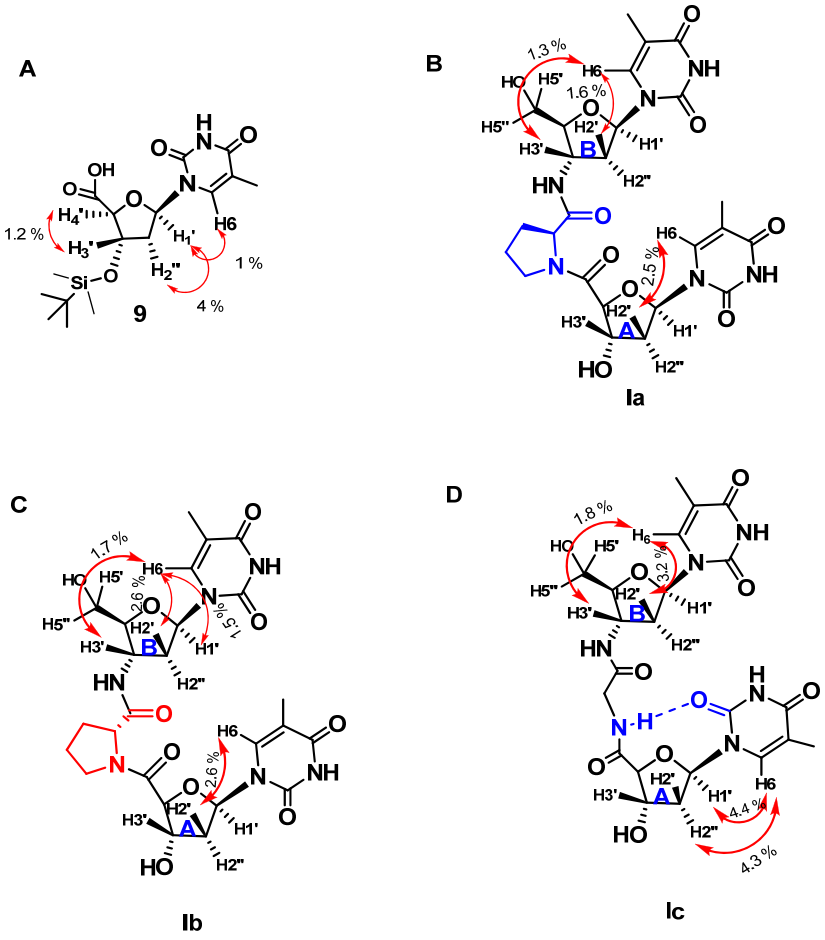

Figure 7. Schematic representation of some of the long range NOE's seen in 2D NOESY spectrum of compound **9** and dimers **Ia, Ib and Ic**

Schematic representation of some of the long range nOe's seen in 2D NOESY spectrum of compound **9** and dimers **Ia**, **Ib** and **Ic** is depicted in Figure 7. In thymidine -4'-carboxylic acid **9**, strong nOe cross peak between H6 and H1' (1 %) and absence of H6 and H3' indicates *syn* conformation of the nucleobase (Figure 9b). Also we have observed nOe cross peaks between the H3' and H4' protons with the methyl group of silyl protecting group of 3' hydroxyl group (Figure 9b). In L-proline containing dimer **Ia**, there are strong nOe cross peaks between H6 with H2' (1.6 %) and H3' (1.3 %) in the 5' terminal sugar (ring B) and strong nOe H6 with H2' (2.5 %) in the 3' terminal sugar (ring A), indicating *anti* glycosidic conformation (Figure 12). In D-proline containing dimer **Ib**, there are strong nOe cross peaks between H6 with H2' (2.6%), H3'

(1.7%) and H6 and H1' (1.5%) in 5' terminal sugar (ring B) indicates both glycosidic conformation with more population of *anti* conformation (Figure 15). In the 3' terminal sugar ring strong nOe between H6 with H2' (2.6%) indicates *anti* glycosidic conformation of thymine (Figure 15).

In glycine containing dimer **Ic,** nOe cross peaks between H6-H3' (1.8 %) and H6-H2' (3.2 %) were observed only in the 5'-end sugar (ring B) which indicate the *anti* glycosidic conformation, whereas in the 3' terminal sugar (ring A) strong nOe between H6-H1'(4.4 %) and H6-H2'' (4.3%) seems to indicate *syn* conformation of thymine as seen in its constituent acid constituent **9** (Figure 18, D). The reason for this could be the possibility of hydrogen bonding between the C2 carbonyl of thymine and the hydrogen atom of the NH-amide bond of the 3' terminal A ring, which restricted the rotation of the glycosidic bond in *syn* conformation (figure 18, D). However absence of such possible hydrogen bonding in proline containing dimer **Ia** and **Ib**, probably allows *anti* conformation of glycosidic bond.

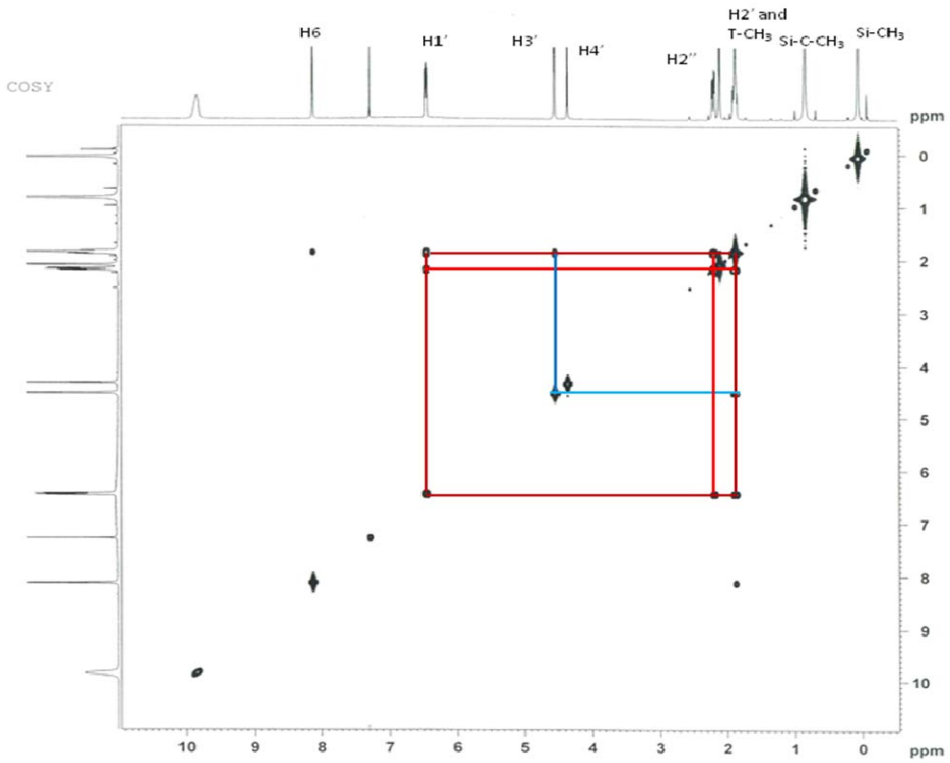

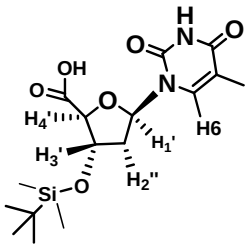

9

Figure 8. Full COSY spectra of compound **9**

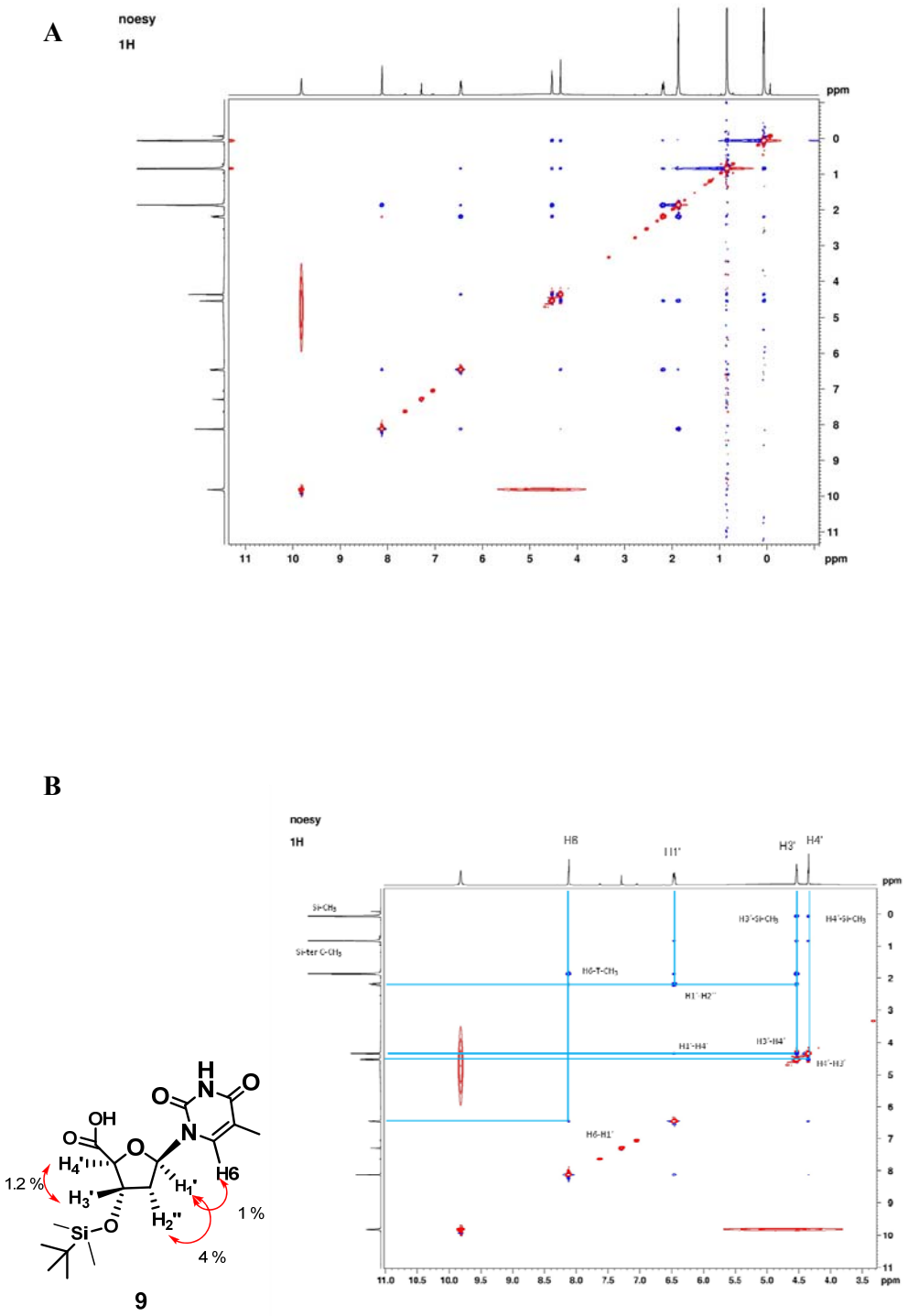

Figure 9. (A) Full NOESY and (B) expanded NOESY NMR spectra of compound **9**

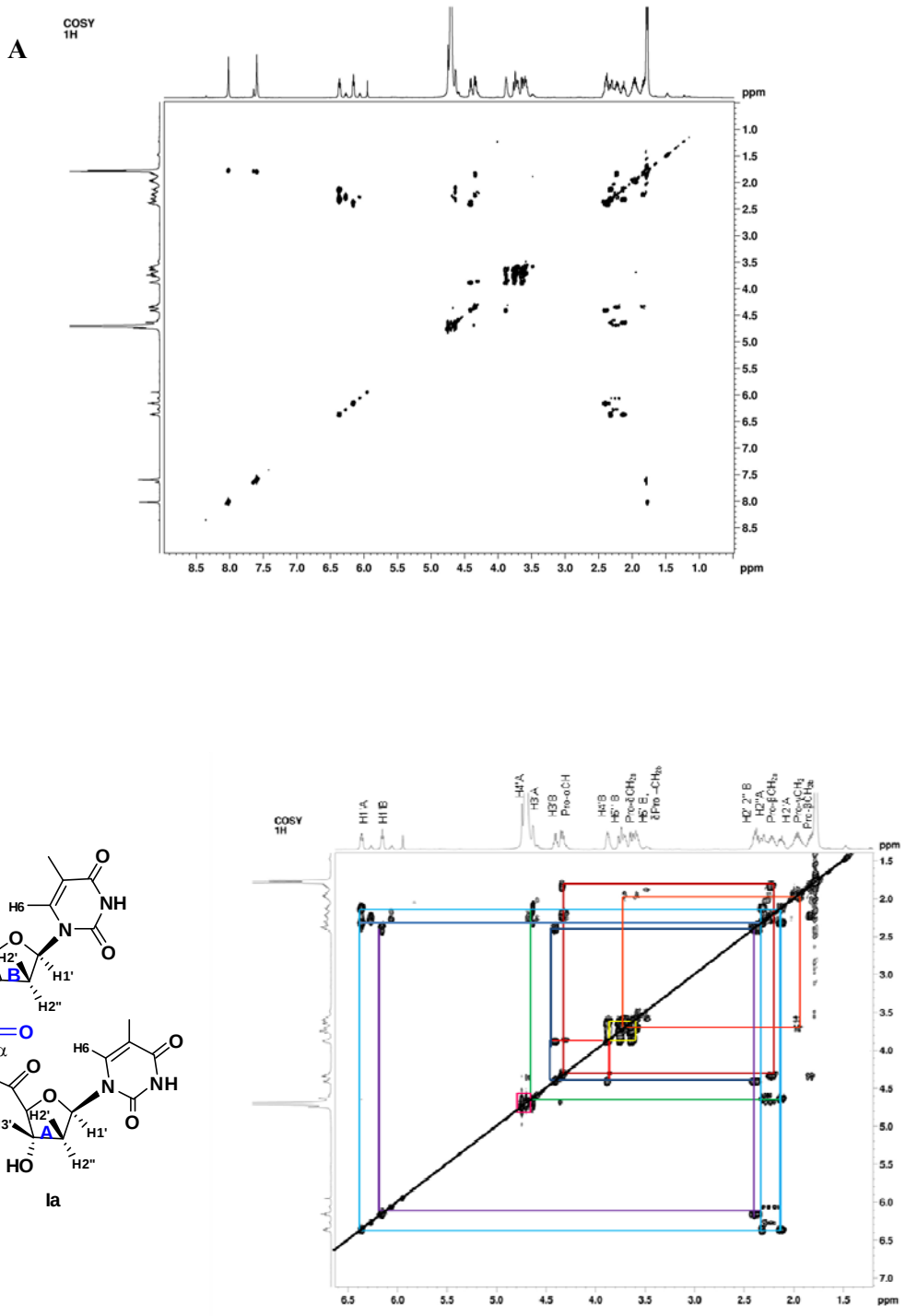

Figure 10. Full COSY and expanded assigned COSY spectra of dimer **Ia**

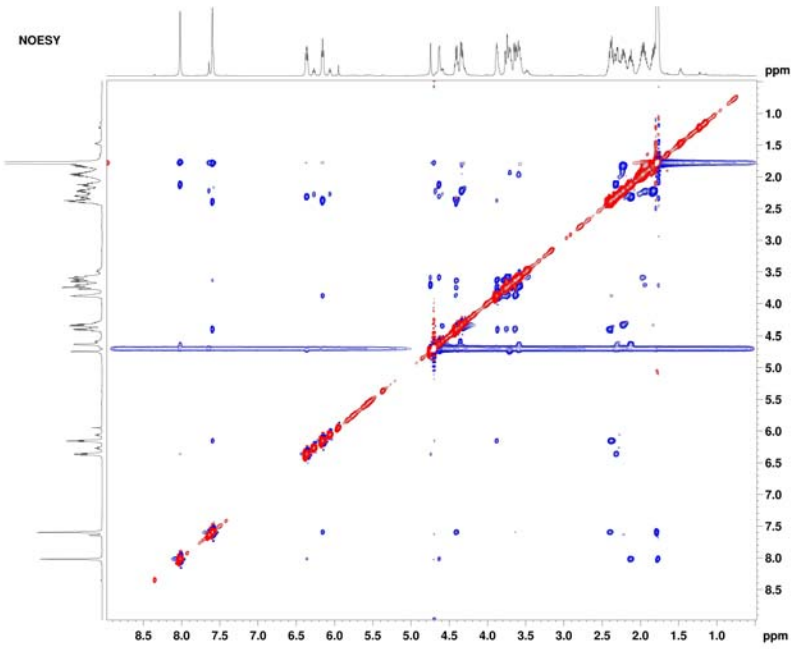

Figure 11. NOESY spectra of dimer **Ia**

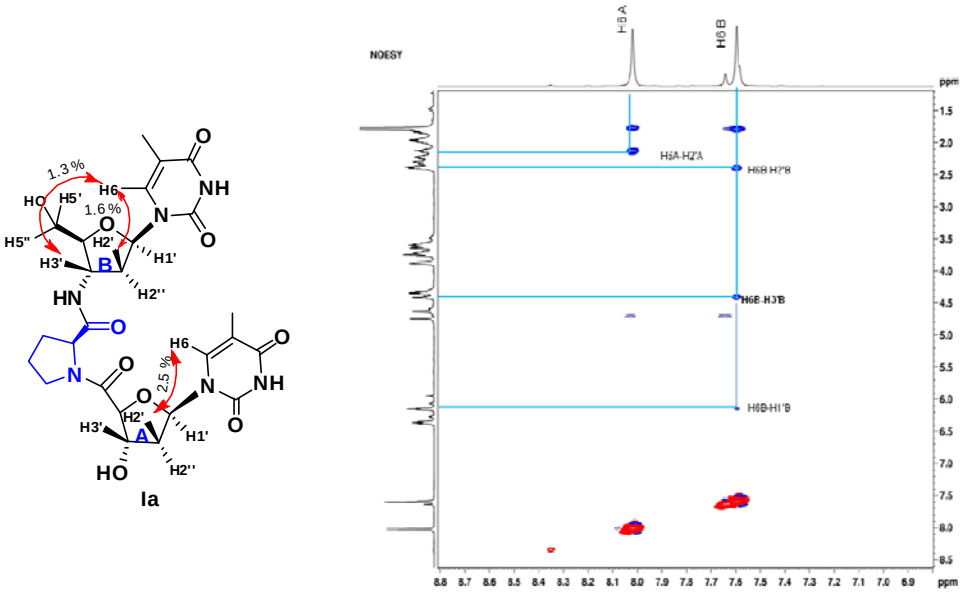

Figure 12. NOESY spectra of dimer **Ia**. The nOe cross peaks between H6-H3', H6-H2' in B- ring and H6-H2' in A-ring indicate *anti* conformation of nucleobase.

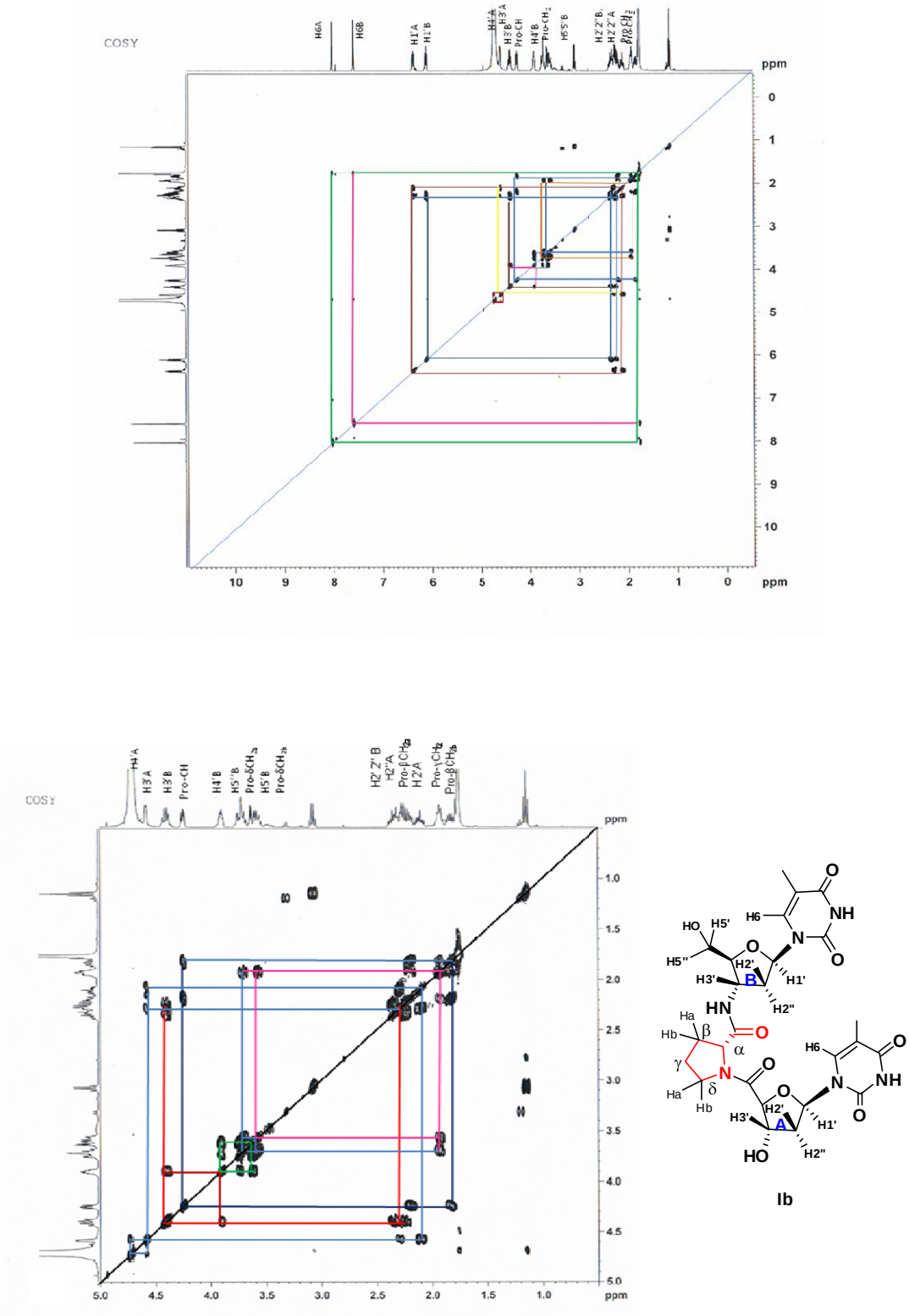

Figure 13. Fully assigned COSY spectra and expanded COSY spectra of dimer **Ib.**

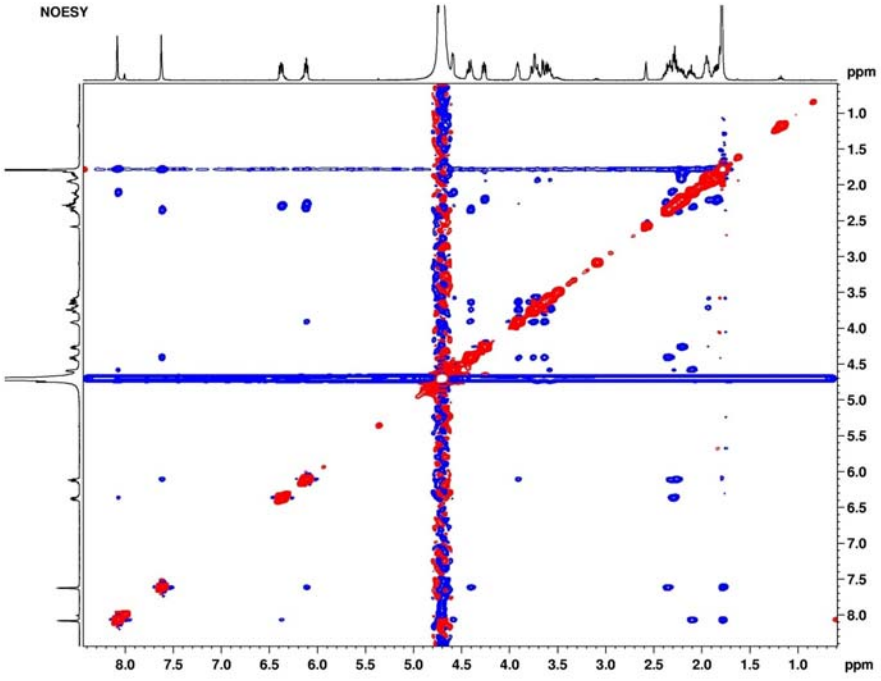

Figure 14. NOESY spectra of dimer **Ib**

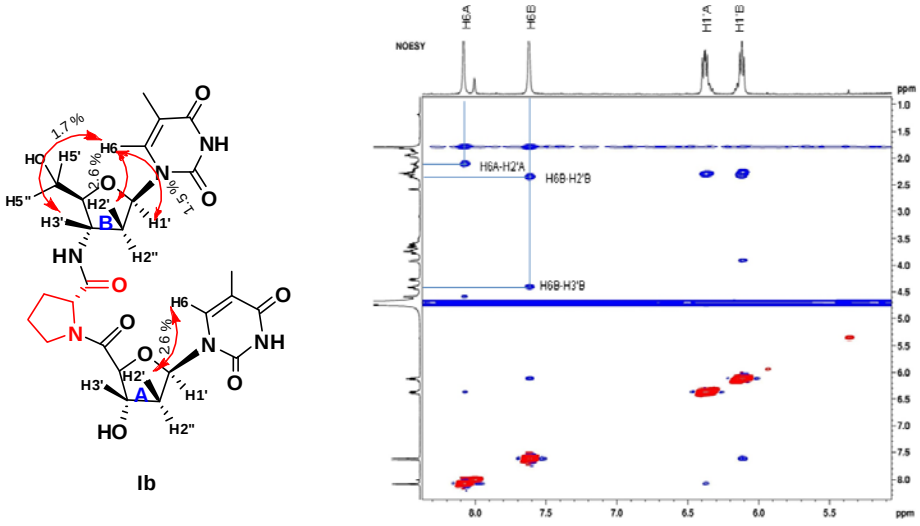

Figure 15. NOESY spectra of dimer **Ib**. The nOe cross peaks between H6-H3', H6-H2' in B- ring and H6-H2' in A-ring indicate *anti* conformation of nucleobase.

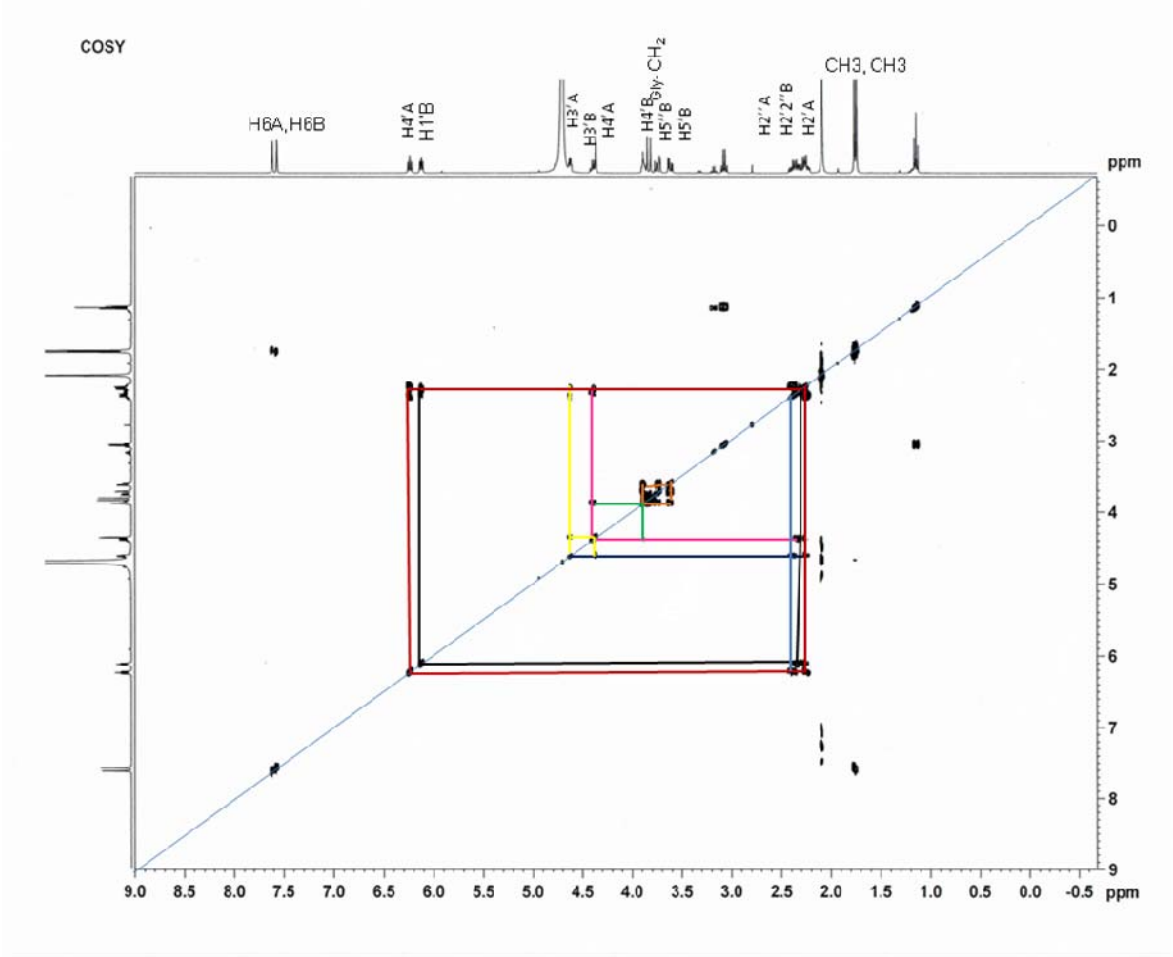

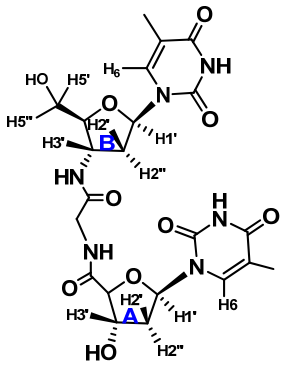

Ic

Figure 16. Fully assigned COSY spectra of dimer **Ic.**

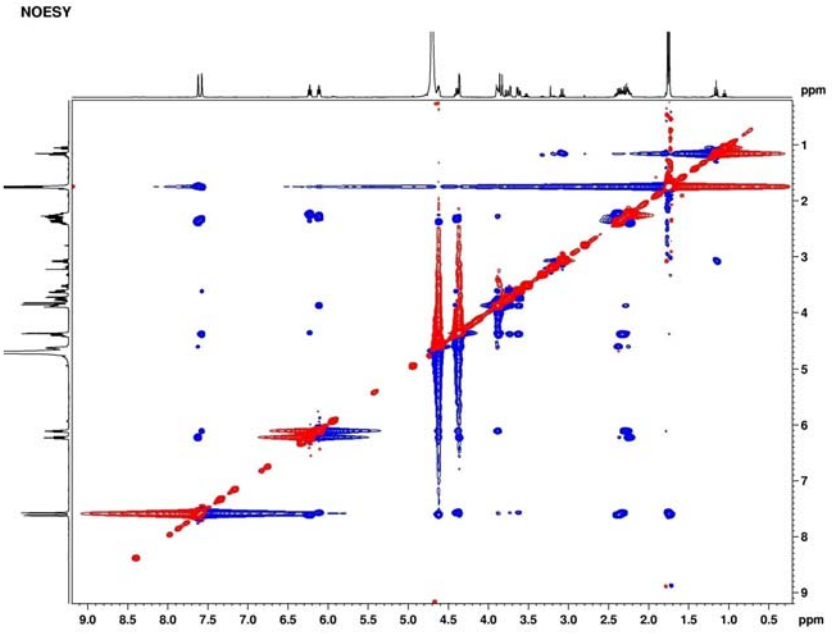

Figure 17. NOESY spectra of dimer **Ic**

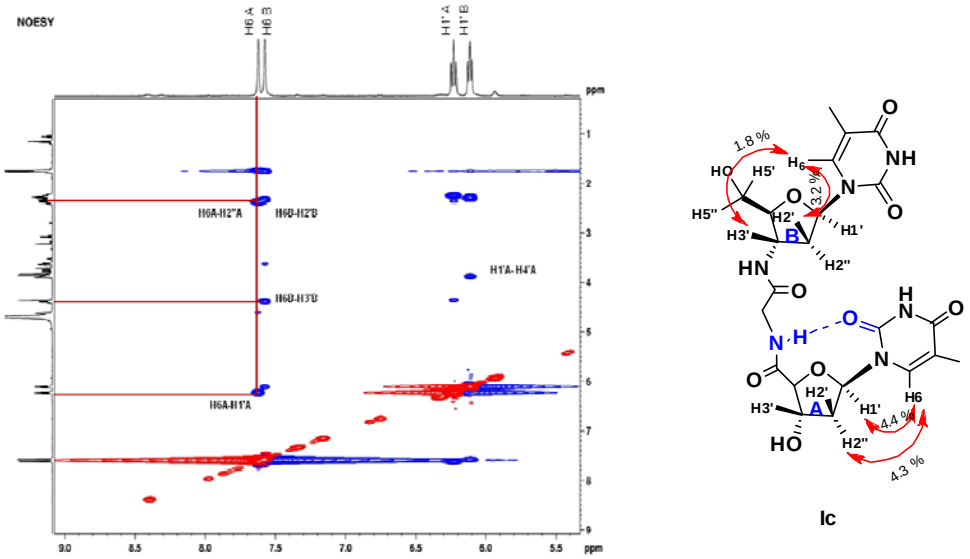

Figure 18. Expanded NOESY spectra of dimer **Ic**. The nOe cross peaks between H6-H3', H6-H2' in B- ring indicates *anti* conformation of nucleobase whereas in A-ring H6-H2'' and H6-H1' indicate *syn* conformation of nucleobase

2.1.5 Conformation of the sugar ring

In natural nucleic acids, the pentose sugars are puckered or twisted to give preferred helical conformations. These pentose sugar moieties are puckered in order to minimize non bonded interactions between their substituents. This puckering is described by identifying the major displacement of carbon C-2' and C-3' from the median plane of *C*1'-*O*4'-*C*-4'. The detailed study of X-ray crystal structures of nucleosides and nucleotides revealed that ribo and deoxyribofuranosyl moieties occur preferentially within two distinct major conformations namely north (C-3' *endo*) and south (C-2' *endo*)[27] [Figure 19]. In solution, N-type and S-type conformations are in rapid equilibrium and are separated by a low energy barrier.

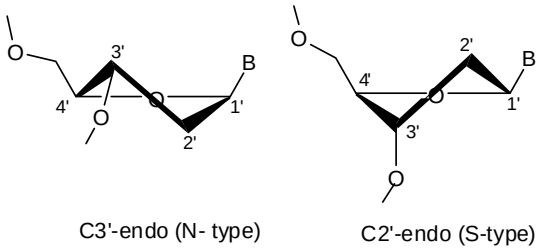

Figure 19. N-type and S-type sugar puckering

The conformation of pentofuranose can be fully described in terms of the phase of pseudorotation (*P*), and puckering amplitude (ν_{max}).[28] For North-type (N) sugars (C3'-endo, C2'-exo), *P* ranges from -1° to 34° and for S-type (S) sugar (C2'-endo, C3'-exo), P ranges from 137°- 194°. The mole fraction of N and S conformers as well as their geometry, expressed by their phase angle of pseudorotation P_N and P_S and puckering amplitude ψ_N and ψ_S, can be calculated from vicinal proton-proton ($^3J_{HH}$) coupling constants $J_{1'-2'}$, $J_{1'-2''}$, $J_{2'-3'}$, $J_{2''-3'}$, $J_{3'-4'}$. These coupling constants can be used as input for pseudorotation analysis of the sugar using PSEUROT.[29] PSEUROT program cannot be used in some cases where it is not possible to get the coupling constants accurately over a range of different temperatures due to spectral overlap.

Alternatively, a semi-empirical method termed as "Sum Rule"[23] can also be employed to have some idea about N↔S equilibrium in the case of sugar conformations. This method was employed in the present work to calculate the conformational preference of pentofuranose moieties of chiral amide linked dimers and

starting material 3'-amino and 4'-carboxalic synthons. The empirical equation to calculate the percentage of S conformer is as below :

$$\% S = (\Sigma H1'\text{-}9.8)/5.9x100 \text{ where } \Sigma H1' = J_{1'2'} + J_{1'2''}$$

The nature of the 3'-α- substituents has an influence on the conformation of the sugar ring. Upon substitution of the 3'-oxygen by a 3'- amine group, the N↔S equilibrium is shifted toward more population of the N-type pseudorotamer (Figure 20 A). This effect is also noticeable when the phosphate functionality is replaced by a sulfonamide functionality, pushing the pseudorotamer equilibrium towards less population of N-type pseudorotamer. This may be partly explained by the *gauche* effect which means that the favored adopted structure could be the one in which the O4' and 3'-α-substituents are in a *gauche* orientation. In S-type 2'-deoxysugars, the O4' and 3'-α substituents are in a *gauche* orientation, and the preference in such cases is for S conformation. The higher electronegativity of oxygen versus nitrogen leads to a greater preference for a X3'-C3'-C4'-O4' *gauche* orientation leading to greater propensity for S-type pucker. The *gauche* effect increases with the higher polarization of the C3'-X bond and therefore the % S increases with the increased electronegativity of the 3'-substituent and vice versa.

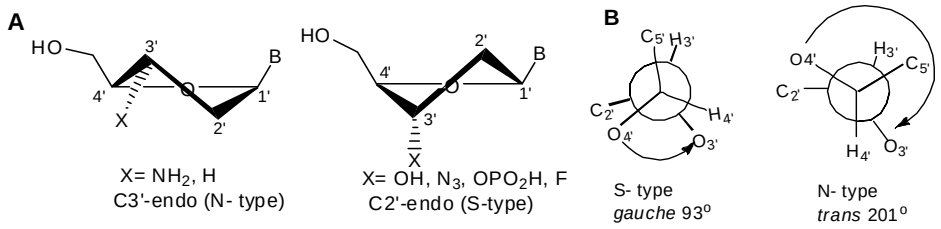

Figure 20. (A) Effect of 3'- substituent on sugar ring conformation and (B) Newman projection for S-type and N-type conformation

The changes in sugar pucker mainly affect the backbone torsion angle δ, which on average is ~80º in A-form duplex and ~120º in B-form duplex.[30] The DNA:DNA duplex is an extended B-form structure whereas RNA:RNA duplex remains in compact A-form, further stabilized by increased base-stacking of axially oriented nucleobases. The relatively low conformational energy barriers of the deoxyribose sugar render flexibility to the 2'-deoxyribose sugar to adopt 3'-*endo* (or O4'-*endo*) conformations in the DNA strand and allow DNA: RNA duplexes also to be in the A-form. The backbone-modified

antisense oligonucleotides with engineered desired conformers of the sugar moiety bind to complementary DNA or RNA sequences depending upon the flexibility of the designed backbone to adopt A, B or intermediate form of duplex structures. The stability is further enhanced by base-stacking interactions and presence or absence of positive/negative charges on the modified backbones.

It is important to study the effect of chirality in the backbone on conformational preferences of deoxyribose sugar in dimers. In the present section the studies towards finding out the conformational preference of the deoxyribose ring in dimer unit and its precursor building units is carried out. The completely deprotected dimers **Ia**, **Ib** and **Ic** were used for the NMR studies in D_2O. The scalar coupling constants were determined from 1D ^1H NMR spectra. %S character was calculated using the Sum rule % S = (Σ H1'- 9.8)/5.9 x 100. The results of NMR studies for 3'-amino 5'-*O*-DMT thymidine **3**, thymidine 4'-carboxylic acid **9** and dimers **Ia**, **Ib** and **Ic** are summarized in Table 2.

Table 2. N-type and S-type preference for the compound **3**, **9** and dimers **Ia**, **Ib**, **Ic**

Compound		$J_{H1'H2'}$ (Hz)	$J_{H1'H2''}$ (Hz)	%S	%N	
3		5.5	5.8	25	75	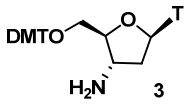
9		5.0	9.3	78	22	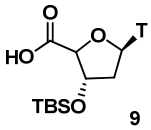
Ia T-L-Proline-T	Ring A	5.6	9.0	82	18	
	Ring B	5.7	7.1	50	50	
Ib T-D-Proline-T	Ring A	5.5	8.6	72	28	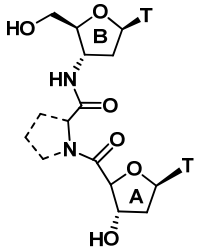
	Ring B	5.5	6.5	36	64	
Ic T-Glycine-T	Ring A	6.9	7.2	73	27	**Ia**, **Ib**, **Ic**
	Ring B	5.6	6.8	44	56	

3'-Amino 5'-*O*-DMT thymidine **3** showed predominantly N-type conformation whereas the thymidine 4'-carboxylic acid **9** showed predominantly S-type conformation. In case of L-proline containing dimer **Ia**, the sugar ring A was found to be predominantly in S-type conformation, while in case of the B ring, equal preference for either S-type or N-type conformation was observed. In the D-Proline containing dimer **Ib**, again the sugar

ring A showed S-type conformation while the ring B showed more percentage of N-type sugar as compared to dimer **Ia**. In case of dimer **Ic,** the ring A showed predominant S-type pucker similar to proline containing dimers **Ia** and **Ib** whereas ring B showed equal preference for either S-type or N-type conformation. The thymidine 4'-carboxylic acid **9** has predominantly S-type conformation and does not show any remarkable change in conformation after coupling. In all the three dimers **Ia**, **Ib** and **Ic**, the 3'-sugar exhibited higher S-type geometry uniformly as compared to the 5'-thymidinyl units. The percentage of N character was found to be higher where C3' of the sugar ring was substituted by nitrogen in the ring B (50–64%) as compared to the 3'-OH sugar (18–28%) in ring A.

2.1.6 *Cis trans* isomers in proline-containing dimer units

In a polypeptide chain, both the amide -CONH- and the imide —CON/peptide groups are intrinsically competent to undergo *cis*/*trans* isomerization by rotation about the torsion angle ω [C^{α}–C(=O)–N–C^{α}] of the peptide bond. Because the lone electron pair of the nitrogen atom is delocalized over the peptide bond, the C-N linkage has a partial double-bond character leading to a planar amide bond (Figure 21 A). The free rotation around the C–N amide bond is drastically restricted because of the partial double bond character with a rotational barrier of ~ 105 kJ mol^{-1}. Consequently, two rotamers of the peptide bond exist: the *trans*-configured peptide bond (ω=180°) and the *cis*-configured peptide bond (ω=0°) [Figure 21 B]. α-Amino acid peptides prefer to be trans oriented with respect to the amide bond, chiefly because the amide hydrogen (*trans* isomer) offers less steric repulsion to the preceding C^{α} atom than does the following C^{α} atom (*cis* isomer) and the E: Z ratio is about 1000: 1 except in proline. The *cis* and *trans* forms of X-Pro (X represents any amino acid) peptide groups are almost isoenergetic, with the trans form being slightly more favored and the E: Z ratio is about 4:1[31] (Figure 21 C).

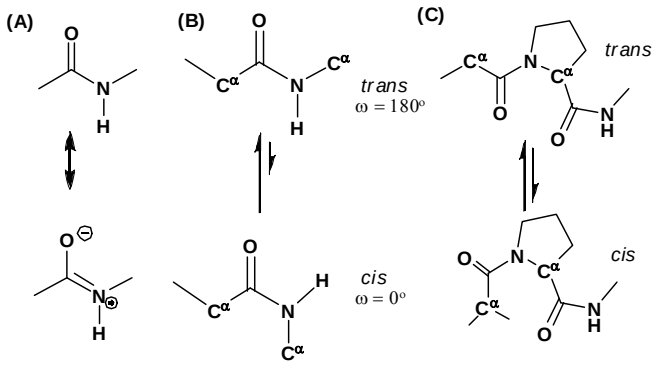

Figure 21. (A) resonance phenomenon in amide bond (B) *cis trans* isomerisation in non-proline peptide bond and (C) *cis-trans* isomerization of an X-Pro peptide bond

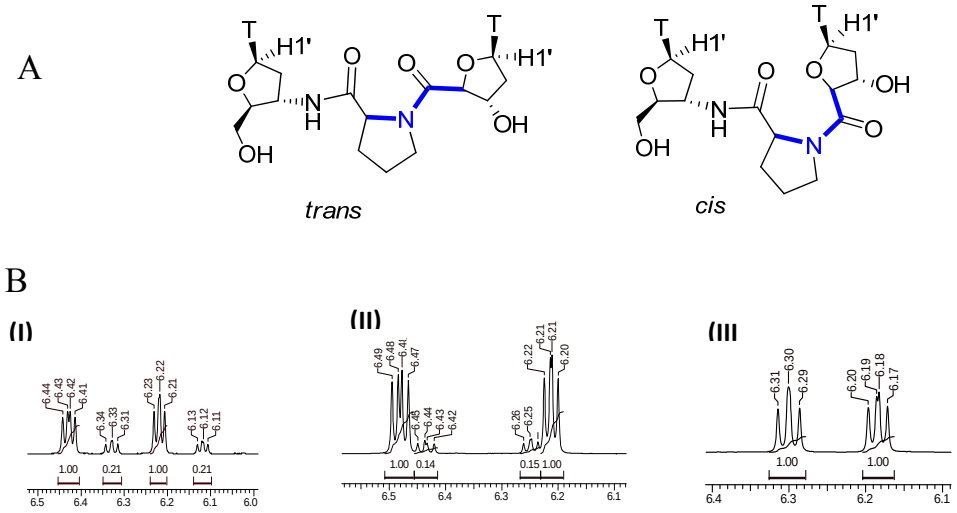

Figure 22. (A) *trans* and *cis* isomers of proline containing dimer (B) H1' NMR resonance corresponding to 3'and 5' thyminyl units of the dimers I) **Ia**, II) **Ib**, III) **Ic**

We also observed this preference in the case of proline-linked nucleoside dimer building blocks **Ia** and **Ib**. The remote sensing of *trans/cis* isomers at the prolyl amide bond is evident from the major : minor isomer ^{1}H NMR resonance in nearly all the protons, but due to spectral overlap the exact ratio could not be calculated, except in the case of H1'. H1' proton showed distinct NMR signals for major: minor isomers (83:17 in **Ia** and 87:13 in **Ib**) corresponding to the 5'- and 3'-thymidinyl units in dimers where the internucleoside amino acid linker is either L- or D-Proline (Figure 22 B, I and II). This difference is absent in **Ic** where glycine is used as the internucleoside amino acid (Figure 22 B, III).

2.1.7 Summary

1. T-$_{(\alpha\text{-amino acid})}$-T dimers have been synthesized using L-proline, D-proline and glycine as the α-amino acid and converted to their phosphoramidite derivatives.

2. 5', 3'-OH free T-$_{(\alpha\text{-amino acid})}$-T dimers were fully characterized using two dimensional COSY and NOESY spectroscopic techniques.

3. NMR studies show that in all the three dimers **Ia**, **Ib** and **Ic**, the 3'-sugar exhibited higher S-type geometry uniformly as compared to the 5'-thyminyl units. The percentage of N character was found to be higher where sugar ring is substituted by nitrogen in the ring B (50–64%) as compared to 3'-OH sugar (18–28%) in ring A.

2.2 Section 2. Synthesis of T-$_{(D\text{-}Proline)}$-$U^{2'\text{-}OMe}$ dimer and T-$_{(\alpha\text{-}Amino\ Acid)}$-T dimers using L-Lysine, D-Lysine

2.2.1 Introduction

In the earlier section 2.1, we have discussed in detail the importance of replacing the phosphodiester linkage with chiral five-atom amide linkage, synthesis of the T-(α-amino acid)-T dimer blocks with L/D-proline and glycine amino acid and N/S sugar conformations in these TT dimers. In this Section, we describe the synthesis of dimer units with a chiral amide backbone along with the 2'-OMe modification in the sugar ring. The presence 2'-OMe nucleosides in DNA or RNA strand is known to enhance thermostability of the resulting duplexes. Also, we have described synthesis of T-(α-amino acid)-T dimer blocks having positively-charged amino acids as L-Lysine and D-Lysine. Electrostatic repulsion disfavours the hybridization of negatively-charged ONs to RNA or DNA targets. ON analogs having neutral backbone such as morpholino derivatives[32] or peptide nucleic acid[33] hybridize with higher affinity than their negatively counterparts without loss of specificity. Along the same lines, it was anticipated that positively-charged oligonucleotide analogs should even be more beneficial in terms of binding efficiency and should also give hybridization with increased association rates. Indeed, several literature studies have shown that the introduction of positively-charged groups at different sites in the base,[34] sugar,[35] or backbone[36] results in stable duplexes and triplexes. However, when the positively-charged group is in the base or the sugar, the duplexes and triplexes are not as stable as those formed when the positively charged group is in the backbone, which is closer to the negatively charged DNA or RNA backbone.

In this Section, we describe the synthesis of TU dimer having 2'-OMe substitution in uridine sugar ring having D-proline as internucleoside amide linker and its conversion to its phosphoramidite derivative, synthesis of TT dimers having D-Lysine and L-Lysine as internucloside amide linker, structural assignment using 2D COSY and NOESY spectroscopic techniques and N$\leftrightarrow$S sugar conformations of the dimers.

2.2.2 Rationale, Design and Objective of the Present Work

A 2'-*O*-alkyl substituent in a ribonucleoside having a phosphodiester or phosphorothioate backbone favors the 3' *endo* conformation of the five-membered rings and increases the melting temperature (*T*m) of the duplexes with an RNA complement.[37] 2'-*O*-methyl oligoribonucleotides were widely studied and are of special interest as antisense probes because i) 2'-OMe RNA: RNA has greater thermal stability than a corresponding DNA:RNA duplex,[38] ii) 2'-OMe RNA: RNA is not a substrate of RNase cleavage[39] and iii) 2'-OMe RNA is resistant to nuclease degradation.[40] De Mesmaeker *et al.* reported four-atom amide linkage backbone modification along with 2'-OMe substitution in one or both the sugar rings[41] (Figure 23). A 2'-OMe substituent on the lower (3') sugar unit of the amides (am-2 and am-3) showed increase in T_m value of the duplexes with RNA with respect to the value of wild type. Pallan *et al.* reported backbone extended amide linkage (five atoms) along with the 2'-OMe modification in the sugar ring[7a] (am-4 and am-5, Figure 23). UV-T_m studies with complementary RNA showed gain in stability (ΔT_m/modification ca 1.5°C) compared to that of wild type.

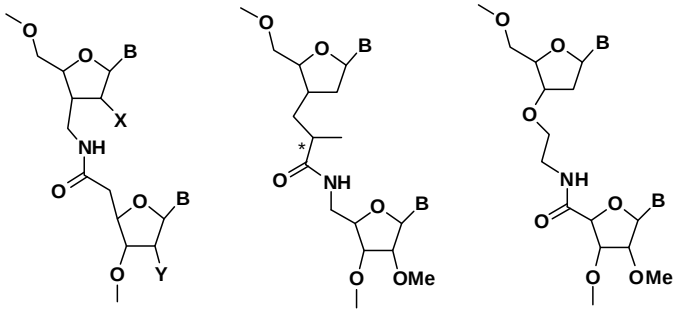

Figure 23. Amide-linked ON analogs

For the incorporation of positive charges in the backbone, strategies have included the incorporation of amino groups prone to protonation under physiological conditions or of the guanidinium group (pKa 12.5), which is highly basic and positively-charged over a wide pH range. An oligonucleotide analog containing alternate phosphodiester and (2-aminoethyl) phosphonate (*R*p) formed a more stable duplex with DNA or RNA than its corresponding natural counterpart[42] (Figure 24, I). These oligonucleotides were resistant to nuclease activity but did not induce RNase H mediated cleavage of a complementary

RNA strand. Partially modified ON analogs with *N*, *N*-dimethylaminoethyl phosphoramidate groups were synthesized (Figure 24, II) and their use as triplex-forming oligonucleotides (TFOs) was shown to produce a decrease in stability with respect to all-phosphodiester oligonucleotide complexes.[43] An oligonucleotide analog containing alternating phosphodiester and stereo-uniform cationic *N*-(dimethylaminopropyl) phosphoramidate linkages, d(T+T–)$_7$T, binds to poly (dA) and poly(A) targets with unusually high affinity in low salt solutions[44] (Figure 24, III). Under the same conditions, the binding affinity of the stereoisomer with opposite chirality at the phosphoramidate linkages is very low. Cationic α-ON (with a non-natural α-anomeric configuration) [Figure 24, IV] bound with high affinity to single-stranded DNA and RNA targets. Duplex stabilization was proportional to the number of cationic modifications, with fully cationic ON having particularly high thermal stability.[45]

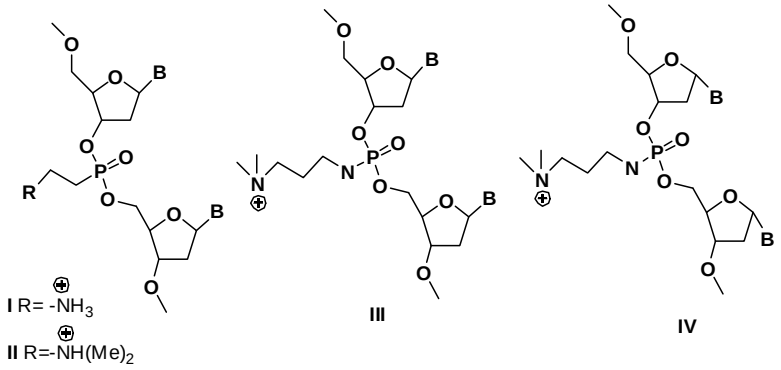

Figure 24. Zwitterionic ON analogs

Bruice *et al* have studied the incorporation of guanidinium linkages into DNA and RNA backbones and the binding affinity towards complementary DNA and RNA.[46] Deoxynucleic guanidine (DNG, Figure 25, I) oligomers in which the internucleoside phosphate linkages are replaced by cationic guanidinium groups have been extensively studied. These DNG analogs are resistant to nucleases and bind to complementary DNA sequences with high affinity without compromising the specificity of binding.[46] The S-methylthiourea linker (DNmt, Figure 25, II), similar to DNG, was designed to lessen the electrostatic attraction compared to DNG and reduce any nonspecific binding with negatively-charged phosphate groups.

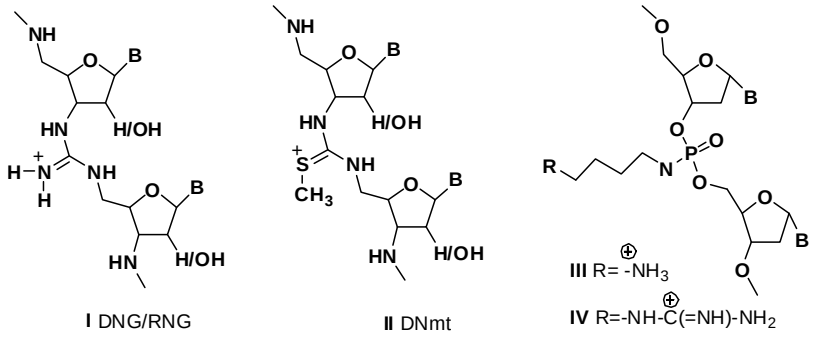

Figure 25. Positively-charged DNA/RNA analogs

The RNG counterpart of DNG containing ribose sugar instead of deoxyribose sugar was shown to bind preferentially to DNA over RNA due to its rigid B-DNA type backbone. The introduction of aminobutylphosphoramidate ($PNHBuNH_2$, Figure 25, III) and guanidinobutylphosphoramidate (PNHBuGua, Figure 25, IV) linkages into α-ONs greatly increased the thermal stabilities of the DNA duplexes.[47] Guanidinium groups as cationic tethers (PNHBuGua) significantly increase the affinity of phosphoramidate α-ONs toward nucleic acid targets, in particular toward RNA. This high affinity could be explained in terms of the dual recognition resulting from Watson–Crick or Hoogsteen base-pairing, combined with cationic/anionic backbone recognition between strands, involving H-bond formation and salt bridging. Moreover, ONs with guanidinium modification increased cellular uptake relative to negatively-charged ONs.

Design of the present work

We have proposed a dinucleotide analog (Figure 26) having D-proline as internucleoside linker and 2'-OMe substitution in one of the sugar rings. As we have already seen from the NMR studies in Section 2.1, the upper ring (5'-end) favors more *N*-type (64%) sugar conformation in TT dimer having D-Proline, 2'-OMe substitution in same ring may not further alter the N-type conformation. On the other hand 2'-OMe substitution in lower ring (3'-end) may favor N-type conformation in this case. Thus, N-type conformation in both the rings may results in better binding to its complementary nucleic acids. Additionally, we have used D-Lysine and L-Lysine as positively-charged amino acids in the internucleoside linker (Figure 26). Lysine provides a covalently attached amino group to the nucleic acid which could be protonated under physiological conditions and may neutralize the anionic phosphate group.

The objectives of this Section are,

1. Synthesis of TU dimer with 2'-OMe substitution in uridine and having D-Proline as the internucleoside amide linker and its conversion to the phosphoramidite derivative.
2. Synthesis of orthogonally protected D-Lysine and L-Lysine.
3. Synthesis of TT dimers having L-Lysine or D-Lysine as the internucleoside amide linker.
4. Structural assignment using 2D COSY and NOESY NMR spectroscopic techniques and N/S sugar conformations of the dimers.

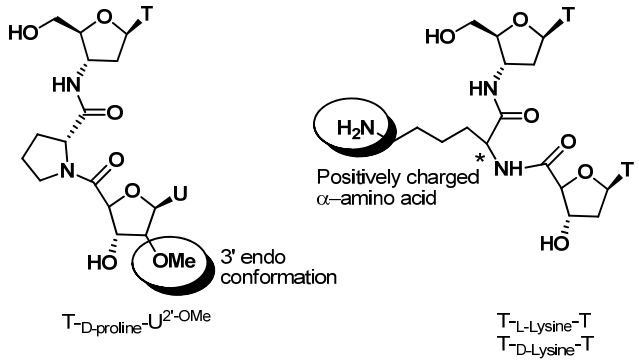

Figure 26. Proposed dinucleotide analogs

2.2.3 Methodology, Results and Discussion

Syntheses of the dimers were accomplished similar to T-$_{(\alpha\text{-amino acid})}$-T dimers. In the case of dimer having 2'-OMe substitution in the 3'-terminal sugar ring, the acid component was synthesized starting from the 2'-OMe-substituted nucleoside. In case of the L-Lysine and D-Lysine dimers, we prepared suitably protected Lysine derivatives.

2.2.3a Synthesis of T-$_{\text{D-Proline}}$-U$^{\text{2'-OMe}}$ dimer

Synthesis of Acid component

The synthesis of acid component was accomplished starting from commercially available 2'-OMe substituted uridine using reported procedure[21] similar to thymidine 4'-carboxylic acid (Scheme 6). Both 3'- and 5'-hydroxyl groups of 2'-OMe-uridine **13** were protected as their silyl ethers to get disilylated product **14**. The 5'-silyl ether was selectively deprotected using pyridinium *p*-toluenesulfonate (PPTS) to give compound **15** which was easily converted to the corresponding acid **16** under TEMPO-BAIB

oxidation conditions. The product was recovered by trituration with ether and acetone. The formation of the product was confirmed by disappearance of the peaks due to the 5' and 5'' protons in the ^{1}H NMR spectra.

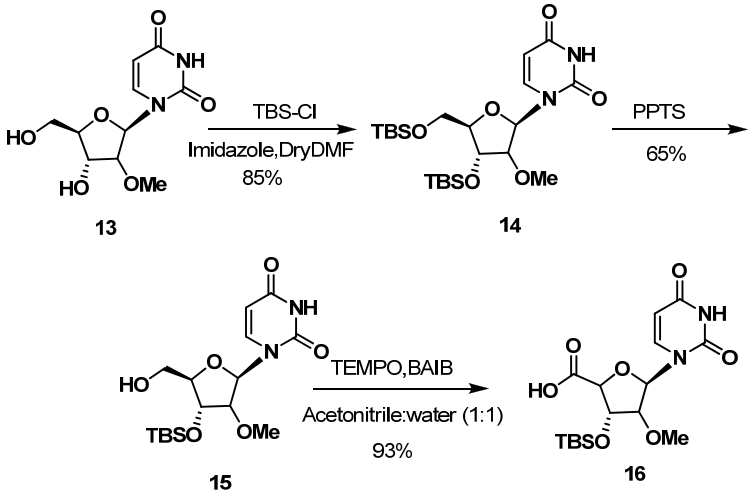

Scheme 6. Synthesis of 2'-OMe Uridine 4'-carboxylic acid

Synthesis of T-$_{D\text{-}Proline}$-U$^{2'\text{-}OMe}$ dimer

Synthesis of the T-$_{D\text{-}proline}$- U$^{2'\text{-}OMe}$ dimer and its conversion to phosphoramidite was achieved as described in Scheme 7. The synthesis of amine component **5b** was accomplished as described in Scheme 1 in Section 1. Coupling of the amine component **5b** with 2'-OMe uridine-4'-carboxylic acid **16** using TBTU/HOBt as coupling reagent and diisopropyl ethyl amine as a base in DMF:ACN mixture (1:1) gave compound **17**. Desilylation of the 3'-OTBS group in **17** using TBAF in THF gave the desilylated dimer **18**. Phosphitylation of the 3'-OH function of **18** was done using the reagent *N*, *N*'-diisopropylcyanoethyl chlorophosphine and base diisopropylethyl amine in DCM as the solvent to obtain the phosphoramidite derivative **19** (Scheme 7). Formation of the product was confirmed by ^{31}P NMR spectroscopy. Detritylation of compound **18** gave the 3', 5'- free dinucleoside **20,** which was purified by successive trituration of the crude product with diethyl ether.

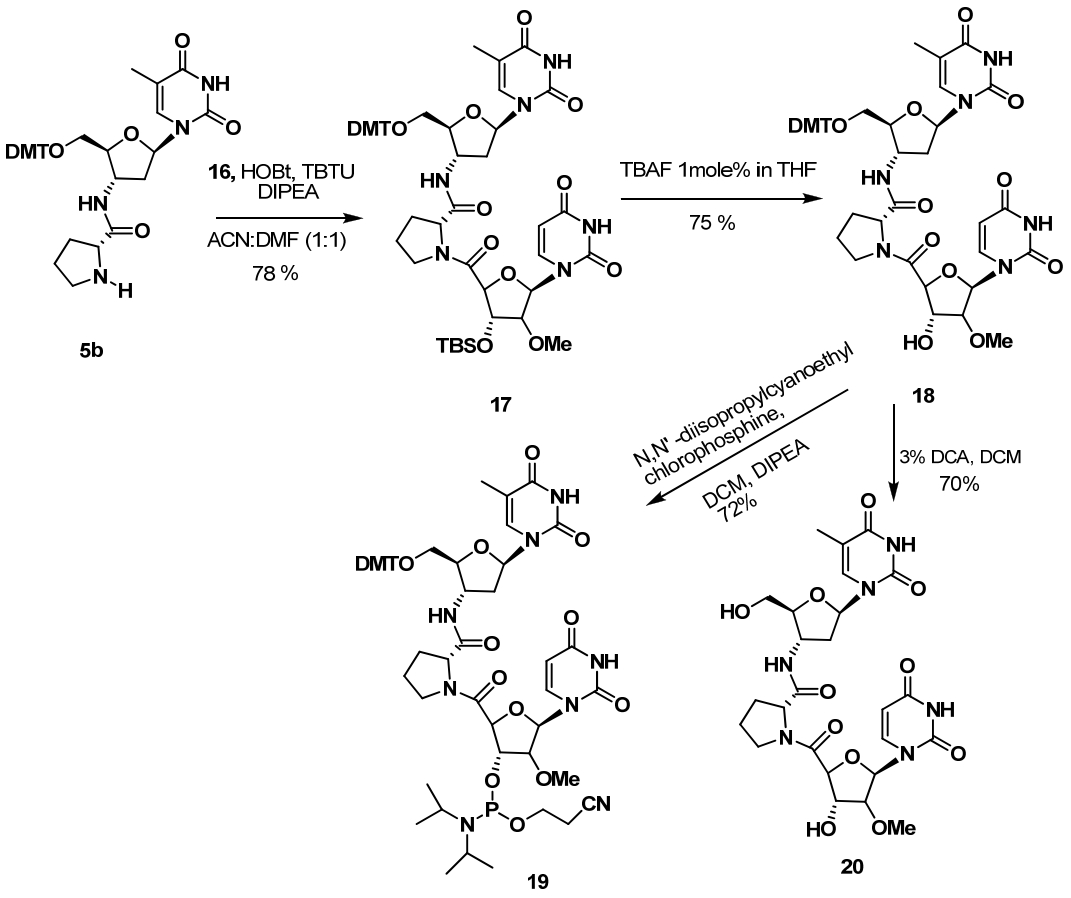

Scheme 7. Synthesis of 3', 5'- protected and 3', 5'- free T-$_{D\text{-}Proline}$-U$^{2'\text{-}OMe}$ dimer

2.2.3b Synthesis of T-$_{L\text{-}Lysine}$-T dimer and T-$_{D\text{-}Lysine}$-T dimer

Orthogonal protection of Lysine

Orthogonal protection of the amino groups of lysine compatible with the synthetic strategy of the dimers and the synthesis of oligomer on automated DNA synthesizer was a prerequisite. We have used trifluoroacetyl protection for the side chain amino (ε) functionality based on the fact that it can be cleaved during final deprotection (ammonolysis) of the ONs. We chose Alloc (allyloxycarbonyl) protection for the α-amino group of lysine as it can be deprotected keeping the trifluoroacetyl protection intact.

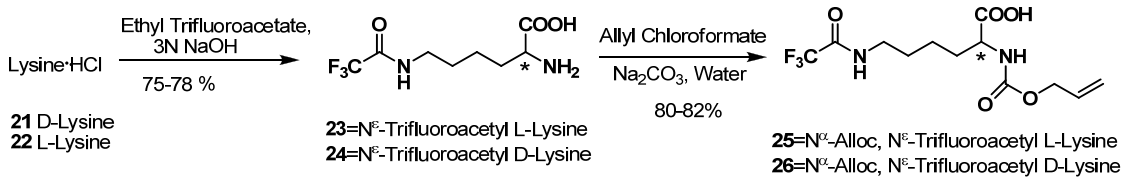

Scheme 8. Synthesis of N^{α}-allyloxycarbonyl N^{ε}-trifluoroacetyl L- and D-Lysine

We have synthesized protected L-Lysine starting from L-Lysine-HCl **21** as shown in Scheme 8. Selective protection of the ε-amino group using trifloroethylacetate in water gave N^{ε}-trifluoroacetyl L-Lysine **23**.[48] We obtained the N^{ε}-trifluoroacetyl L-lysine **23** in 75% yield with trace amount of unreacted lysine. Alloc protection[49] of α-amino group of N^{ε}-trifluoroacetyl L-Lysine **23** using allyl chloroformate gave the N^{α}-allyloxycarbonyl-N^{ε}-trifluoroacetyl L-Lysine **25**. In a similar way, we synthesized the N^{α}-allyloxycarbonyl N^{ε}-trifluoroacetyl D-Lysine **26** starting from D-Lysine HCl **22**.

Synthesis of T-$_{\text{L-Lysine}}$-T dimer and T-$_{\text{D-Lysine}}$-T dimer

The synthesis of T-$_{\text{Lysine}}$-T dimer units was accomplished according to scheme 9. Coupling of the 3'-amino-5'-ODMT thymidine **3** with orthogonally protected L-Lysine **25** using the coupling reagents TBTU/HOBt and diisopropyl ethyl amine as base in acetonitrile: DMF mixture yielded **27**. The Alloc group was removed using tris(dibenzylideneacetone)dipalladium [$Pd_2(dba)_3$] to obtain an intermediate compound **29.** Isolation of **29** with free amino group was done by simple precipitation using petroleum ether. The obtained crude product **29** was used in the next coupling step without further purification. Coupling of **29** with thymidine-4'-carboxylic acid **9** gave dimer **31** which on desilylation furnished desilylated dimer **33**. The DMT group was removed using 3% dichloroacetic acid in DCM and triethyl silane as scavenger followed by removal of the trifluoroacetyl group using aqueous NH_3 to get the completely deprotected dimer **37**. The 3'-, 5'- free dinucleoside formed was purified by successive trituration of the crude product with diethyl ether. In a similar way, we synthesized T-$_{\text{D-Lysine}}$-T dimer **38**.

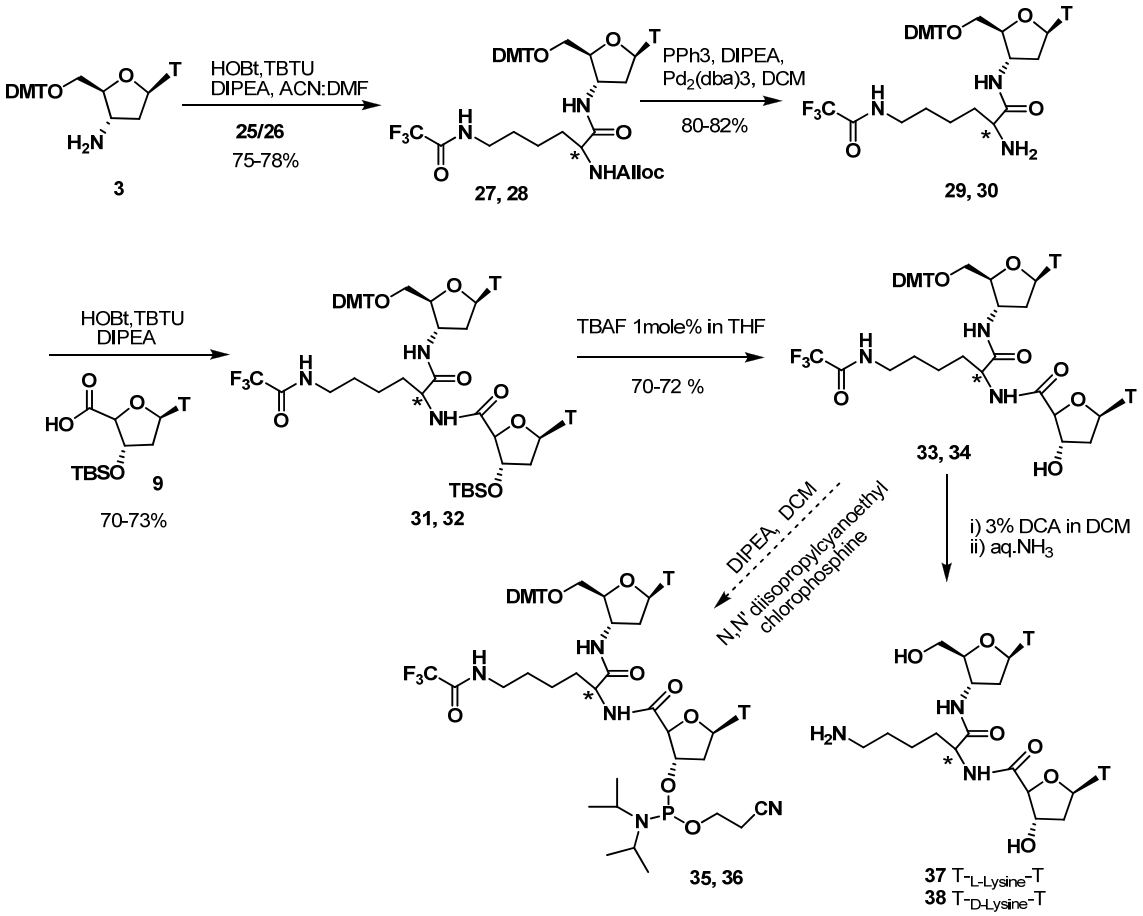

Scheme 9. Synthesis of T-$_{L\text{-}Lysine}$-T dimer and T-$_{D\text{-}Lysine}$-T dimers

2.2.4 Assignments by ^{1}H NMR of 3'-, 5'-OH free T-$_{D\text{-}proline}$-U$^{2'\text{-}OMe}$ and T-$_{Lysine}$-T dimer blocks

^{1}H NMR spectra of 3'-, 5'-free dinucleosides **20**, **37** and **38** were recorded in D_2O. The ^{1}H NMR spectra of dimers **20**, **37** and **38** were fully assigned with the aid of 2D COSY and 2D NOESY experiments and the chemical shift values for dimer **20** are reported in Table 3, and for dimers **37** and **38** in Table 4.

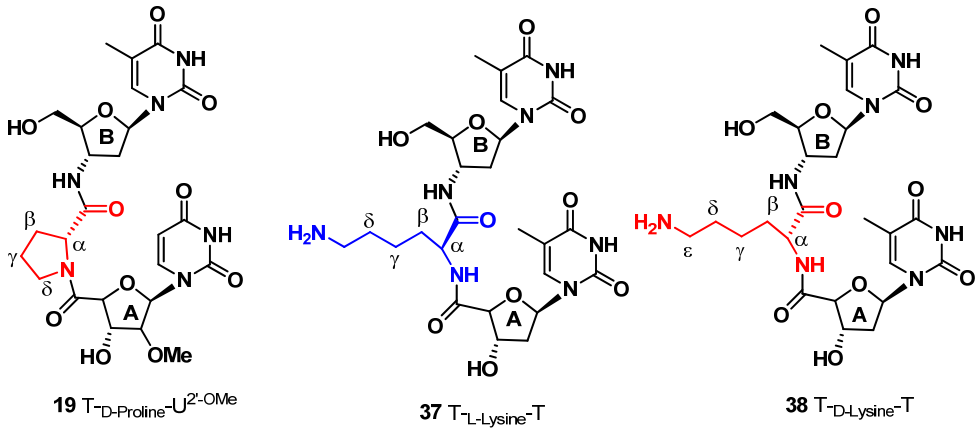

Figure 27. 3', 5'-OH free T-$_{D\text{-Proline}}$-U$^{2'\text{-OMe}}$ and T-$_{Lysine}$-T dimers

H5'/H5" protons were assigned according to the Remin and Shugar rule[22], where the lower field proton was assigned as H5' while the higher field protons were assigned as the H5''. The discrimination between H2' and H2'' protons was made using the rules devised by Altona *et al*.[23] The 5'-and 3'-terminal ribose rings of the dimers were assigned by COSY experiments and distinguished by the absence of H5', H5'' protons at the 3'-terminal sugar. In case of dimer **20**, the H2'-proton in uridine which showed a downfield shift helped to differentiate easily between the two sugar rings. In the proline ring, the two protons attached to the β carbon (diasterotopic protons) and on the δ carbon (attached to tricoordinate nitrogen) showed different chemical shifts. In this case also we observed *cis trans* isomers due to proline ring in the dimer. The H1' proton of the upper ring (5'-end) did not show any distinct separation of the major and minor isomers but H1' of the lower ring (3'-end) and even H5, H6 proton of uridine showed distinction between major and minor isomers (87:13). The other protons in the NMR spectrum did not show any such distinction for *cis-trans* isomers.

Table 3. ^{1}H NMR Chemical shifts of 3', 5'-OH free T-$_{D\text{-proline}}$-U$^{2'\text{-OMe}}$ dimer (**20**)

Entry	Sugar	H1'	H2'	H2''	H3'	H4'	H5'	H5''	H5	H6	T-CH_3/2'-OMe	α Pro-CH	β Pro-CH_2	γ pro-CH_2	δ pro-CH_2
20	Ring A	6.1	4.05	--	4.5	4.9	--	--	5.9	8.2	3.48				
	Ring B	6.2	2.4	2.4	4.5	4.0	3.7	3.8	--	7.6	1.8	4.4	2.3(1H) 1.9(1H)	2.0	3.8(1H) 3.7(1H)

Table 4. ^{1}H NMR Chemical shifts of 3', 5'-OH free T-$_{L\text{-}Lysine}$- T (**37**) and T-$_{D\text{-}Lysine}$-T dimers (**38**)

Entry	Sugar	H1'	H2'	H2''	H3'	H4'	H5'	H5''	H6	CH3	α Lys-CH	β Lys-CH_2	γ Lys-CH_2	δ Lys-CH_2	ω Lys-CH_2
37	Ring A	6.2	2.4	2.5	4.7	4.4	--	--	7.7	1.8	--	--	--	--	--
	Ring B	6.2	2.3	2.5	4.5	3.9	3.7	3.8	7.6	1.8	4.2	1.80	1.42	1.69	2.98
38	Ring A	6.3	2.3	2.5	4.7	4.4	--	--	7.7	1.8	--	--	--	--	
	Ring B	6.2	2.3	2.5	4.5	4.0	3.7	3.8	7.6	1.8	4.2	1.80	1.43	1.68	2.98

2.2.4a Conformation about the glycosidic bond

The conformation about the glycosidic bond in the dimers was determined from 2D NOESY NMR experiments. Schematic representation of some of the long range nOe's seen in 2D Noesy spectrum of compound **20** (T-$_{D\text{-}Proline}$-$U^{2'\text{-}OMe}$), **37** (T-$_{L\text{-}Lysine}$-T) and **38** (T-$_{D\text{-}Lysine}$-T) is depicted in Figure 28. In dimer **20**, the strong nOe between H6 and H2' (1.7 %) indicates *anti* conformation in the 3' terminal sugar. In the 5' terminal sugar, the strong nOe between H6 and H2' (2.4%) and between H6 and H3' (2.3 %) indicate *anti* conformation. In L-Lysine containing dimer **37**, the strong nOe cross peaks between H6-H1' (5.8 %) confirms *syn* orientation of the base in the 3' terminal sugar whereas the nOe cross peaks between H6-H2' (2.5 %) and H6-H3' (3.2 %) with medium intensity indicate *anti* conformation of nucleobase in the 5' terminal sugar ring. In D-Lysine containing dimer **38**, the strong nOe cross peaks between H6-H1' (6 %) confirms *syn* orientation of the base in the 3' terminal sugar whereas the nOe cross peaks between H6-H2' (2.7 %), H6-H3' (2 %) and H6- H1' (2 %) indicate both *syn* and *anti* conformation of nucleobase in the 5' terminal sugar ring. In case of lysine containing dimers **37** and **38**, possibility of hydrogen bonding between the C2 carbonyl of thymine base and hydrogen atom of the NH-amide bond at 3' terminal A ring probably restricted the rotation resulting in *syn* conformation about the glycosidic bond (figure 28) similar to glycine containing dimer **Ic**. However absence of such possible hydrogen bonding in proline containing dimer **20**, probably allows *anti* conformation of glycosidic bond.

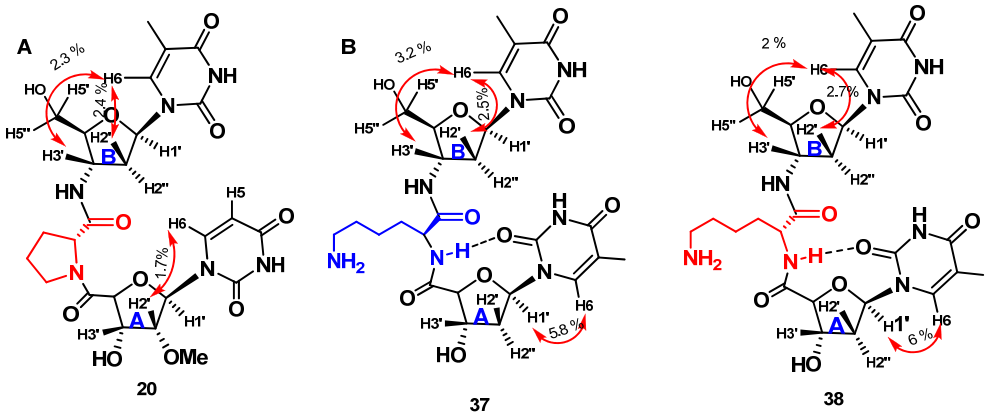

Figure 28. Schematic representation of some of the long range nOe's seen in 2D NOESY NMR spectrum of dimers **20, 37** and **38**

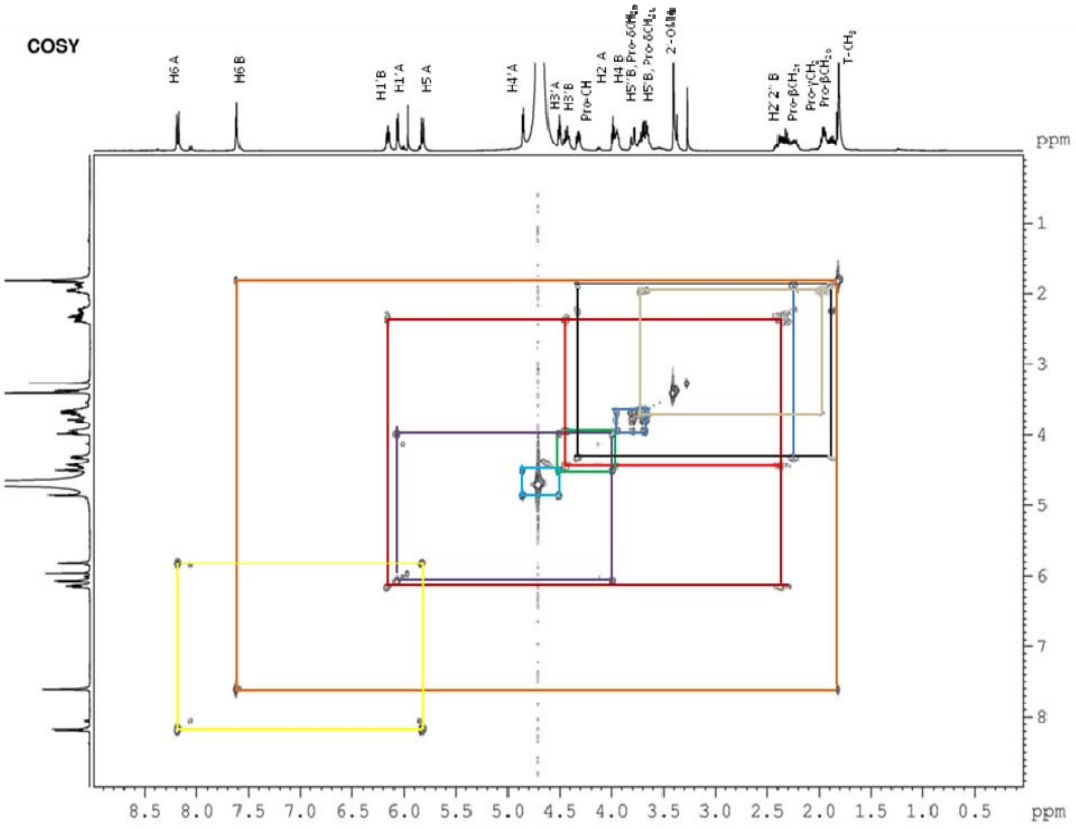

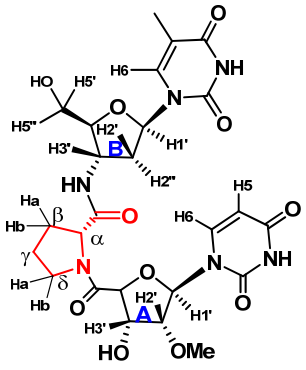

20

Figure 29. Fully assigned COSY spectrum of dimer **20**

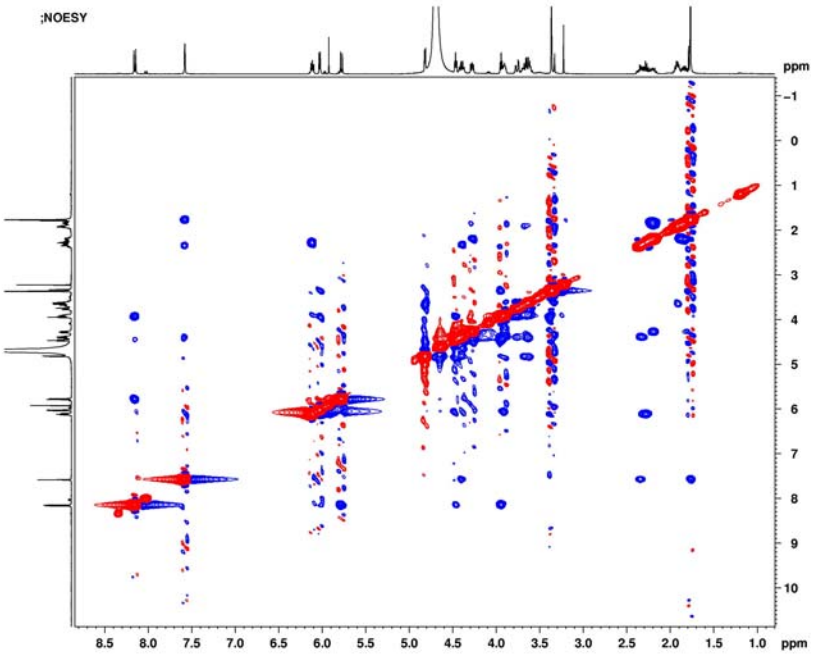

Figure 30. NOESY spectra of dimer **20**

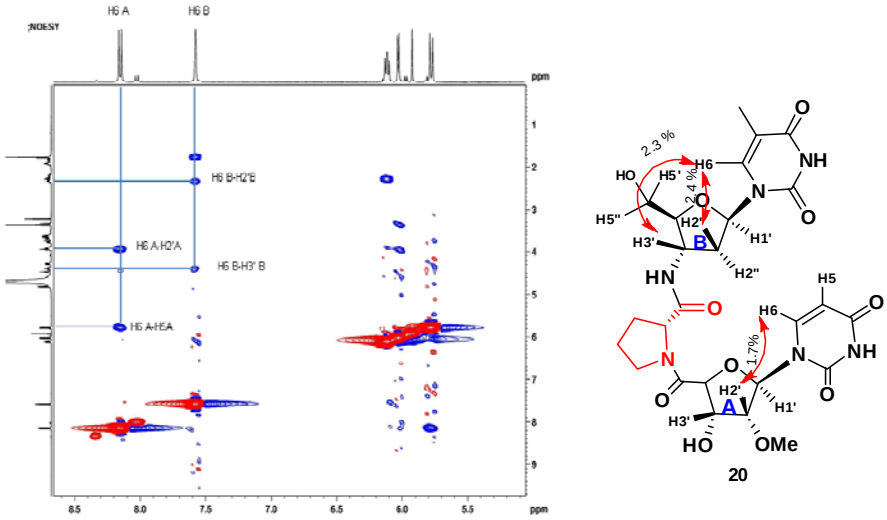

Figure 31. NOESY spectra of dimer **20**. The nOe cross peaks between H6-H2' in A-ring and H6-H2', H6-H3' in B-ring indicate *anti* conformation of nucleobase.

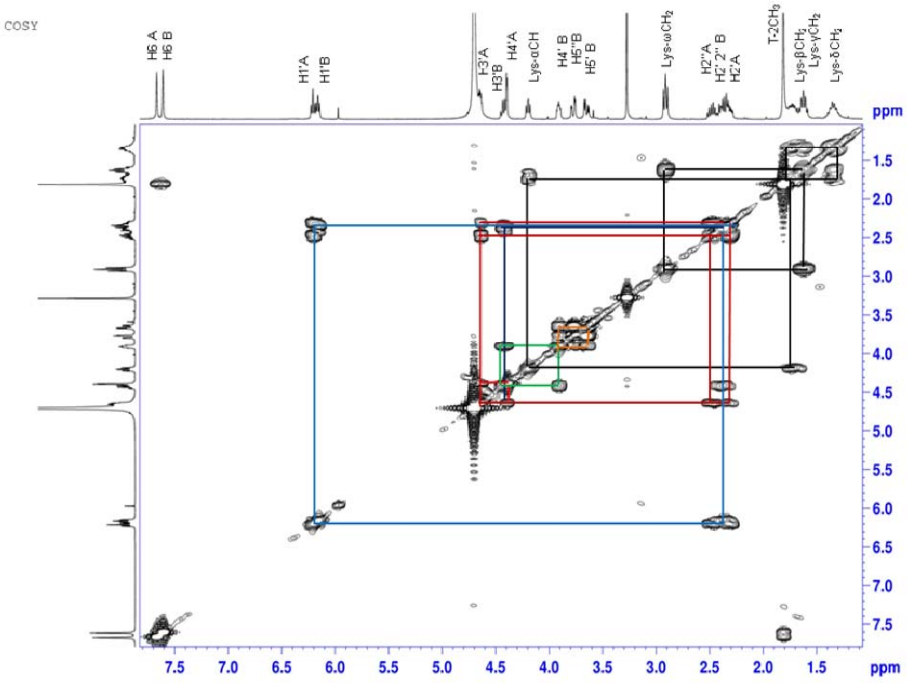

Figure 32. Fully assigned COSY spectra of dimer **37**.

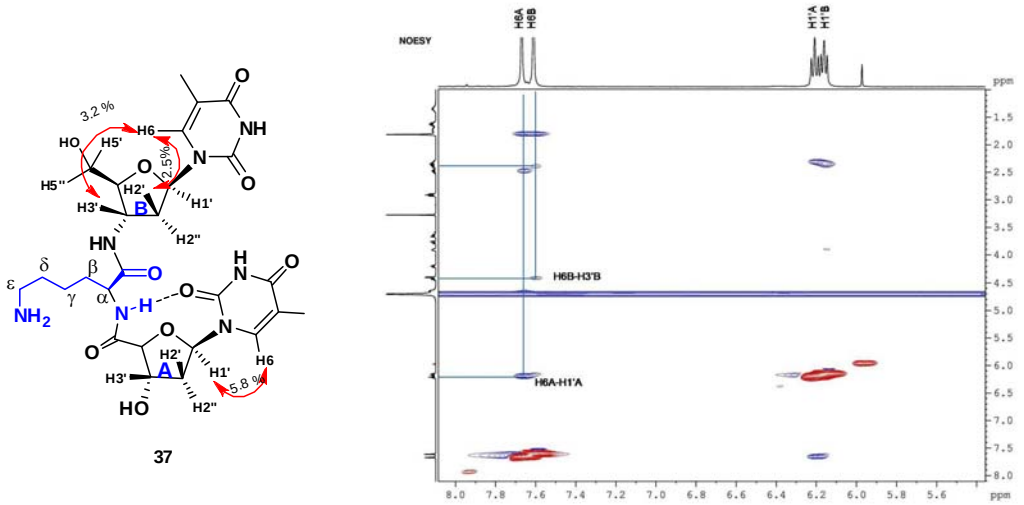

Figure 33. Expanded NOESY spectra of dimer **37**. The strong nOe cross peaks between H6-H1' in the A ring confirms *syn* orientation of base. The H6-H2', H6-H3' nOe with medium intensity indicate *anti* conformation of nucleobase B-ring

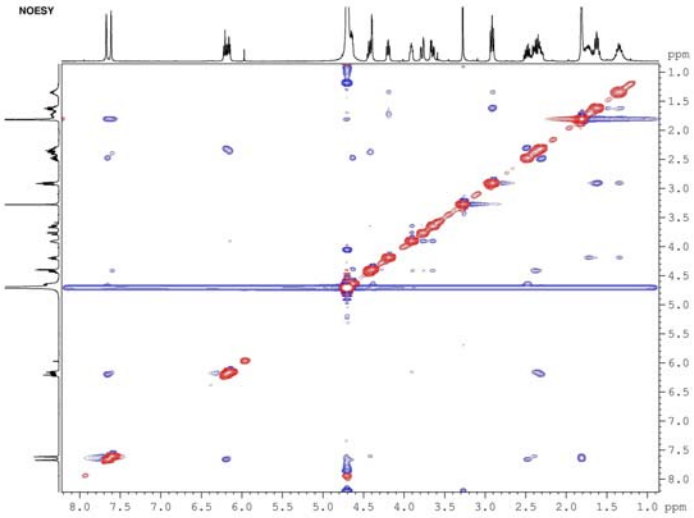

Figure 34. NOESY spectra of dimer **37**

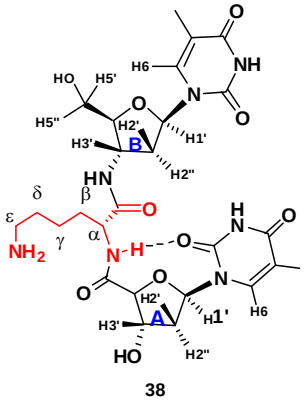

38

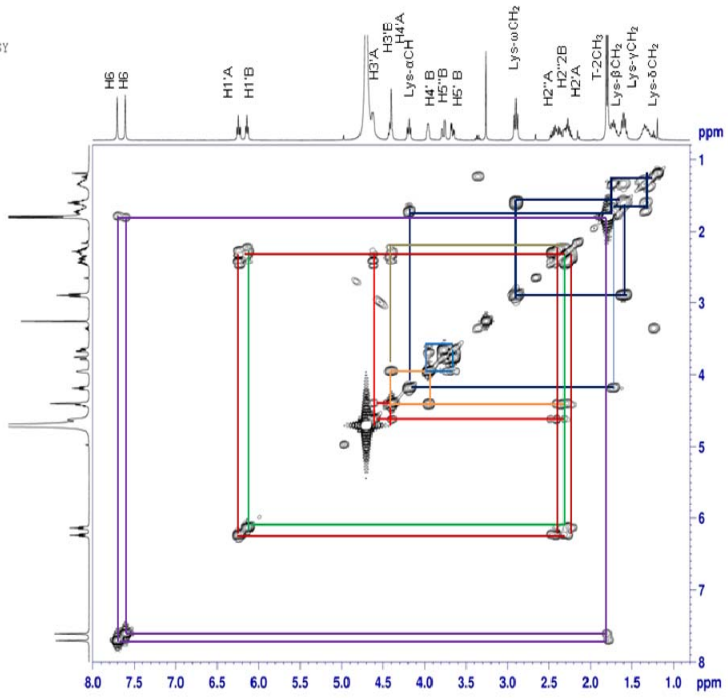

Figure 35. Fully assigned COSY spectra of dimer **38**

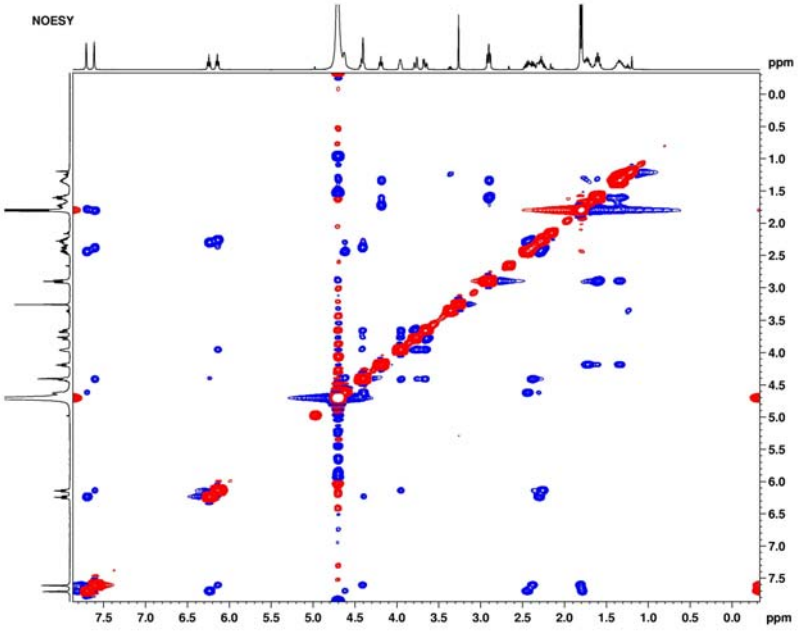

Figure 36. NOESY spectra of dimer **38**

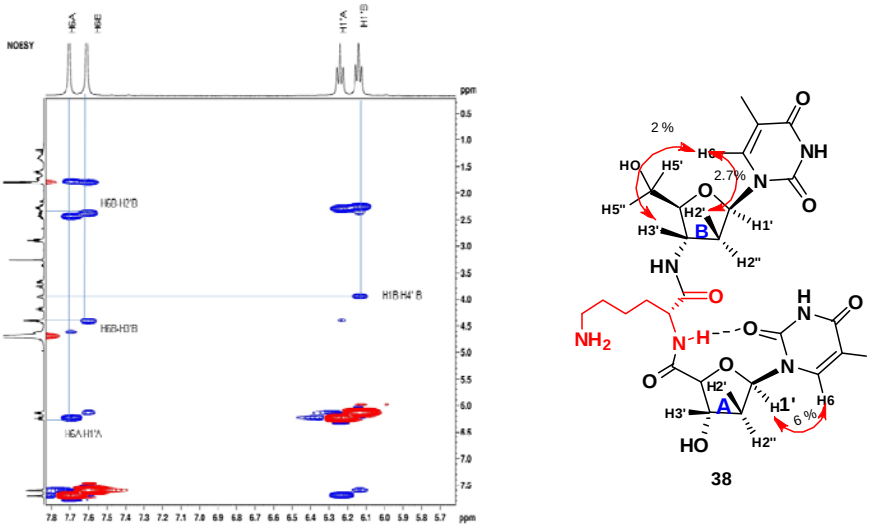

Figure 37. Expanded NOESY spectra of dimer **38**. The strong nOe cross peaks between H6-H1' confirms *syn* orientation of base in A-ring. The H6-H2', H6-H3' and H6-H1' nOe with medium intensity indicate both *syn* and *anti* conformations, however *anti* conformation is predominant of in the B-ring

2.2.5. Conformation of the sugar ring

We have discussed earlier the sugar conformation of the T-(α-amino acid)-T dimers having L-Proline, D-Proline and glycine and constituent nucleosides (Section 2.1). Here we discuss the S-type/N-type geometry preference of the sugar in the $T\text{-}_{D\text{-}Proline}\text{-}U^{2'OMe}$ **20,** TT dimers having L-Lysine **37** and D-Lysine **38** and 2'-OMe-substituted uridine-4'-carboxylic acid **16** (Figure 38). These are given in Table 5.

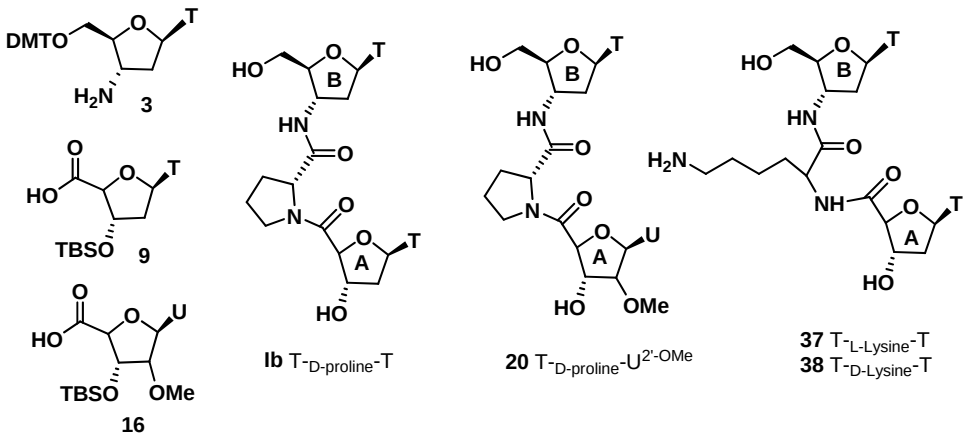

Figure 38. Structure of dimers and their constituent nucleoside units.

In the earlier Section 2.1, we discussed the preference for S-type/N-type geometry in the sugars of compounds **3** and **9.** Here, we have calculated % S sugar conformations of **20**, **37**, **38** and **16** and these are compared with the dimers **Ia**/**Ib**/**Ic**. The % S character was calculated using the Sum rule[23]

$$\% S = (\Sigma J H_{1'} - 9.8)/5.9 \times 100$$

In case of 2'-OMe-uridine- 4'-carboxylic acid **16** and ring A in dimer **20**, we have used the equation[50]

$$\% S = 100 \times (J H_{1'2'} - 1)/6.9$$

The 2'-OMe-uridine-4'-carboxylic acid **16** showed predominantly S-type sugar pucker and its N-type character increased in dimer **20** (ring A) from 27 % to 42%. Ring B in dimer **20** showed major N-type sugar puckering. In dimers containing L-Lysine **37**, the 3' terminal sugar was predominantly S-type whereas the 5' terminal sugar (ring B) was found to have equal proportions of S-type and N-type sugar conformation. In dimers containing D-Lysine **38**, the 3' terminal sugar was predominantly S-type, similar to L-Lysine containing dimer, but the 5' terminal sugar showed major N-type conformation.

Table 5. N-type/S-type sugar geometry preference for the compounds **3**, **9**, **16** and dimers **Ib**, **20**, **37**, **38**

Compound		$J_{H1'H2'}$ (Hz)	$J_{H1'H2''}$ (Hz)	%S	%N	
3		5.5	5.8	25	75	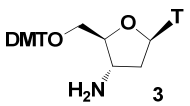
9		5.0	9.3	78	22	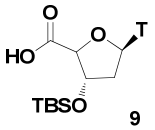
16		6.0	-	73	27	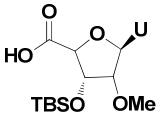
Ib **T-$_{D\text{-}Proline}$-T**	Ring A	5.5	8.6	72	28	
	Ring B	5.5	6.5	36	64	
20 **T-$_{D\text{-}Proline}$-U$^{2'\text{-}OMe}$**	Ring A	5.0	-	58	42	
	Ring B	5.8	7	51	49	
37 **T-$_{L\text{-}Lysine}$-T**	Ring A	6.8	7	68	32	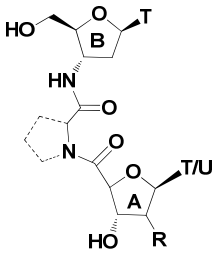
	Ring B	6.5	6.2	49	51	
38 **T-$_{D\text{-}Lysine}$-T**	Ring A	6.8	7	68	32	
	Ring B	5.8	6.5	42	58	

Ib, 37, 38 R=H
20 R=2'-OMe

We anticipated that the 2'-OMe substitution would indicate N-type conformation in the sugar ring and indeed altered sugar conformation from S-type to N-type in compound **20** by about 15%

Section 2.3 of this chapter deals with the CD studies of dimers and biophysical studies of the derived oligomers modified with T-$_{D\text{-}proline}$-U$^{2'\text{-}OMe}$ dimer.

2.2.6 Summary

1. The T-$_{\text{D-proline}}$-U$^{2'\text{-OMe}}$ dimer was synthesized and converted to its phosphoramidite derivative. TT dimers having L-Lysine and D-Lysine as internucleoside linker were synthesized.

2. The 3', 5'-OH free dinucleosides were fully characterized using two-dimensional COSY and NOESY NMR spectroscopic techniques.

3. NMR studies showed that in all the three dimers **20**, **37** and **38**, the 3'-sugar exhibited higher S-type geometry uniformly as compared to the 5'-thymidinyl units.

Section 2.3 CD studies for the dimers and biophysical studies of sequences containing T-$_{(\alpha\text{-Amino Acid})}$-T and T-$_{\text{D-Proline}}$-U$^{2'\text{OMe}}$ dimers

In this Section we discuss circular dichroism studies to study base-stacking interactions in dimers as base-stacking is one of the contributing factors to the duplex stability. UV-T_m studies were carried out in order to investigate the binding preference of the modified sequences towards complementary DNA and RNA.

2.3.1 CD analysis of building units, dimers and comparison study of base-stacking interactions in dimers

Most biological molecules contain a number of electronic units that absorb light nearly independently, called chromophores, which are asymmetrically disposed in the space. Such asymmetric molecules will absorb left circularly polarized light differently from right circularly polarized light. Circular dichroism (CD) is the difference in absorption between left and right circularly polarized light, so that CD spectral bands occur due to the change in the normal electronic absorption bands in an asymmetric molecule.[51] In the earlier Section 2.1 and 2.2, we have seen that the sugar conformations do not drastically differ in the diastereomers formed because of the chirality of the internucleoside linker in the case of the all dimers. The N-type conformational preference of the sugar ring in 2'-OMe or LNA type oligomers is known to dramatically improve the binding efficiency of the oligomers and in these cases, effective base stacking is one of the well-established contributing factors to the duplex stability. Increase in the positive CD band at 275 nm is ascribed to the effective base stacking interactions even at the dimer level.[52] We therefore carried out CD studies on the dimer blocks to evaluate any contributions of chirality of the α-amino acid towards stacking interactions. The CD analysis of monomers was also carried out to see the individual contributions of monomers to the CD pattern of dimers. CD analysis of monomer **3** and **9** were carried out at 25 μmolar concentration in 20:80 acetonitrile: water mixture. CD analyses of all the dimers were carried out at 100 μmolar concentration in water to study base-stacking interaction in aqueous medium. Temperature-dependent change in the base-stacking was studied by scanning CD of the dimer solution with increase in temperature from 10 °C-80 °C.

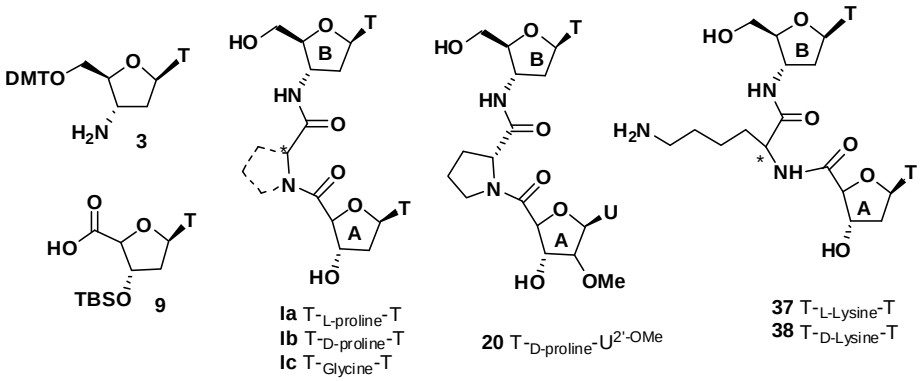

Figure 39. Monomer and T-(α-amino acid)-T/$U^{2'\text{-}OMe}$ dimers

CD spectra of the monomers: CD spectra of the monomers (**3** and **9**) showed a positive band at 270-280 nm. The addition spectra of the two monomers, i.e (**3** + **9**) was recorded, which also gave a positive CD signal at 280 nm (Figure 40A).

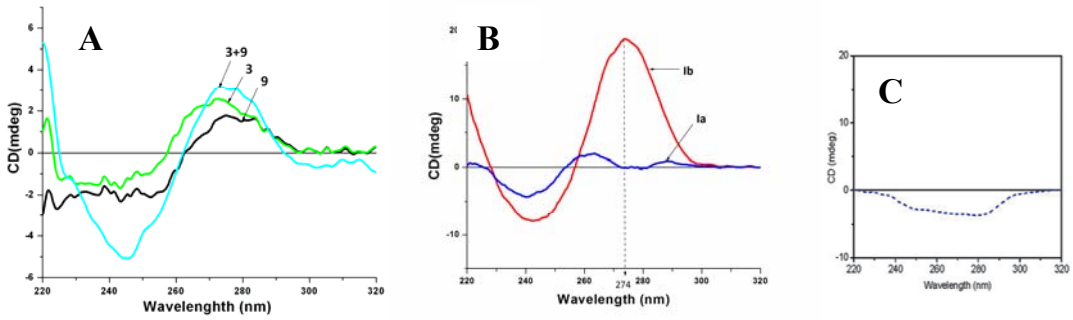

Figure 40. (A) CD spectra of monomers **3**, **9** and their additive CD spectra, (B) CD spectra of T-L-Proline-T **Ia** and T-D-Proline-T **Ib** at a concentration of 100 μM in water. C) CD spectrum of T-[(L-Pro)-T]$_7$

CD spectra of the dimers: The CD studies were carried out for all dimer blocks to investigate the effect of chirality in backbone on the base stacking interactions. The D-proline containing T-D-Proline-T **Ib** showed a strong positive band at 275 nm (Figure 40B) and a negative band at 240 nm. In the T-L-Proline-T dimer **Ia**, along with the negative band at 240 nm, two distinct low intensity CD bands were observed at 265 and 290 nm along with a broad minimum at 275–280 nm (Figure 40B). The T-Glycine-T dimer **Ic** showed low intensity broad bands at 240 and 280 nm (Figure 42). The high intensity of CD signal at ~ 275 nm led us to believe that **Ib** is well stacked even at the dimer level. The minimum at ~ 275 nm in **Ia** is comparable to the negative CD signal at ~ 275 nm in the case of the homogeneous amide-backbone T-[(L-pro-T)]$_7$ octamer (Figure 40C)

earlier reported by our group.[11] Thus, the stacking interactions in **Ia** and **Ib** could be arising from different adopted conformations due to opposite chirality in the internucleoside linker giving rise to opposite CD signals at ~ 275 nm. Glycine, being prochiral, could either result in the existence of both chiral components in equal measure, which cancel each other, or may not contribute to the base-stacked structure, and eventually lead to only a weak maximum at ~ 280 nm.

The strong positive band at ~ 275 nm in the T-$_{D\text{-proline}}$-T dimer **Ib** displayed significant temperature dependence from 10–80 °C (Figure 41B) as reported earlier for the TpT dimer block. For the T-$_{L\text{-proline}}$-T dimer **Ia**, increasing temperature resulted in the reduction of the amplitude of CD minimum band at ~275 nm (Figure 41A). These changes in intensities of CD maxima and minima imply the presence of higher fractions of stacked species in **Ib** and **Ia**.

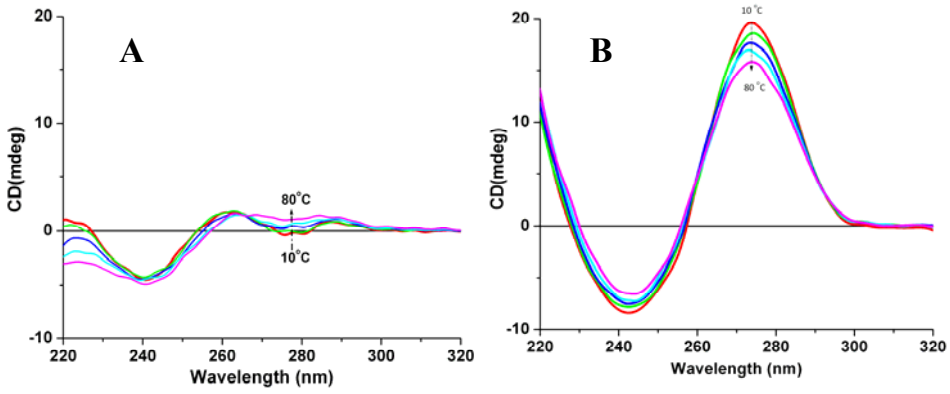

Figure 41. Temperature-dependent CD studies of thymine dimer containing (A) L-Proline **Ia** and (B) D-Proline **Ib** at 100 µM in water at 10 (red), 20 (green), 40 (blue), 60 (light blue) and 80 °C (purple).

No temperature dependent change in CD intensity was observed in the case of T-$_{Glycine}$-T dimer **Ic** (Figure 42) and thus fractions of stacked species are less significant at the dimer level in **Ic.**

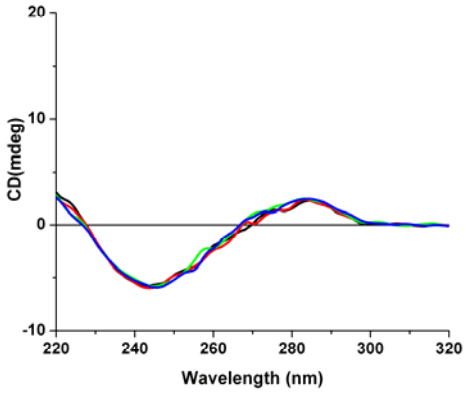

Figure 42. Temperature-dependent CD studies of thymine dimer containing glycine **Ic** at 100 µM in water at 10 (red), 20 (black), 40 (blue), 60 (light blue) and 80°C (purple)

Similarly we carried out CD studies for the dimers containing D-Proline having 2'-OMe modification in the 3' terminal sugar and dimers containing L-Lysine and D-Lysine.

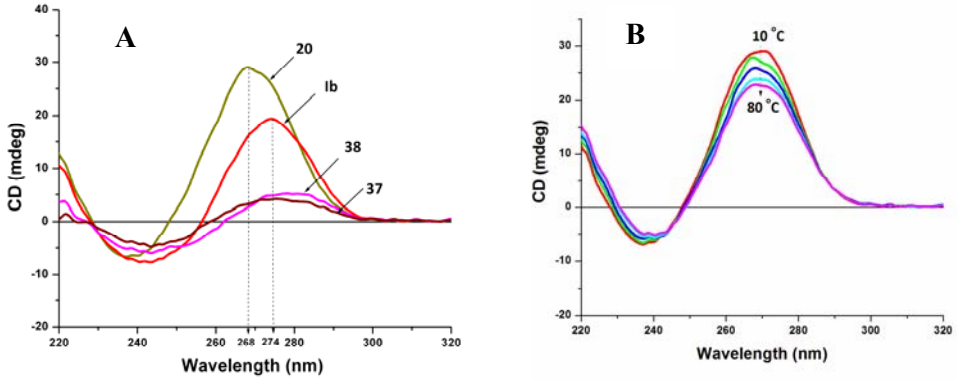

Figure 43. (A) Comparison of the D-Proline containing TT dimer (**Ib**), $TU^{2'\text{-OMe}}$ dimer (**20**) and L/D- Lysine containing TT dimer **37** and **38** at 100 µM concentration in water (B) Temperature-dependent CD studies of TU dimer containing D-proline **20** at 100 µM in water at 10 (red), 30 (green), 50 (blue), 70 (light blue) and 80 °C (purple)

The north/south conformational equilibria of the sugar rings are known to affect the base stacking interactions.[2] 2'-*O*-methylation has been shown to enhance base stacking of dipyrimidine ribodinucleotides[53] which could be a consequence of the C3'-*endo* sugar conformational preference, which is increased in the order 2'-deoxy[54] < ribo[55] < 2-*O*-methylribo.[3] C3' -*endo* conformation was found to be 42 % and 58 % in the 3'-(2'-OMe substituted i.e, ring A) and 5'-(i.e., ring B) terminal sugars respectively in

dimer **20** whereas this was 28% (ring A) and 64% (ring B) respectively in dimer **Ib**. Comparision of the CD for the T-$_{D\text{-}Proline}$-T **Ib** and T-$_{D\text{-}Proline}$-U$^{2'\text{-}OMe}$ **20** indicate that T-$_{D\text{-}Proline}$-U$^{2'\text{-}OMe}$ **20** is better stacked than T-$_{D\text{-}Proline}$-T **Ib** (figure 43A). The increased N-type propensity in 2'-OMe substituted sugar could be the reason for increase in CD intensity band at ~ 270 nm. The strong positive band at ~ 270 nm in the T-$_{D\text{-}proline}$-U$^{2'\text{-}OMe}$ dimer **20** displayed significant temperature dependence from 10–80 °C (Figure 43B) also indicating the presence of stacking interactions.

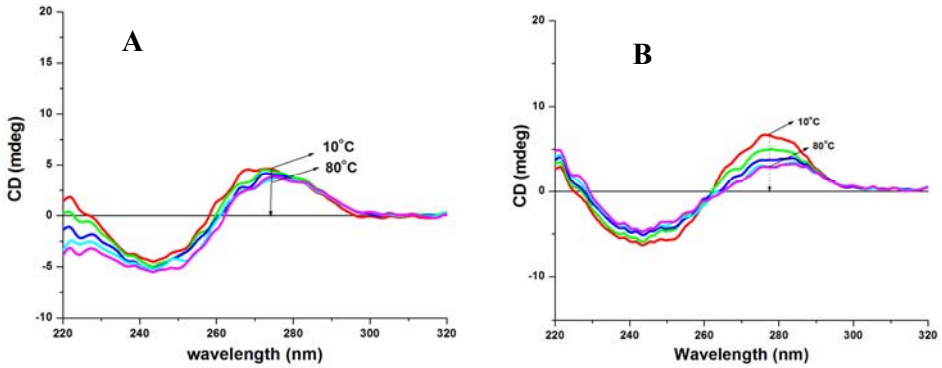

Figure 44. Temperature-dependent CD studies of thymine dimer containing (A) L-Lysine **37** and (B) D-Lysine **38** at 100 μM in water

The acyclic L-Lysine and D-Lysine containing dimer **37** and **38** showed similar CD pattern as achiral glycine containing dimer **Ic**. Dimer **37** and **38** showed weak and broad positive band at ~ 275 and negative band at ~ 240 nm (Figure 43). The D-Lysine containing dimers **38** showed decrease in CD amplitude with increase in temperature from 10-80 °C indicating base stacking interaction (Figure 44B).

2.3.2 Solid phase synthesis of DNA Oligonucleotides by phosphoramidite method

General solid phase synthesis on automated synthesizer of oligonucleotides by β–cyanoethyl phosphoramidite method[56] is given in Scheme 10. Chemical synthesis takes place in the 3'-5' direction (reverse of the biological polymerization reaction) and uses phosphoramidite building blocks derived from protected 2'-deoxynucleosides (dA, dC, dG, and T), ribonucleosides (A, C, G, and U). To obtain the desired oligonucleotide, the building blocks are sequentially coupled to the growing oligonucleotide chain in the order required by the sequence of the product. Upon

completion of the chain assembly, the product is released from the solid phase to solution, deprotected, and collected.

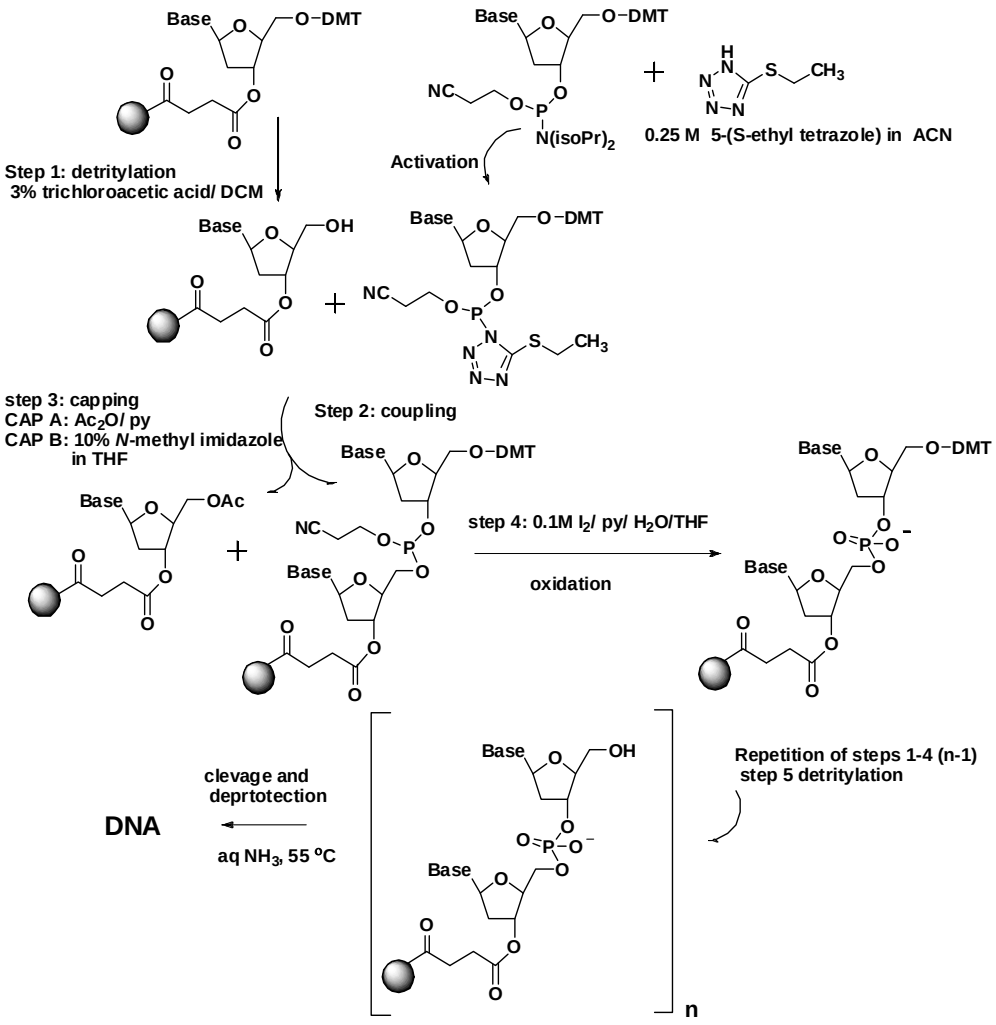

Scheme 10. Solid phase synthesis of DNA

A series of chimeric oligonucleotides (Table 6) containing one or two dimer blocks incorporated at predetermined positions were synthesized using the phosphoramidite approach on an automated Bioautomation MM4 DNA synthesizer. We used extended coupling time for the modified dimer phosophoramidites **12a, 12b**, **12c** and **19** (Figure 45). The modifications are abbrivated as **T-$_{D\text{-}Pro}$-T**, **T-$_{L\text{-}Pro}$-T**, **T-$_{Gly}$-T** and **T-$_{D\text{-}Pro}$-U$^{2'\text{-}OMe}$** in modified oligonucleotides. Control 18mer oligonucleotide **DNA1** chosen was specific for the Splice correction of an aberrant β-globin intron (705 site). Chronic myeloid leukemia (CML) is probably the most extensively studied human malignancy. The discovery of the Philadelphia (Ph) chromosome in 1960 as the first consistent

chromosomal abnormality associated with a specific type of leukemia was a breakthrough in cancer biology.[57] The control 19mer oligonucleotide **DNA2** is the antisense sequence for bcr/abl gene which is responsible for chronic myeloid leukemia.[58] To study the antisense activity modified ONs have been synthesized and are listed in Table 6.

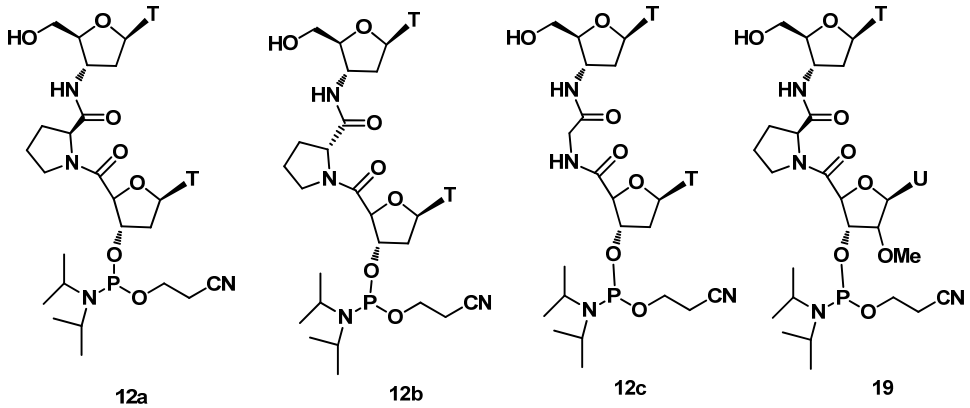

Figure 45. Modified dimer phosphoramidite building blocks

2.3.2a Purification and MALDI-TOF characterization of modified oligomers

The synthesized oligonucleotides were cleaved from the solid support with conc. NH_4OH, lyophilized and desalted to get the crude oligonucleotides. The purity of the oligomers listed in Table 6 was checked by analytical RP-HPLC (C18 column, 0.1 N TEAA Buffer-acetonitrile) which showed more than 75-80% purity. These oligomers were subsequently purified by reverse phase HPLC on a C18 column. The purity of the oligomers was again ascertained by analytical RP-HPLC and found to be > 95%. Their integrity was confirmed by MALDI-TOF mass spectrometric analysis. THAP (2,4,6-trihydroxy acetophenone) matrix with diammonium citrate as additive was used for MALDI-TOF (matrix assisted laser desorption ionization time-of-flight) mass analysis of oligomers. HPLC retention time and observed values of mass in MALDI-TOF spectrometry are listed in Table 6.

Table 6. List of Oligomers synthesized with their HPLC retention times and MALDI - TOF values

Code	Sequences	HPLC t_R (min)	Exp Mass	Obs Mass
ON1	5'CCT CTT ACC TCA G**T$_{D\text{-}Pro}$T** ACA3'	11.2	5400.65	5403.41
ON2	5'CCT CTT ACC TCA G**T$_{L\text{-}Pro}$T** ACA3'	11.4	5400.65	5403.62
ON3	5'CCT CTT ACC TCA G**T$_{Gly}$T** ACA3	11.0	5360.62	5354.46
ON4	5'CCT CTT ACC TCA G**T$_{D\text{-}Pro}$U$^{2'OMe}$** ACA3	13.7	5416.64	5417.32
ON5	5'CCT C**T$_{D\text{-}Pro}$T** ACC TCA G**T$_{D\text{-}Pro}$T** ACA3'	11.3	5431.74	5429.07
ON6	5'CCT C**T$_{L\text{-}Pro}$T** ACC TCA G**T$_{L\text{-}Pro}$T** ACA3'	11.5	5431.74	5433.63
ON7	5'CCT C**T$_{Gly}$T** ACC TCA G**T$_{Gly}$T** ACA3'	11.2	5351.68	5341.43
ON8	5'GAA GGG CTT **T$_{D\text{-}Pro}$T**G AAC TCT T3'	10.8	5864.95	5866.67
ON9	5'GAA GGG CTT **T$_{L\text{-}Pro}$T**G AAC TCT T3'	10.9	5864.95	5868.31
ON10	5'GAA GGG CTT **T$_{Gly}$T**G AAC TCT T3'	10.6	5824.91	5814.90
ON11	5'GAA GGG CTT **T$_{D\text{-}Pro}$U$^{2'OMe}$** G AAC TCT T3'	13.1	5880.95	5880.57
ON12	5'GAA GGG C**T$_{D\text{-}Pro}$U$^{2'OMe}$ T$_{D\text{-}Pro}$U$^{2'OMe}$** G AAC TCT T3'	12.9	5928.03	5926.96

2.3.2b Synthesis of complementary oligonucleotides

The DNA oligonucleotides **DNA1-DNA6** were synthesized on a Bioautomation MM4 DNA synthesizer using standard β-cyanoethyl phophoramidate chemistry (Table 7). The oligomers were synthesized in the 3' to 5' direction on a polystyrene solid support, followed by ammonia treatment. The oligonucleotides were desalted by gel filtration; their purity ascertained by RP-HPLC on a C18 column was found to be more than 95% and these were used without further purification in the biophysical studies of T-$_{(\alpha\text{-amino acid})}$-T/U$^{2'\text{-}OMe}$ modified sequences. The RNA oligonucleotides **RNA1-RNA4** were obtained commercially.

Table 7. DNA/RNA oligonucleotides used in present work

Entry	Sequence(5'→3')	Type
DNA1	5'CCT CTT ACC TCA GTT ACA 3'	Control 18mer seq
DNA2	5' TGT AAC TGA GGT AAG AGG 3'	Complementary to 18mer seq
DNA3	5' TGT AAC TGA GGT ATG AGG 3'	Mismatch to 18mer seq
DNA4	5'GAA GGG CTT TTG AAC TCT T 3'	Control 19mer seq
DNA5	5'AAG AGT TCA AAA GCC CTT C 3'	Complementary to 19mer seq
DNA6	5'AAG AGT TCT AAA GCC CTT C 3'	Mismatch to 19mer seq
RNA1	5'UGU AAC UGA GGU AAG AGG 3'	Complementary to 18mer seq
RNA2	5'UGU AAC UGC GGU AAG AGG 3'	Mismatch to 18mer seq
RNA3	5'AAG AGU UCA AAA GCC CUU C 3'	Complementary to 19mer seq
RNA4	5'AAG AGU UCU AAA GCC CUU C 3'	Mismatch to 19mer seq

2.3.3 Biophysical studies of T-$_{(\alpha\text{-amino acid})}$-T/U$^{2'\text{-OMe}}$ modified oligomers

UV-T_m studies were carried out to investigate the effect of chiral amino acid that replace the phosphodiester linker acids in the dimers, on the binding efficiency of the modified oligomers to complementary DNA and RNA sequences. The T_m experiments of duplexes were carried out in 10 mM sodium phosphate buffer (pH 7.2) containing 100 mM NaCl and 0.1 mM EDTA. Chimeric DNA oligonucleotides were individually hybridized with the complementary DNA and RNA strands, to obtain duplexes.

2.3.3a UV-T_m of T-$_{(\alpha\text{-amino acid})}$-T/U$^{2'\text{-OMe}}$ modified 18mer oligonucleotides

The binding affinity of 18mer chimeric ONs (**ON2-ON8**) with complementary DNA and RNA was investigated by measuring the melting temperatures (T_m) of the duplexes and the results are summarized in Table 8**.** The unmodified 18 mer **DNA1** sequence forms complexes with complementary **DNA2** and **RNA1** with higher melting temperature for DNA:RNA complex over DNA:DNA (ΔT_m= +3.8 ºC, Table 8, entry 1). Oligomer **ON1** bearing single T-$_{D\text{-proline}}$-T dimer unit towards 3'-end was found to have affinity with DNA and RNA similar to the unmodified oligomers (ΔT_m = -1.1°C, Table 8, entry 2). In comparison, T-$_{L\text{-Proline}}$-T dimer-bearing oligomer **ON2** destabilized the

duplexes (ΔT_m = -5-6°C, Table 8, entry 3). The T-$_{Glycine}$-T dimer-bearing oligomer **ON3** was less destabilized the duplexes (ΔT_m = -2.2-3.2°C, Table 8, entry 4) as compared to T-$_{L\text{-}Proline}$-T dimer modified oligonucleotide. The **ON4**:**DNA2** and **ON4**:**RNA1** duplexes were slightly destabilized (ΔTm = -1.3 and -1.4 °C respectively, Table 8, entry 5) and this could be because of the incorporation of uridine in place of thymidine.[59]

Table **8**. T_m (°C) values of 18mer chimeric ONs with complementary DNA/RNA duplexes

Entry	**Sequences**	**UV-T_m °C (ΔT_m °C)**	
		DNA 2	**RNA1**
1	**DNA1** 5'CCT CTT ACC TCA GTT ACA3'	52.8	56.6
2	**ON1** 5'CCT CTT ACC TCA G**T$_{D\text{-}pro}$T** ACA3'	**52.4** (-0.4)	**55.5** (-1.1)
3	**ON2** 5'CCT CTT ACC TCA G**T$_{L\text{-}pro}$T** ACA3'	47.8 (-5.0)	51.5 (-5.1)
4	**ON3** 5'CCT CTT ACC TCA G**T$_{Gly}$T** ACA3	49.6 (-3.2)	54.4 (-2.2)
5	**ON4** 5'CCT CTT ACC TCA G**T$_{D\text{-}pro}$U$^{2'OMe}$** ACA3'	**51.5** (-1.3)	**55.2** (-1.4)
6	**ON5** 5'CCT C**T$_{D\text{-}Pro}$T** ACC TCA G**T$_{D\text{-}Pro}$T** ACA3'	47.2 (-5.6)	53.2 (-3.4)
7	**ON6** 5'CCT C**T$_{L\text{-}Pro}$T** ACC TCA G**T$_{L\text{-}Pro}$T** ACA3'	40.3 (-12.5)	43.5 (-13.1)
8	**ON7** 5'CCT C**T$_{Gly}$T** ACC TCA G**T$_{Gly}$T** ACA3'	47.3 (-5.5)	48.8 (-7.8)

DNA2=5' TGT AAC TGA GGT AAG AGG 3'; **RNA1** = 5'UGU AAC UGA GGU AAG AGG 3', T_m = melting temperature (measured in the buffer 10 mM sodium phosphate, 100 mM NaCl, pH = 7.2), of T-$_{(\alpha\text{-amino acid})}$-T/U$^{2'\text{-}OMe}$ modified ONs:DNA/RNA complexes. The values reported here are the average of 3 independent experiments and are accurate to ±1.0°C. $\Delta T_m = T_m - T_{m(control)}$

Incorporation of two units of the modified dimers (**ON5-ON7**, Table 8, entries 6-8) were found to destabilize the duplexes, however the degree of destabilization was less with complementary **RNA1** in case of T-$_{D\text{-}Proline}$-T modified oligomers **ON5** (ΔT_m = -3.4 ºC, Table 8, entry 6) as compared to T-$_{L\text{-}Proline}$-T modified **ON6** (ΔT_m = -13.1 ºC, Table 8, entry 7) and T-$_{Glycine}$-T modified oligomer **ON7** (ΔT_m = -13.1 ºC, Table 8, entry 8).

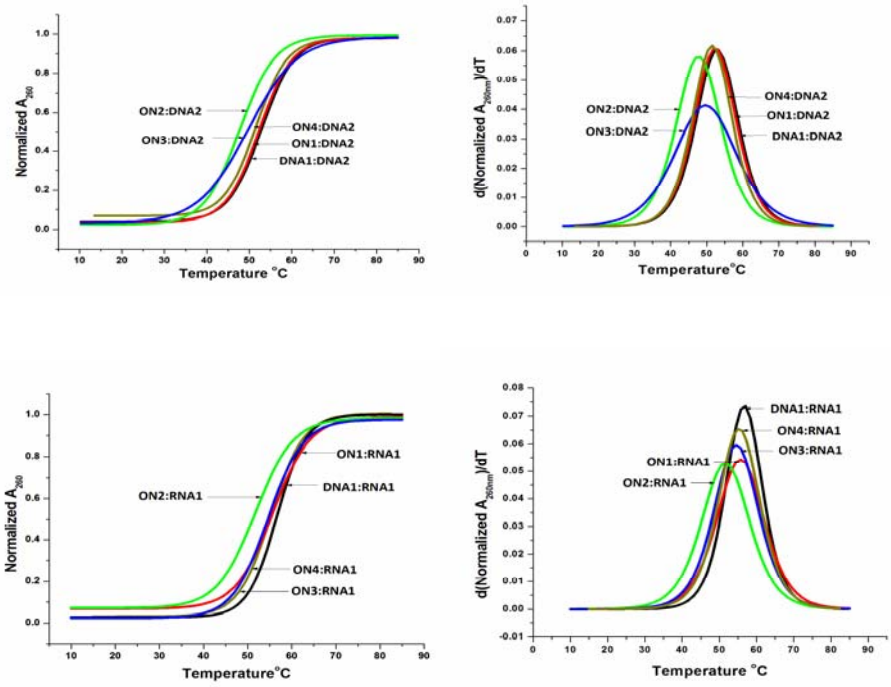

Figure 46: Melting curves for **ON1-ON4** oligomers with complementary DNA/RNA and corresponding first derivative curves.

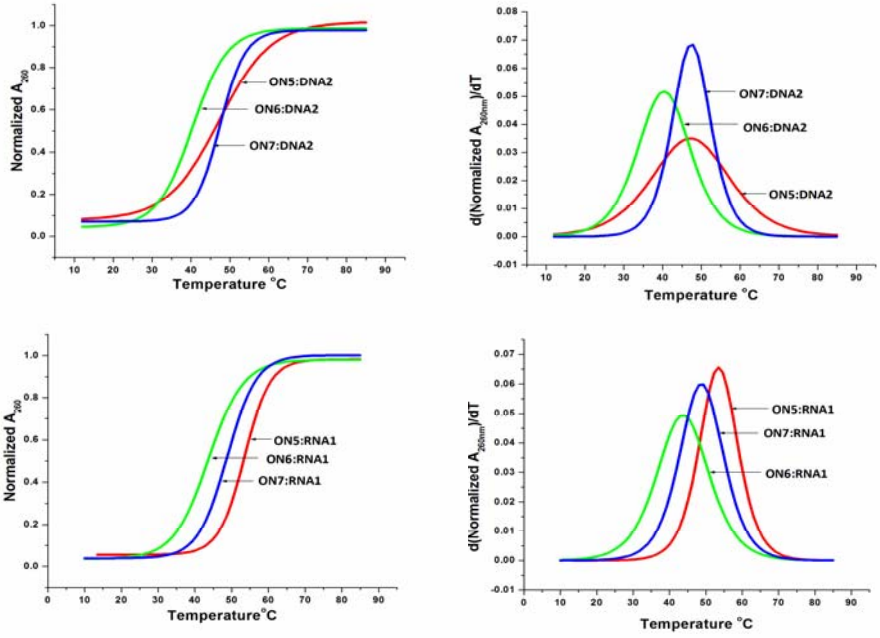

Figure 47: Melting curves for **ON5-ON7** oligomers with complementary DNA/RNA and corresponding first derivative curves.

The thermal stabilities of T-$_{(\alpha\text{-amino acid})}$-T/U$^{2'\text{-OMe}}$ oligonucleotides **ON1-ON7** with **DNA3** and **RNA3** containing single mismatch in the sequence were studied (Table 9). For oligonucleotides **ON1-ON4**, the decrease of binding affinity was 8.4 ºC, 7.9 ºC, 8.2 ºC and 7.9 ºC respectively when they are hybridized mismatch **DNA3** (Table 9, entries 2-5). Increase in destabilization is more (9 °C to 12 °C), when we studied the binding with single base mismatch **RNA2** (Table 9, entries 2-5). For **ON5**, **6** and **7** having double modifications, there was a decrease of UV-melting temperature 10.9 ºC, 10.8 ºC and 12.4 ºC respectively with the single base mismatch **RNA 2** (Table 9, entries 6-8). The destabilization is less when they hybridized with single base mismatch **DNA3** (6.5 to 8.5 ºC, Table 9, entries 6-8). These results clearly indicate that these chimeric oligonucleotides hybridize with their complementary DNA/RNA through Watson-Crick H-bonding.

Table **9**. T_m (°C) values of 18mer chimeric ONs with mismatch complementary DNA/RNA

Entry	**Sequence**	**UV-T_m ^{o}C**	
		DNA3	**RNA2**
1	**DNA1** 5'CCT CTT ACC TCA GTT ACA3'	45.2 (-7.6)	46.2 (-10.4)
2	**ON1** 5'CCT CTT ACC TCA G**T$_{D\text{-}pro}$T** ACA3'	44.0 (-8.4)	44.8 (-10.7)
3	**ON2** 5'CCT CTT ACC TCA G**T$_{L\text{-}pro}$T** ACA3'	39.9 (-7.9)	40.6 (-10.9)
4	**ON3** 5'CCT CTT ACC TCA G**T$_{Gly}$T** ACA3	41.49 (-8.2)	42.3 (-12.1)
5	**ON4** 5'CCT CTT ACC TCA G**T$_{D\text{-}pro}$U$^{2'OMe}$** ACA3'	43.6 (-7.9)	45.7 (-9.5)
6	**ON5** 5'CCT C**T$_{D\text{-}Pro}$T** ACC TCA G**T$_{D\text{-}Pro}$T** ACA3'	40.7 (-6.5)	42.3 (-10.9)
7	**ON6** 5'CCT C**T$_{L\text{-}Pro}$T** ACC TCA G**T$_{L\text{-}Pro}$T** ACA3'	32.0 (-8.3)	32.7 (-10.8)
8	**ON7** 5'CCT C**T$_{Gly}$T** ACC TCA G**T$_{Gly}$T** ACA3'	40.5 (-6.8)	36.4 (-12.4)

DNA3=5' TGT AAC TGA GGT ATG AGG 3'; **RNA2** = 5'UGU AAC UGC GGU AAG AGG 3', T_m = melting temperature (measured in the buffer 10 mM sodium phosphate, 100 mM NaCl, pH = 7.2), of T-$_{(\alpha\text{-amino acid})}$-T/U$^{2'\text{-OMe}}$ modified ONs:mismatch DNA/RNA complexes. The values reported here are the average of 3 independent experiments and are accurate to ±1.0°C. Values in the parentheses denote the difference in the T_m due to mismatch in the DNA/RNA sequence.

2.3.3b UV-T_m of T-$_{(\alpha\text{-amino acid})}$-T/U$^{2'\text{-OMe}}$ modified 19mer oligonucleotides

The T-$_{(\alpha\text{-amino acid})}$-T/U$^{2'\text{-OMe}}$ dimers were also incorporated into a 19mer oligonucleotide sequence to study the effect on binding affinity and the results are tabulated in Table 10.

Table **10**. T_m (°C) values of 19mer chimeric ONs with complementary DNA/RNA

Entry	Sequences	UV-T_m ^{o}C (Δ T_m ^{o}C)	
		DNA 5	**RNA3**
1	**DNA4** 5'GAA GGG CTT TTG AAC TCT T3'	55.9 --	56.5 --
2	**ON8** 5'GAA GGG CTT **T-$_{D\text{-Pro}}$TG** AAC TCT T3'	**56.5** **(+0.6)**	**56.0** **(-0.5)**
3	**ON9** 5'GAA GGG CTT **T-$_{L\text{-Pro}}$-T** G AAC TCT T3'	50.9 (-5.0)	50.7 (-5.8)
4	**ON10** 5'GAA GGG CTT **T-$_{Gly}$-T** G AAC TCT T3'	53.5 (-2.4)	53.1 (-3.4)
5	**ON11** 5'GAA GGG CTT **T-$_{D\text{-Pro}}$-U$^{2'OMe}$** G AAC TCT T3'	**54.5** **(-1.4)**	**54.3** **(-1.7)**
6	**ON12** 5'GAA GGG C**T-$_{D\text{-Pro}}$-U$^{2'OMe}$ T$_{D\text{-pro}}$U$^{2'OMe}$** G AAC TCT T3'	50.5 (-5.4)	50.2 (-6.3)

DNA5=5'AAG AGT TCA AAA GCC CTT C 3'; **RNA3** = 5'AAG AGU UCA AAA GCC CUU C 3', T_m = melting temperature (measured in the buffer 10 mM sodium phosphate, 100 mM NaCl, pH = 7.2), of T-$_{(\alpha\text{-amino acid})}$-T/U$^{2'\text{-OMe}}$ modified ONs:DNA/RNA complexes. The values reported here are the average of 3 independent experiments and are accurate to ±1.0°C. $\Delta T_m = T_m - T_{m(control)}$

The unmodified 19mer **DNA4** sequence forms complexes with complementary **DNA5** and **RNA3** with nearly similar melting temperature (Table 10, entry 1). The duplexes of **ON8** with single modified dimer block having D-proline (Table 10, entry 2) showed binding with complementary **DNA5** and **RNA3** (ΔT_m = +0.6 ºC and -0.5 ºC respectively, Table 10, entry 2) as good as the control sequence. The **ON9** modified with T-$_{L\text{-Proline}}$-T dimer showed destabilization of the duplexes both with **DNA5** and **RNA3** (ΔT_m= -5 and -5.8 ºC respectively, Table 10, entry 3). The T-$_{Glycine}$-T modified **ON10** also showed little destabilization both with **DNA5** (ΔT_m = -2.4 ºC, Table 10, entry 4) and **RNA3** (ΔT_m = -3.4 ºC, Table 10, entry 4), but the degree of destabilization was less as compared to **ON9**. Introduction of a single T-$_{D\text{-Proline}}$-U$^{2'\text{-OMe}}$ dimer unit in **ON11 (**Table 10, entry 5), showed a destabilization of 1.4 ºC and 1.7 ºC with complementary **DNA5** and **RNA3** respectively. A cumulative effect was observed in destabilization in the **ON12:DNA5/RNA3** when two units of T-$_{D\text{-Proline}}$-U$^{2'\text{-OMe}}$ dimer

units were incorporated (Table 10, entry 6). Overall, in **ON9-ON12** showed more destabilization with RNA as compared to DNA.

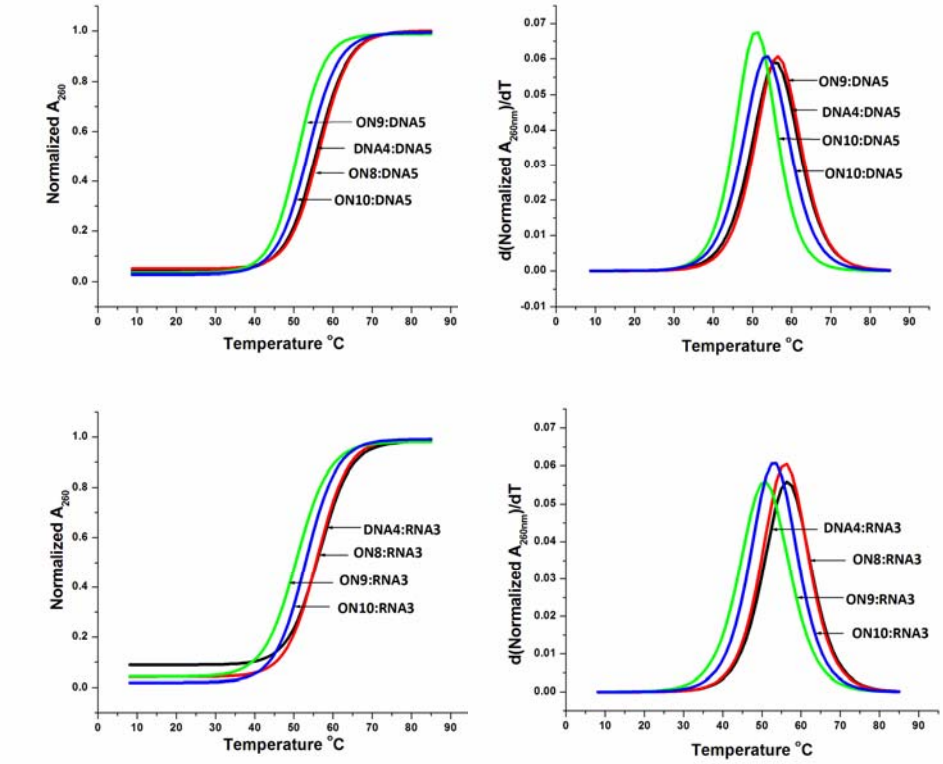

Figure 48: Melting curves for **ON8-ON10** oligomers with complementary **DNA5/RNA3** and corresponding first derivative curves.

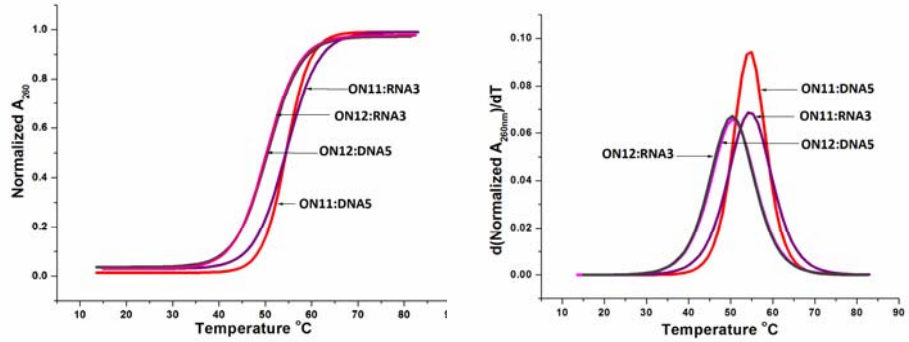

Figure 49: Melting curves for **ON11-ON12** oligomers with complementary **DNA5/RNA3** and corresponding first derivative curves.

The thermal stabilities of T-$_{(\alpha\text{-amino acid})}$-T/U$^{2'\text{-OMe}}$ oligonucleotides **ON8-ON11** with **DNA6** and **RNA4** containing single mismatch in the middle of sequence were studied

(Table 11, entries 2-5). Oligomer with either D-proline or glycine containing dimer which stabilizes duplexes with DNA and RNA, showed discrimination in mismatch binding studies with both single mismatch **DNA6** and **RNA4** with destabilization of 6 °C to 9 °C (Table 11, entry 2, 4 and 5). Melting studies indicate that single modified T-$_{D\text{-Proline}}$-T sequences showed better binding to DNA and RNA as compared to T-$_{L\text{-Proline}}$-T and T-$_{Glycine}$-T modified oligomers.

Table **11**. T_m (°C) values of 19mer chimeric ONs with mismatch complementary DNA/RNA

Entry	**Sequences**	**UV-T_m °C**	
		DNA6	**RNA4**
1	**DNA4** 5'GAA GGG CTT TTG AAC TCT T3'	50.3 (-5.6)	48.3 (-8.2)
2	**ON8** 5'GAA GGG CTT **T-$_{D\text{-Pro}}$TG** AAC TCT T3'	50.4 (-6.1)	48.7 (-7.3)
3	**ON9** 5'GAA GGG CTT **T-$_{L\text{-Pro}}$-T** G AAC TCT T3'	47.7 (-3.2)	47.9 (-2.8)
4	**ON10** 5'GAA GGG CTT **T-$_{Gly}$-T** G AAC TCT T3'	47.0 (-6.5)	46.1 (-7.0)
5	**ON11** 5'GAA GGG CTT **T-$_{D\text{-Pro}}$-U$^{2'OMe}$** G AAC TCT T3'	45.6 (-8.9)	47.0 (-7.3)

DNA6=5'AAG AGT TCT AAA GCC CTT C 3'; **RNA4** = 5'AAG AGU UCU AAA GCC CUU C 3', T_m = melting temperature (measured in the buffer 10 mM sodium phosphate, 100 mM NaCl, pH = 7.2), of T-$_{(\alpha\text{-amino acid})}$-T/U$^{2'\text{-OMe}}$ modified ONs with mismatch DNA/RNA complexes. The values reported here are the average of 3 independent experiments and are accurate to ±1.0°C. Values in the parentheses denote the difference in the T_m due to mismatch in the DNA/RNA sequence.

In summary, incorporation of the single dimer block containing D-Proline was found to be well accommodated in DNA:DNA and DNA:RNA duplexes as there no change in the UV-T_m values was observed (Table 8, entry 2 and 5 and Table 10, entry 2 and 5). Incorporation of second dimer block caused destabilization of duplexes, in most cases (Table 8, entry 6-8 and Table 10, entry 6). The intermittent replacement of the phosphodiester linkages probably causes discontinuity of the backbone structures, further destabilizing the duplexes. It is therefore necessary to study the fully amide linked backbone modified sequences with amino acids as internucleoside linker.

2.3.4 Summary

1. CD studies at the dimer level showed that D-Proline containing-dimer is well stacked as compared to L-Proline- or Glycine-containing dimers.

2. The stacking interactions in D-Proline and L-Proline containing dimers could be arising from differently adopted conformations due to opposite chirality of the linker.

3. L-Lysine and D-Lysine dimers didnot show any drastic change in CD pattern due to opposite chirality as observed in case of D-Proline and L-Proline.

4. Chiral amide-linked dimers were incorporated into the DNA backbone by partial replacement of selected phosphodiester linkages.

5. The UV-T_m data shows that the dimer block having D-Proline as an internucleoside linker in the DNA backbone to stabilizes the ON:DNA and ON:RNA complexes better than L-Proline or glycine.

2.4 Experimental

General: All the reagents were purchased from Sigma-Aldrich and used without purification. DMF, CH_3CN were dried over P_2O_5 and CaH_2 respectively and stored by adding 4 Å molecular sieves. Pyridine, TEA were dried over KOH and stored by adding KOH. THF was passed over basic alumina and dried by distillation over sodium. Analytical TLCs were performed on Merck 5554 silica 60 aluminium sheets. Column chromatography was performed for purification of compounds on silica gel (60-120 mesh, Merck). TLCs were performed using dichloromethane-methanol or petroleum ether-ethyl acetate solvent systems. Visualization was accomplished with UV light and/or by spraying with perchloric acid reagent and heating. ^1H and ^{13}C NMR spectra were obtained using Bruker ACF 200 (200 MHz) or 400 (400 MHz) spectrometers and all the chemical shifts (δ/ppm) are referred to internal TMS/DMSO-d_6 for ^1H and chloroform-*d*/DMSO-d_6 for ^{13}C NMR. ^1H NMR data are reported in the order of chemical shift, multiplicity (s, singlet; d, doublet; t, triplet; br, broad; br s, broad singlet; m, multiplet and/ or multiple resonance), number of protons. Mass spectra were recorded on Thermo Finnigan Surveyor MS-Q spectrometer, while HRMS was recorded by using a Micromass Q-Tof micro (YA-105) spectrometer. RP-HPLC was carried out on a C18 column using Waters system (Waters Delta 600e quaternary solvent delivery system and 2998 photodiode array detector and Empower2 chromatography software). MALDI-TOF spectra were recorded on a Voyager-De-STR (Applied Biosystems) MALDI-TOF instrument. UV experiments were performed on a Varian Cary 300 UV-VIS spectrophotometer fitted with a Peltier-controlled temperature programmer and a water circulator.

Section 1

3'-Azido-5'-*O*-(4, 4'-dimethoxytrityl)-3'-deoxythymidine (2)

A mixture of Azidothymidine **1** (1 g, 3.74 mmol), dimethoxytrityl chloride (1.52 g, 4.49 mmol), DMAP (catalytic amount), triethyl amine (2.61 mL, 18.7 mmol) in 8 mL anhydrous pyridine was stirred at RT for 3 h. Pyridine was removed in *vacuo* and residue dissolved in 100 mL of ethyl acetate. The organic layer was washed with 10% $NaHCO_3$ solution (2 x 15mL) followed by water (2 x 30 mL). The organic layer was dried over anhydrous Na_2SO_4 and concentrated to

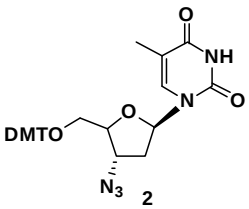

2

dryness. Column purification using 1% methanol-dichloromethane gave compound **2** (1.82 g, 90 %) as yellow foam.

^{1}H NMR (200MHz, $CDCl_3$): 8.68 (bs, 1H), 7.60 (s, 1H), 7.24-7.43 (m, 10H), 6.83-6.87 (d, 4H), 6.26 (t, *J*=6.44 Hz, 1H), 4.34 (q, 1H), 3.97 (m, 1H), 3.8 (s, 6H), 3.54-3.60 (m, 1H), 3.39-3.35 (m, 1H), 2.44 (m, 2H), 1.49 (s, 3H); **^{13}C NMR** (50MHz, $CDCl_3$): 163.7, 158.7, 150.2, 144.1, 135.1, 130.0, 128.0, 127.1, 113.3, 111.3, 87.0, 84.4, 83.4, 62.7, 60.5, 55.2, 37.9, 11.8; **MS (EI)** *m/z* 569.2274, found 592.50 (M+ Na^+).

3'-Amino-5'-*O*-(4, 4'-dimethoxytrityl)-3'-deoxythymidine (3)

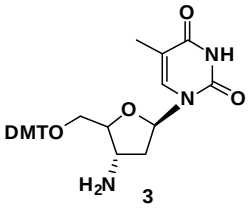

3

A mixture of 3'-azido-5'-*O*-(4, 4'-dimethoxytrityl)-3'-deoxythymidine **1** (1.8 g, 3.16 mmol) and 10% palladium on charcoal (0.180 g) in 10 mL ethyl acetate was stirred under hydrogen atmosphere (40 psi) at room temperature for 4 h. The reaction mixture was filtered through celite and the solvent was evaporated in vacuo to give 3'-amino-5'-*O*-(4, 4'-dimethoxytrityl)-3'-deoxythymidine 3 (1.46 g, 85%) as yellow foam.

^{1}H NMR (200MHz, $CDCl_3$): 7.60 (s, 1H), 7.27-7.44 (m, 10H), 6.82-6.86 (d, 4H), 6.28 (t, *J*=5.67 Hz, 1H), 3.78 (8H, singlet for 6H merged with other 2H), 3.33-3.59 (m, 2H), 2.23-2.36 (m, 2H), 1.50 (s, 3H).

5'-*O*-(4, 4'-dimethoxytrityl)-3'-[(*N*-Fmoc-L-prolyl)-amino]-3'-deoxythymidine (4a)

To *N*-Fmoc-L-proline (1.00 g, 2.96 mmol) in dry acetonitrile : dry DMF (4:1, 5mL), HBTU (1.34 g, 3.55 mmol), HOBt (0.20 g, 1.48 mmol) and diisopropyl ethyl amine (1.52 mL, 8.89mmol) were added under nitrogen atmosphere. This reaction mixture was allowed to stir for 15 min. 3'-Amino-5'-*O*-(4, 4'-dimethoxytrityl)-3'-deoxythymidine **3** (1.44 g, 2.66 mmol) dissolved in dry acetonitrile (5 ml) was added to the reaction mixture and further stirred for 2 h. The reaction mixture was concentrated to dryness, dissolved in ethyl acetate (100 mL) and washed with 5% $NaHCO_3$ solution (2 x 30 mL). The organic layer was dried over Na_2SO_4 and concentrated. Compound was purified by column chromatography using 1.5-2.0% methanol in dichloromethane to afford **4a** (1.78 g, 78%) as a pale yellow foam.

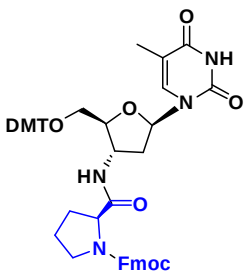

4a

^{1}H NMR (200MHz, $CDCl_3$): 9.95 (s, 1H), 8.33 (s, 1H), 7.78 (s, 1H), 7.75 (s, 1H), 7.65 (m, 2H), 7.25-7.41 (m, 17 H), 6.81 (d, *J*=8.84 Hz, 4H), 6.63 (t, *J*=8.4 Hz, 1H), 4.70 (s, 1H), 4.54 (m, 1H), 4.18-4.32 (m, 2H), 4.05 (s, 1H), 3.78 (s, 6H), 3.40-3.57 (m, 4H), 2.40-2.60 (m, 1H), 2,26-2.40 (m, 1H), 2.06-2.23 (m, 2H), 1.93 (m, 2H), 1.70 (s, 3H); **MS (EI)** *m/z* 862.3578, found 885.90 ($M+Na^+$).

5'-*O*-(4, 4'-dimethoxytrityl)-3'-[(*N*-Fmoc-D-prolyl)-amino]-3'-deoxythymidine (4b)

This compound was obtained in 82% yield as pale yellow foam by an analogous method described above in the synthesis of **4a**, except *N*-Fmoc-D-Proline as α-amino acid was utilized as the starting material.

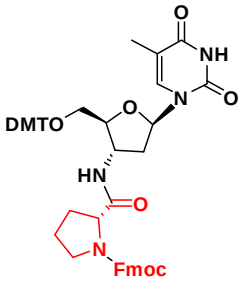

4b

^{1}H NMR (200MHz, $CDCl_3$): 9.88 (s, 1H), 8.34 (s, 1H), 7.78 (s, 1H), 7.75 (s, 1H), 7.65 (m, 2H), 7.25-7.44 (m, 16H), 6.79-6.84 (d, *J*=8.84 Hz, 4H), 6.63 (m, 1H), 4.69 (bs, 1H), 4.54 (m, 1H), 4.20-4.32 (m, 2H), 4.05 (s, 1H), 3.78 (s, 6H), 3.40-3.57 (m, 4H), 2.49-2.64 (m, 1H), 2.11-2.39 (m, 3H), 1.86-2.06 (m, 3H), 1.63 (s, 3H).

MS (EI) *m/z* 862.3578, found 885.87 ($M+Na^+$).

5'-*O*-(4, 4'-dimethoxytrityl)-3'-[(*N*-Fmoc-glycyl)-amino]-3'-deoxythymidine (4c)

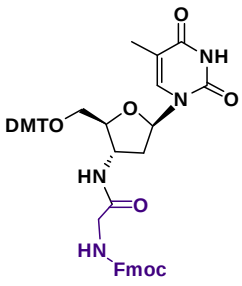

4c

This compound was obtained in 76% yield as pale yellow foam by an analogous method described above in the synthesis of **4a**, except *N*-Fmoc-Glycine as α-amino acid was utilized.

^{1}H NMR (200MHz, $CDCl_3$): 7.92 (s, 1H), 7.74 (s, 1H), 7.70 (s, 1H), 7.53 -7.62 (m, 3H), 7.19-7.40 (m, 15H), 6.77-6.82 (m, 4H), 6.40 (dd, *J*=7.96, 5.68 Hz, 1H), 5.80 (bs, 1H), 4.71 (s, 1H), 4.37 (s, 1H), 4.34 (s, 1H), 4.01-4.19 (m, 2H), 3.87 (m, 2H), 3.74 (s, 6H), 3.41 (m, 2H), 2.38 (m, 2H), 1.35 (s, 3H). **MS (EI)** *m/z* 822.3265, found 845.87 ($M+Na^+$).

5'-*O*-(4, 4'-dimethoxytrityl)-3'-(aminoacyl-amino]-3'-deoxythymidine (5a, 5b and 5c): Deprotection of Fmoc group, general procedure

5'-*O*-(4,4'-dimethoxytrityl)-3'-[(*N*-Fmoc-aminoacyl)-amino]-3'-deoxythymidine **4a**/**4b**/**4c** (1.00 g) was dissolved in dry dichloromethane (10 mL). To it, diethyl amine (10 mL) was added and the reaction mixture was allowed to stir for 45 min.

Dichloromethane and diethyl amine were removed in vacuo and the residue co-distilled with dichloromethane. Isolation of the product **5a**/**5b**/**5c** with free amino group was obtained by simple precipitation using petroleum ether and used in next coupling reaction without further purification.

3', 5'-di-*O*-(*tert*-butyldimethylsilyl)thymidine (7)

Thymidine **6** (1.0 g, 4.13 mmol) was dissolved in dry DMF (10 mL), then TBS-Cl (1.49 g, 9.91mmol) and imidazole (1.40 g, 20.66 mmol) was added under nitrogen atmosphere. The reaction mixture was stirred at room temperature for 6 h. DMF was removed in vacuo. The residue was dissolved into ethyl acetate (100 mL), washed with several portions of water, dried over Na_2SO_4 and on concentration gave **7** (1.90 g, 95%) as a white solid.

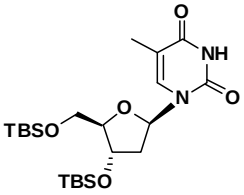

7

^{1}H NMR (200MHz, $CDCl_3$): 8.70 (bs, 1H), 7.49 (d, 1H, *J*=1.13Hz), 6.34 (dd, *J*=7.83, 5.81 Hz, 1H), 4.41 (m, 1H), 3.94 (m, 1H), 3.77-3.86 (m, 2H), 2.20-2-31(m, 1H), 1.96-2.07 (m, 1H), 1.92 (d, , *J*=1.13 Hz, 3H), 0.93 (s, 9H), 0.90 (s, 9H), 0.12 (s, 6H), 0.08 (s, 6H); **MS (EI)** *m/z* 470.2732, found 471.46 (M+ H^+), 493.45 (M+ Na^+).

3'-*O*-(*tert*-butyldimethylsilyl)thymidine (8)

Compound **7** (1.80 g, 3.82 mmol) was dissolved into 30 mL methanol and Pyridinium-p-toluene sulphonate (3.88 g, 15.28 mmol) was added. The reaction mixture was stirred at room temperature for 20 hrs. The solvent was removed in vacuo. The residue was dissolved into 50 mL of ethyl acetate, washed with water (3 x 25 mL) and then with brine. The organic layer dried over Na_2SO_4 and concentrated under reduced pressure. The resulting residue was chromatographed on silica gel column. The product was eluted with 30% ethyl acetate in petroleum ether to afford **8** (0.96 g, 70 %) as a white solid.

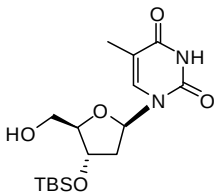

8

^{1}H NMR (200MHz, $CDCl_3$): 9.01 (bs, 1H), 7.38 (d, , *J*=1.26 Hz, 1H), 6.14 (t, J=6.82Hz, 1H), 4.49 (m, 1H), 3.71-3.95 (m, 3H), 2.78 (bs, 1H), 2.15-2.43 (m, 2H), 1.91 (d, *J*= 1.14 Hz, 3H), 0.89 (s, 9H), 0.09 (s, 6H); **^{13}C NMR** (50MHz, $CDCl_3$): 164.0, 150.4, 137.0, 110.9, 87.5, 86.7, 71.5, 61.8, 40.4, 25.6, 17.9, 12.4, -4.91; **MS (EI)** *m/z* 356.1767, found 379.29 (M+ Na^+).

3'-*O*-(*tert*-Butyldimethylsilyl)thymidine-4'-carboxylic acid (9)

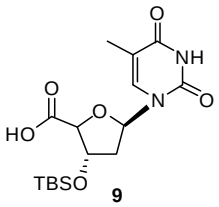

9

TEMPO (0.083 g, 0.53 mmol) and BAIB (1.89 g ,5.87 mmol) were added to the solution of 3'-*O*-(*tert*-butyldimethylsilyl)thymidine **8** (0.950 g, 2.66 mmol) in 1:1 acetonitrile: water (15 mL). The reaction mixture was allowed to stir at room temperature for 2 h. Acetonitrile was removed in vacuo. The reaction mixture was diluted with ethyl acetate (30 mL) and washed with several portions of water, dried over Na_2SO_4 and concentrated. The resulting residue was triturated sequentially with diethyl ether and acetone, filtered and dried in *vacuo*. The product obtained as white solid (0.940 g, 95 %).

^{1}H NMR (200MHz, $CDCl_3$ + drop of DMSO-D_6): 9.46 (bs, 1H), 8.17 (s, 1H), 6.47 (dd, *J*=9.35, 5.18 Hz, 1H), 4.56-4.56 (d, *J*=4.17 Hz, 1H), 4.39 (s, 1H), 2.18-2.28 (dd, 1H, J=13.26, 5.31 Hz, 1H), 1.90 (10H, singlet for 9H merged with multiplet for 1H), 0.10 (s, 3H), 0.08 (s, 3H); **MS (EI)** *m/z* 370.1360, found 393.79 (M+ Na^+).

Synthesis of 5'-*O*-DMT-T-$_{(L\text{-Proline})}$-T- 3'-*O*-TBS dimer (10a)

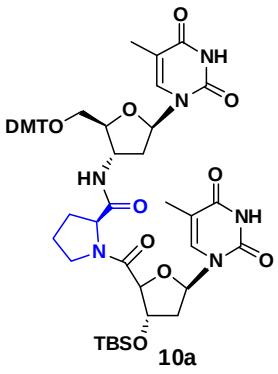

10a

To 3'-*O*-(*tert*-butyldimethylsilyl)thymidine-4'-carboxylic acid **9** (0.43 g, 1.15 mmol) in dry acetonitrile (5 mL), HBTU (0.527 g, 1.39 mmol), HOBt (0.08 g, 0.57 mmol) and DIPEA (0.6 mL, 3.47 mmol) were added and stirred for 15 min. Compound **5a** (0.736 g, 1.15 mmol) dissolved in dry acetonitrile (5 mL) was then added to the reaction mixture and further stirred at room temp for 2 h. The reaction mixture was then concentrated to dryness, dissolved in ethyl acetate (30 mL) and washed with 5% $NaHCO_3$ (10 mL x 2). The organic layer was dried over anhydrous Na_2SO_4 and concentrated. This was purified by column chromatography using 1.5 % MeOH: CH_2Cl_2 to get the product **10a** (0.91 g, 80 %) as a white solid.

^{1}H NMR (200MHz, $CDCl_3$): 8.40 (s, 1H), 7.75 (s, 1H), 7.67 (s, 1H), 7.25 -7.37 (m, 11 H), 6.80-6.84 (d, *J*=8.97 Hz, 4H), 6.58 (dd, *J*= 7.71, 5.05 Hz, 1H), 6.46 (dd, *J*=8.34, 5.81 Hz, 1H), 4.62-4.78 (m, 2H), 4.45-4.54 (m, 2H), 4.05 (s, 1H), 3.79 (s, 6H), 3.69 (m, 2H), 3.42-3.67 (m, 2H), 2.42-2.61 (m, 2H), 2.18-2.33 (m, 2H), 1.93-2.11 (m, 4H), 1.83 (s, 3H), 1.37 (s, 3H), 0.90 (s, 9H), 0.11 (s, 6H); **MS (EI)** *m/z* 992.4351, found 1016.3969 ($M+H^+$+Na^+).

Synthesis of 5'-*O*-DMT-T-$_{(D\text{-}Proline)}$-T- 3'-*O*-TBS dimer (10b)

This compound was obtained in 82% yield as pale yellow foam by an analogous method described above in the synthesis of **10a**, except **5b** was utilized as the starting material.

MS (EI) *m/z* 992.4351, found 1016.6978 ($M+H^+ + Na^+$).

Synthesis of 5'-*O*-DMT-T-$_{(Glycine)}$-T- 3'-*O*-TBS dimer (10c)

This compound was obtained in 82% yield as pale yellow foam by an analogous method described above in the synthesis of **10a**, except **5c** was utilized as the starting material.

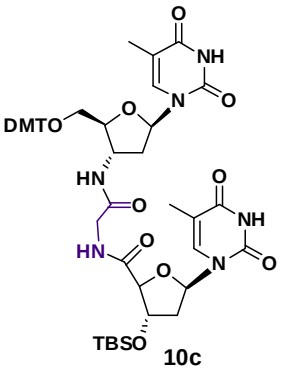

10c

^{1}H NMR (200MHz, $CDCl_3$): 7.72 (bs, 1H), 7.63 (bs, 2H), 7.36-7.41 (m, 2H), 7.20-7.29 (m, 7H), 6.82 (d, *J*=8.84 Hz, 4H), 6.51 (t, *J*= 5.69, 8.21 Hz, 1H), 5.98 (m, 1H), 4.89-5.04 (m, 1H), 4.77 (d, *J*= 4.45 Hz, 1H), 4.64 (s, 1H), 4.36 (s, 1H), 4.19 (s, 1H), 3.77 (s, 6H), 3.36 -3.68 (m, 3H), 2.42 (m, 2H), 2.02 (m, 2H), 1.87 (s, 3H), 1.40 (s, 3H), 0.90 (s, 9H), 0.15 (s, 3H), 0.13 (s, 3H); **MS (EI)** *m/z* 952.4038, found 977.535 ($M+H^+ + Na^+$).

Synthesis of 5'-*O*-DMT-T-$_{(L\text{-}Proline)}$-T-3'-OH dimer (11a)

A solution of compound **10a** (0.878 g, 1 mmol) and TBAF (0.394 g, 1.5 mmol) in anhydrous THF (10 mL) was stirred at RT for 1 h. THF was removed *in vacuo* and the residue redissolved in CH_2Cl_2 (50mL). The solution was washed with water (2 x 20 mL). The organic layer was dried over anhydrous Na_2SO_4 and evaporated to dryness. Silica gel column chromatography gave pure product **11a** (0.789 g, 84 %).

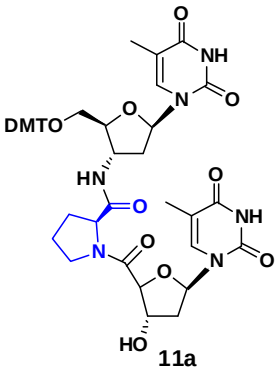

11a

^{1}H NMR (200MHz, $CDCl_3$): 10.47 (s, 1H), 9.91 (s, 1H), 8.05 (s, 1H), 7.64 (s, 1H), 7.28 (m, 9H), 6.81 (d, *J*=8.84 Hz, 4H), 6.47 (t, *J*=6.44, 6.07 Hz), 6.30 (t, *J*=6.45, 5.81 Hz, 1H), 4.68 (m, 3H), 4.53 (m, 1H), 4.05 (s, 1H), 3.78 (s, 8H), 3.43 (m, 2H), 1.90-2.50 (m, 8H), 1.84 (s, 3H), 1.33 (s, 3H); **MS (EI)** *m/z* 878.3487, found 901.7669 ($M+Na^+$).

5'-*O*-DMT-T-$_{(D\text{-}Proline)}$-T- 3'-OH dimer (11b)

This compound was obtained in 72% yield as a white solid via desilylation of **10b** (following the procedure as described in the synthesis of **11a**).

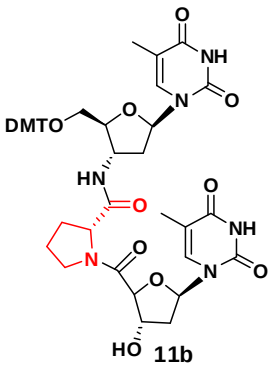

^{1}H NMR (500 MHz, D_2O+drop of DMSO-D_6): 10.04 (bs, 2H), 8.41 (s, 1H), 7.53 (s, 1H), 7.38 (d, *J*=8.37 Hz, 2H), 6.85 (m, 4H), 7.27 (m, 7H), 6.36 (dd, *J*= 9.08, 5.23Hz, 1H), 6.23 (t, *J*=6.53, 6.60 Hz, 1H), 5.84 (d, *J* = 3.54 Hz, 1H), 4.65 (s, 1H), 4.54 (m, 1H), 4.41 (s, 1H), 3.95 (s, 1H), 3.70 (s, 6H), 3.66 (m, 1H), 3.56 (m, 1H), 3.31 (m, 1H), 3.16 (m, 1H), 2.35 (m, 1H), 2.05-2.23 (m, 3H), 1.86 (m, 3H), 1.77 (m, 1H), 1.56 (s, 3H), 1.37 (s, 3H); **MS (EI)** *m/z* 878.3487, found 902.3909 ($M+H^+$+Na^+).

5'-*O*-DMT-T-$_{(Glycine)}$-T-3'-OH dimer (11c)

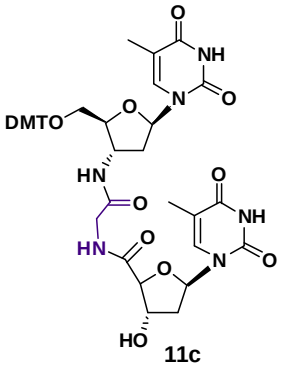

This compound was obtained in 73% yield as a white solid via desilylation of **10c** (following the procedure as described in the synthesis of **11a**).

^{1}H NMR (200MHz, DMSO-D_6): 8.07 (s, 1H), 7.57 (s, 1H), 7.39 (d, *J*= 7.53 Hz, 2H), 7.27 (m, 7H), 6.90 (m, 4H), 6.39 (dd, *J*= 8.28, 6.52 Hz, 1H), 6.24 (t, *J*= 6.53 Hz, 1H), 5.67 (d, *J*=4.02 Hz, 1H), 4.51 (m, 1H), 4.41 (s, 1H), 4.33 (s, 1H), 3.93 (s, 1H), 3.81 (dd, *J*= 16.57, 6.05 Hz, 1H), 3.73 (s, 6H and m, 1H overlapping), 3.30 (m, 1H), 3.31 (m, 1H), 2.39 (m, 1H), 2.21 (m, 1H), 2.09 (m, 2H), 1.72 (s, 3H), 1.46 (s, 3H); **MS (EI)** *m/z* 838.3174, found 862.9564 ($M+H^+$+Na^+).

General procedure for the synthesis of phospharamidite derivatives of amino acid linked dimers (12a, 12b, 12c)

Compound **11a**/**11b**/**11c** (1 mmol) was dissolved in dry DCM (10 mL) followed by the addition of diisopropyl ethyl amine (0.42 mL, 2.5 mmol) and chloro (2-cyanoethoxy) (*N, N*diisopropylamino)-phosphine (0.44 mL, 2 mmol) and the reaction mixture was stirred at room temperature for 2 h. The contents were then diluted with dry DCM and washed with 5% $NaHCO_3$ solution. The organic phase was dried over anhydrous Na_2SO_4 and concentrated to foam. The residue was dissolved in DCM and precipitated

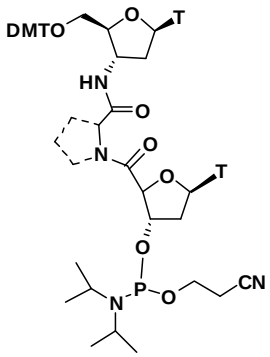

12a, 12b and 12c

with hexane to obtain **12a**/**12b**/**12c**. The phosphoramidite **12a**/**12b**/**12c** was dried overnight over P_2O_5 and KOH in a desiccator before applying on DNA synthesizer. TLC shows two close moving spots for two diastereomers (Rf =0.5, 5 % methanol-dichlromethane).

5'-*O*-(4, 4'-dimethoxy) trityl-T-$_{(L\text{-Proline})}$-T-3'-O-(2-cyanoethyl-*N*, *N*'-diisopropylphoshoramidate)-dimer (12a)

This compound was obtained in 80% yield starting from **11a**.

^{31}P NMR (400MHz, $CDCl_3$) δ 150.28, 148.20

MS (EI) *m/z* 1078.4565, found 1101.71 ($M+Na^+$).

5'-*O*-(4, 4'-dimethoxy) trityl-T-$_{(D\text{-Proline})}$-T-3'-O-(2-cyanoethyl-*N*, *N*-diisopropylphoshoramidate)-dimer (12b)

This compound was obtained in 82% yield starting from **11b**.

^{31}P NMR (400MHz, $CDCl_3$) δ 150.37, 148.44

MS (EI) *m/z* 1078.4565, found 1101.67 ($M+Na^+$).

5'-*O*-(4, 4'-dimethoxy) trityl-T-$_{(Glycine)}$-T-3'-O-(2-cyanoethyl-*N*, *N*-diisopropylphoshoramidate)-dimer (12c)

This compound was obtained in 78% yield starting from **11c**.

^{31}P NMR (400MHz, $CDCl_3$) δ 148.80, 148.28

General procedure for synthesis of 5', 3' –OH free T-$_{(\alpha\text{-amino acid})}$-T (Ia, Ib, Ic)

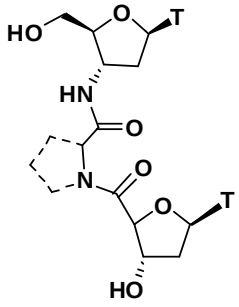

Ia, Ib and Ic

The 5'-*O*-DMT-T-$_{(\alpha\text{-amino acid})}$-T-3'-OH dimer **11a**/**11b**/**11c** (0.2 mmol) was dissolved in 3% dichloroacetic acid (5 mL) and 20 µL triisopropyl silane was added as scavenger. Reaction was stirred for ½ hr. The reaction mixture was concentrated and the product was recovered by successive trituration with acetone and diethyl ether to afford **Ia**/**Ib**/**Ic** as a white solid in 63-65% yield. ^{1}H NMR recorded in D_2O on 400 MHz for these dimers and values are reported in Table 1 in Section 1.

5', 3'–OH free T-$_{(L\text{-}Proline)}$-T (Ia)

^{13}C NMR (100MHz, $CDCl_3$): 173.9, 170.9, 169.8, 166.7, 151.9, 151.7, 137.8, 137.4, 111.3, 111.2, 85.9, 84.6, 84.0, 83.4, 73.4, 68.3, 60.7, 48.7, 47.6, 37.9, 36.1, 29.3, 24.6, 11.6, 11.5; **MS (EI)** *m/z* 576.2180, found 577.56 ($M+H^+$), 599.55 ($M+Na^+$); **HRMS** (ESI) calcd for $C_{25}H_{33}N_6O_{10}$: 577.2258 ($M+H^+$), found 577.2268.

5', 3'–OH free T-$_{(D\text{-}Proline)}$-T (Ib)

MS (EI) *m/z* 576.2180, found 577.48 ($M+H^+$), 599.47 ($M+Na^+$);

HRMS (ESI) calcd for $C_{25}H_{33}N_6O_{10}$: 577.2258 ($M+H^+$), found 577.2263

5', 3'–OH free T-$_{(Glycine)}$-T (Ic)

MS (EI) *m/z* 536.1867, found 537.44 ($M+H^+$), 559.42 ($M+Na^+$);

HRMS (ESI) calcd for $C_{22}H_{28}N_6O_{10}$: 537.1945 ($M+H^+$), found 537.1969

Section 2

3', 5'-di-*O*-(*tert*-butyldimethylsilyl)-2'-OMe-uridine (14)

This compound was obtained in 80% yield as a white solid by an analogous method described above in the synthesis of **7**, except 2'-OMe-uridine **(13)** was utilized as the starting material.

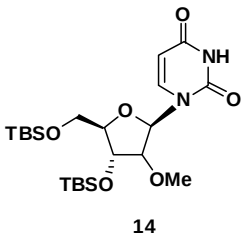

14

^{1}H NMR (200MHz, $CDCl_3$): 8.68 (s, 1H, exchanges with D_2O), 8.05 (d, *J*= 8.08 Hz, 1H), 5.94 (d, *J*= 1.52 Hz, 1H), 5.74 (d, *J*= 8.08 Hz, 1H), 4.21-4.27 (m, 1H), 4.02-4.07 (m, 2H), 3.75-3.80 (m, 1H), 3.59-3.62 (m, 1H), 3.56 (s, 3H), 0.94 (s, 9H), 0.91 (s, 9H), 0.09-0.13 (s, 12H); **^{13}C NMR** (50MH*z*, $CDCl_3$): 163.4, 150.1, 140.1, 101.9, 87.4, 84.3, 83.8, 68.4, 60.7, 58.2, 25.9, 25.7, 18.4, 18.1, -5.5, -5.4, -4.8, - 4.5; **MS (EI)** *m/z* 486.2581, found 509.29 ($M+ Na^+$).

3'-*O*-(*tert*-butyldimethylsilyl)-2'-OMe-uridine (15)

This compound was obtained in 65% yield as a white solid by an analogous method described above in the synthesis of **8**, except 3', 5'-di-*O*-(*tert*-butyldimethylsilyl)-2'-OMe-uridine **(14)** was utilized as the starting material.

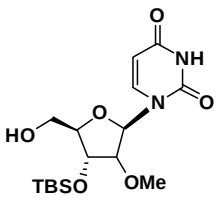

15

^{1}H NMR (200MHz, $CDCl_3$): 8.92 (s, 1H, exchanges with D_2O), 7.67 (d, *J*= 8.09 Hz, 1H), 5.72 (d, *J*= 8.08 Hz, 1H), 5.62 (d, *J*= 4.04 Hz, 1H), 4.36 (m, 1H), 3.95-4.08 (m, 3H), 3.76 (m, 1H), 3.49 (s, 3H), 2.74 (bs, 1H, exchanges with D_2O), 0.94 (s, 9H), 0.12 (s, 6H); **^{13}C NMR** (50MHz, $CDCl_3$): 163.7, 150.3, 142.0, 102.2, 90.7, 85.2, 82.6, 69.4, 60.8, 58.4, 25.6, 18.0, -4.7, -4.8; **MS (EI)** *m/z* 372.1717, found 395.08 (M+ Na^+).

3'-*O*-(*tert*-butyldimethylsilyl)-2'-OMe-uridine-4'-carboxylic acid (16)

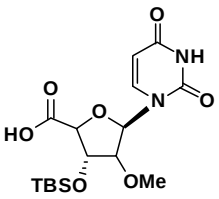

16

This compound was obtained in 93% yield as a white solid by an analogous method described above in the synthesis of **9**, except 3'-*O*-(*tert*-butyldimethylsilyl)-2'-OMe-uridine **(15)** was utilized as the starting materials.

^{1}H NMR (200MH*z*, $CDCl_3$): 8.22 (d, *J*= 8.21 Hz, 1H), 6.11 (d, J= 6.07 Hz, 1H), 5.77 (d, *J*= 8.08 Hz, 1H), 4.46 (m, 1H), 4.38 (m, 1H), 3.72 (m, 1H), 3.40 (s, 3H), 0.91 (s, 9H), 0.12 (s, 6H); **^{13}C NMR** (50MH*z*, $CDCl_3$): 172.8**,** 163.9, 150.6, 141.1, 102.8, 87.7, 87.6, 82.6, 73.1, 58.2, 25.4, 17.4, -5.05, -5.10; **MS (EI)** *m/z* 386.1509, found 385.23 (M^+ -1).

5'-ODMT-T-$_{(D\text{-}Proline)}$-U$^{2'\text{-}OMe}$-3'-OTBDMS (17)

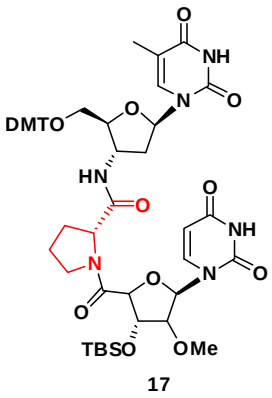

17

To 3'-*O*-(*tert*-butyldimethylsilyl)-2'-OMe-uridine-4'-carboxylic acid **16** (0.44 g, 1.15 mmol) in dry acetonitrile (5 mL), HBTU (0.44 g, 1.39 mmol), HOBt (0.08 g, 0.57 mmol) and DIPEA (0.6 mL, 3.47 mmol) were added and stirred for 15 min. Compound **5b** (0.736 g, 1.15 mmol) dissolved in dry acetonitrile (5 mL) was then added to the reaction mixture and further stirred at room temp for 2 h. The reaction mixture was then concentrated to dryness, dissolved in ethyl acetate (30 mL) and washed with 5% $NaHCO_3$ (10 mL x 2). The organic layer was dried over anhydrous Na_2SO_4 and concentrated. This was purified by column chromatography using 1.3% methanol in dichloromethane to get the product **17** (0.90 g, 78% %) as a white solid.

MS (EI) *m/z* 1008.4301, found 1031.60 (M+ Na^+).

5'-ODMT-T-$_{(D\text{-}Proline)}$-U$^{2'\text{-}OMe}$-3'-OH (18)

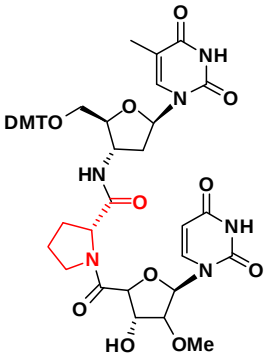

18

This compound was obtained in 75% yield as a white solid via desilylation of **17** (following the procedure as described in the synthesis of **11a**).

^{1}H NMR ($CDCl_3$, 200MHz): 8.26 (b, 1H), 7.78 (bs, 1H), 7.69 (s, 1H), 7.40 (d, I= 7.83 Hz, 2H), 7.26-7.30 (m, 8H), 6.82-6.85 (m, 4H), 6.65 (m, 1H), 5.96 (s, 1H), 5.55 (d, *J*= 8.07 Hz, 1H), 4.88 (m, 1H), 4.68 (m, 1H), 4.61 (m, 1H), 4.41 (t, *J*= 6.36 Hz, 1H), 4.05 (m, 2H), 3.77 (s, 6H), 3.65-3.74 (m, 2H), 3.58 (s, 3H), 3.40-3.47 (m, 2H), 2.48 (m, 1H), 2.23-2.36 (m, 2H), 2.11-2.16 (m, 2H), 1.97 (m, 1H), 1.23 (s, 3H); **MS (EI)** *m/z* 894.3436, found 917.45 (M+ Na^+).

5'-*O*-(4, 4'-dimethoxy) trityl-T-$_{(D\text{-}Proline)}$-U$^{2'\text{-}OMe}$-3'-O-(2-cyanoethyl-*N*, *N*-diisopropylphoshoramidate)-dimer (19)

This compound was obtained in 72% yield as white solid by an analogous method described above in the synthesis of **12a-12c**, except **18** was utilized as the starting material.

^{31}P NMR (400MHz, $CDCl_3$): 151.27, 149.91.

Synthesis of 5', 3'-free T-$_{(D\text{-}Proline)}$-U$^{2'\text{-}OMe}$ dimer (20)

Compound **20** was obtained in 70 % yield as a white solid by an analogous method described above in the synthesis of **Ia-Ic**, except **18** was utilized as the starting material.

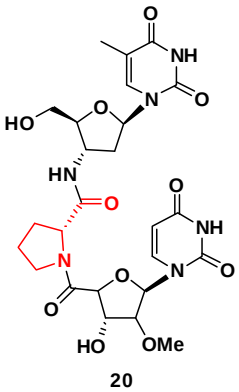

20

^{1}H NMR (400MHz, D_2O): 8.24 (d, *J*=8.28 Hz, 1H), 7.68 (s, 1H), 6.22 (dd, *J*= 5.8, 7.0 Hz, 1H), 6.15 (d, *J*= 5.02 Hz, 1H), 5.88 (d, *J*= 8.08 Hz, 1H), 4.92 (d, *J*= 4.02 Hz, 1H), 4.57 (d, *J*= 4.26 Hz, 1H), 4.48-4.53 (m, 1H), 4.39 (m, 1H), 4.00-4.06 (m, 2H), 3.85-3.89 (m, 1H), 3.71-3.81 (m, 3H), 3.48 (s, 3H), 2.27-2.49 (m, 3H), 1.90-2.05 (m, 3H), 1.88 (s, 3H); **^{13}C NMR** (100MHz, $CDCl_3$): 173.9, 169.2, 167.3, 166.8, 152.5, 151.8, 141.6, 137.4, 111.3, 102.4, 87.3, 84.6, 83.9, 82.5, 81.1, 70.7, 61.0, 60.7, 58.0, 48.6, 47.7, 36.1, 28.3, 24.4, 11.5 (extra peaks at 171.1 and 68.3 counts for dichloroacetic acid). **MS (EI)** *m/z* 592.2129, found 615.17 (M+ Na^+); **HRMS** (ESI) calcd for $C_{25}H_{33}N_6O_{11}$: 593.2207 (M+H^+), found 593.2196.

N^{ε} -Trifluoroacetyl-L-Lysine (23)

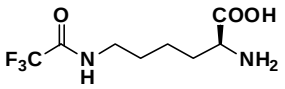

23

A solution of L-Lysine **21** (2 g, 10.92 mmol) in 7.64 mL of water and 4N aqueous sodium hydroxide (10.92 mmol) was cooled to about 5°C. To this solution (pH 10.4) ethyl trifluoroacetate (1.308 mL, 10.92 mL) was rapidly added with fast stirring. After the addition, the stirring was continued for two hours while maintaining inner temperature 5˚C. Finally the reaction mixture was filtered and washed with chilled water (50 mL) and 20 mL 99.5% ethanol. The resulting solid was desiccated overnight to give white powdery solid (1.62 g, 78%) with a trace amount of unreacted L-Lysine.

^{1}H NMR (200MHz, D_2O): 3.59 (t, 1H), 3.20 (t, 2H), 1.71 (m, 2H), 1.50 (m, 2H), 1.30 (m, 2H); **^{13}C NMR** (50MHz, $CDCl_3$): 174.7, 158.4, 118.6, 54.5, 39.3, 29.9, 27.3, 21.6; **MS (EI)** *m/z* 242.0878, found 242.95 (M^+).

N^{α}-Alloc-N^{ε} -Trifluoroacetyl-L-Lysine (25)

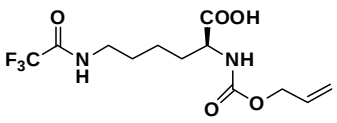

25

Allyl chloroformate (0.406 mL, 4.54 mmol) was added slowly to a stirred solution of N^{ε} -Trifluoroacetyl-L-Lysine (1 g, 4.13 mmol) and sodium carbonate (1.31 g, 12.39 mmol) in water (25 mL) at 0°C. The mixture was stirred for 12h during which time it was allowed to slowly attain room temperature. The reaction mixture was washed with ethyl acetate and the separated aqueous phase was acidified by addition of conc HCl. The resulting suspension was extracted with 2 % methanol in ethyl acetate two to three times. Ethyl acetate layer combined together dried over sodium sulphate and concentrated to afford N^{α}-Alloc-N^{ε} -Trifluoroacetyl-L-Lysine **25** (1.07 g, 80 %) as white solid.

^{1}H NMR (200MHz, $CDCl_3$): 6.68 (b, 1H), 5.90 (m, 1H), 5.21-5.40 (m, 2H), 4.60 (d, *J*= 5.56 Hz, 2H), 4.41 (m, 1H), 3.33-3.43 (dd, *J*= 12.88, 6.57 Hz, 2H), 1.40-1.99 (m, 6H); **^{13}C NMR** (50MHz, $CDCl_3$): 174.5, 158.0, 156.3, 132.3, 118.6, 117.8, 65.8, 53.2, 39.4, 31.8, 27.7, 22.1.

N^{ε} -Trifluoroacetyl-D-Lysine (24)

N^{ε} -Trifluoroacetyl-D-Lysine **24** was obtained in 78% yield as a white solid starting from D-Lysine **22** by an analogous method described for compound **23**.

N^{α}-Alloc-N^{ε} -Trifluoroacetyl-D-Lysine (26)

N^{ε}-Trifluoroacetyl-D-Lysine **26** was obtained in 81% yield as a white solid starting from N^{ε}-Trifluoroacetyl-D-Lysine **24** by an analogous method described for compound **25**.

5'-*O*-(4, 4'-dimethoxytrityl)-3'-[(N^{α}-Alloc-N^{ε}-Trifluoroacetyl-L-Lysyl)-amino]-3'-deoxythymidine (27)

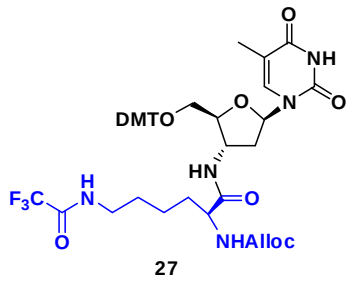

27

To N^{α}-Alloc-N^{ε}-Trifluoroacetyl-L-Lysine **25** (1.00 g, 2.92 mmol) in dry acetonitrile : dry DMF (4:1, 5mL), TBTU (1.12 g, 3.50 mmol), HOBt (0.197 g, 1.46 mmol) and diisopropyl ethyl amine (1.51 mL, 8.76 mmol) were added under nitrogen atmosphere. This reaction mixture was allowed to stir for 15 min. 3'-Amino-5'-*O*-(4, 4'-dimethoxytrityl)-3'-deoxythymidine **3** (1.42 g, 2.62 mmol) dissolved in dry acetonitrile (5 ml) was added to the reaction mixture and further stirred for 2 h. The reaction mixture was concentrated to dryness, dissolved in ethyl acetate (100 mL) and washed with 5% $NaHCO_3$ solution (2 x 30 mL). The organic layer was dried over Na_2SO_4 and concentrated. Compound was purified by column chromatography using 35% ethyl acetate in petroleum ether to afford **27** (1.78 g, 80%) as a pale yellow foam.

^{1}H NMR (200MH*z*, $CDCl_3$): 8.03 (bs, 1H), 7.64 (s, 1H), 7.37 (m, 2H), 7.21-7.27 (m, 8H), 6.79 (m, 4H), 6.46 (m, 1H), 5.80-5.92 (m, 1H), 5.70 (m, 1H), 5.25 (d, *J*= 17.07 Hz, 1H), 5.17 (d, *J*= 10.29 Hz, 1H), 4.72 (m, 1H), 4.50-4.57 (m, 2H), 4.17 (m, 1H), 3.98 (s, 1H), 3.77 (s, 6H), 3.25-3.30 (m, 2H), 3.17 (m, 1H), 2.47-2.52 (m, 1H), 2.27-2.32 (m, 1H), 1.69-1.77 (m, 1H), 1.52-1.65 (m, 3H), 1.33 (s, 3H); **^{13}C NMR** (100MHz, $CDCl_3$): 172.1, 164.0, 158.6, 156.4, 151.4, 144.1, 135.5, 135.2, 135.1, 132.2, 130.1, 129.0, 128.1, 127.9, 127.1, 118.1, 113.2, 112.2, 87.0, 85.3, 84.2, 66.1, 64.1, 55.2, 54.1, 51.4, 39.4, 38.5, 31.9, 27.9, 22.3, 11.3; **MS (EI)** *m/z* 851.3353, found 874.37 ($M+Na^+$).

5'-*O*-(4,4'-dimethoxytrityl)-3'-[(N^{α}-Alloc-N^{ε}-Trifluoroacetyl-D-Lysyl)-amino]-3'-deoxythymidine (28)

Compound **28** was obtained in 80% yield as a pale yellow foam by an analogous method described for compound **27**, except N^{α}-Alloc-N^{ε}-Trifluoroacetyl-D-Lysine **26** was utilized as starting material

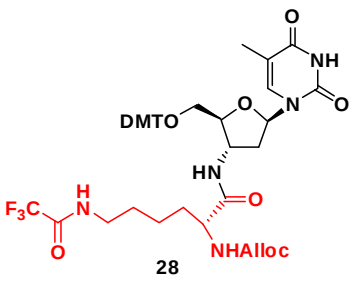

28

.**^{1}H NMR** (200MHz, $CDCl_3$): 7.90 (bs, 1H), 7.62 (s, 1H), 7.39 (m, 2H), 7.22-7.29 (m, 8H), 6.81 (d, *J*= 8.78 Hz, 4H), 6.41 (m, 1H), 5.85 (m, 1H), 5.57 (m, 1H), 5.24 (d, *J*=17.32 Hz, 1H), 5.18 (d, *J*= 10.29 Hz, 1H), 4.81 (m, 1H), 4.51-4.57 (m, 2H), 4.18 (m, 1H), 3.97 (s, 1H), 3.78 (s, 6H), 3.31-3.45 (m, 3H), 3.17 (m, 1H), 2.43 (m, 1H), 2.29 (m, 1H), 1.84 (m, 2H), 1.51-1.68 (m, 3H), 1.35 (s, 3H). **^{13}C NMR** (100MHz, $CDCl_3$)**:** 171.5, 163.8, 158.7, 156.3, 151.3, 144.2, 135.3, 135.3, 135.2, 132.2, 130.1, 129.1, 128.1, 127.9, 127.1, 118.0, 113.2, 113.1, 87.0, 84.7, 84.4, 66.2, 64.1, 55.2, 54.4, 50.8, 39.4, 38.5, 31.9, 28.1, 22.3, 11.6; **MS (EI)** *m/z* 851.3353, found 874.37 ($M+Na^+$).

5'-*O*-(4,4'-dimethoxytrityl)-3'-[(N^{ε}-Trifluoroacetyl-L-Lysyl)-amino]-3'-deoxythymidine (29): Deprotection of Alloc group

5'-*O*-(4,4'-dimethoxytrityl)-3'-[(N^{ε}-Trifluoroacetyl-L-Lysyl)-amino]-3'-deoxythymidine **27** (1.00 g, 1.17 mmol) was dissolved in dry dichloromethane (10 mL). To it, DIPEA (0.8 mL, 8.22 mmol) and PPh_3 (0.215 g, 0.82 mmol) was added. To it $Pd(dba)_3$ (37 mg, 0.11 mmol) and the reaction mixture was allowed to stir for 2 h. Dichloromethane and DIPEA were removed in vacuo and the residue co-distilled with dichloromethane. Crude products were obtained in quantitative (80-82 % crude) yield by trituration with diethyl ether and acetone. Upon drying in vacuo, a foamy solid was obtained, that was used for the next reaction without further purification.

5'-*O*-(4,4'-dimethoxytrityl)-3'-[(N^{ε}-Trifluoroacetyl-D-Lysyl)-amino]-3'-deoxythymidine (30)

This compound was obtained as a pale yellow foam by an analogous method described above for synthesis of **29**, except 5'-*O*-(4,4'-dimethoxytrityl)-3'-[(N^{α}-Alloc-N^{ε}-Trifluoroacetyl-D-Lysyl)-amino]-3'-deoxythymidine **28** was used as starting material.

Synthesis of 5'-*O*-DMT-T-$_{(N^{\varepsilon}\text{-Trifluoroacetyl-L-Lysine})}$-T- 3'-*O*-TBS dimer (31)

To 3'-*O*-(*tert*-butyldimethylsilyl)thymidine-4'-carboxylic acid **9** (0.37 g, 1 mmol) in dry acetonitrile (5 mL), TBTU (0.385 g, 1.2 mmol), HOBt (67 mg, 0.5 mmol) and DIPEA (0.51 mL, 3 mmol) were added and stirred for 15 min. Compound **29** (0.690 g, 0.9 mmol) dissolved in dry acetonitrile (5 mL) was then added to the reaction mixture and further stirred at room temp for 2 h. The reaction mixture was then concentrated to dryness, dissolved in ethyl acetate (30 mL) and washed with 5% $NaHCO_3$ (10 mL x 2).

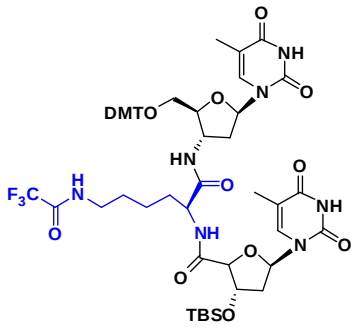

31

The ethyl acetate layer was dried over anhydrous Na_2SO_4 and concentrated. This was purified by column chromatography using 1.5 % MeOH: CH_2Cl_2 to get the product **31** (0.724 g, 72 %) as a white solid.

MS (EI) *m/z* 1119.4596, found 1142.62 (M+ Na^+)

Synthesis of 5'-*O*-DMT-T-$_{(N^{\varepsilon}\text{-Trifluoroacetyl-D-Lysine})}$-T- 3'-*O*-TBS dimer (32)

Compound **32** was obtained in 73% yield as a white foam starting from 5'-*O*-(4,4'-dimethoxytrityl)-3'-[(N^{ε}-Trifluoroacetyl-D-Lysyl)-amino]-3'-deoxythymidine **(30)** and 3'-*O*-(*tert*-butyldimethylsilyl)thymidine-4'-carboxylic acid **9** by an analogous method described for compound **31.**

MS (EI) *m/z* 1119.4596, found 1142.63 (M+ Na^+)

Synthesis of 5'-*O*-DMT-T-$_{(N^{\varepsilon}\text{-Trifluoroacetyl-L-Lysine})}$-T- 3'-OH dimer (33) and 5'-*O*-DMT-T-$_{(N^{\varepsilon}\text{-Trifluoroacetyl-D-Lysine})}$-T- 3'-OH dimer (34)

A solution of compound **31**/ **32** (0.700 g, 0.62 mmol) and TBAF (0.93 mL, 0.93 mmol) in anhydrous THF (10 mL) was stirred at RT for 1 h. THF was removed *in vacuo* and the residue redissolved in CH_2Cl_2 (50mL). The solution was washed with water (2 x 20 mL). The organic layer was dried over anhydrous Na_2SO_4 and evaporated to dryness. Silica gel column chromatography using 2.5 % methanol in dichloromethane afford pure product **33** (0.452 g, 72 %)/ **34** (0.438 g, 70 %) respectively.

5'-*O*-DMT-T-$_{(N^{\varepsilon}\text{-Trifluoroacetyl-L-Lysine})}$-T- 3'-OH dimer (33)

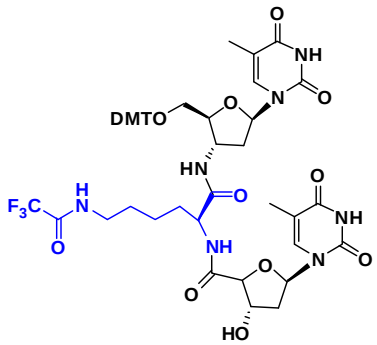

33

^{1}H NMR (400MHz, MeOH-D_4): 7.99 (s, 1H), 7.77 (s, 1H), 7.46-7.50 (d, *J*= 7.09 Hz, 2H), 7.28-7.37 (m, 7H), 6.87 (d, *J*= 8.71 Hz, 4H), 6.31-6.40 (m, 2H), 4.83 (m, 1H), 4.69 (m, 1H), 4.56 (m, 1H), 4.41 (m, 1H), 4.30-4.37 (m, 1H), 4.09 (m, 1H), 3.79 (s, 6H), 3.47 (m, 2H), 3.31 (m, 1H), 2.16-2.60 (m, 4H), 1.93 (m, 1H), 1.83 (s, 3H), 1.55-1.78 (m, 5H), 1.39 (s, 3H); **MS (EI)** *m/z* 1005.3732, found 1028.54 (M+ Na^+).

5'-*O*-DMT-T-(N^{ε}-Trifluoroacetyl-D-Lysine)-T- 3'-OH dimer (34)

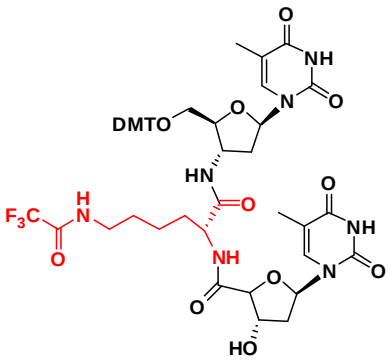

34

^{1}H NMR (400MHz, MeOH-D_4): 7.96 (s, 1H), 7.75 (s, 1H), 7.48 (d, *J*= 7.09 Hz, 2H), 7.23-7.35 (m, 7H), 6.86-6.89 (d, *J*= 8.07 Hz, 4H), 6.31-6.37 (m, 2H), 4.83 (m, 1H), 4.57 (m, 1H), 4.40 (m, 1H), 4.32 (m, 1H), 4.09 (m, 1H), 3.79 (s, 6H), 3.46 (m, 2H), 3.30 (m, 1H), 2.51 (m, 1H), 2.36-2.43 (m, 2H), 2.18-2.23 (m, 1H), 1.83 (s, 3H), 1.68-1.80 (m, 2H), 1.61 (m, 2H), 1.46 (m, 1H), 1.40 (s, 3H); **^{13}C NMR** (MeOH-D_4, 100MHz): 174.2, 172.9, 166.7, 166.6, 160.4, 160.3, 152.9, 152.5, 146.2, 139.9, 137.7, 136.9, 131.6, 131.5, 129.6, 129.1, 128.2, 114.3, 112.1, 111.9, 89.6, 88.2, 87.3, 85.9, 85.3, 75.8, 64.3, 55.8, 54.9 51.1, 40.5, 39.1, 38.9, 32.8, 29.6, 24.2, 12.6, 12.2; **MS (EI)** *m/z* 1005.3732, found 1028.57 ($M+ Na^+$).

General procedure for the deprotection of DMT and Trifluoroacetyl group : Synthesis of 5', 3'-OH free T-(L-Lysine)-T (37) and 5', 3'-OH free T-(D-Lysine)-T (38)

Compound **33**/**34** (0.200 g, 0.2 mmol) was dissolved in 3% dichloroacetic acid (5 mL) and 20 µL triisopropyl silane was added as scavenger. Reaction was stirred for ½ hr. The reaction mixture was concentrated. To the obtained solid 30 % aq.ammonia solution was added (5 mL) and the reaction was stirred for 1 hr. Reaction mixture was concentrated and the product was recovered by successive trituration with acetone and diethyl ether to afford **37**/**38** as a white solid in 70 % yield.

5', 3'-OH free T-(L-Lysine)-T (37)

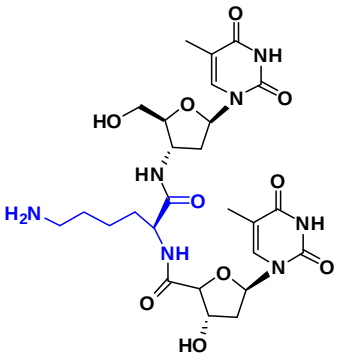

37

^{1}H NMR (400MHz, D_2O): 7.74 (s, 1H), 7.68 (s, 1H), 6.27 (dd, *J*= 7.02, 6.78 Hz, 1H), 6.23 (dd, *J*= 7.03, 5.81 Hz 1H), 4.71 (m, 1H), 4.46-4.52 (m, 2H), 4.26 (m, 1H), 3.97 (m, 1H), 3.82-3.86 (m, 1H), 3.69-3.74 (m, 1H), 2.98 (t, *J*= 7.78 Hz, 2H), 2.35-2.58 (m, 4H), 1.88 (s, 6H), 1.80-1.84 (m, 2H), 1.65-1.76 (m, 2H), 1.36-1.46 (s, 2H); **^{13}C NMR** (100MHz, $CDCl_3$): 173.5, 172.2, 166.4, 151.6, 151.5, 139.1, 137.5, 111.3, 111.0, 88.2, 85.0, 84.7, 83.9, 73.7,

60.8, 53.8, 49.8, 39.1, 37.3, 36.1, 30.5, 26.3, 22.2, 11.52, 11.50; **MS (EI)** *m/z* 607.2602, found 608.24 (M+ H^+); **HRMS** (ESI) calcd for $C_{26}H_{38}N_7O_{10}$: 608.2680 (M+H^+), found 608.2658.

5', 3'-OH free T-$_{(D\text{-}Lysine)}$-T (38)

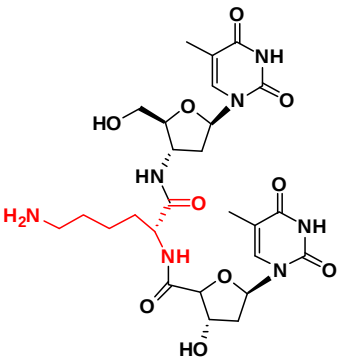

38

^{1}H NMR (400MHz, D_2O)**:** 7.78 (s, 1H), 7.69 (s, 1H), 6.32 (dd, *J*= 7.03, 6.78 Hz, 1H), 6.22 (dd, *J*= 6.52, 6.27 Hz, 1H), 4.71 (m, 1H), 4.47-4.52 (m, 2H), 4.27 (m, 1H), 4.04 (m, 1H), 3.83-3.87 (m, 1H), 3.72-3.76 (m, 1H), 2.98 (t, J= 7.78 Hz, 2H), 2.30-2.56 (m, 4H), 1.89 (s, 3H), 1.87 (s, 3H), 1.76-1.85 (m, 2H), 1.64-1.72 (m, 2H), 1.37-1.47 (s, 2H); **^{13}C NMR** (100MHz, $CDCl_3$): 173.3, 172.0, 166.6, 166.3, 151.6, 151.5, 138.9, 137.3, 111.4, 111.2, 87.9, 85.0, 84.6, 83.7, 73.7, 60.8, 53.8, 49.0, 39.1, 37.4, 36.7, 30.4, 26.3, 22.0, 11.53, 11.50; **MS (EI)** *m/z* 607.2602, found 608.27 (M+ H^+); **HRMS** (ESI) calcd for $C_{26}H_{38}N_7O_{10}$: 608.2680 (M+H^+), found 608.2680.

2.5 Appendix

Compounds	Page Number
Section 1	
Compound 2: ^{1}H, ^{13}C, DEPT NMR	132
Compound 3: ^{1}H NMR	133
Compound 4a: ^{1}H NMR	133
Compound 4b: ^{1}H NMR	134
Compound 4c: ^{1}H NMR	134
Compound 7: ^{1}H NMR	135
Compound 8: ^{1}H and **^{13}C** NMR	135
Compound 8 : ^{13}C DEPT NMR	136
Compound 9: ^{1}H NMR	136
Compound 10a: ^{1}H NMR	137
Compound 10b: ^{1}H NMR	137
Compound 11a: ^{1}H NMR and Mass	138
Compound 11b: ^{1}H NMR and Mass	139
Compound 11c: ^{1}H NMR and Mass	140
Compound 12a: ^{31}P NMR and Mass	141
Compound 12b: ^{31}P NMR and Mass	142
Compound 12c: ^{31}P NMR	143
Compound Ia: ^{1}H, ^{13}C NMR	144
Compound Ia: ^{13}C DEPT NMR and HRMS	145
Compound Ib: ^{1}H NMR and HRMS	146
Compound Ic: ^{1}H NMR and HRMS	147
Section 2	
Compound 14 ^{1}H, ^{13}C and DEPT NMR	148
Compound 15 ^{1}H and **^{13}C** and **DEPT**	149
Compound 16 ^{1}H and **^{13}C** and **DEPT**	150
Compound 16 ^{1}H NMR and Mass	151
Compound 19 ^{31}P NMR	152
Compound 20 ^{1}H and **^{13}C** NMR	153
Compound 20 ^{13}C DEPT NMR and HRMS	154

Compound 23 ^{1}**H and** ^{13}**C and DEPT** 155
Compound 25 ^{1}**H and** ^{13}**C and DEPT** 156
Compound 27 ^{1}**H and** ^{13}**C** 157
Compound 27 DEPT 158
Compound 28 ^{1}**H** 158
Compound 28 ^{13}**C** and **DEPT** 159
Compound 33 1H NMR and mass 160
Compound 34 ^{1}**H** and ^{13}**C** 161
Compound 34 ^{13}**C DEPT** and mass 162
Compound 37 ^{1}**H** and ^{13}**C** 163
Compound 37 ^{13}**C DEPT** and HRMS 164
Compound 38 ^{1}**H** and ^{13}**C** and 165
Compound 38 ^{13}**C DEPT** and HRMS 166
ON1-ON12 HPLC chromatogram 167-169
ON1-ON12 MALDI-TOF spectra 170-175

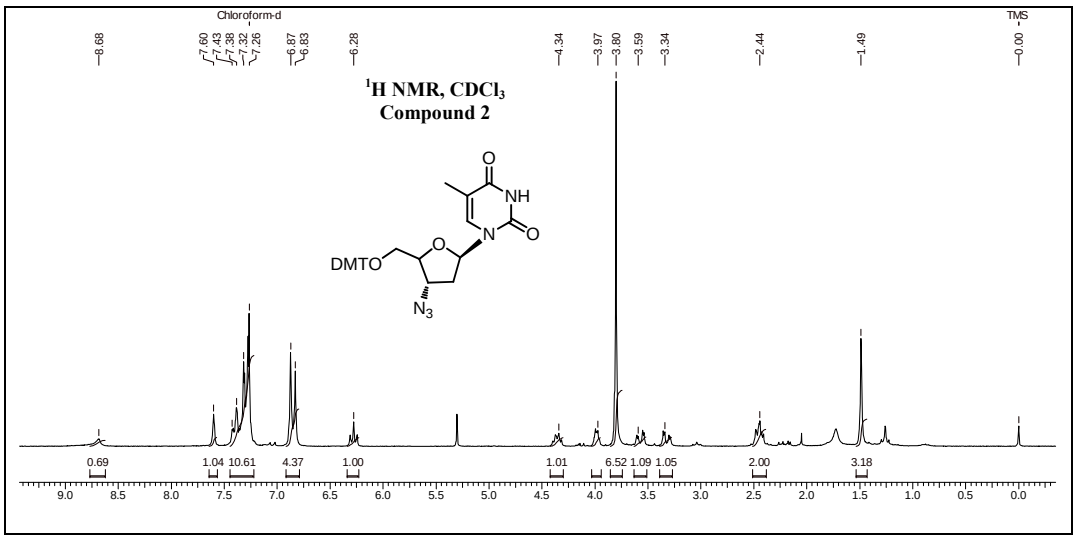
Chloroform-d
TMS
8.68
7.60
7.43
7.38
7.32
7.26
6.87
6.83
6.28
4.34
3.97
3.80
3.59
3.34
2.44
1.49
0.00
^{1}H NMR, CDCl$_3$
Compound 2
O
NH
N
O
O
DMTO
N$_3$
0.69
1.04
10.61
4.37
1.00
1.01
6.52
1.09
1.05
2.00
3.18

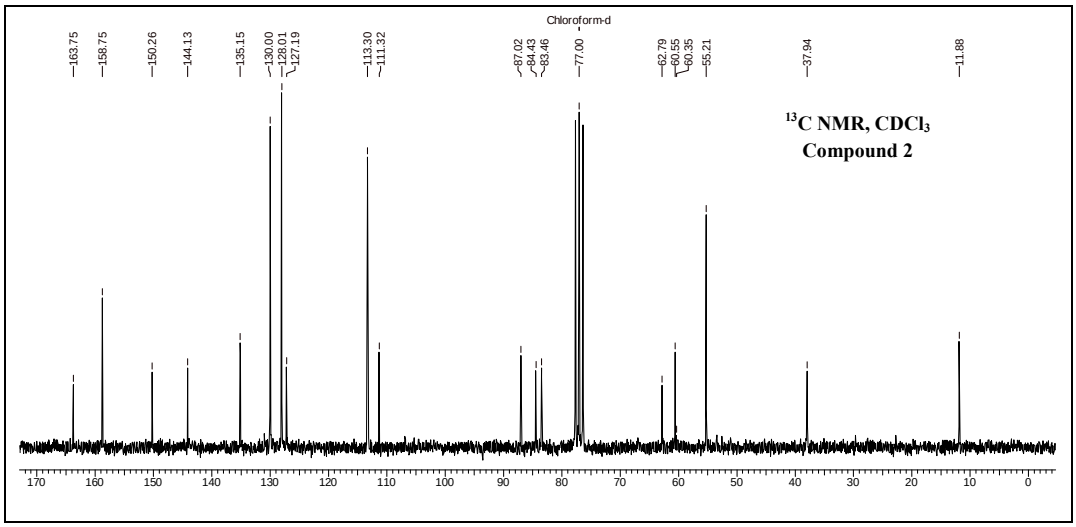
Chloroform-d
163.75
158.75
150.26
144.13
135.15
130.00
128.01
127.19
113.30
111.32
87.02
84.43
83.46
77.00
62.79
60.55
60.35
55.21
37.94
11.88
^{13}C NMR, CDCl$_3$
Compound 2

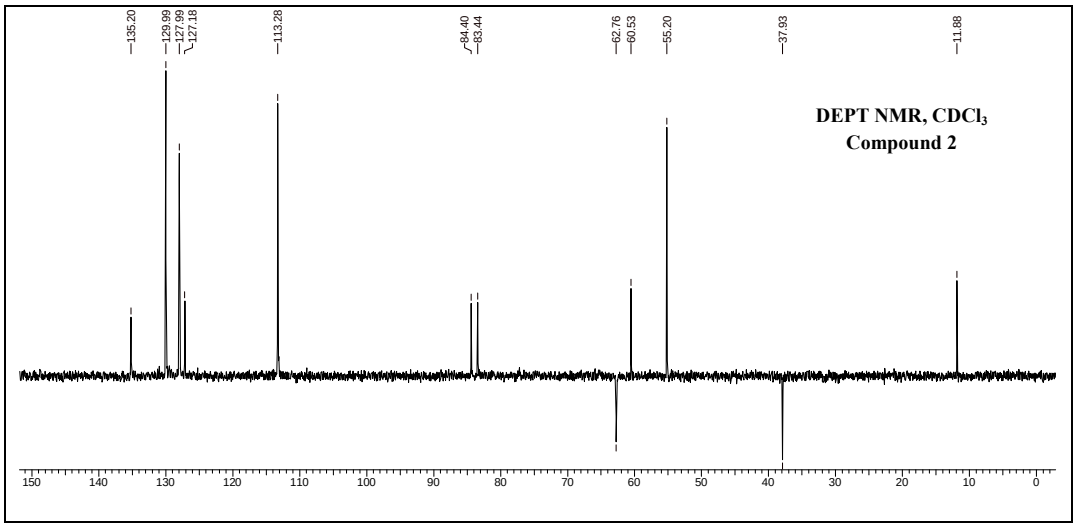
135.20
129.99
127.99
127.18
113.28
84.40
83.44
62.76
60.53
55.20
37.93
11.88
DEPT NMR, CDCl$_3$
Compound 2

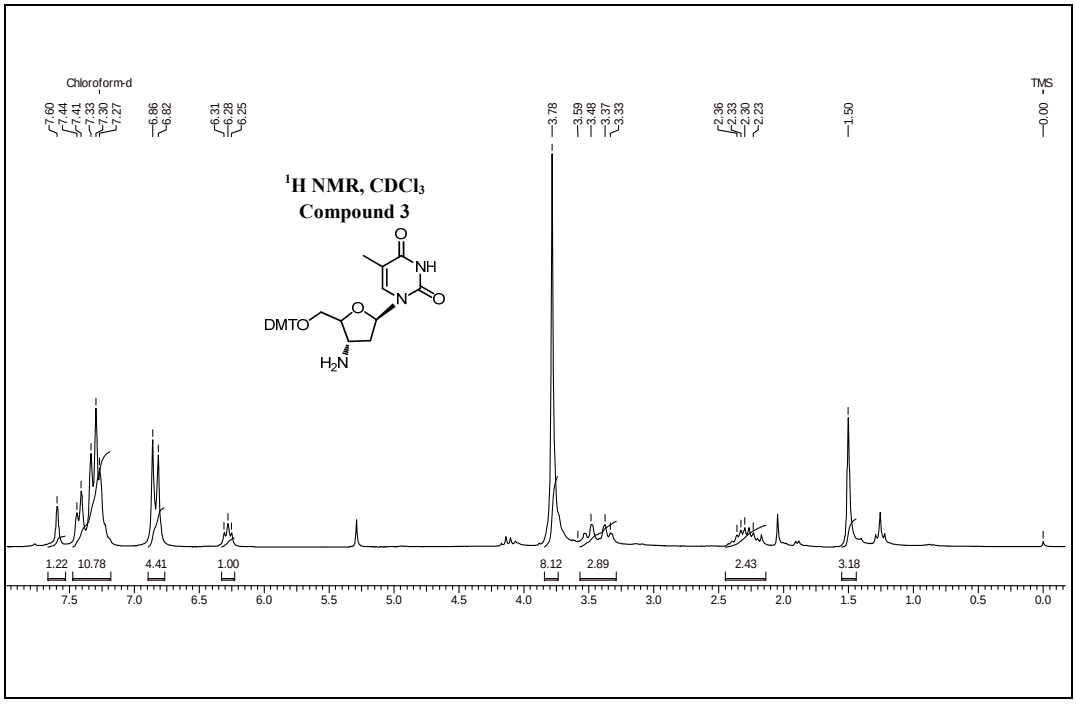
Chloroform-d
TMS
7.60
7.44
7.41
7.33
7.30
7.27
6.86
6.82
6.31
6.28
6.25
3.78
3.59
3.48
3.37
3.33
2.36
2.33
2.30
2.23
1.50
0.00
^{1}H NMR, CDCl$_3$
Compound 3
O
NH
N
O
O
DMTO
H$_2$N
1.22
10.78
4.41
1.00
8.12
2.89
2.43
3.18
7.5
7.0
6.5
6.0
5.5
5.0
4.5
4.0
3.5
3.0
2.5
2.0
1.5
1.0
0.5
0.0

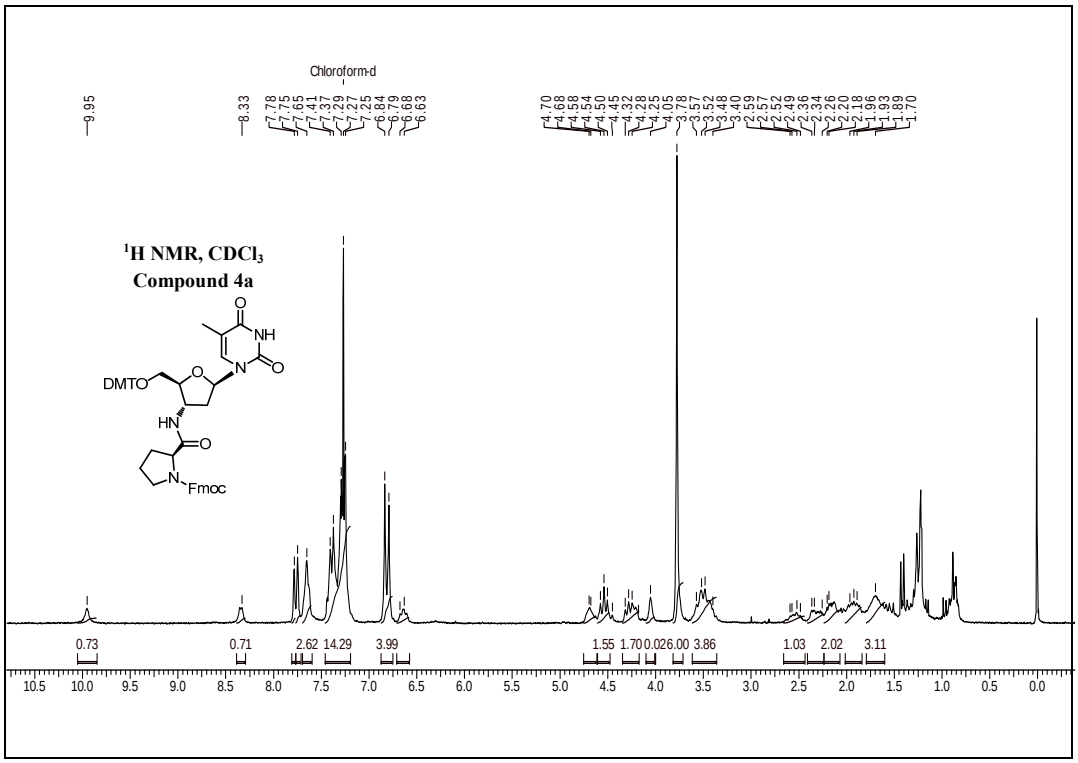
Chloroform-d
9.95
8.33
7.78
7.75
7.65
7.41
7.37
7.29
7.27
7.25
6.84
6.79
6.68
6.63
4.70
4.68
4.58
4.54
4.50
4.45
4.32
4.28
4.25
4.05
3.78
3.57
3.52
3.48
3.40
3.59
2.57
2.52
2.49
2.36
2.34
2.26
2.20
2.18
1.96
1.93
1.89
1.70
^{1}H NMR, CDCl$_3$
Compound 4a
O
NH
N
O
DMTO
HN
O
N
Fmoc
0.73
0.71
2.62
14.29
3.99
1.55
1.70
0.02
6.00
3.86
1.03
2.02
3.11
10.5
10.0
9.5
9.0
8.5
8.0
7.5
7.0
6.5
6.0
5.5
5.0
4.5
4.0
3.5
3.0
2.5
2.0
1.5
1.0
0.5
0.0

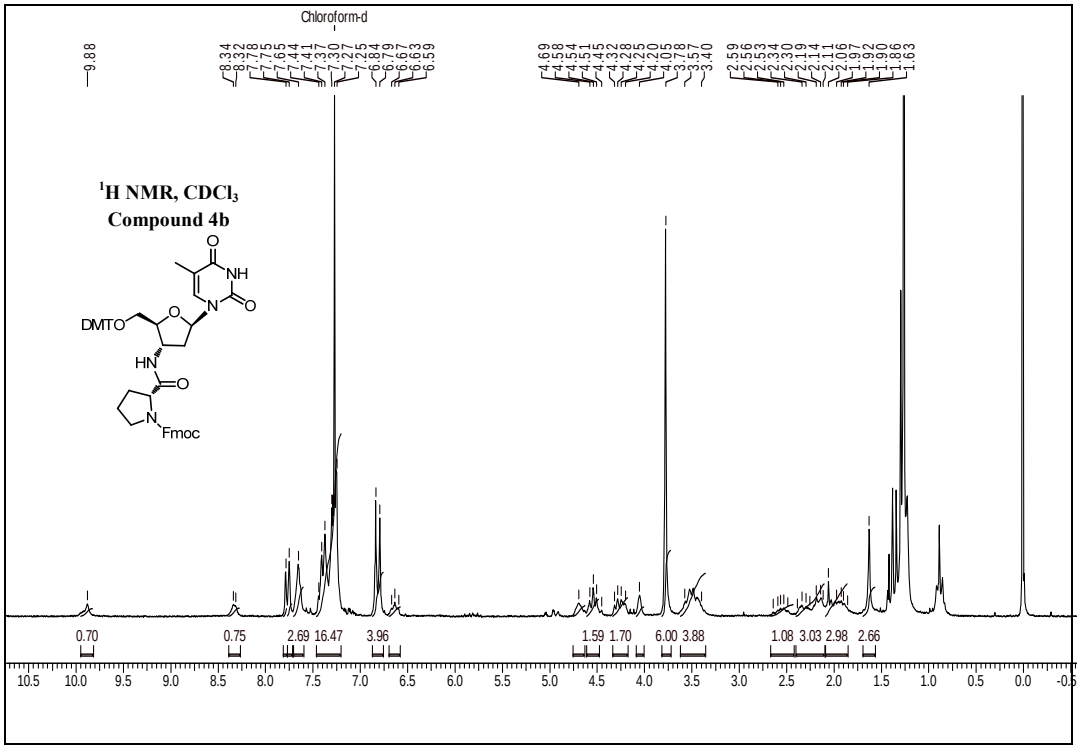
Chloroform-d
^{1}H NMR, CDCl$_3$
Compound 4b
DMTO
NH
HN
Fmoc

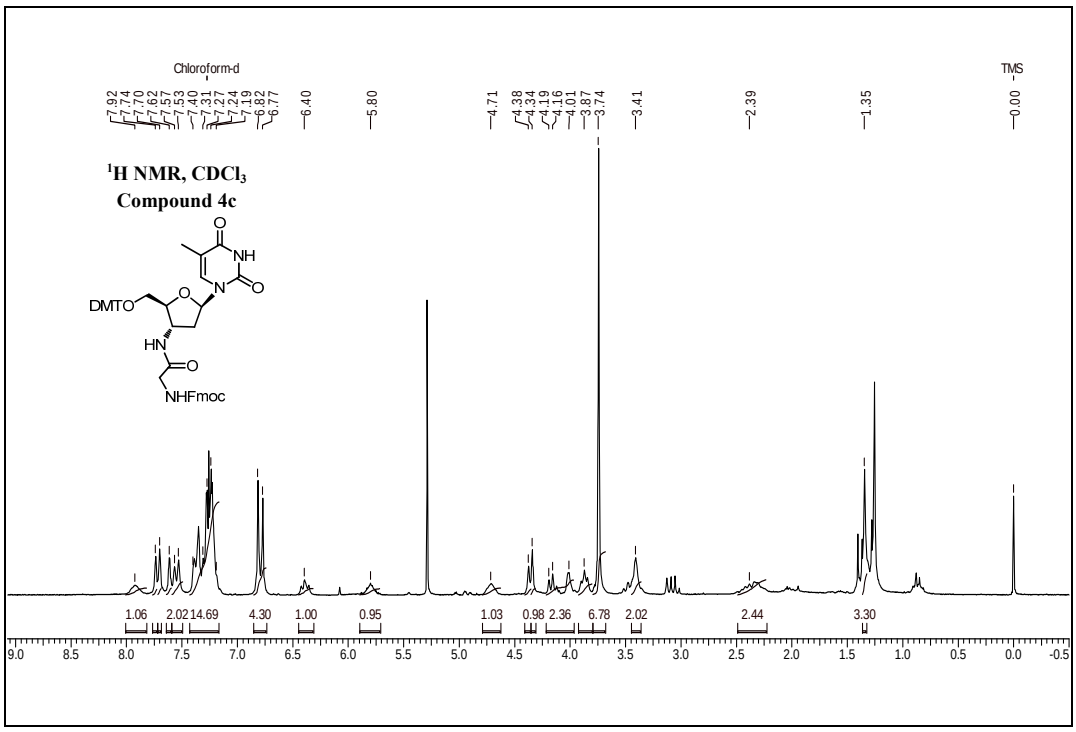
Chloroform-d
TMS
^{1}H NMR, CDCl$_3$
Compound 4c
DMTO
NH
HN
NHFmoc

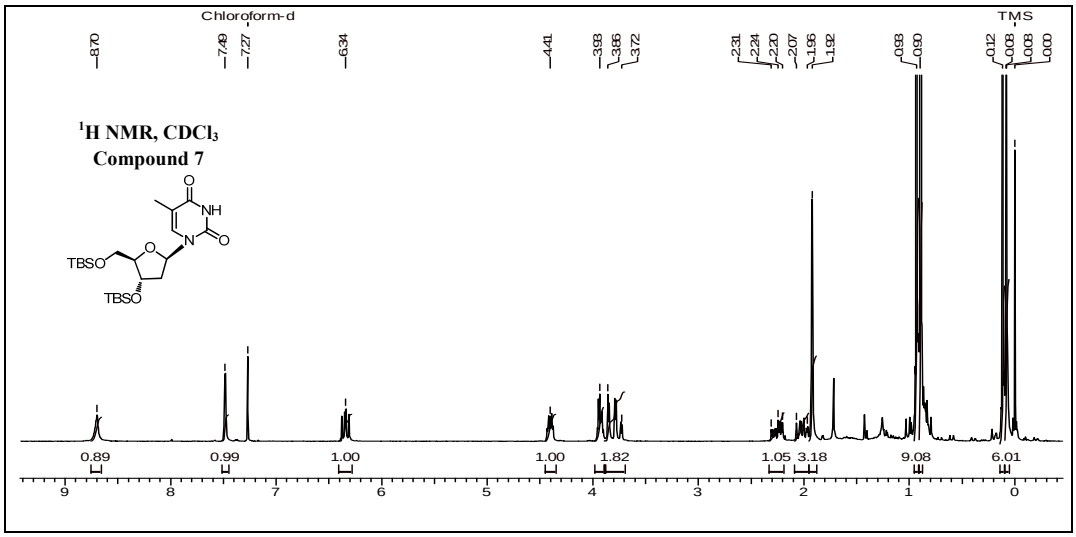
Chloroform-d
TMS
^{1}H NMR, CDCl$_3$
Compound 7
TBSO
TBSO
NH
O
N
O
0.89
0.99
1.00
1.00
1.82
1.05
3.18
9.08
6.01

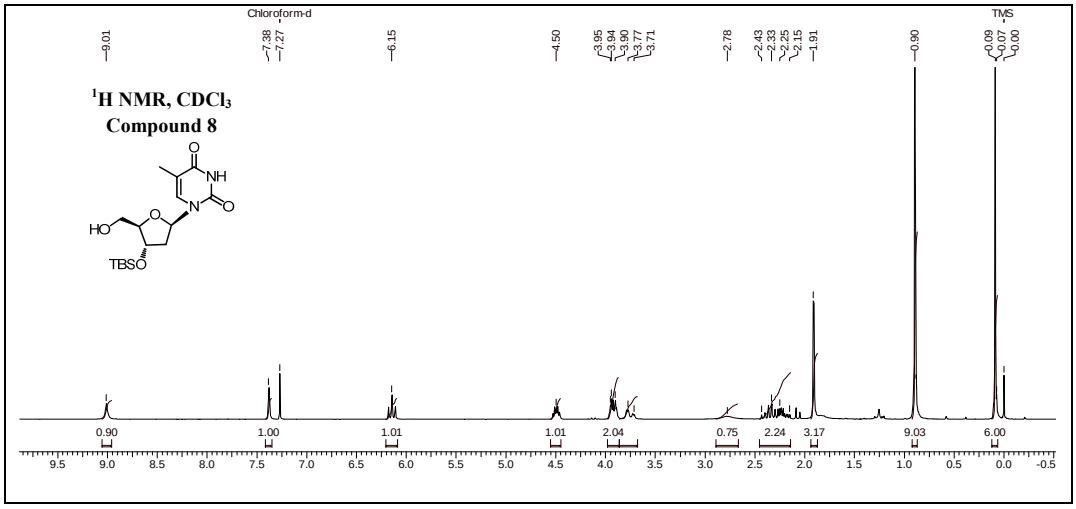
Chloroform-d
TMS
^{1}H NMR, CDCl$_3$
Compound 8
HO
TBSO
NH
O
N
O
0.90
1.00
1.01
1.01
2.04
0.75
2.24
3.17
9.03
6.00

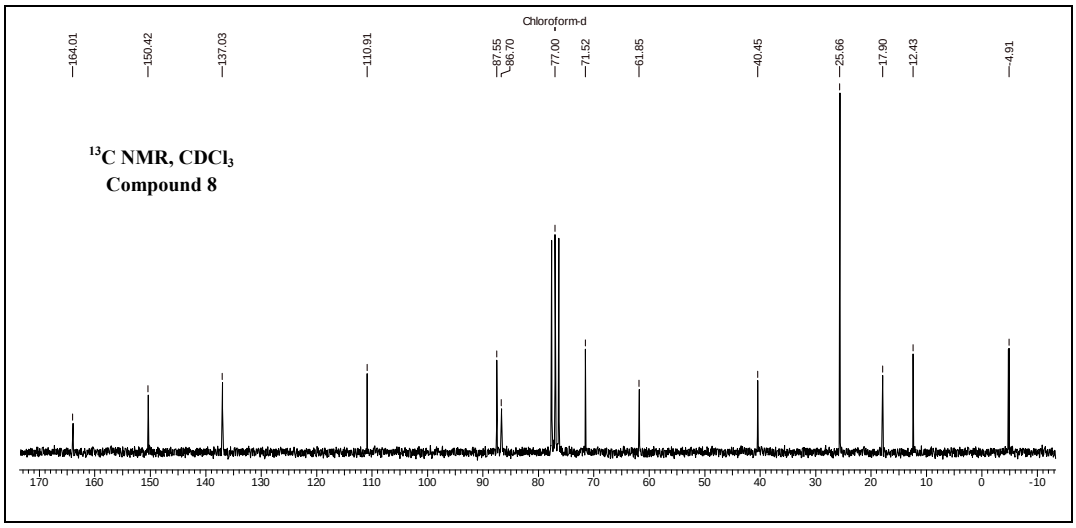
Chloroform-d
^{13}C NMR, CDCl$_3$
Compound 8

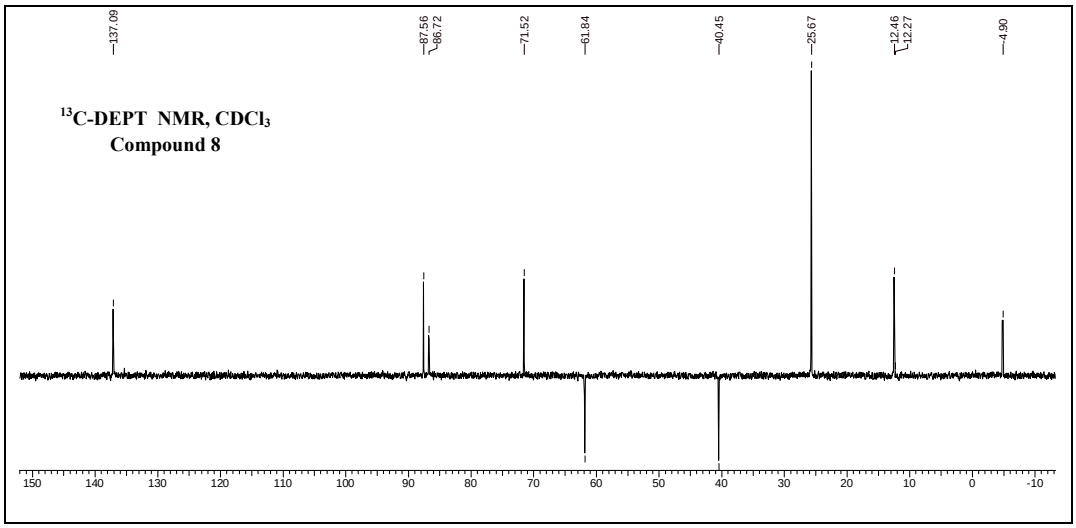
137.09
87.56
86.72
71.52
61.84
40.45
25.67
12.46
12.27
4.90
13C-DEPT NMR, CDCl3
Compound 8
150 140 130 120 110 100 90 80 70 60 50 40 30 20 10 0 -10

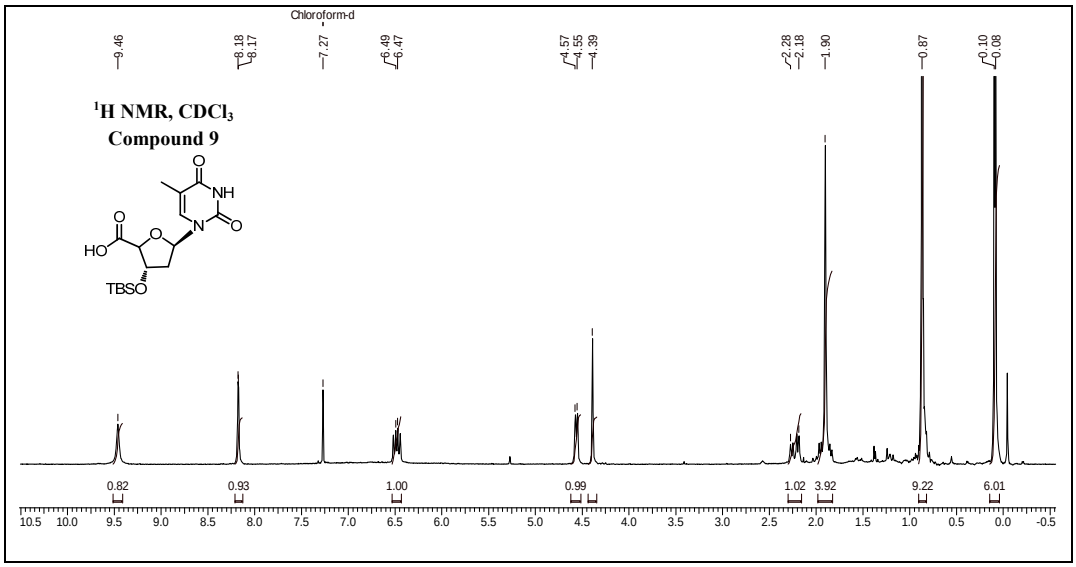
Chloroform-d
9.46
8.18
8.17
7.27
6.49
6.47
4.57
4.55
4.39
2.28
2.18
1.90
0.87
0.10
0.08
1H NMR, CDCl3
Compound 9
O
NH
N
O
O
HO
O
TBSO
0.82
0.93
1.00
0.99
1.02
3.92
9.22
6.01
10.5 10.0 9.5 9.0 8.5 8.0 7.5 7.0 6.5 6.0 5.5 5.0 4.5 4.0 3.5 3.0 2.5 2.0 1.5 1.0 0.5 0.0 -0.5

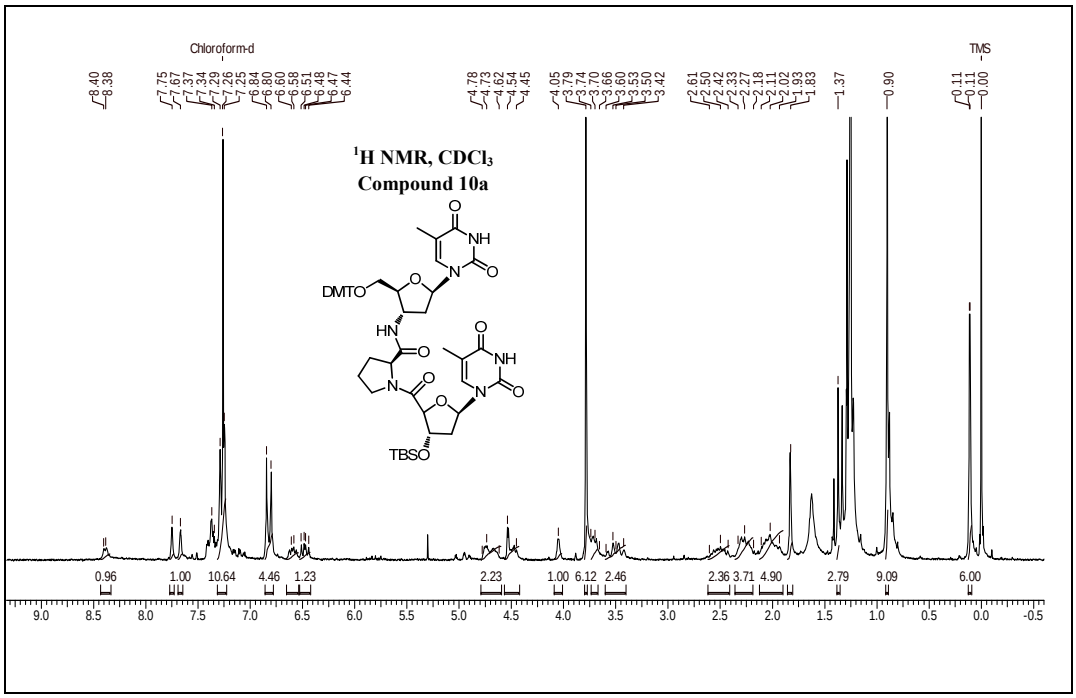
Chloroform-d
TMS
^{1}H NMR, CDCl$_3$
Compound 10a
DMTO
TBSO

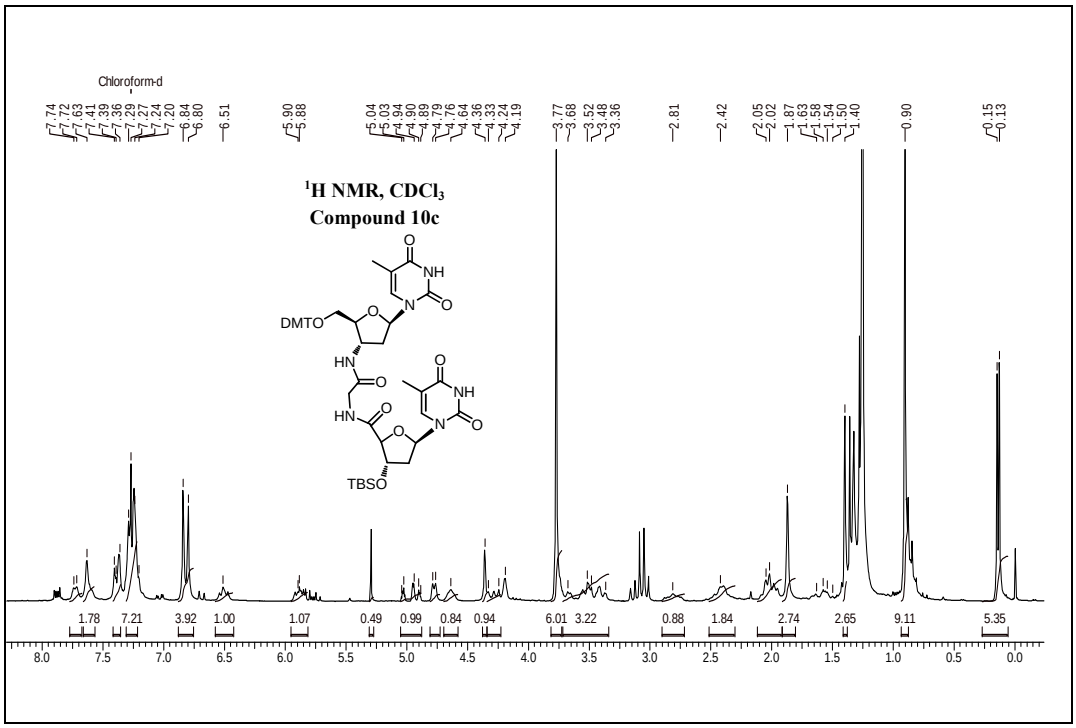
Chloroform-d
^{1}H NMR, CDCl$_3$
Compound 10c
DMTO
TBSO

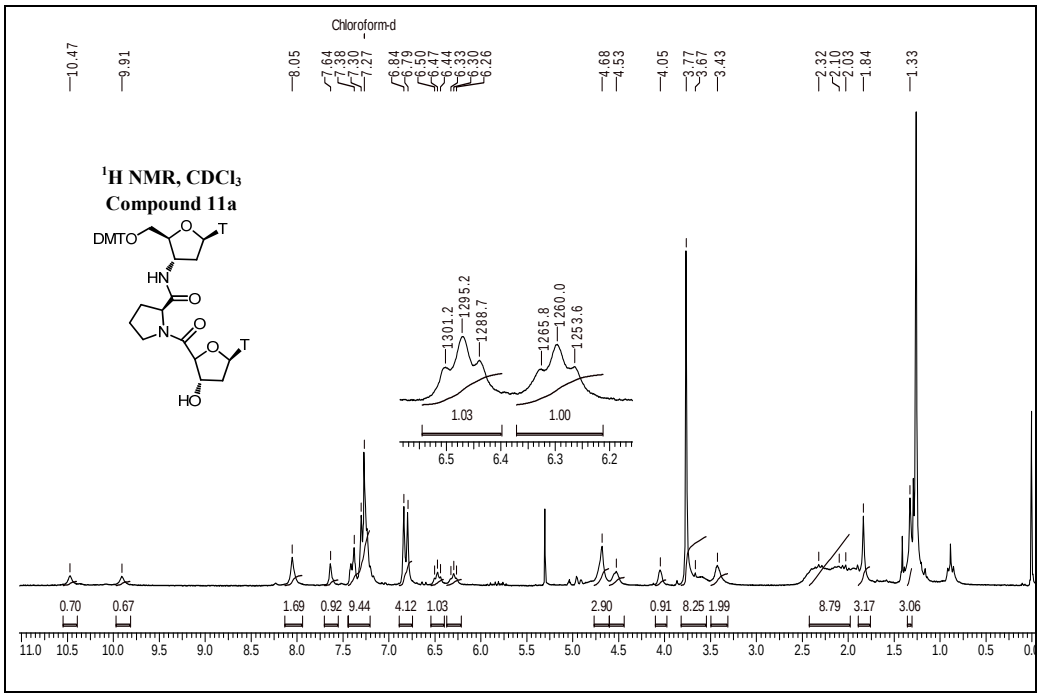
Chloroform-d
10.47
9.91
8.05
7.64
7.38
7.30
7.27
6.84
6.79
6.50
6.47
6.44
6.33
6.30
6.26
4.68
4.53
4.05
3.77
3.67
3.43
2.32
2.10
2.03
1.84
1.33
1H NMR, CDCl3
Compound 11a
DMTO
T
HN
O
N
HO
1301.2
1295.2
1288.7
1265.8
1260.0
1253.6
1.03
1.00
6.5
6.4
6.3
6.2
0.70
0.67
1.69
0.92
9.44
4.12
1.03
2.90
0.91
8.25
1.99
8.79
3.17
3.06

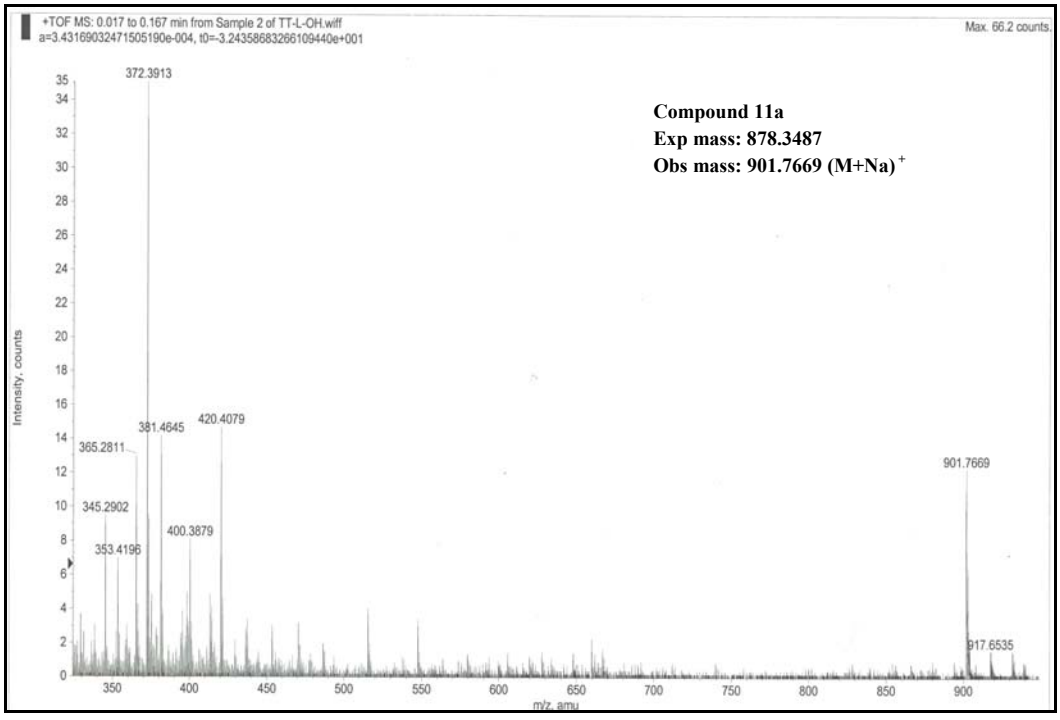
+TOF MS: 0.017 to 0.167 min from Sample 2 of TT-L-OH.wiff
a=3.43169032471505190e-004, t0=-3.24358683266109440e+001
Max. 66.2 counts.
Intensity, counts
m/z, amu
372.3913
381.4645
420.4079
365.2811
345.2902
353.4196
400.3879
901.7669
917.6535
Compound 11a
Exp mass: 878.3487
Obs mass: 901.7669 (M+Na)+

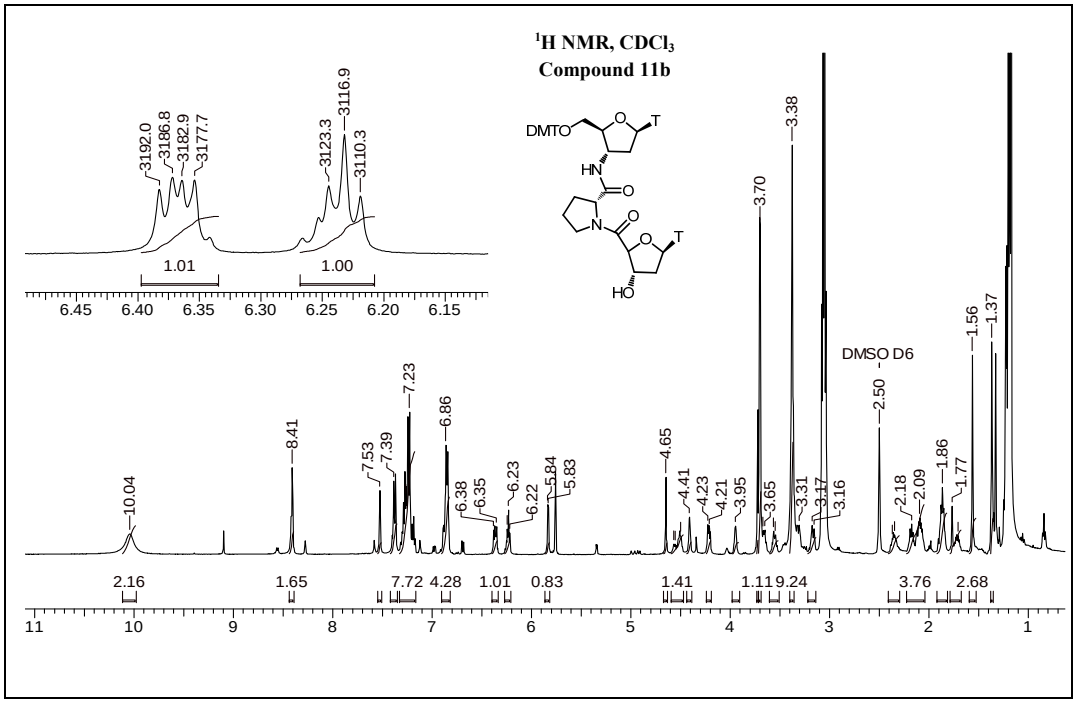
^{1}H NMR, CDCl$_3$
Compound 11b
DMTO
T
HN
O
N
HO
DMSO D6
3192.0
3186.8
3182.9
3177.7
3123.3
3116.9
3110.3
1.01
1.00
10.04
8.41
7.53
7.39
7.23
6.86
6.38
6.35
6.23
6.22
5.84
5.83
4.65
4.41
4.23
4.21
3.95
3.70
3.65
3.38
3.31
3.17
3.16
2.50
2.18
2.09
1.86
1.77
1.56
1.37
2.16
1.65
7.72
4.28
1.01
0.83
1.41
1.11
9.24
3.76
2.68

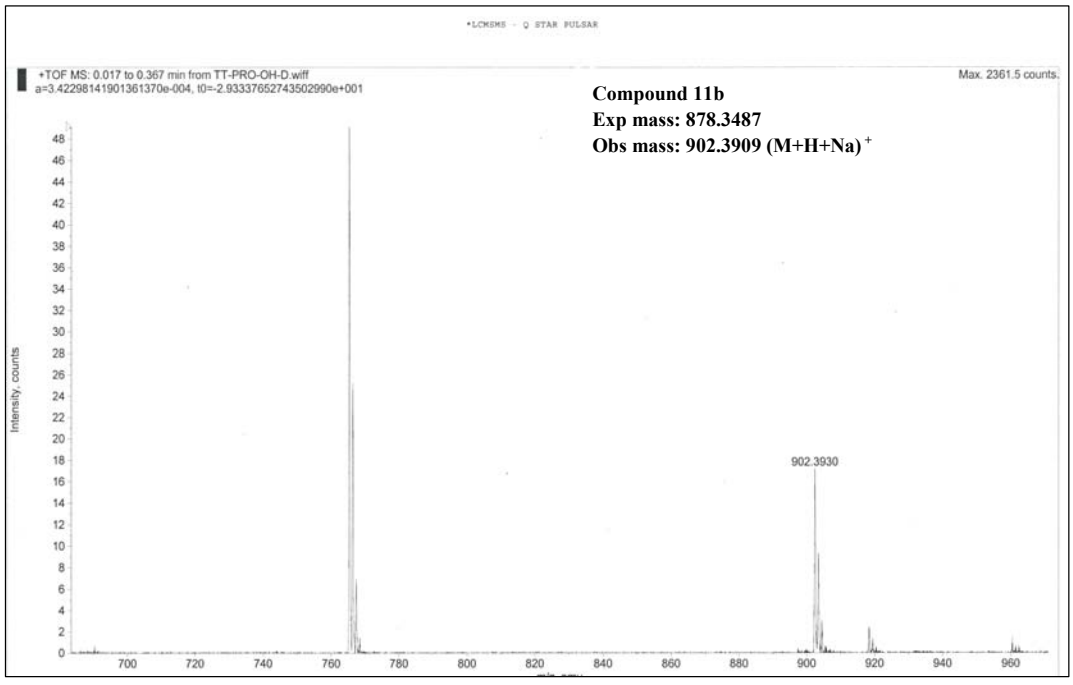
+TOF MS: 0.017 to 0.367 min from TT-PRO-OH-D.wiff
Max. 2361.5 counts.
Compound 11b
Exp mass: 878.3487
Obs mass: 902.3909 (M+H+Na)$^+$
Intensity, counts
902.3930

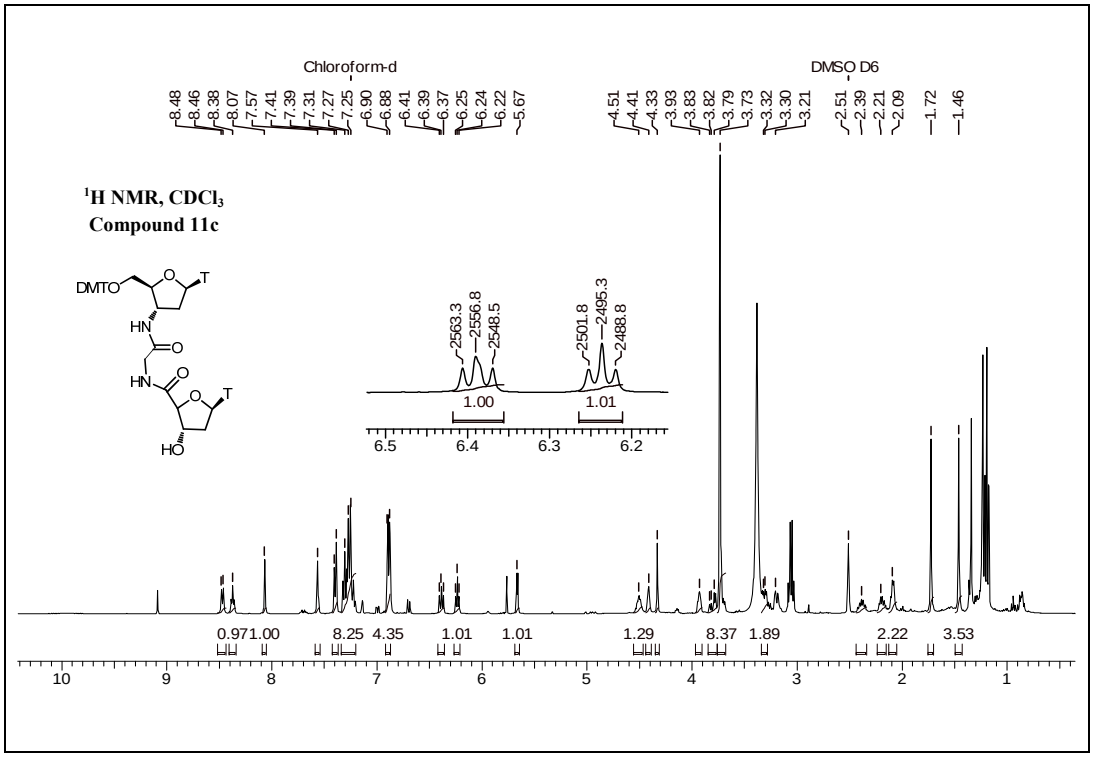
Chloroform-d
DMSO D6
8.48
8.46
8.38
8.07
7.57
7.41
7.39
7.31
7.27
7.25
6.90
6.88
6.41
6.39
6.37
6.25
6.24
6.22
5.67
4.51
4.41
4.33
3.93
3.83
3.82
3.79
3.73
3.32
3.30
3.21
2.51
2.39
2.21
2.09
1.72
1.46
^{1}H NMR, CDCl$_3$
Compound 11c
DMTO
T
HN
O
HN
O
T
HO
2563.3
2556.8
2548.5
2501.8
2495.3
2488.8
1.00
1.01
6.5
6.4
6.3
6.2
0.97
1.00
8.25
4.35
1.01
1.01
1.29
8.37
1.89
2.22
3.53
10
9
8
7
6
5
4
3
2
1

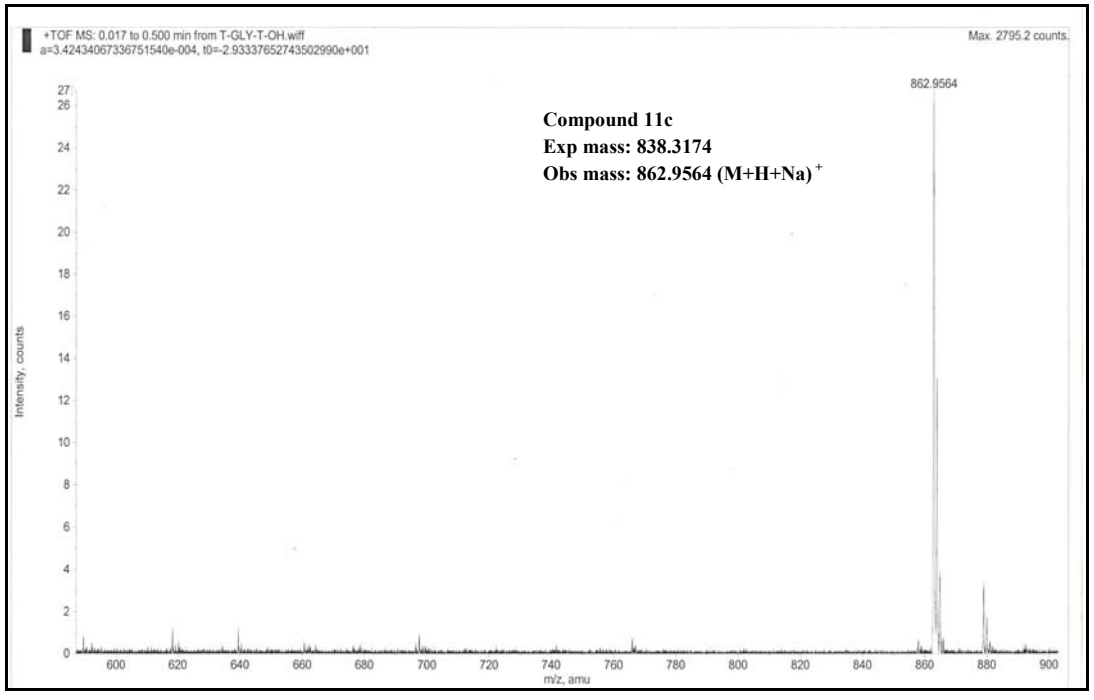
+TOF MS: 0.017 to 0.500 min from T-GLY-T-OH.wiff
a=3.42434067336751540e-004, t0=-2.93337652743502990e+001
Max. 2795.2 counts.
862.9564
Compound 11c
Exp mass: 838.3174
Obs mass: 862.9564 (M+H+Na)$^+$
Intensity, counts
m/z, amu
600
620
640
660
680
700
720
740
760
780
800
820
840
860
880
900

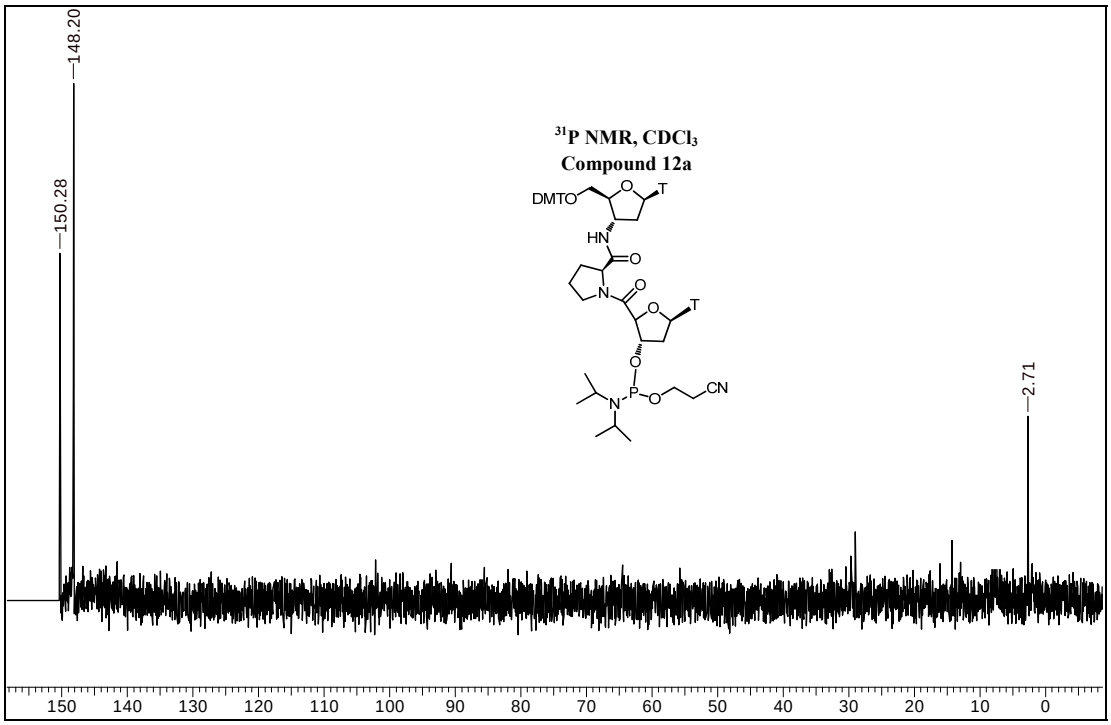
148.20
150.28
2.71
31P NMR, CDCl3
Compound 12a
DMTO
T
HN
O
N
O
O
T
O
P
O
CN
150 140 130 120 110 100 90 80 70 60 50 40 30 20 10 0

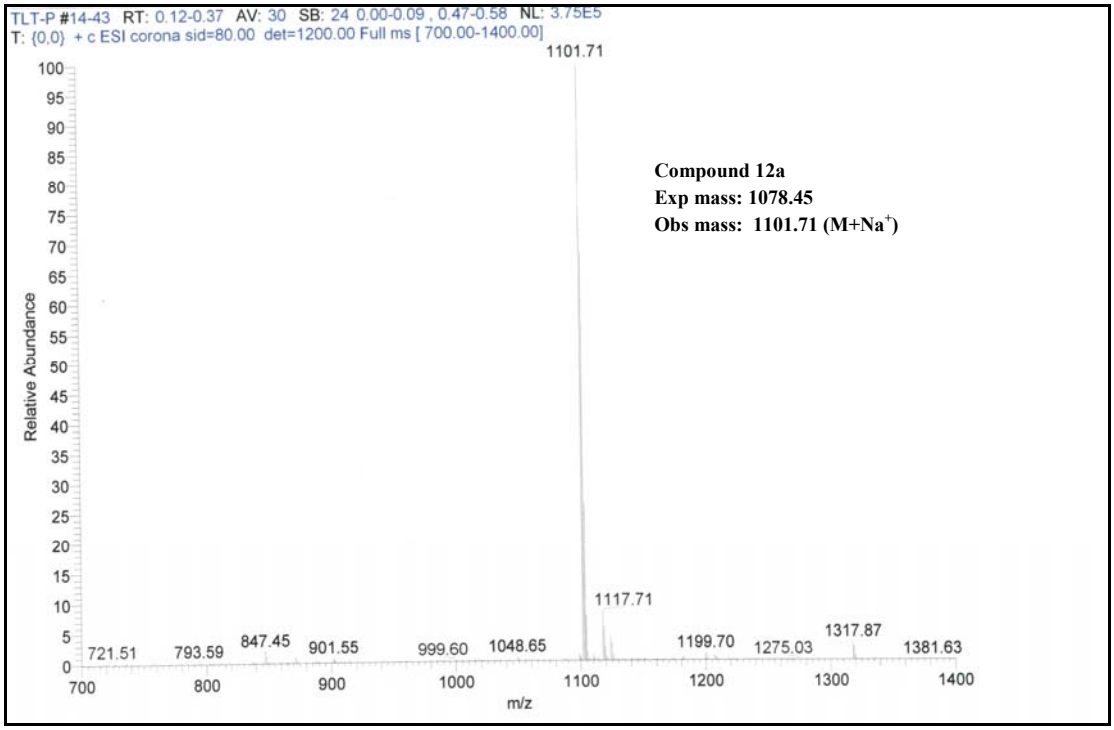
TLT-P #14-43 RT: 0.12-0.37 AV: 30 SB: 24 0.00-0.09 , 0.47-0.58 NL: 3.75E5
T: {0,0} + c ESI corona sid=80.00 det=1200.00 Full ms [700.00-1400.00]
1101.71
Compound 12a
Exp mass: 1078.45
Obs mass: 1101.71 (M+Na+)
Relative Abundance
1117.71
721.51
793.59
847.45
901.55
999.60
1048.65
1199.70
1275.03
1317.87
1381.63
m/z
700 800 900 1000 1100 1200 1300 1400

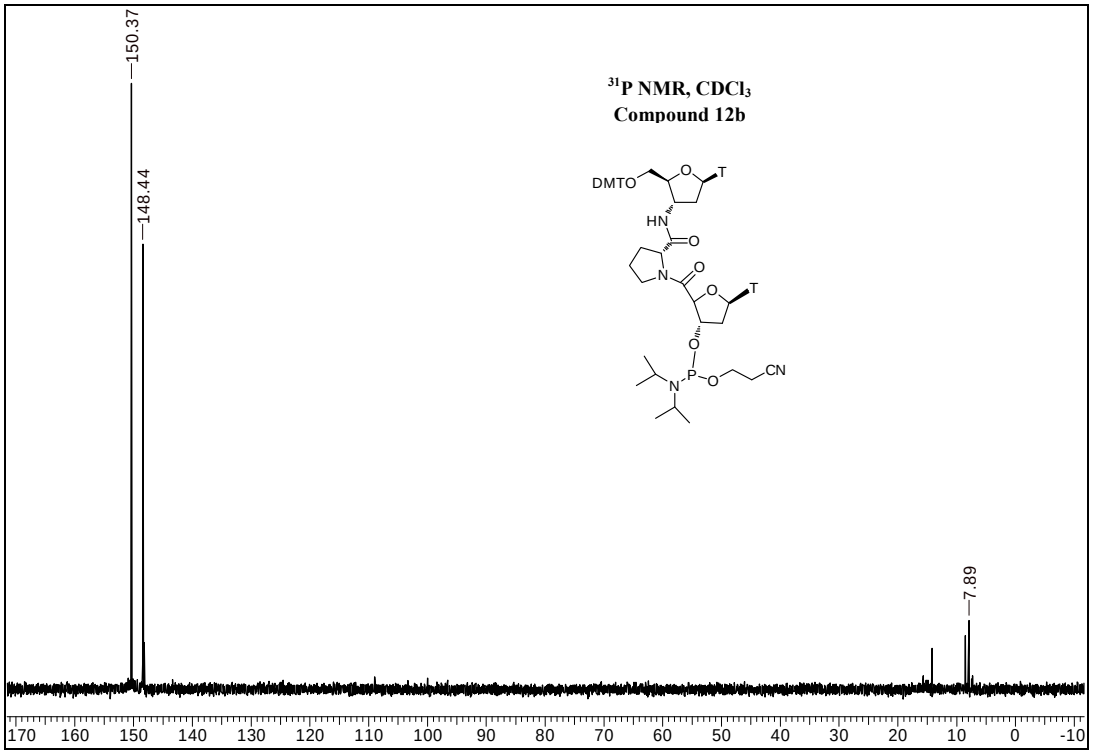
150.37
148.44
7.89
31P NMR, CDCl3
Compound 12b
DMTO
T
HN
O
N
O
O
T
O
P
O
CN
170 160 150 140 130 120 110 100 90 80 70 60 50 40 30 20 10 0 -10

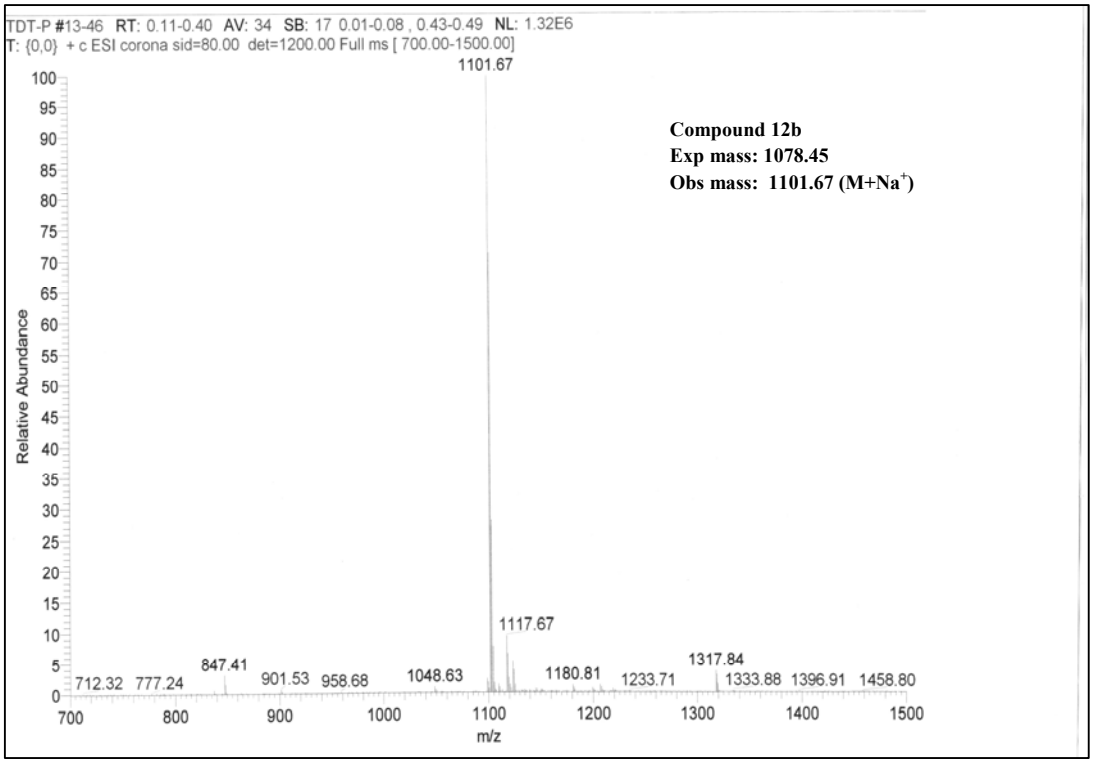
TDT-P #13-46 RT: 0.11-0.40 AV: 34 SB: 17 0.01-0.08 , 0.43-0.49 NL: 1.32E6
T: {0,0} + c ESI corona sid=80.00 det=1200.00 Full ms [700.00-1500.00]
1101.67
Compound 12b
Exp mass: 1078.45
Obs mass: 1101.67 (M+Na+)
Relative Abundance
1117.67
847.41
1317.84
712.32 777.24 901.53 958.68 1048.63 1180.81 1233.71 1333.88 1396.91 1458.80
700 800 900 1000 1100 1200 1300 1400 1500
m/z

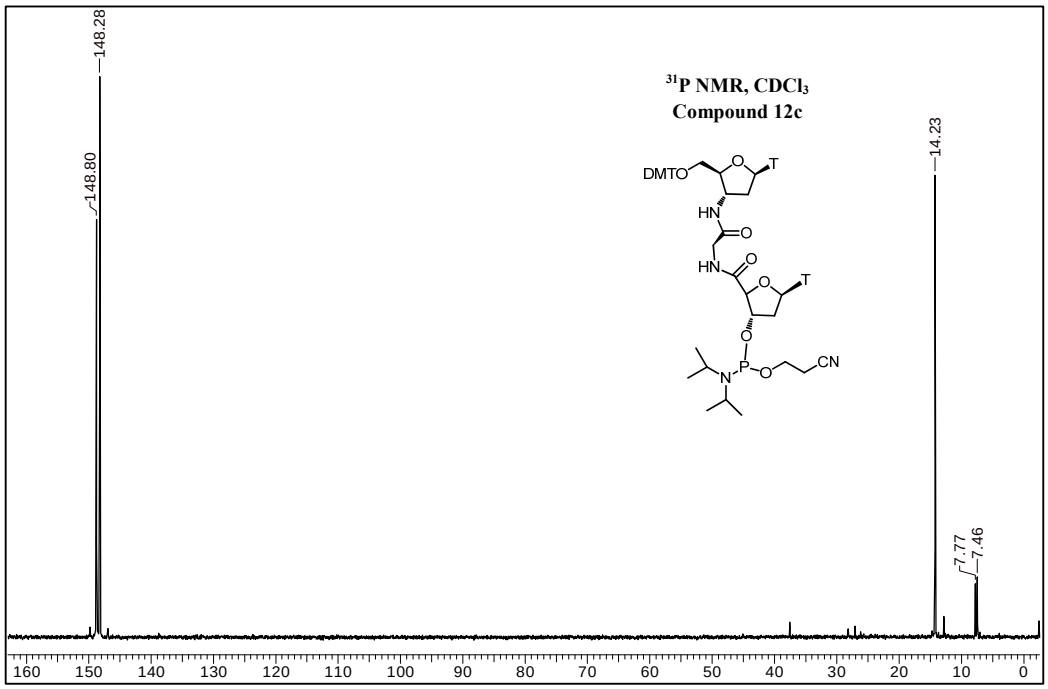

^{31}P NMR, $CDCl_3$
Compound 12c

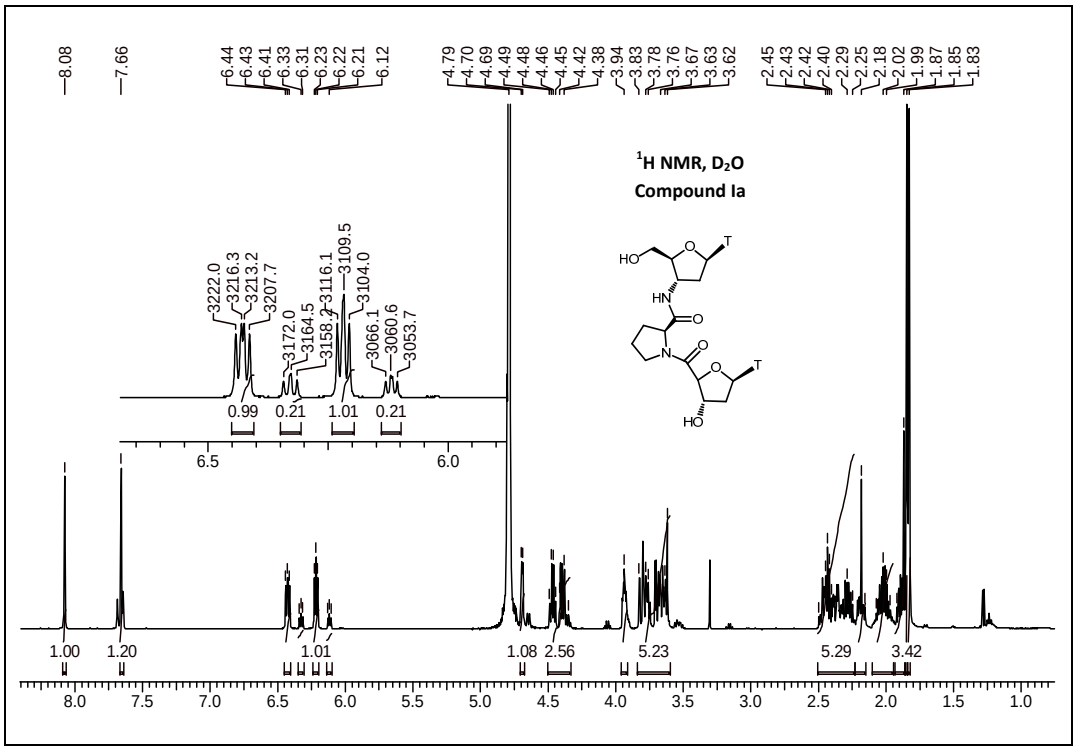
^{1}H NMR, D$_2$O
Compound Ia

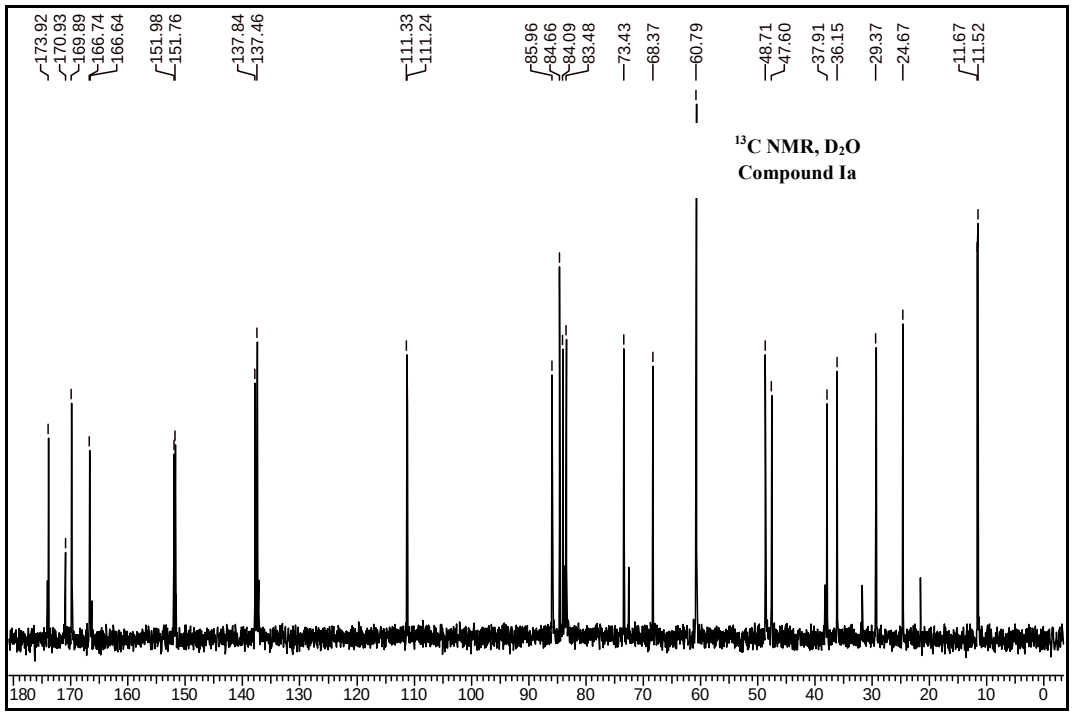
^{13}C NMR, D$_2$O
Compound Ia

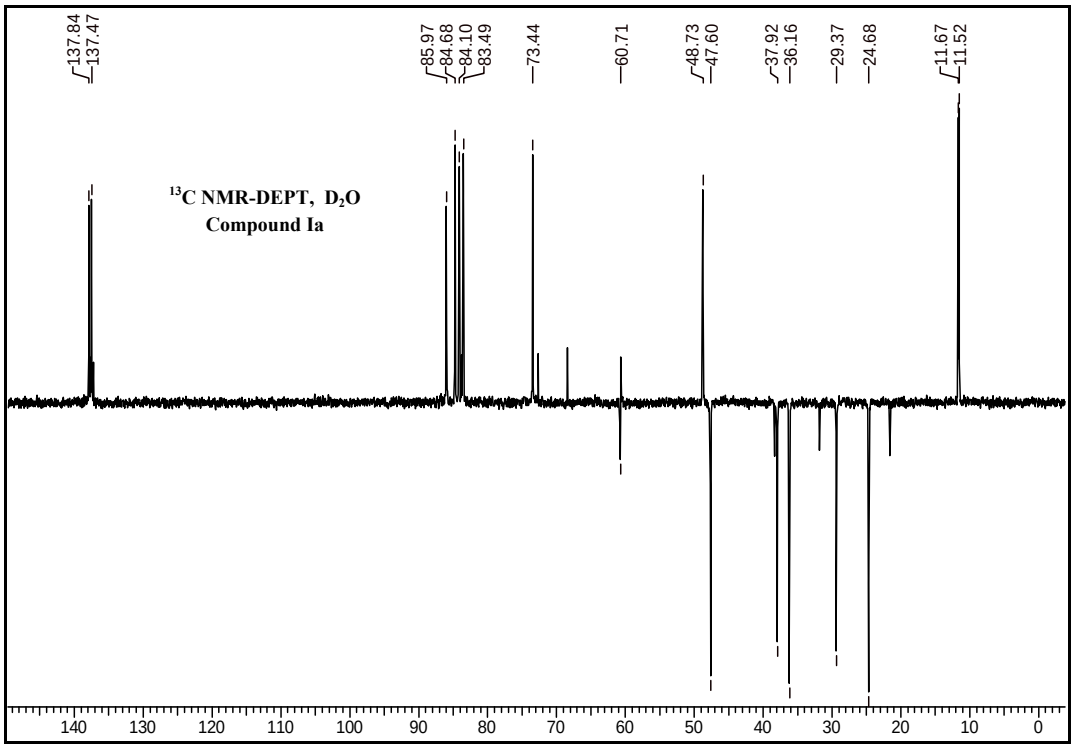

Compound Ia
Exp mass: 577.2258
Obs mass: 577.2268

Elemental Composition Report

Single Mass Analysis (displaying only valid results)
Tolerance = 5.0 PPM / DBE: min = -1.5, max = 100.0
Isotope cluster parameters: Separation = 1.0 Abundance = 1.0%

Monoisotopic Mass, Odd and Even Electron Ions
72 formula(e) evaluated with 1 results within limits (up to 50 closest results for each mass)

Micromass : Q-Tof micro (YA-105) Dept. Of Chemistry I.I.T.(B) 20-Jan-201210:34:32
C25H32N6O10
NCL-VAK-A (HO-T-L-PRO-T-OH) 19 (0.190) AM (Cen,5, 80.00, Ht,5000.0,556.28,1.00); Sb (5,40.00); Cm (17:57) TOF MS ES+
1.68e3

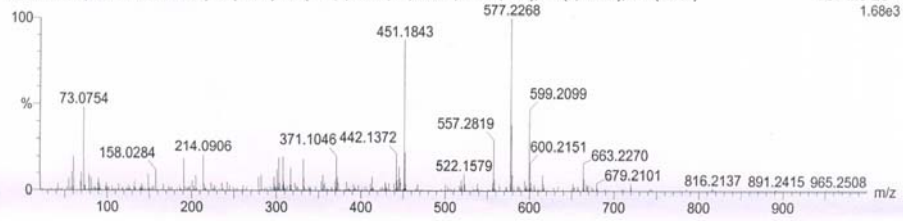

Minimum:				-1.5		
Maximum:		200.0	5.0	100.0		
Mass	Calc. Mass	mDa	PPM	DBE	Score	Formula
577.2268	577.2258	1.0	1.7	12.5	1	C25 H33 N6 O10

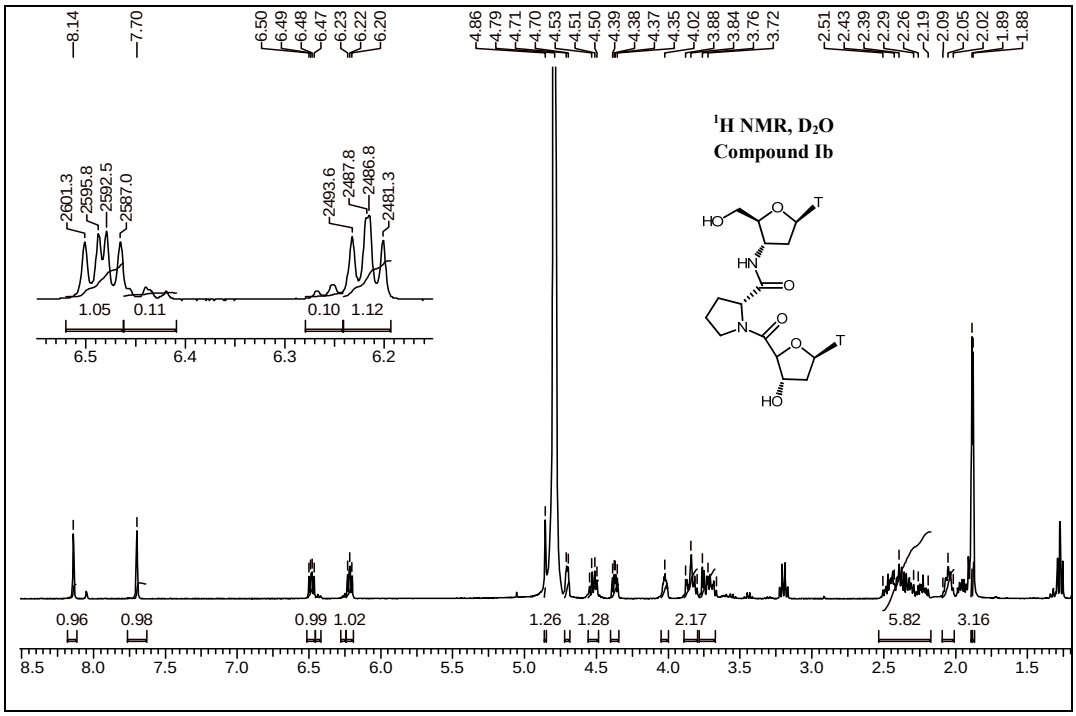

Elemental Composition Report Page 1

Single Mass Analysis (displaying only valid results)
Tolerance = 5.0 PPM / DBE: min = -1.5, max = 100.0
Isotope cluster parameters: Separation = 1.0 Abundance = 1.0%

Compound Ib
Exp mass: 577.2258
Obs mass: 577.2263

Monoisotopic Mass, Odd and Even Electron Ions
72 formula(e) evaluated with 1 results within limits (up to 50 closest results for each mass)

Micromass : Q-Tof micro (YA-105) Dept. Of Chemistry I.I.T.(B) 20-Jan-201210:47:59
C25H32N6O10
NCL-VAK-B (HO-T-D-PRO-T-OH) 2 (0.020) AM (Cen,5, 80.00, Ht,5000.0,556.28,1.00); Sm (Md, 6.00); Sb (5,40.00); Cm (1:33) TOF MS ES+
3.23e3

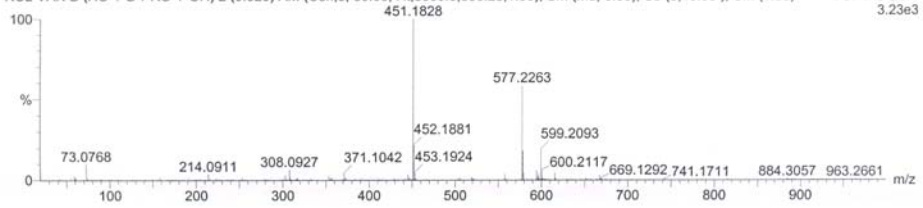

Minimum:				-1.5		
Maximum:		200.0	5.0	100.0		
Mass	Calc. Mass	mDa	PPM	DBE	Score	Formula
577.2263	577.2258	0.5	0.9	12.5	1	C25 H33 N6 O10

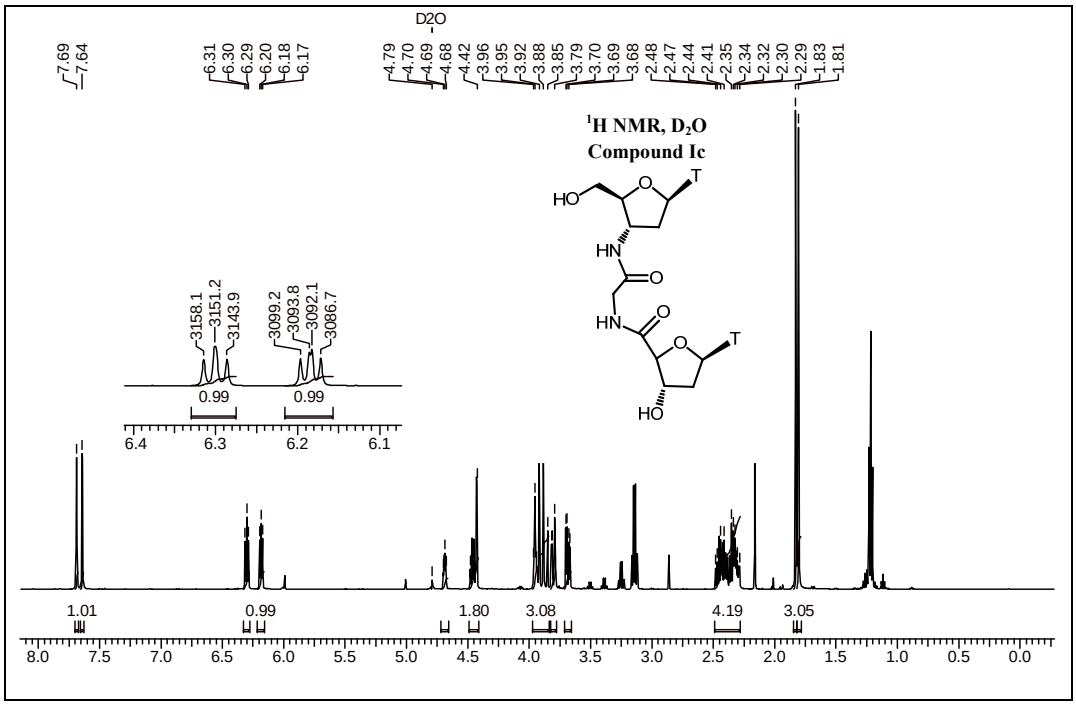

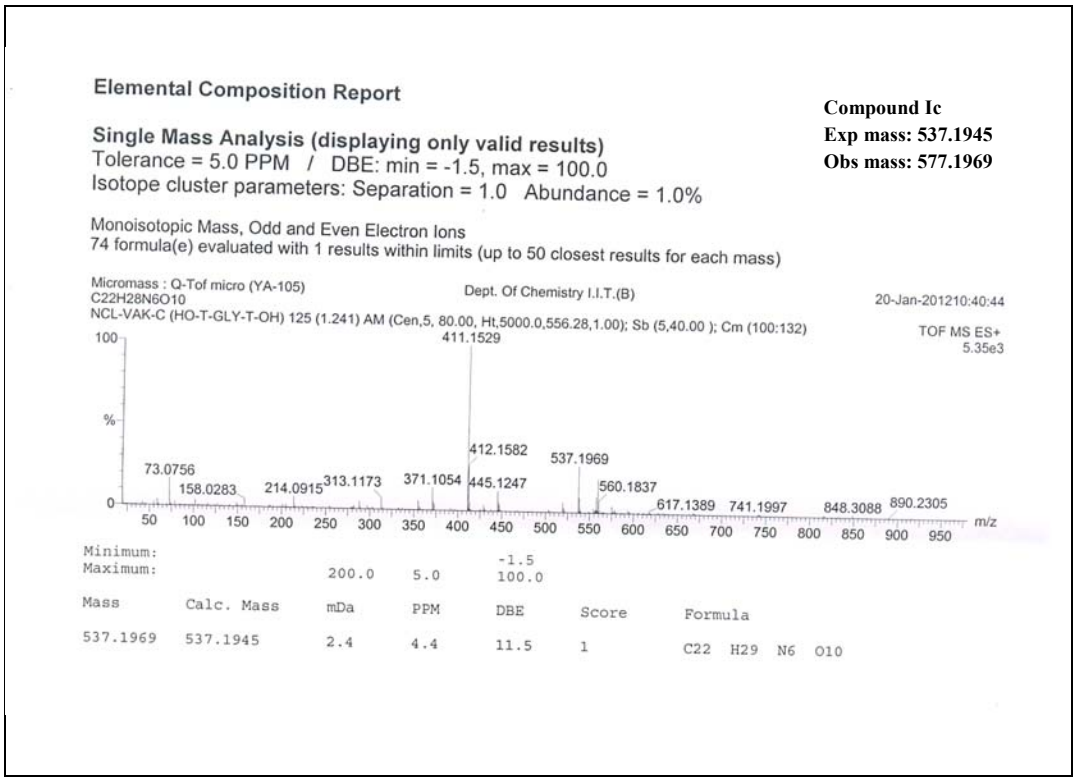

Compound Ic
Exp mass: 537.1945
Obs mass: 577.1969

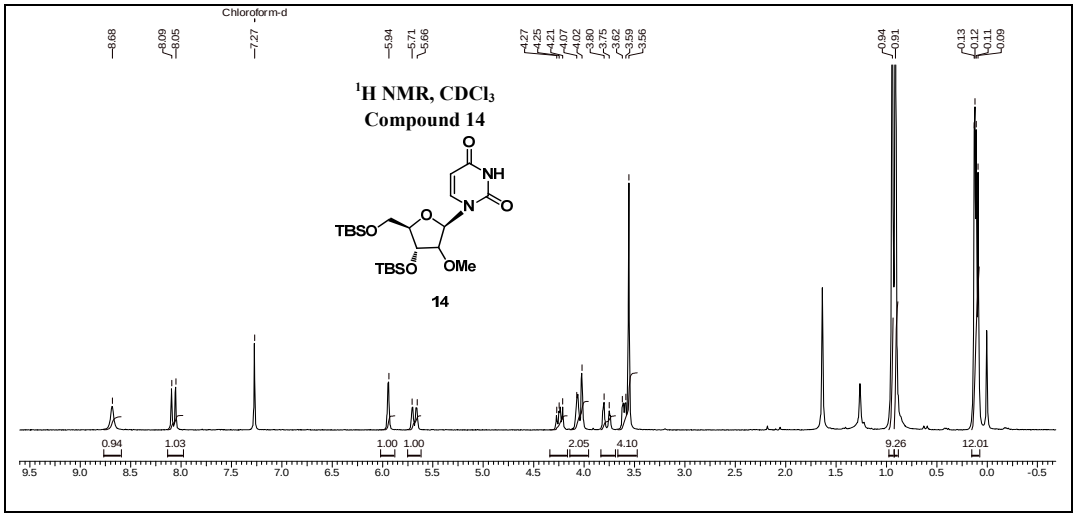
Chloroform-d
8.68
8.09
8.05
7.27
5.94
5.71
5.66
4.27
4.25
4.21
4.07
4.02
3.80
3.75
3.62
3.59
3.56
0.94
0.91
0.13
0.12
0.11
0.09
^{1}H NMR, CDCl$_3$
Compound 14
NH
N
O
TBSO
TBSO
OMe
14
0.94
1.03
1.00
1.00
2.05
4.10
9.26
12.01

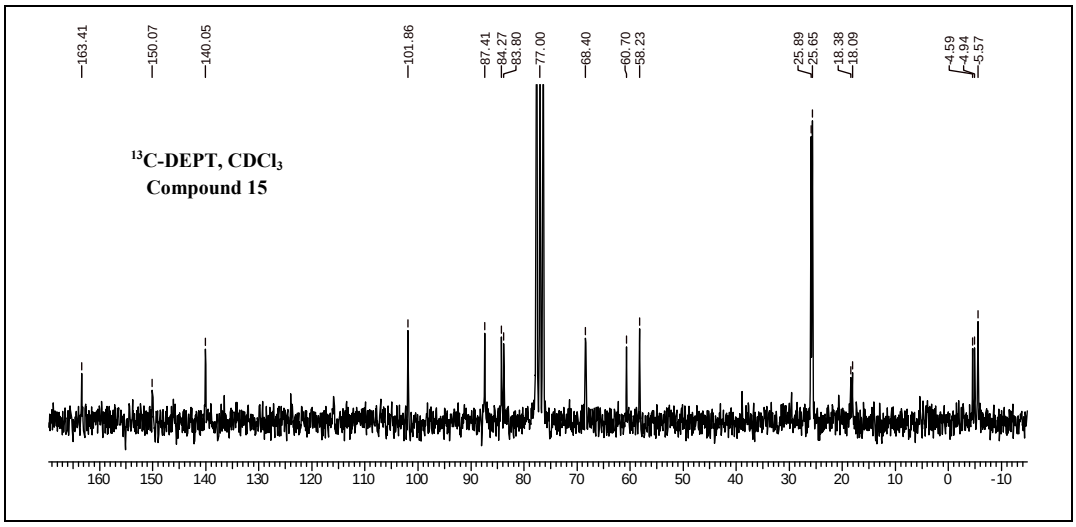
163.41
150.07
140.05
101.86
87.41
84.27
83.80
77.00
68.40
60.70
58.23
25.89
25.65
18.38
18.09
4.59
4.94
5.57
^{13}C-DEPT, CDCl$_3$
Compound 15

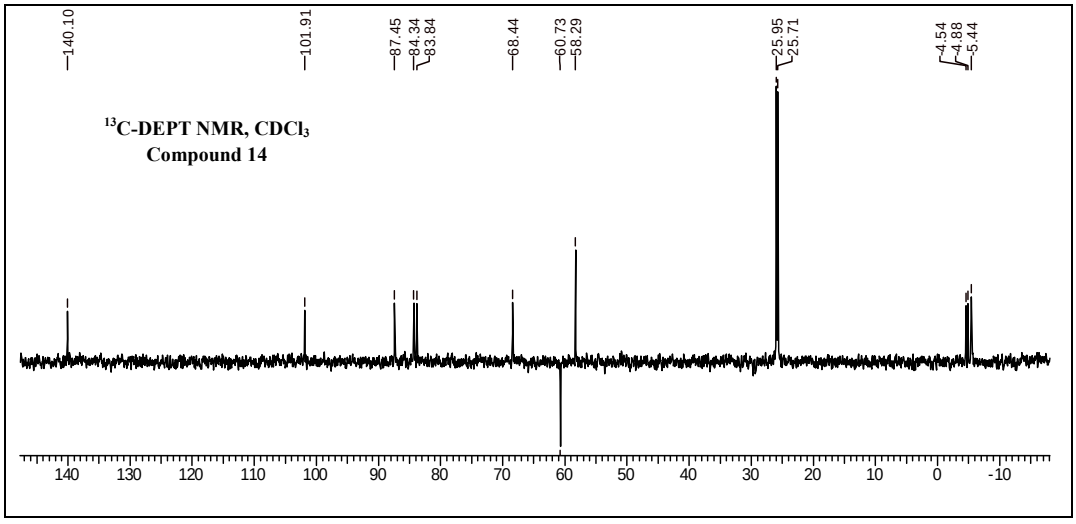
140.10
101.91
87.45
84.34
83.84
68.44
60.73
58.29
25.95
25.71
4.54
4.88
5.44
^{13}C-DEPT NMR, CDCl$_3$
Compound 14

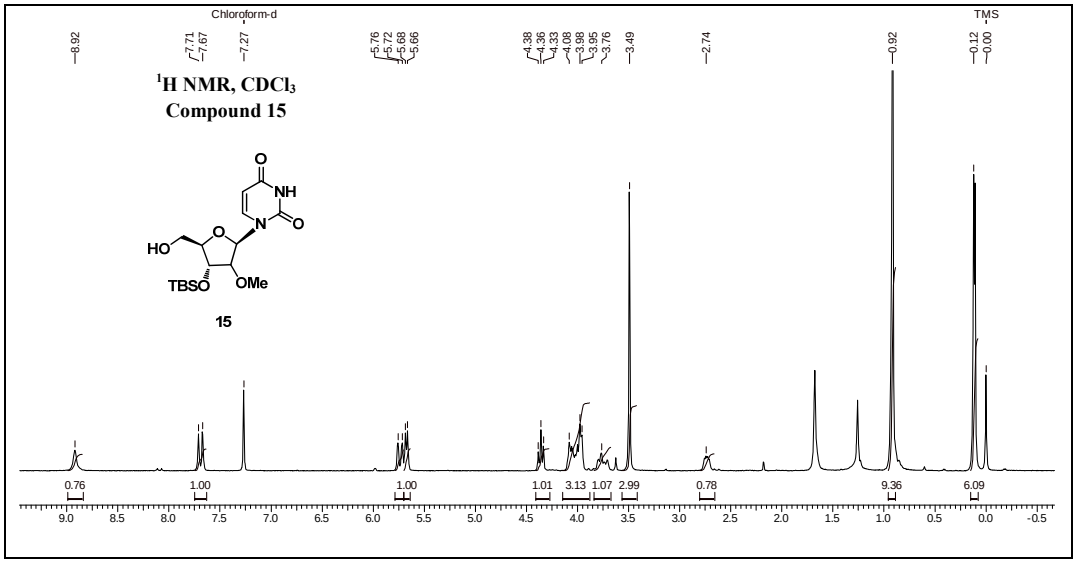
Chloroform-d
TMS
8.92
7.71
7.67
7.27
5.76
5.72
5.68
5.66
4.38
4.36
4.33
4.08
3.98
3.95
3.76
3.49
2.74
0.92
0.12
0.00
^{1}H NMR, CDCl$_3$
Compound 15
NH
O
N
HO
TBSO
OMe
15
0.76
1.00
1.00
1.01
3.13
1.07
2.99
0.78
9.36
6.09

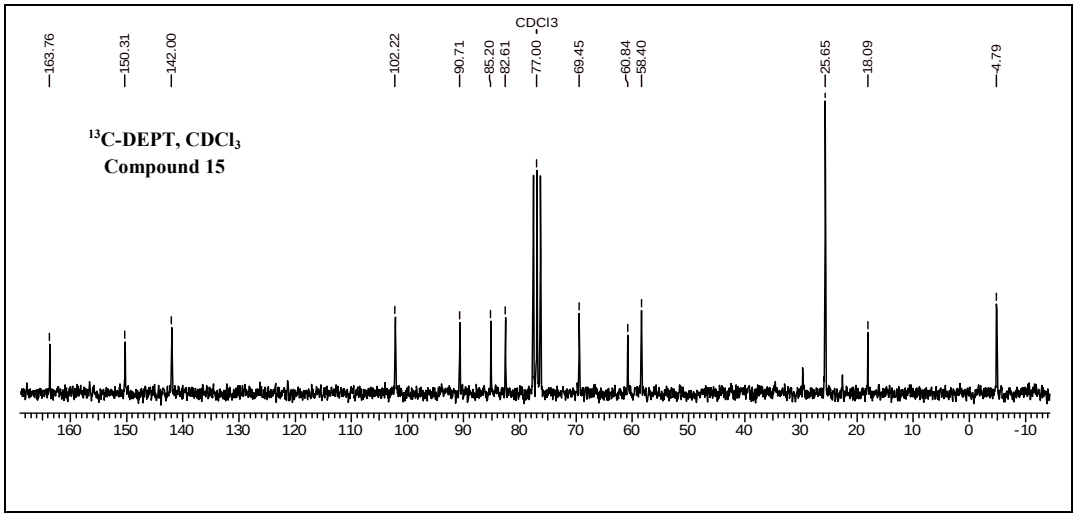
CDCl3
163.76
150.31
142.00
102.22
90.71
85.20
82.61
77.00
69.45
60.84
58.40
25.65
18.09
4.79
^{13}C-DEPT, CDCl$_3$
Compound 15

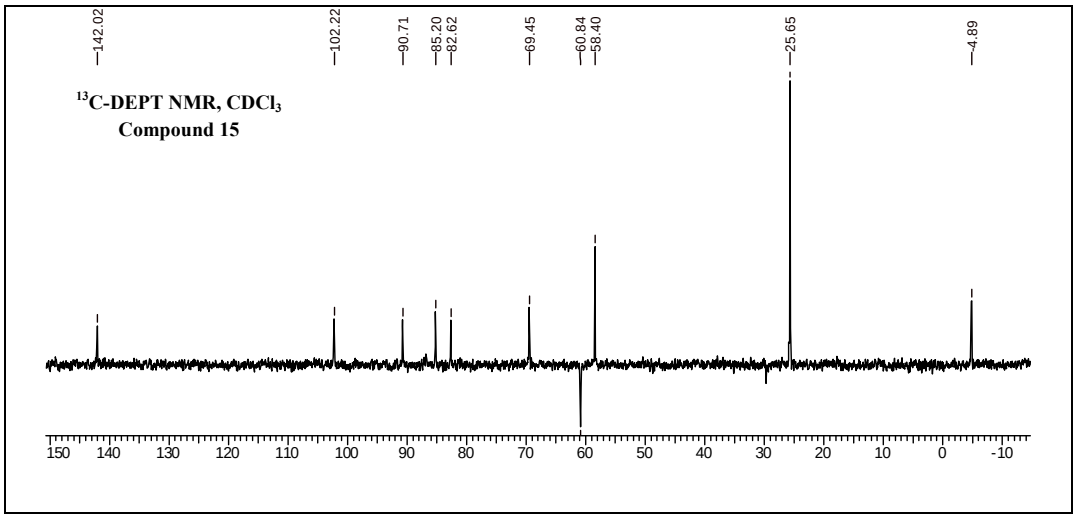
142.02
102.22
90.71
85.20
82.62
69.45
60.84
58.40
25.65
4.89
^{13}C-DEPT NMR, CDCl$_3$
Compound 15

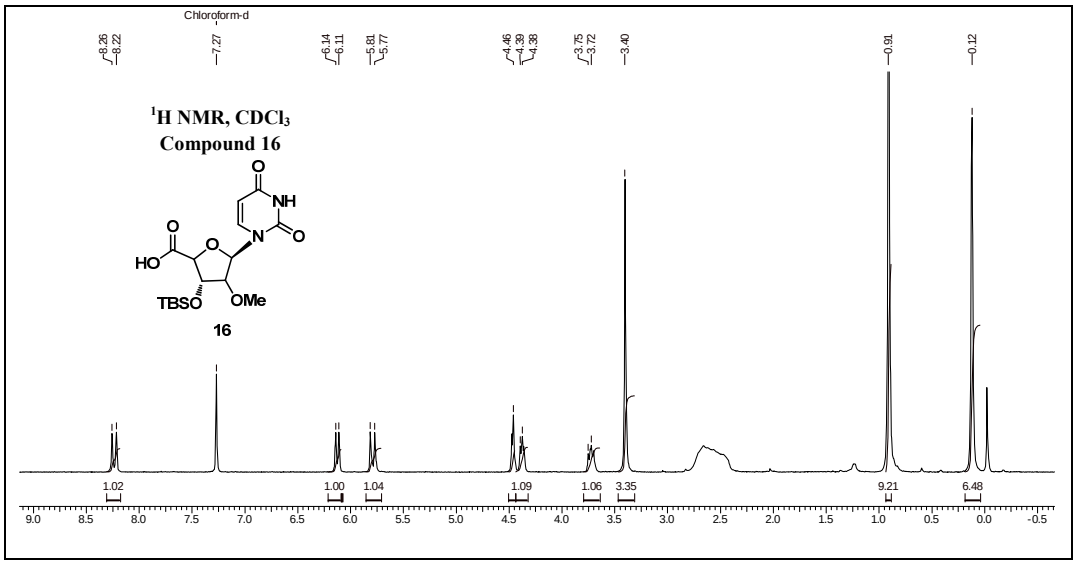
Chloroform-d
8.26
8.22
7.27
6.14
6.11
5.81
5.77
4.46
4.39
4.38
3.75
3.72
3.40
0.91
0.12
^{1}H NMR, CDCl$_3$
Compound 16
O
NH
N
O
O
HO
O
TBSO
OMe
16
1.02
1.00
1.04
1.09
1.06
3.35
9.21
6.48
9.0 8.5 8.0 7.5 7.0 6.5 6.0 5.5 5.0 4.5 4.0 3.5 3.0 2.5 2.0 1.5 1.0 0.5 0.0 -0.5

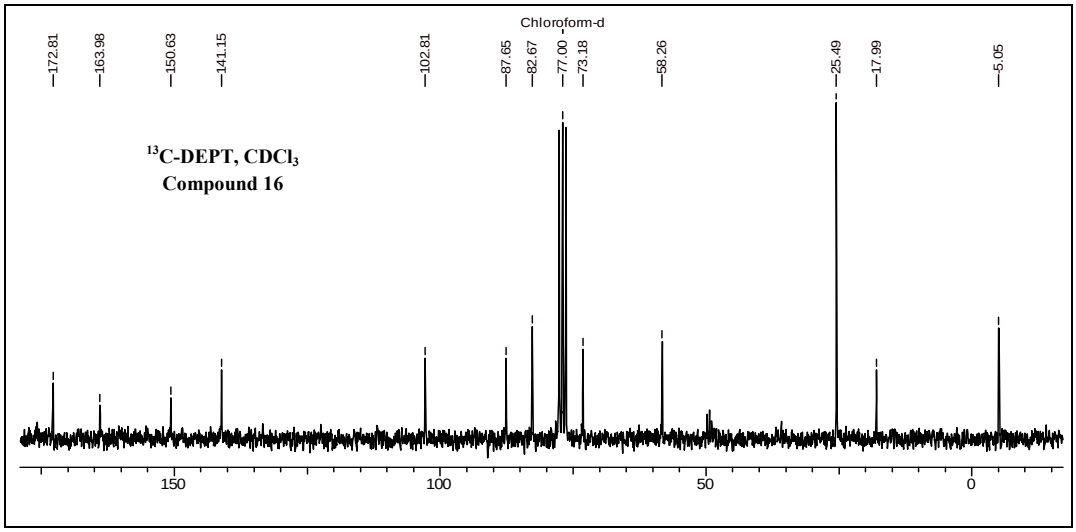
Chloroform-d
172.81
163.98
150.63
141.15
102.81
87.65
82.67
77.00
73.18
58.26
25.49
17.99
5.05
^{13}C-DEPT, CDCl$_3$
Compound 16
150
100
50
0

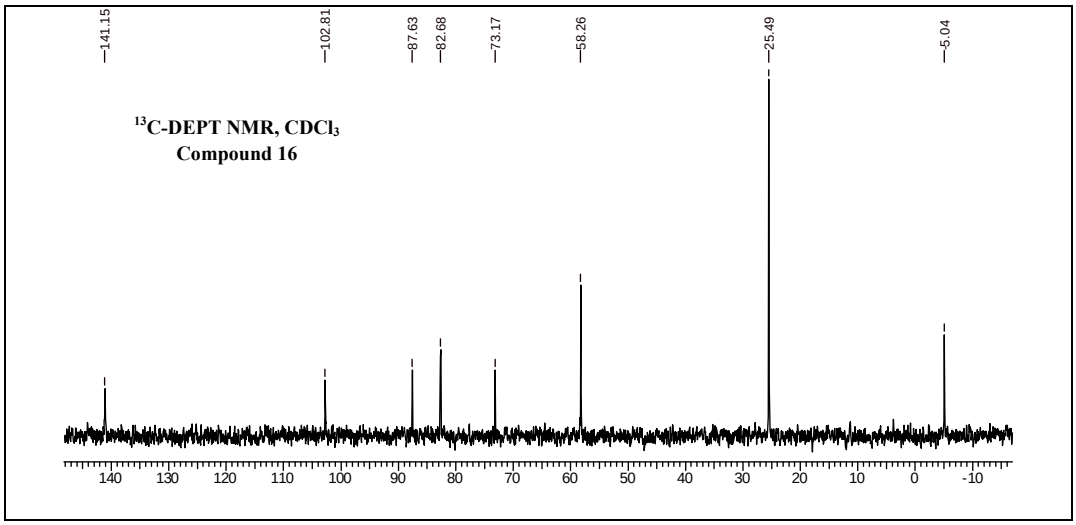
141.15
102.81
87.63
82.68
73.17
58.26
25.49
5.04
^{13}C-DEPT NMR, CDCl$_3$
Compound 16
140 130 120 110 100 90 80 70 60 50 40 30 20 10 0 -10

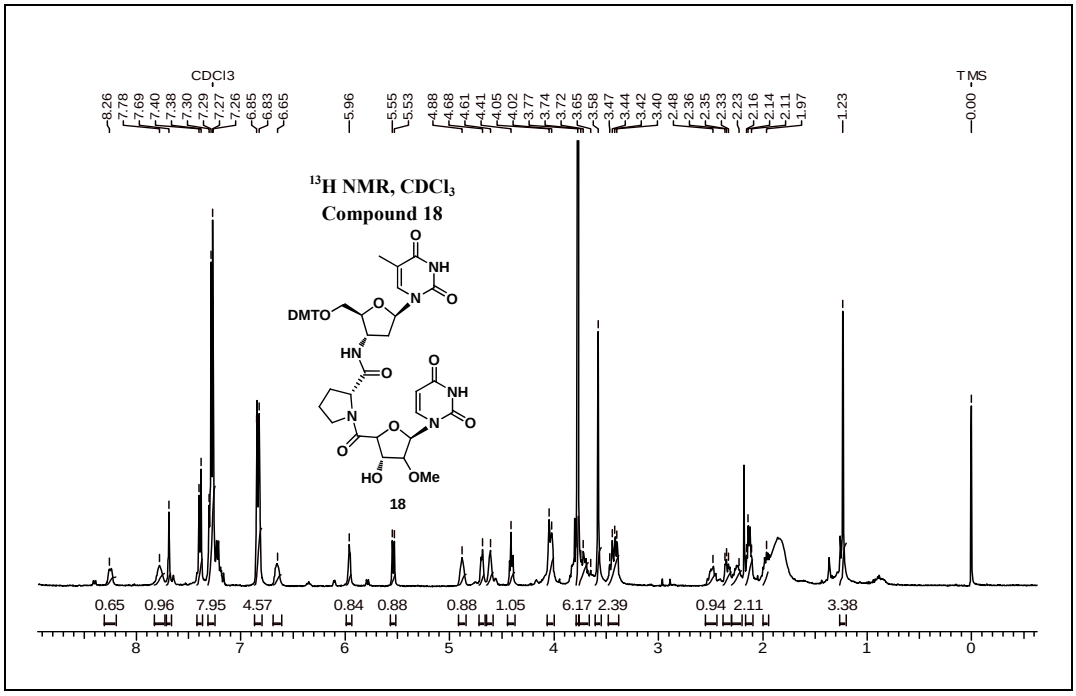
CDCl3
TMS
^{13}H NMR, CDCl$_3$
Compound 18
DMTO
HO
OMe
18

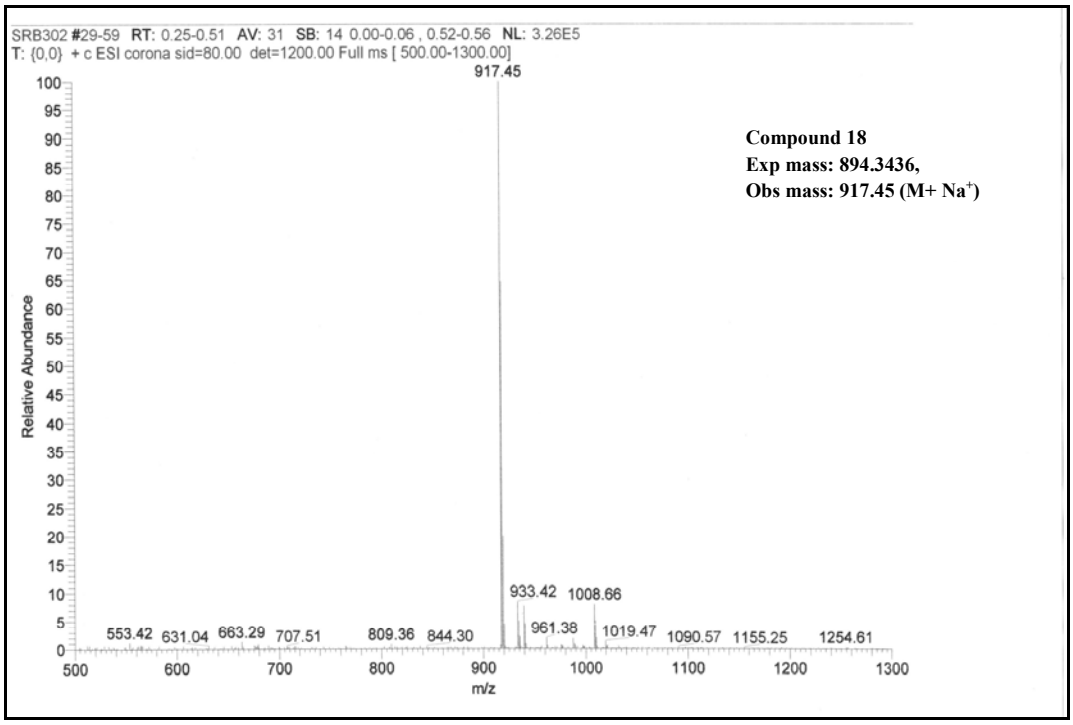
SRB302 #29-59 RT: 0.25-0.51 AV: 31 SB: 14 0.00-0.06 , 0.52-0.56 NL: 3.26E5
T: {0,0} + c ESI corona sid=80.00 det=1200.00 Full ms [500.00-1300.00]
917.45
Relative Abundance
m/z
Compound 18
Exp mass: 894.3436,
Obs mass: 917.45 (M+ Na+)

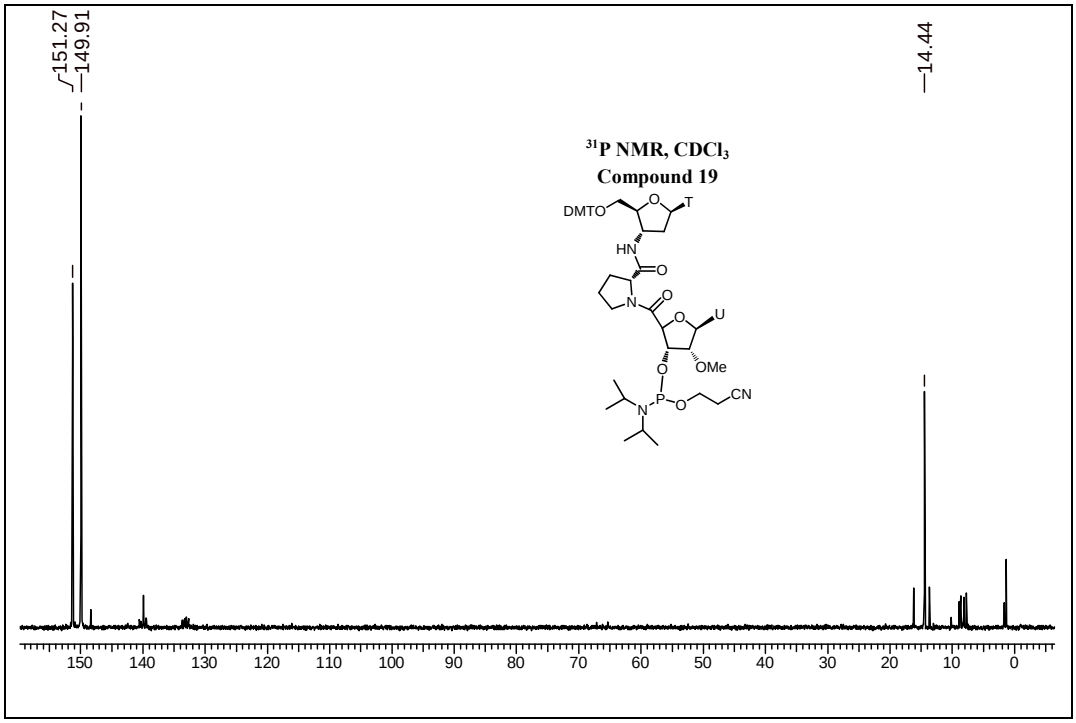
151.27
149.91
14.44
31P NMR, CDCl3
Compound 19
DMTO
T
HN
O
N
O
O
U
OMe
O
N
P
O
CN
150
140
130
120
110
100
90
80
70
60
50
40
30
20
10
0

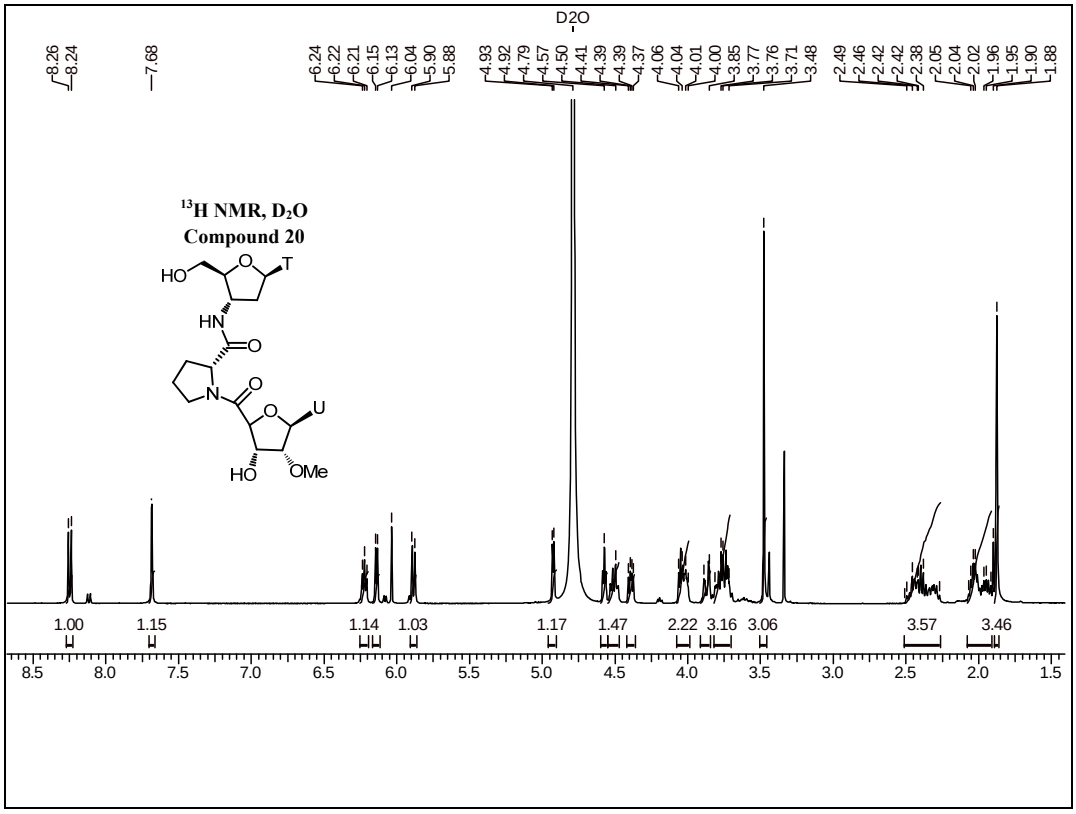
D2O
8.26
8.24
7.68
6.24
6.22
6.21
6.15
6.13
6.04
5.90
5.88
4.93
4.92
4.79
4.57
4.50
4.41
4.39
4.39
4.37
4.06
4.04
4.01
4.00
3.85
3.77
3.76
3.71
3.48
2.49
2.46
2.42
2.42
2.38
2.05
2.04
2.02
1.96
1.95
1.90
1.88
^{13}H NMR, D$_2$O
Compound 20
HO
T
HN
O
N
O
O
U
HO
OMe
1.00
1.15
1.14
1.03
1.17
1.47
2.22
3.16
3.06
3.57
3.46
8.5
8.0
7.5
7.0
6.5
6.0
5.5
5.0
4.5
4.0
3.5
3.0
2.5
2.0
1.5

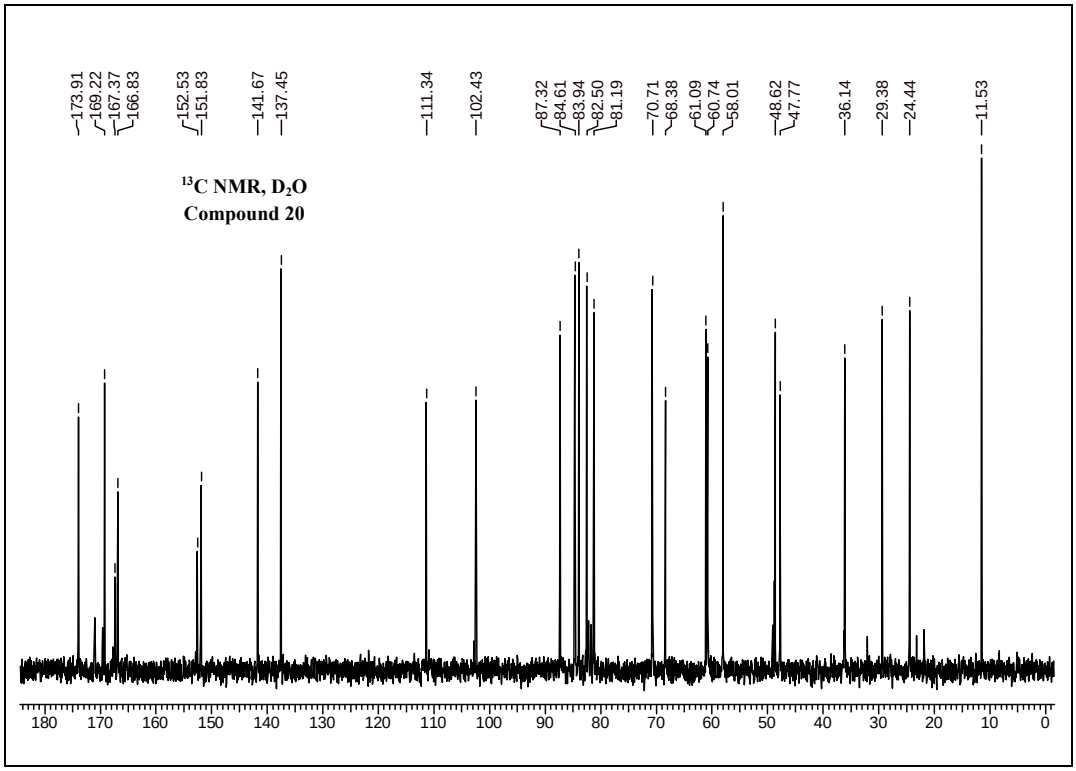
173.91
169.22
167.37
166.83
152.53
151.83
141.67
137.45
111.34
102.43
87.32
84.61
83.94
82.50
81.19
70.71
68.38
61.09
60.74
58.01
48.62
47.77
36.14
29.38
24.44
11.53
^{13}C NMR, D$_2$O
Compound 20
180
170
160
150
140
130
120
110
100
90
80
70
60
50
40
30
20
10
0

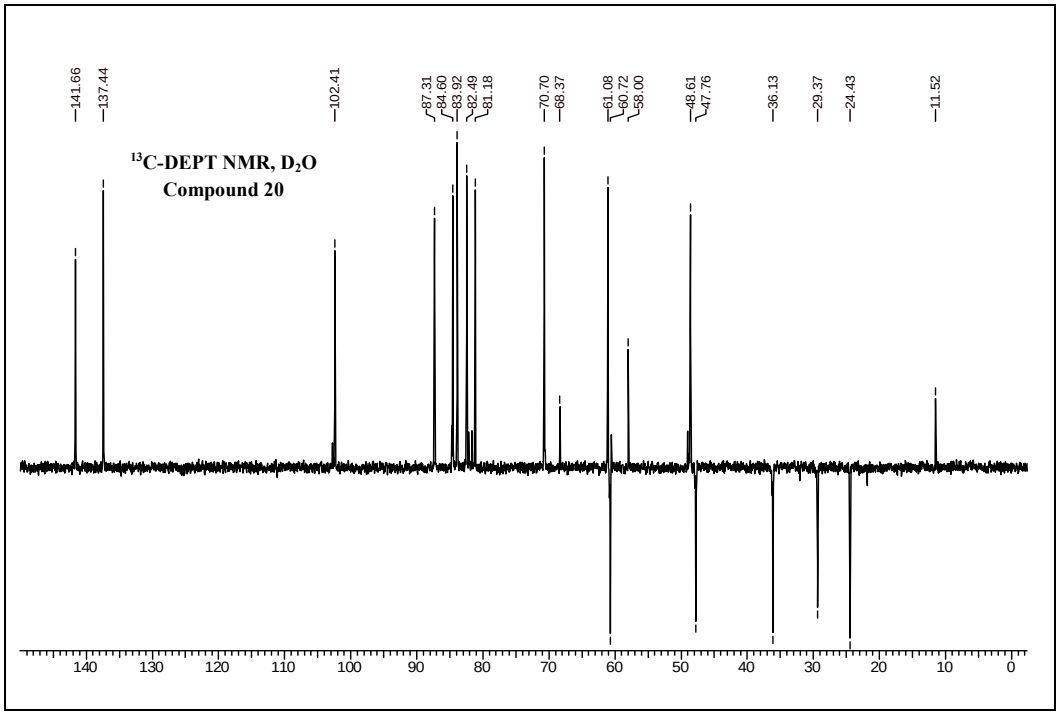

Elemental Composition Report Page 1

Single Mass Analysis (displaying only valid results)
Tolerance = 10.0 PPM / DBE: min = -1.5, max = 100.0
Isotope cluster parameters: Separation = 1.0 Abundance = 1.0%

Compound 20
Exp mass: 593.2207
Obs mass: 593.2196

Monoisotopic Mass, Odd and Even Electron Ions
79 formula(e) evaluated with 1 results within limits (up to 50 closest results for each mass)

Micromass : Q-Tof micro (YA-105) Dept. Of Chemistry I.I.T.(B) 20-Jan-201211:11:02
C25H32N6O11
NCL-VAK-D (HO-T-D-PRO-U-OH) 10 (0.099) AM (Cen,5, 80.00, Ht,5000.0,556.28,1.00); Sm (Md, 4.00); Cm (1:33) TOF MS ES+
4.68e3

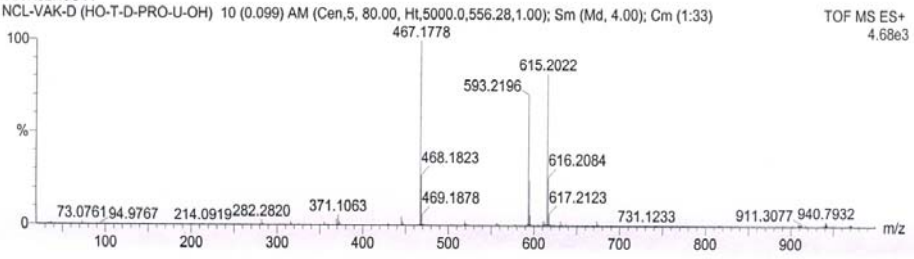

Minimum:				-1.5		
Maximum:		200.0	10.0	100.0		
Mass	Calc. Mass	mDa	PPM	DBE	Score	Formula
593.2196	593.2207	-1.1	-1.9	12.5	1	C25 H33 N6 O11

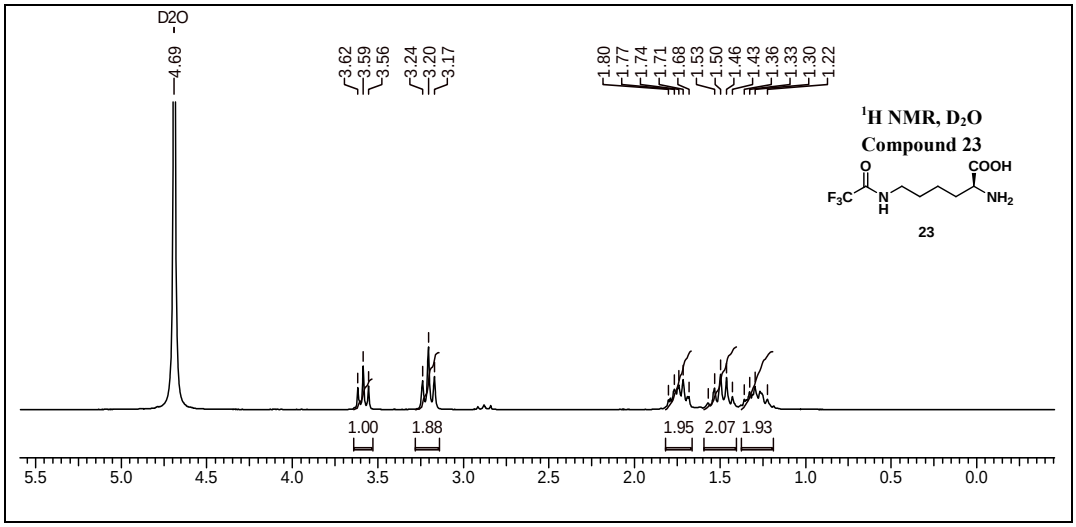
D2O
4.69
3.62
3.59
3.56
3.24
3.20
3.17
1.80
1.77
1.74
1.71
1.68
1.53
1.50
1.46
1.43
1.36
1.33
1.30
1.22
1H NMR, D2O
Compound 23
O
COOH
F3C
N
H
NH2
23
1.00
1.88
1.95
2.07
1.93
5.5
5.0
4.5
4.0
3.5
3.0
2.5
2.0
1.5
1.0
0.5
0.0

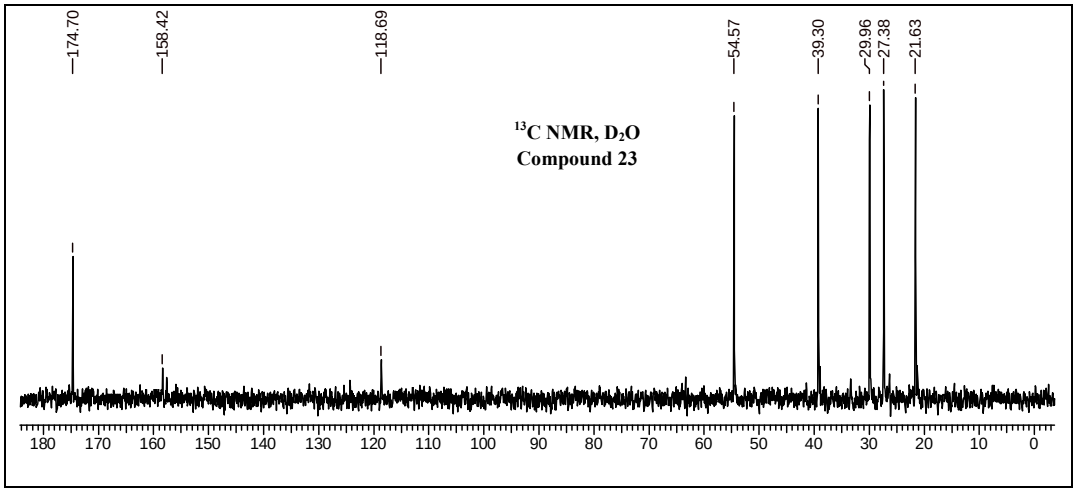
174.70
158.42
118.69
54.57
39.30
29.96
27.38
21.63
13C NMR, D2O
Compound 23
180
170
160
150
140
130
120
110
100
90
80
70
60
50
40
30
20
10
0

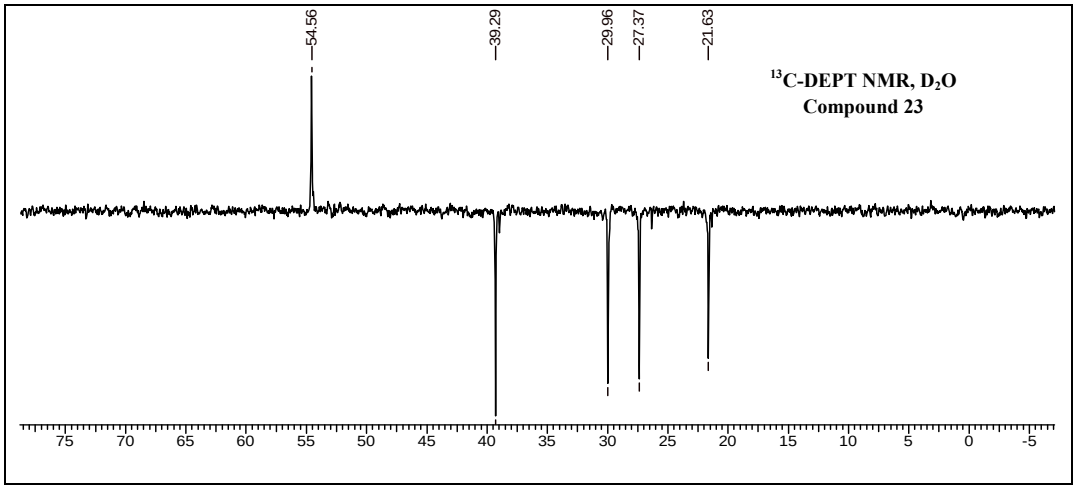
54.56
39.29
29.96
27.37
21.63
13C-DEPT NMR, D2O
Compound 23
75
70
65
60
55
50
45
40
35
30
25
20
15
10
5
0
-5

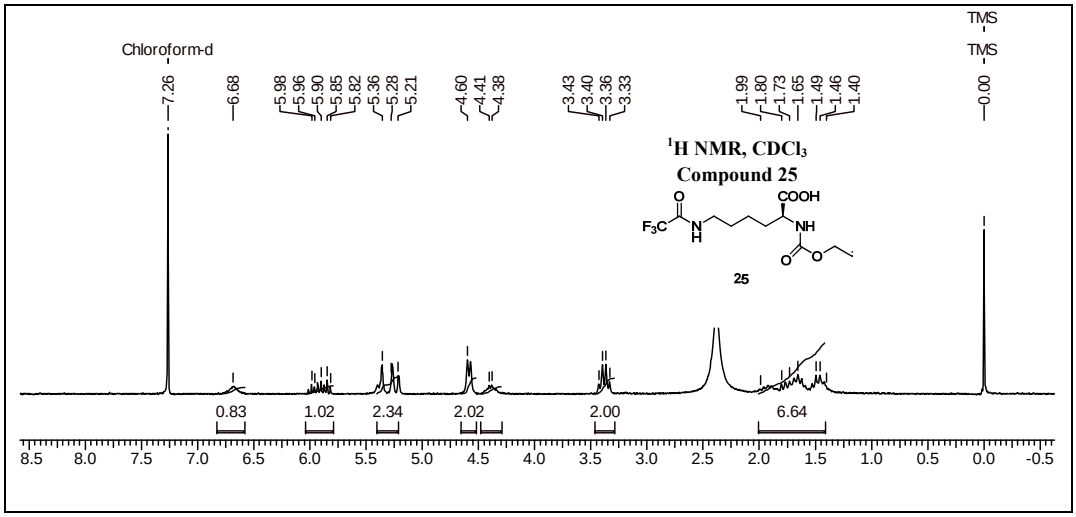
TMS
TMS
Chloroform-d
7.26
6.68
5.98
5.96
5.90
5.85
5.82
5.36
5.28
5.21
4.60
4.41
4.38
3.43
3.40
3.36
3.33
1.99
1.80
1.73
1.65
1.49
1.46
1.40
0.00
^{1}H NMR, CDCl$_3$
Compound 25
COOH
NH
F_3C
25
0.83
1.02
2.34
2.02
2.00
6.64

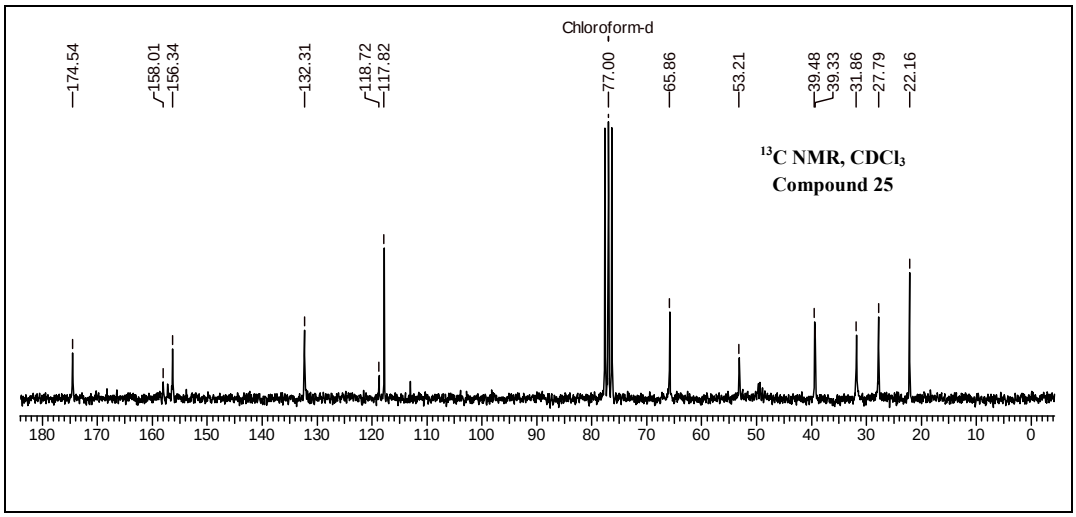
Chloroform-d
174.54
158.01
156.34
132.31
118.72
117.82
77.00
65.86
53.21
39.48
39.33
31.86
27.79
22.16
^{13}C NMR, CDCl$_3$
Compound 25

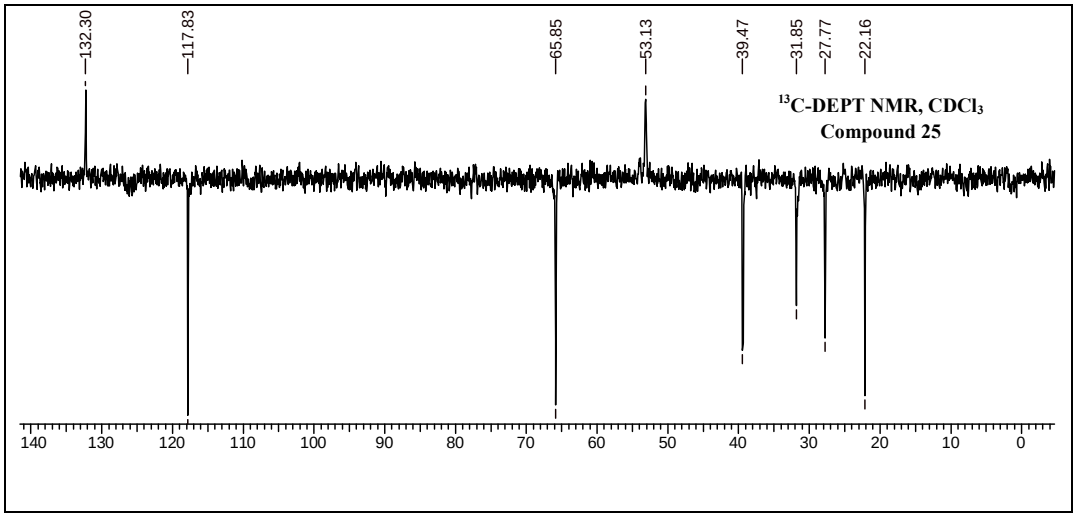
132.30
117.83
65.85
53.13
39.47
31.85
27.77
22.16
^{13}C-DEPT NMR, CDCl$_3$
Compound 25

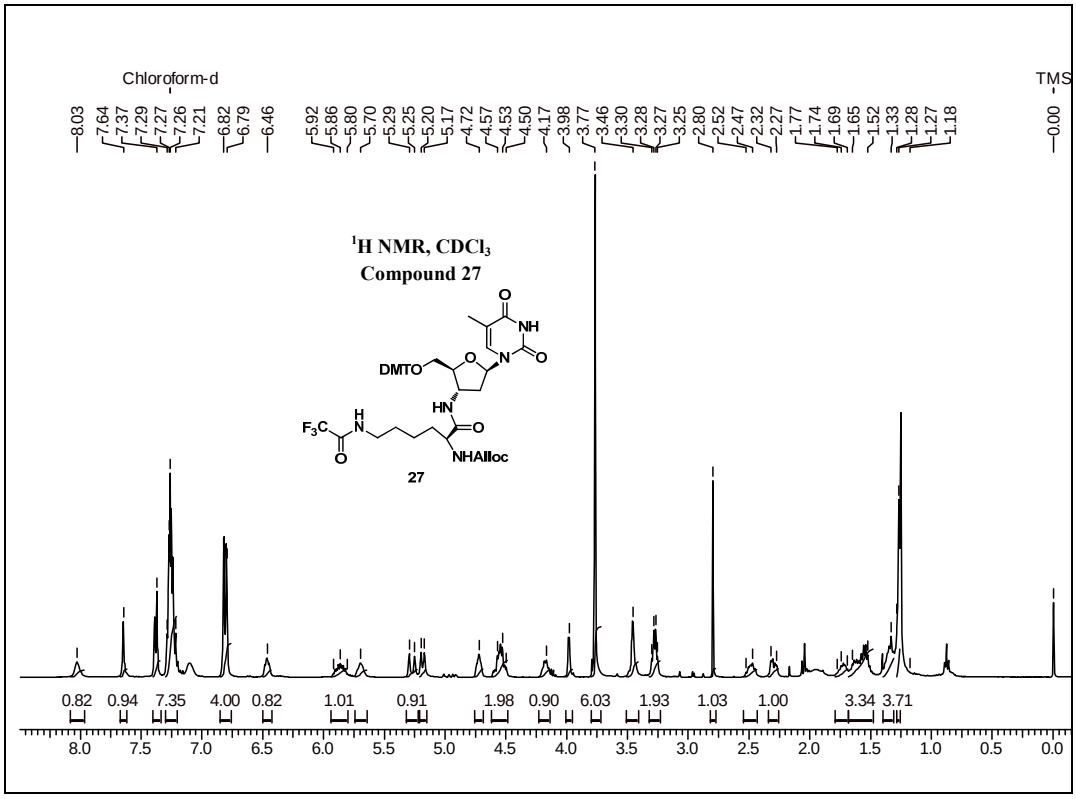
Chloroform-d
TMS
8.03 7.64 7.37 7.29 7.27 7.26 7.21 6.82 6.79 6.46 5.92 5.86 5.80 5.70 5.29 5.25 5.20 5.17 4.72 4.57 4.53 4.50 4.17 3.98 3.77 3.46 3.30 3.28 3.27 3.25 2.80 2.52 2.47 2.32 2.27 1.77 1.74 1.69 1.65 1.52 1.33 1.28 1.27 1.18 0.00
^{1}H NMR, $CDCl_3$
Compound 27
DMTO
HN
F_3C
NHAlloc
27
0.82 0.94 7.35 4.00 0.82 1.01 0.91 1.98 0.90 6.03 1.93 1.03 1.00 3.34 3.71
8.0 7.5 7.0 6.5 6.0 5.5 5.0 4.5 4.0 3.5 3.0 2.5 2.0 1.5 1.0 0.5 0.0

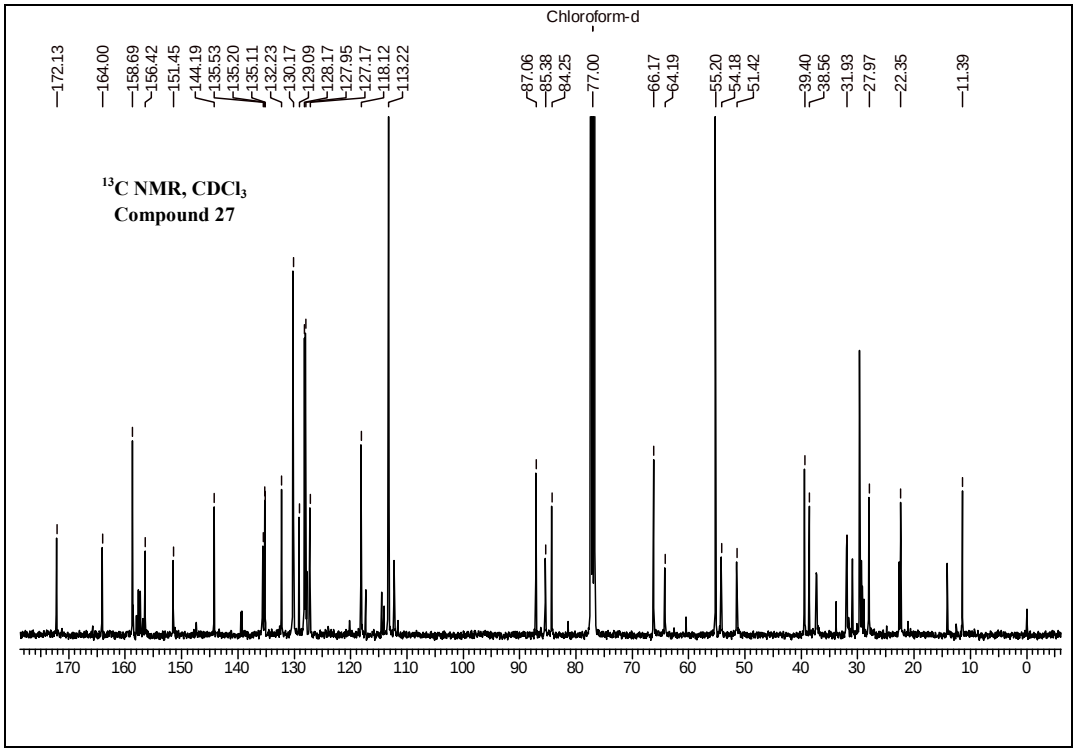
Chloroform-d
172.13 164.00 158.69 156.42 151.45 144.19 135.53 135.20 135.11 132.23 130.17 129.09 128.17 127.95 127.17 118.12 113.22 87.06 85.38 84.25 77.00 66.17 64.19 55.20 54.18 51.42 39.40 38.56 31.93 27.97 22.35 11.39
^{13}C NMR, $CDCl_3$
Compound 27
170 160 150 140 130 120 110 100 90 80 70 60 50 40 30 20 10 0

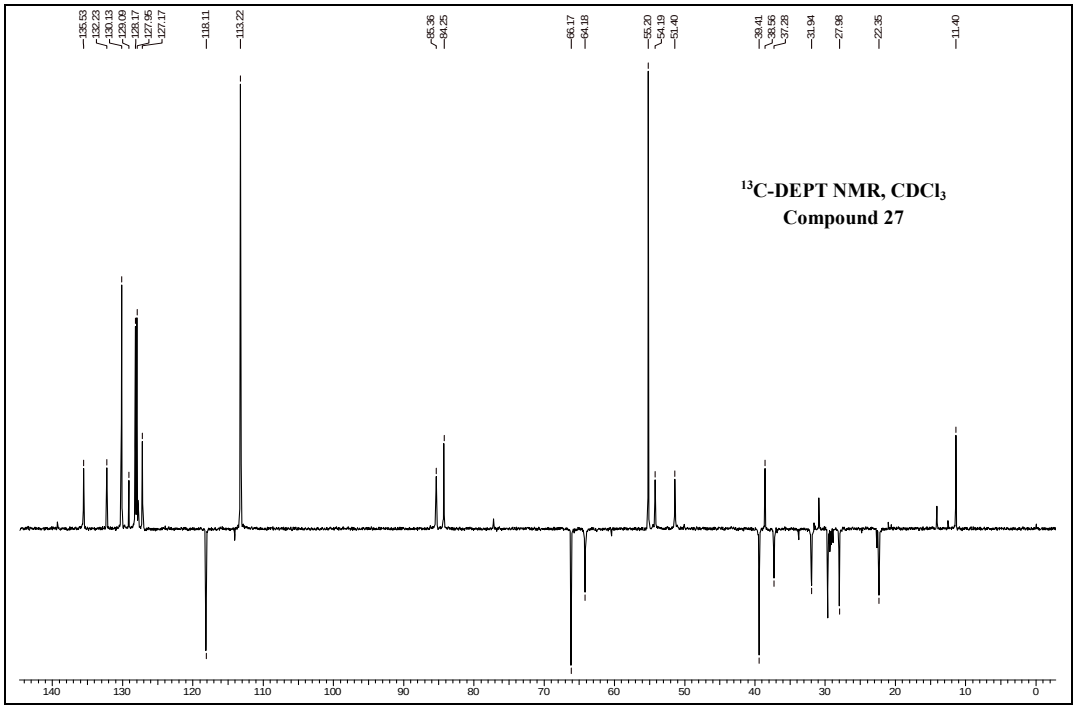
135.53
132.23
130.13
128.09
128.17
127.85
127.17
118.11
113.22
85.36
84.25
66.17
64.18
55.20
54.19
51.40
39.41
38.56
37.28
31.94
27.98
22.35
11.40
13C-DEPT NMR, CDCl3
Compound 27

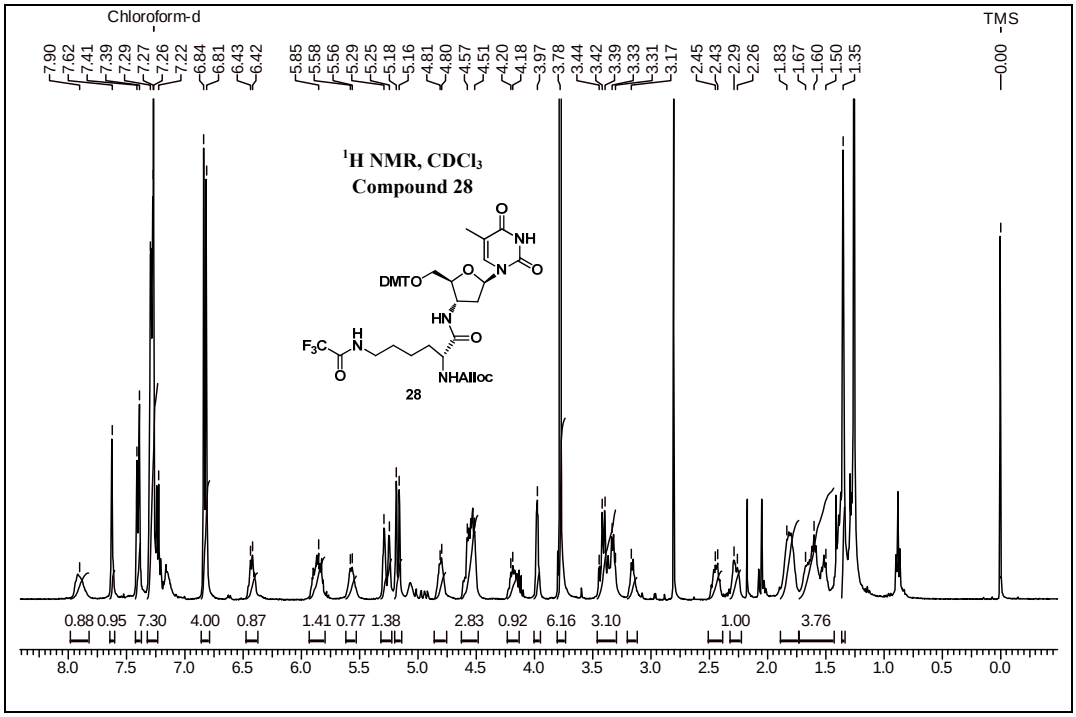
Chloroform-d
TMS
1H NMR, CDCl3
Compound 28
DMTO
NH
HN
F3C
NHAlloc
28
0.88 0.95 7.30 4.00 0.87 1.41 0.77 1.38 2.83 0.92 6.16 3.10 1.00 3.76

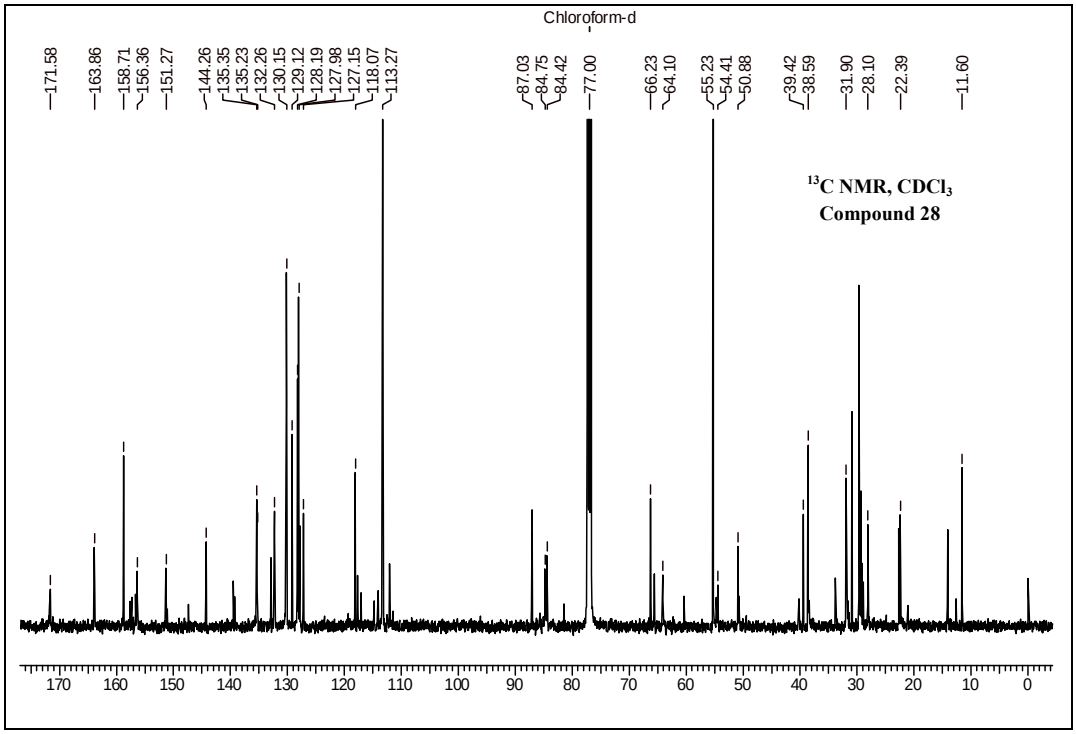
Chloroform-d
171.58
163.86
158.71
156.36
151.27
144.26
135.35
135.23
132.26
130.15
129.12
128.19
127.98
127.15
118.07
113.27
87.03
84.75
84.42
77.00
66.23
64.10
55.23
54.41
50.88
39.42
38.59
31.90
28.10
22.39
11.60
13C NMR, CDCl3
Compound 28
170 160 150 140 130 120 110 100 90 80 70 60 50 40 30 20 10 0

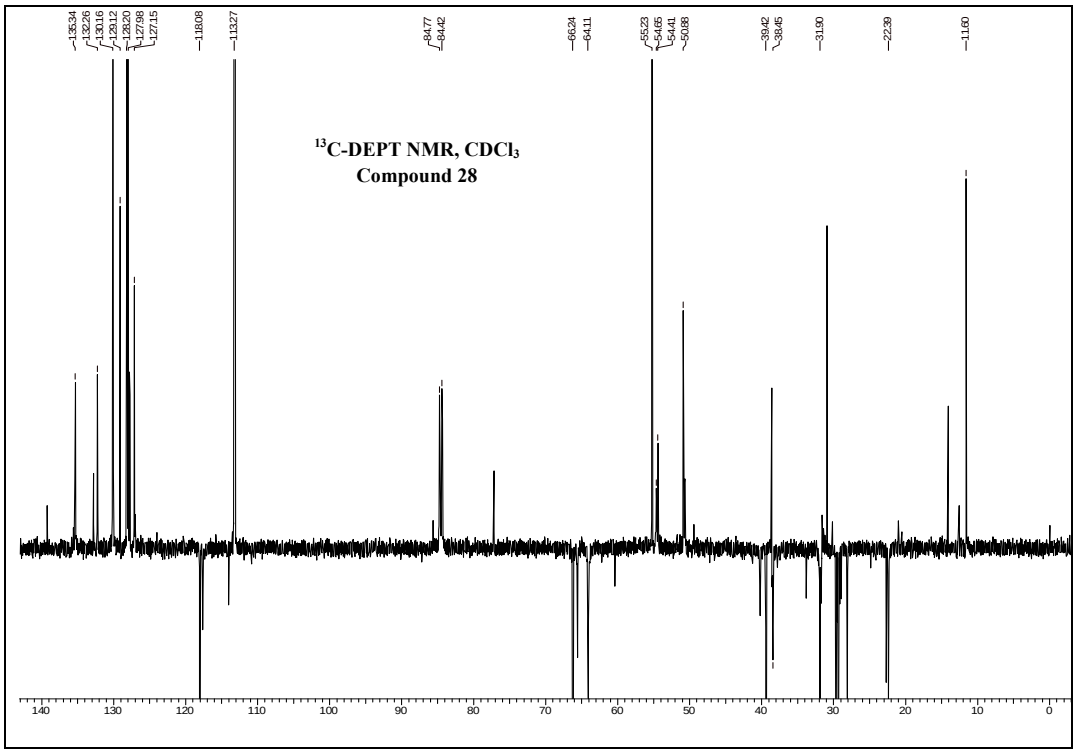
135.34
132.26
130.16
129.12
128.20
127.98
127.15
118.08
113.27
84.77
84.42
66.24
64.11
55.23
54.65
54.41
50.88
39.42
38.45
31.90
22.39
11.60
13C-DEPT NMR, CDCl3
Compound 28
140 130 120 110 100 90 80 70 60 50 40 30 20 10 0

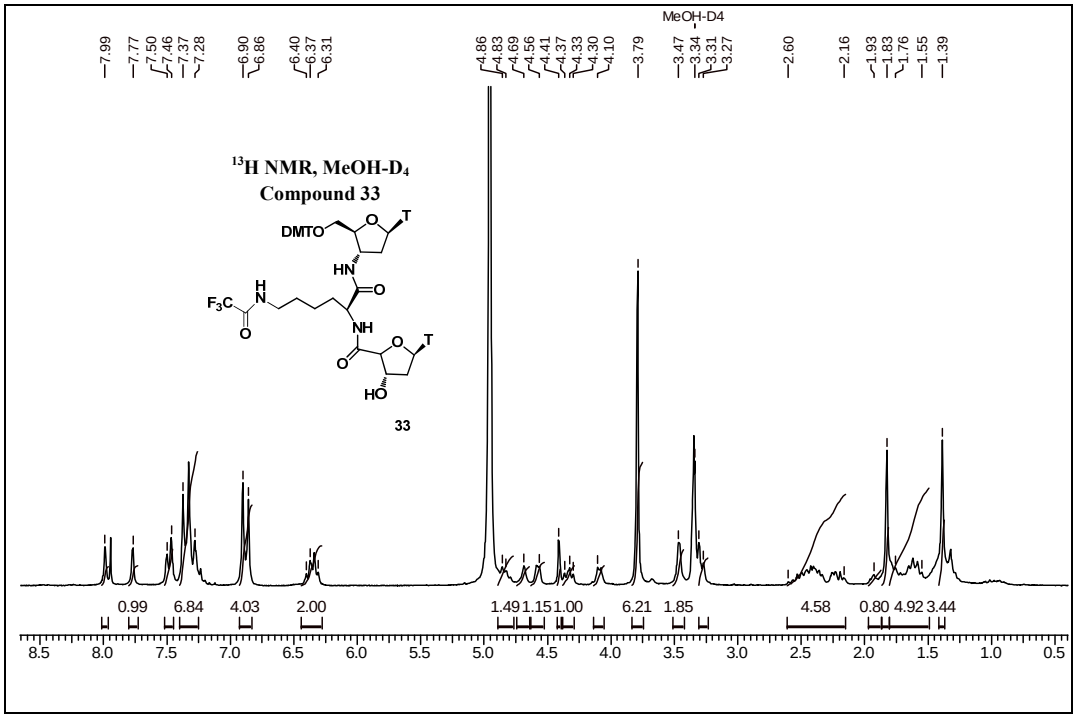
MeOH-D4
7.99
7.77
7.50
7.46
7.37
7.28
6.90
6.86
6.40
6.37
6.31
4.86
4.83
4.69
4.56
4.41
4.37
4.33
4.30
4.10
3.79
3.47
3.34
3.31
3.27
2.60
2.16
1.93
1.83
1.76
1.55
1.39
13H NMR, MeOH-D4
Compound 33
DMTO
T
HN
H
N
F3C
O
NH
HO
33
0.99
6.84
4.03
2.00
1.49
1.15
1.00
6.21
1.85
4.58
0.80
4.92
3.44
8.5
8.0
7.5
7.0
6.5
6.0
5.5
5.0
4.5
4.0
3.5
3.0
2.5
2.0
1.5
1.0
0.5

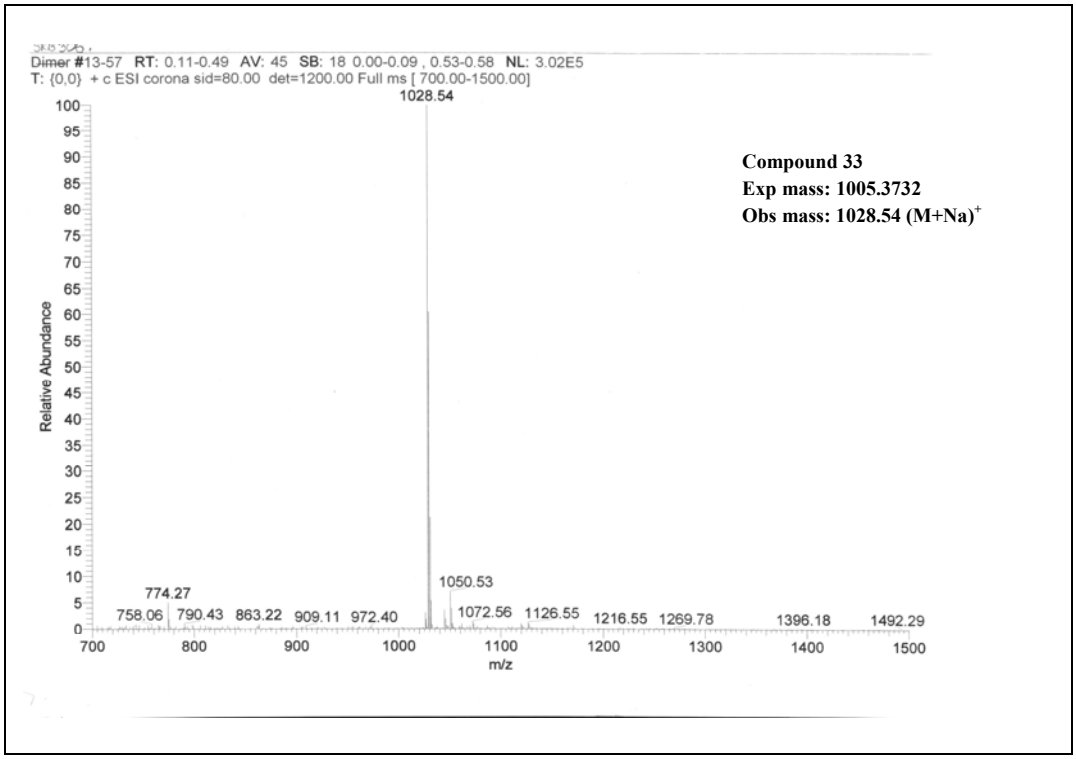
Dimer #13-57 RT: 0.11-0.49 AV: 45 SB: 18 0.00-0.09 , 0.53-0.58 NL: 3.02E5
T: {0,0} + c ESI corona sid=80.00 det=1200.00 Full ms [700.00-1500.00]
1028.54
Relative Abundance
774.27
758.06
790.43
863.22
909.11
972.40
1050.53
1072.56
1126.55
1216.55
1269.78
1396.18
1492.29
m/z
Compound 33
Exp mass: 1005.3732
Obs mass: 1028.54 (M+Na)+

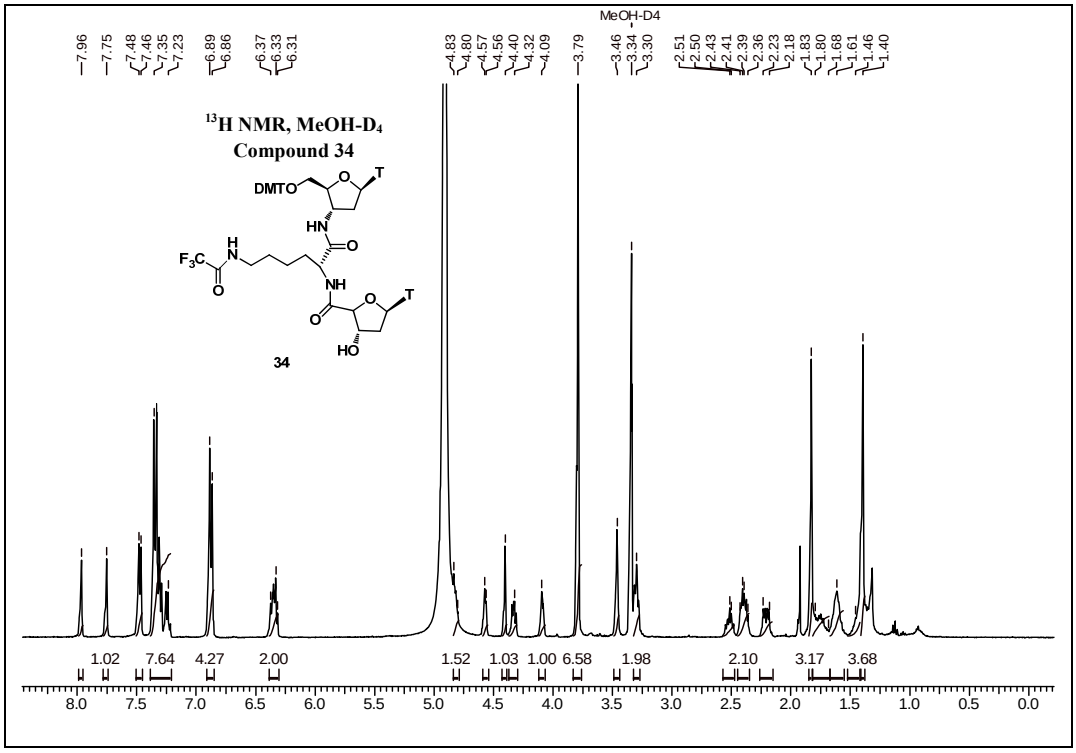
MeOH-D4
7.96
7.75
7.48
7.46
7.35
7.23
6.89
6.86
6.37
6.33
6.31
4.83
4.80
4.57
4.56
4.40
4.32
4.09
3.79
3.46
3.34
3.30
2.51
2.50
2.43
2.41
2.39
2.36
2.23
2.18
1.83
1.80
1.68
1.61
1.46
1.40
13H NMR, MeOH-D4
Compound 34
DMTO
T
HN
O
H
N
F3C
O
NH
O
T
HO
34
1.02
7.64
4.27
2.00
1.52
1.03
1.00
6.58
1.98
2.10
3.17
3.68
8.0
7.5
7.0
6.5
6.0
5.5
5.0
4.5
4.0
3.5
3.0
2.5
2.0
1.5
1.0
0.5
0.0

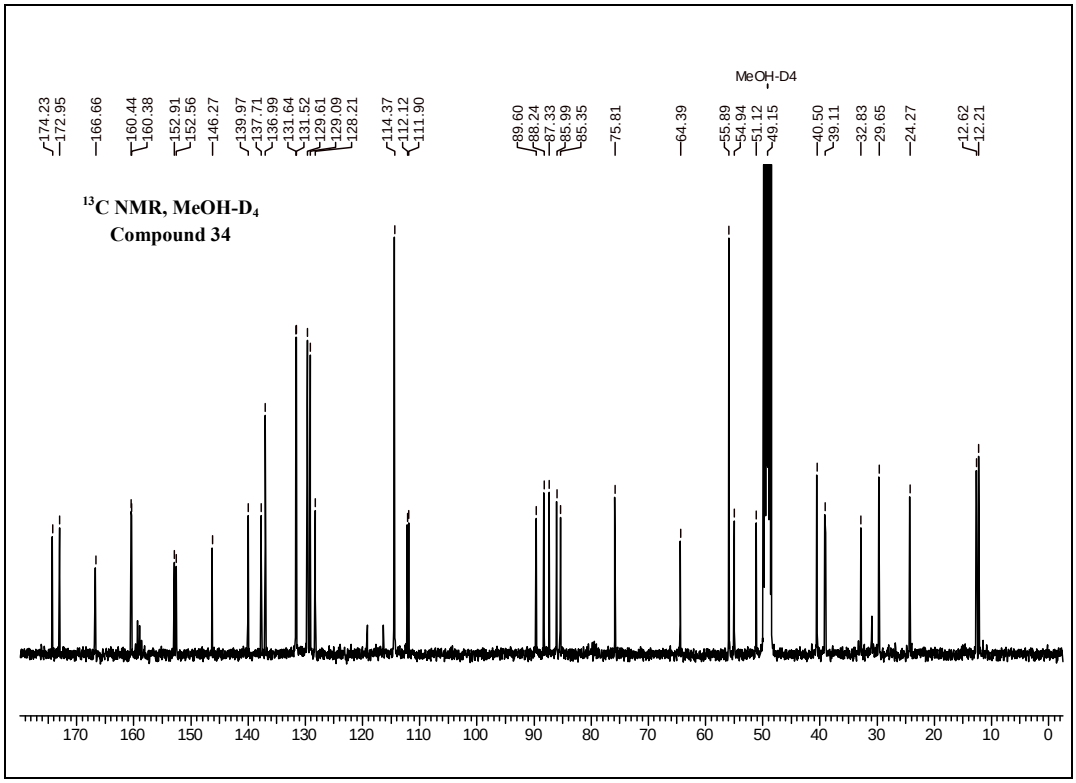
MeOH-D4
174.23
172.95
166.66
160.44
160.38
152.91
152.56
146.27
139.97
137.71
136.99
131.64
131.52
129.61
129.09
128.21
114.37
112.12
111.90
89.60
88.24
87.33
85.99
85.35
75.81
64.39
55.89
54.94
51.12
49.15
40.50
39.11
32.83
29.65
24.27
12.62
12.21
13C NMR, MeOH-D4
Compound 34
170
160
150
140
130
120
110
100
90
80
70
60
50
40
30
20
10
0

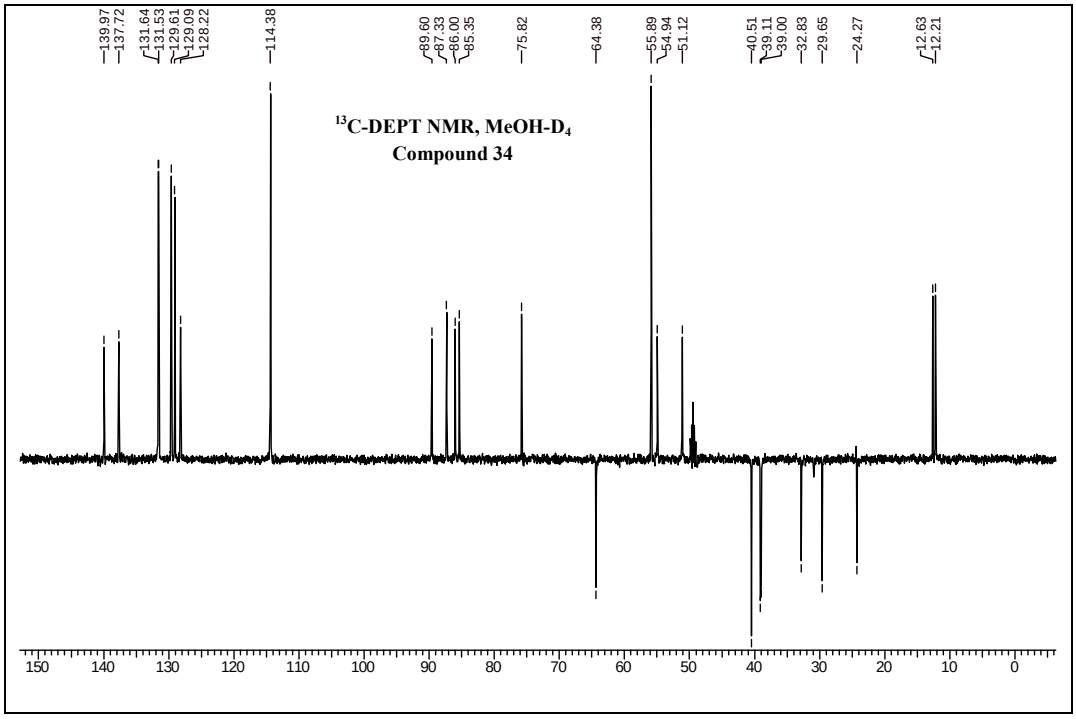
139.97
137.72
131.64
131.53
129.61
129.09
128.22
114.38
89.60
87.33
86.00
85.35
75.82
64.38
55.89
54.94
51.12
40.51
39.11
39.00
32.83
29.65
24.27
12.63
12.21
13C-DEPT NMR, MeOH-D4
Compound 34
150 140 130 120 110 100 90 80 70 60 50 40 30 20 10 0

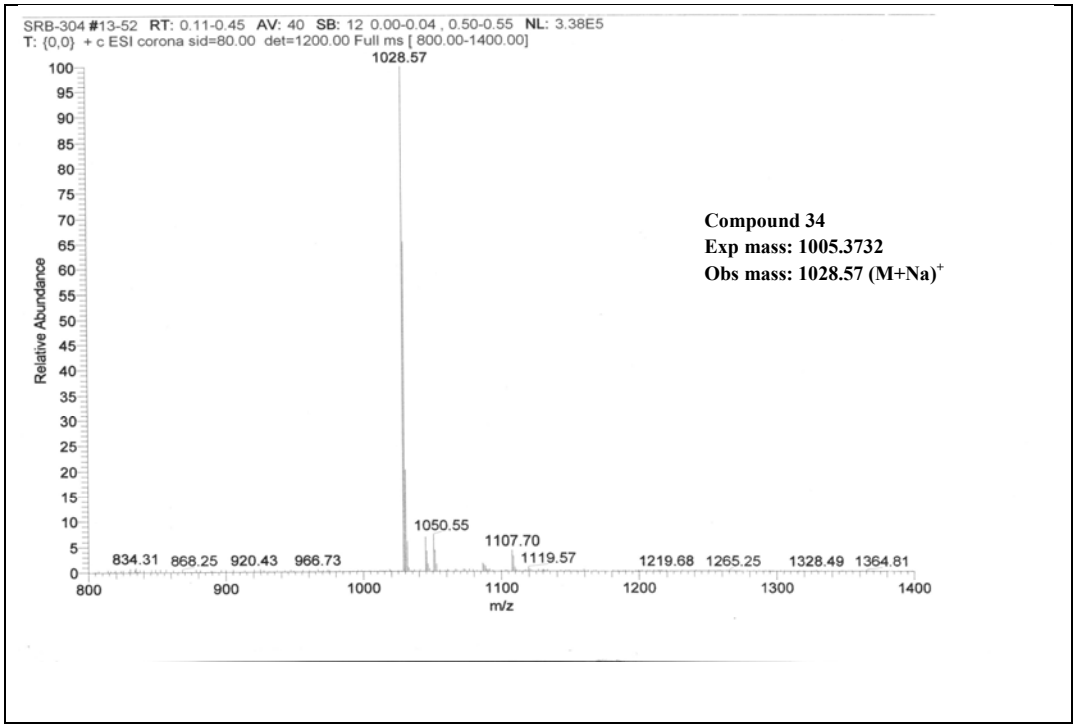
SRB-304 #13-52 RT: 0.11-0.45 AV: 40 SB: 12 0.00-0.04 , 0.50-0.55 NL: 3.38E5
T: {0,0} + c ESI corona sid=80.00 det=1200.00 Full ms [800.00-1400.00]
1028.57
Relative Abundance
m/z
1050.55
1107.70
1119.57
834.31
868.25
920.43
966.73
1219.68
1265.25
1328.49
1364.81
Compound 34
Exp mass: 1005.3732
Obs mass: 1028.57 (M+Na)+

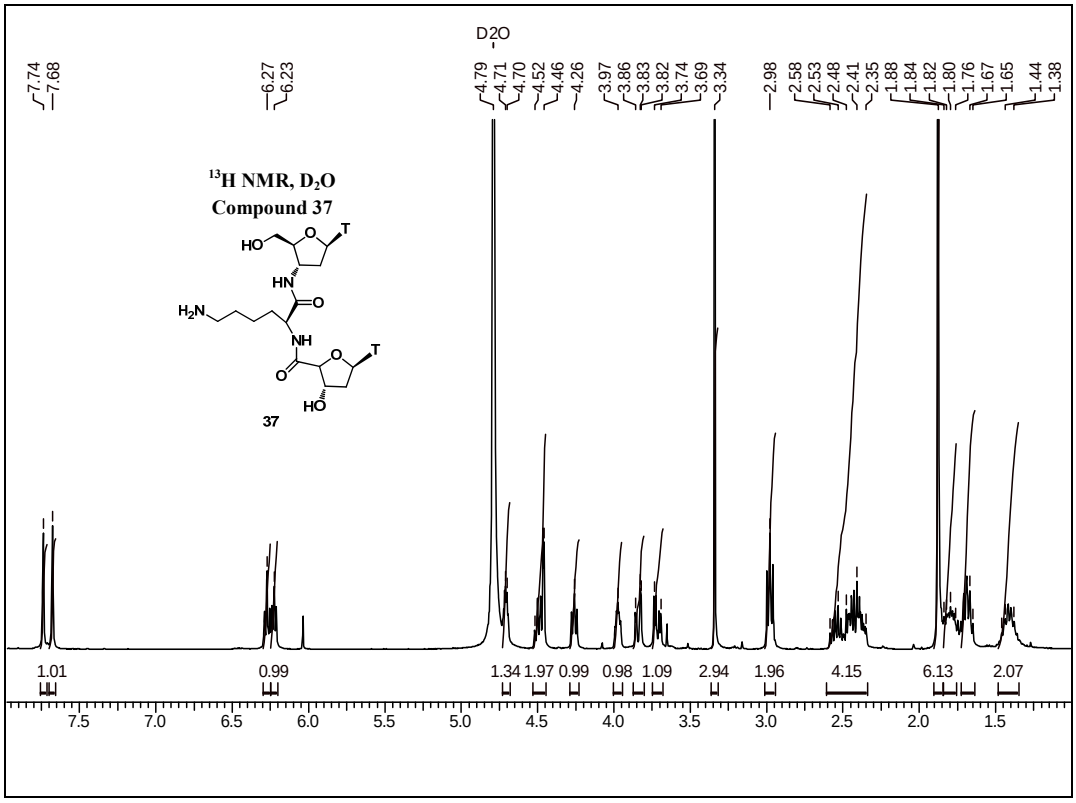
D2O
7.74
7.68
6.27
6.23
4.79
4.71
4.70
4.52
4.46
4.26
3.97
3.86
3.83
3.82
3.74
3.69
3.34
2.98
2.58
2.53
2.48
2.41
2.35
1.88
1.84
1.82
1.80
1.76
1.67
1.65
1.44
1.38
13H NMR, D2O
Compound 37
37
1.01
0.99
1.34
1.97
0.99
0.98
1.09
2.94
1.96
4.15
6.13
2.07
7.5
7.0
6.5
6.0
5.5
5.0
4.5
4.0
3.5
3.0
2.5
2.0
1.5

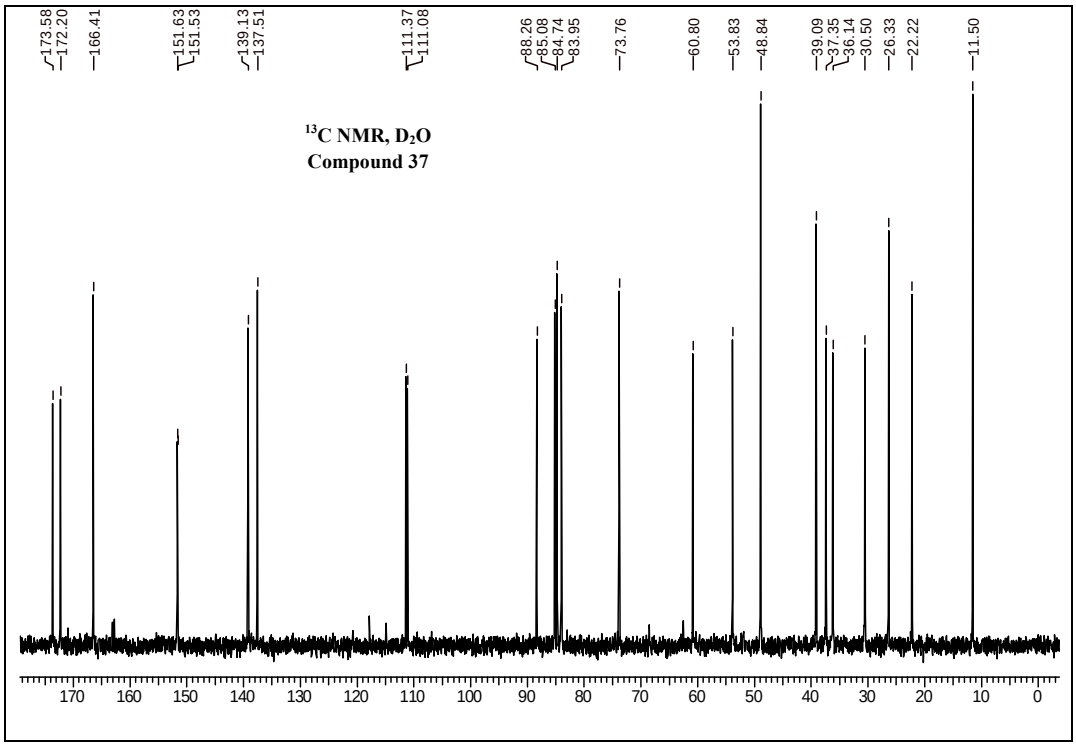
173.58
172.20
166.41
151.63
151.53
139.13
137.51
111.37
111.08
88.26
85.08
84.74
83.95
73.76
60.80
53.83
48.84
39.09
37.35
36.14
30.50
26.33
22.22
11.50
13C NMR, D2O
Compound 37
170
160
150
140
130
120
110
100
90
80
70
60
50
40
30
20
10
0

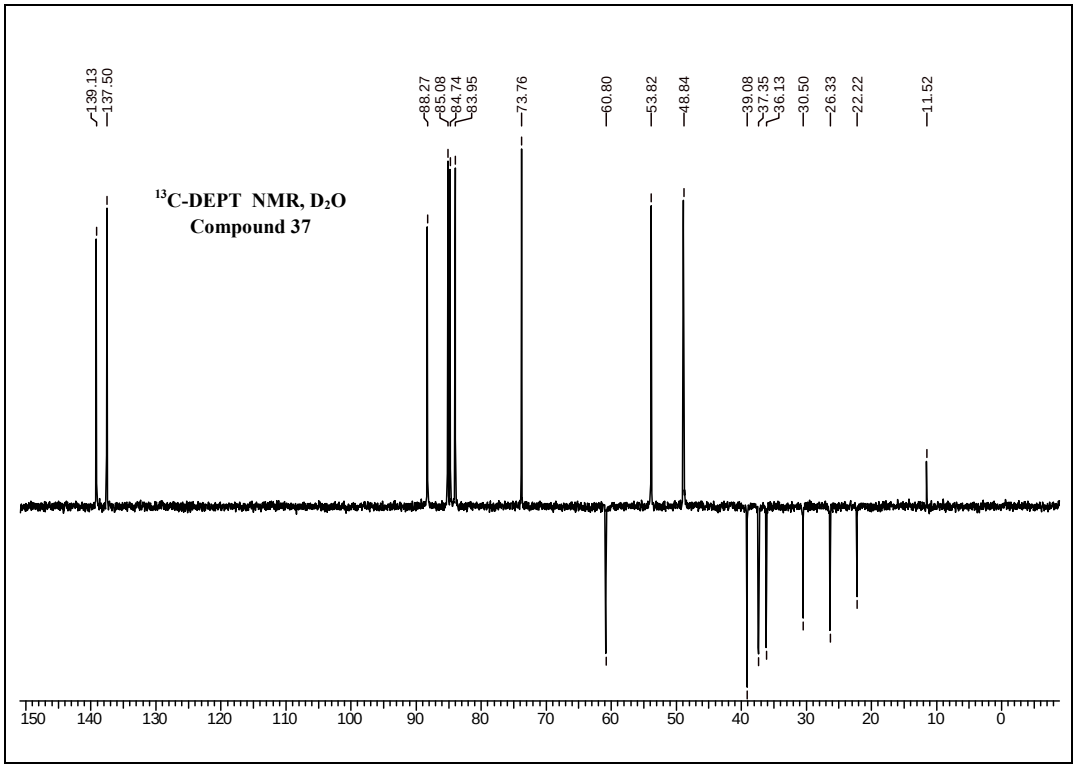

Elemental Composition Report Page 1

Single Mass Analysis (displaying only valid results)
Tolerance = 10.0 PPM / DBE: min = -1.5, max = 100.0
Isotope cluster parameters: Separation = 1.0 Abundance = 1.0%

Compound 37
Exp mass: 608.2680
Obs mass: 608.2658

Monoisotopic Mass, Odd and Even Electron Ions
83 formula(e) evaluated with 1 results within limits (up to 50 closest results for each mass)

Micromass : Q-Tof micro (YA-105) Dept. Of Chemistry I.I.T.(B) 20-Jan-201210:54:11
C26H37N7O10
NCL-VAK-E (HO-T-L-LYS-T-OH) 61 (0.605) AM (Cen,5, 80.00, Ht,5000.0,556.28,1.00); Sb (5,40.00); Cm (28:73) TOF MS ES+
6.49e3

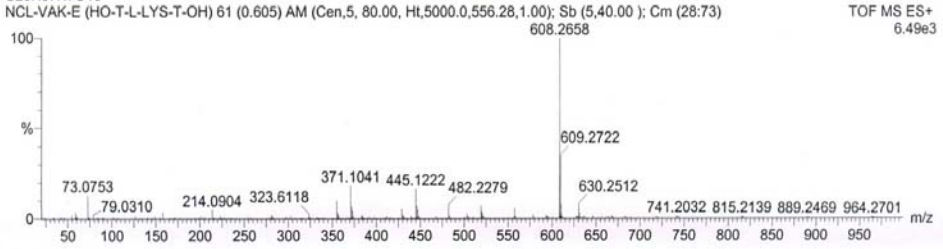

Minimum:				-1.5		
Maximum:		200.0	10.0	100.0		
Mass	Calc. Mass	mDa	PPM	DBE	Score	Formula
608.2658	608.2680	-2.2	-3.6	11.5	1	C26 H38 N7 O10

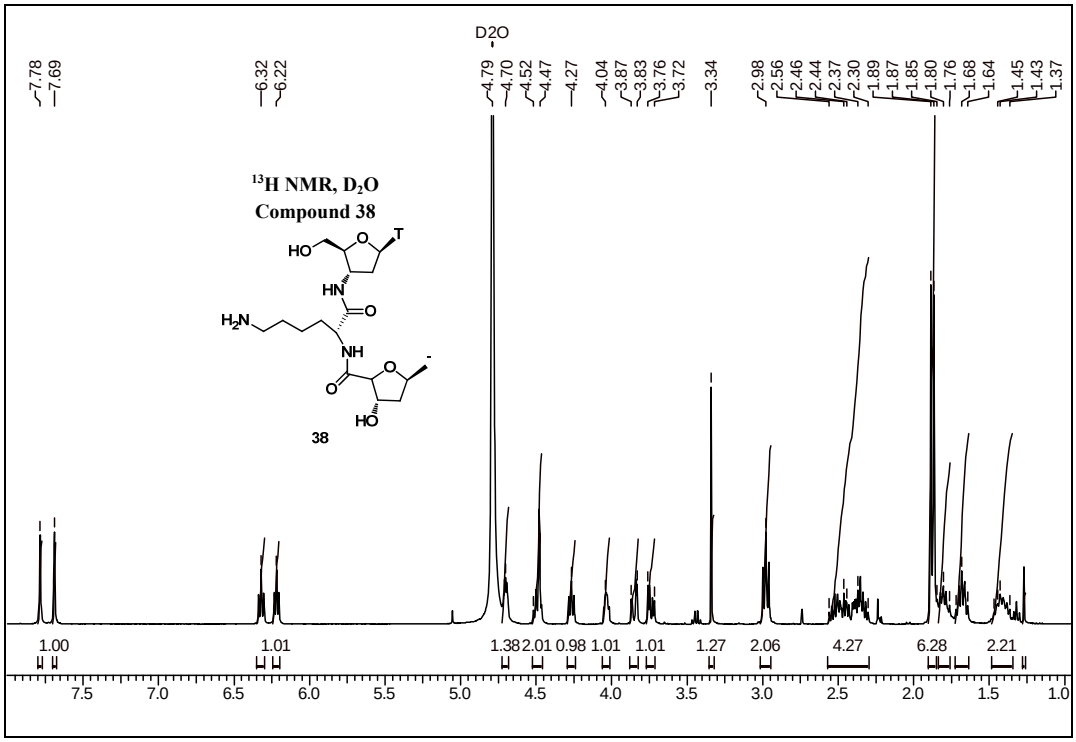
D2O
7.78
7.69
6.32
6.22
4.79
4.70
4.52
4.47
4.27
4.04
3.87
3.83
3.76
3.72
3.34
2.98
2.56
2.46
2.44
2.37
2.30
1.89
1.87
1.85
1.80
1.76
1.68
1.64
1.45
1.43
1.37
^{13}H NMR, D$_2$O
Compound 38
38
1.00
1.01
1.38
2.01
0.98
1.01
1.01
1.27
2.06
4.27
6.28
2.21

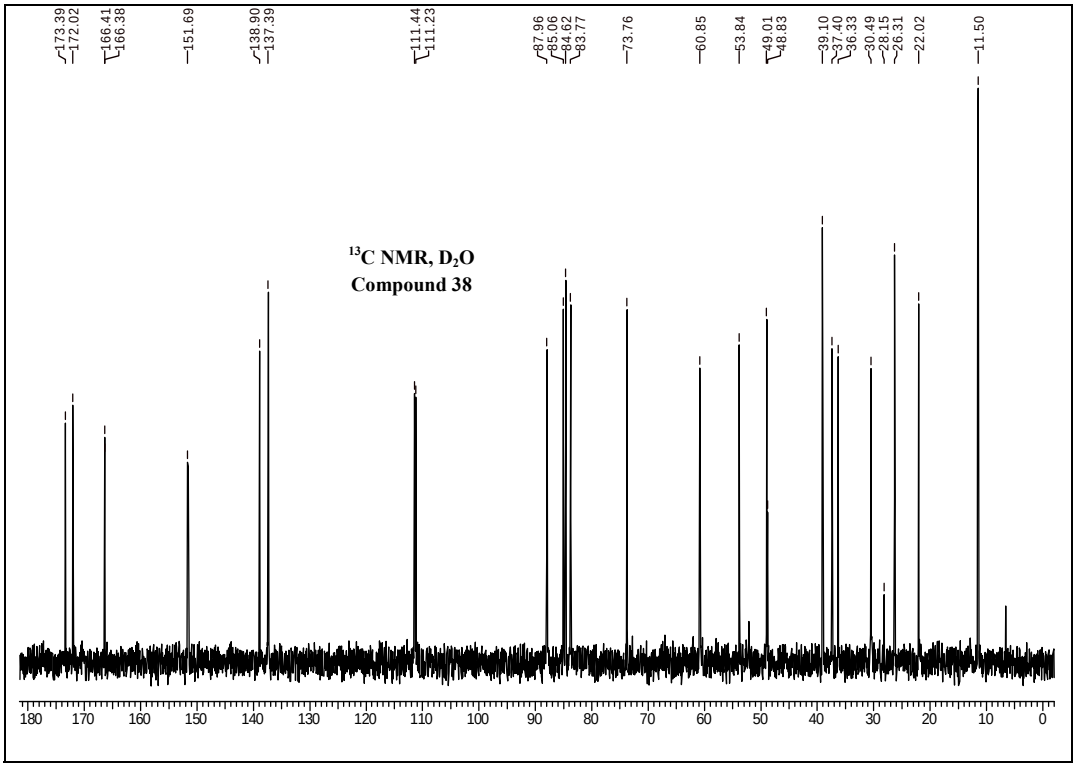
173.39
172.02
166.41
166.38
151.69
138.90
137.39
111.44
111.23
87.96
85.06
84.62
83.77
73.76
60.85
53.84
49.01
48.83
39.10
37.40
36.33
30.49
28.15
26.31
22.02
11.50
^{13}C NMR, D$_2$O
Compound 38

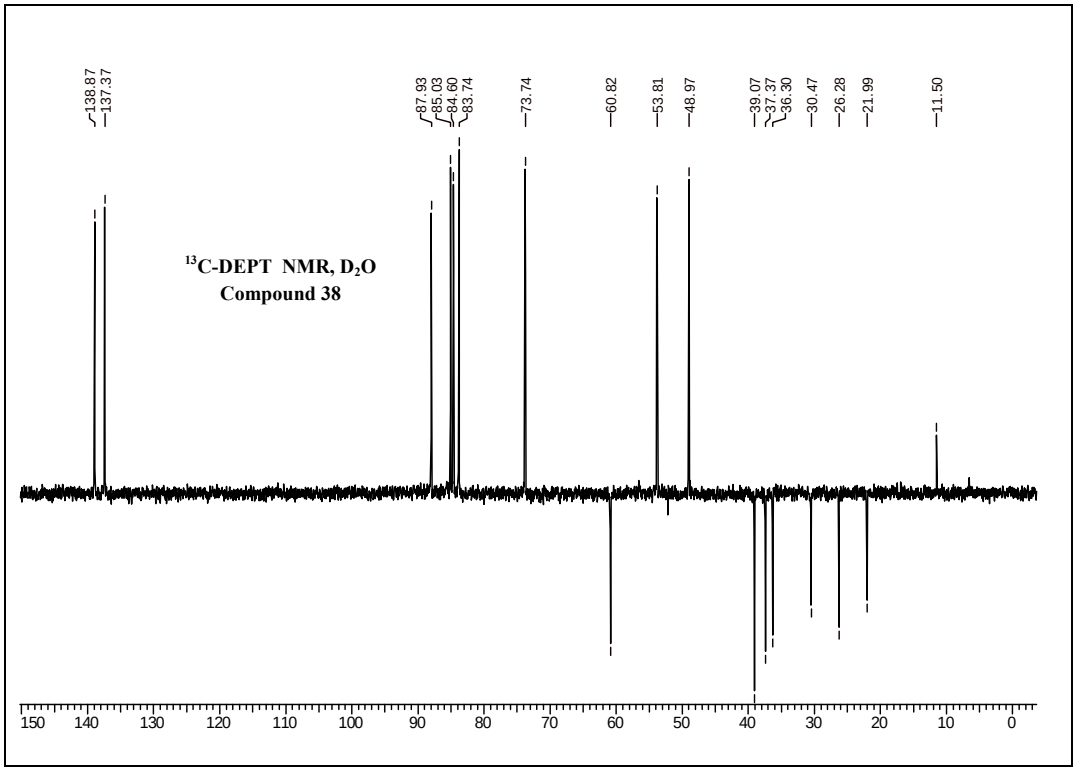

Elemental Composition Report **Page 1**

Single Mass Analysis (displaying only valid results)
Tolerance = 10.0 PPM / DBE: min = -1.5, max = 100.0
Isotope cluster parameters: Separation = 1.0 Abundance = 1.0%

Compound 38
Exp mass: 608.2680
Obs mass: 608.2680

Monoisotopic Mass, Odd and Even Electron Ions
83 formula(e) evaluated with 1 results within limits (up to 50 closest results for each mass)

Micromass : Q-Tof micro (YA-105) Dept. Of Chemistry I.I.T.(B) 20-Jan-201211:15:36
C26H37N7O10
NCL-VAK-F (HO-T-D-LYS-T-OH) 56 (0.554) AM (Cen,5, 80.00, Ht,5000.0,556.28,1.00); Sm (Mn, 2x4.00); Sb (5,40.00); Cm (1:62) TOF MS ES+
1.97e3

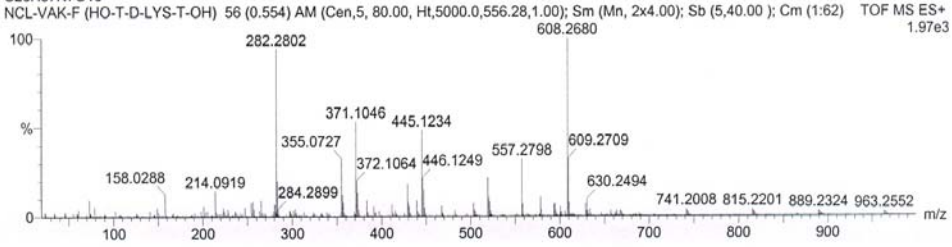

Minimum:				-1.5		
Maximum:		200.0	10.0	100.0		
Mass	Calc. Mass	mDa	PPM	DBE	Score	Formula
608.2680	608.2680	0.0	0.0	11.5	1	C26 H38 N7 O10

HPLC chromatogram of ON1 to ON4

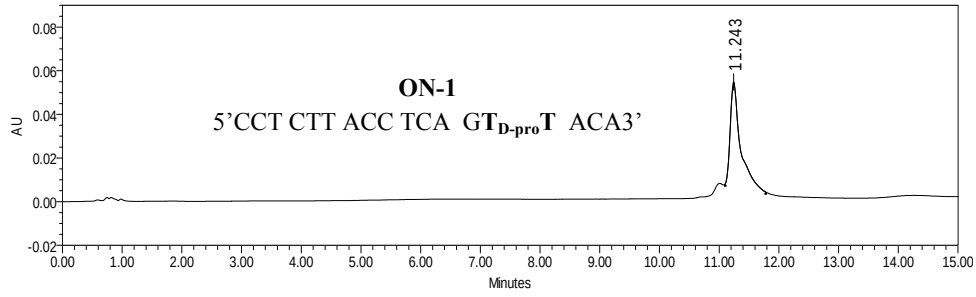

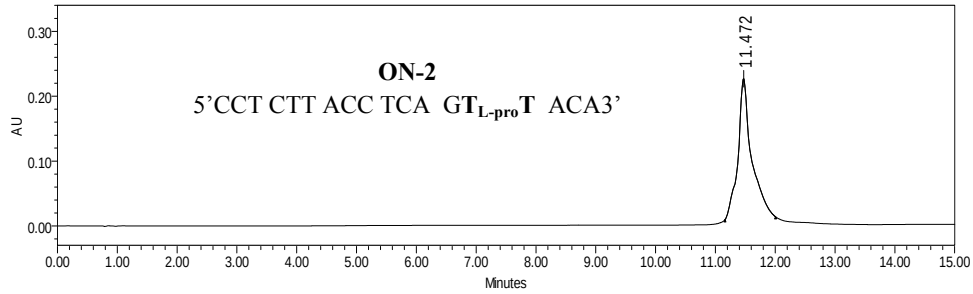

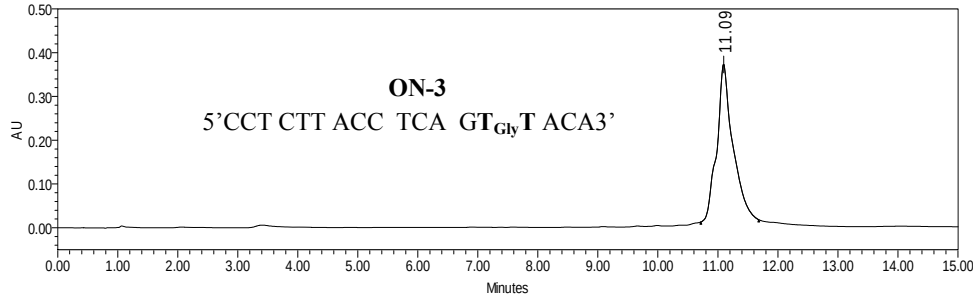

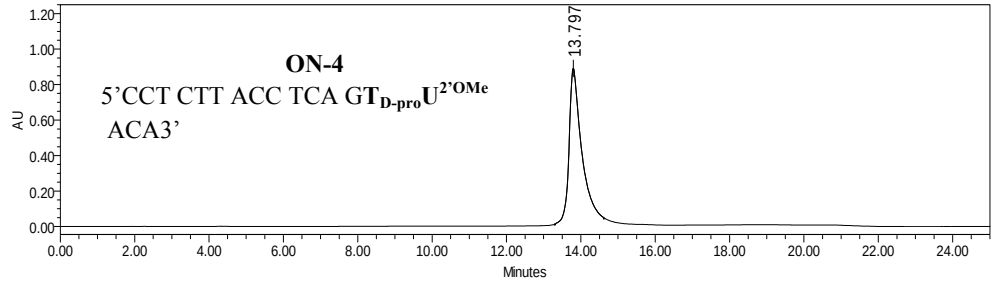

HPLC chromatogram of ON5-ON8

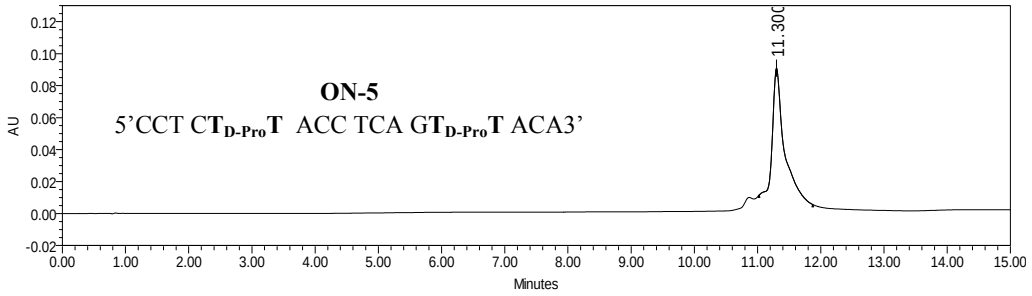

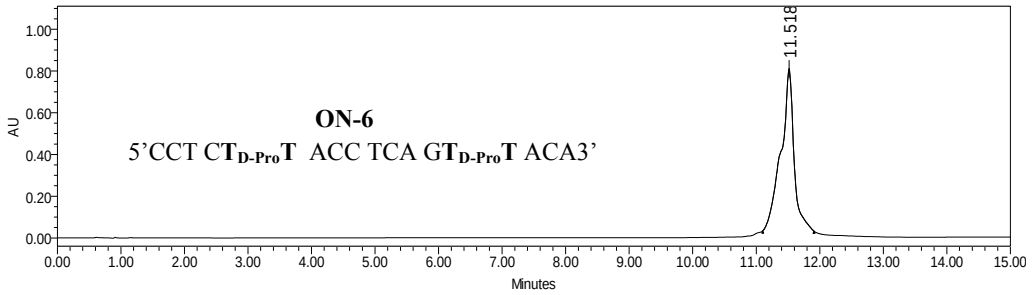

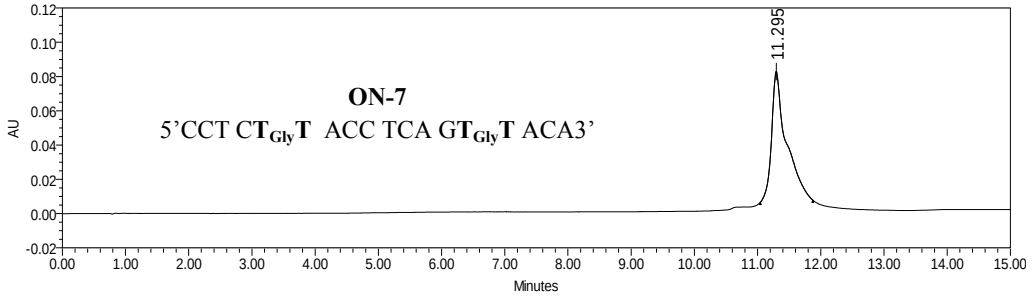

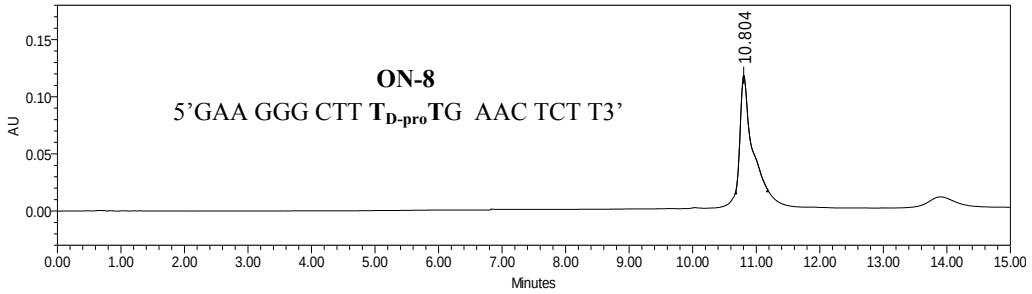

HPLC chromatogram of ON9 to ON12

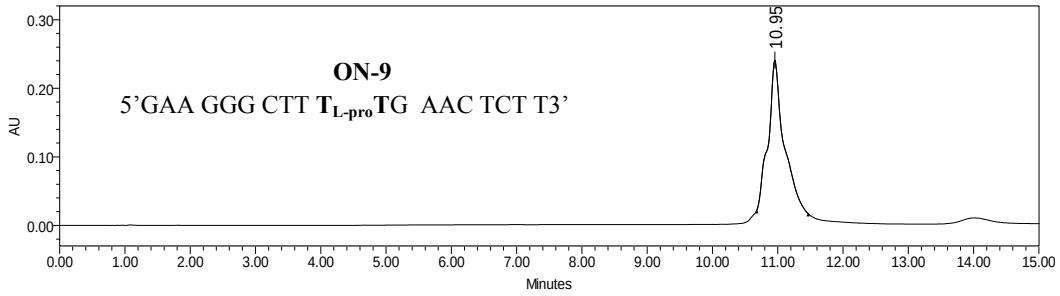

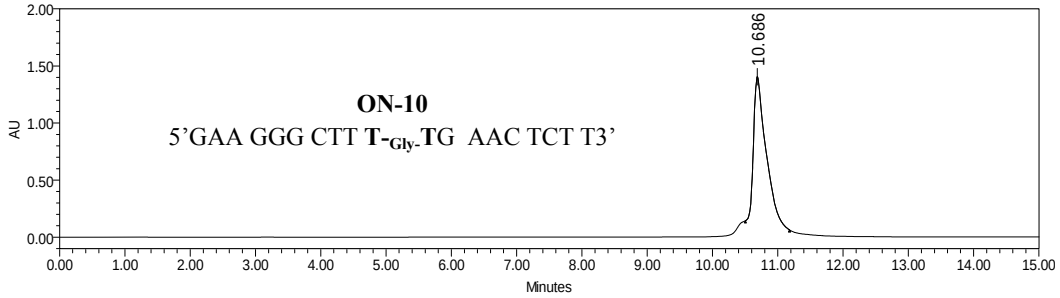

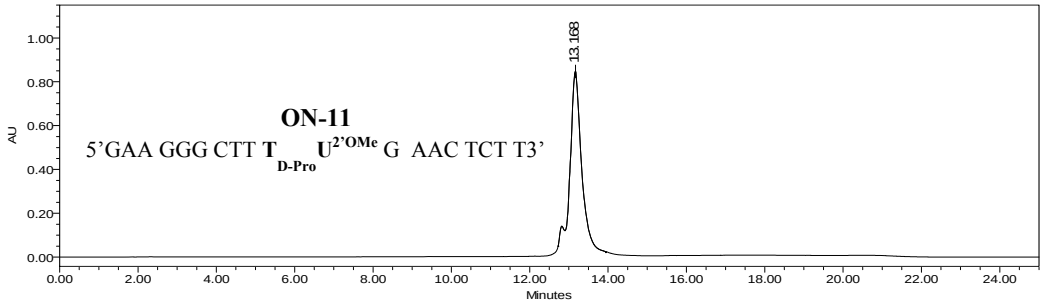

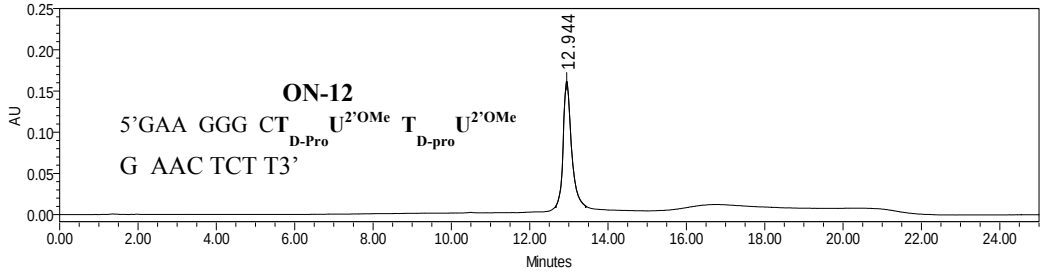

MALDI TOF spectra of ON1-ON12

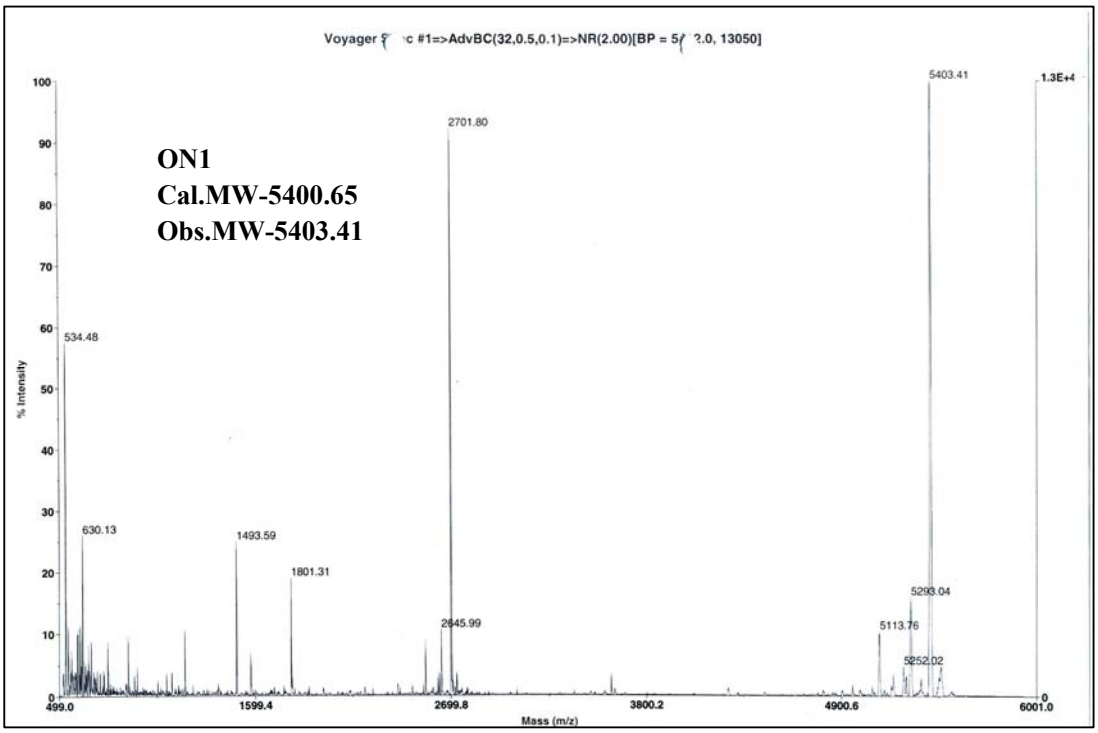

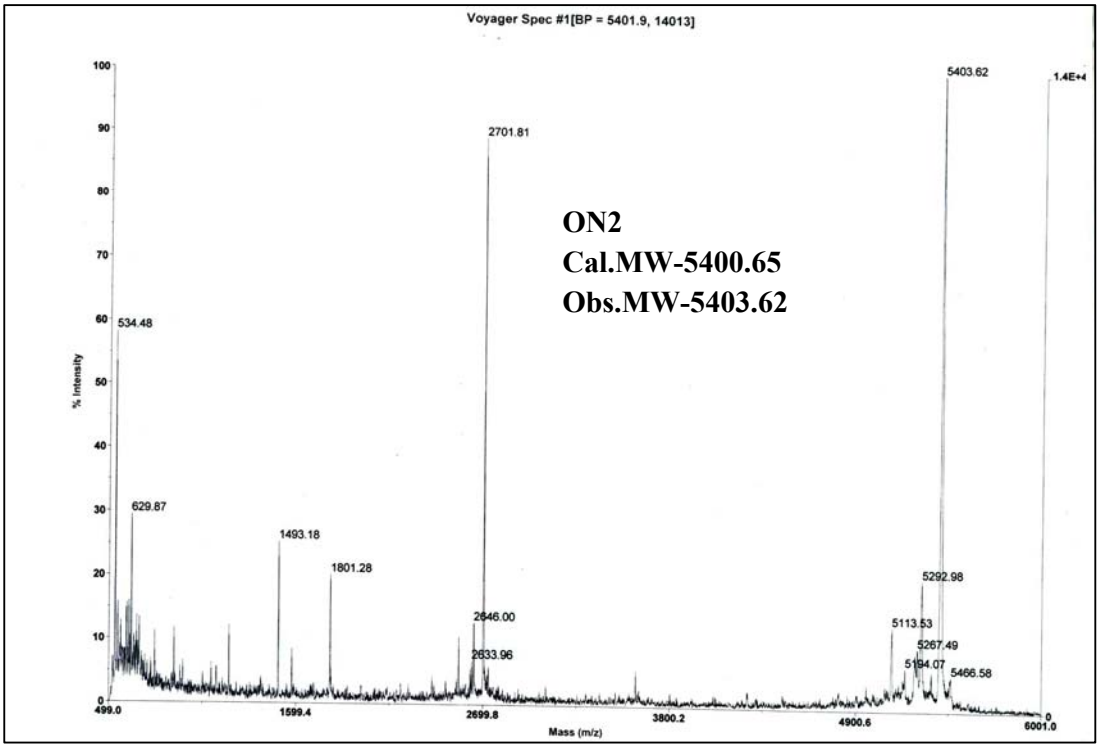

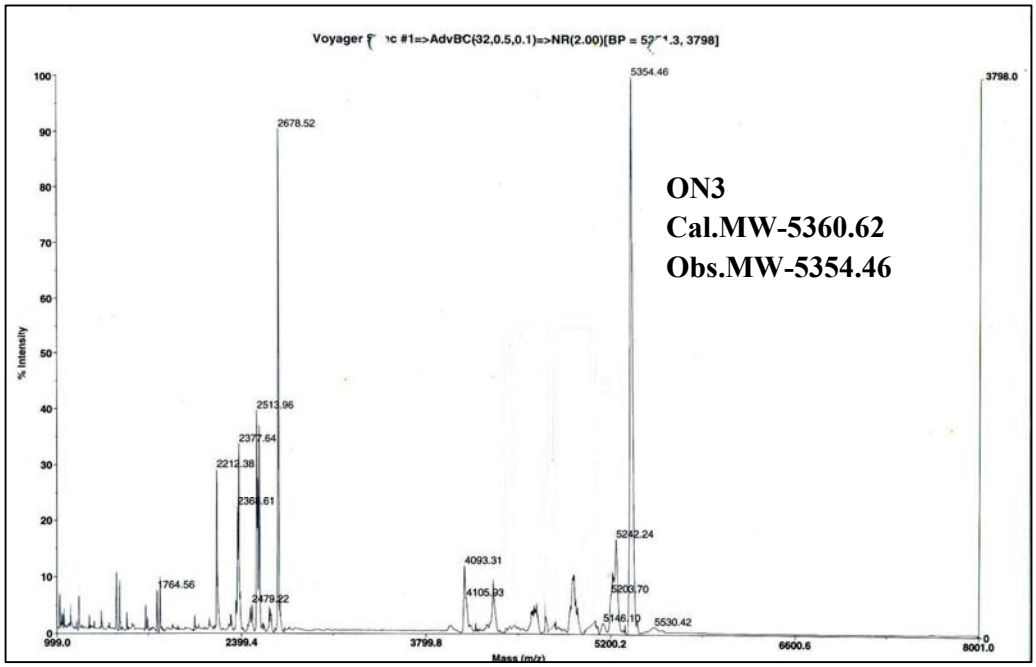
Voyager Spec #1=>AdvBC(32,0.5,0.1)=>NR(2.00)[BP = 5354.46, 3798]
% Intensity
Mass (m/z)
5354.46
3798.0
2678.52
2513.96
2377.64
2212.38
2368.61
5242.24
4093.31
4105.93
1764.56
2479.22
5200.70
5146.10
5530.42
999.0
2399.4
3799.8
5200.2
6600.6
8001.0
ON3
Cal.MW-5360.62
Obs.MW-5354.46

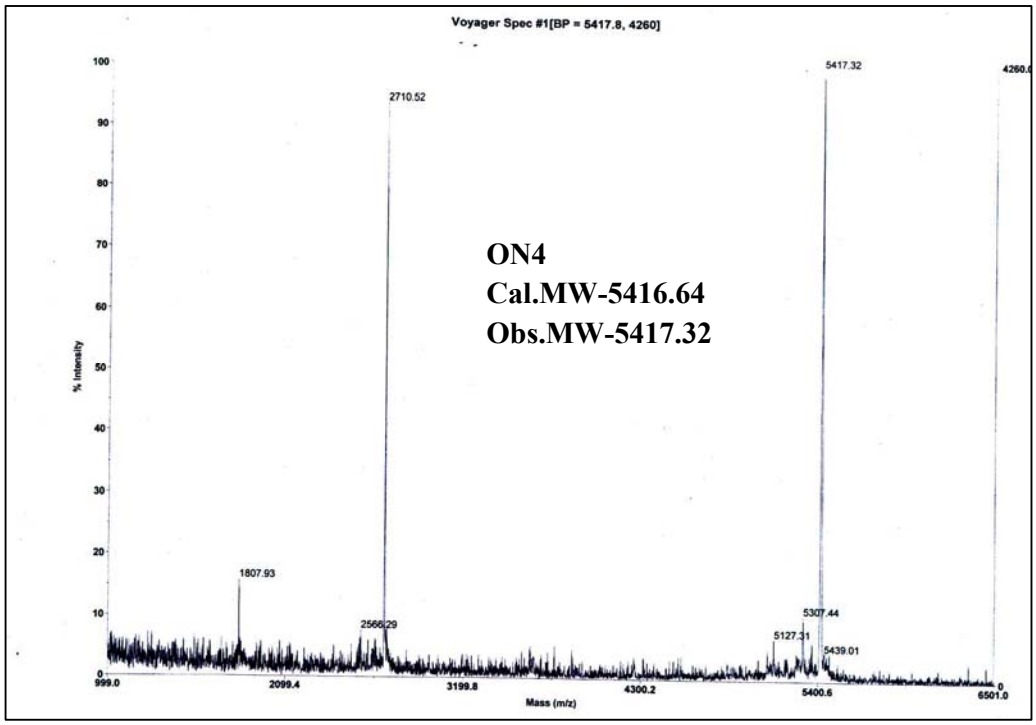
Voyager Spec #1[BP = 5417.8, 4260]
% Intensity
Mass (m/z)
5417.32
4260.0
2710.52
1807.93
2566.29
5307.44
5127.31
5439.01
999.0
2099.4
3199.8
4300.2
5400.6
6501.0
ON4
Cal.MW-5416.64
Obs.MW-5417.32

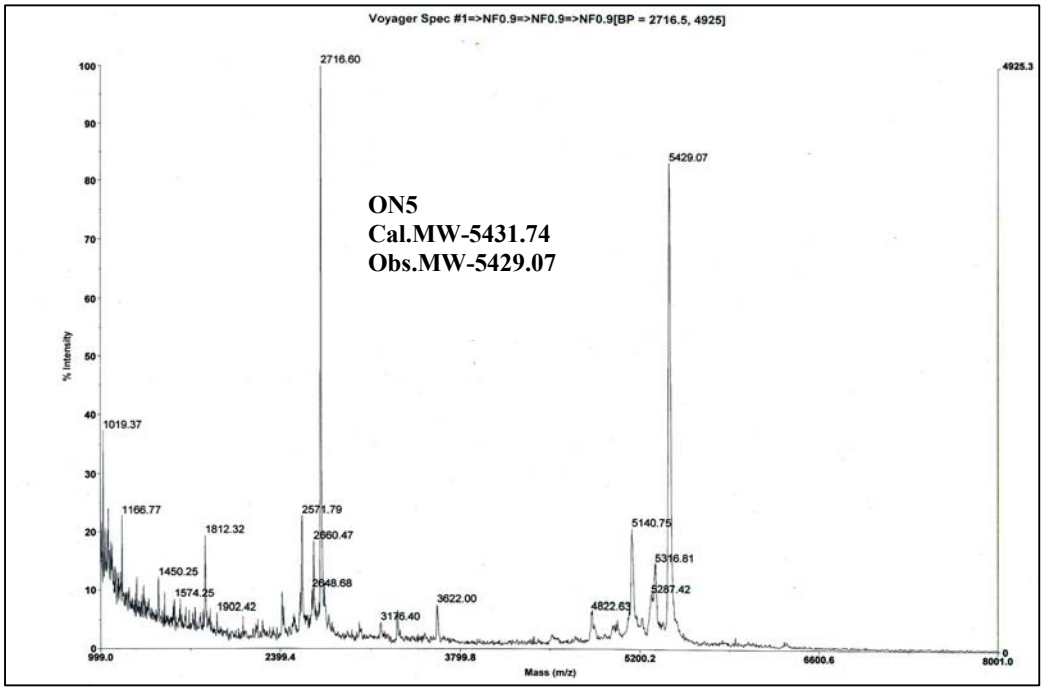
Voyager Spec #1=>NF0.9=>NF0.9=>NF0.9[BP = 2716.5, 4925]
ON5
Cal.MW-5431.74
Obs.MW-5429.07
% Intensity
Mass (m/z)
2716.60
4925.3
5429.07
1019.37
1166.77
1812.32
2571.79
2660.47
1450.25
1574.25
1902.42
2648.68
3176.40
3622.00
5140.75
5316.81
5287.42
4822.63
999.0
2399.4
3799.8
5200.2
6600.6
8001.0

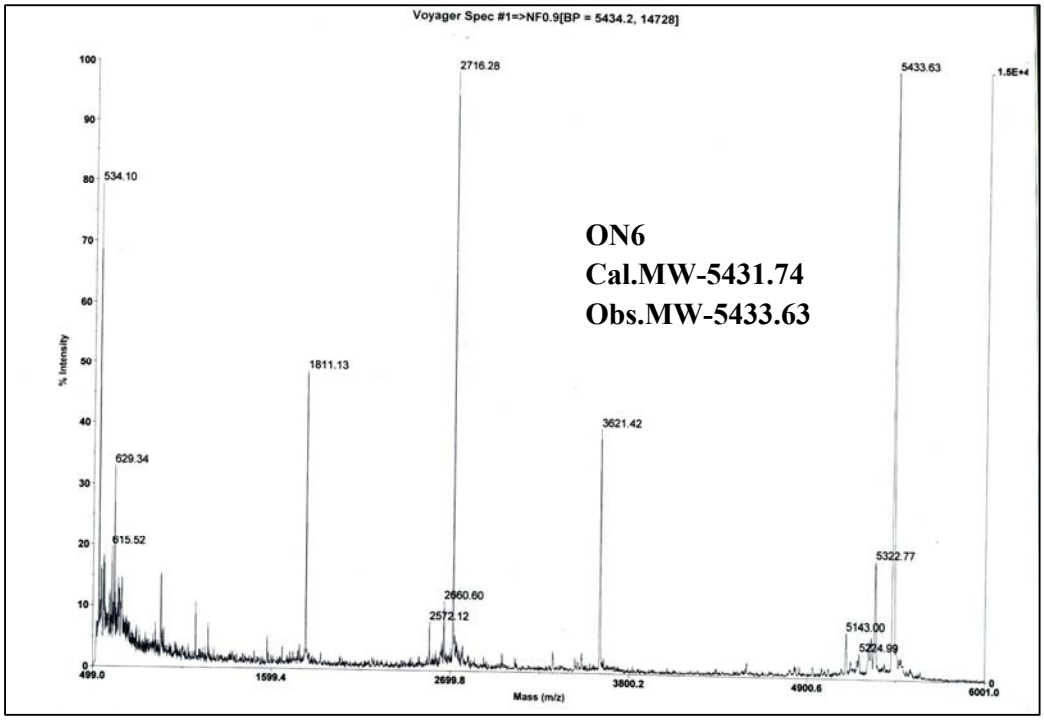
Voyager Spec #1=>NF0.9[BP = 5434.2, 14728]
ON6
Cal.MW-5431.74
Obs.MW-5433.63
% Intensity
Mass (m/z)
2716.28
5433.63
1.5E+4
534.10
1811.13
3621.42
629.34
615.52
5322.77
2660.60
2572.12
5143.00
5224.99
499.0
1599.4
2699.8
3800.2
4900.6
6001.0

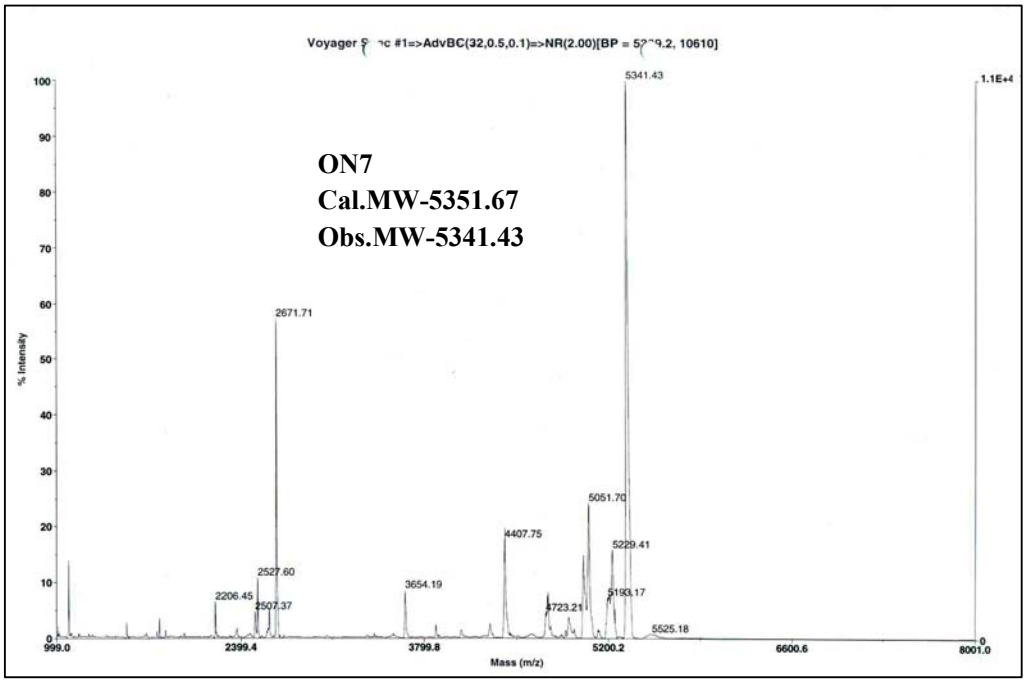
Voyager Spec #1=>AdvBC(32,0.5,0.1)=>NR(2.00)[BP = 5?79.2, 10610]
ON7
Cal.MW-5351.67
Obs.MW-5341.43
5341.43
1.1E+4
2671.71
5051.70
4407.75
5229.41
2527.60
2206.45
3654.19
2507.37
4723.21
5193.17
5525.18
% Intensity
Mass (m/z)
999.0
2399.4
3799.8
5200.2
6600.6
8001.0

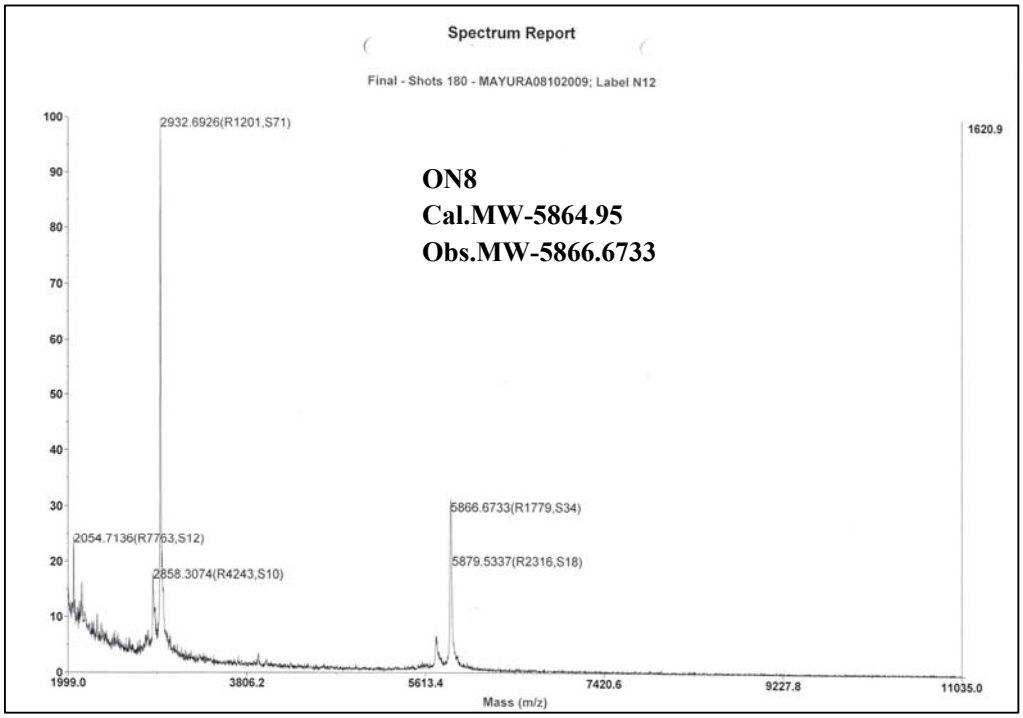
Spectrum Report
Final - Shots 180 - MAYURA08102009; Label N12
ON8
Cal.MW-5864.95
Obs.MW-5866.6733
2932.6926(R1201,S71)
1620.9
5866.6733(R1779,S34)
2054.7136(R7763,S12)
5879.5337(R2316,S18)
2858.3074(R4243,S10)
Mass (m/z)
1999.0
3806.2
5613.4
7420.6
9227.8
11035.0

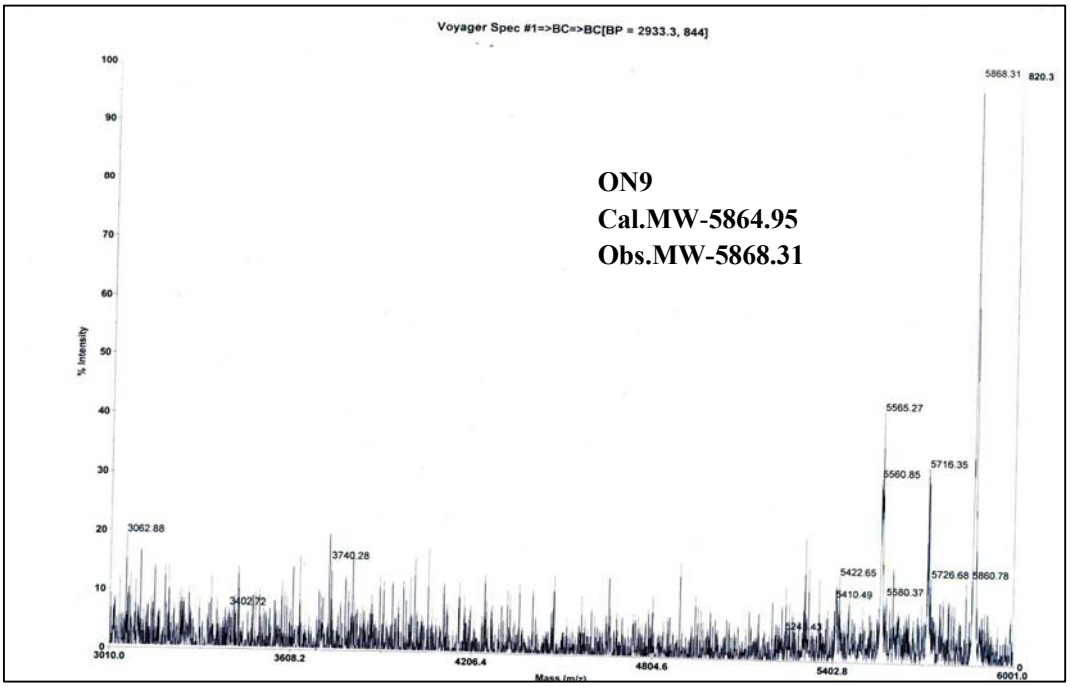
Voyager Spec #1=>BC=>BC[BP = 2933.3, 844]
% Intensity
Mass (m/z)
ON9
Cal.MW-5864.95
Obs.MW-5868.31
5868.31
820.3
5565.27
5560.85
5716.35
3062.88
3740.28
3402.72
5422.65
5410.49
5580.37
5726.68
5860.78
3010.0
3608.2
4206.4
4804.6
5402.8
6001.0

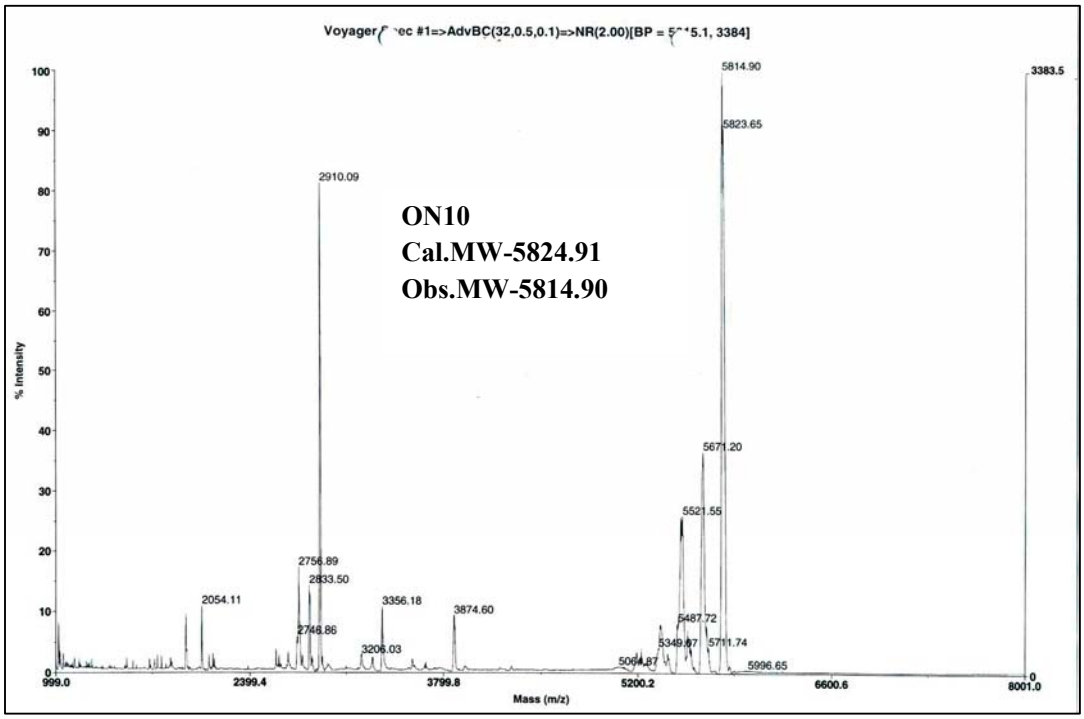
Voyager Spec #1=>AdvBC(32,0.5,0.1)=>NR(2.00)[BP = 5?*5.1, 3384]
% Intensity
Mass (m/z)
ON10
Cal.MW-5824.91
Obs.MW-5814.90
5814.90
3383.5
5823.65
2910.09
5671.20
5521.55
2756.89
2833.50
2054.11
3356.18
3874.60
2746.86
3206.03
5487.72
5349.67
5711.74
5064.87
5996.65
999.0
2399.4
3799.8
5200.2
6600.6
8001.0

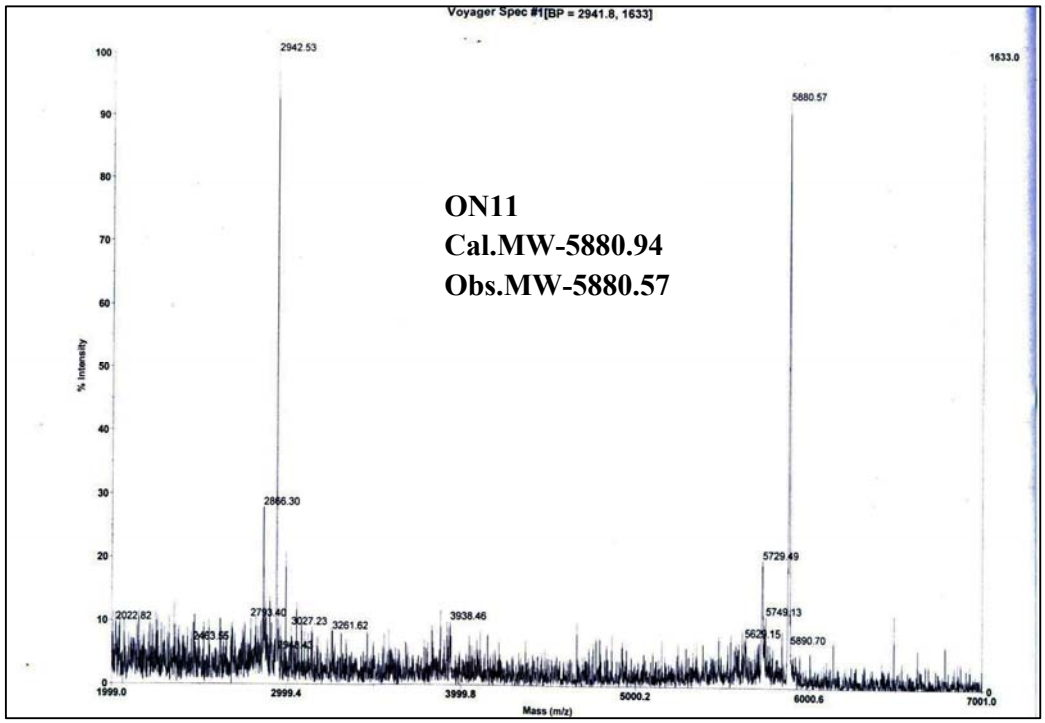
Voyager Spec #1[BP = 2941.8, 1633]
ON11
Cal.MW-5880.94
Obs.MW-5880.57
% Intensity
Mass (m/z)
2942.53
1633.0
5880.57
2866.30
5729.49
2022.82
2793.40
3027.23
3261.62
3938.46
5749.13
5629.15
5890.70
1999.0
2999.4
3999.8
5000.2
6000.6
7001.0

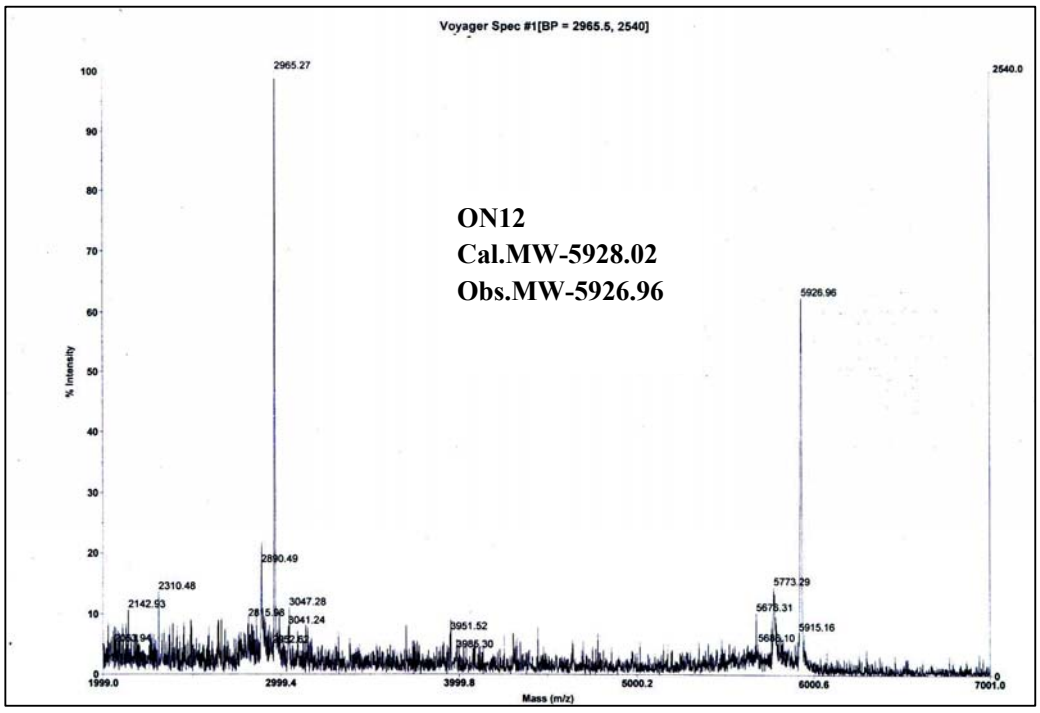
Voyager Spec #1[BP = 2965.5, 2540]
ON12
Cal.MW-5928.02
Obs.MW-5926.96
% Intensity
Mass (m/z)
2965.27
2540.0
5926.96
2890.49
2310.48
2142.93
3047.28
3041.24
3951.52
5773.29
5915.16
1999.0
2999.4
3999.8
5000.2
6000.6
7001.0

2.6 References

1. (a) Kole, R.; Krainer, A.R.; Altman, S. RNA therapeutics: beyond RNA interference and antisense oligonucleotides, *Nature Rev-Drug Discov.* **2012**, *11*, 125; (b) J. Kurreck, Antisense technologies. Improvement through novel chemical modifications. *Eur. J. Biochem*. **2003**, *270*, 1628.
2. (a) Shukla, S.; Sumaria, C. S.; Pradeepkumar, P.I. Exploring Chemical Modifications for siRNA Therapeutics: A Structural and Functional outlook. *Chem. Med. Chem*, **2010**, *5*, 328; (b) Kurreck J. RNA interference: from basic research to therapeutic applications. *Angew. Chem., Int. Ed. Engl.* **2009**, *48*, 1378.
3. (a) Sun, W.; Li, Y. S. H.; Huang, H. D.; John Y-J. Shyy.; Chien, S. microRNA: A Master Regulator of Cellular Processes for Bioengineering Systems, *Annu. Rev. Biomed. Eng.* **2010**. *12*, 1; (b) Turner, J. J.; Fabani, M.; Arzumano, A. A.; Ivanova, G.; Gait, M. J. Targeting the HIV-1 RNA leader sequence with synthetic oligonucleotides and siRNA: Chemistry and cell delivery. *Biochim. Biophys. Acta, Biomembr,* **2006**, *1758*, 290.
4. (a) Bauman J.; Jearawiriyapaisam, N.; Kole R. Therapeutic potential of splice switching oligonucleotides. *Oligonucleotides*, **2009**, *19*, 1; (b) Sazani, P.; Kole, R. Therapeutic potential of antisense oligonucleotides as modulators of alternative splicing. *J. Clin. Invest,* **2003**, *112*, 481.
5. Bendifallah, N.; Rasmussen, F. W.; Zachar, V.; Ebbesen, P.; Nielsen, P. E.; Koppelhus, U., Evaluation of Cell-Penetrating Peptides (CPPs) as vehicles for intracellular delivery of antisense Peptide Nucleic Acid (PNA), *Bioconjugate Chem.* **2006***, 17*, 750.
6. (a) Zhou, P.; Wang, M.; Du, L.; Fisher, G. W.; Waggoner, A.; Ly, D. H. Novel Binding and Efficient Cellular Uptake of Guanidine-Based Peptide Nucleic Acids (GPNA) *J. Am. Chem. Soc*., **2003**, *125*, 6878; (b) Englund, E. A.; Appella, D. H. γ-Substituted Peptide Nucleic Acids Constructed from L-Lysine are a versatile scaffold for multifunctional display. *Angew. Chem. Int. Ed*, **2007**, *46*, 1414.
7. (a) Pallan, P. S.; von Matt, P.; Wilds, C. J.; Altmann, K.-H. and Egli, M. RNA-Binding affinities and crystal structure of oligonucleotides containing five-atom amide-based backbone structures. *Biochemistry*, **2006**, *45*, 8048; (b) Wilds, C. J., Minasov, G.; von Matt, P.; Altmann K.-H. and Egli, M. Studies of a chemically modified oligodeoxynycleotide containing a 5-atom amide backbone which

exhibits improved binding to RNA. *Nucleosides, Nucleosides and Nucleic Acids,* **2001**, *20*, 991.

8. (a) Burgers, P. M.; Eckstein, F. Diastereomers of 5'-O-adenosyl 3'-O-uridyl phosphorothioate: chemical synthesis and enzymic properties. *Biochemistry*, **1979**, 18, 592; (b) Almer, H.; Stawinski, J.; Str□mberg, R.; Thelin, M. Synthesis of diribonucleoside phosphorothioates via stereospecific sulfurization of H-phosphonate diesters. *J. Org. Chem.* **1992**, *57*, 6163; (c) Oivanen, M.; Ora, M.; Almer, H.; Strömberg, R.; Lönnberg, H. Hydrolytic reactions of the diastereomeric phosphoromonothioate analogs of uridylyl (3',5') uridine: kinetics and mechanisms for desulfurization, phosphoester hydrolysis, and transesterification to the 2',5'-isomers. *J. Org. Chem.* **1995**, *60*, 5620; (d) Miller, P. S.; Dreon, N.;. Pulford S. M.; McParland, K. B. *J. Biol. Chem.*, **1980**, *255*, 9659; (e) Oka, N.; Kondo, T.; Fujiwara, S.; Maizuru, Y.; Wada, T. Stereocontrolled synthesis of oligoribonucleoside phosphorothioate by an oxazaphospholidine Approach *Org. Lett.* **2009**, *11*, 967.
9. (a) Yano, J.; Ohgi, T.; Ueda, T. WO2006/043521-A1, CAN: 144: 450874; b) Yano, J.; Smyth, G. E. New Antisense Strategies: Chemical Synthesis of RNA Oligomers *Adv Polym Sci.* **2012**, *249*, 1.
10. (a) Gokhale, S.S.; Gogoi, K.; Kumar, V. A. Probing binding preferences of DNA and RNA: backbone chirality of thioacetamido-linked nucleic acids and iso-thioacetamido-linked nucleic acids to differentiate DNA versus RNA selective binding. *J. Org. Chem.*, **2010**, *75*, 7431; (b) Gogoi, K.; Gunjal, A.D.; Kumar, V.A. Sugar–thioacetamide backbone in oligodeoxyribonucleosides for specific recognition of nucleic acids. *Chem. Commun*. **2006**, 2373.
11. Gogoi, K.; Kumar, V. A. Chimeric (α-amino acid + nucleoside-β-amino acid)n peptide oligomers show sequence specific DNA/RNA recognition *Chem. Commun*. **2008**, 706.
12. (a) Micklefield, J. Backbone Modification of Nucleic Acids: Synthesis, Structure and Therapeutic Applications. *Curr. Med. Chem*. **2001**, *8*, 1157; (b) Kumar, V. A.; Ganesh, K.N. Structure-editing of nucleic acids for selective targeting of RNA. *Curr. Top. Med. Chem*. **2007**, *7*, 715; (c) Kumar, V. A. Structural preorganization of Peptide Nucleic Acids: chiral cationic analogues with five- or six-membered ring structures. *Eur. J. Org. Chem.*, **2002**, 2012; (d) Kumar, V. A.; Ganesh, K. N.

Conformationally constrained PNA analogues: Structural evolution toward DNA/RNA binding selectivity. *Acc. Chem. Res*., **2005**, *38*, 404.

13. (a) Govindaraju, T.; Kumar, V. A. Backbone-extended pyrrolidine peptide nucleic acids (bepPNA): design, synthesis and DNA/RNA binding studies. *Chem. Commun*. **2005**, 495; (b) Govindaraju, T. and Kumar, V. A. Backbone extended pyrrolidine PNA (*bep*PNA): a chiral PNA for selective RNA recognition. *Tetrahedron*, **2006**, 60, 2321.
14. Gokhale, S.S.; Kumar, V. A. Amino/guanidino-functionalized N-(pyrrolidin-2-ethyl) glycine-based pet-PNA: Design, synthesis and binding with DNA/RNA. *Org. Biomol. Chem*. **2010**, *8*, 3742.
15. Vilaivan, T.; Lowe, G. A novel pyrrolidinyl PNA showing high sequence specificity and preferential binding to DNA over RNA. *J. Am. Chem. Soc*. **2002**, *124*, 9326.
16. Vilaivan, C.; Srisuwannaket, C.; Ananthanawat, C.; Suparpprom, C.; Kawakami, J.; Yamaguchi, Y.; Tanaka, Y. and Tirayut Vilaivan. Pyrrolidinyl peptide nucleic acid with α/β-peptide backbone: A conformationally constrained PNA with unusual hybridization properties, *Artificial DNA: PNA & XNA*, **2011**, *2*, 50.
17. Balgopala, M. I.; Ollapally, A. P.; Lee, H. J. An improved synthesis of azidothymidine. *Nucleosides and nucleotides*, **1996**, *15*, 899.
18. Montevecchi, P. C.; Manetto, A.; Navacchia M. L. and Chatgilialoglu, C. Thermal decomposition of the tert-butyl perester of thymidine-5'-carboxylic acid. Formation and fate of the pseudo-C4' radical. *Tetrahedron*, **2004**, *60*, 4303.
19. Miyashita, M.; Yoshikoshi, A.; Griecolb, P. A. Pyridinium p-Toluenesulfonate. A Mild and Efficient Catalyst for the Tetrahydropyranylation of Alcohols. *J. Org.Chem*.**1997**, *42*, 3772.
20. Zhang, J.; Matteucci. M. D. Synthesis of a *N*-Acylsulfamide linked dinucleoside and its incorporation into an oligonucleotide. *Bioorg. Med. Chem. Lett*. **1999**, *9*, 2213-2216.
21. (a) De Mico, A.; Margarita, R.; Parlanti, L.; Vescovi, A. and Piancatelli, G. A Versatile and Highly Selective Hypervalent Iodine (III)/2,2,6,6-Tetramethyl-1-piperidinyloxyl-Mediated Oxidation of Alcohols to Carbonyl Compounds. *J. Org. Chem.,* **1997**, *62*, 6974. (b) Epp, J. B. and Widlanski, T. S. Facile preparation of nucleoside -5'-carboxylic acid. *J. Org. Chem*. **1999**, *64*, 293.

22. Remin, M. and Shuger, D. Conformation of exocyclic 5' CH2OH in nucleosides and nucleotides in aqueous solutions from specific assignments of the H5' and 5'' signals in the NMR spectra. *Biochem. Biophys. Res. Commun*. **1972**, *48*, 636.

23. Rinkel L.J.; Altona, C. Conformation analysis of the deoxyfuranose ring in DNA by means of sum of proton-proton coupling constant. *J. Biomol. Struct. Dync*. **1987**, *4*, 621.

24. Donohue, J .; Trueblood K.N. Base pairing In DNA . *J. Mol. Biol*. **1960**, *3*, 363.

25. Glemarec, C., Nyllas, A., Sund, C. and Chattopadhyaya, J. A comparative conformational study of thymidylyl (3' → 5')thymidine, thymidylyl(3' → 5')-5'-thio-5'-deoxy thymidine, & thymidinylacetamido-[3'(O)→5'(C)]-5'-deoxythymidine by NMR spectroscopy. *J Biochem Biophys Methods*, **1990**, *12*, 311.

26. (a) Glemarec, C.; Reynolds, R. C.; Crooks, P. A.; Maddry, J. A.; Akhtar, M. S., Montgomery, J. A., Secrist III, J. A. and Chattopadhyaya, J. Conformational studies of thymidine dimers containing sulphonate and sulphonamide linkages By NMR spectroscopy. *Tetrahedron*, **1993**, *49*, 2287. (b) Plavec, J., Koole, L.H., Sandstrom, A. and Chattopadhyaya, J. Structural studies of Anti HIV 3'-α-Fluorothymidine and 3'-α-Azidothymidine By 500 MHz ^{1}H NMR spectroscopy and molecular mechanics (MM2) calculations. *Terahedron*, **1991,** *47*,7363.

27. Sundaralingam, M. *Biopolymers* **1969**, *7*, 821.

28. (a) Altona, C.; Sundaralingam, M. Coformational-analysis of sugar ring in nucleosides and nucleotides-improved method for interpretation of proton magnetic–resonance coupling-constants *J. Am. Chem. Soc*. **1973**, *95*, 2333. (b) Altona, C.; Sundaralingam, M. Conformational-analysis of sugar ring in nucleosides and nucleotides-new description using concept of pseudorotation. *J. Am. Chem. Soc*. **1972**, *94*, 8205.

29. (a) van Wijk, J.; Haasnoot, C.A. G.; de Leeuw, F. A. A. M.; Huckriede, B. D.; Westra Hoeckzema, A.; Altona, C. PSEUROT 6.2 1993, PSEUROT 6.3 1999; Leiden Institute of Chemistry, Leiden University. (b) de Leeuw, F. A. A. M. ; Altona, C. J. computer-assisted pseudorotation analysis of 5-Membered rings by means of proton spin spin coupling –constants- program PSEUROT *Comput. Chem*. **1983,** *4*, 428.

30. Eschenmoser, A. and Dobler, M. Why pentose and not hexose nucleic acids? Part I. Introduction to the problem, conformational analysis of oligonucleotide single strands containing 2', 3'-dideoxyglucopyranosyl building blocks ('homo-DNA') and reflections on the conformation of A- and B-DNA. *Helvetica Chimica Acta*, **1992** *75*, 218.
31. T. E. Creighton, Proteins, W. H. Freeman & Co., 2nd edn, 1993, pp. 173–174.
32. Iversen, P. L, Phosphoroamidate morpholino oligomers: favorable properties for sequence-specific gene inactivation. *Curr. Opin. Mol. Ther*. **2001**, *3*, 235.
33. P. E. Nielsen in Methods in Enzymology: Antisense Technology Part A: General Methods, Methods of Delivery, and RNA Studies, Vol. 313 (Ed.: M. I. Phillips), Academic Press, San Diego, **2000**, pp. 156–164
34. (a) Barawkar, D.; Rajeev, K.; Kumar, V.; Ganesh, K. Triplex formation at physiological pH by 5-Me-dC-N4-(spermine) [X] oligodeoxynucleotides: non protonation of N3 in X of X*G:C triad and effect of base mismatch/ionic strength on triplex stabilities. *Nucleic Acids Res*. **1996**, *24*, 1229; (b) Bijapur, J.; Keppler, M.; Bergqvist, S.; Brown, T.; Fox, K. 5-(1-propargylamino)-2′-deoxyuridine (U^P): a novel thymidine analogue for generating DNA triplexes with increased stability. *Nucleic Acids Res*. **1999**, *27*, 1802; (c) Robles, J.; Grandas, A.; Pedroso, E. Tetrahedron 2001, 57, 179; (d) Roig, V.; Asseline, U. *J. Am. Chem. Soc*. **2003**, *125*, 4416; (e) Ueno, Y.; Mikawa, M.; Matsuda, A. *Bioconj. Chem*. **1998**, *9*, 33
35. (a) Cuenoud, B.; Casset, F.; Hüsken, D.; Natt, F.; Wolf, R. M.; Altmann, K.-H.; Martin, P.; Moser, H. E. Dual Recognition of Double-Stranded DNA by 2′-Aminoethoxy-Modified Oligonucleotides *Angew. Chem., Int. Ed*. **1998**, *37*, 1288; (b) Kanazaki, M.; Ueno, Y.; Shuto, S.; Matsuda, A. *J. Am. Chem. Soc*. **2000**, *122*, 2422; (c) Prakash, T. P.; Manoharan, M.; Fraser, A. S.; Kawasaki, A. M.; Lesnik, E. A.; Owens, S. R. *Tetrahedron Lett*. **2000**, *41*, 4855; (d) Puri, N.; Majumdar, A.; Cuenoud, B.; Natt, F.; Martin, P.; Boyd, A.; Miller, P. S.; Seidman, M. M. *Biochemistry* **2002**, *41*, 7716.
36. (a) Bailey, C.; Dagle, J.; Weeks, D. *Nucleic Acids Res*. **1998**, *26*, 4860; (b) Chaturvedi, S.; Horn, T.; Letsinger, R. *Nucleic Acids Res*. **1996**, *24*, 2318;(b) Dagle, J. M.; Littig, J. L.; Sutherland, L. B.; Weeks, D. L. *Nucleic Acids Res*. **2000**, *28*, 2153; (c) Kore, A.; Salunkhe, M. *Ind. J. Chem. Sec*t. *B* **1998**, 37, 536;(d) Letsinger, R. L.; Singman, C. N.; Histand, G.; Salunkhe, M. *J. Am. Chem. Soc.*

1988, *110*, 4470; (e) Michel, T.; Debart, F.; Vasseur, J.-J. *Tetrahedron Lett*. **2003**, *44*, 6579; (f) Robles, J.; Ib_a~nez, V.; Grandas, A.; Pedroso, E. *Tetrahedron Lett*.**1999**, *40*, 7131; (g) Vasquez, K. M.; Dagle, J. M.; Weeks, D. L.; Glazer, P. M. *J. Biol. Chem*. **2001**, *276*, 38536.

37. Guschlbauer, W.; Jankowski, K.Nucleoside conformation is determined by the electronegativity of the sugar substituent. *Nucleic Acids Res*. **1980**, *8*, 1421.
38. Inoue, H.; Hayase, Y.; Imura, A.; Iwai, S.; Miura, K.; Ohtsuka, E. Synthesis and hybridization studies on two complementary nona(2'-O-methyl)ribonucleotides *Nucleic Acids Res*. **1987**, *15*, 6131.
39. Inoue, H.; Hayase, Y.; Iwai, S.; Ohtsuka, E. RNase H cleavage for processing of in vitro transcribed RNA for NMR studies and RNA ligation. FEBS *Lett*. **1987**, *215*, 327.
40. Sproat, B. S., Lamond, A. I., Beijer, B., Neuner, P. & Ryder, U. Highly efficient chemical synthesis of 2′-O-methyloligoribonucleotides and tetrabiotinylated derivatives; novel probes that are resistant to degradation by RNA or DNA specific nucleases. *Nucleic Acids Res.* **1989**, *17*, 3373.
41. DeMesmaeker, A.; Lesueur, C.; Bevierre, M. O.; Waldner, A.; Fritsch, V.; Wolf, R. M. Amide Backbones with Conformationally Restricted Furanose Rings: Highly Improved Affinity of the Modified Oligonucleotides for Their RNA Complements, *Angew. Chem. Int. Ed. Engl*. **1996**, *35*, 2790.
42. Fathi, R.; Huang, Q.; Coppola, G.; Delaney, W.; Teasdale, R.; Krieg A.M.; Cook, A.F. Oligonucleotides with novel, cationic backbone substituents: aminoethylphosphonates. *Nucleic Acids Res*. **1994**, *22*, 5416.
43. Robles, J.; Ibanez, V.; Grandas, A.; Pedroso, E. Synthesis and triple helix-forming ability of oligonucleotides with N, N-Dimethylaminoethyl Phosphoramidate Linkages. *Tetrahedron Let.*, **1999**, *40*, 7131.
44. Horn, T.; Chaturvedi, S.; Balasubramaniam, T. N.; Letsinger, R. L. Oligonucleotides with Alternating Anionic and Cationic Phosphoramidate Linkages:Synthesis and hybridization of Stereo-uniform Isomers. *Tetrahedron Lett.* **1996**, *37*, 743.
45. Michel, T.; Martinand-Mari, C.; Debart, F.; Lebleu, B.; Robbins, I.; Vasseur, J. J.

Cationic phosphoramidate α-oligonucleotides efficiently target single-stranded DNA and RNA and inhibit hepatitis C virus IRES-mediated translation. *Nucleic Acids Res.* **2003**, *31*, 5282.

46. Jain, M. L.; Bruice, P. Y.; Szabo, I. E.; Bruice, T. C. Incorporation of Positively Charged Linkages into DNA and RNA Backbones: A Novel Strategy for Antigene and Antisense Agents *Chem. Rev.* **2012**, *112*, 1284 and reference theiein.
47. Deglane, G.; Abes, S.; Michel, T.; Prevot, P.; Vives, E.; Debart, F.; Barvik, I.; Lebleu, B.; Vasseur, J. J. Impact of the Guanidinium Group on Hybridization and Cellular Uptake of Cationic Oligonucleotides. *Chem.bio.chem.* **2006**, *7*, 684.
48. (a) Ueda, Y.; Manabe, H.; Mitsuda, M.; Kitamura, M. On the production of N^{ε}-trifluoroacetyl-L-lysine. *Chem .Eng. Res. Design* **2000**, *78*, 756; (b) Qian, X. H.; Zheng, B.; Burke, B.; Saindane, M. T.; Kronenthal, D. R. A stereoselective synthesis of BMS-262084, an azetidinone-based tryptase inhibitor *J. Org. Chem.* **2002**, *67*, 3595.
49. Shibata, N.; Baldwin, J. E.; Jacobs, A.; Wood, M. E. Electrophilic Sulfenylation in a Stereocontrolled Synthesis of Protected *(2R,3R)-3.*Mercaptoaspartic Acid from L-Aspartic Acid. *Tetrahedron.* **1996**, *52*, 12839.
50. Obika, S.; Morio, K.-I.; Nanbu, D.; Imanishi, T. Synthesis and conformation of 3'-*O*,4'-*C*-methyleneribonucleosides, novel bicyclic nucleoside analogues for 2',5'-linked oligonucleotide modification *Chem.Commun*. **1997**, 1643.
51. Analysis of circular dichroism spectra. Methods of enzymology vol .210, **1992**, 426.
52. Desnous, C.; Babu, B. R .; Moriou, C.; Mayo, J. U. O.; Favre, A.; Wengel, J.; Clivio, P. The sugar conformation governs (6-4) photoproduct formation at the dinucleotide level. *J. Am. Chem. Soc.* **2008**, *130*, 30.
53. (a) Cheng, D. M.; Sarma, R. H. Nuclear magnetic resonance study of the impact of ribose 2′-*O*-methylation on the aqueous solution conformation of cytidylyl-(3′ → 5′)-cytidine. *Biopolymers.* **1977**, *16*, 1687; (b) Kawai, G.; Yamamoto, Y.; Kamimura, T.; Masegi, T.; Sekine,M.; Hata, T.; Iimori, T.; Watanabe, T.; Miyazawa, T.; Yokoyama, S. Conformational rigidity of specific pyrimidine residues in tRNA arises from posttranscriptional modifications that enhance steric interaction between the base and the 2'- hydroxyl group. *Biochemistry*. **1992**, *31*, 1040.

54. Cheng, D. M.; Sarma, R. H. Intimate details of the conformational characteristics of deoxyribodinucleoside monophosphates in aqueous solution J. Am. Chem. Soc. **1977**, *99*, 7333.

55. Lee, C.-H.; Ezra, F. S.; Kondo, N. S.; Sarma, R. H.; Danyluk, S. S. Conformational properties of dinucleoside monophosphates in solution—dipurines and dipyrimidines . *Biochemistry.* **1976**, *15*, 3627.

56. (a) Gait, M. J. Oligonucleotide synthesis: A practical approach. IRL Press Oxford, UK 217 (b) Agrawal, S. PROTOCOLS for oligonucleotides and analogs Synthesis and Properties Methods in Molecular Biology. (ed): vol.20 Totowa, NJ,. Humana Press, Inc

57. (a) Nowell, P. and Hungerford, D. A minute chromosome in human chronic granulo cytic leukemia. *Science*, **1960**, *132*, 1497; (b) Deininger, M. W. N.; Goldman J. M.; Melo J. V. The molecular biology of chronic myeloid leukemia. *Blood*, **2000**, *96*, 3343.

58. Kang, S-H.; Cho, M-J.; Kole, R. Up-regulation of luciferase gene expression with antisense oligonucleotides: Implications and Applications in functional assay development. *Biochemistry*, **1998**, *37*, 6235.

59. Howard, F. B. The Stabilizing Contribution of Thymine in Duplexes of $(dA)_{24}$ with $(dU)_{24}$, $(dT)_{24}$, $(dU_{12}–dT_{12})$, $(dU–dT)_{12}$, $(dU_2–dT_2)_6$, or $(dU_3– dT_3)_4$: Nearest Neighbor and Next-Nearest Neighbor Effects. *Biopolymers*, **2005**, *78*, 221

Chapter 3

Synthesis of all four Nucleoside-based-β-amino acid monomers for the synthesis of polyamide-DNA with alternating α-amino acid and nucleoside-β-aminoacids

3.1 Introduction

Novel oligonucleotide (ON) analogues that can form stable duplexes or triplexes with target nucleic acids are highly desired synthetic objectives because of their use as therapeutic agents.[1] Various types of modified oligonucleotides[2] have been developed over the last two decades as potential antisense and antigene agents. The more recent developments such as splice correcting and exon skipping[3] strategies require highly robust nucleic acid analogues that are stable under physiological conditions as single strands as well as in the form of duplexes with complementary RNA sequences. The study of unnatural dephosphono nucleic acid oligomers would be highly beneficial for siRNA applications as well.[4] This approach would maintain the chirality and 3'–5' directionality of the backbone, along with the enzymatic stability of the replaced phosphate linkage by unnatural linker group. The replacement of the internucleoside sugar–phosphate linkages by the robust amide,[4-8] carbamate,[9] guanidino-[10] linkages is studied in the literature. The exploration of an amide bond for this purpose may be an interesting choice because the well established solid phase peptide synthesis (SPPS) methodology can be directly extended and could be advantageous as in case of synthesis of peptide nucleic acids (PNA)[8a-c] and analogues containing chiral α-amino acids.[8d-i] Several four- and five-atom amide-linked (6/7 atom repeating units) deoxyribo/ribo[4-7] ON analogues are studied till date, but the chemistry development in most instances has been restricted to the synthesis of thymine (T-T dimers). The other dephosphono linkers also have not been extensively explored for the synthesis of mixed purine-pyrimidine sequences probably because of the difficulties encountered during the synthesis of building blocks corresponding to all four nucleobases required for the synthesis of any desired nucleobase sequence. In this chapter, we present the synthesis of all four appropriately protected nucleoside based β-amino acids and their utility in the synthesis of a model (α-amino acid + nucleoside-β-amino acid) tetrameric sequence of dephosphono polyamide-DNA.

3.2 Rationale, Design and Objectives of the Present Work

The complete replacement of sugar phosphate backbone as in PNA has been extremely successful[8] and has found advantages in diagnostic applications[11] as well as in splice correction antisense applications.[3] The development of cyclic, chiral analogues of PNA containing 6/7-atom repeating units was an offshoot aimed at either getting

better RNA selectivity as antisense agents, or directional selectivity for binding to specific RNA sequences.[8] The relevant examples are those of pyrrolidine-based NA analogues such as pyrrolidinyl[12]/POM-PNA[13] and bepPNA[14] or those comprising prolyl-aminopyrrolidine-2-carboxylic acid[15] and prolyl-2-aminocyclopentanecarboxylic acid (prolyl-ACPC backbone) (Figure 1).[16,17] The prolyl-ACPC backbone and its homologues[17b] are the alternating α/β amino acid backbone exhibited preferential binding with complementary DNA. Initial work from our group was based on the prolyl-ACPC backbone and in that case the alternating nucleoside-β-amino acids with natural α-amino acids (Figure 1) gave rise to similar alternating α/β amino acid backbone scaffolds using well-established peptide chemistry.[18] We studied thyminyl homooligomer sequences in which thyminyl-β-amino acid was used in conjunction with natural α-L-amino acids and found that these sequences displayed RNA selective binding.

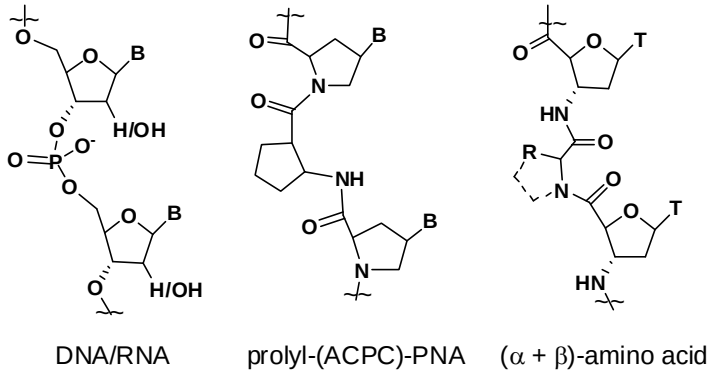

Figure 1: DNA/RNA and backbone alteration

The thyminyl-β-amino acids were also synthesized by others for synthesizing phoshonamide internucleoside linkages [19] and also for their use in sequences for studies in foldamer chemistry.[20] For our interests in synthesizing α + β- amino acid backbone, we further studied the effect of chirality of the α-amino acids by synthesizing the thymine dimers linked with L-proline, D-proline and prochiral glycine units on base stacking interactions.[21] To further exploit this interesting backbone, synthesis of all four natural nucleoside-based β-amino acids as building blocks was required. In this chapter, we describe the first approach toward the synthesis of all four appropriately protected natural nucleoside-based β-amino acids (Figure 2) and show their utility in the synthesis

of a model (α-amino acid + nucleoside-β-amino acid) tetrameric sequence of dephosphono polyamide-DNA.

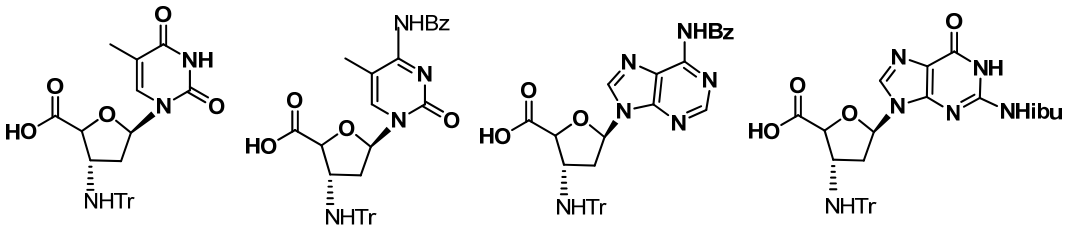

Figure 2. All four nucleoside based-β-amino acid

The specific objectives of this chapter are

i) Synthesis of all four trityl protected nucleoside -β-amino acid.

ii) Solid phase synthesis of chimeric [α-amino acid + nucleoside -β-amino acid] oligomer.

iii) Cleavage from the solid support and purification, characterization of the oligomer.

3.3 Methodology, Results and Discussion

In our earlier strategy, we used Fmoc protected 3'-deoxy-3'-aminothymidine as nucleoside-β-amino acid monomer and rink amide resin as the solid support.[18] Exocyclic amino protection is not required for thymine nucleobase during oligomer synthesis, and Fmoc strategy worked well. Also cleavage from the rink amide MBHA resin requires strongly acidic conditions (TFA:TFMSA/20% TFA in DCM), which may not be compatible for mixed base sequences containing purine nucleosides due to likely depurination in strongly acidic medium. We decided to use the trityl protection for 3'-sugar-amino function to be deprotected by trichloroacetic acid at each coupling step. This altered strategy would accommodate the orthogonal protection of nucleobases (benzoyl for adenine/cytosine and isobutyryl for guanine). We chose the succinate ester at 5'-end as a linker of the growing oligomer *via* succinamide linker to the support. The succinate ester can be cleaved concomitantly with the nucleobase deprotection, using aqueous/methanolic ammonia at the end of synthesis leaving a 5'-OH group. This strategy has been previously applied successfully for the synthesis of oligonucleotide phosphonamidates on Controlled Pore Glass (CPG) support[22] The MBHA-succinate linker strategy has been previously used for the synthesis of glycopeptides[23] but has not been employed for the synthesis of oligopeptides.

The TEMPO–BAIB method[24] used earlier by us[18,21] and others[20] for oxidation of 5'-primary hydroxyl group in 3'-deoxy-3'-azidothymidine to get the 4'-carboxylic acid was followed for the synthesis of protected tritylaminonucleosides. This method of general procedure for the production of 4'-carboxylic acids of nucleosides is very mild and the desired products were obtained in good yields and separated from TEMPO and reaction byproducts by trituration with diethyl ether. The mildness of this reaction and its tolerance of acid sensitive, base sensitive and oxidatively labile functional groups should make it an attractive method for the oxidation of primary alcohols to carboxylic acids for both nucleosides. In our case, we found that the protecting group such as benzoyl of cytocine and adenine base, and isobutyryl for guanine are also stable towards the oxidation reaction conditions.

3.3.1 Synthesis of Thymine monomer

The 3'-deoxy-3'-tritylamino-thymidine-4'-carboxylic acid **4** was obtained as follows (Scheme 1). The 5'-TBS-protected 3'-deoxy-3'-azidothymidine **1**[22a] was hydrogenated over Pd-C for reduction of azide to amine to get compound **2.** Reaction of **2** with trityl chloride, followed by deprotection of 5'-silyl ether gave compound **3** in good yield. The 3'-tritylamino-3'-deoxythymidine **3** was obtained in comparable yields and purity as reported earlier.[22] Compound **3** was easily converted to the corresponding acid **4** under TEMPO–BAIB oxidation conditions and the product was recovered by trituration with ether and acetone (60 % overall yield).

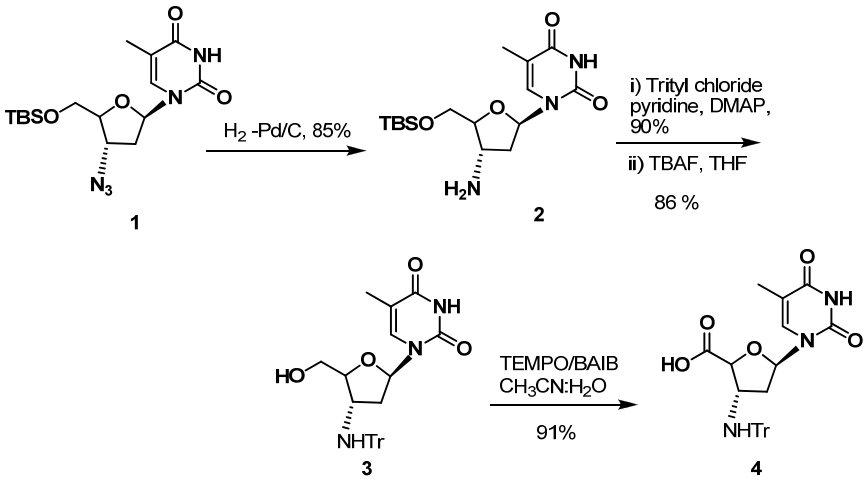

Scheme 1. Synthesis of thymidine-β-amino acid

3.3.2 Synthesis of 5-methylcytosine monomer

The 3'-tritylamino-3'-dideoxy-N^4-benzoyl-5-methylcytidine was synthesized from **1** as shown in Scheme 2. Compound **1** was converted to 1,2,4-triazolyl nucleoside derivative **5** by treatment with $POCl_3$ and 1,2,4-triazole in the presence of triethylamine.[22b] The cytidine derivative **6** was obtained upon treatment of **5** with aq.ammonia in dioxane. The free exocyclic amino group was further protected by treatment with benzoyl chloride in dry pyridine to get N^4-Bz protected cytidine derivative **7** in good yield. Compound **7** was further reduced to 3'-amino-5-methylcytidine derivative **8** which was subsequently protected as 3'-tritylamino group followed by the removal of silyl ether to get compound **9**.[22a] These altered reaction sequence as compared to the reported route[22b] avoided formation of 3'-NHTr-benzoyl derivative which was formed during N^4-benzoylation. We used H_2S/pyridine for the reduction of azide to amine[7a] as reduction with Pd-C was found to be sluggish and less efficient. Oxidation to 4'-carboxylic acid derivative **10** was accomplished using TEMPO–BAIB oxidation conditions and the product was recovered by trituration with ether and acetone (42 % overall yield).

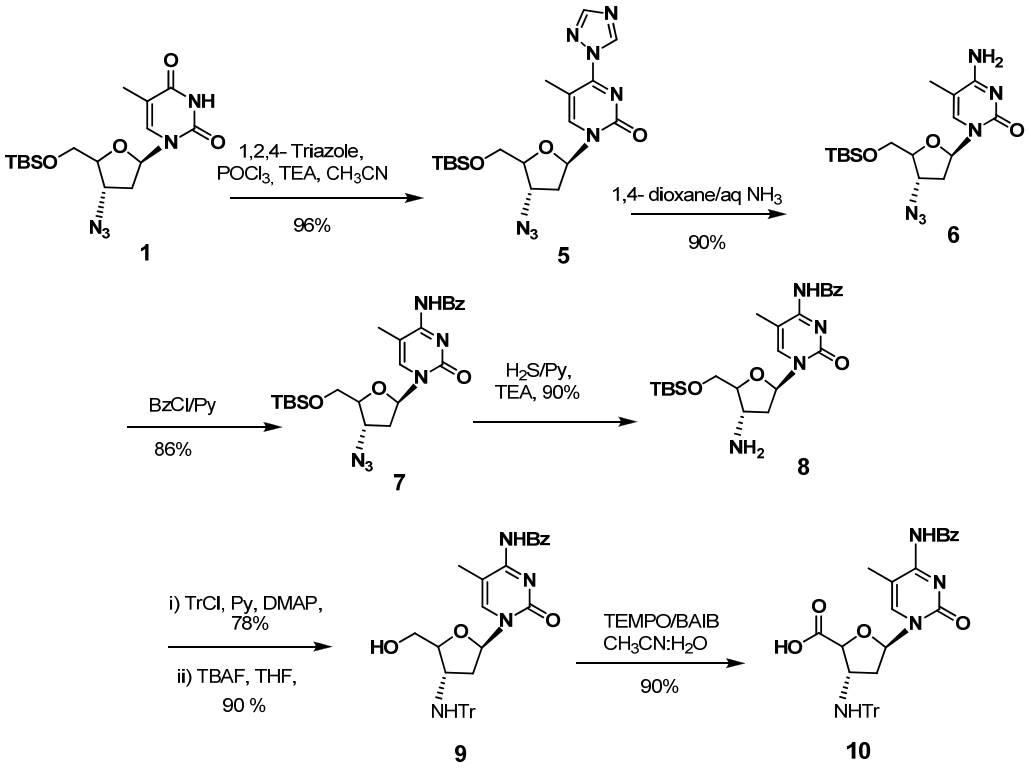

Scheme 2. Synthesis of 5- Methylcytidine -β-amino acid

3.3.3 Synthesis of Adenine monomer

For the synthesis of β-amino acid derivatives of adenine and guanine nucleosides, we used the commercially available 3'-amino-2',3'-deoxy purine nucleosides as starting materials. The synthesis of the starting nucleoside derivatives is earlier reported from exocyclic amino protected 2'-deoxyxylo nucleosides.[22] Studies are also reported using commercial 3'-tritylamino-2',3'-dideoxy purine nucleosides, when exocyclic amino protection involved either transient protection using TMS-chloride or peracylation/ hydrolysis.[25] In either case, some undesired side products were obtained. The reactivity of nucleosides is quite sensitive to the substituent groups and we had to consider appropriate changes in the route to get the desired products in good yields. To get clean reaction products, we decided to use 5'-*O*-TBDMS protection as for the pyrimidine derivatives.

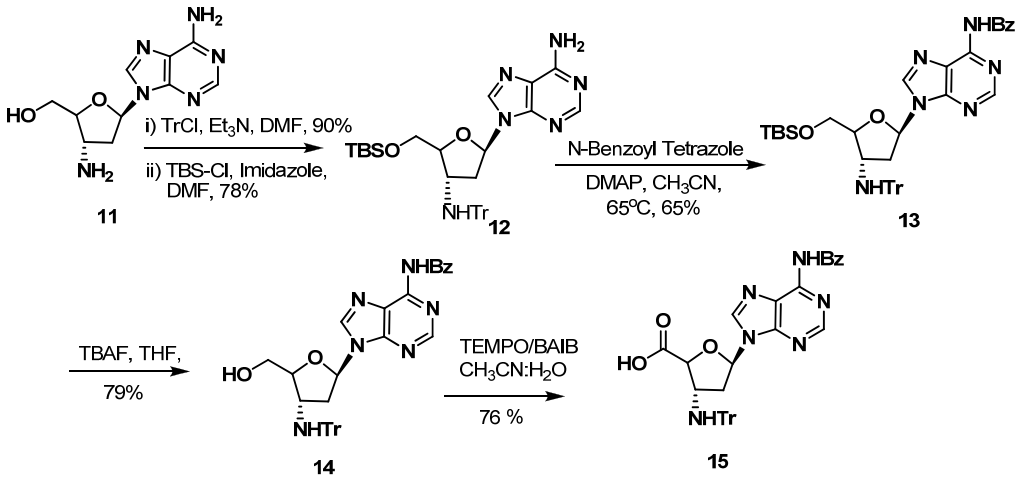

Scheme 3. Synthesis of Adenine-β-amino acid

The 3'-amino-2',3'-dideoxyadenosine **11** (Scheme 3) was converted to 3'-tritylamino derivative[25] by treatment with trityl chloride in DMF followed by silylation of 5'-OH with TBS-chloride to get the desired 3'-and 5'- protected derivative **12.** Subsequent protection of the exocyclic amino functionality with N-benzoyl tetrazole at higher temperature[26] afforded **13** in good yields. The protection of exocyclic amino group proved to be challenging as extensive depurination was encountered even at -5 to -10 ºC when benzoyl chloride was used as the acylating reagent. Benzoylation of 3'-NH-trityl group was not observed under these conditions. Compound **13** was then desilylated to get the free hydroxyl function at 5' position in **14** which was further

subjected to oxidation using TEMPO–BAIB conditions to afford corresponding acid **15** (27% overall yield).

3.3.4 Synthesis of Guanine monomer

The 3'-amino-2',3'-dideoxyguanosine **16** (Scheme 4) was converted to 3'-tritylamino derivative[25] by treatment with trityl chloride followed by treatment with TBS-chloride to afford 3'-and 5'- protected derivative **17**. Exocyclic amino group was protected with isobutyryl chloride in pyridine to get **18**. Removal of the 5'-silyl protecting group in **18** gave compound **19** which on oxidation with TEMBO-BAIB afforded 4'-carboxylic acid derivative **20** (37% overall yield) (Scheme 4).

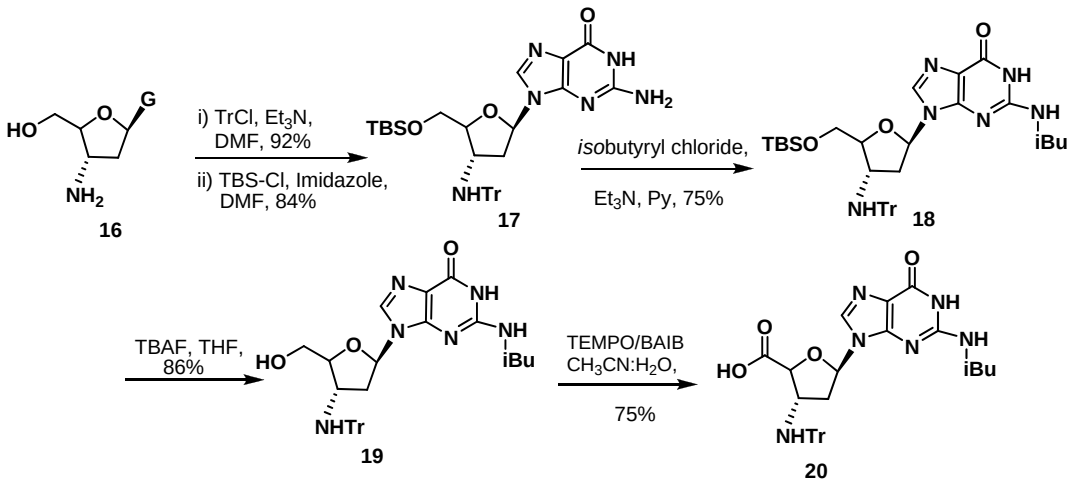

Scheme 4. Synthesis of Guanine-β-amino acid

To rule out the possibility of epimerization at C4' during TEMPO-BAIB oxidation, compound **4** was treated with aq. NaOH and the chiral HPLC chromatogram was compared with of compound **4** (without NaOH treatment) [figure 3] and did not observe any additional peak for epimerized product. These results were also supported by 2D NMR of compound **4** which showed that H4' proton exhibit NOE cross peak with H1' proton confirming α-orientation of H4' proton.

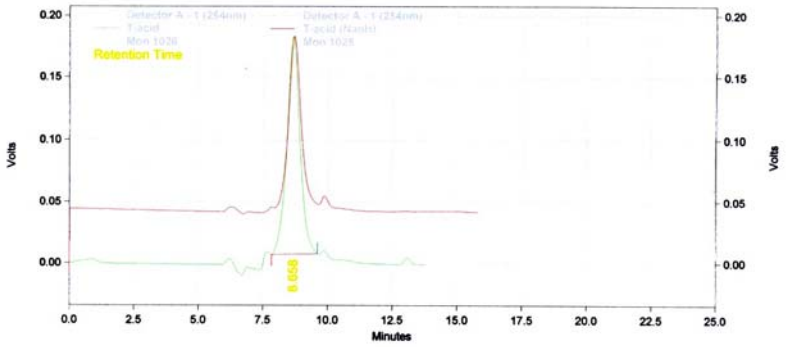

Figure 3. HPLC chromatogram of compound **4** before (green) and after NaOH (purple) treatment

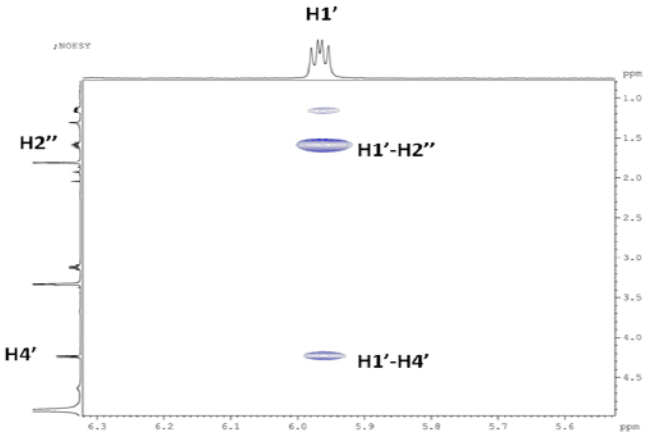

Figure 4. Expanded NOESY spectrum of compound **4** shows nOe cross peaks between H1' and H4' indicating H4' is α to the plane of furanose ring.

All the purified compounds in schemes 1-4 were characterized by ^{1}H, ^{13}C and mass spectrometry analysis and by comparing with the known compounds. The new compounds β-amino acid monomers **4**, **10**, **15** and **20** were further characterized by HRMS analysis.

3.4 Solid Phase synthesis of polyamide DNA oligomer

Synthesis of a model tetrameric nucleoside sequence 5'-^{Me}C(gly)A(gly)^{Me}C(gly)T (**23**) was done using synthesized monomeric units and trityl glycine (**22**).[27] Choice of the resin for solid phase synthesis was influenced by the swelling properties of the resin and avoiding harsh acidic deprotection conditions

considering sensitivity of the glycosidic bond towards acid. Amino functionalized resin has to be selected such that the final cleavage conditions are compatible towards stability of glycosidic bond. With this in mind, the first building block was modified with succinate ester linker at its 5' position and was loaded on the resin through an amide bond. The resulting ester bond at 5' position can be hydrolysed under basic condition after oligomer synthesis. We used both CPG[22] and MBHA[23] resin for solid phase synthesis. The MBHA resin which has better swelling properties gave much higher yield compared (coupling yield ~ 80% at each step) to the synthesis when CPG was used. The coupling efficiencies at each step could be monitored using Kaiser test[28] or by measurement of trityl cation. Thus, the succinate modified monomer[22] **21** was loaded on the MBHA resin using solid phase peptide coupling protocol (Scheme 5).[23] Tetrameric sequence was assembled using repetitive cycles, purified (21% isolated yield) and analyzed by mass spectrometry using ESI-MS technique.

3.4.1 Pre-loading of MBHA resin

MBHA resin (60 mg, 1.75mmol/g, 0.024mmol) was washed and swelled in DCM for 1 hr in solid phase flask. The resin was drained and washed with DMF. To a solution of N^4-Benzoyl-5-methyl 3'-tritylamino-2',3'-dideoxycytidine-5'-succinylate[20] **21** (16.19 mg, 0.024 mmol) in 500 μL DMF , DIPEA (12.47 μL, 0.072 mmol) and TBTU(9.63 mg, 0.028 mmol) was added. To this solution HOBt (3.24 mg, 0.024 mmol) in 100μL of DMF was added. This activated monomer solution was added to the resin and the suspension was allowed for gentle shaking for 12 hrs. Resin was drained and washed with DMF (2 x), DCM (2 x) and pyridine (2 x).Unreacted amino groups capped with 10% acetic anhydride in pyridine for 1 hr. The nucleoside loading on solid support was determined by spectrophotometric determination of the concentration of trityl cation at 410 nm released after detritylation using 3 % TCA in DCM. Calculated loading value for resin using molar extinction coefficient[29] 35300 M^{-1} cm^{-1} at 410 nm for trityl cation was 35.2 μmol/g which was good enough for next synthesis.

3.4.2 Solid Phase synthesis of model tetramer 23

Synthesis of a model tetrameric nucleoside sequence 5'-C(gly)A(gly)C(gly)T was then undertaken using protected nucleoside β amino acid monomeric units and

trityl glycine (**22**) on preloaded MBHA resin. The tetramer was synthesized using repetitive cycles (Scheme 5), each comprising the following steps:

i) Deprotection of trityl group using 3% trichloroacetic acid (3 min x 3)

ii) Neutraization using 5% DIPEA in DCM (3min X 2)

iii) coupling using 3 equivalent of monomer, 9 equivalent DIPEA, 3 equivalent TBTU and 1.5 equivalent of HOBt as activator with respect to loading value of resin. All are premixed in DMF prior to addition to resin. This suspension was added to the resin. Reaction time 5 hrs.

iv) Capping of unreacted amino groups using 10% acetic anhydride in pyridine (10 min x 2).

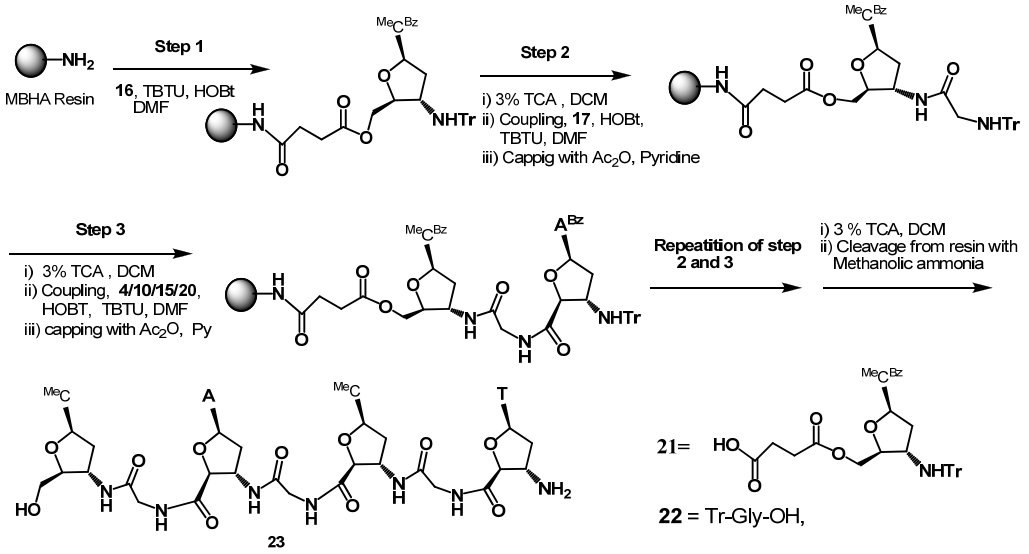

Scheme 5: Schematic representation of solid phase synthesis of (α + β amino acid) tetramer

3.4.3 Cleavage and purification of tetramer

After the synthesis was complete, the oligomer **23** was cleaved from solid support using aqueous methanolic ammonia at 55°C for 8 hrs. The terminal trityl group was deprotected before cleavage using 3 % TCA in DCM or after cleavage using 80% aqueous acetic acid. Oligomer was extracted from resin in 20% methanol in water. Analytical purification was achieved on reverse phase C18 column using 5% acetonitrile in 0.1 M TEAA buffer as eluent system and monitored at 260 nm (retention

time for tetramer 3.54 min) and further characterized by ESI-mass spectrometry. Mass calc. for $C_{46}H_{58}N_{20}O_{15}$ 1130.4391 ESI mass observed *m\z* for ($C_{46}H_{58}N_{20}O_{15}^{+1}$ 1129.7) $C_{46}H_{58}N_{20}O_{15}^{+2}$), 565.22.

3.5 Conclusion

In conclusion, the synthesis of all four protected natural nucleoside-β-amino acids was accomplished using simple TEMPO/BAIB method and we further tested the synthesis of a model tetrameric nucleobase sequence 5'-^{Me}C(gly)A(gly)^{Me}C(gly)T **23** where ^{Me}C, A and T are nucleoside-β-amino acids corresponding to the 5-methyl-cytosine, adenine and thymine, and glycine is used as the alternating α-amino acid. Synthesis of longer oligomer needs small changes in our protocols. Current studies are going on for optimizing condition for solid phase synthesis for improving coupling reactions and yield of the final oligomers so that the synthesis of longer oligomers can be achieved in greater purity.

3.6 Summary

1. All four nucleoside-β-amino acids were synthesized using the simple **TEMPO-BAIB** method for oxidation.

2. A tetrameric nucleoside sequence 5'-C(gly)A(gly)C(gly)T was accomplished using synthesized monomeric units.

3.7 Experimental

General-All the reagents were purchased from Sigma-Aldrich and used without purification. 3'-Amino purine nucleosides were purchased from Metkinen Chemistry, Finland. All solvents used were dried and distilled according to standard protocols. Analytical TLCs were performed on Merck 5554 silica 60 aluminium sheets. Column chromatography was performed for purification of compounds on silica gel (60-120 mesh, Merck). For acid-sensitive (trityl-containing) compounds, the column packed and equilibrated with 0.5% triethylamine. TLCs were performed using dichloromethane-methanol or petroleum ether-ethyl acetate solvent systems. Visualization was accomplished with UV light and/or by spraying with perchloric acid reagent and heating. ^{1}H and ^{13}C NMR spectra were obtained using Bruker ACF 200 (200 MHz) or 400 (400 MHz) spectrometers and chemical shifts are reported on δ scale in parts per million (ppm) with the solvent indicated as the internal reference. The IR spectra were recorded on a Perkin Elmer Spectrum one-FT-IR spectrophotometer in chloroform.^{1}H NMR data are reported in the order of chemical shift, multiplicity (s, singlet; d, doublet; t, triplet; br, broad; br s, broad singlet; m, multiplet and/ or multiple resonance), number of protons. Mass spectra were recorded on Thermo Finnigan Surveyor MS-Q spectrometer (Mass spectra for tetramer was recorded on Aquity Ultra performance LC-MS, Waters), while HRMS was recorded by using a Micromass Q-Tof micro (YA-105) spectrometer and Thermo Scientific Q-exactive mass spectrometer. Specific rotation was recorded on Bellingham +Stanley Ltd, ADP 220 polarimeter and the concentration (c) is expressed in gram per 100 mL. HPLC done on Chiralcel OJ-H (250 x 4.6 mm) column and ethanol: pet ether: DEA (30:70:0.1) as mobile phase.

(1'R, 3'S, 4'R)-3'-amino-5'-*O*-(*tert*-butyldimethylsilyl)-3'-deoxythymidine (**2**)

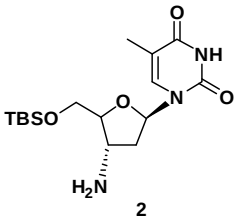

2

A mixture of 3'-azido-5'-*O*-(*tert*-butyldimethylsilyl)-3'-deoxythymidine **1** (3 g, 7.87 mmol) and 10% palladium on charcoal (0.3 g) in 30 mL methanol: ethyl acetate mixture (1:1, v/v) was stirred under hydrogen atmosphere (60 psi) at room temperature for 4 h. The reaction mixture was filtered through celite and the solvent was evaporated in vacuo to give 3'-amino-5'-*O*-(*tert*-butyldimethylsilyl)-3'-deoxythymidine **2** (2.37 g, 85%) as white foam.

^{1}H NMR (200MHz, $CDCl_3$): 7.51 (s, 1H), 6.26 (t, *J*= 6.07 Hz, 1H), 3.90 (m, 2H), 3.72 (m, 1H), 3.64 (m, 1H), 2.19 (m, 2H), 1.91 (s, 3H), 0.93 (s, 9H), 0.11 (s, 6H); **^{13}C NMR** (50MHz, $CDCl_3$): 164.1, 150.5, 135.4, 110.5, 87.4, 84.3, 62.9, 51.4, 41.7, 25.8, 18.3, 12.5, -5.42, -5.47; **MS (EI)** *m/z* 355.19 found 378.12 (M+ Na^+).

(1'R, 3'S, 4'R)-3'-Tritylamino-3'-deoxythymidine (3)

Compound **2** (2 g, 5.63 mmol) was dissolved in dry pyridine (10 mL) and to it trityl chloride (2.04 g, 7.32 mmol) and catalytic amount of DMAP was added. Reaction mixture was allowed to stir at room temperature for 8 h. Solvent was removed under reduced pressure to afford crude 5'-*O*-(*tert*-butyldimethylsilyl)-3'-tritylamino-3'-deoxythymidine (3.03 g, 90%) which was then dissolved in 15 mL anhydrous THF and to it 1N TBAF in THF (5.41 mL, 5.41 mmol) was added. Reaction was stirred at RT for 1 h. THF was removed in vacuo and residue dissolved in dichloromethane, washed with water. Organic layer was dried over Na_2SO_4 and concentrated. Compound was purified by column chromatography using 30% ethyl acetate in petroleum ether to afford 3'-Tritylamino-3'-deoxythymidine **3** (1.49 g, 90%) as a white foam.

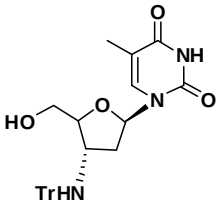

3

^{1}H NMR (200MHz, $CDCl_3$): 8.72 (br s, 1H), 7.54 (m, 6H), 7.14-7.33 (m, 10H), 6.02 (dd, *J*=6.57, 6.19 Hz, 1H), 3.60-3.87 (m, 3H), 3.32 (m, 1H), 2.26 (br s, 1H), 1.81 (s, 3H), 1.26-1.52 (m, 2H); **^{13}C NMR** (50MHz, $CDCl_3$): 163.8, 150.3, 146.0, 135.9, 128.5, 128.0, 126.7, 110.8, 86.6, 84.5, 71.1, 61.9, 53.2, 39.7, 12.4; **MS (EI)** *m/z* 483.21, found 506.20 (M+ Na^+).

(1'R, 3'S, 4'R)-3'-azido-5'-*O*-(*tert*-butyldimethylsilyl)- 5-methyl-2',3'-dideoxy-4-(1,2,4-triazol-1-yl)thymidine (5)

Triethylamine (10.95 mL, 78.94 mmol) was added drop wise over a portion of 10 min to a stirred mixture 1, 2, 4-triazole (5.97 g, 86.61 mmol) and phosphorus oxychloride (1.83 mL, 19.68 mmol) in 60 mL CH_3CN at 0°C. The solution of compound **1** (3 g, 7.87 mmol) in 15 mL dry CH_3CN was then added drop wise and reaction mixture was allowed to stir at room temp for 2.5 h. The solvent was evaporated in vacuo. The resulting brown solid was dissolved in ethyl acetate (100 mL). Organic layer washed with saturated $NaHCO_3$

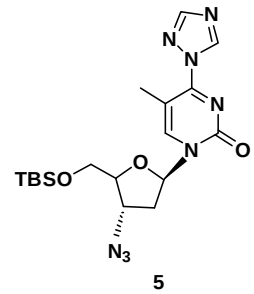

5

solution followed by water, dried over Na_2SO_4 and concentrated to afford crude product **5** (3.26 g, 96 %) as a white solid, which was used immediately for next reaction.

(1'R, 3'S, 4'R)- 3'-azido-5'-*O*-(*tert*-butyldimethylsilyl)- 5-methyl-2',3'-dideoxycytidine (6)

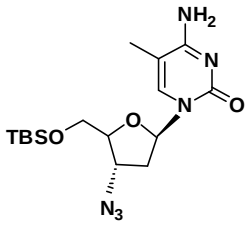

6

Compound **5** (3.26 g, 7.54 mmol) was dissolved in 1, 4-dioxane (30 mL) and 15 mL concentrated aqueous ammonia was added. Reaction mixture was allowed to stir at RT for 2 h. After completion of the reaction, solvents were removed in vacuo. The residue was dissolved in dichloromethane and washed with water. Organic layer was dried over Na_2SO_4, concentrated in vacuo. Compound was purified by column chromatography using 3-5% methanol in dichloromethane to afford 3'-azido-5'-*O*-(*tert*-butyldimethylsilyl)-5-methyl-2',3'-dideoxycytidine **6** (2.56 g, 90%) as a white foam.

^{1}H NMR (200MHz, $CDCl_3$): 7.56 (s, 1H), 6.22 (t, *J*= 6.19 Hz, 1H), 4.17 (m, 1H), 3.94-4.01 (m, 2H), 3.84 (m, 1H), 2.52 (m, 1H), 2.22 (m, 1H), 1.93 (s, 3H), 0.93 (s, 9H), 0.13 (s, 6H); **MS (EI)** m/z 380.1992, found 403.05 (M+ Na^+).

(1'R, 3'S, 4'R)- N^4-Benzoyl -3'-azido-5'-*O*-(*tert*-butyldimethylsilyl)-5-methyl-2',3'-dideoxycytidine (7)

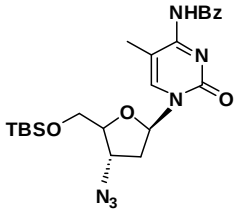

7

Compound **6** (2.56 g, 6.73 mmol) was azeotroped with pyridine and redissolved in pyridine (15 mL), and cooled externally at 0 °C. To this solution, benzoyl chloride (0.938 mL, 8.08 mmol) was added drop wise and the mixture was then allowed to attain RT and stir additionally for 14 h at RT. The reaction was quenched with 2N NH_3 (5 mL) and was further stirred for 30 min. The solvent was evaporated in vacuo and residue was dissolved in ethyl acetate, washed with saturated $NaHCO_3$ solution, dried over Na_2SO_4 and concentrated in vacuo. This crude product was purified on column chromatography using 25% ethyl acetate in petroleum ether to afford **7** (2.79 g, 86%) as a colourless foam.

^{1}H NMR (200MHz, $CDCl_3$): 8.33 (m, 2H), 7.66 (s, 1H), 7.44-7.58 (m, 3H), 6.23 (t, *J*=6.31 Hz, 1H), 4.27 (m, 1H), 3.90-4.02 (m, 2H), 3.80-3.86 (m, 1H), 2.49-2.58 (m, 1H), 2.30 (m, 1H), 2.12 (s, 3H), 0.95 (s, 9H), 0.15 (s, 6H).

(1'R, 3'S, 4'R)-N^4-Benzoyl-3'-amino-5'-*O*-(*tert*-butyldimethylsilyl)-5-methyl-2',3'-dideoxycytidine (8)

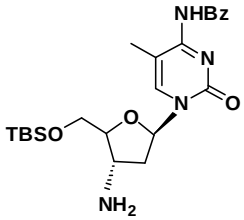

8

Compound **7** (2.7 g, 5.57 mmol) was dissolved in 15 % Et_3N in dry pyridine (10 mL) and H_2S gas was bubbled into the solution at 0 °C for 10 minutes. Reaction mixture was then stirred at room temperature for 30 minutes. Solvent was removed in vacuo and the residue was purified by column chromatography using 5% methanol in DCM to afford of compound **8** (2.29 g, 90%) as yellow foam.

^{1}H NMR (200MHz, $CDCl_3$): 8.34 (m, 2H), 7.75 (s, 1H), 7.50 (m, 3H), 6.25 (t, *J*=5.94 Hz, 1H), 3.95 (m, 2H), 3,76 (m, 1H), 3.65 (q, *J*=12.26, 6.57 Hz, 1H), 2.25 (m, 1H), 2.30 (m, 1H), 2.12 (s, 3H), 0.95 (s, 9H), 0.15 (s, 6H); **^{13}C NMR** (50MHz, $CDCl_3$): 179.5, 159.8, 147.8, 137.2, 136.9, 132.3, 129.8, 128.0, 111.2, 87.8, 85.2, 62.7, 51.2, 42.3, 25.9, 18.4, 13.7, -5.37, -5.36; **MS (EI)** *m/z* 458.2349, found 481.24 (M+ Na^+).

(1'R, 3'S, 4'R)-N^4-Benzoyl-3'-tritylamino-5-methyl -2',3'-dideoxycytidine (9)

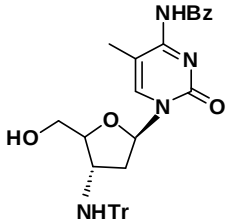

9

Compound **8** (2.29 g, 4.99 mmol) was azeotroped with pyridine and redissovled in 15 mL anhydrous pyridine. Trityl chloride (1.58 g, 5.67 mmol) and catalytic amount of DMAP was added to reaction mixture and was allowed to stir at room temperature for 8 hr. Solvent was removed in vacuo and the residue was purified by column chromatography using 30% ethyl acetate in petroleum ether to afford N^4-Benzoyl-3'-tritylamino-5'-*O*-(*tert*-butyldimethylsilyl)-5-methyl-2',3'-dideoxycytidine (2.90 g, 78%) which was then subjected for desilylation. Following amounts were used in desilyation reaction; N^4-Benzoyl-5'-*O*-(*tert*-butyldimethylsilyl)-3'-tritylamino-5-methyl-2',3'-dideoxycytidine (2.90 g, 4.14 mmol), 15 ml anhydrous THF as a solvent and TBAF 1N in THF (6.21 mL , 6.21 mmol). Reaction was stirred at RT for 1 h. THF was removed in vacuo and residue dissolved in dichloromethane, washed with water. Organic layer was dried over Na_2SO_4 and concentrated. Compound was purified by column chromatography using 35 % ethyl acetate in petroleum ether to give product **9** (2.18 g, yield 90%) as a white solid.

^{1}H NMR (200MHz, $CDCl_3$): 8.31 (s, 1H), 8.28 (m, 1H), 7.39-7.55 (m, 10H), 7.18-7.39 (m, 10H), 6.03 (dd, *J*=6.70, 5.30 Hz, 1H), 3.66-3.93 (m, 3H), 3.32 (q, *J*=13.26, 6.94 Hz,

1H), 2.03 (s, 3H), 1.73 (br s, 1H), 1.25-1.42 (m, 2H); **^{13}C NMR** (50MHz, $CDCl_3$): 179.4, 159.6, 147.8, 146.0, 137.2, 137.0, 132.4, 129.8, 129.5, 128.1, 126.8, 111.6, 86.7, 85.4, 71.1, 61.8, 52.9, 40.3, 13.5; **MS (EI)** *m/z* 586.2560, found 609.21 (M+ Na^+).

General procedure for synthesis of 3'-tritylamino-2',3'-dideoxy-purine nucleosides[25]

Et_3N (1.15 mL, 8.26 mmol) was added to a stirred solution of 3'-Amino-2',3'-dideoxy purine nucleoside **11**/ **16** (7.51 mmol) in dry DMF (80 mL). The reaction mixture was stirred at 60°C for 30 min. Trityl chloride (2.24 g, 8.26 mmol) was added to reaction mixture in two portions and allowed to stir for 3 h at room temp. The reaction mixture poured on 120 mL cold water and the flask kept in freezer for 2 h. The obtained precipitate was filtered and washed thoroughly with cold water. White solid desiccated overnight to give crude 3'-Tritylamino-2',3'-dideoxyadenosine (3.32 g, 90%)/ 3'-Tritylamino-2',3'-dideoxyguanosine (4.13 g, 92%) which was used as such for next reaction.

(1'R, 3'S, 4'R)-5'-*O*-(*tert*-butyldimethylsilyl)-3'-tritylamino-2',3'-dideoxyadenosine (12)

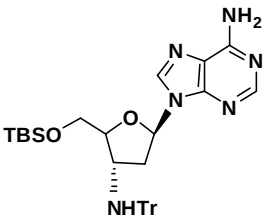

12

3'-Tritylamino-2',3'-dideoxyadenosine (3.32 g, 6.74 mmol), TBS-Cl (1.32 g, 8.77 mmol) and imidazole (1.37 g, 20.22 mmol) was suspended in 15 mL dry DMF and the reaction was allowed to stir overnight at RT. DMF was removed in vacuo and the residue was redissolved in ethyl acetate (150 mL). Organic layer was washed with water followed by brine, dried over Na_2SO_4 and concentrated in vacuo. Product was purified by column chromatography using 3% methanol in dichloromethane to afford 5'-*O*-(*tert*-butyldimethylsilyl)-3'-tritylamino-2',3'-dideoxyadenosine **12** (3.19 g, 78%). **^{1}H NMR** (200MHz, $CDCl_3$): 8.30 (s, 1H), 7.91 (s, 1H), 7.51-7.56 (m, 6H), 7.17-7.32 (m, 9H), 6.29 (dd, *J*=6.19, 5.93 Hz, 1H), 5.71 (br s, 2H), 3.87 (m, 1H), 3.60-3.82 (m, 2H), 3.44 (m, 1H), 2.02 (br s, 1H), 1.71-1.79 (m, 2H), 0.82 (s, 9H), -0.03 (s, 3H), -0.04 (s, 3H); **^{13}C NMR** (50MHz, $CDCl_3$): 155.3, 152.8, 149.4, 146.1, 138.4, 128.6, 128.0, 126.6, 119.4, 87.1, 83.6, 71.2, 63.6, 54.7, 41.1, 25.8, 18.3, -5.4; **MS (EI)** *m/z* 606.3139, found 607.23 (M+ H^+), 629.29 (M+Na^+); HRMS (ESI): calcd for $C_{35}H_{42}N_6O_2Si$: 607.3211, found: 607.3205.

(1'R, 3'S, 4'R)- N^6-benzoyl-5'-*O*-(*tert*-butyldimethylsilyl)-3'-tritylamino-2',3'-dideoxyadenosine (13)

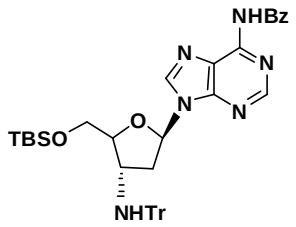

13

5'-*O*-(*tert*-butyldimethylsilyl)-3'-tritylamino-2',3'-dideoxyadenosine **12** (3.19 g, 5.26 mmol) dissolved in dry acetonitrile (40 mL). To it *N*-benzoyl tetrazole (1.82 g, 9.89 mmol) and 4-dimethylaminopyridine (0.604 g, 5.25 mmol) was added. The reaction mixture is allowed to stir at 65 °C for 90 min. After completion of reaction, solvent was removed in vacuo and residue dissolved in dichloromethane. Organic layer washed with saturated $NaHCO_3$ solution, dried over Na_2SO_4 and concentrated to give crude product. This crude was purified by column chromatography using 1% methanol in dichloromethane to afford **13** (2.42 g, 65 %) as a white solid.

^{1}H NMR (200MHz, $CDCl_3$): 9.15 (bs, 1H), 8.75 (s, 1H), 8.13 (s, 1H), 8.00 (d, *J*=6.70 Hz, 2H), 7.49-7.59 (m, 8H), 7.15-7.32 (m, 10H), 6.36 (dd, *J*=6.06, 5.69 Hz, 1H), 3.64-3.91 (m, 3H), 3.51 (m, 1H), 2.08 (br s, 1H), 1.64-1.88 (m, 2H), 0.81 (s, 9H), -0.02 (s, 3H), -0.03 (s, 3H); **^{13}C NMR** (50MHz, $CDCl_3$): 164.6, 152.4, 151.1, 149.2, 146.0, 140.9, 133.6, 132.6, 128.7, 128.5, 128.0, 127.8, 126.6, 122.8, 87.2, 83.9, 71.1, 63.4, 54.5, 41.0, 25.8, 18.3, -5.45, -5.53; **MS (EI)** *m/z* 710.3401, found 711.26 ($M+ H^+$), 733.31($M+Na^+$).

(1'R, 3'S, 4'R)- N^6-benzoyl-3'-tritylamino-2',3'-dideoxyadenosine (14)

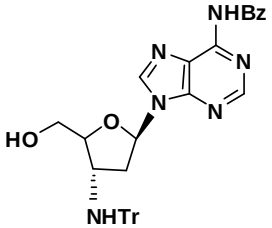

14

Compound **13** (2.4 g, 3.38 mmol) dissolved in anhydrous THF (15 mL) and 1N TBAF in THF (5.07 mL, 5.07 mmol) was added. Reaction was stirred at RT for 1 h. THF was removed in vacuo and the residue was dissolved in dichloromethane, washed with water and then brine. Organic layer was dried over Na_2SO_4, concentrated in vacuo and purified by column chromatography using 3% methanol in DCM to get product **14** (1.59 g, 79%) as a white solid.

^{1}H NMR (200MHz, $CDCl_3$): 9.26 (br s, 1H), 8.61 (s, 1H), 8.03 (m, 3H), 7.49-7.56 (m, 8H), 7.20-7.33 (m, 10H), 6.24 (dd, *J*=7.45, 6.31 Hz, 1H), 3.68-3.78 (m, 3H), 3.55 (d, *J*=11.32 Hz, 1H), 2.30 (m, 1H), 2.04 (br s, 1H), 1.76 (m, 1H); **MS (ESI)** *m/z* 596.2536, found 597 ($M +H^+$), 619 ($M+ Na^+$).

(1'R, 3'S, 4'R)-5'-*O*-(*tert*-butyldimethylsilyl)-3'-tritylamino-2',3'-dideoxyguanosine (17)

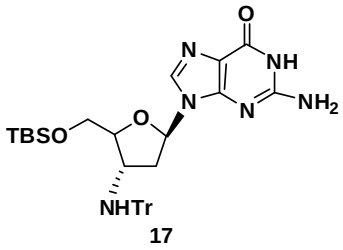

17

3'-Tritylamino-2',3'-dideoxyguanosine (4.13 g, 8.12 mmol), TBS-Cl (1.59 g, 10.56 mmol) and imidazole (1.65 g, 24.36 mmol) was suspended in 15 mL dry DMF and the reaction was allowed to stir overnight at RT. DMF was removed in vacuo and the residue was dissolved in ethyl acetate (150 mL). Organic layer was washed with water, dried over Na_2SO_4 and concentrated in vacuo The crude product was purified by column chromatography using 3% methanol in dichloromethane to afford **17** (4.23 g, 84%) as a white solid.

^{1}H NMR (200MHz, DMSO-D_6): 10.64 (br s, 1H), 7.46-7.50 (m, 7H), 7.14-7.32 (m, 9H), 6.45 (br s, 1H), 5.89-5.95 (t, *J*=6.19 Hz, 1H), 3.74-3.80 (m, 1H), 3.46-3.68 (m, 2H), 3.34 (m, 1H, merged with H_2O), 1.45-1.58 (m, 1H), 1.23-1.30 (m, 1H), 0.79 (s, 9H), -0.07 (s, 6H); **^{13}C NMR** (50MHz, $CDCl_3$): 159.1, 153.3, 151.3, 146.2, 135.4, 128.6, 128.0, 126.7, 117.0, 87.0, 83.0, 71.1, 63.5, 54.6, 40.3, 25.9, 18.4, -5.40, -5.52; **MS (EI)** *m/z* 622.3088, found 623.27 (M+ H^+), 645.32 (M+Na^+); HRMS (ESI): calcd for $C_{35}H_{42}N_6O_3Si$: 623.3160, found: 623.3145.

5'-*O*-(*tert*-butyldimethylsilyl)-N^2-isobutyryl-3'-tritylamino-2',3'-dideoxyguanosine (18)

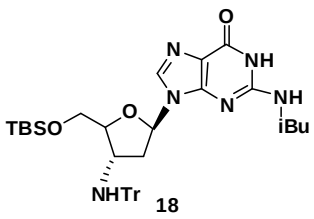

18

To solution of compound **17** (4.23 g, 6.80 mmol) in anhydrous pyridine (20 mL), triethyl amine (0.95 mL, 6.80 mmol) was added and the mixture was stirred for 15 min. To this reaction mixture *iso*butyryl chloride (1.43 mL, 13.6 mmol) was added drop-wise and reaction was allowed to stir for 1 h. Pyridine was removed in vacuo and reaction mixture dissolved in ethyl acetate, washed with saturated $NaHCO_3$ solution, then water. Organic layer dried over Na_2SO_4 and concentrated to give crude product. The product was purified by column chromatography using 1% methanol in DCM to afford **18** (3.53 g, 75%) as a white solid.

^{1}H NMR (200MHz, $CDCl_3$): 7.58 (s, 1H), 7.52 (d, *J*=7.93 Hz, 6H), 7.28 (t, *J*=7.93 Hz , 6H), 7.20 (t, *J*=7.32 Hz , 3H), 5.97 (dd, *J*=6.72, 4.88 Hz, 1H), 3.83 (m, 1H), 3.67-3.77

(ABX, J_{AB}=11.30 Hz, 2H), 3.47 (m, 1H), 2.57-2.59 (septet, *J*= 6.41 Hz, 1H), 1.68-1.71 (m, 1H), 1.54-1.57 (m, 1H), 1.21-1.25 (m, 6H) 0.80 (s, 9H), -0.05 (s, 3H), -0.06 (s, 3H); **^{13}C NMR** (50MHz, $CDCl_3$): 178.1, 155.4, 147.7, 147.2, 146.1, 136.5, 128.6, 128.1, 127.9, 126.7, 121.1, 87.1, 83.0, 71.1, 63.4, 54.6, 40.4, 36.5, 25.9, 18.9, 18.4, -5.45, -5.55; **MS (EI)** *m/z* 692.3506, found 693.43 (M+ H^+), 715.45 (M+ Na^+).

(1'R, 3'S, 4'R)-*N*^{2}-isobutyryl-3'-tritylamino-2',3'-dideoxyguanosine (19)

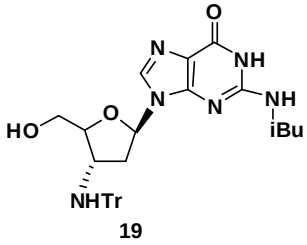

19

This compound is obtained in 91 % yield via desilylation of **18** as described in the synthesis of **14**. Compound was purified by column chromatography using 3% methanol in DCM to afford **19** as white solid.

^{1}H NMR (200MHz, $CDCl_3$): 7.60 (s, 1H), 7.52 (d, J=7.93 Hz, 6H), 7.18-7.38 (m, 9H), 5.98 (dd, *J*=6.44, 6.57 Hz, 1H), 3.85-3.96 (m, 2H), 3.53-3.64 (m, 2H), 2.68 (septet, *J*= 6.95 Hz, 1H), 2.06 (br s, 1H), 1.83 (m, 1H), 1.52 (m, 1H), 1.20 (dd, *J*= 6.82, 3.28 Hz, 6H); **MS (EI)** *m/z* 578.2642, found 579.25 (M+H^+), 601.28 (M+Na^+).

General Procedure for synthesis of nucleoside-β-amino acids

(Diacetoxyiodo)benzene (2.2 mmol) and TEMPO (0.25 mmol), were added to the solution of protected 2' 3'-deoxy-3'-tritylamino nucleosides **3**/**9**/**14**/**19** (1 mmol) in 5 mL CH_3CN/H_2O mixture (1:1). The reaction mixture was stirred at 25 °C for 3 h. Acetonitrile was removed completely in vacuo. The crude product was extracted with ethyl acetate. The organic phase was dried over anhydrous Na_2SO_4 and concentrated. The resulting residue was triturated sequentially with diethyl ether and acetone, filtered and dried in vacuo.

(1'R, 3'S, 4'S) 3'-deoxy-3'-tritylamino-thymidin-4'-carboxylic acid (4)

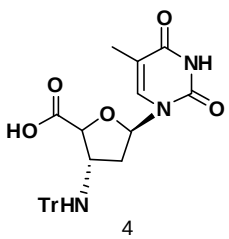

4

This compound is obtained as a white solid (0.45 g, 91%) starting from compound **3** by general procedure described above. Rf (10% MeOH/DCM) 0.51; MP: 214-217 °C; $[\alpha]_D^{25}$: +30.9 º (*c* = 1.03, MeOH); **^{1}H NMR** (400MHz, DMSO-D_6 + drop of D_2O): 8.73 (s, 1H, H6), 7.42-7.44 (m, 6H, aromatic), 7.22-7.26 (m, 6H, aromatic), 7.12-7.16 (m, 3H, aromatic), 5.87 (dd, *J*= 5.52,5.02 Hz, 1H, H1'), 4.08 (d, *J* = 5.78 Hz, 1H, H4'), 2.89 (dd, *J*= 11.54, 5.52 Hz, 1H, H3'), 1.64 (s, 3H, CH_3), 1.21 (m, 1H, H2''),

1.00 (m, 1H, H2'); **^{13}C NMR** (100 MHz, DMSO-D_6 + drop of D_2O): 173.9, 164.0, 150.1, 146.5, 138.5, 128.7, 127.6, 126.1, 107.5, 86.2, 85.6, 70.7, 56.6, 38.9, 12.3; **IR** (υ_{max}, cm^{-1}) ($CHCl_3$): 3620, 3399, 3018, 2975, 2896, 1690, 1215; **HRMS** (ESI): calcd for $C_{29}H_{27}N_3O_5$: 520.1848, found: 520.1846.

(1'R, 3'S, 4'S)-2',3'-dideoxy-3'-tritylamino-*N*^{4}-benzoyl-5-methylcytidin-4'-carboxylic acid (10)

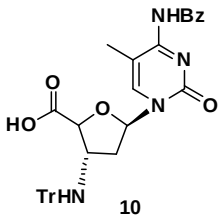

10

This compound is obtained as a white solid (0.54g, 90%) starting from compound **9** by general procedure described above. Rf (10% MeOH/DCM) 0.59; MP: 204-207 °C; $[\alpha]_D^{26}$: +115.9 º (*c* = 1.07, MeOH); **^{1}H NMR** (400MHz, DMSO-D_6 + drop of D_2O): 8.84 (br s, 1H, NH), 8.12 (s, 2H, aromatic), 7.57 (m, 1H, aromatic), 7.43-7.47 (m, 9H, aromatic), 7.23-7.27 (m, 6H, aromatic), 7.13-7.16 (m, 3H, aromatic), 5.96 (t, *J*= 4.77 Hz, 1H, H1'), 4.22 (d, *J*= 5.77 Hz, 1H, H4'), 3.05 (m, 1H, H3'), 1.89 (s, 3H, CH_3), 1.40 (m, 1H, H2''), 1.06 (m, 1H, H2'); **^{13}C NMR** (100 MHz, DMSO-D_6 + drop of D_2O): 174.4, 173.7, 160.4, 147.9, 146.6, 142.7, 136.6, 132.7, 129.4, 128.9, 128.0, 127.0, 126.4, 108.7, 87.3, 86.5, 70.8, 56.5, 39.1, 13.5; **IR** (υ_{max}, cm^{-1})($CHCl_3$): 3619, 3318, 3018, 2976, 2897, 1703, 1652, 1215; **HRMS**(ESI): calcd for $C_{36}H_{32}N_4O_5$: 601.2451, found: 601.2452.

(1'R, 3'S, 4'S)-2',3'-dideoxy-3'-tritylamino-*N*^{6}-benzoyl-adenin-4'-carboxylic acid (15)

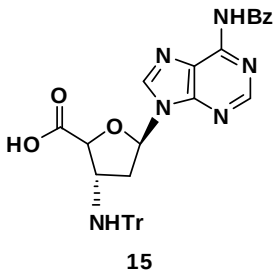

15

This compound was obtained as a white solid (0.46g, 76%) starting from compound **14** by general procedure described above. Rf (10% MeOH/DCM) 0.52; MP: 262-270 °C; $[\alpha]_D^{26}$: +5.1 º (*c* = 0.79, MeOH); **^{1}H NMR** (400MHz, DMSO-D_6 + drop of D_2O): 8.63 (s, 1H, C2-H), 8.46 (s, 1H, C8-H), 7.97 (d, *J* = 7.28 Hz, 2H, aromatic), 7.66 (m, 1H, aromatic), 7.51-7.55 (m, 2H, aromatic), 7.44-7.46 (m, 6H, aromatic), 7.24 (m, 6H, aromatic) 7.07-7.16 (m, 3H, aromatic), 6.35-6.38 (dd, *J*= 6.27, 4.52 Hz, 1H, H1'), 4.30 (d, *J*= 6.27 Hz, 1H, H4'), 3.47(dd, *J*=13.05, 6.53 Hz, 1H, H3'), 1.62-1.69 (m, 1H, H2''), 1.31-1.34 (m, 1H, H2'); **^{13}C NMR** (100MHz, DMSO-D_6 + drop of D_2O): 173.0, 165.5, 151.7, 151.5, 150.1, 146.2, 142.4, 133.3, 132.4, 128.58, 128.50, 128.4, 127.8, 126.3, 125.5, 84.6, 83.5, 70.7, 58.1, 37.3; **IR** (υ_{max}, cm^{-1}) ($CHCl_3$): 3619, 3399, 3018, 2976, 2896, 1707, 1216; **HRMS**(ESI): calcd for $C_{36}H_{30}N_6O_4$: 611.2407, found: 611.2404.

(1'R, 3'S, 4'S)-2',3'-dideoxy-3'-tritylamino-*N*^{2}-isobutyryl-guanosin-4'-carboxylic acid (20)

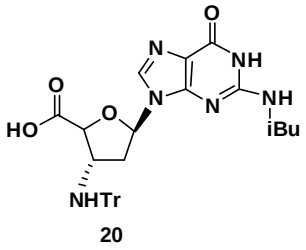

20

Analogous method was used for the synthesis of this compound starting from compound **19**. In this case, after completion of the reaction mixture directly diluted with ethyl acetate and extracted with water. The organic phase was dried over anhydrous Na_2SO_4 and concentrated. The resulting residue was triturated sequentially with diethyl ether and acetone, filtered and dried in vacuo to get white solid (0.44g, 75%). Rf (10% MeOH/DCM) 0.51; MP: 235-238 °C ; $[\alpha]_D^{26}$: +33.0 º (*c* = 1.75, MeOH); **^{1}H NMR** (400MHz, DMSO-D_6 + drop of D_2O): 8.49 (s, 1H, C8-H), 7.40 (d, *J*= 7.78 Hz, 6H, aromatic), 7.10-7.23 (m, 10H, aromatic), 5.96-5.99 (dd, *J*=5.52, 3.76 Hz, 1H, H1'), 4.17 (d, *J*=6.77 Hz, 1H, H4'), 3.11-3.16 (m, 1H, H3'), 2.72-2.75 (m, 1H, iBu-CH), 1.50-1.53 (m, 1H, H2''), 1.08-1.12 (2d, 6H, iBu-CH_3), 0.99 (m, 1H, H2'); **^{13}C NMR** (100MHz, DMSO-D_6 + drop of D_2O): 180.4, 174.0, 155.2, 147.8, 146.6, 138.83, 128.9, 128.1, 127.9, 126.6, 120.3, 85.2, 84.8, 70.7, 57.0, 39.5, 35.0, 19.2, 19.1; **IR** (υ_{max}, cm^{-1}) ($CHCl_3$): 3393, 3016, 2975, 2895, 1685, 1609, 1215; **HRMS** (ESI): calcd for $C_{33}H_{32}N_6O_5$: 593.2512, found: 593.2510.

3.8 Appendix

Compounds	Page No.
Compound 2: ^{1}H, ^{13}C NMR and DEPT	207
Compound 3: ^{1}H, ^{13}C NMR and DEPT	208
Compound 4: ^{1}H, ^{13}C NMR and DEPT	209
Compound 6: ^{1}H NMR	210
Compound 7: ^{1}H NMR	210
Compound 8: ^{1}H NMR	210
Compound 8: ^{13}C NMR	211
Compound 9: ^{1}H, ^{13}C NMR	211
Compound 10: ^{1}H, ^{13}C NMR and DEPT	212
Compound 12: ^{1}H, ^{13}C NMR and DEPT	213
Compound 13: ^{1}H, ^{13}C NMR	214
Compound 14: ^{1}H NMR	214
Compound 15: ^{1}H, ^{13}C NMR and DEPT	215
Compound 17: ^{1}H, ^{13}C NMR and DEPT	216
Compound 18: ^{1}H, ^{13}C NMR	217
Compound 19: ^{1}H NMR	217
Compound 20: ^{1}H, ^{13}C NMR and DEPT	218
Compound 4, 10 : HRMS spectra	219
Compound 15, 20 : HRMS spectra	220
NOESY spectrum of compound **4**	221
HPLC Chromatogram of tetramer **23**	221-222
ESI Mass Spectra of tetramer **23**	223

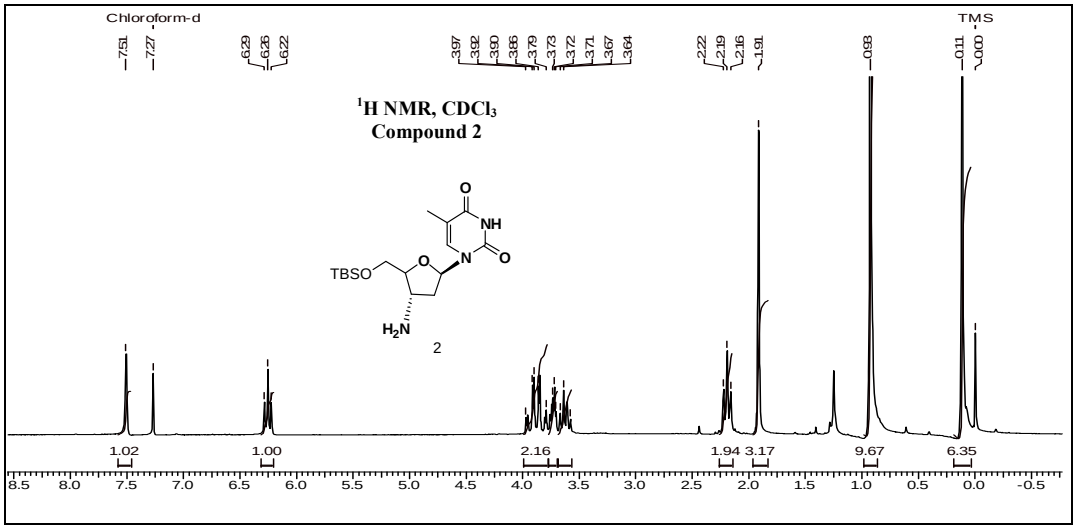
Chloroform-d
TMS
7.51
7.27
6.29
6.26
6.22
3.97
3.92
3.90
3.86
3.79
3.73
3.72
3.71
3.67
3.64
2.22
2.19
2.16
1.91
0.93
0.11
0.00
^{1}H NMR, CDCl$_3$
Compound 2
O
NH
N
O
O
TBSO
H_2N
2
1.02
1.00
2.16
1.94
3.17
9.67
6.35
8.5 8.0 7.5 7.0 6.5 6.0 5.5 5.0 4.5 4.0 3.5 3.0 2.5 2.0 1.5 1.0 0.5 0.0 -0.5

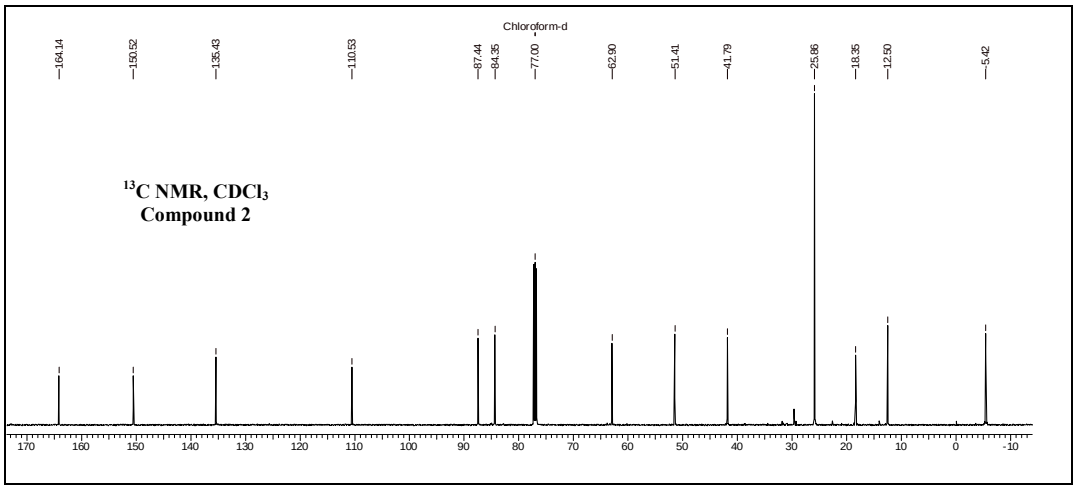
Chloroform-d
164.14
150.52
135.43
110.53
87.44
84.35
77.00
62.90
51.41
41.79
25.86
18.35
12.50
5.42
^{13}C NMR, CDCl$_3$
Compound 2
170 160 150 140 130 120 110 100 90 80 70 60 50 40 30 20 10 0 -10

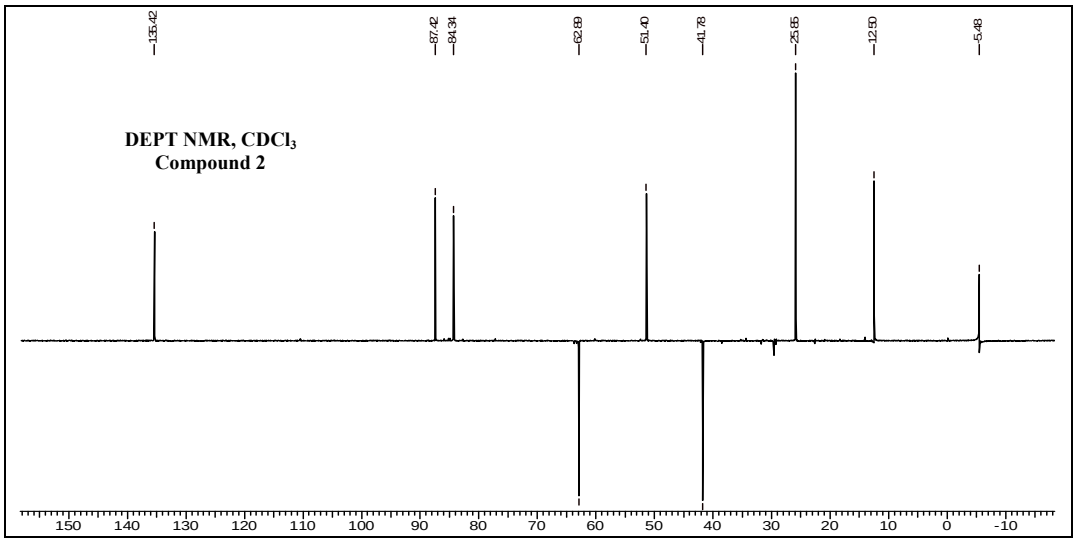
135.42
87.42
84.34
62.89
51.40
41.78
25.85
12.50
5.48
DEPT NMR, CDCl$_3$
Compound 2
150 140 130 120 110 100 90 80 70 60 50 40 30 20 10 0 -10

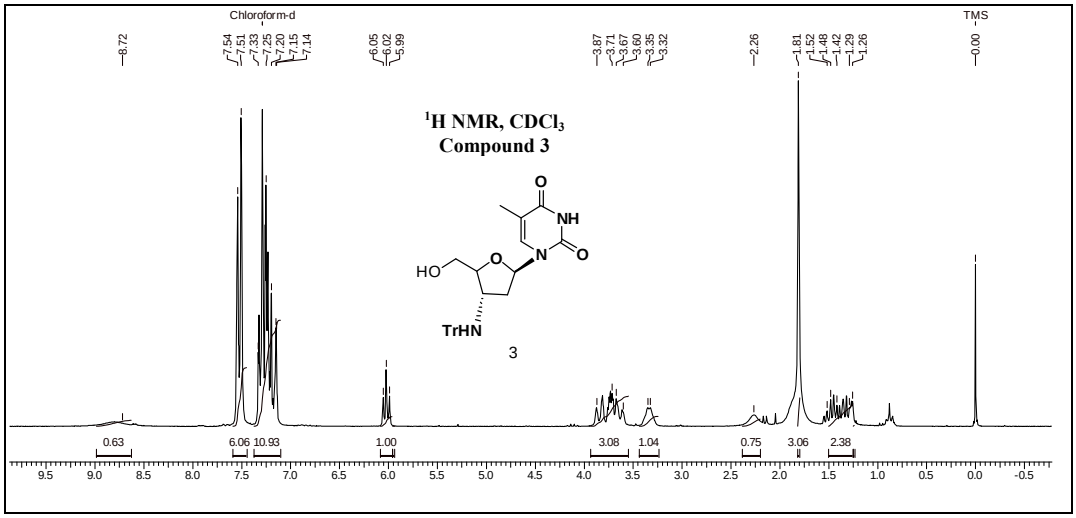
Chloroform-d
TMS
8.72
7.54
7.51
7.33
7.25
7.20
7.15
7.14
6.05
6.02
5.99
3.87
3.71
3.67
3.60
3.35
3.32
2.26
1.81
1.52
1.48
1.42
1.29
1.26
0.00
^{1}H NMR, CDCl$_3$
Compound 3
O
NH
N
O
O
HO
TrHN
3
0.63
6.06
10.93
1.00
3.08
1.04
0.75
3.06
2.38

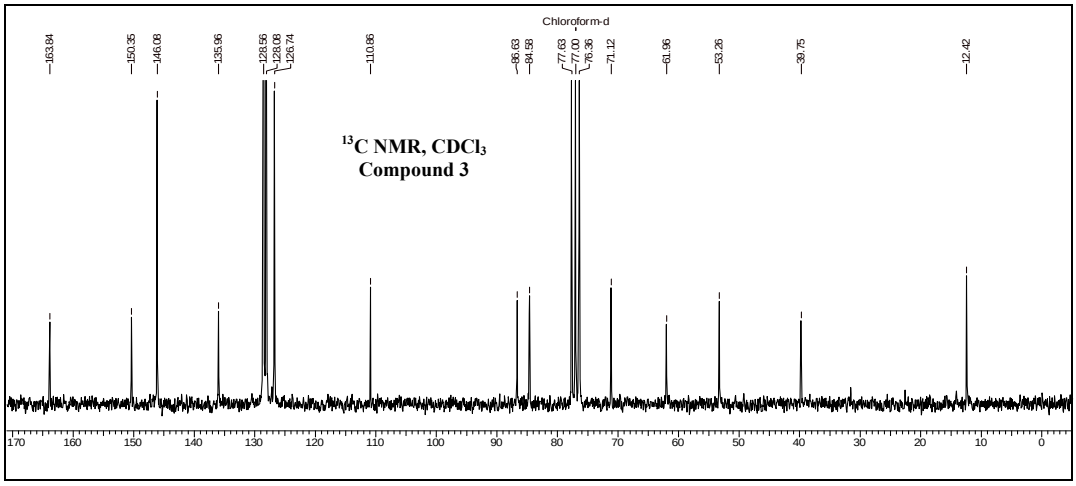
Chloroform-d
163.84
150.35
146.09
135.96
128.56
128.08
126.74
110.86
86.63
84.38
77.63
77.00
76.36
71.12
61.96
53.26
39.75
12.42
^{13}C NMR, CDCl$_3$
Compound 3

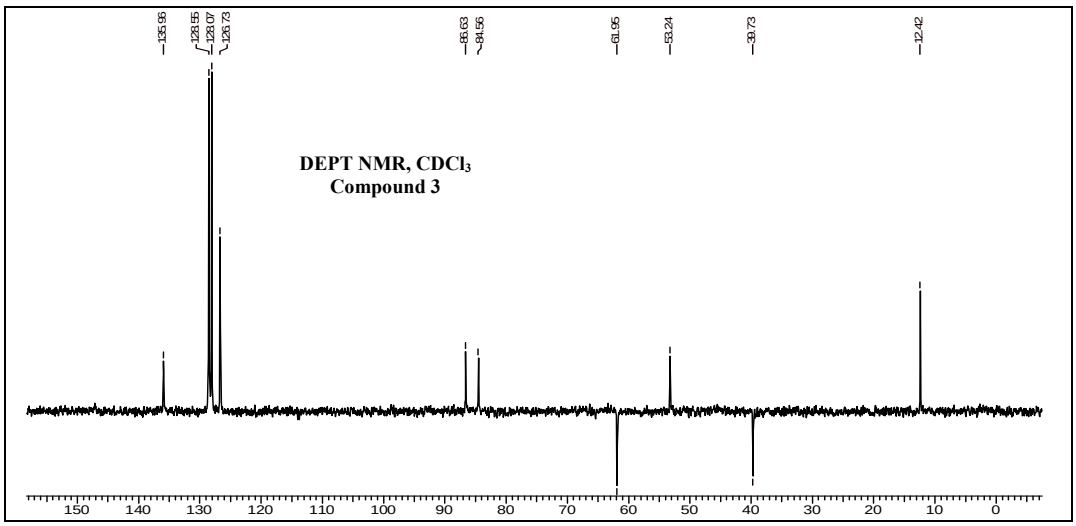
135.96
128.55
128.07
126.73
86.63
84.56
61.95
53.24
39.73
12.42
DEPT NMR, CDCl$_3$
Compound 3

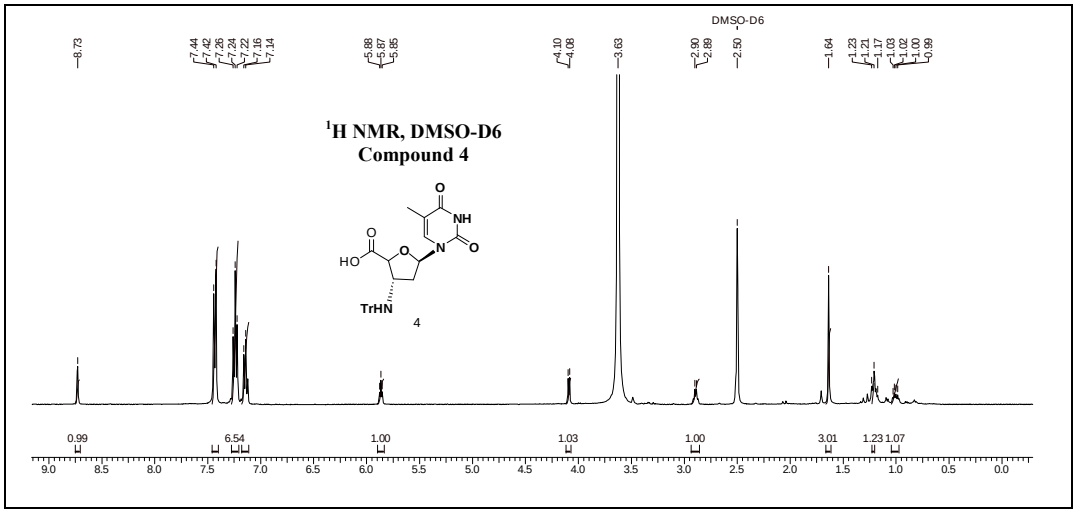
DMSO-D6
8.73
7.44
7.42
7.26
7.24
7.22
7.16
7.14
5.88
5.87
5.85
4.10
4.08
3.63
2.90
2.89
2.50
1.64
1.23
1.21
1.17
1.03
1.02
1.00
0.99
^{1}H NMR, DMSO-D6
Compound 4
O
NH
O
HO
O
N
O
TrHN
4
0.99
6.54
1.00
1.03
1.00
3.01
1.23
1.07
9.0
8.5
8.0
7.5
7.0
6.5
6.0
5.5
5.0
4.5
4.0
3.5
3.0
2.5
2.0
1.5
1.0
0.5
0.0

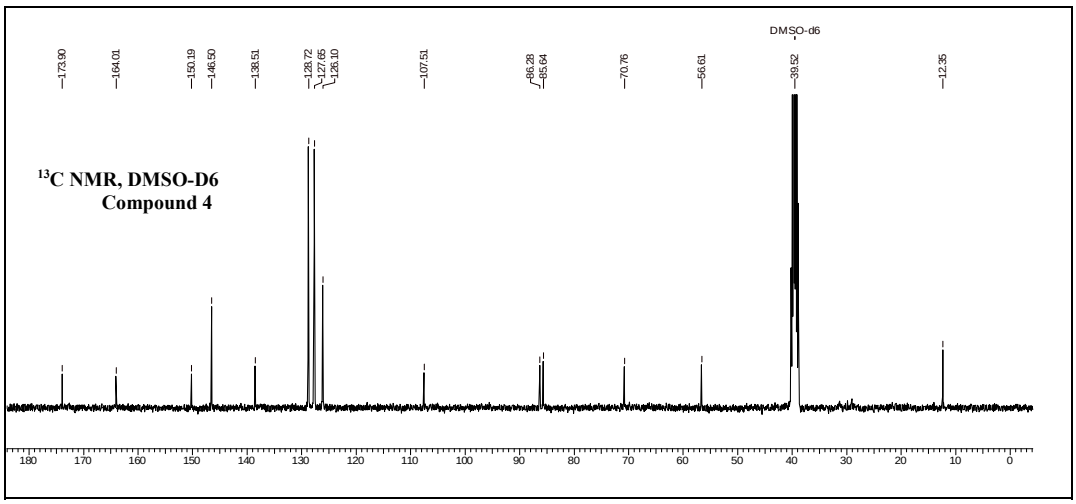
DMSO-d6
173.90
164.01
150.19
146.50
138.51
128.72
127.65
126.10
107.51
86.28
85.64
70.76
56.61
39.52
12.35
^{13}C NMR, DMSO-D6
Compound 4
180
170
160
150
140
130
120
110
100
90
80
70
60
50
40
30
20
10
0

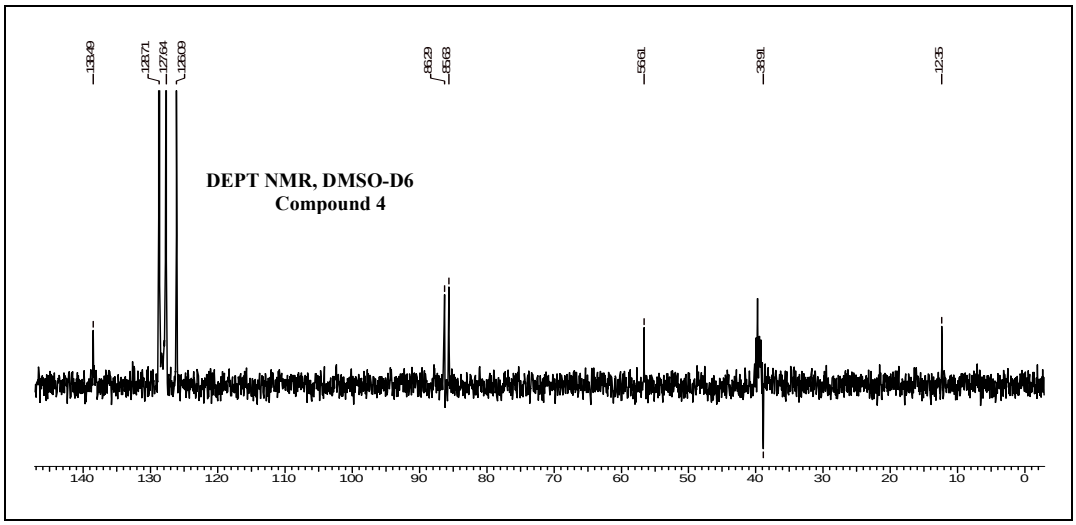
138.49
128.71
127.64
126.09
86.29
85.63
56.61
39.91
12.35
DEPT NMR, DMSO-D6
Compound 4
140
130
120
110
100
90
80
70
60
50
40
30
20
10
0

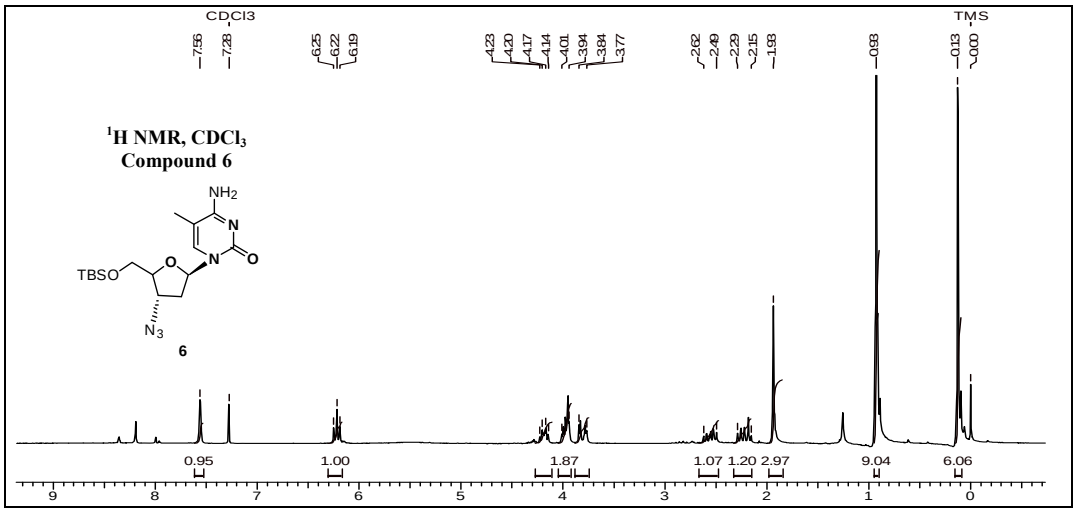
CDCl3
TMS
7.56
7.28
6.25
6.22
6.19
4.23
4.20
4.17
4.14
4.01
3.94
3.84
3.77
2.62
2.49
2.23
2.15
1.98
0.93
0.13
0.00
^{1}H NMR, CDCl$_3$
Compound 6
NH$_2$
N
O
N
O
TBSO
N$_3$
6
0.95
1.00
1.87
1.07
1.20
2.97
9.04
6.06

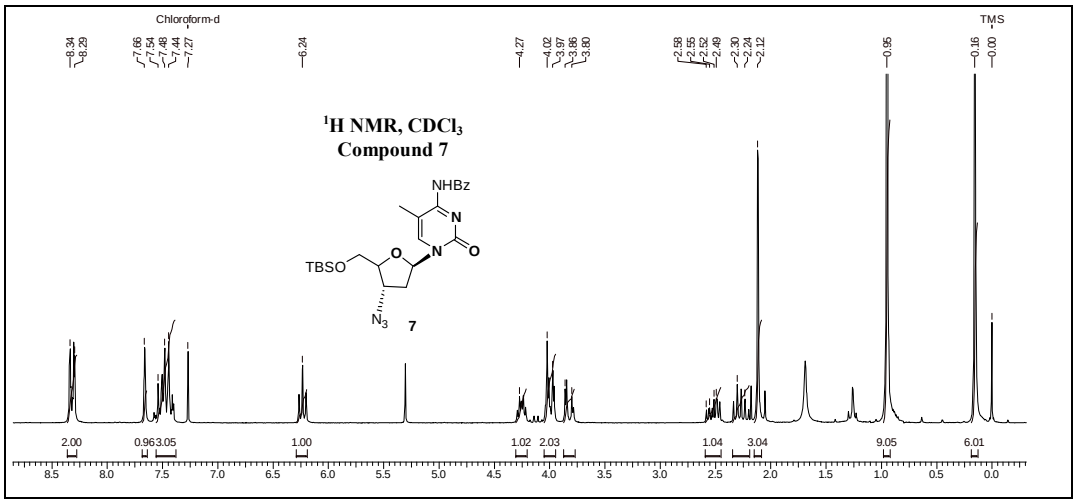
Chloroform-d
TMS
8.34
8.29
7.66
7.54
7.48
7.44
7.27
6.24
4.27
4.02
3.97
3.86
3.80
2.59
2.55
2.52
2.49
2.30
2.24
2.12
0.95
0.16
0.00
^{1}H NMR, CDCl$_3$
Compound 7
NHBz
N
O
N
O
TBSO
N$_3$
7
2.00
0.96
3.05
1.00
1.02
2.03
1.04
3.04
9.05
6.01

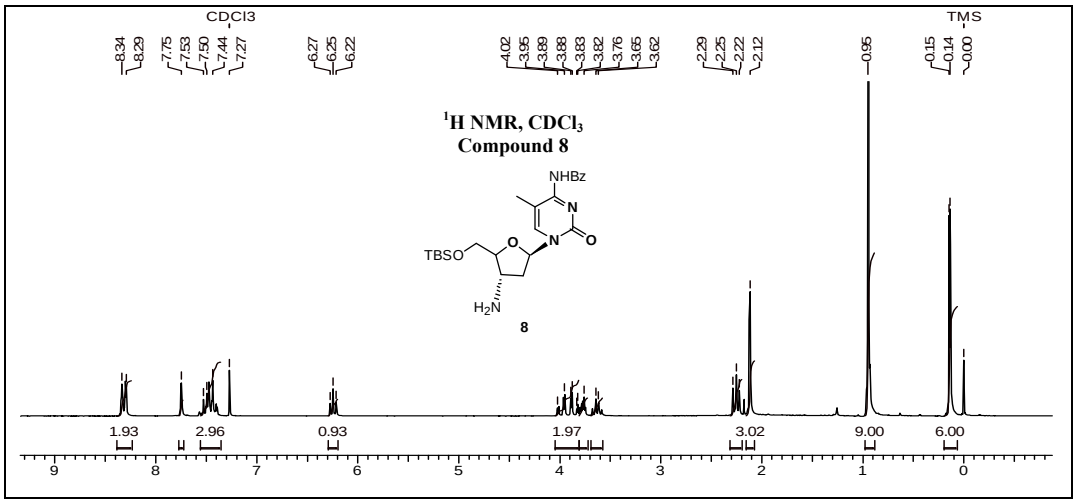
CDCl3
TMS
8.34
8.29
7.75
7.53
7.50
7.44
7.27
6.27
6.25
6.22
4.02
3.95
3.89
3.88
3.83
3.82
3.76
3.65
3.62
2.29
2.25
2.22
2.12
0.95
0.15
0.14
0.00
^{1}H NMR, CDCl$_3$
Compound 8
NHBz
N
O
N
O
TBSO
H$_2$N
8
1.93
2.96
0.93
1.97
3.02
9.00
6.00

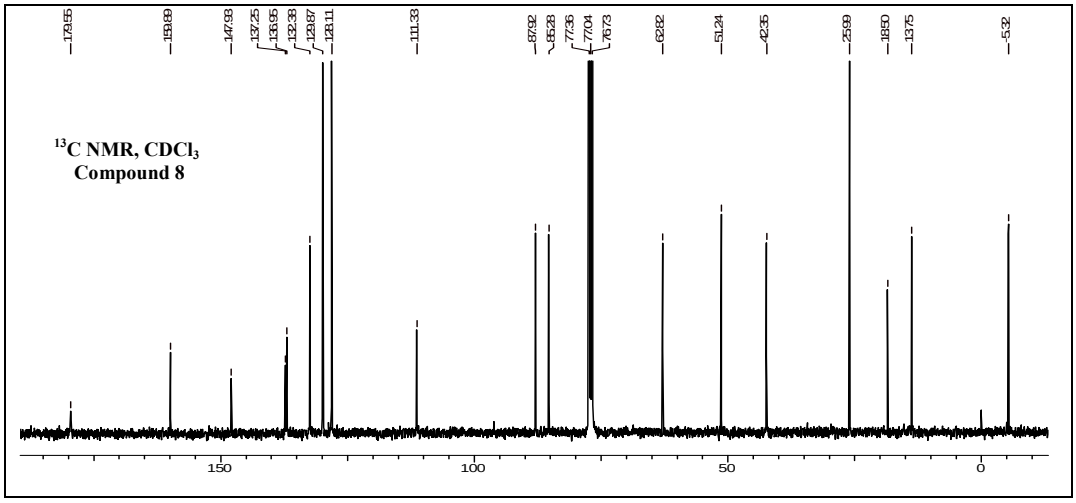
^{13}C NMR, CDCl$_3$
Compound 8

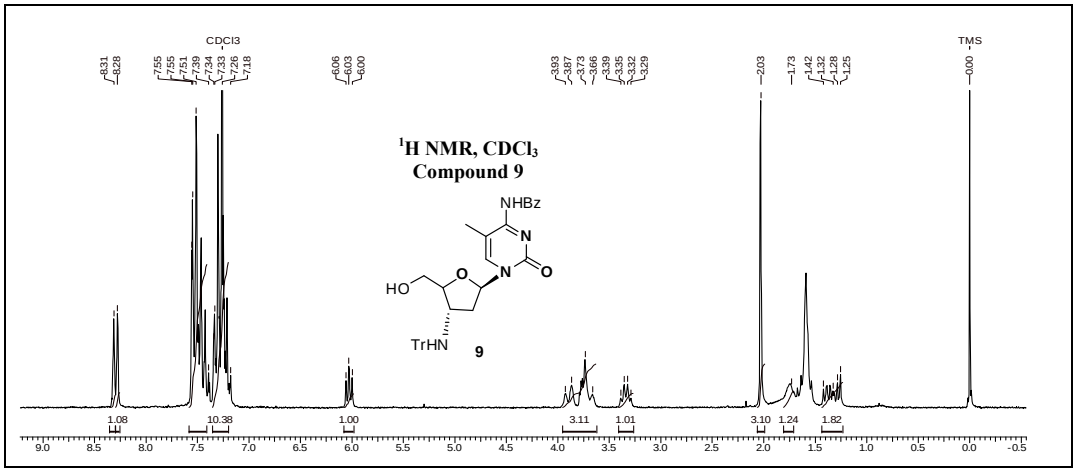
^{1}H NMR, CDCl$_3$
Compound 9
NHBz
HO
TrHN
9
CDCl3
TMS

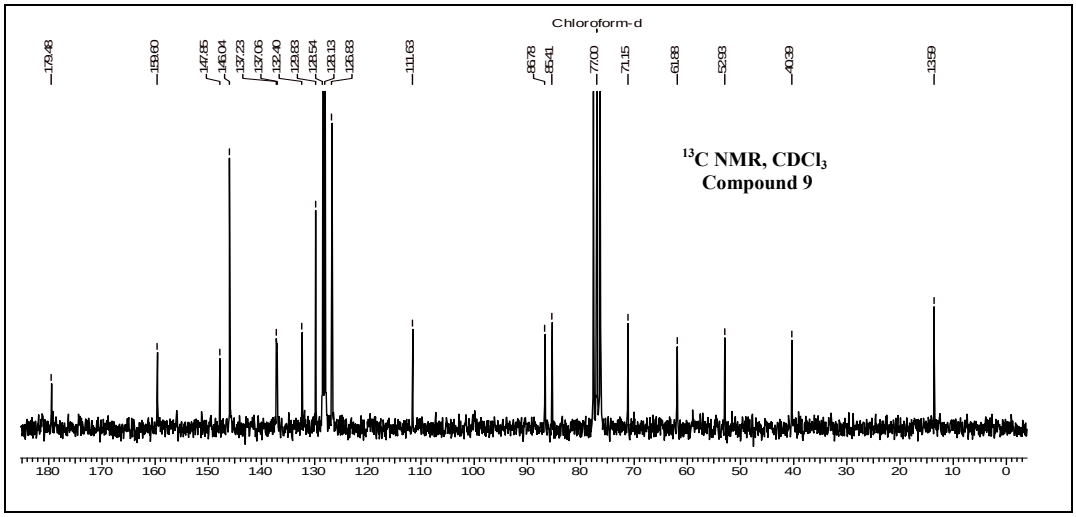
^{13}C NMR, CDCl$_3$
Compound 9
Chloroform-d

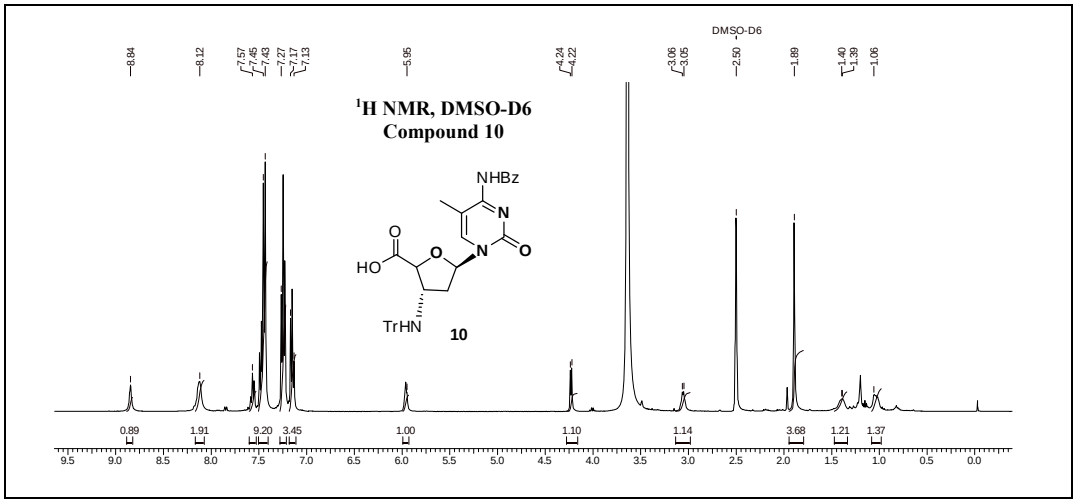
DMSO-D6
8.84
8.12
7.57
7.45
7.43
7.27
7.17
7.13
5.95
4.24
4.22
3.06
3.05
2.50
1.89
1.40
1.39
1.06
[1]H NMR, DMSO-D6
Compound 10
NHBz
N
O
HO
O
N
O
TrHN
10
0.89
1.91
9.20
3.45
1.00
1.10
1.14
3.68
1.21
1.37

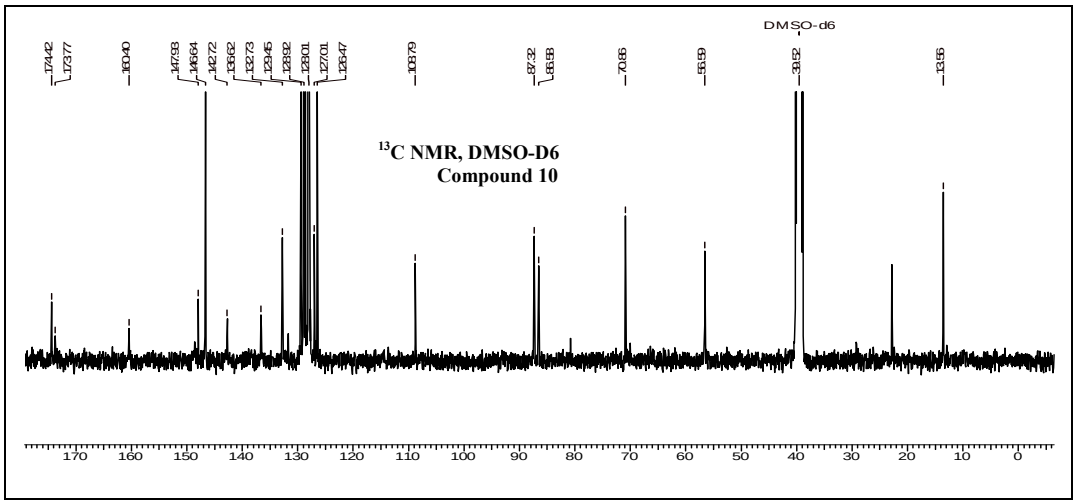
DMSO-d6
174.42
173.77
160.40
147.93
146.64
142.72
136.62
132.73
129.45
128.92
128.01
127.01
126.47
109.79
87.32
86.58
70.86
56.59
39.32
13.56
[13]C NMR, DMSO-D6
Compound 10

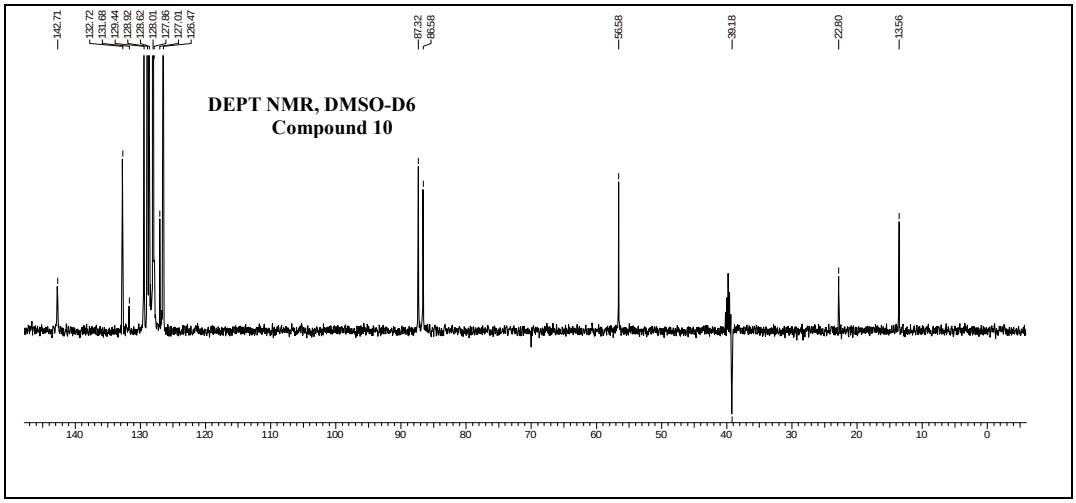
142.71
132.72
131.68
129.44
128.92
128.62
128.01
127.86
127.01
126.47
87.32
86.58
56.59
39.18
22.80
13.56
DEPT NMR, DMSO-D6
Compound 10

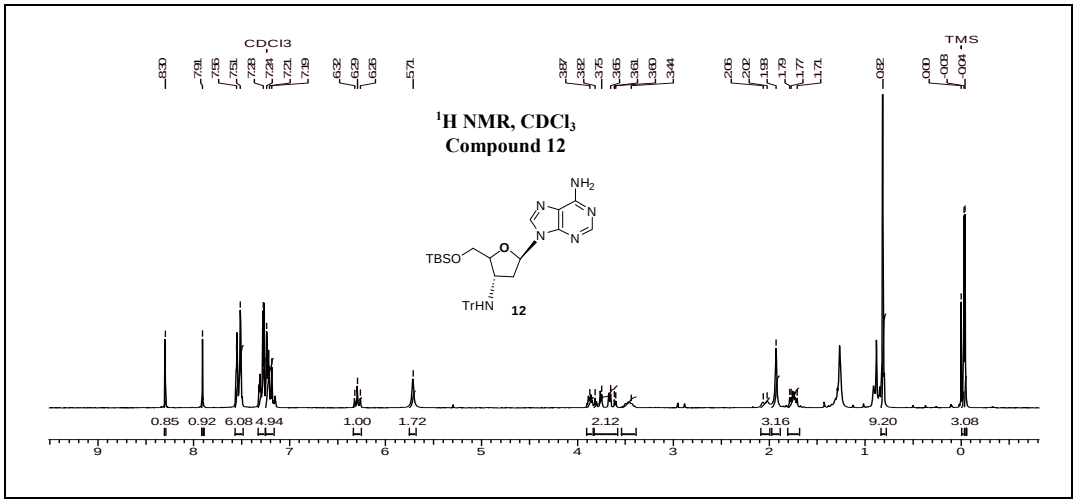
CDCl3
TMS
^{1}H NMR, CDCl$_3$
Compound 12
NH$_2$
TBSO
TrHN
12
0.85 0.92 6.08 4.94 1.00 1.72 2.12 3.16 9.20 3.08

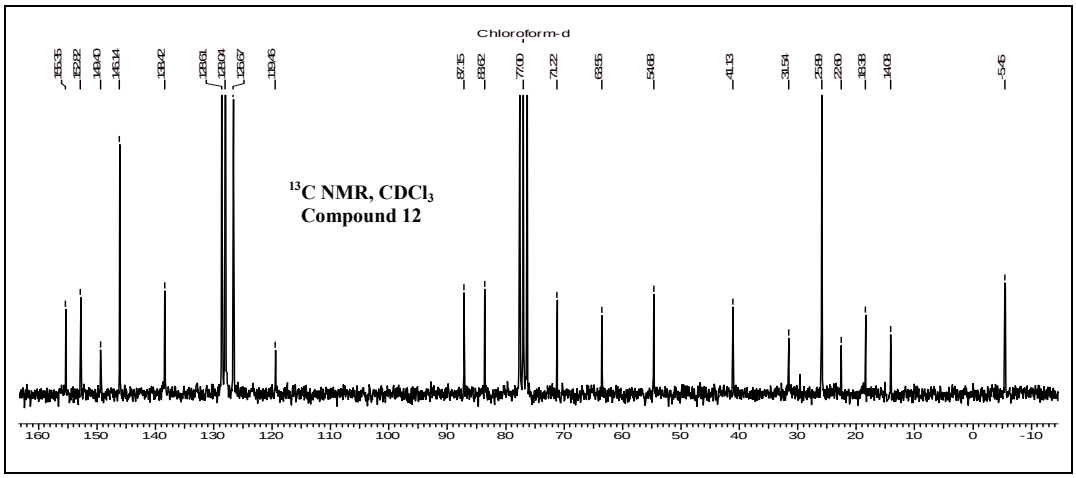
Chloroform-d
^{13}C NMR, CDCl$_3$
Compound 12

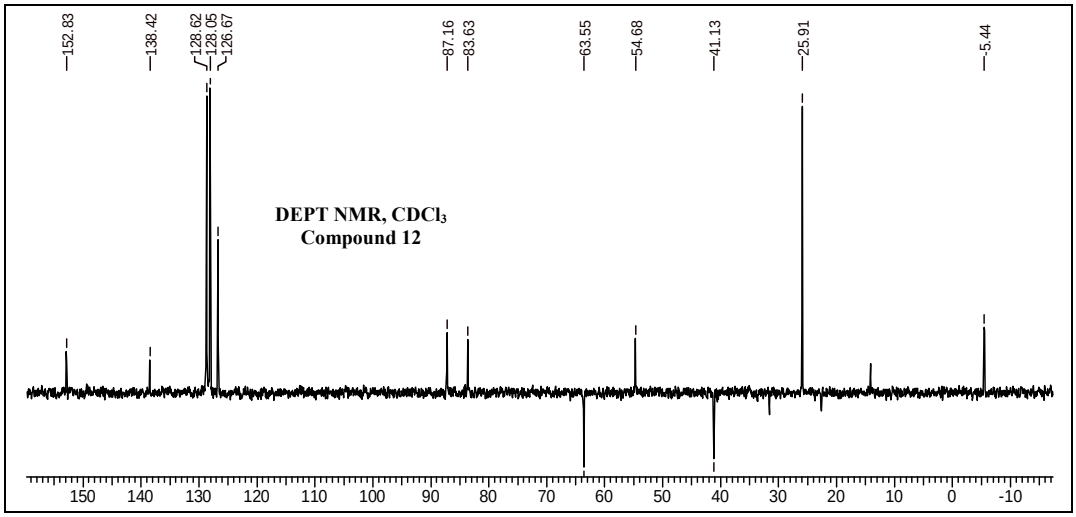
152.83
138.42
128.62
128.05
126.67
87.16
83.63
63.55
54.68
41.13
25.91
-5.44
DEPT NMR, CDCl$_3$
Compound 12

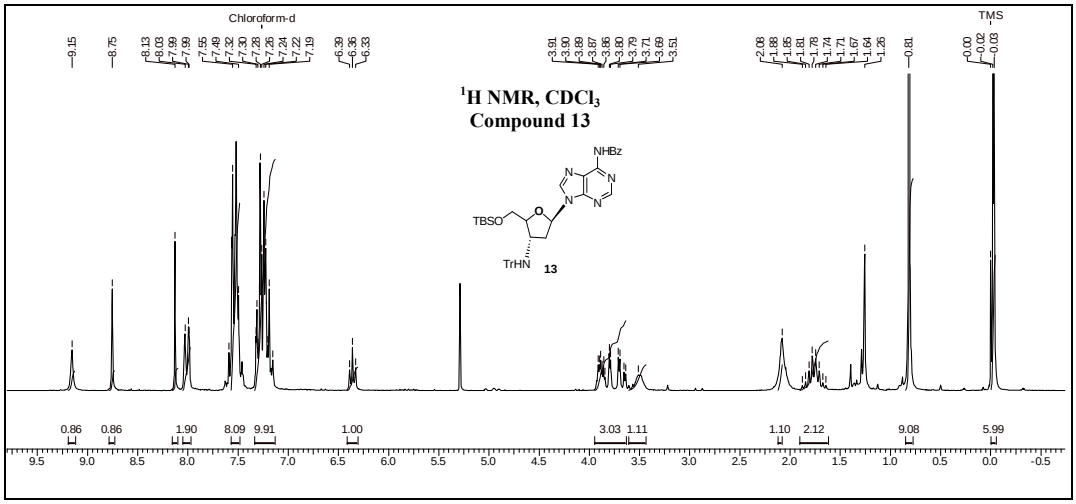
Chloroform-d
TMS
^{1}H NMR, CDCl$_3$
Compound 13
NHBz
TBSO
TrHN
13

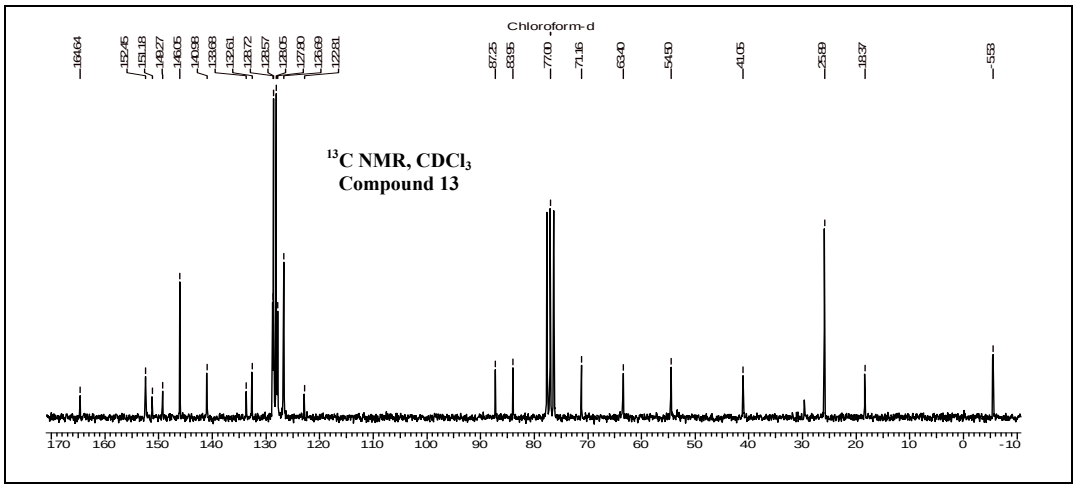
Chloroform-d
^{13}C NMR, CDCl$_3$
Compound 13

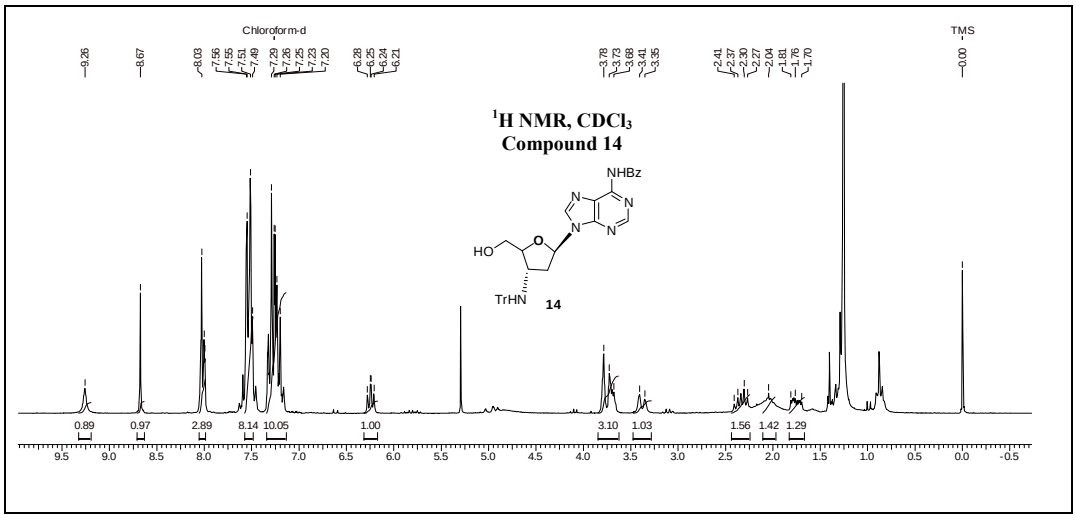
Chloroform-d
TMS
^{1}H NMR, CDCl$_3$
Compound 14
NHBz
HO
TrHN
14

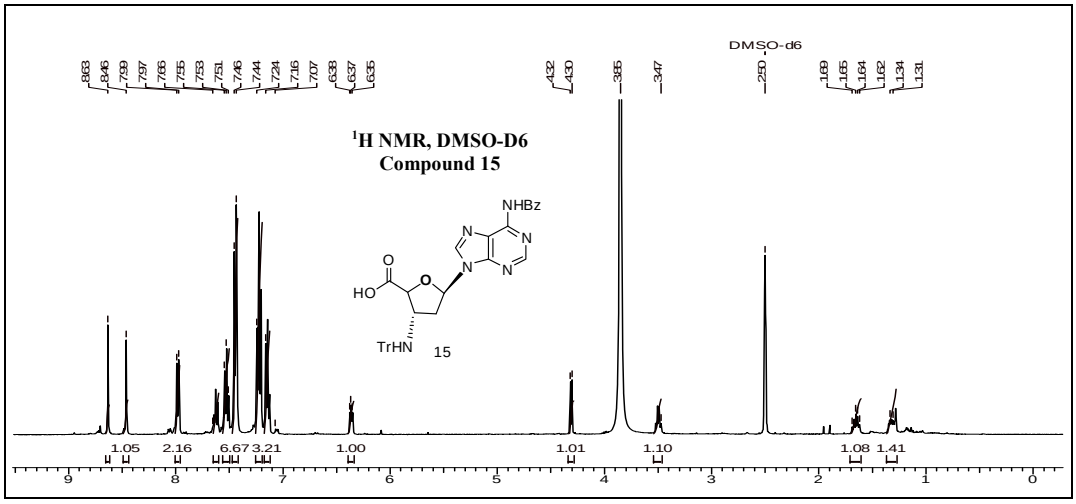
DMSO-d6
8.63
8.46
7.99
7.97
7.66
7.55
7.53
7.51
7.46
7.44
7.24
7.16
7.07
6.38
6.37
6.35
4.32
4.30
3.95
3.47
2.50
1.69
1.65
1.64
1.62
1.34
1.31
1H NMR, DMSO-D6
Compound 15
NHBz
HO
TrHN
15
1.05
2.16
6.67
3.21
1.00
1.01
1.10
1.08
1.41

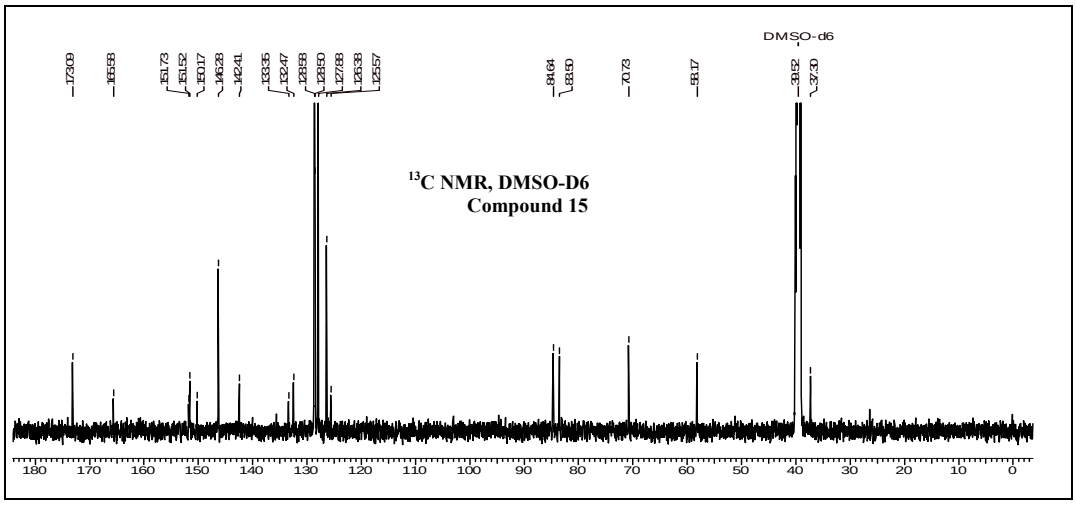
DMSO-d6
173.09
166.58
151.73
151.52
150.17
146.28
142.41
133.35
132.47
128.93
128.80
127.88
126.33
125.57
84.64
83.50
70.73
58.17
39.52
37.30
13C NMR, DMSO-D6
Compound 15

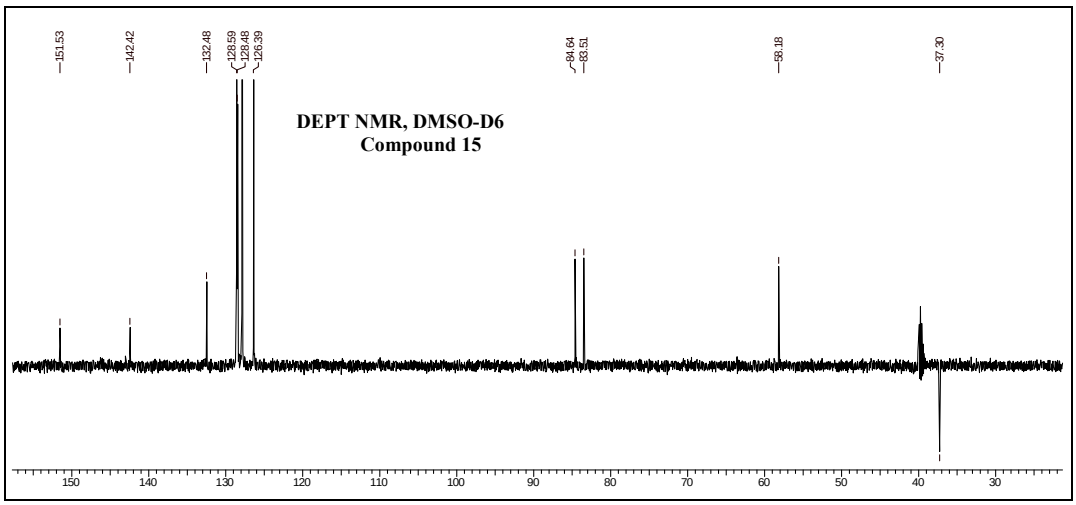
151.53
142.42
132.48
128.59
128.48
126.39
84.64
83.51
58.18
37.30
DEPT NMR, DMSO-D6
Compound 15

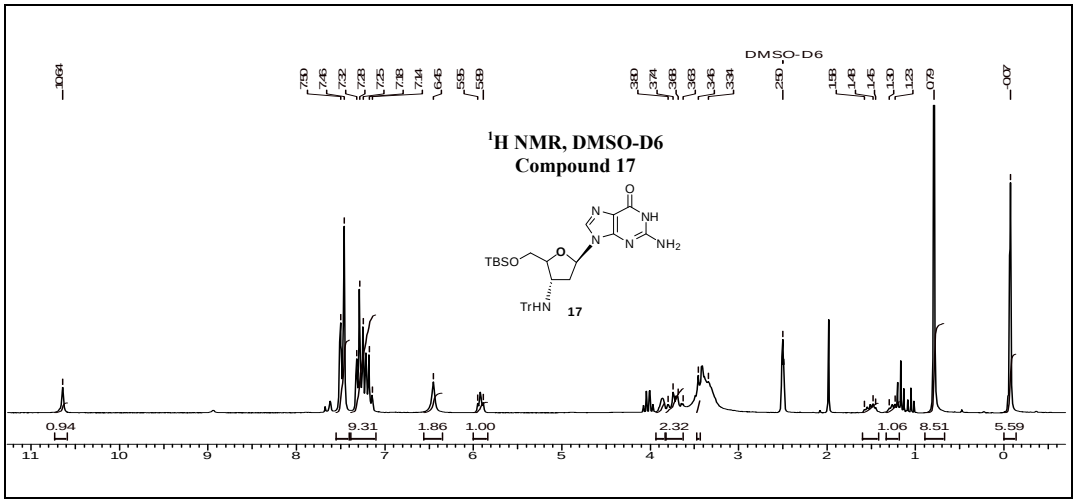
DMSO-D6
^{1}H NMR, DMSO-D6
Compound 17
TBSO
TrHN
17
0.94
9.31
1.86
1.00
2.32
1.06
8.51
5.59

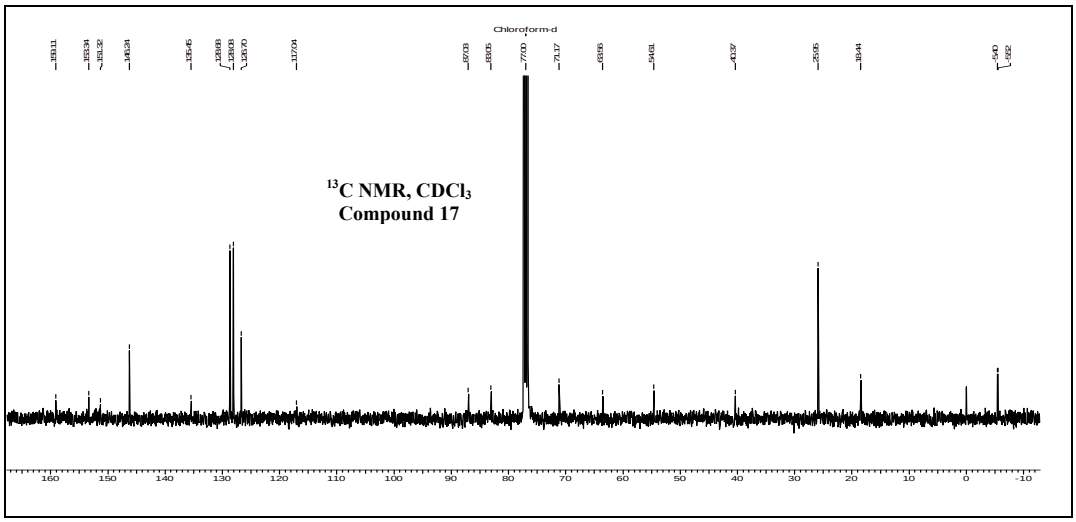
Chloroform-d
^{13}C NMR, CDCl$_3$
Compound 17

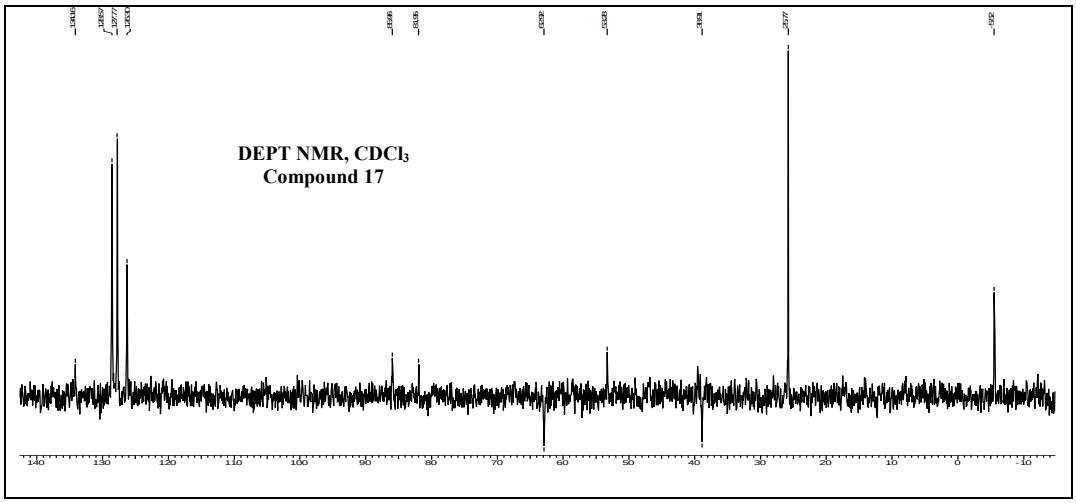
DEPT NMR, CDCl$_3$
Compound 17

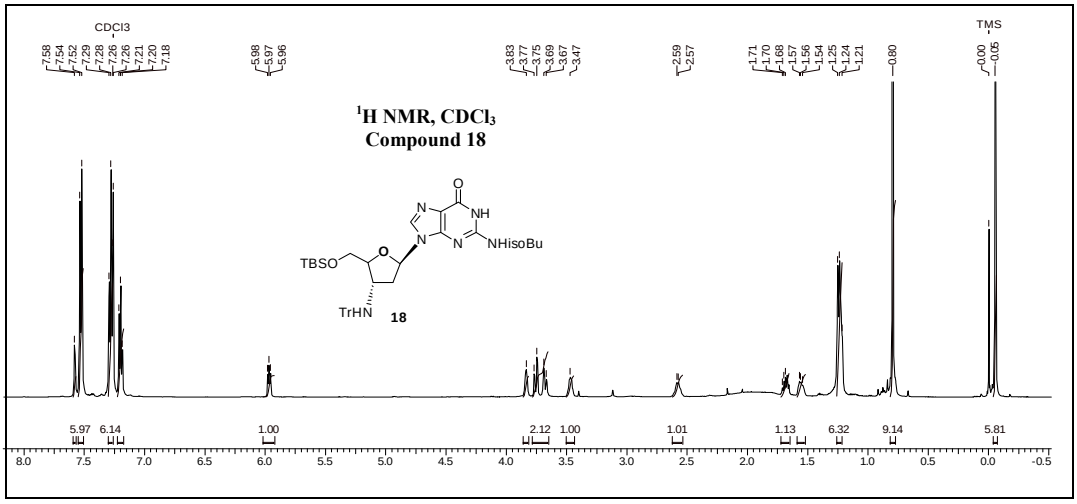
CDCl3
TMS
^{1}H NMR, CDCl$_3$
Compound 18
TBSO
TrHN
NHisoBu
18

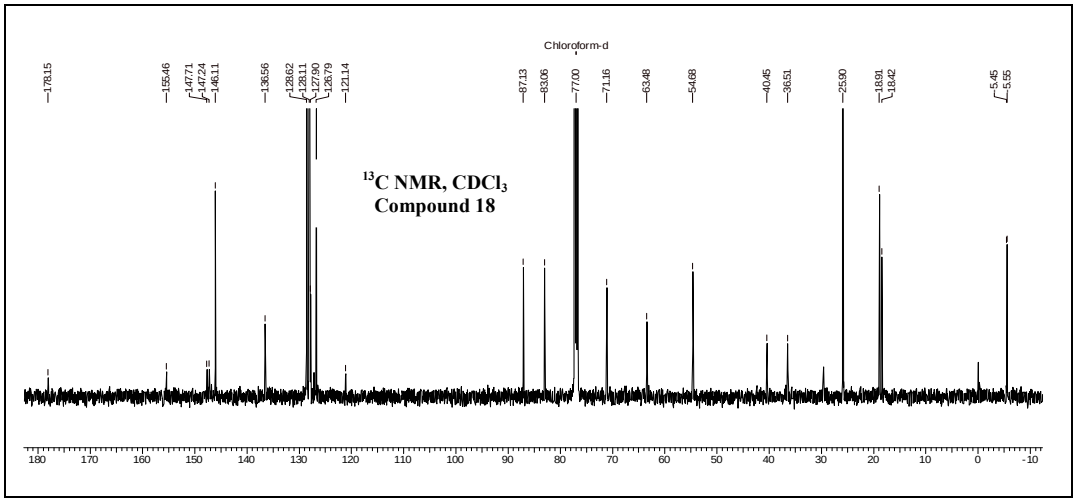
Chloroform-d
^{13}C NMR, CDCl$_3$
Compound 18

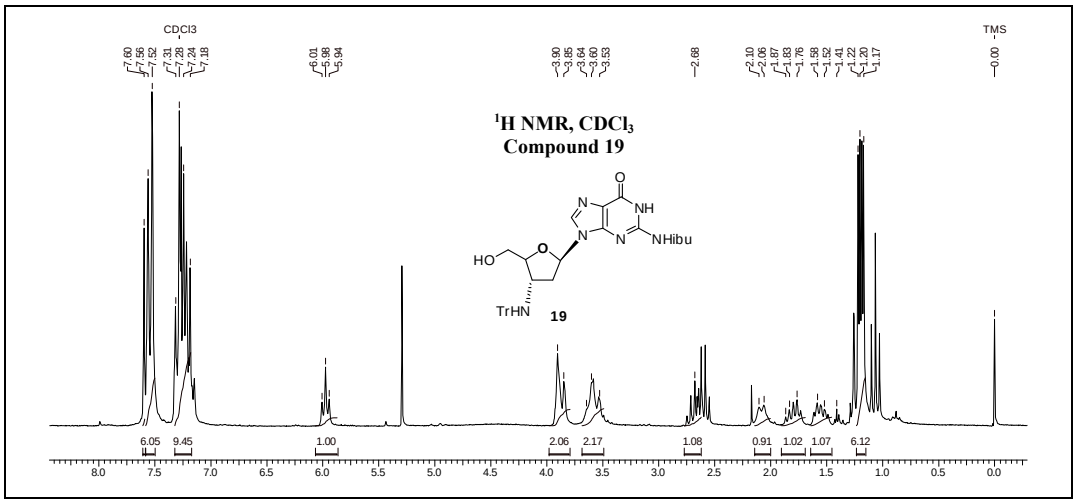
CDCl3
TMS
^{1}H NMR, CDCl$_3$
Compound 19
HO
TrHN
NHibu
19

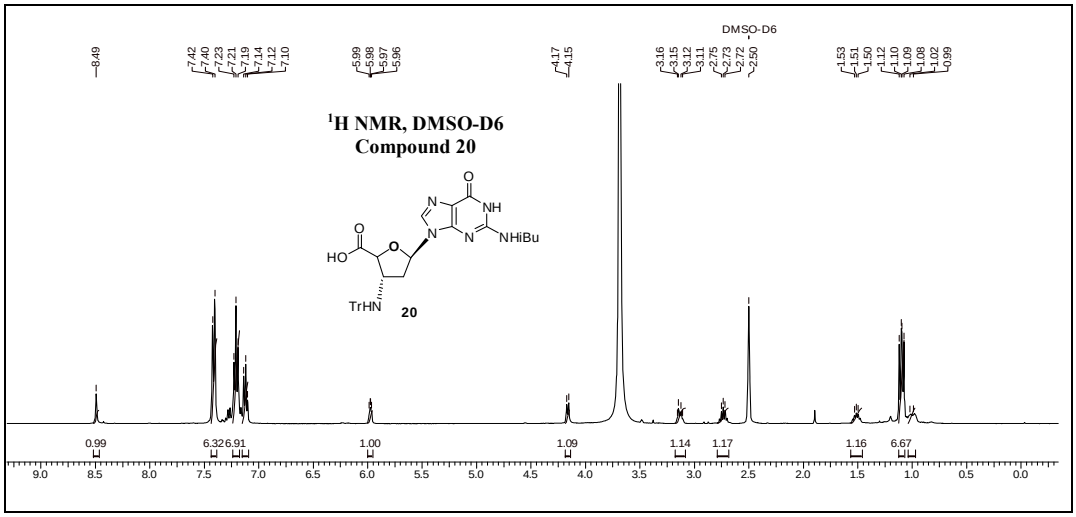

^{1}H NMR, DMSO-D6
Compound 20

20

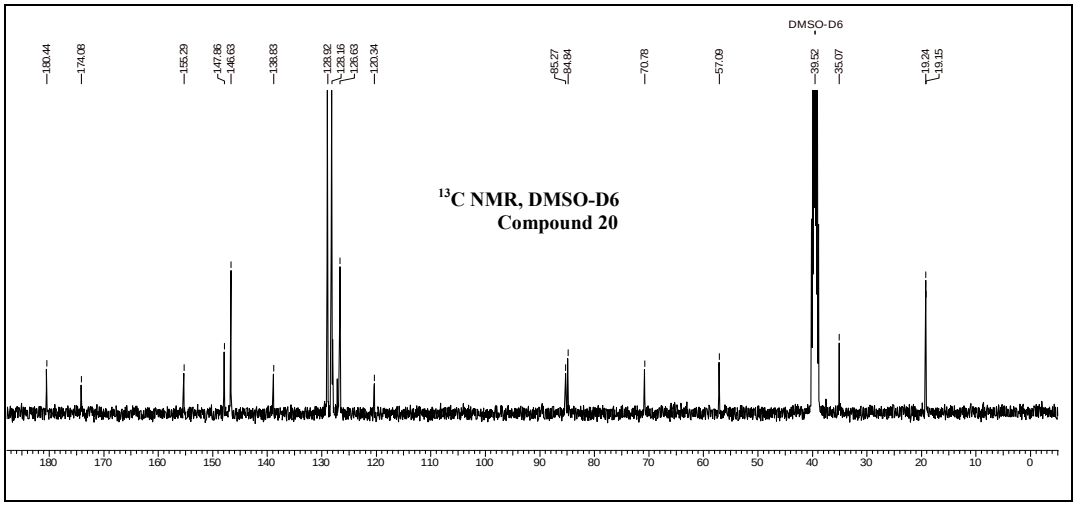

^{13}C NMR, DMSO-D6
Compound 20

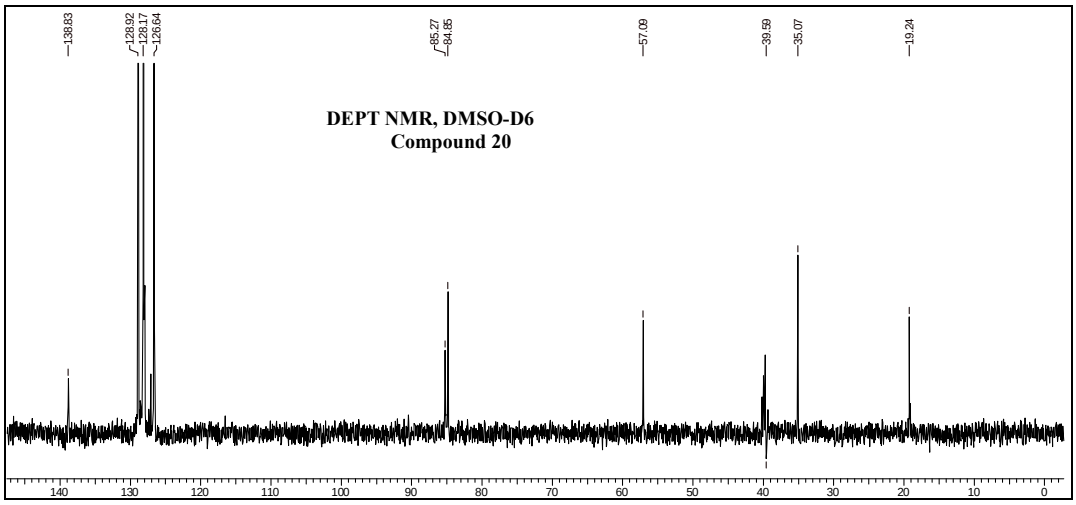

DEPT NMR, DMSO-D6
Compound 20

HRMS spectra's

Elemental Composition Report Page 1

Single Mass Analysis (displaying only valid results)
Tolerance = 10.0 PPM / DBE: min = -1.5, max = 100.0
Isotope cluster parameters: Separation = 1.0 Abundance = 1.0%

Monoisotopic Mass, Odd and Even Electron Ions
39 formula(e) evaluated with 1 results within limits (up to 50 closest results for each mass)

Compound 4
Exp mass: 520.1848
Obs mass: 520.1846

Micromass : Q-Tof micro (YA-105) Dept. Of Chemistry I.I.T.(B) 20-Jan-201211:24:53
C29H27N3O5
NCL-VAK-T-ACID 65 (0.647) AM (Med,5, Ht,5000.0,556.28,1.00); Sm (SG, 2x4.00); Cm (1:81) TOF MS ES+
1.77e4

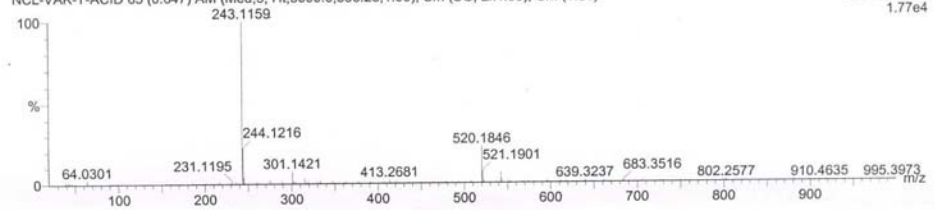

Minimum:				-1.5		
Maximum:		200.0	10.0	100.0		
Mass	Calc. Mass	mDa	PPM	DBE	Score	Formula
520.1846	520.1848	-0.3	-0.5	17.5	1	C29 H27 N3 O5 Na

Elemental Composition Report Page 1

Single Mass Analysis (displaying only valid results)
Tolerance = 10.0 PPM / DBE: min = -1.5, max = 100.0
Isotope cluster parameters: Separation = 1.0 Abundance = 1.0%

Monoisotopic Mass, Odd and Even Electron Ions
21 formula(e) evaluated with 1 results within limits (up to 50 closest results for each mass)

Compound 10
Exp mass: 601.2451
Obs mass: 601.2452

Micromass : Q-Tof micro (YA-105) Dept. Of Chemistry I.I.T.(B) 20-Dec-201111:21:14
C36H32N4O5
NCL-VAK-C-ACID 28 (0.277) AM (Cen,5, 80.00, Ht,5000.0,556.28,1.00); Sm (SG, 2x4.00); Sb (5,40.00); Cm (17:54) TOF MS ES+
6.93e3

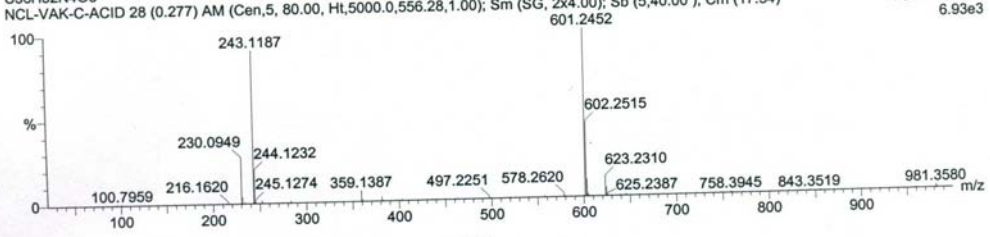

Minimum:				-1.5		
Maximum:		200.0	10.0	100.0		
Mass	Calc. Mass	mDa	PPM	DBE	Score	Formula
601.2452	601.2451	0.1	0.1	22.5	1	C36 H33 N4 O5

Elemental Composition Report Page 1

Single Mass Analysis (displaying only valid results)
Tolerance = 10.0 PPM / DBE: min = -1.5, max = 100.0
Isotope cluster parameters: Separation = 1.0 Abundance = 1.0%

Monoisotopic Mass, Odd and Even Electron Ions
26 formula(e) evaluated with 1 results within limits (up to 50 closest results for each mass)

Compound 15
Exp mass: 611.2407
Obs mass: 611.2404

Micromass : Q-Tof micro (YA-105) Dept. Of Chemistry I.I.T.(B) 20-Dec-201111:34:55
C36H30N6O4
NCL-VAK-A-ACID 65 (0.639) AM (Cen,5, 80.00, Ht,5000.0,556.28,1.00); Sm (Md, 4.00); Sb (5,40.00); Cm (43:79) TOF MS ES+
4.29e3

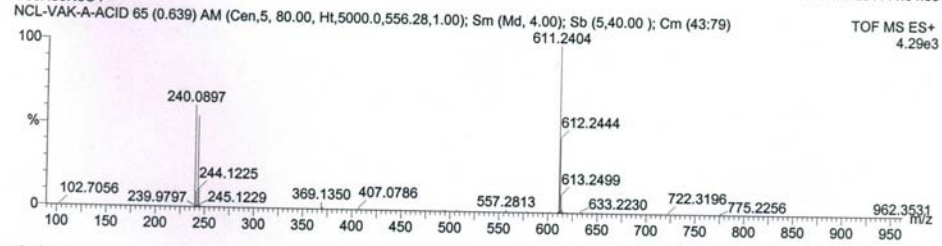

Minimum:				-1.5		
Maximum:		200.0	10.0	100.0		
Mass	Calc. Mass	mDa	PPM	DBE	Score	Formula
611.2404	611.2407	-0.3	-0.4	24.5	1	C36 H31 N6 O4

Elemental Composition Report Page 1

Single Mass Analysis (displaying only valid results)
Tolerance = 10.0 PPM / DBE: min = -1.5, max = 100.0
Isotope cluster parameters: Separation = 1.0 Abundance = 1.0%

Monoisotopic Mass, Odd and Even Electron Ions
27 formula(e) evaluated with 1 results within limits (up to 50 closest results for each mass)

Compound 20
Exp mass: 593.2510
Obs mass: 593.2510

Micromass : Q-Tof micro (YA-105) Dept. Of Chemistry I.I.T.(B) 20-Dec-201111:49:26
C33H32N6O5
NCL-VAK-G-ACID 29 (0.289) AM (Cen,5, 80.00, Ht,5000.0,556.28,1.00); Sm (Mn, 2x4.00); Sb (5,40.00); Cm (1:36) TOF MS ES+
3.51e3

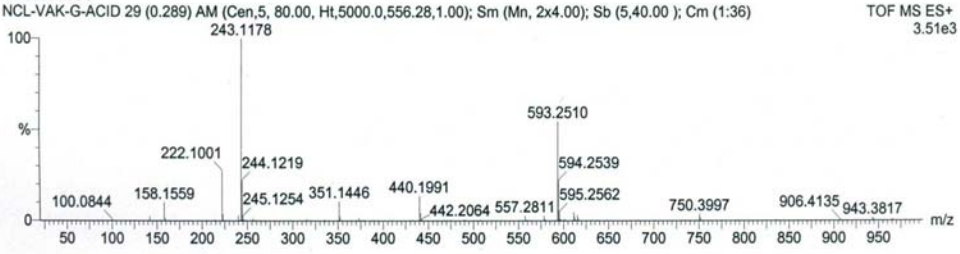

Minimum:				-1.5		
Maximum:		200.0	10.0	100.0		
Mass	Calc. Mass	mDa	PPM	DBE	Score	Formula
593.2510	593.2512	-0.2	-0.3	20.5	1	C33 H33 N6 O5

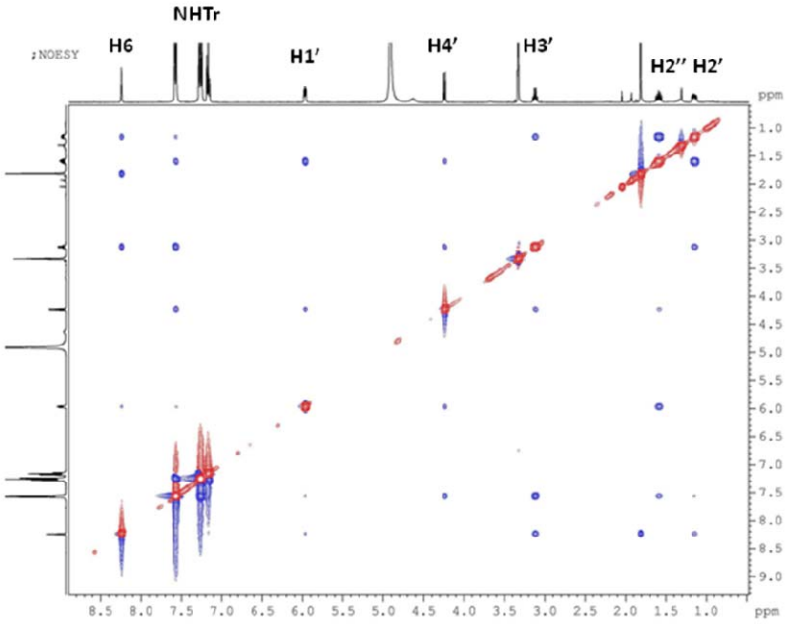

Full NOESY spectra of compound **4**

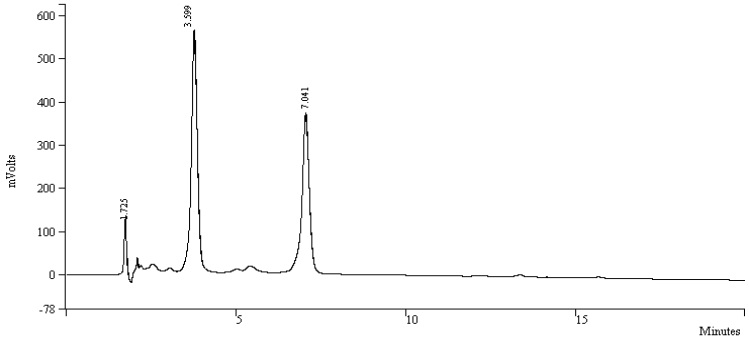

Peak No	Ret. Time (min)	Width 1/2 (sec)	Peak Area (counts)	Result ()
1	1.725	4.8	856030	6.2358
2	3.599	0.0	7108052	51.7791
3	7.041	12.7	5763575	41.9851
			13727657	**100.0000**

HPLC Chromatogram for crude tetramer **23** sample

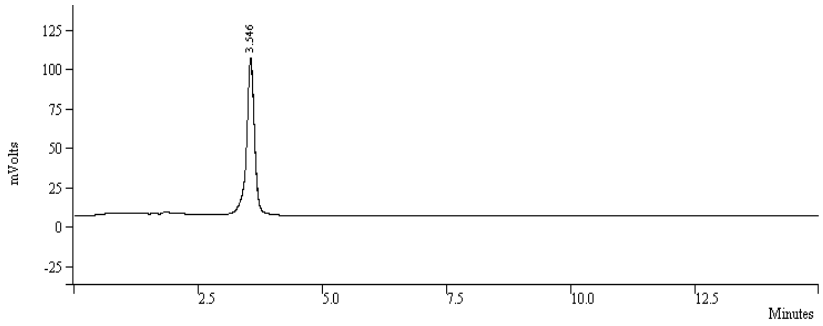

Peak No	Ret. Time (min)	Width 1/2 (sec)	Peak Area (counts)	Result ()
1	3.546	9.3	1091035	100.0000
			1091035	**100.0000**

HPLC Chromatogram for purified tetramer **23**

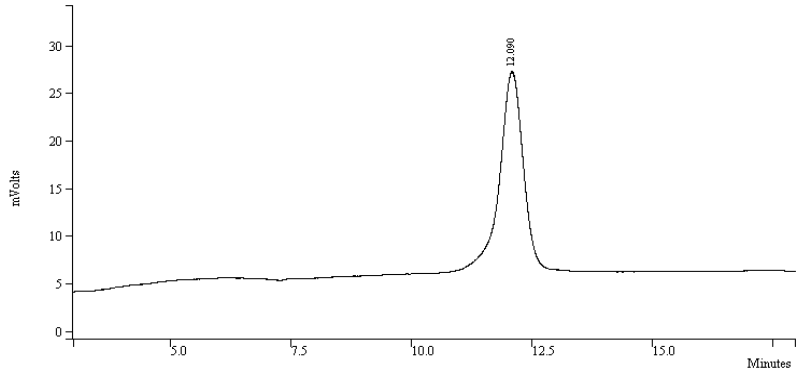

Peak No	Ret. Time (min)	Width 1/2 (sec)	Peak Area (counts)	Result ()
1	12.090	29.4	712684	100.0000
			712684	**100.0000**

HPLC Chromatogram of Tetramer **23** with a longer retention time

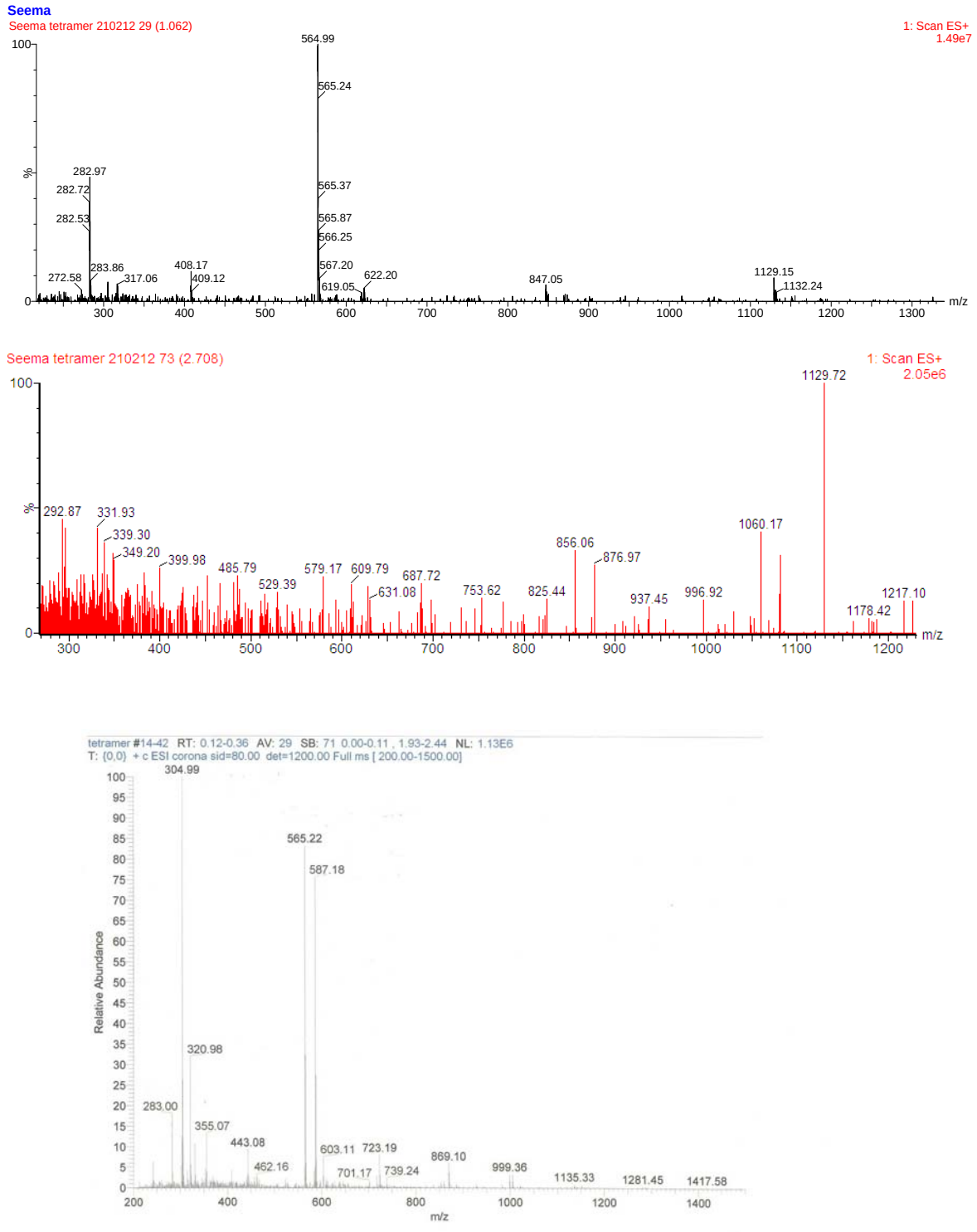

ESI mass spectra of tetramer **23**

3.9 References

1. (a) Uhlmann, E.; Peyman, A. *Chem. Rev*. **1990**, *90*, 543; (b) Freier, S. M.; Altmann, K.H. The ups and downs of nucleic acid duplex stability: structure_stability studies on chemically-modified DNA:RNA duplexes . *Nucleic Acids Res*. **1997**, 25, 4429; (c) Shukla, S.; Sumaria, C. S.; Pradeepkumar, P.I. Exploring chemical modifications for siRNA therapeutics: A structural and functional outlook *Chem. Med. Chem*, **2010**, *5*, 328; (d) Bennet, C. F.; Swayze, E. E. RNA targeting therapeutics: molecular mechanisms of antisense oligonucleotides as a therapeutic platform. *Annu. Rev. Pharmacol. Toxicol.* **2010**, *50*, 259; (e) Kole, R.; Krainer, A. R.; Altman, S. RNA therapeutics: beyond RNA interference and antisense oligonucleotides *Nature Revs. Drug Discov*. **2012,** *11,* 125**.**
2. (a) Micklefield, J. Backbone modification of nucleic acids: Synthesis, structure and therapeutic applications. *Curr. Med. Chem.* **2001**, *8*, 1157; (b) Kurreck, J. Antisense technologies. Improvement through novel chemical modifications. *Eur. J. Biochem*. **2003**, *270*, 1628; (c) Turner, J. J.; Fabani, M.; Arzumanov, A. A.; Ivanova, G.; Gait, M. J. Targeting the HIV-1 RNA leader sequence with synthetic oligonucleotides and siRNA: chemistry and cell delivery*Biochim. Biophys. Acta.* **2006**, *1758*, 290; (d) Kumar, V. A.; Ganesh, K. N. Structure-Editing of Nucleic Acids for Selective Targeting of RNA. *Curr. Top. Med. Chem*. **2007**, *7*, 715; (e) Prakash, T. P. *Chem.* An Overview of Sugar-Modified Oligonucleotides for Antisense Therapeutics. *Biodiversity*, **2011**, *8*, 1616. (f) Kumar, V. A. Structural pre-organization of peptide nucleic acids: chiral cationic analogues with five- or six- membered ring structures . *Eur. J. Org. Chem*. **2002**, 2021.
3. (a) Dominski, Z.; Kole, R.; Restoration of correct splicing in thalassemic pre-mRNA by antisense oligonucleotides. *Proc. Natl. Acad. Sci*. U. S. A., **1993**, *90*, 8673; (b) Sazani P.; Kole, R. Therapeutic potential of antisense oligonucleotides as modulators of alternative splicing. *J. Clin. Invest*. **2003**, *112*, 481.
4. (a) Tanui, P.; Kullberg, M.; Song, N.; Chivate, Y.; Rozners, E. Monomers for preparation of amide linked RNA: Synthesis of C3'-homologated nucleoside amino acids from d-xylose. *Tetrahedron.* **2010**, *66*, 4961; (b) Rozners, E.;

Katkevica, D.; Bizdena E.; Stromberg, R. Synthesis and Properties of RNA Analogs Having Amides as Interuridine Linkages at Selected Positions*J. Am. Chem. Soc*. **2003**, *125*, 12125; (c) Rozners E.; Liu, Y. Monomers for preparation of amide linked RNA: Asymmetric synthesis of all four nucleoside 5'-azido 3'-carboxylic acids. *J. Org. Chem*. **2005**, *70*, 9841; (d) Xu, Q.; Katkevica,D.; Rozners, E. Toward Amide Modified RNA: Synthesis of 3'-Aminomethyl-5'-Carboxy-3',5'-Dideoxy Nucleosides. *J. Org. Chem*. **2006**, *71*, 5906–5913.

5. De Mesmaeker, A.; Lesueur, C.; Btvikrre, M.O.; Waldner, A.; Fritsch, V.; Wolf, R. M. Amide Backbones with Conformationally Restricted Furanose Rings: Highly Improved Affinity of the Modified Oligonucleotides for Their RNA Complements. *Angew. Chem., Int. Ed. Engl.* **1996**, *35*, 2790.
6. Pallan, P. S.; von Matt P.; Wilds, C. J.; Altmann, K.-H.; Egli, M. RNA binding affinities and crystal structure of oligonucleotides containing five-atom amide-based backbone structures. *Biochemistry*, **2006**, *45*, 8048; (b) Wilds, C. J.; Minasov, G.; von Matt, P.; Altmann K.-H.; Egli, M. Studies of a chemically modified oligodeoxynucleotide containing a 5-atom amide backbone which exhibits improved binding to RNA. *Nucleosides, Nucleotides, Nucleic Acids.* **2001**, *20*, 991.
7. (a) Gogoi, K.; Gunjal, A. D.; Phalgune, U. D.; Kumar V. A. Synthesis and RNA binding selectivity of oligonucleotides modified with five atom thioacetamido Nucleic Acid backone structures .*Org. Lett*. **2007**, *9*, 2697; (b) Chakraborty, T.K.; Koley, D.; Prabhakar, S.; Ravi R.; Kunwar, A. C. Synthesis and conformational studies of amide-linked cyclic homooligomers of a thymidine-based nucleoside amino acid. *Tetrahedron.* **2005**, *40*, 9506
8. (a) Nielsen, P. E.; Egholm, M.; Berg R. H.; Buchardt,O. Sequence-selective recognition of DNA by strand displacement with a thymine-substituted polyamide *Science*. **1991**, *254*, 1497; (b) Nielsen, P. E.; Egholm M.; Buchardt, O. Peptide nucleic acid (PNA): A DNA mimic with a peptide backbone. *Bioconjugate Chem*. **1994**, *5*, 3; (c) Egholm, M.; Buchardt, O.; Nielsen P. E.; Berg, R. H. Peptide nucleic acids (PNA). Oligonucleotide analogs with an achiral peptide backbone *J. Am. Chem. Soc*. **1992**, *114*, 1895; (d) Uhlmann, E.; Peyman, A.; Breipohl G.; Will, D. W. *Angew. Chem., Int. Ed.* **1998,** *37*, 2796; (e) Kumar, V. A.; Ganesh, K. N. Conformationally constrained PNA analogues:

Structural evolution toward DNA/RNA binding selectivity. *Acc. Chem. Res*. **2005**, *38*, 404; (f) Yeh, J. I.; Shivachev, B.; Rapireddy, S.; Crawford, M. J.; Gil, R. R.; Du, S.; Marcela, M. and Ly D. H. Crystal Structure of Chiral γPNA with Complementary DNA Strand: Insights into the Stability and Specificity of Recognition and Conformational Preorganization. *J. Am. Chem. Soc*. **2010**, 132, 10717; (g) Corradini, R.; Sforza, S.; Tedeschi, T.; Totsingan, F.; Manicardi, A.; Marchelli, R. Peptide nucleic acids with a structurally biased backbone: effects of conformational constraints and stereochemistry. *Curr. Top. Med. Chem.* **2011**, 1535; (h) Eglund, E. A.; Appella, D. H. *γ*-substituted peptide nucleic acids constructed from L-lysine are a versatile scaffold for multifunctional display. *Angew. Chem. Int. Ed*. **2007**, *46,* 1414. (i) Sugiyama, T.; Imamura, Y.; Demizu, Y.; Kurihara, M.; Takano, M.; Kittaka, A. β-PNA: Peptide nucleic acid (PNA) with a chiral center at the β-position of the PNA backbone. *Bioorg. Med. Chem. Lett.* **2011**, *21*, 7317.

9. (*a*) Gait, M. J.; Jones, A. S.; Walker, R. T. Synthetic Analogues of Polynucleotides. Part XII. Synthesis of Thyrnidine Derivatives containing an Oxyacetamido- or an Oxyformamido-linkage instead of a Phosphodiester Group**.** *J. Chem. Soc., Perkin Trans.* **1974**, *1*, 1684; (b) Coull, J. M.; Carlson, D. V.; Weith, H. L. Synthesis and characterization of a carbamate-linked oligonucleotide. *Tetrahedron Lett.* **1987**, *28*, 745; (c) V. Madhuri, Kumar, V. A. Design, synthesis and DNA/RNA binding studies of nucleic acids comprising stereoregular and acyclic polycarbamate backbone: polycarbamate nucleic acids (PCNA).*Org. Biomol.Chem*. **2010**, *8*, 3734
10. .Linkletter, B. A.; Bruice T. C. Solid-phase synthesis of positively charged deoxynucleic guanidine (DNG) modified oligonucleotides containing neutral urea linkages: effect of charge deletions on binding and fidelity. *Bioorg. Med. Chem*. **2000,** *8,* 1893.
11. P. E. Nielsen, Peptide Nucleic Acids Protocols and Applications, Eds. P. E. Nielsen and M. Egholm, Horizon Scientific press, **1999**.
12. Kumar, V. A.; Meena.; Pallan, P. S.; Ganesh, K. N. Pyrrolidine nucleic acids: DNA/PNA oligomers with 2-hydroxy/ aminomethyl-4-(thymin-1yl) pyrrolidine-N-acetic acid. *Org. Lett*. **2001**, *3*, 1269.

13. Worthington, R. J.; O′Rourke, P.; Morral, J. D.; Tan, T. H. S.; Mickelfield, J. Mixed sequence pyrrolidine-amide oligonucleotide mimics: Boc(Z) synthesis and DNA/RNA binding properties. *Org. Biomol. Chem.* **2007**, *5*, 249.
14. (a) Govindaraju, T.; Kumar, V. A. Backbone-extended pyrrolidine peptide nucleic acids (bepPNA): design, synthesis and DNA/RNA binding studies *Chem. Commun*. **2005**, 495; (b) Govindaraju, T.; Kumar, V. A. Backbone extended pyrrolidine PNA (*bep*PNA): a chiral PNA for selective RNA recognition.*Tetrahedron*. **2006**, *62*, 2321.
15. Vilaivan, T.; Lowe G. A Novel Pyrrolidinyl PNA showing high sequence specificity and preferential binding to DNA over RNA *J. Am. Chem. Soc*. **2002**, *124*, 9326
16. Suparpprom, C.; Srisuwannaket, C.; Sangvanich, P.; Vilaivan, T. Hybridization of pyrrolidinyl peptide nucleic acids and DNA: Selectivity, base-pairing specificity, and direction of binding. *Tetrahedron Lett*. **2005**, *46*, 2833.
17. (a) Vilaivan.T.; Srisuwannaket, C. Hybridization of Pyrrolidinyl Peptide Nucleic Acids and DNA: Selectivity, Base-Pairing Specificity, and Direction of Binding *Org. Lett.* **2006**, *8*, 1897; b) Mansawat, W.; Vilaivan, C.; Balázs, Á.; Aitken, David J. and Vilaivan T. Pyrrolidinyl Peptide Nucleic Acid Homologues: Effect of Ring Size on Hybridization Properties *Org. Lett.* **2012**, *14,* 1440.
18. Gogoi, K.; Kumar, V. A. Chimeric (α-amino acid + nucleoside-β-amino acid)n peptide oligomers show sequence specific DNA/RNA recognition *Chem. Commun*. **2008**, 706;
19. Efimov, A.; Buryakova, A.A.; Chakhmakhcheva, O.G. Synthesis of DNA analogues with novel carboxamidomethyl phosphonamide and glycinamide internuceloside linkages. *Bioorg. Med. Chem. Lett*. **1998,** *8,* 1013
20. (a) Chandrasekhar, S.; Reddy, G. P. K.; Kiran, M. U.; Nagesh, Ch.; Jagadeesh, B. Nucleoside derived amino acids (NDA) in foldamer chemistry: synthesis and conformational studies of homooligomers of modified AZT. *Tetrahedron Lett*. **2008**, *49*, 2969; (b) Cosstick, R.; Davies, A.; Howarth, N. M.; Fisher ,J.; Cosstick, R. *Chem. Commun*. **2008**, 585; (c) Threlfall, R.; Davies, A. Howarth, N. M.; Cosstick, R. Foldamers derived from nucleoside β-amino acids: PNA Or DNA? Can we have both in one place?. *Nucleosides, Nucleotides, Nucleic Acids.* **2006**, *26*, 611; (d) Cosstick, R.; Cosstick, R. Foldamers derived from nucleoside

β-amino acids: a new twist on the DNA helix. *Nucleic Acids. Symp. Ser*. **2008**, *52*, 313.

21. Bagmare, S.; D′Costa, M.; Kumar, V. A . Effect of chirality of L/D-proline and prochiral glycine as the linker amino acid in five-atom linked thymidinyl-(a-amino acid)-thymidine dimers . *Chem.Commun.* **2009**, 6646.
22. (a) Fearon, K. L.; Nelson, J. S. Synthesis and Purification of Oligonucleotide: N3′→P5′ Phosphoramidates and their Phosphodiester and Phosphorothioate Chimeras. *Current Protocols in Nucleic Acid Chemistry.* **2001**. *4.7.1– 4.7.40*. (b) Divakar, K. J.; Reese, C. B. 4- (1,2,4-Triazol-1-yl)- and 4-(3- Nitro-l,2,4-triazol-l-yl)-l-(β-D-2,3,5-tri-O-acetylarabinofuranosyl) pyrimidin-2(lH)-ones. Valuable Intermediates in the Synthesis of derivatives of 1-(β-D-Arabinofuranosy1)cytosine (Ara-C). *J. Chem. Soc. Perkin. Trans*. 1, **1982**, 1171.
23. Malkinson, J.P.; Falconer, R. A. Solid-phase synthesis of C-terminal thio-linked glycopeptides. *Tetrahedron Lett,* **2002**, *43*, 9549.
24. (a) Epp, J. B.; Widlanski, T. S. Facile preparation of nucleoside -5'-carboxylic acid *J. Org. Chem*., **1999**, *64*, 293; (b) De Mico, A.; Margarita, R.; Parlanti, L.; Vescovi A.; Piancatelli, G. Versatile and Highly Selective Hypervalent Iodine (III)/2,2,6,6-Tetramethyl-1-piperidinyloxyl-Mediated Oxidation of Alcohols to Carbonyl Compounds *J. Org. Chem*. **1997**, *62*, 6974.
25. Zielinska, D.; Pongracz, K.; Gryaznov, S. M. A new approach to oligonucleotide N3'→ P5' phosphoramidate building blocks. *Tetrahedron Lett.* **2006**, *47*, 4495.
26. Bhat, B.; Sanghvi. Y.S. A mild and highly selective N-benzoylation of cytosine and adenine bases in nucleosides with N-benzoyltetrazole. *Tetrahedron Lett,* **1997**, *38*, 8811.
27. de la Torre, B.G.; Marcos, M. A.; Eritja, R.; Albericio, F. Solid-phase peptide synthesis using Nα-trityl-amino acids. *Lett. Pept. Sci*. **2001**, *8*, 331.
28. Kaiser, E.; Colescott, R. L.; Bossinger, C. D.; Cook, P. Color test for detection of free terminal amino groups in the solid-phase synthesis of peptides *Anal. Biochem.* **1970**, *34,* 595.
29. Rathore, R.; Burns, C, L.; Guzei I. A. Synthesis and isolation of polytrityl cations by utilizing hexaphenylbenzene and tetraphenylmethane Scaffolds *J. Org. Chem.* **2004**, *69*, 1524.

Chapter 4

α-L-DNA: A DNA mimic with a compact backbone like RNA

4.1 Introduction

Antisense oligonucleotides as potential human therapeutics have been explored for more than the last two decades.[1] There are several antisense methodologies currently being pursued. Such mechanisms include RNase H cleavage of target RNA, RNA interference, inhibition of micro-RNA function and alteration of splicing. All these mechanisms are shortly discussed in chapter 1. RNase H (Ribonuclease H) cleavage of target RNA (Figure 1) is a highly effective approach and the most widely used mechanism to downregulate target genes using antisense oligonucleotides, accounting for the majority of drugs in development. RNase H, a ubiquitous enzyme that hydrolyzes the RNA strand of an RNA/DNA duplex and is widely expressed in mammalian cells.[2] An externally delivered antisense molecule must bind to a targeted mRNA according to Watson-Crick recognition rules and also be able to elicit RNase H enzyme activity. The RNase H enzyme interacts with the minor groove of the RNA/DNA hybrid helix and cleaves the RNA strand.[3] The enzyme requires divalent metal ions Mg^{2+} and Mn^{2+} and generates products with 5'-phosphate and 3'-hydroxyl group as final products.

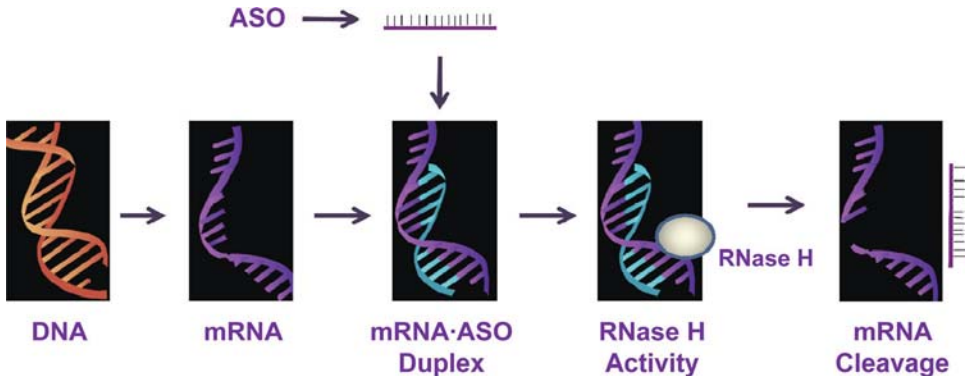

Figure 1. RNase H Cleavage mechanism[4]

The catalytic cleavage by the RNase H enzyme demands a flexible hybrid duplex.[5] For example, in the native DNA-RNA duplex, the conformation of the DNA strand is B type (all nucleotides are in intermediate O4′-*endo*/S-type conformation, Figure 2) whereas the RNA strand adopts a conformation which is very similar to single stranded RNA in which all nucleotides are in C3′-*endo* conformation, i.e., N-type (Figure 2).[6] It has emerged that the RNase H cleavage site retains this intermediate B-type-DNA/A-type RNA conformation in order to be substrate for cleavage reaction by RNase H. The antisense molecule is then free to interact with other target

RNA molecule, thus improving the potency of antisense ONs, resulting in dose reduction.

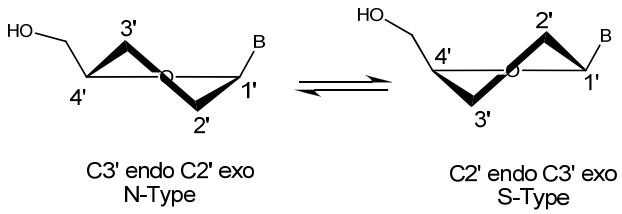

Figure 2. (A) C3'-*endo* and C2' *endo* sugar conformations

Oligonucleotide-assisted RNase H-dependent reduction of targeted RNA expression can be quite efficient, reaching 80–95% down-regulation of protein and mRNA expression. Furthermore, in contrast to the steric-blocker oligonucleotides, RNase H-dependent oligonucleotides can inhibit protein expression when targeted to virtually any region of the mRNA.

The ideal antisense gene inhibitor should display high specificity towards its target sequence, enhanced stability towards intra- and extracellular nucleases and should possess the ability to penetrate the cell membrane. In addition to these requirements, the antisense oligonucleotide should leave the nucleic acid structure relatively unperturbed in order to retain the ability to elicit RNase H degradation of the resulting ON: RNA hybrid.

Several antisense agents have reached the stage of clinical trials and in 1998, the first antisense oligonucleotide (phosphorothioate backbone) drug, Formivirsen was approved by FDA. Though phosphorothioate were able to activate RNase H, they exhibit several disadvantages such as: they have a comparably low binding capacity and show nonspecific binding to proteins[7], causing toxic side effects that limit many applications. In order to overcome these limitations, various modifications of the sugar and nucleobase, as well as of the phosphate backbone, have been investigated, and numerous reports are available about these modified AONs and their antisense action.[1,4,8] Different 2'-*O*-alkyl[9] and 2'-*O*-aminoalkyl[10,11] as well as 2'-fluoro[12] modifications in ribose resulted in significant increase of the duplex stability (about 2 °C per modification). Unfortunately all these modifications drive the sugar into the C3'-*endo* conformation typical for the A-type RNA/RNA duplex[13] which results in complete loss of the RNase H activity. However,

arabinonucleic acids (ANA, Figure 3) and 2'-deoxy-2'-fluoro-arabinonucleic acids (2'F-ANA, Figure 3) were shown[14] to be substrates for RNase H. Lower RNase H activity observed for ANA/RNA duplexes was attributed to the lower thermal stability of the duplex as a result of lesser amount of ANA/RNA duplex available for the enzyme to process. RNase H activity of the duplexes formed by 2'F-ANA was comparable with the corresponding non-modified substrates. In an NMR study, it has been demonstrated that the 2'F-ANA have an eastern *O*-4'-*endo*-sugar conformation, closer to B-type DNA when hybridized to RNA.[15] The small size of the F-atom and its upward position (away from minor grove) may suggest that it may not interfere with the enzyme binding to the heteroduplex, thereby not impairing the activity of the enzyme on 2'-F-ANA/RNA duplex.[14b]

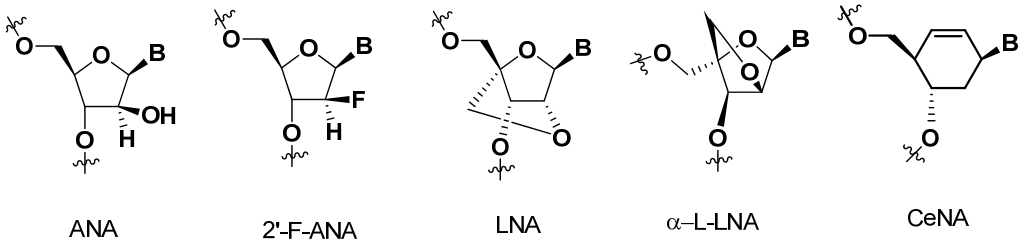

Figure 3. ANA, 2'-F-ANA, LNA and α-L-LNA Analogs

LNA (Locked Nucleic acid, Figure 3) and α-L-LNA (Figure 3) have emerged as useful tools in therapeutics and diagnostics.[16] Both LNA[17] and α-L-LNA[18] sequences have demonstrated unprecedented stability for antiparallel hybridization with both DNA and RNA complements. An LNA nucleotide contains a 2'-*O*, 4'-C-methylene bridge that locks the nucleotide in a C3'-*endo* (N-type) furanose conformation resulting in LNA:RNA duplex in A-type and so do not support RNase H enzyme activity. α-L-LNA, which contains the 2',4'-bridge on the same side of the sugar as the nucleobases, along with an inversion of the 3'-OH group. Structural studies of α-L-LNA were reported and showed that α-L-LNA assumes a DNA-like Southern conformation, resulting in H-form duplexes with target RNA.[18,19] Even though α-L-LNA showed Southern sugar pucker, α-L-LNA does not support RNase H, but has been utilized successfully in gapmer ASO designs.[20] Cyclohexene nucleic acids (CeNA) were shown to have enhanced affinity to the target RNA. The resulting CeNA/RNA duplexes were susceptible to RNase H cleavage and found to be

relatively poorer substrate in comparison with native counterpart.[21] The flexible cyclohexene ring can adopt both S-type and N-type geometries and the energy barrier is low.

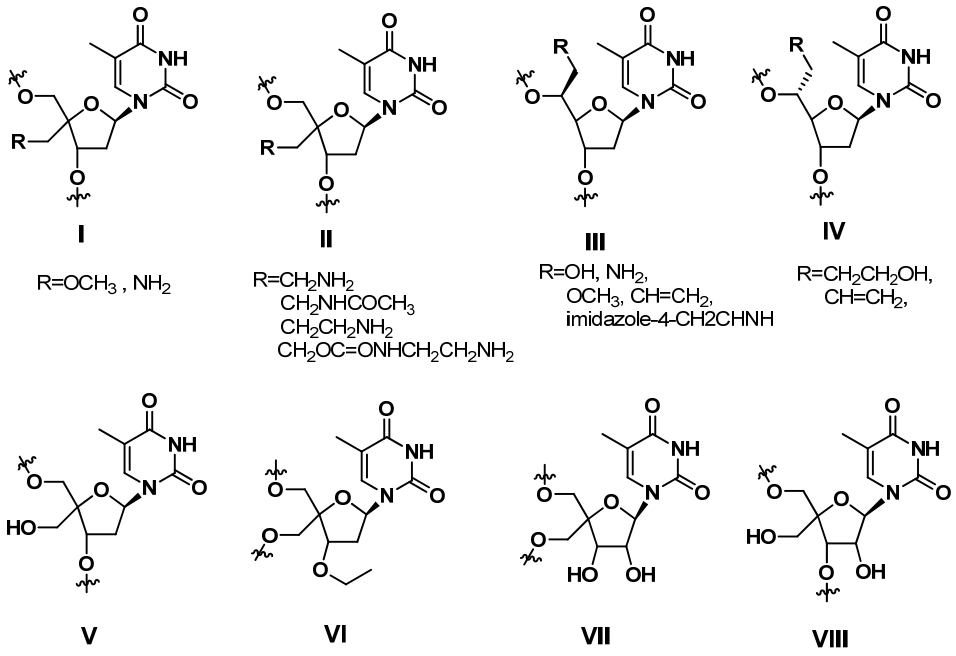

Figure 4. 4'-C and 5'-C-substituted sugar analog

AONs possessing various 4'-*C*[22,23](Figure 4, I and II) and 5'-*C* modifications[22] (Figure 4, III and IV) in 2'-deoxyribose moiety have been reported to serve as substrates for RNase H with efficiency comparable with those of the non-modified DNAs irrespective of their lower affinity to the RNA target. Kanazaki et al. studied the RNase H-eliciting power of AONs containing 4'-α-*C*-amininoalkylthymidines.[23] RNase H-promoted hydrolysis rates for the hybrid duplexes formed by 4'-α-*C*-aminoalkylthymidine-containing AONs were found to be similar to that of unmodified counterpart. Also, it was reported that hydrolysis rates were decreased when five residues of 4'-α-*C*-amininoalkylthymidine have been introduced into the AON. Literature also reports the 4'-*C*-(hydroxymethyl)thymidine[24,25] (Figure 4, V and VI) and 4'-*C*-(hydroxymethyl)uridine[26] (Figure 4, VII and VIII) modifications which have not been further studied for their RNase H activity. 4'-C-(hydroxymethyl)thymidine modified ODNs have shown excellent hybridization properties and this modification leads to significantly improved enzymatic stability. Oligodeoxynucleotide analogues containing 3'-*O*-ethyl-4'-*C*-hydroxymethyl

nucleoside (single modification at 3' end) moderately weaken duplex stability while significantly improved the resistance towards 3'-exonucleolytic degradation.[25] Incorporation of 4'-*C*-(hydroxymethyl)uridine (Figure 3, VII and VIII) in oligonucleotides (both 5'- hydroxyl to 4'-*C*-hydroxymethyl backbone or 5'-hydroxyl to 3'-hydroxy backbone) led to destabilization of the complexes with complementary DNA and RNA.[26] The conformations of the pentofuranose ring in the modified nucleotides VII and VIII are far from ideal when optimal DNA:DNA duplex stability is considered. This was confirmed by modeling studies which revealed distortions in the sugar-phosphate backbone, especially for modification VII.

4.2 Rationale, Design and Present Work

In search for oligonucleotide analogs possessing enhanced hybridization and enzyme stability as well as ability to induce RNase H activity, we have explored a sugar modification at the 4'-postion. From the consideration that the restriction of sugar puckering in nucleosides to a proper conformation would serve as an advantageous strategy to develop a desired antisense molecule, we propose a nucleotide analog in which the sugar was expected to have a 2'-*endo* (S-type) pucker (Figure 5) that is normally observed in DNA. The cis geometry of the phosphodiester linking 4'-α-CH_2OH and 3'-OH group may show internucleoside distance complementarity while binding to A-type RNA geometry. This compact backbone (5''- 3' linkage) was envisaged to be helpful in improving DNA:RNA duplex binding strength.

The L-configuration indicates the configuration about the C4' center, wherein the 5'' CH_2OH group is positioned below the C4'-O4'-C1' furanose plane (which is the carbon atom involved in the backbone linkage). With respect to the 5"CH_2OH group, the base is α-oriented. Therefore, we called this analog as 'α-L-DNA'. In natural DNA, on the other hand, the C5' center (involved in backbone linkage) is D-configured and the base is consequently, β-oriented.

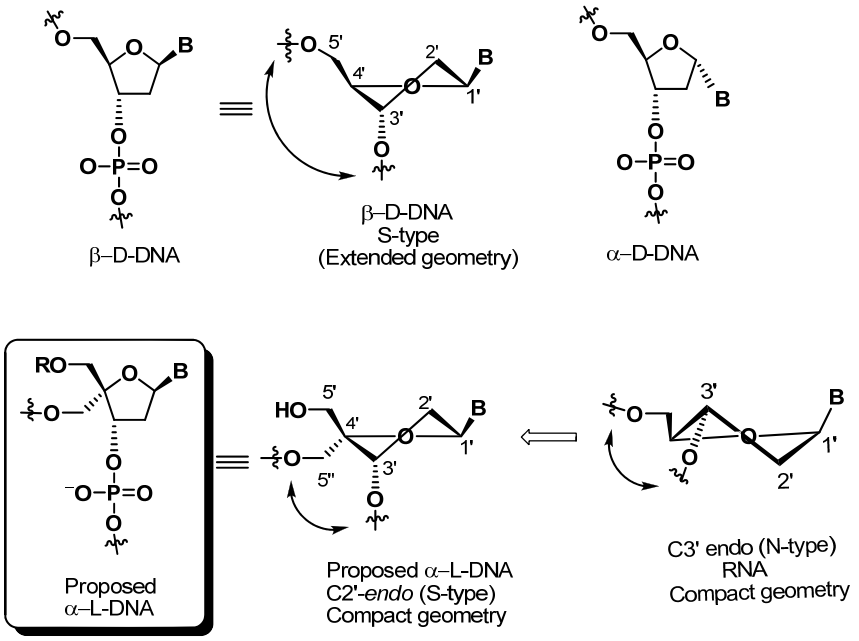

Figure 5. β-D-DNA, α-D-DNA and proposed α-L-DNA with 5''→ 3'-phosphodiester linkage

Specific objectives of this chapter are

1. Synthesis of the α-L-DNA thyminyl monomer
2. Conversion of the monomeric unit to its phosphoramidite derivative
3 Incorporation of these activated monomer into pre-determined oligonucleotide sequences using the automated DNA synthesizer and their characterization by HPLC and MALDI-TOF.
4. Evaluation of these α-L-DNA modified oligomers for their UV-thermal binding stability towards complementary DNA/RNA.
5. Evaluation of RNase H activity of the modified sequences.

4.3 Results and Discussion

4.3.1 Synthesis of α-L-DNA monomer

A number of 4'-C-branched nucleosides have been reported in the literature, either studied for their anti HIV activity[27] or incorporation into oligomers.[24-26] Here, we have synthesized a new α-L-DNA phosphoramidite monomer **11** (scheme 1) and incorporated it into oligomers. The 4' hydroxymethyl carbon was considered as C 5'' and the linkage 5''→ 3'. The synthesis of the monomer was accomplished from

commercially available starting material, thymidine. Compound **4** was obtained following the reaction conditions as per literature.[28] Accordingly the 5'-OH of thymidine **1** was protected as its 5'-*O*-*tert.*butyldimethylsilyl ether to get **2,** which on protection of the 3'-OH group with DMT gave compound **3**. The silyl group of compound **3** was removed by treatment with TBAF to give compound **4**. We applied a simple oxidation protocol for the synthesis of the 5'-aldehyde using IBX[29] rather than Swern oxidation[30] (oxalyl chloride/DMSO/DIPEA) or Moffat's oxidation (DMSO/DCC/TFA/Pyridine) procedure.[31] The latter two oxidation procedures require polar solvents and tedious reaction conditions whereas IBX oxidation was simple, using relatively volatile solvents and offered aldehyde after filteration of the reaction mixture. Oxidation of compound **4** with IBX to corresponding aldehyde **5** proceeded with good yield, followed by aldol condensation between the intermediate nucleoside aldehyde **5** and formaldehyde in the presence of aqueous sodium hydroxide with concomitant reduction using sodium borohydride employing known reaction conditions[32] to give known compound **6**. The 4'-*C*-hydroxymethyl functionality (5'') was regioselectively protected by reaction with DMT-Cl to give nucleoside **7**. This selectivity might be due to steric hindrance from the base moiety and was found to be in accordance with literature reports. Protections of 5'- hydroxyl group as a silyl ether furnished compound **8**. The dimethoxy trityl group of compound **8** was then removed using 2% dichloroacetic acid in DCM to give 5'-*O*-(tert-butyldimethylsilyl)-4'-C-(hydroxymethyl)thymidine **9**. The protection of the 4'-C-hydroxymethyl group by reaction with DMT-Cl furnished the final monomer **10** which was then converted to its phosphoramidite derivative **11**. The formation of the product was confirmed by ^{31}P NMR spectroscopy.

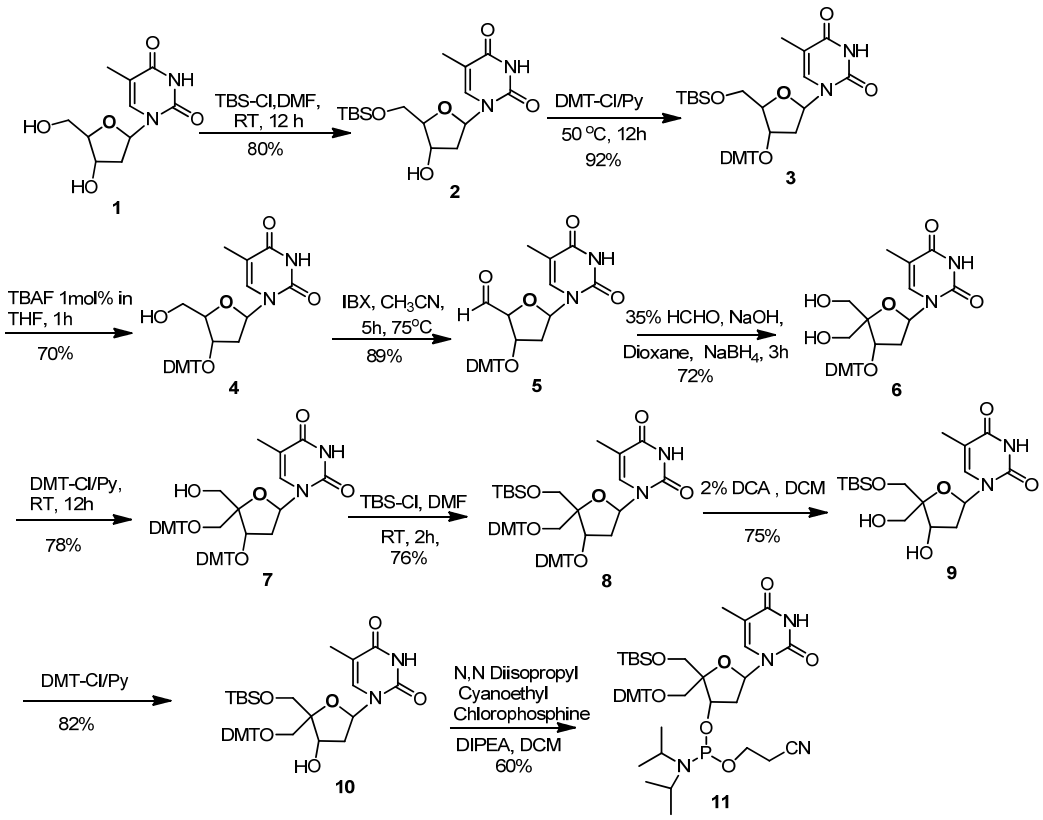

Scheme 1. Synthesis of α-L-DNA monomer

4.3.2 Sugar Conformation and Crystal Structure

In natural nucleic acids, the pentose sugars are puckered or twisted to give preferred helical conformations. In principle, there is a continuum of interconvertible puckers, separated by energy barriers. These various puckers are produced by systematic changes in the ring torsion angles (ν0- ν1)

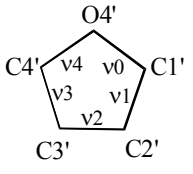

ν0=C4'-O4'-C1'-C2'
ν1=O4'-C1'-C2'-C3'
ν2=C1'-C2'-C3'-C4'
ν3=C2'-C3'-C4'-O4'
ν4=C1'-O4'-C4'-C3'

Figure 6. endocyclic tortional angles ν0-ν4

The puckers can be succinctly defined by the parameters P and $\nu_{max.}$[33] The value of P, the phase angle of pseudorotation, indicates the type of pucker since P is defined in terms of the five torsion angles ν0-ν4:

$$\tan P = \frac{(\nu4+\nu1) - (\nu3+\nu0)}{2\,\nu2\,(\sin32° + \sin 72°)} \qquad \text{…….. } \mathbf{1}$$

and the maximum degree of pucker i.e puckering amplitude ν_{max}:

$$\nu_{max} = \frac{\nu2}{\cos P} \qquad \text{……..} \mathbf{2}$$

The pseudorotation phase angle can take any value between 0° and 360°. If ν2 has a negative value, then 180° is added to the value of P. The pseudorotation phase angle is commonly represented by the pseudorotation wheel, which indicates the continuum of ring puckers (Figure 7). Values of ν_{max} indicate the degree of puckering of the ring; typical experimental values from crystallographic studies on mononucleosides are in the range 25–45°.[34] For North-type (N) sugars (C3'-*endo*, C2'-*exo*), P ranges from -1º to 34º and for S-type (S) sugars (C2'-*endo*, C3'-*exo*), P ranges from 137º to 194º.

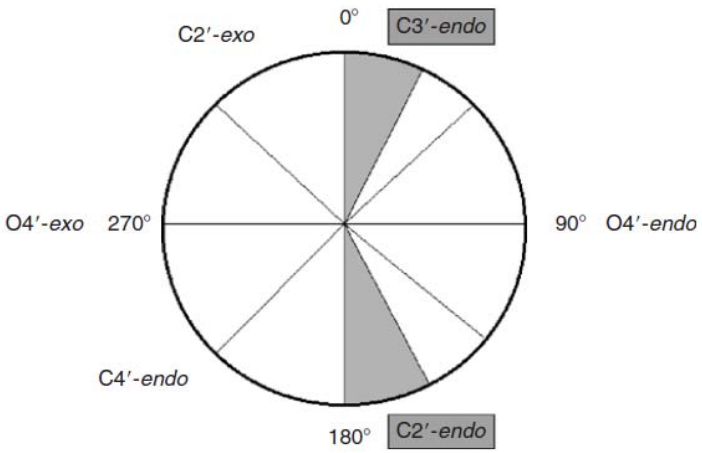

Figure 7. The pseudorotation wheel for a deoxyribose sugar. The shaded areas indicate the preferred ranges of the pseudorotation angle for the two principal sugar conformations.[34]

We have calculated sugar conformation of intermediate compound **9** from NMR H1' coupling constant (*J*H1'= 8.84 and 5.43 Hz) using Sum rule (equation 3) and was found to have 76% S-type sugar pucker.

$$\% S = (\Sigma Hl'-9.8)/ 5.9 \quad \text{where } \Sigma Hl' = J_{1',2'} + J_{1',2''} \quad \ldots\ldots\ldots\ldots\ldots \mathbf{3}$$

We have further confirmed from crystal structure of compound **9** (Figure 8) which clearly indicate S-type sugar conformation.

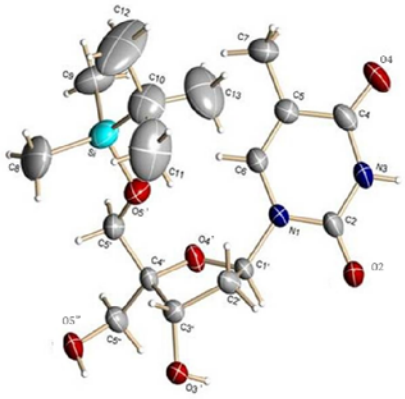

Figure 8. Crystal structure of compound **9**

Phase angle of pseudorotaion (P) and puckering amplitude ν_{max} was calculated from the torsional angle obtained from crystal data (Table 1) using equation 1 and 2 respectively. Phase angle of pseudorotation (P) was found to be 172.14° which again indicates S-type sugar pucker. The puckering amplitude ν_{max} was found to be 33.5° which was in accordance with typical experimental values.

Table 1. Geometrical parameters obtained from X-ray crystal structure for compound **9**

Torsional angles	Torsional angle (deg)
ν0 =[C4'- O4'- C1'- C2']	-15.3
ν1 =[O4'- C1'- C2'- C3']	30.3
ν2 =[C1'- C2'- C3'- C4']	-33.6
ν3 =[C2'- C3'- C4'- O4']	-25.3
ν4 =[C1'- O4'- C4'- C3']	6.7
χ =[O4'- C1'- N1- C2]	-147

The torsion angle χ around the glycosidic bond is defined in terms of four atoms:

O4'–C1'–N9–C4 for purines
O4'–C1'–N1–C2 for pyrimidines

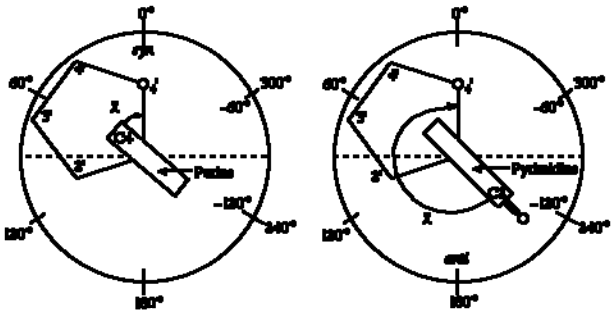

Figure 9. Diagrammatic representation of the N-glycosidic bond torsion angle χ and the *syn* and *anti* regions for purine and pyrimidine derivatives[34]

The *anti* conformation has the N1, C2 face of purines and the C2, N3 face of pyrimidines directed away from the sugar ring so that the hydrogen atoms attached to C8 of purines and C6 of pyrimidines, are lying over the sugar ring (Figure 9). Thus, the Watson–Crick hydrogen-bonding groups of the bases are directed away from the sugar ring. These orientations are reversed for the *syn* conformation, with these hydrogen-bonding groups now oriented toward the sugar. The sterically preferred ranges for these two domains of glycosidic angles are:

Anti: $-120 > \chi > 180°$

Syn: $0 < \chi < 90°$

The χ angle obtained from the X-ray crystal structure of compound **9** was −147°, indicating the *anti* conformation of thymine base.

4.4 Solid Phase Synthesis of DNA Oligonucleotides by Phosphoramidite Method

Control 18mer oligonucleotide **DNA1** chosen was specific for the Splice correction of an aberrant *β*-globin intron (705 site).[35] Chronic myeloid leukemia (CML) is probably the most extensively studied human malignancy. The discovery of the Philadelphia (Ph) chromosome in the 1960 as the first consistent chromosomal abnormality associated with a specific type of leukemia was a breakthrough in cancer biology.[36] The unmodified oligomers were synthesized using an automated

Bioautomation MM4 DNA synthesizer and commercially available 5'-*O*-DMT-2'-deoxy-3'-phosphoramidite building blocks using β–cyanoethyl phosphoramidite method.[37] The modified monomer unit **11** was incorporated at pre-determined positions using an extended coupling time to yield the modified oligomers efficiently. **ON1** and **ON2** were synthesized with one and two modifications respectively.

4.4.1 Purification and MALDI-TOF characterization of modified oligomers

The synthesized oligonucleotides were cleaved from the solid support with conc. NH_4OH, lyophilized. The silyl group was deprotected by adding 0.1 mL desilylation solution (1.5 mL NMP + 0.75 mL TEA + 1 mL 3HF: TEA) and heated at 65 °C for two hours. The reaction mixture was then cooled and neutralized with 0.1 mL NH_4HCO_3 (0.5 M), lyophilized and desalted to get the crude oligonucleotides. The purity of the oligomers listed in Table 2 was checked by analytical RP-HPLC (C18 column, 0.1 N TEAA buffer-acetonitrile) which showed more than 75-80% purity. These oligomers were subsequently purified by reverse phase HPLC on C18 column. The purity of the oligomers was again ascertained by analytical RP-HPLC and found to be > 95%. Their integrity was confirmed by MALDI-TOF mass spectrometric analysis. THAP (2,4,6-trihydroxy acetophenone) matrix with diammonium citrate as additive was used for MALDI-TOF (matrix assisted laser desorption ionization time-of-flight) mass analysis of oligomers. HPLC retention time and observed values of mass in MALDI-TOF spectrometry are listed in Table 2.

Table 2. Oligomers synthesized with their HPLC retention times and MALDI -TOF values

Code	Sequence	HPLC t_R (min)	Mass	
			Exp. Mass	Obs. Mass
ON1	5'CCT CTT ACC TCA GT**T** ACA3'	8.66	5400	5401.91
ON2	5'CCT CTT ACC **T**CA GT**T** ACA3'	7.95	5431	5431.32

T indicate α-L-DNA monomer

4.5 Biophysical studies of α-L-DNA modified oligomers

UV-T_m studies were carried out to investigate the binding of the modified oligomers to complementary DNA and RNA. The T_m experiments of duplexes were carried out in 10 mM sodium phosphate buffer (pH 7.2) containing 100 mM NaCl

and 0.1 mM EDTA. Chimeric DNA oligonucleotides were individually hybridized with the complementary DNA and RNA strands, to obtain duplexes.

The binding affinity of 18mer chimeric ONs (**ON1 and ON2**) with complementary DNA2 and RNA was investigated by measuring the melting temperatures (T_m) of the duplexes and the results are summarized in Table 3**.**

Table 3. T_m (°C) values of 18mer chimeric ONs: DNA/RNA duplexes

Entry	Sequences	UV-T_m °C (Δ T_m °C)	
		DNA 2	RNA
1	**DNA1** 5'CCT CTT ACC TCA GTT ACA3'	**53.1**	**56.5**
2	**ON1** 5'CCT CTT ACC TCA GT**T** ACA3'	50.2 (-2.9)	50.4 (-6.1)
3	**ON2** 5'CCT CTT ACC **T**CA GT**T** ACA3'	46.8 (-6.3)	48.6 (-7.9)

T = α-L-DNA monomer unit, **DNA2**: 5' TGT AAC TGA GGT AAG AGG 3', **RNA:** 5'UGU AAC UGA GGU AAG AGG 3', T_m = melting temperature (measured in the buffer 10 mM sodium phosphate, 100 mM NaCl, pH = 7.2), of α-L-DNA modified ONs:DNA/RNA complexes. The values reported here are the average of 3 independent experiments and are accurate to ±1.0°C. Δ T_m = T_m - $T_{m(control)}$

The unmodified 18mer **DNA1** sequence forms complexes with complementary **DNA2** and **RNA** with higher melting temperature for DNA:RNA complex over DNA:DNA (Δ T_m= +3.5 ºC). Introduction of a single monomeric unit towards the 3' end in 18mer oligomer **ON1**, caused a destabilization of 2.9 ºC and 6.1 ºC with complementary **DNA2** and **RNA**. A cumulative effect was observed in destabilization in the **ON2:DNA2/RNA1** when two monomer units were incorporated. Incorporation of two monomer units into the oligomer showed further increase in destabilization with both **DNA/RNA**. Thus, intermittent change to 3'-5'' linkage in continuous 3'-5' backbone at a single or more positions destabilized the duplexes with both DNA and RNA. It would be perhaps necessary to synthesize a completely modified 3'-5'' phosphodiester linked DNA oligomer to fully understand the usefulness of this designed oligomer backbone.

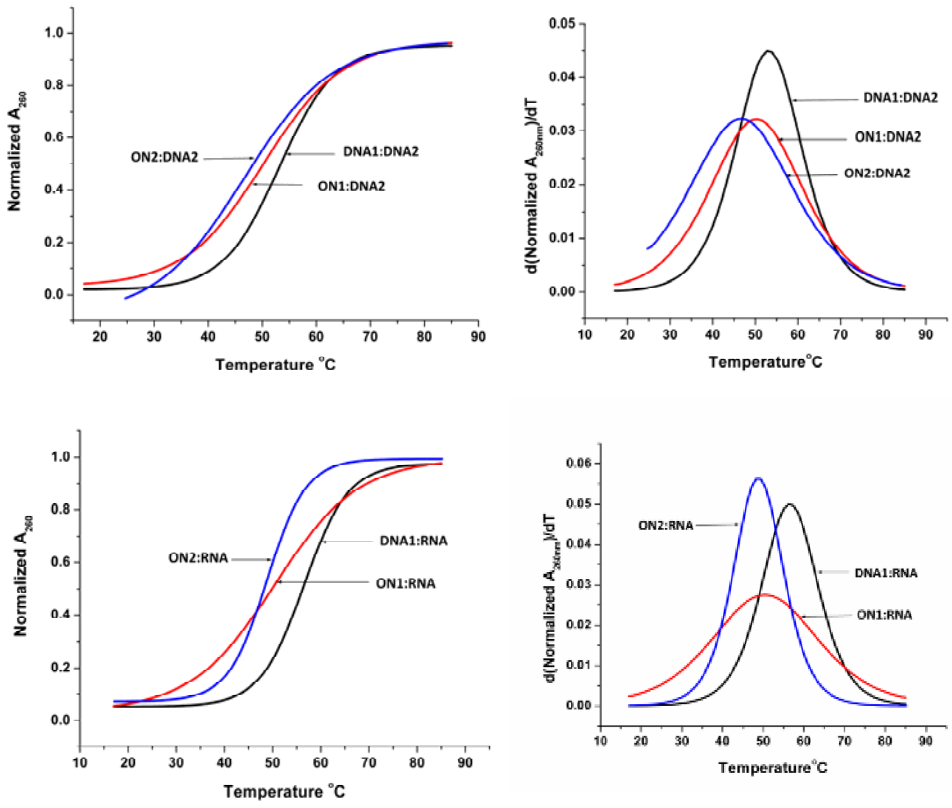

Figure 10: Melting curves for **ON1-ON2** oligomers with complementary DNA/RNA and corresponding first derivative curves.

4.6 RNase H Digestion Assay

We have carried out RNase H digestion assay for the single modified sequence in order to find out its ability to induce RNase H using electrophoretic gel experiment (Figure 11). The control **DNA1, ON1** were mixed separately with complementary **RNA** in 1:1 ratio (300 µM each) in water. The samples were lyophilized to dryness and re-suspended in 10 mM Tris-HCl buffer (pH 7.5, 5 µL) containing 25 mM KCl and 0.5 mM $MgCl_2$. The samples were annealed by heating at 85ºC for 1 min followed by slow cooling to room temperature and refrigeration at 4ºC overnight. Single stranded **DNA1**, **ON1** and **RNA** (300 µM) were also subjected to the same conditions. Annealed samples were centrifuged and then incubated at 37 °C. 1 µL of duplex was taken out prior to addition of enzyme. The remaining 4 µL of duplex were digested with 6 U of RNase H enzyme (total reaction volume was 7 µL). Aliquots (1.5 µL) were taken out after 30, 60, 120 and 240 min; the reaction was

stopped by adding 0.75 µL EDTA, followed by chilling in icebath. Control samples and reaction aliquots were mixed with equal volume of 40% sucrose in TBE buffer (pH 8.0) and loaded on the gel (2 µL each). Bromophenol blue (BPB) was used as the tracer dye separately in an adjacent well. Gel electrophoresis was performed on a 20% non-denaturing polyacrylamide gel (acrylamide:bis-acrylamide, 29:1) with 1X TBE buffer at 200V and 10 mA, until the BPB migrated to three-fourth of the gel length. During electrophoresis the temperature was maintained at 10ºC. The spots were visualized through UV shadowing by illuminating the gel placed on a pre-coated silica gel plate (F_{254}). The gel was stained with ethidium bromide followed by visualization using UV transilluminator.

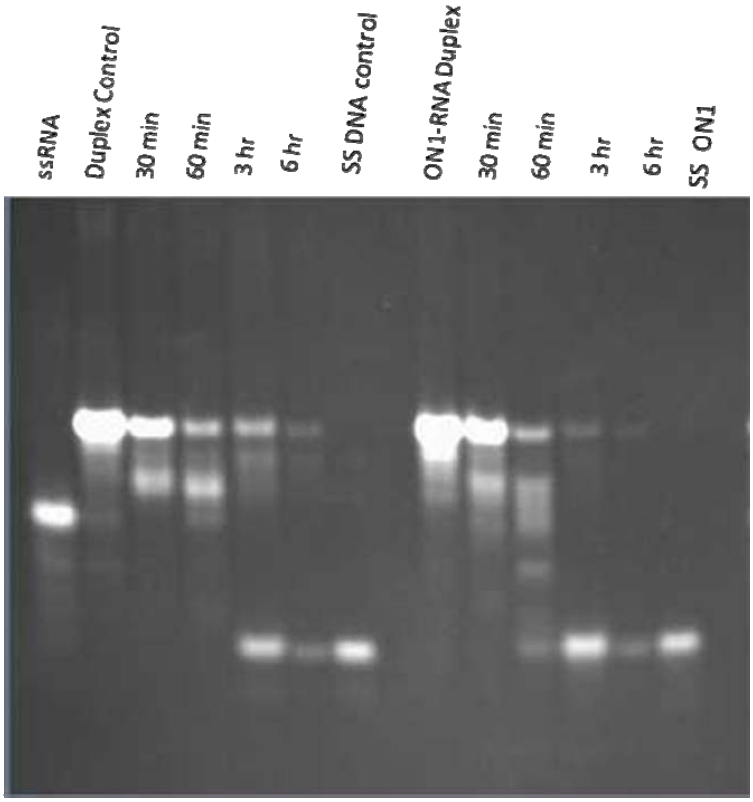

Figure 11. The PAGE analysis of RNase H hydrolysis of the hybrid duplexes control DNA and modified oligomer **ON1** with **RNA**

The PAGE analysis of RNase H hydrolysis of the hybrid duplexes (Figure 11) showed that the modified oligomer **ON1** was found to be as good a substrate for RNase H as the native hybrid duplex, although it showed destabilization of ~ 3 °C with RNA.

4.7 Summary

1. The proposed nucleotide analog shows S-type sugar pucker, confirmed by NMR and crystal structure.

2. Introduction of 4'-substituted sugar monomer into oligomer destabilized complexes with both DNA and RNA.

3. Irrespective of the loss of T_m, the single modified **ON1-RNA** duplex was found to be as good a substrate for RNase H as the native hybrid duplex.

4.8 Experimental Section

General: All the reagents were purchased from Sigma-Aldrich and used without purification. DMF, CH_3CN were dried over P_2O_5 and CaH_2 respectively and stored by adding 4 Å molecular sieves. Pyridine, TEA were dried over KOH and stored by adding KOH. THF was passed over basic alumina and dried by distillation over sodium. Analytical TLCs were performed on Merck 5554 silica 60 aluminium sheets. Column chromatography was performed for purification of compounds on silica gel (60-120 mesh, Merck). For acid-sensitive (trityl-containing) compounds, the column packed and equilibrated with 0.5% triethylamine. TLCs were performed using dichloromethane-methanol or petroleum ether-ethyl acetate solvent systems. Visualization was accomplished with UV light and/or by spraying with perchloric acid reagent and heating. ^1H and ^{13}C NMR spectra were obtained using Bruker ACF 200 (200 MHz) or 400 (400 MHz) spectrometers and all the chemical shifts (δ/ppm) are referred to internal TMS for ^1H and chloroform-*d* for ^{13}C NMR. ^1H NMR data are reported in the order of chemical shift, multiplicity (s, singlet; d, doublet; t, triplet; br, broad; br s, broad singlet; m, multiplet and/ or multiple resonance), number of protons. Mass spectra were recorded on Thermo Finnigan Surveyor MS-Q spectrometer, while HRMS was recorded by using a Thermo Scientific Q-exactive mass spectrometer. Gel experiment was carried using BIO-RAD PROTEAN II xi cell electrophoresis instrument. RP-HPLC was carried out on a C18 column using Waters system (Waters Delta 600e quaternary solvent delivery system and 2998 photodiode array detector and Empower2 chromatography software). MALDI-TOF spectra were recorded on a Voyager-De-STR (Applied Biosystems) MALDI-TOF instrument. UV experiments were performed on a Varian Cary 300 UV-VIS spectrophotometer fitted with a Peltier-controlled temperature programmer and a water circulator.

5'-*O*-(*tert*-butyldimethylsilyl)-thymidine (2)

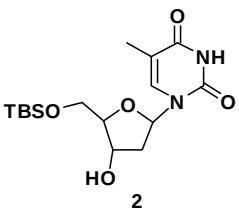

2

Thymidine **1** (10 g, 41.28 mmol) and imidazole (6.0 g, 90.75 mmol) was suspended in 15 mL of dry DMF. TBS-Cl (6.5 g, 41.25 mmol) dissolved in 5 mL of dry DMF was added dropwise at 0 °C and reaction was stirred at RT for 20 h. DMF

was removed under vacuum and product was extracted in ethyl acetate. Organic layer was dried over Na_2SO_4 concentrated and product was purified with column chromatography using 2% methanol in dichloromethane gave product **2** (12.1 g, Yield 80 %).

^{1}H NMR (200MHz, $CDCl_3$): 8.93 (s, 1H, exchanges with D_2O), 7.53 (s, 1H), 6.35-6.42 (dd, *J*=8.21, 5.81 Hz, 1H), 4.48 (m, 1H), 4.05 (m, 1H), 3.89 (m, 2H), 2.65 (bs, 1H, exchanges with D_2O), 2.34-2.44 (m, 1H), 2.03- 2.17 (m, 1H), 1.92 (s, 1H), 0.92 (s, 9H), 0.12 (s, 6H); **^{13}C NMR** (50MHz, $CDCl_3$): 164.1, 150.6, 135.5, 110.9, 87.3, 85.0, 72.7, 63.6, 41.0, 25.8, 18.3, 12.5, -5.4, -5.5; **MS (EI)** *m/z* 356.1767, found 379.11 ($M+Na^+$); **HRMS (ESI):** calcd for $C_{16}H_{28}N_2O_5SiNa$: 379.1659, found 379.1648.

5'-*O*-(*tert*-butyldimethylsilyl)-3'-*O*-(4, 4'-dimethoxytrityl)thymidine (3)

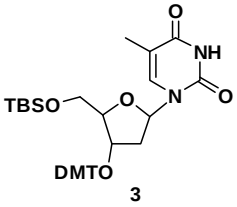

3

A mixture of **2** (10 g, 28 mmol) and DMT-Cl (11.4 g, 33.7 mmol) in 25 mL dry pyridine was heated at 50 °C for 12 h. Pyridine was removed under vacuum and residue was purified by column chromatography on neutralized silica gel using 50% ethyl acetate in petroleum ether to give product **3** (17.1g, Yield 92%).

^{1}H NMR (200MHz, $CDCl_3$): 8.32 (s, 1H, exchanges with D_2O), 7.32-7.47 (m, 10H), 6.82-6.86 (d, *J*=8.85 Hz, 4H), 6.37-6.45 (dd, *J*=9.34, 5.31 Hz, 1H), 4.28 (d, *J*=5.30 Hz, 1H), 4.03 (s, 1H), 3.80 (s, 6H), 3.66 (m, 1H), 3.27 (m, 1H), 1.86 (s, 3H), 1.70 (m, 2H), 0.81 (s, 9H), -0.04 (s, 3H), -0.09 (s, 3H); **^{13}C NMR** (50MHz, $CDCl_3$): 163.6, 158.6, 150.2, 145.0, 136.3, 136.2, 135.5, 130.2, 130.1, 128.2, 127.9, 127.0, 113.2, 110.8, 87.2, 86.6, 84.8, 74.9, 63.5, 55.2, 39.9, 25.7, 18.1, 12.3, -5.4, -5.7; **MS (EI)** *m/z* 658.3074, found 681.34 ($M+ Na^+$); **HRMS (ESI)**: calcd for $C_{37}H_{46}N_2O_7SiNa$: 681.2966, found 681.2956.

3'-*O*-(4, 4'-dimethoxytrityl) thymidine (4)

Compound **3** (15 g, 22.7 mmol) dissolved in 40 mL anhydrous THF and 1N TBAF in THF (34.1 mL, 34.1 mmol) was added. Reaction was stirred at RT for 1 h. THF was removed under reduced pressure and the residue was dissolved in DCM, washed with water and then brine. Organic layer was dried over Na_2SO_4 and concentrated. The

product was purified by column chromatography using 1.5% of methanol in dichloromethane to get product **4** as a white solid (9.8 g, Yield 79%).

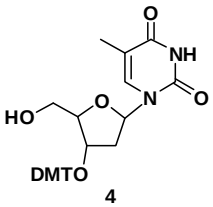

4

^{1}H NMR (200MHz, $CDCl_3$): 8.59 (s, 1H, exchanges with D_2O), 7.24-7.47 (m, 10H), 6.82 (d, *J*=8.46 Hz, 4H), 6.09-6.17 (dd, *J*=8.72, 5.81 Hz, 1H), 4.36 (m, 1H), 3.98 (s, 1H), 3.79 (s, 6H), 3.63-3.69 (m, 1H), 3.35 (m, 1H), 2.50 (bs, 1H, exchanges with D_2O), 1.90-1.95 (m, 1H), 1.85 (s, 3H), 1.69 (s, 1H); **^{13}C NMR** (50MHz, $CDCl_3$): 163.7, 158.8, 150.3, 145.0, 137.1, 136.2, 136.1, 130.1, 128.2, 127.9, 127.0, 113.2, 110.8, 87.2, 87.1, 86.5, 74.2, 62.4, 55.2, 38.5, 12.3; **MS (EI)** *m/z* 544.2210, found 567.21 (M+ Na^+); **HRMS (ESI)**: calcd for $C_{31}H_{32}N_2O_7Na$: 567.2102, found 567.2091.

3'-*O*-(4, 4'-dimethoxytrityl)-5'-formyl Thymidine (5)

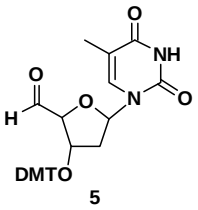

5

Compound **4** (3 g, 5.51 mmol) was dissolved in 20 mL acetonitrile. The flask was equipped with reflux condenser. To it IBX (4.63 g, 16.5 mmol) was added and the reaction mixture was heated at 80 °C for three hrs. After completion of reaction, reaction mixture cooled to room temperature and filtered on bed of celite. Filtrate was concentrated and subjected for filtration column purification on neutralized silica gel. The product eluted at 35-40% acetone in pet ether system to get compound **5** (2.65 g, yield 89%) as a white foam. The product obtained immediately subjected for next reaction.

3'-*O*-(4, 4'-dimethoxytrityl)-4'-hydroxymethylthymidine (6)

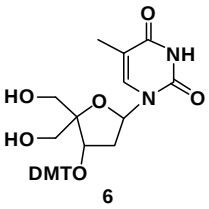

6

To a solution of **5** (2.62 g, 4.83 mmol) in dioxane cooled in waterbath, 35% HCHO (0.787 mL, 9.18 mmol) and 2N NaOH (4.6 mL, 9.18 mmol) were added. Stirring was continued for 5 mins. Reaction mixture was then cooled in ice bath and $NaBH_4$ (0.349 g, 9.18 mmol) was added in portions. Stirring was continued in icebath for 1 hr and then allowed to attain room temperature for 3 h. To the reaction mixture 1 mL water was added and the mixture was neutralized using Dowex H^+ resin. The resin was filtered off and the filtrate evaporated to dryness. The residue was purified by column chromatography with 30% acetone in petroleum ether to give product **6** as a white solid (2 g, Yield 72%).

^{1}H NMR (200MHz, $CDCl_3$): 8.65 (s, 1H, exchanges with D_2O), 7.28-7.46 (m, 10H), 6.98 (s, 1H), 6.83-6.88 (m, 4H), 6.12-6.18 (m, 1H), 4.57 (m, 1H), 4.02 (m, 1H), 3.75-3.80 (m, 8H), 3.39 (m, 1H), 3.08 (bs, 1H, exchanges with D_2O), 2.62 (bs, 1H, exchanges with D_2O), 2.0-2.15 (m, 1H), 1.81 (s, 3H), 1.41-1.55 (m, 1H); **^{13}C NMR** (50MHz, $CDCl_3$): 163.6, 158.8, 150.5, 144.9, 136.6, 135.9, 135.8, 130.3, 128.2, 128.0, 127.2, 113.3, 111.1, 89.1, 87.3, 83.7, 72.6, 63.2, 62.1, 55.2, 38.8, 12.3; **MS (EI)** *m/z* 574.2315, found 597.17 (M+ Na^+); **HRMS (ESI)**: calcd for $C_{32}H_{34}N_2O_8Na$: 597.2207, found 597.2196.

4'-*C*-[(4, 4'-dimethoxytrityl)oxomethyl]-3'-*O*-(4,4'-dimethoxytrityl)thymidine (7)

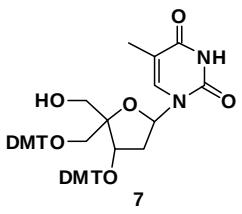

7

To a solution of **6** (1.9 g, 3.31 mmol) in pyridine, DMT-Cl (1.34 g, 3.8 mmol) was added and reaction mixture was allowed to stirr 12 h. Pyridine was removed under vacuum and residue was purified by column chromatography on neutralized silica gel using 45% ethyl acetate in petroleum ether to give product **7** (2.25 g, Yield 78%).

^{1}H NMR (200MHz, $CDCl_3$): 8.60 (s, 1H, exchanges with D_2O), 7.51-7.54 (m, 2H), 7.39-7.45 (m, 4H), 7.16-7.33 (m, 12H), 7.09 (m, 1H), 6.84-6.89 (m, 4H), 6.71-6.77 (m, 4H), 6.26-6.32 (m, 1H), 4.33 (t, *J*=8.09 Hz, 1H), 3.83 (m, 1H), 3.77 (s, 12H), 3.55 (d, *J*=10.36 Hz, 1H), 3.30 (d, *J*=10.36 Hz, 1H), 2.96-3.09 (m, 1H), 2.32-2.47 (m,1H), 2.08 (bs, 1H, exchanges with D_2O), 1.84 (s, 3H), 1.49-1.62 (m, 1H); **^{13}C NMR** (100MHz, $CDCl_3$): 163.6, 158.6, 158.6, 158.4, 158.4, 150.0, 145.1, 144.8, 136.5, 136.0, 135.9, 134.8, 135.7, 130.2, 130.1, 128.1, 127.9, 127.7, 127.0, 126.7, 113.2, 113.2, 113.0, 110.7, 88.5, 87.0, 86.7, 84.1, 71.6, 64.8, 62.9, 55.1, 38.8, 12.4; **MS (EI)** *m/z* 876.3622, found 875.50 (M^+-1).

5'-*O*-(*tert*-butyldimethylsilyl)-4'-*C*-[(4, 4'-dimethoxytrityl) oxomethyl]-3'-*O*-(4, 4'-dimethoxytrityl)thymidine (8)

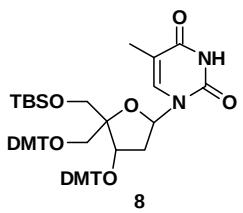

8

Compound **7** (2 g, 2.28 mmol), imidazole (0.446 g, 6.84mmol) and TBS-Cl (0.515 g, 3.42 mmol) was suspended in 4 mL of dry DMF. Reaction mixture was stirred at RT for 3 hrs. DMF was removed under vacuum and product was extracted in ethyl acetate. Organic layer was dried over

Na_2SO_4, concentrated and product was purified by column chromatography using 30% ethyl acetate in petroleum ether to give product **8** (1.71 g, Yield 76 %).

^{1}H NMR (200MHz, $CDCl_3$): 8.27 (s, 1H, exchanges with D_2O), 7.50-7.53 (m, 2H), 7.34-7.43 (m, 4H), 7.22-7.31 (m, 3H), 7.07-7.18 (m, 9H), 7.09 (m, 1H), 6.80-6.86 (m, 4H), 6.67-6.72 (m, 4H), 6.38 (t, *J*=6.84 Hz, 1H), 4.21-4.27 (dd, *J*=7.70, 4.55 Hz, 1H), 3.92 (d, *J*=10.7 Hz, 1H), 3.76 (s, 12H), 3.68 (d, merged with 3.76 peak, 1H), 3.24-2.31 (m, 2H), 1.87 (s, 3H), 1.63 (m, 2H), 0.77 (s, 9H), -0.07 (s, 3H), -0.16 (s, 3H); **^{13}C NMR** (50MHz, $CDCl_3$): 163.5, 158.5, 158.4, 150.0, 145.3, 144.9, 136.0, 135.8, 130.3, 130.2, 130.2, 130.1, 128.2, 128.1, 127.8, 127.7, 126.8, 126.7, 113.1, 113.1, 113.0, 110.7, 88.7, 86.9, 86.5, 83.0, 77.3, 65.1, 64.5, 55.1, 39.2, 25.8, 18.2, 12.5, -5.4, -5.6; **MS (EI)** *m/z* 990.4487, found 1013.54 (M+ Na^+); **HRMS (ESI):** calcd for $C_{59}H_{66}N_2O_{10}SiNa$: 1013.4383, found 1013.4421.

5'-*O*-(*tert*-butyldimethylsilyl)-4'-hydroxymethylthymidine (9)

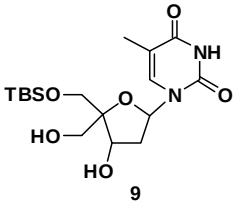

9

Compound **8** (1.5 g, 1.51 mmol) was dissolved in minimum quantity of DCM and to it 2 % dichloroacetic acid in DCM (total 18 mL + 0.3 mL of triisopropyl silane as scavenger) was added in portions. Reaction was monitored by TLC. After completion of reaction mixture was diluted with DCM and saturated Na_2CO_3 wash was given to organic layer. Organic layer dried over Na_2SO_4 and concentrated. The product was purified by column chromatography using 60% ethyl acetate in petroleum ether to give **9** as a white solid (0.438 g, Yield 75%).

^{1}H NMR (200MHz, $CDCl_3$): 9.87 (s, 1H, exchanges with D_2O), 7.55 (s, 1H), 6.45-6.52 (dd, *J*=8.84, 5.43 Hz, 1H), 4.50 (d, *J*=5.05 Hz, 1H), 4.32 (bs, exchanges with D_2O, 1H), 3.70-3.88 (m, 5H), 2.39-2.48 (m, 1H), 2.16-2.30 (m, 1H), 1.90 (s, 3H), 0.92 (s, 9H), 0.12 (s, 6H); **^{13}C NMR** (50MHz, $CDCl_3$): 163.9, 150.7, 135.4, 111.3, 88.8, 84.7, 74.0, 66.1, 63.2, 41.4, 25.8, 18.3, 12.4. -5.4, -5.5; **MS (EI)** *m/z* 386.1873, found 409.16 (M+ Na^+); **HRMS (ESI)**: calcd for $C_{17}H_{30}N_2O_6SiNa$: 409.1771, found 409.1771.

5'-*O*-(*tert*-butyldimethylsilyl)-4'-*C*-[(4, 4'-dimethoxytrityl) oxomethyl]thymidine (10)

To a solution of **9** (0.4 g, 1.03 mmol) in pyridine, DMTr-Cl (0.42 g, 1.24 mmol) was added and reaction mixture was allowed to stirr 12 h. Pyridine was removed under

vacuum and residue was purified by column chromatography on neutralized silica gel using 40% ethyl acetate in petroleum ether to give product **10** (0.583 g, Yield 82%).

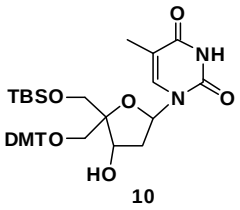

10

^{1}H NMR (500MHz, $CDCl_3$): 8.43 (s, 1H, exchanges with D_2O), 7.55 (s, 1H), 7.88 (d, *J*=7.33 Hz, 2H), 7.22-7.33 (m, 8H), 6.84 (m, 4H), 6.43-6.46 (m, 1H), 4.50 (s, 1H), 3.90 (d, *J*=10.68 Hz, 1H), 3.80 (s, 6H), 3.62 (d, *J*=10.68 Hz, 1H), 3.35 (d, *J*=9.77 Hz, 1H), 3.24 (d, *J*=9.46 Hz, 1H), 2.88 (bs, exchanges with D_2O, 1H), 2.34-2.38 (m, 1H), 2.20-2.26 (m, 1H), 1.91 (s, 3H), 0.92 (s, 9H), 0.12 (s, 3H), 0.11 (s, 3H); **^{13}C NMR** (125MHz, $CDCl_3$): 163.5, 158.7, 150.1, 143.8, 135.5, 134.8, 134.7, 129.8, 129.8, 128.1, 127.7, 127.1, 113.4, 110.8, 88.8, 87.2, 84.6, 73.9, 66.5, 63.2, 55.2, 40.8, 25.9, 18.4, 12.4, -5.42, -5.45; **MS (EI)** *m/z* 688.3180, found 711.38 (M+ Na^+); **HRMS (ESI)**: calcd for $C_{38}H_{48}N_2O_8SiNa$: 711.3078, found 711.3098.

5'-*O*-(*tert*-butyldimethylsilyl)-3'-*O*-[(2-cyanoethoxy) diisopropylaminophosphino]-4'-*C*-[(4,4'-dimethoxytrityl)oxomethyl]thymidine (11)

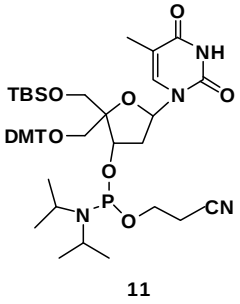

11

Compound **10** (0.200 g, 0.29 mmol) was dissolved in dry dichloromethane (5 mL) followed by the addition of diisopropylethylamine (0.126 mL, 0.726mmol). Then 2-cynoethyl-*N*, *N'*-diisopropyl-chloro phosphine (77 µL, 0.34 mmol) was added to the solution at 0 °C and reaction mixture was stirred at room temperature for 3 hours. The contents were then diluted with DCM and washed with 5% $NaHCO_3$ solution. The product was purified by column chromatography using 1% Triethylamine in 30% petroleum ether in DCM to give (0.153 g, yield 60%).

^{31}P NMR (400MHz, $CDCl_3$) 149.3, 148.5.

Crystal Data:

Single crystals of the compound were grown by slow evaporation of the solution in $CDCl_3$. Colourless crystal of approximate size 0.19 x 0.14 x 0.11 mm^3, was used for data collection on *Bruker SMART APEX* CCD diffractometer using Mo K_α radiation with fine focus tube with 50kV and 30mA. Crystal to detector distance 6.05 cm, 512 x 512 pixels / frame, quadrant data acquisition. Total frames = 2424,

Oscillation/frame -0.3º, exposure/frame = 10.0 sec/frame, maximum detector swing angle = –30.0º, beam center = (260.2, 252.5), in plane spot width = 1.24, SAINT integration, θ range = 1.69 to 25.00 º, completeness to θ of 25.0 º is 99.9.0 %. SADABS correction applied , C17 H30 N2 O6 Si, *M* = 386.52. Crystals belong to Monoclinic, space group $P2_1$, a = 10.4579(5), *b* = 16.8927(8)), *c* = 12.7383(6) Å, *V* = 2125.20(17) $Å^3$, *Z* = 4, D_c = 1.208 g /cc, μ (MoK_α) = 0.143 mm^{-1}, *T* = 293(2) K, 20740 reflections measured, 7468 unique [I>2σ(I)], R value 0.0543, wR2 = 0.1285. All the data were corrected for Lorentzian, polarisation and absorption effects. SHELX-97 (ShelxTL)[38] was used for structure solution and full matrix least squares refinement on F^2. Hydrogen atoms were included in the refinement as per the riding model. Largest diff. peak and hole 0.353 and -0.289 e.$Å^{-3}$. Data collection and refinement parameters are listed in table 1. The conformation of the molecule at C1', C3' and C4' is *R*, *S* and *R* respectively.

Table 1. Crystal data and structure refinement for compound **9**

Empirical formula	C_{17} H_{30} N_2 O_6 Si
Formula weight	386.52
Temperature	273(2) K
Wavelength	0.71073 Å
Crystal system	Monoclinic
Space group	P21
Unit cell dimensions	a = 10.4579(5) Å α= 90°.
	b = 16.8927(8) Å β= 109.200(1)°.
	c = 12.7383(6) Å γ= 90°.
Volume	2125.20(17) $Å^3$
Z	4
Density (calculated)	1.208 g/cc
Absorption coefficient	0.143 mm^{-1}
F(000)	832
Crystal size	0.19 x 0.14 x 0.11 mm^3
Theta range for data collection	1.69 to 25.00°.
Index ranges	-12<=h<=12, -20<=k<=20, -15<=l<=15
Reflections collected	20740
Independent reflections	7468 [R(int) = 0.0265]
Completeness to theta = 25.00°	99.9 %

Absorption correction	Semi-empirical from equivalents
Max. and min. transmission	0.9845 and 0.9734
Refinement method	Full-matrix least-squares on F^2
Data / restraints / parameters	7468 / 1 / 485
Goodness-of-fit on F^2	1.071
Final R indices [I>2sigma(I)]	R1 = 0.0543, wR2 = 0.1285
R indices (all data)	R1 = 0.0656, wR2 = 0.1360
Absolute structure parameter	0.22(14)
Largest diff. peak and hole	0.353 and -0.289 e.$Å^{-3}$

Making buffers and gel for RNase H experiment

All buffer, gel and dye were stored in refrigerator.

1) Tris-HCl buffer (10 mM, 100 mL, pH 7.5)

Tris-HCl (157 mg, 10mM), $MgCl_2 \cdot 6H_2O$ (10 mg, 0.5 mM) and KCl (186 mg, 25 mM) were dissolved in total 100 mL of autoclaved DI water. pH was adjusted with Tris base and HCl.

2) 29:1 acrylamide: N, N'-methylene bis acryl amide gel (100 mL)

29 g of acrylamide and 1 g of N, N'-methylene bis acryl amide was dissolved in total 100 mL of autoclaved DI water.

3) 5X TBE buffer (500 mL, pH 8)

Tris (hydroxymethyl)methyl amine i.e., Tris base (27 g) , boric acid (13.75 g) and EDTA (1.462 g) was dissolived in total 500 mL of autoclaved DI water. pH was adjusted with tris base or HCl.

4) 1X TBE buffer (500 mL)

100 mL of 5X TBE buffer diluted to 500 mL volume with autoclaved DI water.

5) Bromophenol dye

40% of glycerol solution in DI water (V/V) + 0.25 % bromophenol blue dye was used as tracer dye.

6) 40% sucrose solution in DI water (w/v): equal volume of this solution was added to dye and samples before loading on the gel.

7) 10% ammonium persulphate solution: 50 mg ammonium pursulphate solution in 500 µL autoclaved DI water. This solution was prepared freshly at the time of preparing 20 % acryl amide gel.

8) 100 mM EDTA solution: 36 mg in 1 mL of DI water. This solution was used as stop activity of RNase H enzyme.

9) 20% acrylamide gel (40 mL)

26.64 mL of acrylamide: N, N'-methylene bis acryl amide solution (29:1), 5.08 mL of autoclaved DI water and 8 mL of 5X TBE were added together in a conical, degassed it for 20-25 min by applying vaccum. Then to it 280 µL of freshely prepared 10% ammonium persulphate solution and 18.4 µL of TMEDA was added. After shaking for 30 second to 1min, immediately poured it in blank gel plates and left it for 30 mins to form a proper gel.

4.9 Appendix

Compounds	Page No.
Compound 2: ^{1}H, ^{13}C NMR and DEPT NMR	256
Compound 3: ^{1}H, ^{13}C NMR and DEPT NMR	257
Compound 4: ^{1}H, ^{13}C NMR and DEPT NMR	258
Compound 6: ^{1}H, ^{13}C NMR and DEPT NMR	259
Compound 7: ^{1}H, ^{13}C NMR and DEPT NMR	260
Compound 8: ^{1}H, ^{13}C NMR and DEPT NMR	261
Compound 9: ^{1}H, ^{13}C NMR and DEPT NMR	262
Compound 10: ^{1}H, ^{13}C NMR and DEPT NMR	263
Compound 10 : HRMS	264
Compound 10 : ^{31}P NMR	264
HPLC chromatogram of ON1 and ON2	265
MALDI-TOF spectra of ON1 and ON2	266

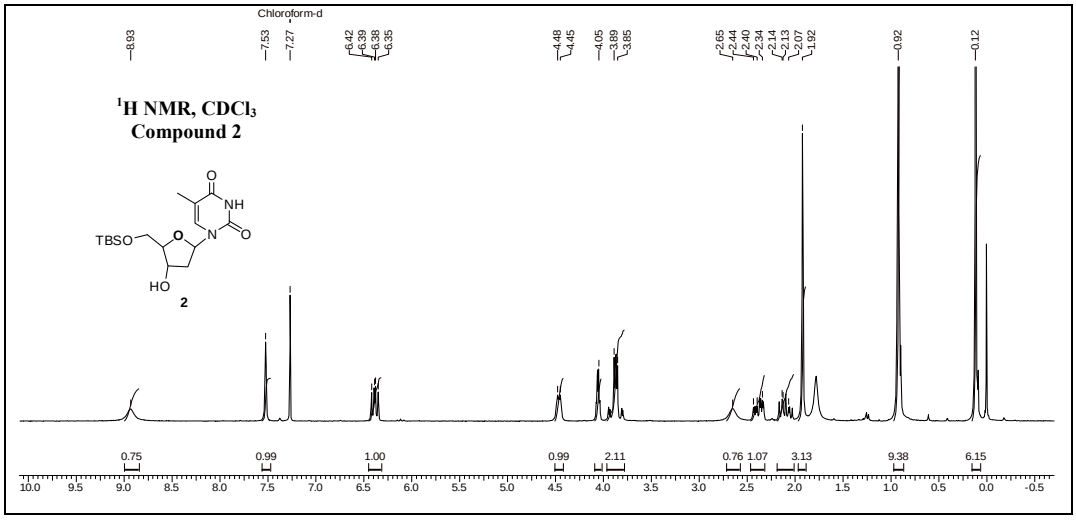
Chloroform-d
8.93
7.53
7.27
6.42
6.39
6.38
6.35
4.48
4.45
4.05
3.89
3.85
2.65
2.44
2.40
2.34
2.14
2.13
2.07
1.92
0.92
0.12
^{1}H NMR, CDCl$_3$
Compound 2
TBSO
HO
NH
2
0.75
0.99
1.00
0.99
2.11
0.76
1.07
3.13
9.38
6.15

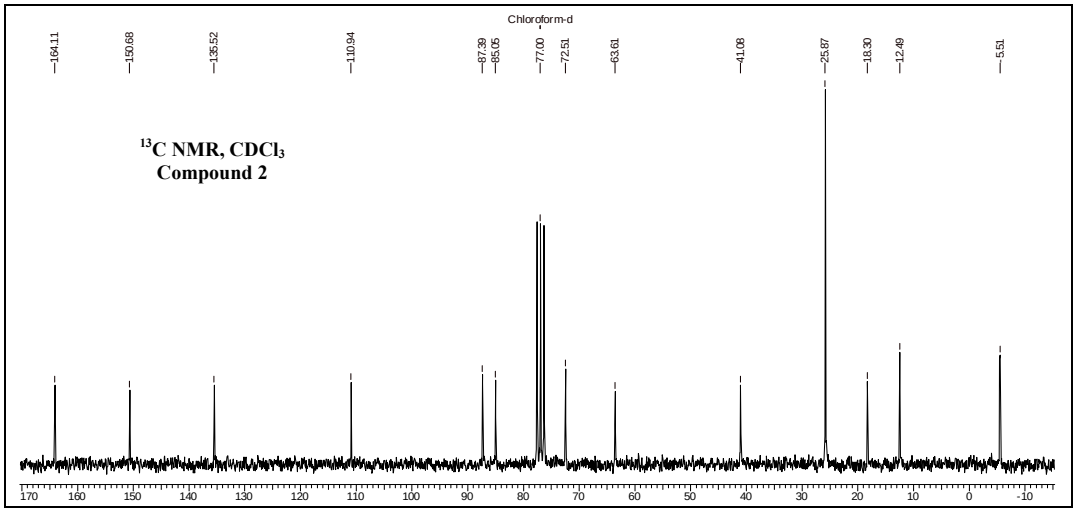
Chloroform-d
164.11
150.68
135.52
110.94
87.39
85.05
77.00
72.51
63.61
41.08
25.87
18.30
12.49
5.51
^{13}C NMR, CDCl$_3$
Compound 2

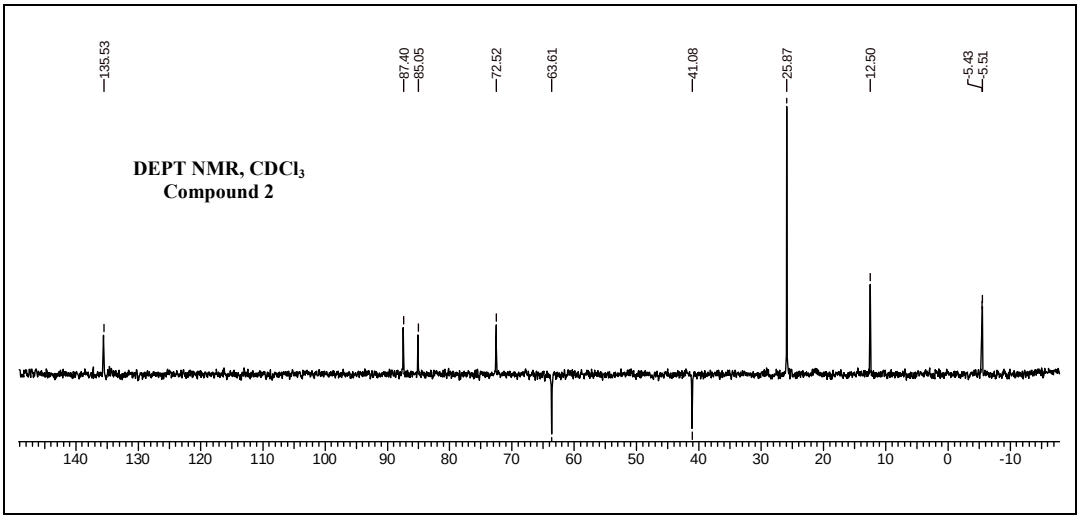
135.53
87.40
85.05
72.52
63.61
41.08
25.87
12.50
5.43
5.51
DEPT NMR, CDCl$_3$
Compound 2

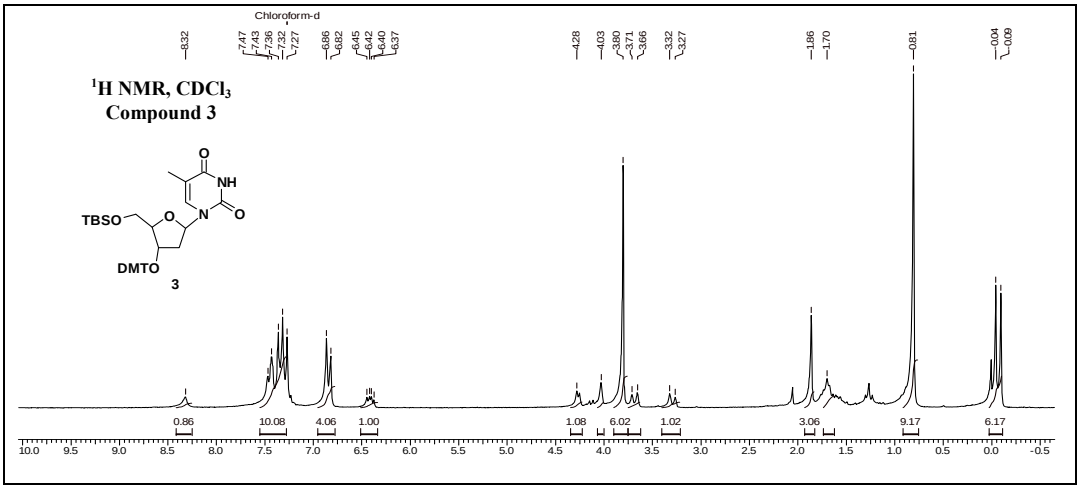
Chloroform-d
8.32
7.47
7.43
7.36
7.32
7.27
6.86
6.82
6.45
6.42
6.40
6.37
4.28
4.03
3.80
3.71
3.66
3.32
3.27
1.86
1.70
0.81
0.04
0.09
^{1}H NMR, CDCl$_3$
Compound 3
O
NH
N
O
TBSO
O
DMTO
3
0.86
10.08
4.06
1.00
1.08
6.02
1.02
3.06
9.17
6.17
10.0 9.5 9.0 8.5 8.0 7.5 7.0 6.5 6.0 5.5 5.0 4.5 4.0 3.5 3.0 2.5 2.0 1.5 1.0 0.5 0.0 -0.5

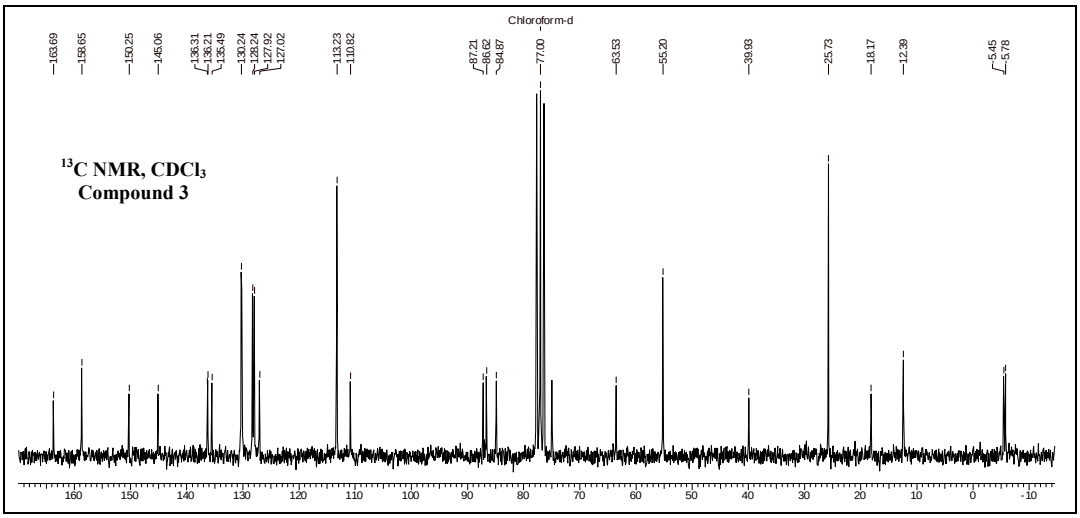
Chloroform-d
163.69
158.65
150.25
145.06
136.31
136.21
135.49
130.24
128.24
127.92
127.02
113.23
110.82
87.21
86.62
84.87
77.00
63.53
55.20
39.93
25.73
18.17
12.39
5.45
5.78
^{13}C NMR, CDCl$_3$
Compound 3
160 150 140 130 120 110 100 90 80 70 60 50 40 30 20 10 0 -10

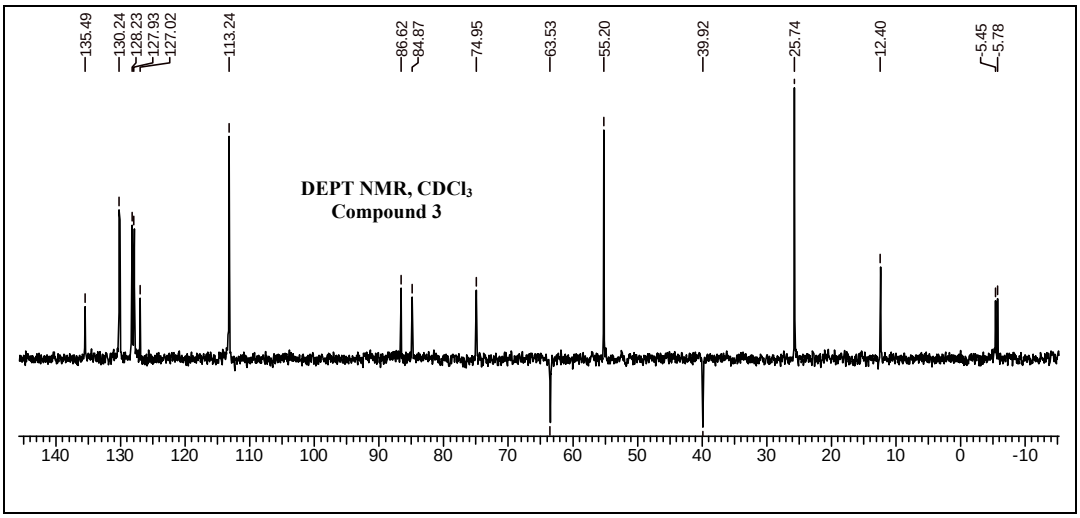
135.49
130.24
128.23
127.93
127.02
113.24
86.62
84.87
74.95
63.53
55.20
39.92
25.74
12.40
5.45
5.78
DEPT NMR, CDCl$_3$
Compound 3
140 130 120 110 100 90 80 70 60 50 40 30 20 10 0 -10

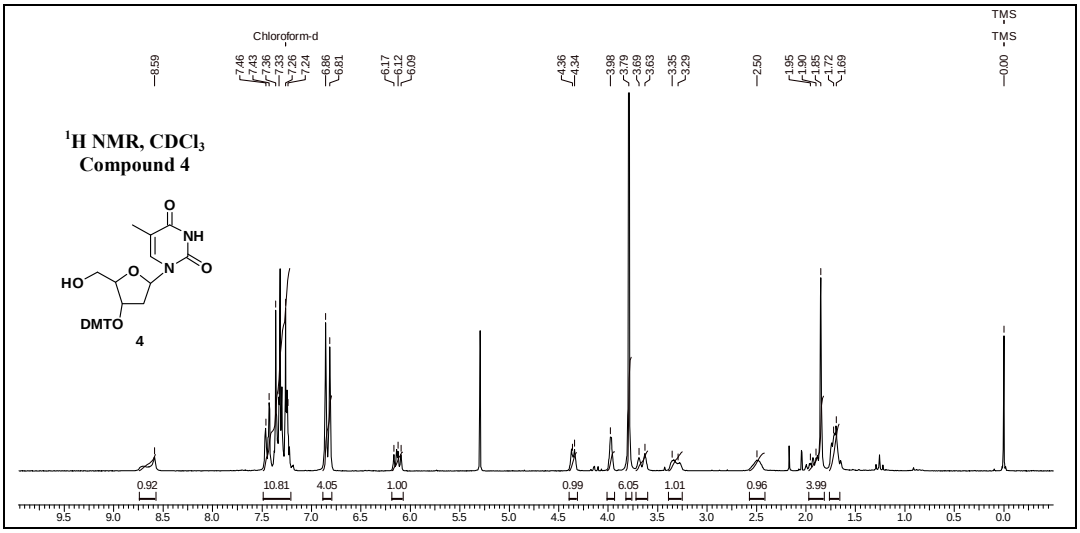
Chloroform-d
TMS
TMS
8.59
7.46
7.43
7.36
7.33
7.26
7.24
6.86
6.81
6.17
6.12
6.09
4.36
4.34
3.98
3.79
3.69
3.63
3.35
3.29
2.50
1.95
1.90
1.85
1.72
1.69
0.00
^{1}H NMR, CDCl$_3$
Compound 4
O
NH
N
O
HO
O
DMTO
4
0.92
10.81
4.05
1.00
0.99
6.05
1.01
0.96
3.99

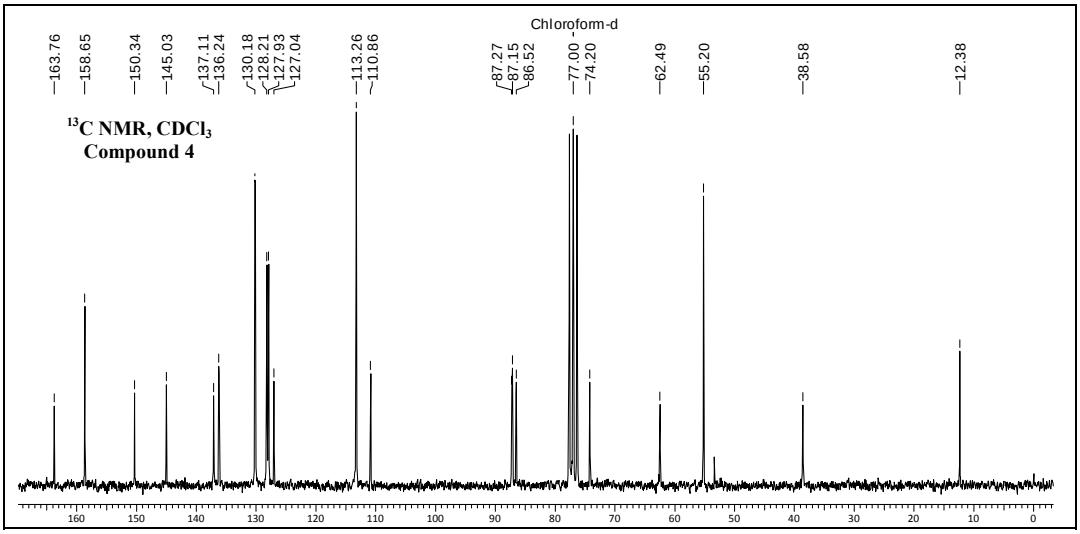
Chloroform-d
163.76
158.65
150.34
145.03
137.11
136.24
130.18
128.21
127.93
127.04
113.26
110.86
87.27
87.15
86.52
77.00
74.20
62.49
55.20
38.58
12.38
^{13}C NMR, CDCl$_3$
Compound 4

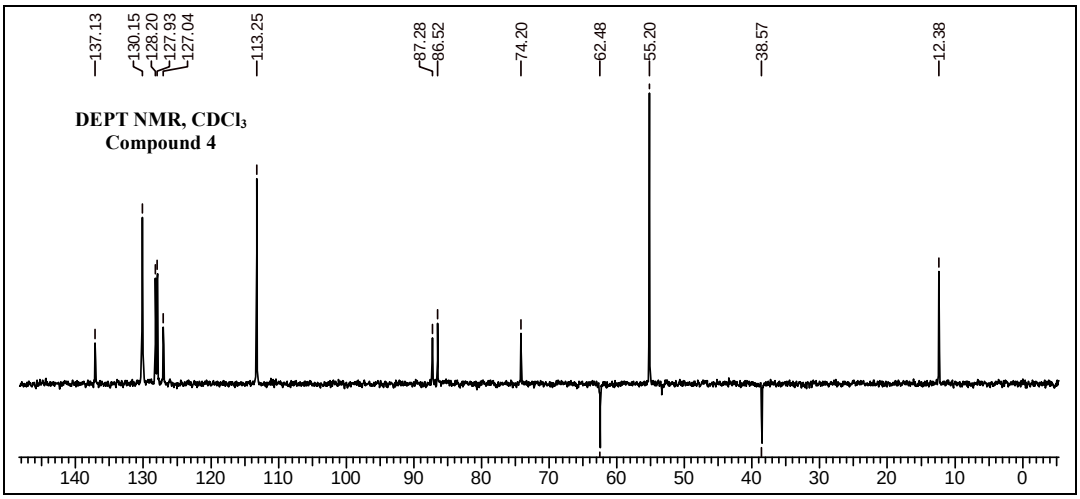
137.13
130.15
128.20
127.93
127.04
113.25
87.28
86.52
74.20
62.48
55.20
38.57
12.38
DEPT NMR, CDCl$_3$
Compound 4

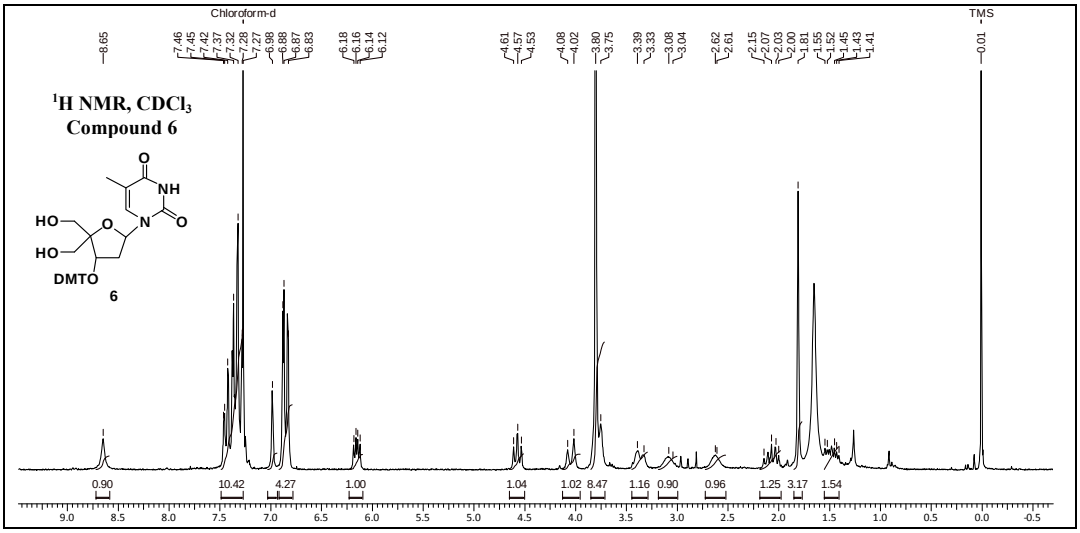
Chloroform-d
TMS
8.65
7.46
7.45
7.42
7.37
7.32
7.28
7.27
6.98
6.88
6.87
6.83
6.18
6.16
6.14
6.12
4.61
4.57
4.53
4.08
4.02
3.90
3.75
3.39
3.33
3.08
3.04
2.62
2.61
2.15
2.07
2.03
2.00
1.81
1.55
1.52
1.45
1.43
1.41
0.01
0.90
10.42
4.27
1.00
1.04
1.02
8.47
1.16
0.90
0.96
1.25
3.17
1.54
^{1}H NMR, CDCl$_3$
Compound 6
HO
HO
DMTO
O
NH
N
O
6

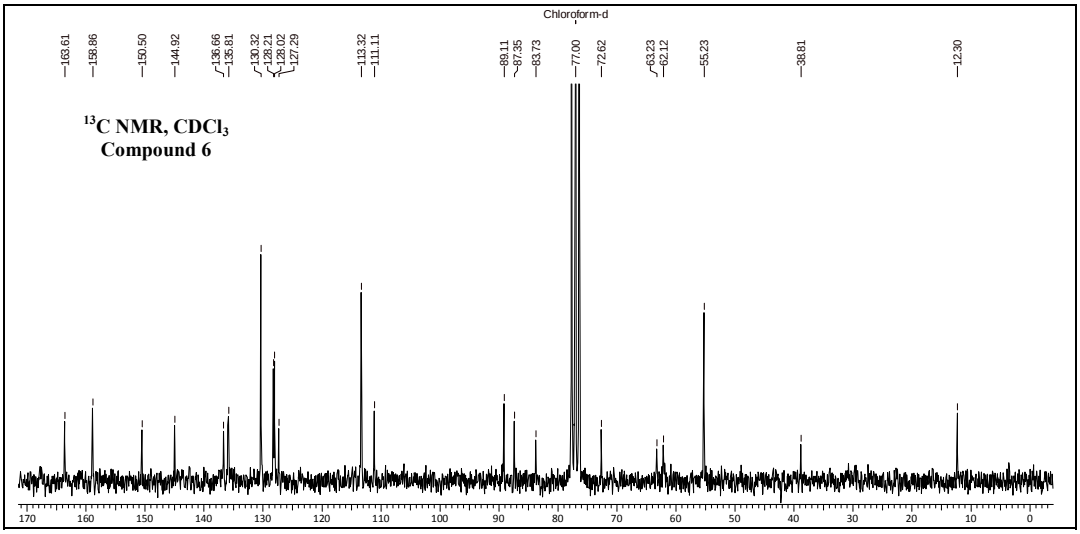
Chloroform-d
163.61
158.86
150.50
144.92
136.66
135.81
130.32
128.21
128.02
127.29
113.32
111.11
89.11
87.35
83.73
77.00
72.62
63.23
62.12
55.23
38.81
12.30
^{13}C NMR, CDCl$_3$
Compound 6

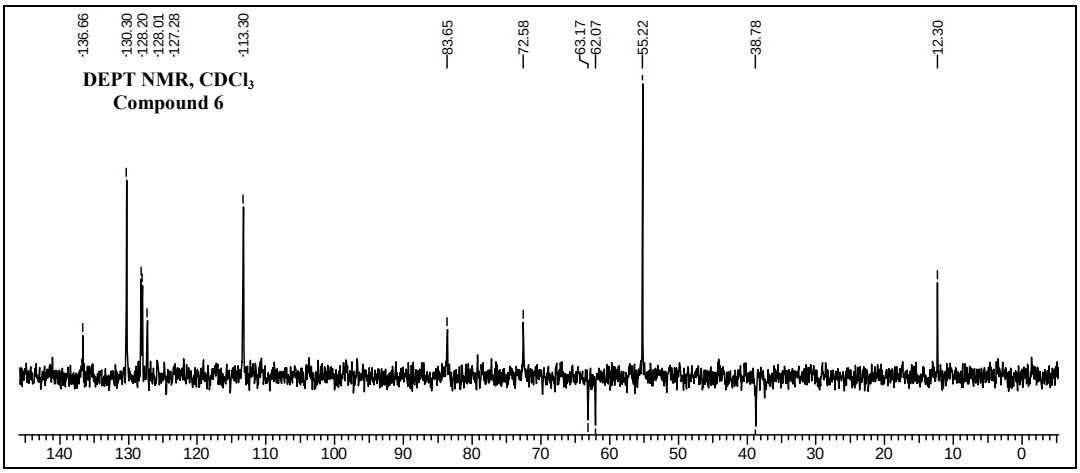
136.66
130.30
128.20
128.01
127.28
113.30
83.65
72.58
63.17
62.07
55.22
38.78
12.30
DEPT NMR, CDCl$_3$
Compound 6

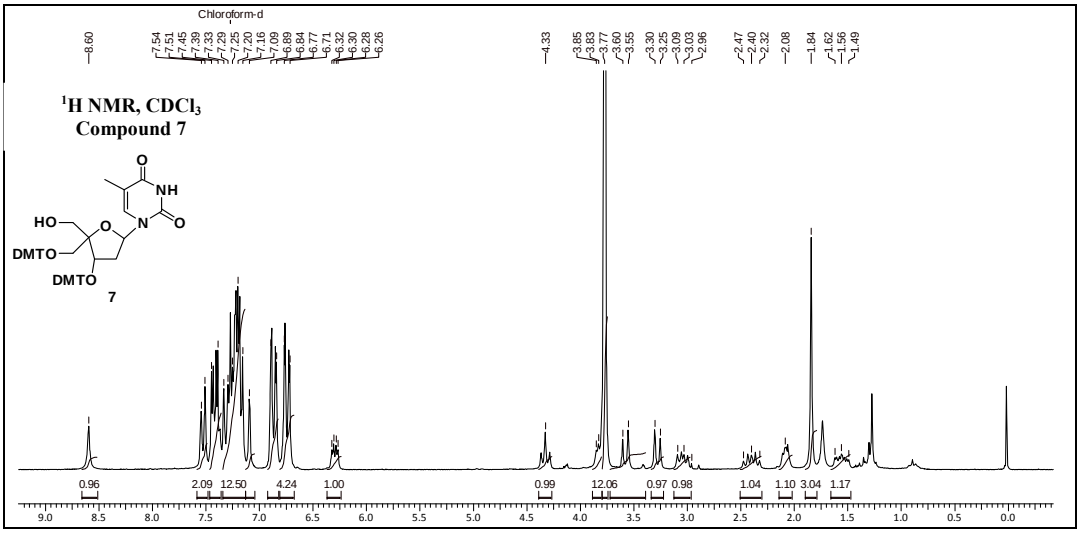
Chloroform-d
8.60
7.54
7.51
7.45
7.39
7.33
7.29
7.25
7.20
7.16
7.09
6.89
6.84
6.77
6.71
6.32
6.30
6.28
6.26
4.33
3.85
3.83
3.77
3.60
3.55
3.30
3.25
3.09
3.03
2.96
2.47
2.40
2.32
2.08
1.84
1.62
1.56
1.49
^{1}H NMR, CDCl$_3$
Compound 7
O
NH
N
O
HO
O
DMTO
DMTO
7
0.96
2.09
12.50
4.24
1.00
0.99
12.06
0.97
0.98
1.04
1.10
3.04
1.17
9.0
8.5
8.0
7.5
7.0
6.5
6.0
5.5
5.0
4.5
4.0
3.5
3.0
2.5
2.0
1.5
1.0
0.5
0.0

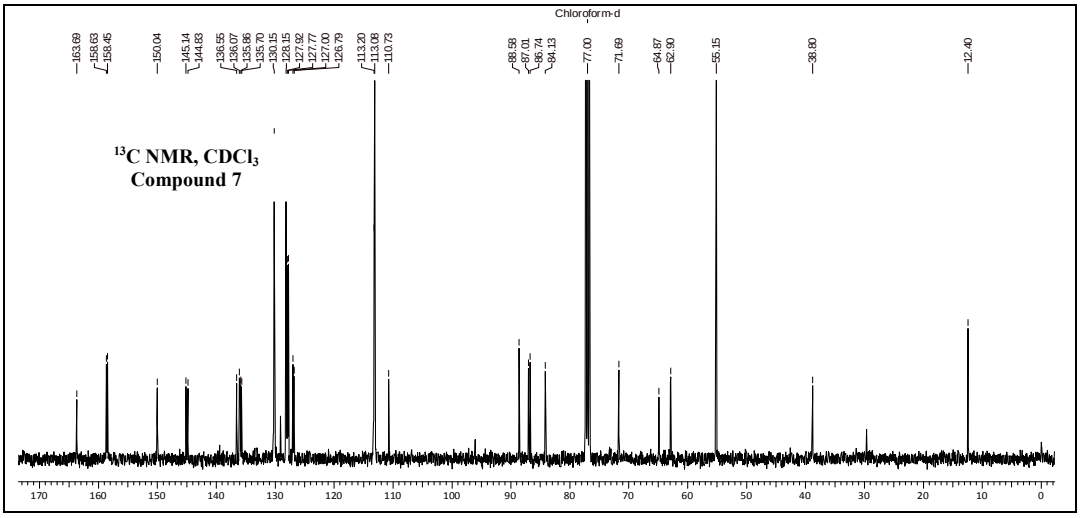
Chloroform-d
163.69
158.63
158.45
150.04
145.14
144.83
136.55
136.07
135.86
135.70
130.15
128.15
127.92
127.77
127.00
126.79
113.20
113.08
110.73
88.58
87.01
86.74
84.13
77.00
71.69
64.87
62.90
55.15
38.80
12.40
^{13}C NMR, CDCl$_3$
Compound 7
170
160
150
140
130
120
110
100
90
80
70
60
50
40
30
20
10
0

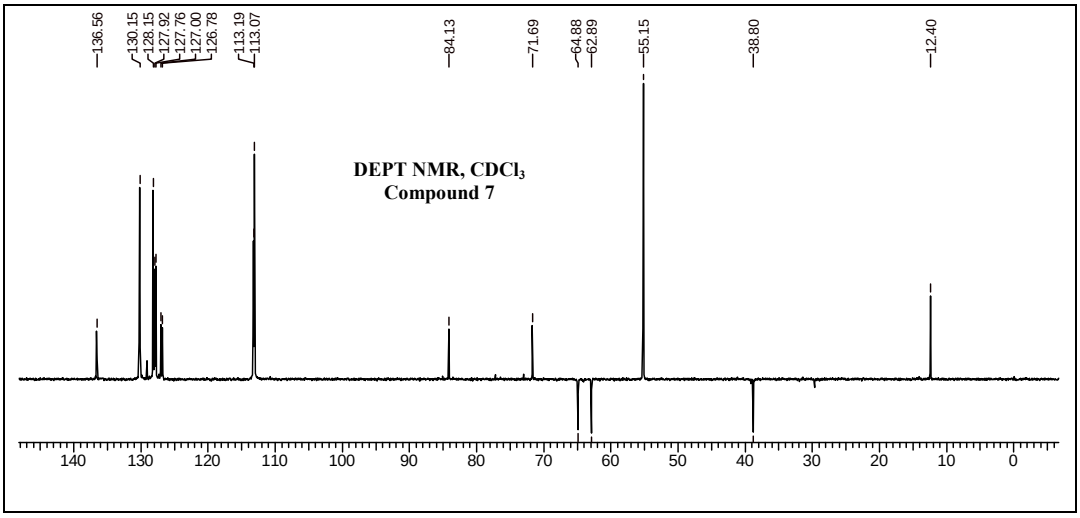
136.56
130.15
128.15
127.92
127.76
127.00
126.78
113.19
113.07
84.13
71.69
64.88
62.89
55.15
38.80
12.40
DEPT NMR, CDCl$_3$
Compound 7
140
130
120
110
100
90
80
70
60
50
40
30
20
10
0

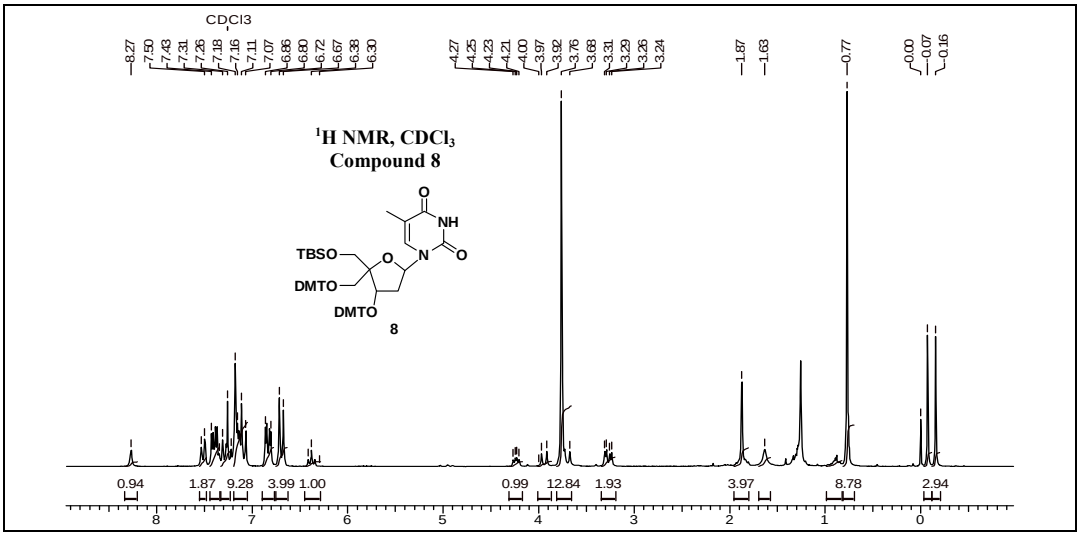
CDCl3
^{1}H NMR, CDCl$_3$
Compound 8
TBSO
DMTO
DMTO
8
0.94 1.87 9.28 3.99 1.00 0.99 12.84 1.93 3.97 8.78 2.94

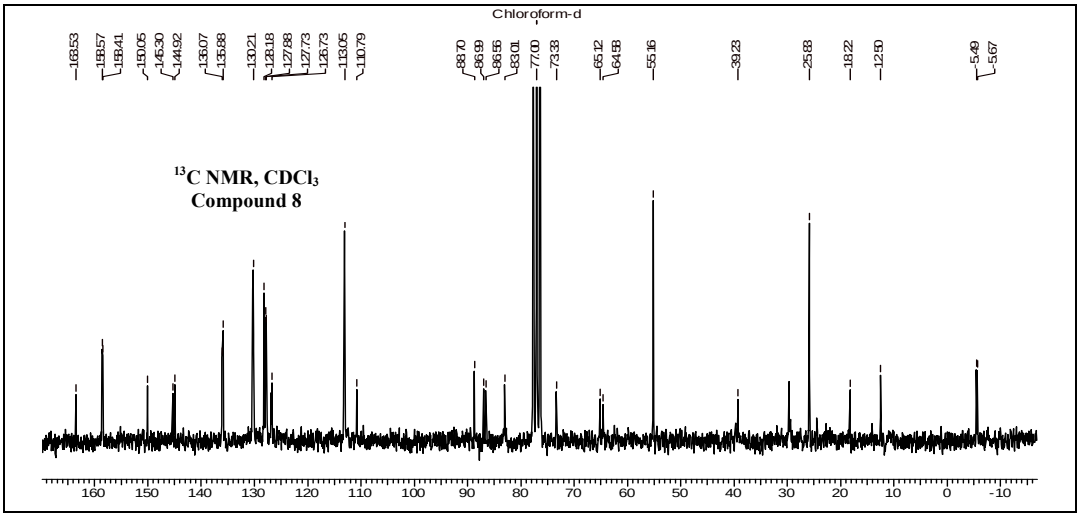
Chloroform-d
^{13}C NMR, CDCl$_3$
Compound 8

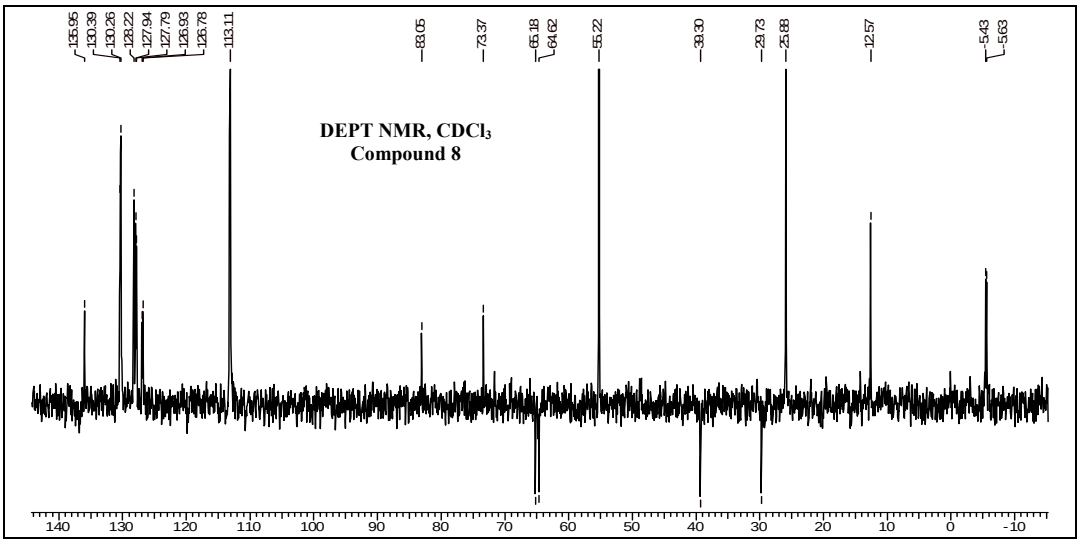
DEPT NMR, CDCl$_3$
Compound 8

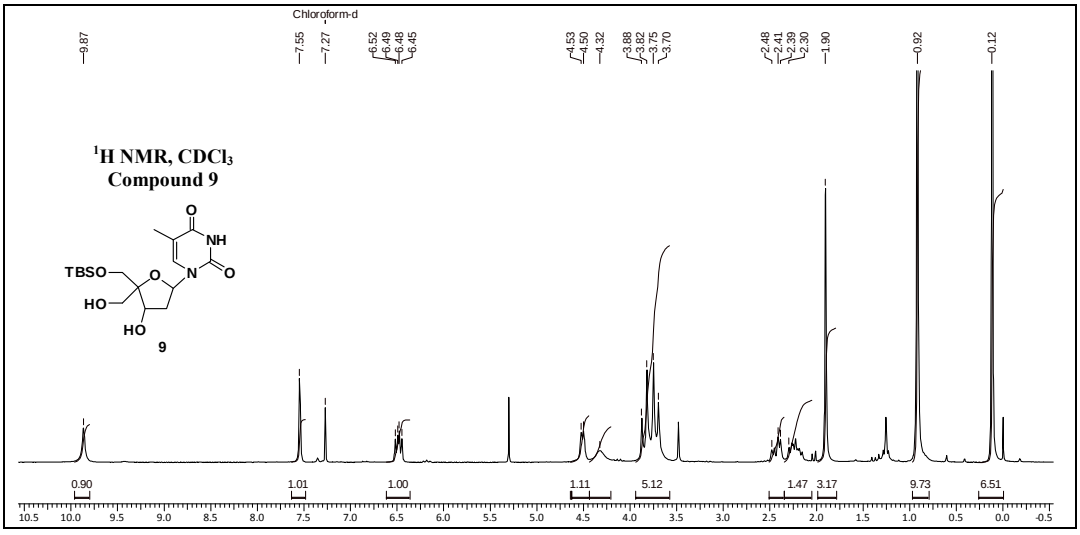
Chloroform-d
9.87
7.55
7.27
6.52
6.49
6.48
6.45
4.53
4.50
4.32
3.88
3.82
3.75
3.70
2.48
2.41
2.39
2.30
1.90
0.92
0.12
^{1}H NMR, CDCl$_3$
Compound 9
TBSO
HO
HO
9
0.90
1.01
1.00
1.11
5.12
1.47
3.17
9.73
6.51

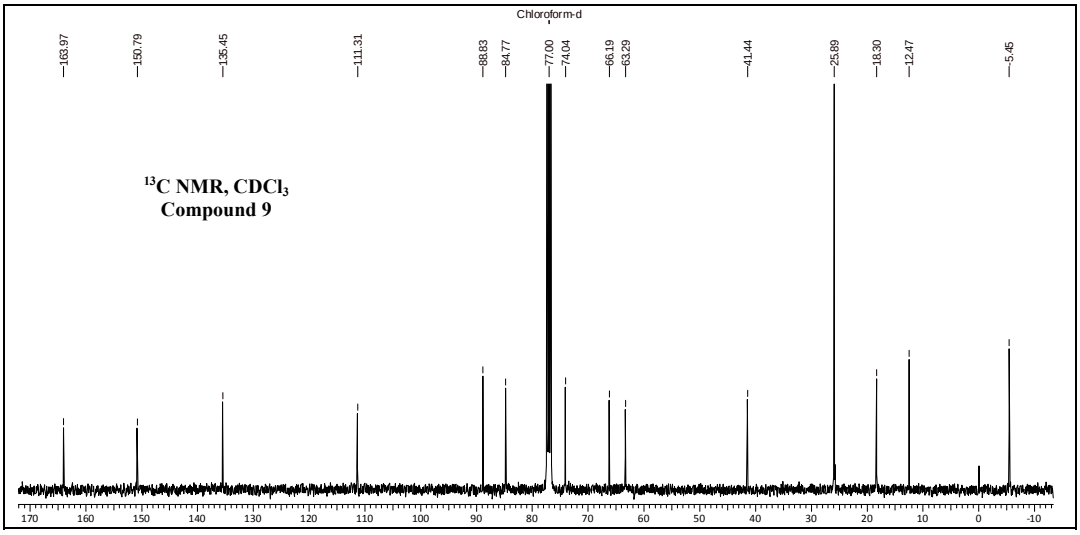
Chloroform-d
163.97
150.79
135.45
111.31
88.83
84.77
77.00
74.04
66.19
63.29
41.44
25.89
18.30
12.47
5.45
^{13}C NMR, CDCl$_3$
Compound 9

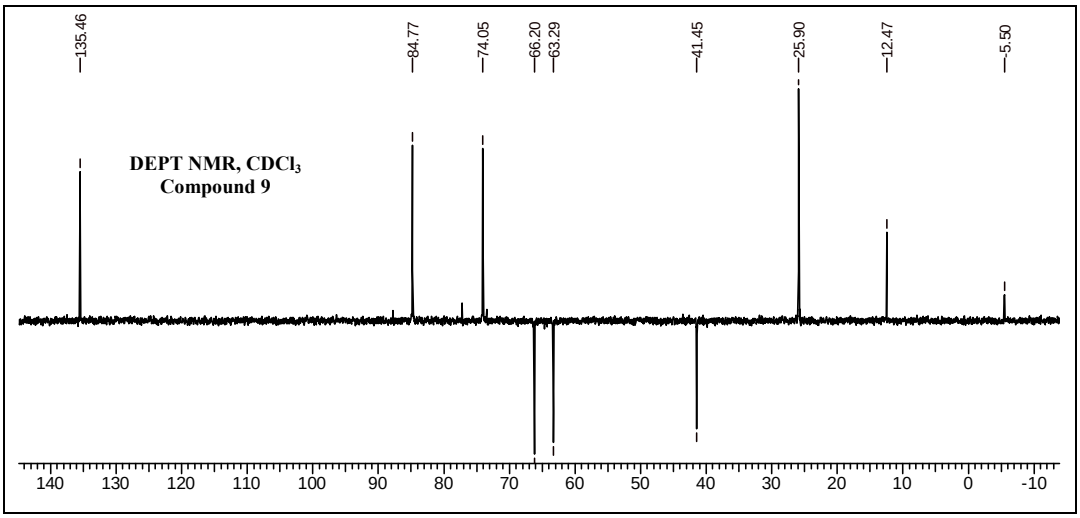
135.46
84.77
74.05
66.20
63.29
41.45
25.90
12.47
5.50
DEPT NMR, CDCl$_3$
Compound 9

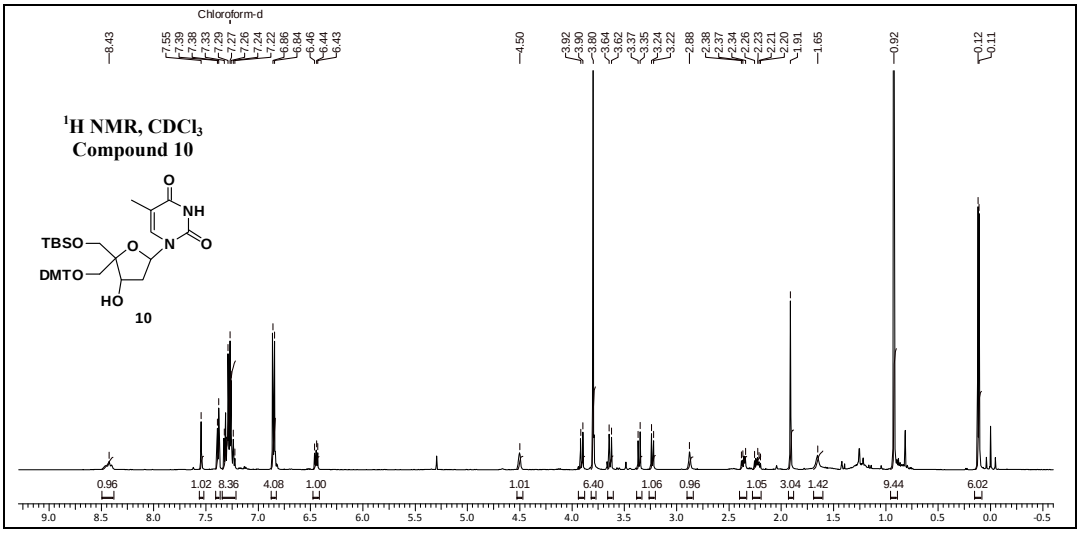
Chloroform-d
^{1}H NMR, CDCl$_3$
Compound 10
TBSO
DMTO
HO
NH
O
N
10

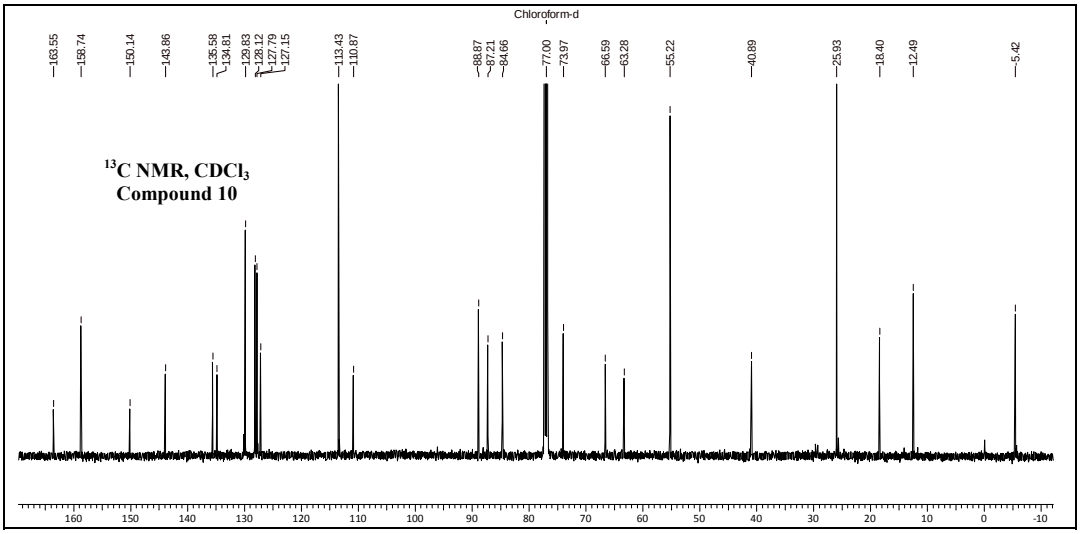
Chloroform-d
^{13}C NMR, CDCl$_3$
Compound 10

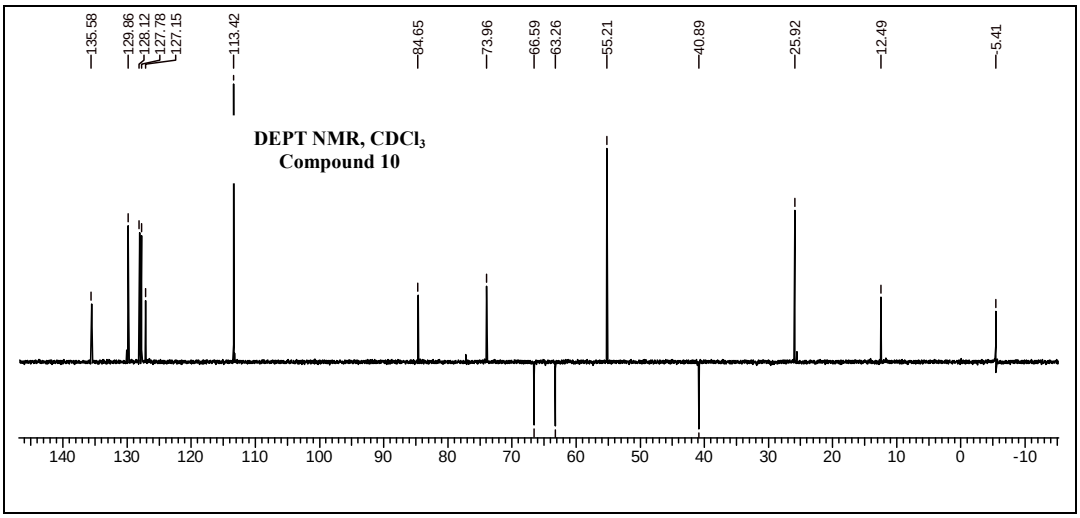
DEPT NMR, CDCl$_3$
Compound 10

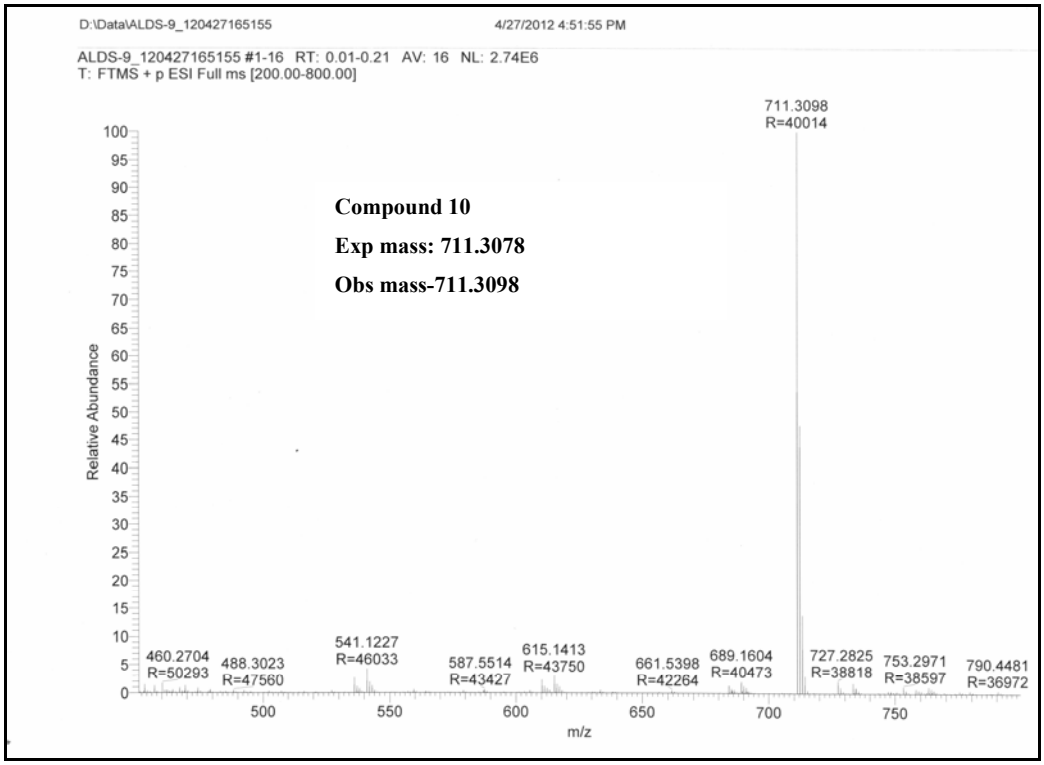
D:\Data\ALDS-9_120427165155
4/27/2012 4:51:55 PM
ALDS-9_120427165155 #1-16 RT: 0.01-0.21 AV: 16 NL: 2.74E6
T: FTMS + p ESI Full ms [200.00-800.00]
711.3098
R=40014
Compound 10
Exp mass: 711.3078
Obs mass-711.3098
Relative Abundance
460.2704 R=50293
488.3023 R=47560
541.1227 R=46033
587.5514 R=43427
615.1413 R=43750
661.5398 R=42264
689.1604 R=40473
727.2825 R=38818
753.2971 R=38597
790.4481 R=36972
m/z

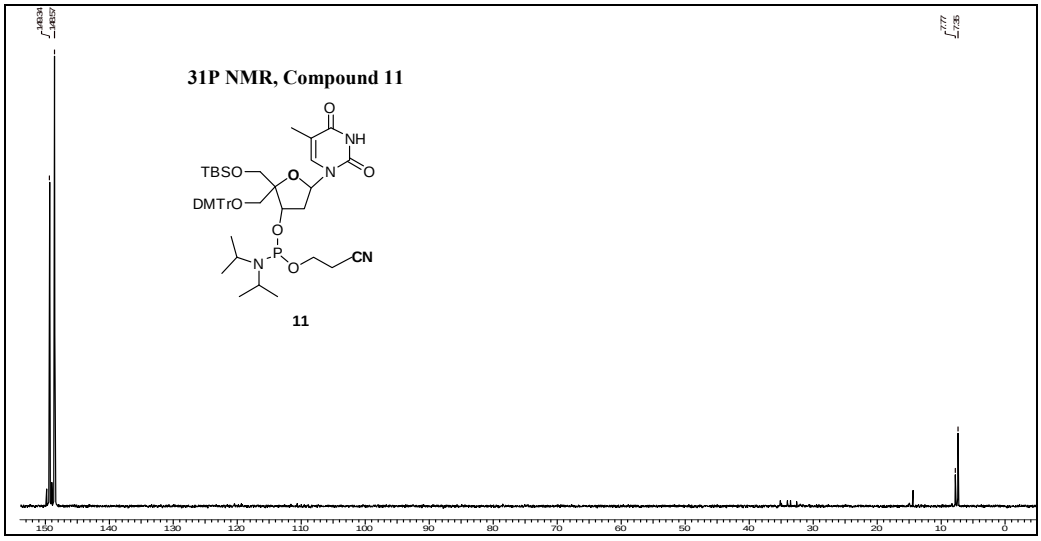
31P NMR, Compound 11
TBSO
DMTrO
NH
N
O
P
CN
11

HPLC chromatogram for **ON1** and **ON2**

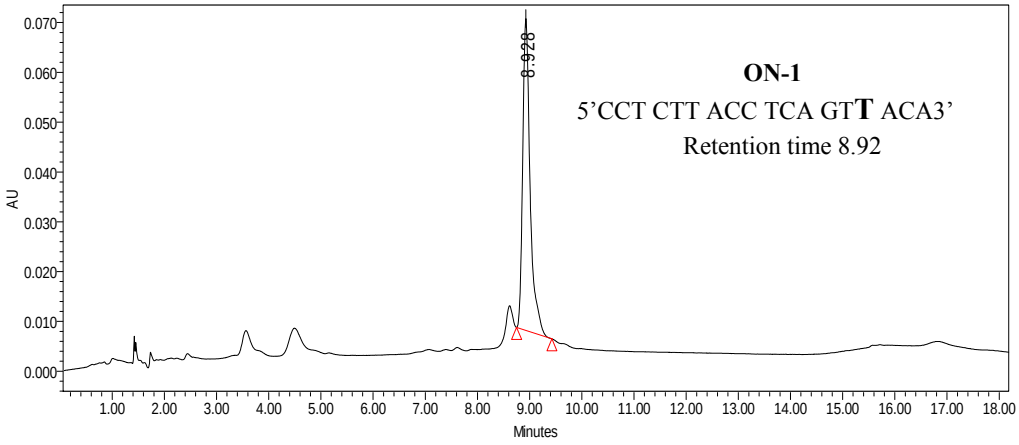

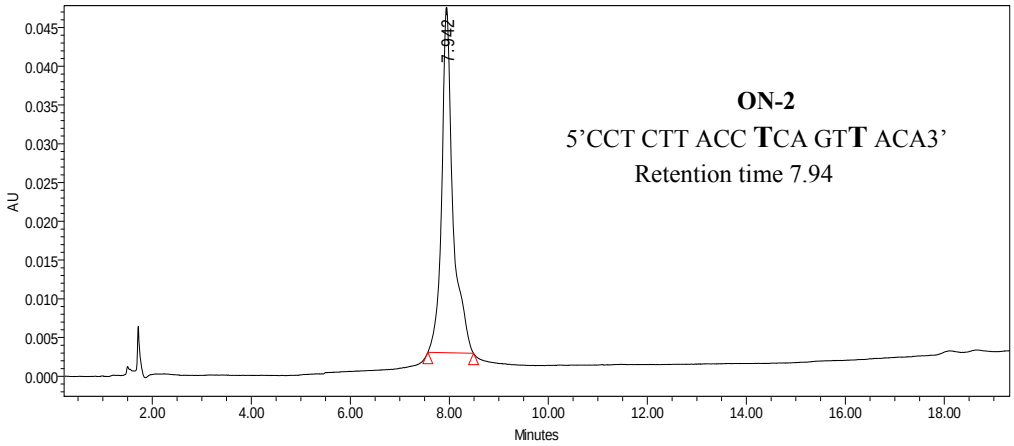

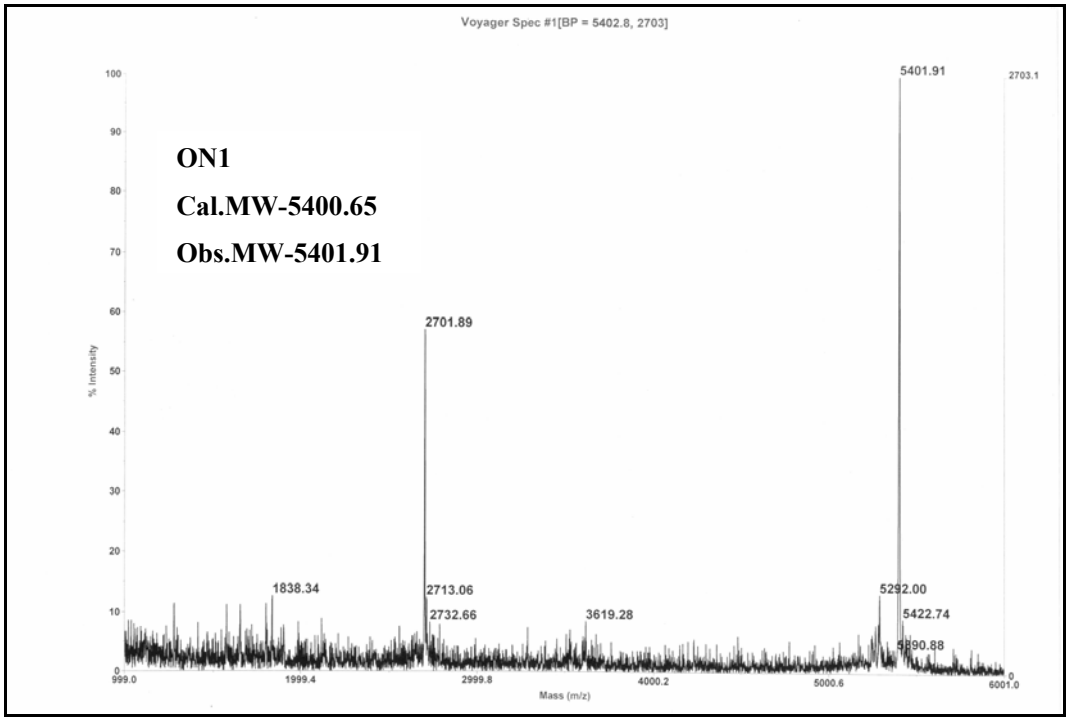
Voyager Spec #1[BP = 5402.8, 2703]
ON1
Cal.MW-5400.65
Obs.MW-5401.91
5401.91
2703.1
2701.89
1838.34
2713.06
2732.66
3619.28
5292.00
5422.74
5890.88
% Intensity
Mass (m/z)

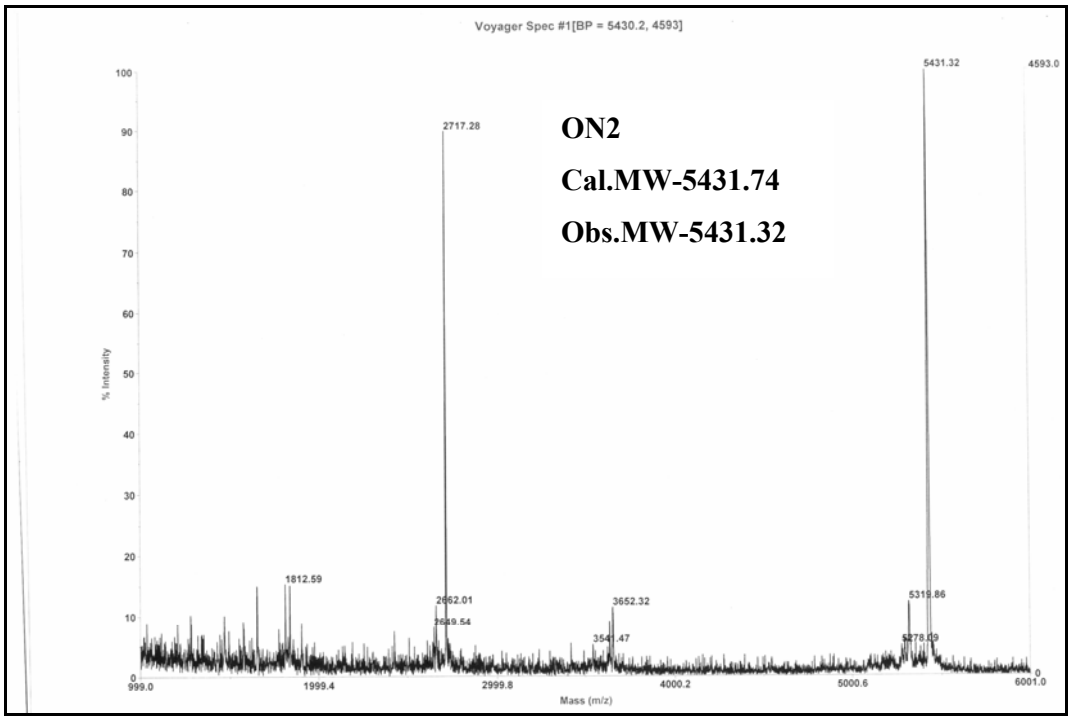
Voyager Spec #1[BP = 5430.2, 4593]
ON2
Cal.MW-5431.74
Obs.MW-5431.32
5431.32
4593.0
2717.28
1812.59
2662.01
3652.32
3541.47
5319.86
% Intensity
Mass (m/z)

4.10 References

1. (a) Bennet, C. F.; Swayze, E. E. RNA targeting therapeutics: molecular mechanisms of antisense oligonucleotides as a therapeutic platform. *Annu. Rev. Pharmacol. Toxicol.* **2010**, *50*, 259; (b) Kole, R.; Krainer, A. R.; Altman, S. RNA therapeutics: beyond RNA interference and antisense oligonucleotides *Nature Rev. Drug Discov.* **2012**, *11*, 125.
2. Crouch, R. J.; Dirksen, M. L. in Nucleases, Vol. 14, Cold Spring Harbor Monograph Series, Plainview, **1982**, 211.
3. Nakamura, H.; Oda, Y.; Iwai, S.; Inoue, H.; Ohtsuka, E.; Kanaya, S.; Kimura, S.; Katsuda, C.; Katayanagi, K.; Morikawa, K.; Miyashiro, H.; Ikehara, M. How does RNase H recognize DNA·RNA. Hybrid ?. *Proc. Natl. Acad. Sci. U.S.A*. **1991**, *88*, 11535.
4. Prakash, T. P. An Overview of Sugar-Modified Oligonucleotides for Antisense Therapeutics. *Biodiversity,* **2011**, *8*, 1616.
5. Fedoroff, O.-Y.; Salazar M.; Reid B. R. Structure of a DNA:RNA hybrid duplex. Why RNase H does not cleave pure RNA. *J. Mol. Biol.* **1993**, *233*, 509.
6. Zamaratski, E.; Pradeepkumar, P. I.; Chattopadhyaya, J. A. critical survey of the structure-function of the antisense oligo/RNA heteroduplex as substrate for RNase H. *J. Biochem. Biophys. Methods.* **2001**, *48*, 189.
7. Levin, A. A. A review of issues in the pharmacokinetics and toxicology of phosphorothioate antisense oligonucleotides. *Biochim. Biophys. Acta*. **1999**, *1489*, 69.
8. (a) Kurreck, J. Antisense technologies. Improvement through novel chemical modifications. *Eur. J. Biochem.* **2003**, *270*, 1628; (b) Shukla, S.; Sumaria, C. S.; Pradeepkumar, P. I. Exploring chemical modifications for siRNA therapeutics: A structural and functional outlook. *Chem. Med. Chem*, **2010**, *5*, 328; (c) Micklefield, J. Backbone modification of nucleic acids: Synthesis, structure and therapeutic applications. *Curr. Med. Chem.* **2001**, *8*, 1157.
9. Lesnik, E. A.; Guinosso, C. J.; Kawasaki, A. M.; Sasmor, H.; Zounes, M.; Cummins, L. L.; Ecker, D. J.; Cook, P. D.; Freier, S. M. Oligodeoxynucleotides containing 2'-*O*-modified adenosine: synthesis and effects on stability of DNA:RNA duplexes. *Biochemistry* **1993**, *32*, 7832.

10. Manoharan, M. 2'-Carbohydrate modifications in antisense oligonucleotide therapy: importance of conformation, configuration and conjugation. *Biochim. Biophysi. Acta.* **1999**, *1489*, 117.

11. Martin, P. A new access to 2'-*O*-alkylated ribonucleosides and properties of 2'-*O*-alkylated Oligoribonucleotides. *Helv. Chim. Acta* **1995**, *78*, 486.

12. Kawasaki, A. M.; Casper, M. D.; Freier, S. M.; Lesnik, E. A.; Zounes, M. C.; Cummins, L. L.; Gonzalez, C.; Cook, P.D. Uniformly modified 2'-deoxy-2'-fluoro-phosphorothioate oligonucleotides as nuclease-resistant antisense compounds with high affinity and specificity for RNA targets. *J. Med. Chem*. **1993**, *36*, 831.

13. Ramasamy K. S.; Zounes, M.; Gonzalez, C.; Freier, S. M.; Lesnik, E. A.; Cummins, L. L.; Griffeu, R. H.; Monia, B. P.; Cook, P. D. Remarkable enhancement of binding affinity of Heterocycle-modified DNA to DNA and RNA. Synthesis, characterization and biophysical evaluation of N^2-imidazolylpropylguanine and N^2-imidazolylpropyl-2-aminoadenine modified oligonucleotides. *Tetrahedron Lett*. **1994**, *2*, 215.

14. (a) Noronha, A. M.; Wilds, C. J.; Lok C-N.; Viazovkina K, Arion D, Parniak, M. A. Masad, M. J. Synthesis and properties of arabinonucleic acids (ANA).: circular dichroic spectra, melting temperatures, and RNase H susceptibility of ANA:RNA hybrid duplexes. *Biochemistry* **2000**, *39*, 7050; (b) Lima, W. F.; Nichols, J. G.; Wu, H.; Prakash, T. P.; Migawa, M. T.; Wyrzykiewicz, T. K.; Bhat, B.; Crooke, S. T. Structural Requirements at the Catalytic Site of the Heteroduplex Substrate for Human RNase H1 Catalysis. *J. Biol. Chem*. **2004**, *279*, 36317; (c) Minasov, G.; Teplova, M.; Nielsen, P.; Wengel, J.; Egli M. Structural basis of cleavage by RNase H of hybrids of arabinonucleic acids and RNA. *Biochemistry* **2000**, *39*, 3525; (d) Damha, M. J.; Wilds, C. J.; Noronha, A. M.; Bruckner, I.; Borkow, G.; Arion, D.; Parnaik, M. A.; Hybrids of RNA and arabinonucleic acids (ANA and 2'F–ANA) are substrates of ribonuclease H. *J. Am. Chem. Soc.* **1998**, *120*, 12976.

15. Denisov, A.Y.; Noronha, A. M.; Wilds, C. J.; Trempe, J.-F.; Pon, R. T.; Gehring, K.; Damha, M. J. Solution structure of an arabinonucleic acid (ANA)/RNA duplex in a chimeric hairpin: comparison with 2'-fluoro-ANA/RNA and DNA/RNA hybrids. *Nucleic Acids Res*. **2001**, *29*, 4284.

16. Bennett, C. F.; Swayze, E. E. RNA Targeting Therapeutics: Molecular Mechanisms of Antisense Oligonucleotides as a Therapeutic Platform. *Annu. Rev. Pharmacol. Toxicol.* **2010**, *50*, 259.
17. Kurreck, J.; Wyszko, E.; Gillen, C.; Erdmann V. A. Design of antisense oligonucleotides stabilized by locked nucleic acids. *Nucleic Acid Res.* **2002**, *30*, 1911.
18. Rajwanshi, V. K.; Ha˚kansson, A. E.; Sørensen, M. D.; Pitsch, S.; Singh, S. K.; Kumar, R.; Nielsen, P.; Wengel, J. The Eight Stereoisomers of LNA (Locked Nucleic Acid): A Remarkable Family of Strong RNA Binding Molecules. *Angew. Chem., Int. Ed.* **2000**, *39*, 1656.
19. Nielsen, K. M. E.; Petersen, M.; Ha˚kansson, A. E.; Wengel, J.; Jacobsen, J. P. α -L-LNA (α-L-ribo Configured Locked Nucleic Acid) Recognition of DNA: An NMR Spectroscopic Study, *Chemistry* **2002**, *8*, 3001.
20. Nielsen, J. T.; Stein, P. C.; Petersen, M. NMR structure of an α-L-LNA:RNA hybrid: structural implications for RNase H recognition. *Nucleic Acids Res*. **2003**, *31*, 5858.
21. Wang, J.; Verbeure, B.; Luyten, I.; Lescrinier, E.; Froeyen, M.;, Hendrix C.; Rosemeyer, H.; Seela, F.; Van Aerschot, A.; Herdewijn, P. Cyclohexene nucleic acids CeNA: serum stable oligonucleotides that activate Rnase H and increase duplex stability with complementary RNA. *J. Am. Chem. Soc.* **2000***, 122,* 8595.
22. Wang, G.; Middleton, P. J.; Lin, C.; Pietrzkowski, Z. Biophysical and biochemical properties oligonucleotides containing 4'-C- and 5'-C- substituted thymidines. *Bioorg. Med. Chem. Lett*. **1999**, *9*, 885.
23. Kanazaki, M.; Ueno, Y.; Shuto, S.; Matsuda, A. Highly nuclease-resistant phosphodiester-type oligodeoxynucleotides containing 4'-α-*C*-aminoalkylthymidines form thermally stable duplexes with DNA and RNA. A candidate for potent antisense molecules. *J. Am. Chem. Soc*. **2000**, *122*, 2422.
24. Fensholdt, J.; Thrane, H.; Wengel, J. Synthesis of oligodeoxynucleotides containing 4'-C-(hydroxymethyl)thymidine: Novel promising antisense molecules. *Tetrahedron Lett*. **1995**, *36*, 2535.
25. DreioØea, L. H.; Wengel, J. Synthesis and evaluation of oligodeoxynucleotides containing 3′-*O*-ethyl- 4′-*C*-(hydroxymethyl)thymidine: Introduction of a novel

class of phosphodiester internucleoside linkages, *Nucleosides and Nucleotides*. **1994**, *13*, 1939.

26. Nielsen, K. D.; Kirpekar, F.; Roepstorft, P.; Wengel, J. Oligonucleotide analogues containing 4'-C-(hydroxymethyl)uridine: Synthesis, evaluation and mass spectrometric analysis. *Bio. Med. Chem.* **1995**, *3*, 1493.
27. (a) O-Yang, C.; Kurz, W.; Elsie M. Eugui, E. M.; McRoberts, M. J.; Verheyden, J. P. H.; Kurz, L. J.; Walker, K. A. M. 4'-substituted Nucleosides as Inhibitors of HIV: An Unusal Oxetane Derivative *Tetrahedron Lett*, **1992**, *33*, 41; (b) Synthesis of 4'-cynothymidine and analogs of Potent Inhibitors of HIV. Couade O-Yang.; Helen Y. Wu.; Elizabeth, B.; Smith, F.; Walker, K. A. M. *Tetrahedron Lett*, **1992**, *33*. 37.
28. Wang, G.; Seifert, W.E. Synthesis and evaluation of oligodeoxynucleotides containing 4'-C-substituted thymidines. *Tetrahedron Lett*. **1996**, *36*, 6515.
29. More J. D.; Finney, N. S. A Simple and Advantageous protocol for the oxidation of alcohols with o-Iodoxybenzoic Acid (IBX). *Org. Lett.* **2002**, *4*, 3001.
30. (a) Omura, K.; Swern, D. Oxidation of alcohols by "activated'' dimethyl sulphoxide. A preparative, steric and mechanistic study . *Tetrahedron* **1978**, *34*, 1651; (b) Mancuso, A. J.; Swern, D. Activated dimethyl sulphoxide: Useful reagents for synthesis. *Synthesis* **1981**, 165.
31. Pfitzer K. E.; Moffatt, J.G. Sulfoxide-Carbodiimide reactions. I. A facile oxidation of alcohols. *J. Am. Chem. Soc*, **1965**, *87*, 5661.
32. Jones, G. H.; Taniguchi, M.; Tegg, D.; Moffatt, J. G. 4'-Substituted nucleosides. Hydroxymethylation of nucleoside 5'-aldehydes. *J. Org. Chem*. **1979,** *44*, 1309.
33. Altona, C.; Sundaralingam, M. Conformational analysis of the sugar ring in nucleosides and nucleotides. A new description using the concept of pseudorotation. *J. Am. Chem. Soc*. ***1972***, *94*, 8205.
34. Neidle, S. Principles of nucleic acid structure, 1st Edition , **2007**, Academic Press
35. Abes, S.; Turner, J. J.; Ivanova, G. D.; Owen, D.; Williams, D.; Arzumanov, A.; Clair, P.; Gait, M. J.; Lebleu, B. Efficient splicing correction by PNA conjugation to an R6-Penetratin delivery peptide, *Nucleic Acids Res.* **2007**, *13*, 4495.
36. (a) Nowell, P.; Hungerford, D. A minute chromosome in human chronic granulo cytic leukemia. *Science*, **1960**, *132*, 1497; (b) Deininger, M. W. N., Goldman J.

M. and Melo J. V. The molecular biology of chronic myeloid leukemia. *Blood*, **2000**, *96*, 3343.

37. (a) Gait, M. J. Oligonucleotide synthesis: A practical approach. IRL Press Oxford, UK 217; (b) Agrawal, S. PROTOCOLS for oligonucleotides and analogs Synthesis and Properties Methods in Molecular Biology. (ed): vol.20 Totowa, NJ,. Humana Press, Inc.
38. G. M. Sheldrick, SHELX-97 program for crystal structure solution and refinement, University of Gottingen, Germany, 1997